SOME ASPECTS OF THE INJECTION MOULDING OF ALUMINA AND OTHER ENGINEERING CERAMICS.

BY

M. YOUSEFFI, B.Sc. (Hons.), M.Sc.,

A Doctoral Thesis submitted in
partial fulfilment of the requirements for the award of
Doctor of Philosophy of the Loughborough
University of Technology
July 1992

Supervisor: Prof. Ian A. Menzies, BSc St Andrews, MBA CNAA, PhD London, DSc Manchester, DIC, FBIM, CChem, FRSC, FIM, FICorr, FIMF, CEng, MIMM, AInst.Pkg
(Institute of Polymer Technology and Materials Engineering)

ACKNOWLEDGEMENTS

I would like to express my sincere thanks to the following people and organisations without whom this thesis would not have been written:-

Dr. D. Gabe, for use of Departmental facilities;
Dr. P. J. James, for use of equipments in the Powder Metallurgy Laboratory and discussions on powder injection moulding (PIM);
Dr. Michael T. Martyn, for discussions on PIM;
Prof. Ian A. Menzies, for arranging the finance and very kind and useful supervision of this work;
Mr. R. Owen, for technical advice and assistance with various laboratory equipments;
Mr. F. Page, for discussion and help with scanning electron microscope;
Mr. P. Ramsey, for the use of various laboratory equipments;
Loughborough University of Technology, for the provision of all kinds of facilities within the University Campass;

and to the many other members of I.P.T.M.E. who have helped in various ways. I am also very grateful to my parents for their support throughout my studies and ,of course, thanks to God for everything and without whom this world would not exist.

ABSTRACT

The literature concerning the injection moulding of engineering ceramics has been reviewed. This indicated that a number of claims had been made for the successful use of different organic binders during moulding and their removal prior to sintering. However, many of the claims were not supported by detailed/exact experimental evidence as to powder-binder compositions, moulding conditions, moulded properties, debinding times/cycles, or details of the structure and properties of the solid ceramic bodies produced. From the available information it was clear that there were few systematic and scientific investigations concerning the understanding of each stage of the injection moulding process.

The present research programme has been carried out in two phases as follows. The first phase was concerned with the re-investigation and re-evaluation of binder systems claimed to be successful for the injection moulding of alumina ceramics. The binders re-investigated included the thermoplastic-based binders such as polystyrene, polyacetal and atactic polypropylene and the water-based methylcellulose (Rivers) binder system. Alumina was chosen as the main powder to be investigated due to its simple handling and highest applications amongst ceramic materials and on the basis that there is incomplete published work for almost every step of the injection moulding process. During the first stage of this work the optimum properties such as powder-binder compositions, mixing and moulding conditions, debinding properties, green and sintered densities provided by each binder system were determined. The results of these investigations showed that all the previous (re-evaluated) binder systems had major limitations and disadvantages. These included low volume loading (64 % maximum) of the alumina powder resulting in rather low sintered densities (96 % maximum-of theoretical density) and very long debinding times in the case of the thermoplastic-based binders. Very low alumina volume loading (55 % maximum resulting in a 94 % sintered theoretical density) and long moulding cycle time (-5 min) along with adhesion and distortion problems during demoulding occurred in the case of the water-based methylcellulose binder system. Further work did not appear worthwhile.

The second phase of the present work has involved the development of new binder systems in order to obtain better properties such as higher volume loadings of the alumina powder (to obtain higher sintered densities and hence better mechanical properties), better moulding and demoulding properties, shorter moulding cycle times and shorter debinding times (where possible) than those of the existing/re-evaluated binder systems. These new systems were a thermoplastic+wax based binder system (polyisobutylene+montanester wax+liquid paraffin) and a water-based (polyvinyl alcohol) binder system. This phase has involved studies of powder-binder compositions and rheological properties, studies of thermogravimetric behaviour of the binders and also their removal processes, determination of

moulding and sintering conditions, microstructural studies and determination of mechanical and thermal properties. The use of these new binder systems has led to higher moulded and sintered densities of alumina which resulted in improved flexural and compressive strengths (27-35 %), as compared with the best results claimed in the literature for injection moulded alumina. A maximum possible volume loading of 70 % of the alumina powder resulting in a 98.5 % sintered theoretical density were achieved by the newly developed thermoplastic+wax based binder system. With the newly developed water-based binder system a 56 % volume loading resulting in a 96 % sintered theoretical density with a moulding cycle time of < 1 min was achieved without any adhesion and distortion problems. Thermal conductivity data have been determined experimentally for injection moulded alumina ceramics (having different compositions) for the first time and the results are as good as, if not marginally better than those claimed for alumina produced by compaction techniques.

The newly developed binder systems have been used with a number of other powders such as zirconia, silicon nitride, silicon carbide, tungsten carbide-6 weight % cobalt and iron-2 weight % nickel, to establish whether injection moulding is feasible. Optimum properties such as powder volume loadings, mixing, moulding, demoulding, moulded densities, debinding and some sintered density results showed that these new binder systems can also be used successfully for the injection moulding of other ceramic and metallic powders, although a fuller evaluation of the properties such as optimum sintered densities and mechanical properties is required.

CONTENTS

CHAPTER FOUR

CHAPTER FIVE

CHAPTER ONE

CHAPTER ONE

1- INTRODUCTION

Ceramic/metallic powder injection moulding technique has gained universal attraction for the production of near-net shape components with complex shapes, high dimensional accuracy, high strength and uniformity, low scrap rates and reasonable cost at highly automated production rates (1). Due to such properties the powder injection moulding (PIM) technique is considered superior to the other powder fabrication techniques such as the present die compaction technique which can only be used for the production of simple shapes with low aspect, i.e. length/diameter, ratios. Cold or hot isostatic pressing techniques can be used for the production of more complex shapes but these techniques are very expensive for mass production. It is also very well known (2) that the PIM technique can be used for the production of any fine ceramic or metallic powder that can be sintered and that this technique offers more benefit than the usual thermo-mechanical methods for the production of certain powders which are hard, brittle, non-plastic and have relatively high melting points and rely almost entirely on powder metallurgy techniques as the only viable fabrication method. Oxide ceramics such as alumina, cermets such as tungsten carbide-cobalt alloys, nitrides such as silicon nitride and carbides such as silicon carbide are typical examples of such powders which have been injection moulded.

From this background it is quite clear that the PIM process will have a better future provided that it is understood more scientifically and technically and also accepted more economically as a viable production technique (1). It is partly for these reasons that the present research program was commenced.

The present injection moulding process originated from the die-casting technique for non-ferrous alloys which were melted and then injected into closed dies to form the desired shapes. This technique was later applied successfully in the plastic moulding

industry with its first application being the production of continuous rod, sheet or tube made out of cellulose nitrate plasticised with camphor by extruding it through a nozzle into a cooled mould. The first commercial application of the PIM process in its present form is attributed to Schwartzwalder (4) in 1937, who injection moulded ceramic spark plug insulators. This technique was replaced later by isostatic pressing as a more efficient technique. The ceramic injection moulding (CIM) industry gained its wide acceptance only within the last two decades (1-7). The injection moulding of metallic powders was started in the 1960's (2) and has not yet been accepted as an economically and technically viable process due mainly to lack of detailed scientific and technical (experimental) information which is also true for the CIM process (1).

The application of the PIM process to alumina powder (which is the main powder investigated during this research work) has only recently received some systematic and scientific attention only in few areas of the CIM process which consists essentially of the following steps: (i)- tailoring the ceramic powder; (ii)- developing suitable organic binder formulations; (iii)- producing a homogeneous ceramic and organic binder mixture; (iv)- moulding the ceramic-binder mixture; (v)-removing the organic binders; (vi)- sintering (densifying) the debonded body after binder removal. The recent scietific and systematic approach has resulted in the publications of number of papers on agglomeration effects, ceramic-binder formulations, compounding and on ceramic moulding and debinding defects and their remedies which will be covered in detail in the detailed literature review which follows.

The literature review (chapter two) has indicated clearly the fragmentary pattern of published work of which is lacking in detail in many or all the process steps indicated above, whatever the particular ceramic system which is considered. Individual groups of research workers have provided isolated pockets of information on particular aspects of individual steps and industrial reviews have described process and products in qualitative terms only. Overall it is clear that few

quantitative relationships have been established between the processing steps and the properties of fully processed test pieces or components. One of the development objectives is to shorten processing times in the binder burn-out stage and to reduce overall processing times and hence costs.

In view of these general features it was decided to select a simple oxide ceramic system with available starting materials to avoid difficulties with controlled atmospheres during processing. Alumina was selected since there is a base of incomplete published work. The technical/experimental information available so far for the injection moulded alumina ceramics is incomplete and does not give the exact details necessary for each stage of the CIM process. The informations available in the present literature can be summarised as follows: (i)- some scattered informations are available concerning the effects of powder characteristics on the rheology of a typical alumina powder using an ethylene vinyl acetate (EVA) copolymer as the binder which, as will be seen in the results chapter, was found to be unsuitable as a major binder for the injection moulding of alumina ceramics due to its crumbling and cracking problems during the debinding stage; (ii)- different binder systems which have technical and economical limitations as will be seen in the results chapter for each re-evaluated binder system; (iii)- few injection moulding operations which do not give the exact moulding conditions and almost no information is available about the moulded densities; (iv)- some general debinding conditions which do not specify the exact debinding times and do not provide the exact detail of the debinding cycle; and (v)- some general sintering conditions which may not be entirely valid for every injection moulded alumina ceramic and therefore have to be re-evaluated as is the case for the other properties.

One of the objectives of the present work is therefore to provide a complete experimental/practical detail for each step of the injection moulding of alumina powder using the available binder systems for which some success have been claimed for in the literature. These binder systems can be divided into two

groups. One group is based on the usual thermoplastic/wax binders and the other on water-soluble polymers. The most popular binder systems in each group are re-investigated and re-evaluated during the first part of this research work in order to obtain the exact/detailed properties such as: (a)- maximum possible volume loading of the alumina powder into the binder system; (b)- mixing; (c)- moulding and demoulding properties; (d)- the detailed debinding cycle characteristics; and (e)- green and sintered densities achievable by each binder system. The binder systems investigated were as follows: (1)- ethylene vinyl acetate copolymer; (2)- polystyrene; (3)- polyacetal copolymer; (4)- atactic polypropylene; and (5)- the water-soluble methylcellulose (Rivers) binder system.

As will be seen in the results chapter (chapter four) all of these re-evaluated binder systems proved to have serious shortcomings and some major limitations and therefore did not appear to be worthy of furthur development. These limitations can be summarised as follows: low volume loadings of the alumina powder resulting in low sintered densities, and quite long debinding times particularly for thick sections (> 3 mm) in the case of thermoplastic-based binder systems; the maximum achievable volume loading was 64 % of the alumina powder into the atactic polypropylene (APP) binder system which resulted in a sintered density of only 96 % of theoretical density; the shortest possible debinding times were 78 and 107 h for the 3 and 6 mm thick samples respectively provided by the APP binder system. The re-evaluated water-based binder system provided a much longer moulding cycle time (5 min total) and much lower volume loading (55 % maximum) of the alumina powder (resulting in a lower sintered density of 94 % theoretical) than the re-evaluated thermoplastic-based binder systems and also there were adhesion and distortion problems during the demoulding (ejection) process. However, the re-investigated water-based binder system provided much shorter debinding time (20 h for 5 mm thick samples) than the thermoplastic-based binder systems which is quite typical. The re-evaluated properties for each re-investigated binder system are quite originl since they are not available in the present literature.

However, these re-evaluated properties suggested quite strongly that there is a need for developing new binder systems which can provide better properties such as higher volume loadings of the alumina powder (so that to obtain higher sintered densities), reasonable debinding and cycle times, better moulding and demoulding properties than the existing/re-evaluated binder systems. This was another major objective of the present work which resulted in the development of two new binder systems during the second part of this research programme, i.e. the polyisobutylene-montanester wax-liquid paraffin (PIB-MEW-LP) binder system which is based on thermoplastic + wax binders and the water-based polyvinyl alcohol (PVA) binder system, for the injection moulding of alumina ceramics. The newly developed PIB-MEW-LP binder system provided a maximum possible volume loading of 70 % of the alumina powder which resulted in a sintered density of 98.5 % of theoretical with very similar debinding times to those of the APP binder system. The newly developed water-based PVA binder system provided a maximum possible volume loading of 56 % of the alumina powder resulting in a sintered density of 96 % of theoretical with a very short debinding time of 12 h and without any adhesion and distortion problems with a moulding cycle of < 1 min. As can be seen these properties are much better than those provided by the existing/re-evaluated binder systems.

Sintered and fractured microstructures, flexural (or bend) and compressive strengths and thermal conductivities of the injection moulded (99.5, 95 and 88 %) alumina ceramics obtained during this work using the best binder systems (PIB-MEW-LP, 60/40 APP and the water-based PVA) are also investigated and compared with those obtained by other workers (104, 173) for the injection moulded and compacted alumina ceramics having similar chemical compositions. The results of these investigations showed very similar properties to those of the standard microstructures, flexural and compressive strengths and thermal conductivities of the compacted alumina ceramics and that the flexural strength results obtained during this work for the injection moulded 99.5 % alumina ceramics using the newly developed binder systems are higher (27-35 %) than that obtained

by another worker (173) for an injection moulded alumina ceramic having a similar chemical composition.
Bend and compressive strengths of 401 and 4400 MN/m^2 were obtained for the injection moulded 99.5 % alumina ceramics using the newly developed PIB-MEW-LP binder system. These values are very similar to those reported in the alumina book (104) and in the Handbook of Materials Science (see chapter five-Table 5.1) for the compacted alumina ceramics having similar chemical compositions. The newly developed water-based PVA binder system provided bend and compressive strengths of 360 and 4000 MN/m^2 respectively which are quite satisfactory and comparable to the standard 99.5 % alumina ceramics (see chapter five-Table 5.1). Thermal conductivities of 23.3 and 20.8 KW/m^oC were obtained for the injection moulded 99.5 % alumina ceramics using the newly developed PIB-MEW-LP and the water-based PVA binder systems respectively. These results are also in good agreement with those reported by other workers (see chapter five-Table 5.2) for the compacted 99.5 % alumina ceramics.

The newly developed PIB-MEW-LP and the water-based PVA binder systems were sufficiently promising to suggest that it would be worthwhile to carry out some preliminary evaluation (such as formulation, mixing, moulding, demoulding, debinding and sintering) of these binder systems for other ceramic and metallic powders. The results of these investigations suggest that the newly developed binder systems can also be used successfully for the injection moulding of other powders such as zirconia, silicon nitride, silicon carbide, hardmetals and iron-nickel (metallic) powders, although a fuller evaluation of the systems is required to establish a more complete results such as sintered and mechanical properties.

As already mentioned the main powder investigated during this research work is a 99.5 % alumina powder with an average particle size of 1.4 μm and a particle size distribution of 0.1-10 μm having almost spherical shapes which is a typical alumina/ceramic powder used for the injection moulding process (1-2). This alumina powder along with other powders used during this work will be described in detail in the material section of

chapter three of this thesis. It is also useful to mention that there are mainly three grades of alumina ceramics available in the market and they are as follows: the 88 % aluminas which are used for general purpose applications; the 95 % plus aluminas which also cover the bulk of the market and the 99.5 % plus alumina grades used widely for particular applications. There are many applications of alumina ceramics which can be classified mainly into three groups, mechanical, electrical/electronic and medical applications which are described in detail during the literature review. Alumina ceramics have the highest number of applications among ceramic materials and are the strongest among oxide ceramics.

The production technique of alumina ceramics depends on the purity of the alumina powder. Lower grades of alumina (e.g. porcelain) are generally produced by the more conventional compacting techniques such as slip casting whereas the high purity alumina ceramics are normally produced by other compacting techniques such as dry pressing, hydrostatic moulding, extrusion, injection moulding and hot pressing. The slip casting process cannot be used for the production of high purity aluminas due to lack of precompaction (104). Dry pressing is the most economical compacting process for the production of high purity aluminas but can only be applied to small parts with simple shapes. Parts with larger dimensions and aspect ratios more than 4:1 are preferably manufactured by hydrostatic moulding. Extrusion process is restricted to production of long rods and tubes with small diameters but various profiles, as well as flat ribbons for special applications. The injection moulding technique is just recently being applied to the production of small/medium parts with complicated shapes (e.g. for the textile industry). The hot pressing method is reserved for relatively small parts for special applications with extreme requirements and is the most expensive powder compacting process and therefore economically the least viable technique.

The dry compaction technique at different compaction pressures (30-200 MN/m^2) is used during this work for the production of alumina ceramics with simple rectangular shapes and their sintered densities are compared with the alumina ceramics

obtained during this work by the injection moulding process (using the best binder systems) having similar shapes with the same chemical compositions as the compacted alumina samples. It is found that both production techniques provided very similar sintered densities (and very near to their theoretical densities). However, it is very well known (1-7) that density variations are easily introduced during the die compaction process by stress gradients set up by differences in frictional forces specially in the case of hard, brittle and non-plastic powders. This density variation can result in differential shrinkage during sintering (1) which will ultimately affect the dimensional accuracy and can also cause internal cracks which will have a deleterious effect on mechanical properties. It follows therefore that in order to avoid this problem the production of parts is limited to simple geometries with low aspect ratios of ~1.0. Complex shapes are then usually machined from these simple pre-sintered parts produced by a pressing operation. Such processes are quite expensive, take considerable time and energy and also require expensive diamond coated tooling which leads to a lot of material wastage (often . 30-60 %). In contrast, the PIM technique does not have the as-mentioned problems and can be used quite successfully for the production of small, medium or large components with very complex shapes and uniform properties which requires the correct conditions for each stage of the injection moulding process. It is part of the objectives of this work to provide such correct conditions for each stage of the injection moulding of alumina (and other) powders. The most immediate area for investigation is the optimisation of the powder-binder composition which requires a proper powder and a correct binder formulation. This leads to optimum properties such as maximum possible volume loading of the powder into the binder system which provides maximum green (as-moulded) and sintered densities. Such optimised properties are obtained for each powder-binder mixture used during this work. It is believed (1-2) that the most important and vital stage of the injection moulding process is the debinding (binder removal) stage which influences to a great extent the final sintered properties. This stage is investigated thoroughly using thermogravimetric analysis. Optimised debinding

times and conditions are obtained for each moulded powder-binder composition having different thicknesses.

This thesis consists of six chapters. The first chapter as already covered was the introduction to the present research programme. The second chapter is devoted to the literature review covering in detail the related theoretical, technical and experimental background of the injection moulding process. This chapter ends with the general review of some injection moulded nitride, carbide, cermet and metallic powders and finally in more detail it covers the history of the injection moulded alumina ceramics using different binder systems, the characteristics and limitations of these binder systems, sintering, mechanical, thermal and electrical properties and applications of alumina ceramics. Chapter three of this thesis covers the materials and equipments used during this work. This chapter provides the relevant properties for each material and also the relevant procedure for each equipment used during the experimental work. Chapter four covers the experimental results and their interpretations. Chapter five covers the discussion of the results and compares them with the results already available from the literature and finally conclusions and suggestions for future work are covered in chapter six of this thesis.

CHAPTER TWO

CHAPTER TWO

2- REVIEW OF RELEVANT LITERATURE

This chapter is devoted to the review of the available literature concerning the injection moulding of powders. First section of this chapter gives a summary of the injection moulding process for ceramic/metallic powders. The second part covers in detail the literature on the properties of the individual stages of the injection moulding process. The third part is devoted to the available literature on the injection moulding of different ceramics, metallics and cermets in general. The fourth part covers the injection moulding of alumina ceramics in more detail since it is the major ceramic powder investigated during this research work. The fifth (last) part of this chapter gives an introduction to the present work which describes the linkage between this work and the shortcomings of the literature.

2.1- Summary of the injection moulding process and its applications

Ceramic/metallic injection moulding (C/MIM) consists, basically, of the following stages (1).

1-Mixing, which involves mixing of a ceramic/metallic powder (C/MP) with temporary organic additives (i.e. binders) to form a ceramic/metallic-binder mixture (C/MBM) which flows under heat and pressure to fill the cavity of a closed mould.

2-Injecting the heated mixture into the mould cavity using an injection moulding machine to form a precision component.

3-Opening the mould and removing the moulded article (i.e. demoulding).

4-Removing the organic binders (i.e. debinding) either by solvent extraction or by thermal decomposition.

5-Sintering of the debonded body to achieve strength and near full density.

6-Finishing of the sintered body if necessary.

A process flow chart illustrating the above stages in more detail is shown in Fig. 2.1 which must be followed completely for a successful injection moulding process. As can be seen from this flow chart powder and binder characterisations are essential parts of the injection moulding process prior to the mixing stage. Powder characterisation includes determination of : chemical composition, particle size, particle size distribution, particle shape, specific surface area, tap and full densities. Binder characterisation includes : thermophysical properties, burning characteristics (i.e. thermogravimetric analysis), chemical or corrosive behaviour, wetting characteristics and rheological properties. Characterisation of the binder mixture includes : miscibility of the components, chemical reactions of the components and thermogravimetric properties of the mixture. After the mixing process characterisation of the powder-binder mixture and mould design are necessary so as to obtain the correct flow properties for the C/MBM. Characterisation of the powder-binder mixture (or feedstock) includes: rheological analysis and mouldability

studies of the feedstock so that to obtain the correct rheological and moulding properties. The mould should be designed in such a way that: it provides the correct flow (i.e. plug flow) and to prevent jetting of the feedstock
Weld lines which are the source of weakness and cracks are formed due to jetting of the feedstock. By choosing the right moulding conditions (i.e. moulding and mould temperatures, injection and hold pressures) the feedstock can then be injection moulded. After removal from the mould the moulded parts must be inspected visually, optically and by non-destructive testing methods for defects such as cracks, pores and bubbles. The cause of defects, if any, must be found and eliminated prior to the debinding (binder removal) process. It is also necessary to know the burning characteristics of each binder used in order to programme the correct debinding cycle. After debinding the debonded parts must be inspected for defects. Inspection of the debonded parts includes: visual inspection for visible debinding defects such as macro-cracks, blistering and swelling. For the inspection of the micro-cracks and bubbles x-ray tests are carried out. Dimensional, geometrical and chemical stability should also be checked. The debinding defects should be eliminated by choosing the correct debinding conditions which must be programmed according to the thermogravimetric analysis (TGA) results. The debinding process is commonly carried out either by solvent extraction or by thermal treatment to break down and vaporise the binders. Binders are usually designed to come off sequentially so as not to disturb the geometry of the part, leaving just enough binder to hold the ceramic/metallic shape together. Finally the debonded parts are sintered to achieve strength and near full density. After sintering the sintered parts should be inspected for dimensions, density, porosity, cracks, pores and surface finish (3). Any sintering defects and short comings must be eliminated by choosing the right sintering conditions. Finishing (e.g. machinning) of the sintered part, if necessary, may then be carried out. The very fine powder particles provide a very strong thermodynamic driving force and parts undergo shrinkage

during sintering which must be considered during the mould design stage . Reproducibility of the sintered parts is achieved through close control over the feedstock and moulding variables (2). The metal injection moulded parts, once sintered, can then be given supplementary treatments exactly like wrought products, including heat treatment, plating or machining (2).

Applications of the powder injection moulding process

Injection moulding of powders (ceramic, metallic and cermets) has been a useful technique for producing components with complex shapes, high dimensional accuracy, high strength and uniformity, low scrap rates and reasonable cost (1). Injection moulding also offers an automated process at high rates. It has been known (2) that almost any metal or ceramic which can be obtained as fine particles and which can be sintered can be injection moulded.

However, ceramic injection moulding in its present form was first used for the fabrication of spark plug insulators in 1937 (4), which was replaced later by isostatic pressing as a more effective and more efficient forming method. Since the 1930's there has been a continuous record of the developments and applications of injection moulded ceramic materials in the literature. From the available literature and many small and large industries it is quite clear that the injection moulding technique is the most suitable manufacturing technique for the production of complex structural ceramic/metallic shapes at high production rates and that this technique has replaced the expensive high pressure techniques and machining processes (1). The main application fields of ceramic injection moulding has been as follows: 1-In the electrical and electronic industries as a whole and particularly in the telecommunications industry, there is a wide variety of applications for ceramic parts of complex shape, high dimensional accuracy and specialised compositions (5). Among these ceramics aluminium oxide (or alumina) ceramics have been used more widely than any other ceramic material.

2-As aerospace refractory and structural components (6).
3-In medical and dental industries, e.g. partially stabilised zirconia (PSZ) and alumina are produced as dental brackets by the injection moulding process.
4-For applications in gas turbine, diesel engines, turbochargers, heat exchangers, etc. where corrosion, oxidation, creep/stress rupture and thermal fatigue affect the integrity of the component. Examples are injection moulded silicon nitride and silicon carbide engine parts (7).
5-In non-chip-forming applications, such as in stamping and forming as shearing, bending and deep-drawing tools and in reducing and extrusion dies. The main material for these applications is the tungsten carbide-(6-10) weight % cobalt (also known as hardmetal or cemented carbide) which is a cermet. This material is also used widely as a cutting tool.
<u>For the metallic materials the main applications of the injection moulding process are :</u> 1-Nickel-Iron in guns and armaments, office equipment, light machine tools, drill blank bits, computer peripherals, magnetic armatures, fasteners, etc. (8).
2-Stainless steels in medical and dental instrumentations, orthodontic devices, valve components, chemical machinery, electronic armatures, food and beverage machines, etc. (8).
3-Kovar and tungsten-copper in hermetic packages, heat sinks and flanges, eyelets and headers, power packages, microwave packages, etc. (8).
4-Specialty alloys, e.g. stellite for high temperature parts, Si-Fe for magnetic armatures, Hastelloy for high temperature and corrosion, low-alloy steels, etc. (8).
It has been reported that injection moulding can also be used to form ceramic/metallic matrix composites with particulates, fibre or whisker reinforcements (9-11). With these materials one of the main difficulties is homogeneous mixing of different constituents without changing their properties. In this area the development seems to be in its infancy (12).

2.2- Injection moulding of powders

This section covers in detail the available literature on the individual stages of the injection moulding process as described in the previous section (section 2.1).

2.2.1- Powder properties

This includes: average particle size, particle size distribution, particle shape, specific surface area, surface chemistry, dispersion, wettability and surface tension forces. For a successful powder injection moulding process these parametric variables should be characterised, examined and related in a systematic manner (13). For an ideal powder injection moulding the powder property requirements can be summarised as follows (14):

First powders have to be tailored for maximum packing so as to achieve high green densities and to minimise the binder content without seriously affecting basic rheology requirements (15). The packing density of multiparticle systems can be increased when the particle size distribution is extended (16). The mean particle size must be between 0.1 and 30 microns. A particle size < 10 μm would lead to a greater degree of homogeneity within a filled powder system as opposed to a coarse particle system (15), and because the rate of diffusion during sintering is inversely proportional to the square of particle size, therefore shrinkage and densification of a porous body will proceed more rapidly with finer powders and also the pores will be removed more effectively (15). Within such a particle system the remaining void volume must be more than sufficiently filled by the binder ingredients in order that flow is possible under injection moulding conditions (17). The particle's shape should be equiaxed to spherical so as to obtain maximum prefired densities (18). Particle size effects for some properties depend on the diameter of the particle directly and for others on the reciprocal of the particle diameter (14). For example, the ability of the material to replicate the detail of the mould, to achieve good surface finish and to retain shape in the green

compact during subsequent processes like debinding and sintering are all proportional to the reciprocal of the diameter. On the other hand, the rate of debinding, mixing rate and the packing density are all related directly to the diameter (14). It follows therefore that some compromise is required.

There are some other desirable and important properties of the powder which can be summarised as follows (14). There should be no agglomeration of powder particles before and during mixing because the presence of agglomerates can have damaging effects on sintering kinetics and final density (19) and are also capable of introducing strength limiting flaws. The surface of the powder particles should be clean and the powder particles themselves should be discrete and fully dense. Finally there should be sufficient interparticle friction that the dry powder exhibits an angle of repose of - 45°, or otherwise shape retention, in particular, becomes a problem. Besides shape, interparticle friction also affects mixing which later affects the green strength (14).

Considering the above summary of powder property requirements for an ideal powder injection moulding process it is now more feasible to describe each parameter individually. The parameters to be described are as follows: the effect of agglomerates, the effect of particle size distribution, the effect of particle size and shape, the effect of powder properties on viscosity and also some shrinkage effects.

Effect of agglomerates

In order to increase the driving force and the kinetics for sintering, the use of fine powders in the sub-micron size range has been recommended for the fabrication of components (20). Such powders, however, have a tendency to agglomerate under the influence of strong forces (21). Notably, London dispersion forces (22) provide a universal force of attraction between matter. The adsorbed water layers characteristic of high surface energy solids exposed to ambient humidities have an ice-like

structure and are capable of strong hydrogen bonding (23). If adsorbed multi-molecular layers are present these may adopt the properties of liquid water and provide liquid bridges (21). Hydrostatic tension in the liquid lens between particles arising from the high curvature provides a force tending to hold particles together. Drying of powder which has encountered impurities or additives in solution may produce solid bridge agglomeration. Similarly, particles which are partially water-soluble such as those bearing silica film may become cemented after contact with water in ambient humidities (20).

As suggested by Lange (19) the presence of agglomerates may have a damaging effect on sintering kinetics and final density. Agglomerates are also capable of introducing strength limiting flaws (24-26). Under conditions where agglomerates sinter more rapidly than the surrounding matrix, circumferential cracks are produced with dimensions comparable to the original agglomerate diameter. At high temperatures, where the matrix shrinkage rate is greater, hoop stresses are set up around the agglomerate producing radial cracks.

For these reasons, where powders are assembled by pressing operations, the compaction of agglomerates attracts serious attention. Stress transmission in pressing (27) and compaction of agglomerates have recently recieved more attention (28) and prefired densities are substantially reduced by the presence of agglomerates even at higher pressures (29).

It has been suggested that the uniformity of powder packing influences sintering kinetics (19). Prefired density on the other hand, being an average quantity, conceals wide variations in local density and gives less guidance on achievable sintered density. It is argued that since pores surrounded by a large number of grains can be thermodynamically stable, aggregation of particles in the prefired state will not allow full density to be achieved (19). Thus Lange makes comment that Alcoa A16 alumina would reach full density at temperatures below 1000°C if the prefired particle arrangement were ideal.

For these reasons viable technologies for the creation of shape

and form from assemblies of fine particles must be capable of dispersing agglomerated powders. Aqueous slip casting techniques are generally able to disperse non-solid bridge agglomerates and dispersion in non-aqueous low viscosity liquids is influenced by the hydrogen bonding capability of the liquid (30) or by the use of surfactants.

In the injection moulding of fine powders two approaches for dispersion are possible (20): the use of surfactants and coupling agents (31) and the use of mechanical action (20). The coupling agents are added as pre-treatments to the powder or directly to the ceramic-polymer melt so that to modify the interfacial interactions and then to break down the agglomerates. Surfactants can improve the wetting characteristics between binder and ceramic/metallic powder during mixing and coupling agents increase the flexural strength and lower the viscosity so that significant reductions in energy needed for processing are made possible. Examples of surfactants and/or coupling agents are: stearic acid, silane and organic titanate which are typically added in the range 0.2-2 % by weight based on the filler (1).

Edirisinghe and Evans (20) found that the agglomerates in as-recieved fine ceramic powders persist in die pressed bodies and may produce defects which appear in the fired ceramic. They reported that viable processes for assembling fine particles into complex shapes must be capable of dispersing agglomerates. In their work on compounding ceramic powders prior to injection moulding they found that low shear mixers such as the z-blade type, do not disperse the powder effectively and some agglomerates persist. They also found that high shear mixers such as the twin roll mill (developed in Brunel University for mixing of ceramic-polymer blends) and twin screw extruder are effective in dispersing soft agglomerates in alumina powder. The latter device provided rapid continuous mixing and, if connected to a granulator, provides extrudate in a ready state for injection moulding. However, the extruder was not able to disperse artificial solid-bridge hard agglomerates completely.

Effect of particle size distribution

The green density of an injection moulded compact is a function of the volume percent binder and can be expressed as follows (32): $D_G = V_p / V_T \times SG_p$ ——— (1)

where D_G = green density (g/cm^3), V_p = volume of powder (cc), V_T = volume of powder + binder (cc), SG_p = specific gravity of powder (g/cm^3).

According to Mangels et al (32) the major problem arises in obtaining a batch composition which will not only yield a sufficiently high density but also have a viscosity which is low enough to be processed by injection moulding. Mooney (33) showed that the relative viscosity, Σ_r, of a monomodal distribution of solids in an organic binder system can be expressed in terms of the volume fractions of solids V (where $V = V_p / V_T$) as follows:

$\Sigma_r = \exp (2.5V / 1-KV)$ ——— (2)

where K is an exponential constant which will vary between 1.9 and 1.0 depending on the volume fraction of solids (K = 1.0 where V = 100 % solids). Fig. 2.2 shows that compositions with $V_p / V_T < 0.5$, the relative viscosity of the system ($\Sigma_r = \Sigma / \Sigma_o$ where Σ = viscosity of the suspension and Σ_o = viscosity of the fluid) is only increased by about one order of magnitude by the addition of the solids to the binder. For values of $V_p / V_T > 0.6$, the relative viscosity increases asymtotically (approaching infinity at V = 0.74).

The problem of increasing the solids concentration of a suspension without increasing its viscosity has been treated by Farris (16). He first showed that the viscosity of highly concentrated suspension could be altered by blending solids of different particle sizes. Increasing the difference in mean particle size between coarse and fine fractions increased the amount of solids that could be incorporated in the system. Fig. 2.3 shows that the volume fractions of solids can be increased by - 17 % in a mix containing 75 % coarse and 25 % fines by progressively decreasing the size ratio, without causing any change in the viscosity of the suspension. Farris also showed that the viscosity could be furthur optimised by varying the

blend ratio (percent coarse / percent fine). This is shown in Fig. 2.4 for the case of a bimodal particle distribution. These results are similar to the curves obtained for the packing density of bimodally distributed spheres; where the maximum packing density is achieved at a ratio of ~ 70 % coarse / 30 % fines (34). Finally he showed that the ultimate system would be composed of an infinite-modal particle distribution, with size ratios and blend ratios being optimised. Fig. 2.5 shows the calculated relative viscosity for a number of theoretical particle distribution curves. The general equation describing the relative viscosity is of the form: $\Sigma_r = (1-V)^{-K}$ ——— (3)
where K is a constant which varies according to the particle size distribution. In practice, K ranges from 21 for monomodal, to 3 for infinite-modal distributions. Farris therefore pointed out that, in practice, a very broad particle distribution should result in a minimum viscosity system.

Similar requirements have been noted by Adams (35) for slip cast ceramics where he stated that maximum green densities would be obtained when distributions are as broad as possible without an excessive concentration of particles in any narrow particle size range. Both of these samples require optimising the particle packing efficiency of the powders in order to reach a maximum solids content, minimum viscosity system.

Sweeny and Geckler (36) also stated that the viscosity of a system can be decreased as the bulk (or packing) density of the powders are increased. They also mentioned that absolute particle size is critical; finer particle sizes result in increased viscosities due to the increased surface area of the powders.

Brodnyan (37) extended Mooney's equation, shown as equation (2), to ellipsoidal particles as follows:

$\Sigma_r = \exp [2.5V + 0.399 (p-1)^{1.48} V] / 1-KV$ ——— (4)

where p is the axial ratio. This equation was found to fit experimental data up to V = 0.55. This was extended on an empirical basis by Kitano et al (38) to give a relationship for acicular particles as follows:

$\Sigma_r = 1 - V/0.54-0.0125p$ ——————— (5)

Krieger and Dougherty (39) derived an equation by a modification of Mooney's analysis as follows:

$\Sigma_r = (1 - KV)^{-2.5}$ ——————— (6) and this has found experimental justification (40).

The work of Chong et al (41) has shown good fit between experimental results and an equation of the type:

$\Sigma_r = [1 + 0.75V/V_{max} \;/\; 1-(V/V_{max})]^2$ ——————— (7) for V/V_{max} close to unity, where V_{max} is the maximum space filling efficiency for uniform sized spheres (= 0.74 maximum).

Equations (1)-(7) are valid for particles of uniform diameter and near spherical shape and it is pertinent to note that modern developments in ceramic powders are yielding materials which closely meet those conditions (1, 42, 43). In fact the requirement for uniform shrinkage without discontinuous grain growth during sintering imposes the requirement of near uniform particle size, for which, given sphericity, V_{max} ~0.74. The disadvantages of this approach is the low green density and consequent high sintering shrinkage compared to the more traditional approach of achieving high green density by blending of different particle sizes.

Clearly if a range of particle sizes is present the K value in Mooney's equation [equation (2)] changes. Unfortunately fit with experiment has usually been obtained by choosing rather than deriving a suitable value of K (1). Theories on the viscosity of polydisperse systems have been developed by Lee (44) and by Farris (16). Chong (41) has also developed his own equation to consider more complex particle size distributions. In general, the incorporation of more than one particle size leads to a decrease in viscosity for the same volume fraction of powder but it is generally insufficient to replace K with a new, higher packing efficiency (1).

There are cases in the fabrication of ceramics where a wide distribution of particle sizes can be accommodated without consequent grain growth during sintering (1). One such case is the fabrication of reaction-bonded silicon nitride where vapour

phase reactions refine the grain size during nitriding (45) and Mangels (46) has made use of the reduced viscosity of wide size distribution powders to produce injection moulding blends of high powder loading (73.5 volume %).

Effect of particle size and shape

It was found by Matsumoto and Sherman (47) that the K value (also referred to as the crowding factor) in Mooney's equation (Σ_r = exp (2.5V / 1-KV , where $K=1/V_{max}$ and V_{max} is the volume fraction for maximum packing) is very sensitive to mean particle size. It is considered that spheres in a cubic close-packed lattice (V_{max} = 0.74) exhibit infinite viscosity because of mechanical interlocking. Simple cubic packing (V_{max} = $\pi/6$) is taken to provide the greatest density which would permit continuous movement. Thus the lower and upper limits of K are: $1.35 < K < 1.91$.

In contrast to the findings of Matsumoto and Sherman (47), Barsted et al (48) found only a small variation in K over a broader particle size range than that employed by Matsumoto and Sherman. Thus the value of K does not vary systematically with particle size. This is not surprising as equations (1)-(7) do not allow for an effect of overall particle size on viscosity (1). Yet this effect has been noticed. It was found that viscosity sometimes increased as particle diameter decreased and this has been attributed to an adsorbed immobile layer on fine particles which effectively increases particle diameter (36) and hence total filler loading.

Willermet et al (49) report a halving of spiral flow length during moulding, caused by a decrease in mean particle diameter from 28 to 10 μm. There does not appear to be a sound explanation for this and also the respective particle size distribution were not given (1). However, the spiral flow testing was used as a testing method to assess the injection mouldability of their powder-binder mixture. It is generally accepted that the greater the spiral flow distance, the better the injection mouldability of a material.

Considering the combined effects of particle size and shape on viscosity it is known (1) that non-spherical morphology may influence both the packing efficiency of the powder (i.e. V_{max}) and the effective radius of rotating particles in shear. The effect of particle shape on V_{max} is shown in a study of vibratory compaction of spheres and angular particles (50). For spherical particles the packing efficiency was not influenced by particle diameter, but as the number of sides of the particles became more angular, the effect of particle diameter on the packing efficiency became more pronounced and packing efficiency decreased with decreasing particle diameter. This may help to explain the results of Willermet (49). An apparent contradiction to this effect was noted by Mutsuddy (13) who found that a higher proportion of angular alumina particles than spherical zirconia particles could be accommodated in injection moulding blends. However, since the particle size distribution of the two powders was different, this is inconclusive (1).

Shrinkage considerations

From the previous discussions it is quite clear that the powder characteristics have a strong influence on the green density and handling strength of the body after binder removal and also on the viscosity of the moulding mixture (1). It is therefore very important to achieve a high green density for a given powder so that to lower the error in firing shrinkage as the overall shrinkage decreases (5). Also failure to achieve a near-maximum powder volume fraction in a binder may result in the body slumping or distorting during removal of the organic binder (1). It is perhaps more important to achieve a uniform powder packing throughout the moulded body. Non-uniform mixing of the powder and binder will result in non-uniform shrinkage during sintering which may result in a type of distortion that cannot be corrected by subsequent machining (1).

There are several contributions to shrinkage in the injection moulding process which must be taken into account in die design.

In the first place there is a shrinkage of the moulded body by thermal contraction during cooling in the cavity. If the binder (polymer) is partially crystalline there is a shrinkage associated with solidification. Secondly, when the binder is removed there is a furthur slight shrinkage associated with the drawing together of particles by capillary action. In a moulding composition there must be excess binder to prevent the powder particles contacting or the composition would be too viscous to enter the mould. Finally the largest shrinkage contribution is caused by pore removal during sintering (1).

In practice, using conventional metrology equipment the moulding shrinkage (S_m) can be calculated from the dimensions of the of the moulded body (L_m) and the mould itself (L_o):

i.e., using $S_m = L_o - L_m / L_o$ ——————— (8)

The small shrinkage due to binder removal involves accurate measurements on an extremely fragile body and is normally included in the sintering shrinkage (S_s):

$S_s = L_m - L_s / L_m$ ——————— (9)

where L_s is the dimensions of the as-sintered body (1). Thus the final dimensions are related to the die dimensions by:

$S_s = 1 - L_s/L_o(1-S_m)$ ——————— (10)

If the final relative density D_s is known the volume fraction V of powder in the moulded body can be related to the sintering shrinkage S_s by:

$1 - V/D_s = 3S_s - 3S_s^2 + S_s^3$ ——————— (11)

The common approximation $1 - V/D_s = 3S_s$ should be avoided as it introduces a large error, e.g. 17 % for a linear shrinkage of 15 %. Equation (11) assumes that shrinkage is uniform in all directions and that there are no volume dilations associated with phase changes during sintering (1).

Effect of powder volume loading

The volume loading of powder in the organic suspension should be as high as possible (1) for the following reasons.

1- To reduce shrinkage and slumping during binder removal.

2- To improve handling by increasing the mechanical strength after binder removal.

3- To reduce shrinkage and distortion during sintering.

4- To provide high as-moulded and sintered densities.

However, a high volume loading of powder increases the viscosity of the powder-binder mixture and this makes processing more difficult (1). It is therefore important that the volume loading of powder should be fixed at a level at which the mixture has acceptable flow properties, i.e. the optimised powder-binder composition should show pseudoplasticity throughout the extrusion/moulding process (see section 2.2.4 and Fig. 2.10), have a fluidity greater than 10^3 $(N/m^2)^{-1}$ s^{-1} and a low temperature dependency of viscosity. This last property helps to produce high-integrity mouldings by allowing the post-injection hold pressure to pack the mouldings more efficiently during solidification (51).

2.2.2- Types and selection of organic binders

Criteria for the addition of the organic binders

Ceramic/metallic powders are nonplastic and do not flow sufficiently under heat and pressure and are therefore impossible to form into any shape without the use of a binder. Organic binders are therefore added as temporary bonding media to provide the correct rheological properties (1), i.e. the correct plasticity, green and wet strength, viscosity, cohesiveness, lubricity (for die and interparticle friction), etc., for the injection moulding of the ceramic/metallic-binder mixtures. After injection moulding they should be removed successfully without leaving any defects in the debonded part.

Selection criteria, types and properties of the organic binders

Organic binder systems used for the injection moulding of ceramic/metallic powders are mostly composed of two or more components (1). The components used can be classified into one of four categories (1) as follows.

(i)- Major binder component; this component should have the following properties: (a)- provide sufficient fluidity upon the powder for defect-free filling of the cavity; (b)- wetting of the solid powder particles so that to help dispersion and remove entrapped gas; (c)- stability under mixing and moulding conditions; (d)- provide enough strength to the body during and after binder removal; (e)- leave as little residue as possible in the product after removal; and (f)- be readily available at acceptable cost.

Examples of such major binders are: thermoplastic polymers (e.g. polyolefins such as polyethylene, polypropylene or polybutene; polystyrene; atactic polypropylene; styrene-butadiene and polyacetal copolymers; etc.), thermosetting polymers (e.g. epoxy resin; phenylformaldehyde resin; phenolfurfural phenolformaldehyde resin; etc.) and other organic binders (e.g. water-soluble polymers such as methylcellulose and polyvinyl alcohol; etc.).

(ii)- Minor binder component; this is usually a thermoplastic,

wax or oil which is removed early in the binder removal cycle and therefore generates pore channels within the body allowing easier removal of the other components.

(iii)- Plasticisers; these are also considered as minor additives and should have the following properties: (a)- increase the fluidity of the ceramic/metallic-binder mixture; (b)- should be compatible with the binders, i.e. they should not react but form an intimate mixture with the binders increasing the free volume of the polymer and thereby lowering the viscosity; and (c)- they should have a high boiling point and low volatility so that they are retained during processing and therefore will provide the necessary consistency for the ceramic/metallic powder volume loading.

Some examples of plasticisers are: diethyl, dibutyl, dioctyl and diallyl phthalates, light oil, beeswax, naphthanic or paraffinic oils or waxes, butyl stearate, metal stearates (such as calcium, magnesium, zinc and aluminium stearates), liquid paraffin, etc.

(iv)- Processing aids; these minor additives are used mainly as surfactants to improve the wetting characteristics between binder and ceramic/metallic powder during mixing and ideally they should perform the following functions: (a)- modify adhesive forces between binder and powder, thus dispersing the organic components throughout the mix and enhancing deagglomeration of the powder particles; (b)- reducing the viscosity of the melt; and (c)- allowing easy mould release.

Some examples of processing aids are: stearic acid, polyethylene wax, mixtures of natural waxes and wax derivatives, different types of vegetable fat, partially oxidised polyethylene, paraffinic and ester wax, hydrogenated peanut oil (which acts as the diluent and lubricant and therefore reduces viscosity significantly), methyl acetylricinoleate, etc.

2.2.3- Mixing processes

Properties of ceramic/metallic-binder mixtures

It is very important to have a uniform mixture of the ceramic/metallic (C/M) powder with the organic binder because failure to disperse the powder in the binder uniformly may result in non-uniform shrinkage at a microscopic or even macroscopic scale during sintering (51). A non-uniform shrinkage during sintering may result in a type of distortion that cannot be corrected by subsequent machining (1). A non-uniform powder-binder mixture will also cause internal and surface moulding defects such as macro/micro voids and sink marks which cannot be removed by sintering/machining and therefore will remain as part of the final product causing microstructural and mechanical damage.

The C/M injection moulding blends usually consists of a C/M powder mixture in a multicomponent binder matrix (1) as described previously. In most cases incomplete solubility can be expected to take place and the degree of dispersion of one binder phase in the other will influence the properties of the blend, in particular its decomposition kinetics (51). It follows therefore that the mixing of C/M injection moulding blends involves the dispersion of powder particles and a minor polymer binder in a continuous matrix of the major polymer binder.

Mixing is defined as a process that reduces compositional non-uniformity and in viscous polymeric fluids the influence of molecular and eddy diffusion is generally negligible for useful time scales, leaving forced convective flow as the main mixing process (52). If convection causes the movement of fluid or solid particles from one spatial location to another such that the interfacial area between liquid particles and the matrix increases, or that solid particles are distributed throughout the matrix, then distributive mixing is said to have occurred (52).

Distributive mixing is influenced by the strain imposed on the mixture. However, in the case of viscoelastic polymers and agglomerated fine particles which show yield point characteristics, the application of strain is necessary, but insufficient, to achieve mixing. The strain rate and hence shear

stress imposed on the material determine the extent of mixing and this is known as dispersive mixing (52).

The importance of dispersive mixing in ceramic systems is illustrated by the recent work of Lange (53) on uniformity of prefired density in ceramics. If agglomerates start at a different prefired density from the dispersed particles in a ceramic body then very high stresses are set up during firing (54) and these can produce circumferential or radial cracks in the region of agglomerates depending on whether the agglomerates shrink faster or slower than the matrix respectively (26). Furthurmore failure to disperse agglomerates may influence the sintering kinetics and reduce the fired density by leaving thermodynamically stable pores with a large grain co-ordination number (19).

The characteristic volume (or scale of segregation) is an important parameter in defining mixture quality. It may be defined (55) as the amount of material at every location throughout the mixture within which the position of individual particles is unimportant. Its size depends on the properties demanded of the mixture. For example the characteristic volume of an engineering ceramic injection moulding composition could be calculated from the dimensions of the flaw size defined by Griffith's equation for a desired mechanical strength. This would mean that compositional uniformity would be expected among random samples of typically 1000 mm^3 volume. Since such samples are well below the limits of practical analysis resort to microscopical methods (56) is necessary in defining mixture quality. Since flaws produced by firing agglomerated powders are typically of the same dimensions as the starting agglomerates (53) the characteristic volume will be smaller than the volume of agglomerates often found in ceramic powders. The break down of agglomerates in shear flow is described quantitatively by Tadmor and Gogos (52).

There is increasing interest in ultrafine monosized spherical powders which can be packed into ordered arrays for ceramic fabrication (57). In this case the characteristic volume would

be of particle dimensions. The best that can be expected from injection moulding of such particles is a uniform random packing throughout the mouldings (51).

Effect of mixing conditions on tolerance capability

It was found by Billiet (58) during a statistical process control of the production of a ceramic part for a computer application that final product's dimensions were gradually becoming smaller, while the standard deviation, initially stable, went haywire. Sequentially, the sintering, dewaxing and moulding steps were suspected and thoroughly checked out, only to discover that everything was under control. Reluctantly, the investigation was extended into the moulding feedstock preparation area, believed to be beyond suspicion. The result was dramatic and immediate. The standard deviation stabilised and reduced in magnitude resulting in a consistent and record 0.0007 process tolerance capability. It was also noticed that the part had now slightly grown in size, as compared to the average size before the onset of the problem. The latter was eventually traced to adulteration of the feedstock formulation by human error, and prompted the determination of the maximum mixing error $|\epsilon\phi|=3T/2(1-\phi)$——(12) where T is the targeted process tolerance capability (which can be set arbitarily) and ϕ is the volumetric loading =

V_d/V_d+V_c with V_d being the volume occupied by the powder and V_c the volume occupied by the organic binder. The author (58) therefore showed the need for extreme care in weight determination and handling at the moulding feedstock preparation.

Time dependency of mixing

It was reported by Billiet (58) that time-dependent, three dimensional, non-linear flows, such as the mixing of filled organic fluids to produce moulding feedstocks for C/M injection moulding, most necessarily involve efficient, stretching-and-folding mechanisms essential for good homogenisation. Such flow

system, where regions of outflow (the so-called hyperbolic points) are able to display chaotic behaviour.
Billiet again used an actual process tolerance capability as an indicator of mixing efficiency and prepared several batches of moulding feedstock mixed for variable durations of time, then moulded into test parts which were sintered in order to determine the actual process tolerance as a function of mixing time. He obtained the results shown in Fig. 2.6, where σ is the standard deviation and L is the final sintered dimension in $3X10^3\sigma/L$ equation. As expected, insufficient mixing time negatively affected the process tolerance capability. There is an optimum mixing time, for which this capability is greatest, i.e. the tolerance which can be held confidently reaches the lowest value. Extending mixing time beyond this time period produces a negative effect on tolerance capability. It was therefore postulated that two time regions: a chaotic net randomising area where increased mixing time has the effect of homogenising the mixture, and a chaotic symmetrical region where period doubling occurs and the mixture shows areas of inhomogeneity.
These effects clearly depend on moulding feedstock formulation, the design of the mixing equipment and the operational conditions. It is believed (58) that chaotic mixing is the only way to effectively mix particulates in a fluid matrix. Its study offers plenty of room for both basic research and technological exploitation (58).

Mixing techniques

A range of double-blade batch mixers such as the 'Z' or 'Sigma' blade mixers are used extensively for the mixing of C/M powder-binder blends (51). The Z or Sigma-blade mixers are usually heated by oil to a temperature < 250°C. Early experts on ceramic injection moulding such as Schwartzwalder (4) and Taylor (59) favoured such mixers and some recent research has also relied on these types (60). The limitations of the double-blade mixers are the tendency for filled polymers which show yield point

behaviour to reside in dead spaces in the mixer and there is insufficient dispersive mixing to break down ceramic powder agglomerates (20).

Banbury-type mixers provide higher intensity batch mixing and are used on high-viscosity fluids for pigment and filler dispersion (51). They consist of a figure of eight section mixing chamber containing two-counter rotating lobed rotors. Quackenbush et al (61) employed a torque rheometer of similar design to prepare ceramic moulding compositions.

The Brabender torque rheometer, either the Plastograph or the plasti-corder types, are also used extensively for the batch mixing of C/M powder-binder blends (62). It consists of a mixing head/chamber which is heated electrically having two counter rotating roller blades with different speeds for better mixing. The blades are removable which makes cleaning much easier. The Brabender torque rheometer Plastograph and Plasti-corder function according to a practice related dynamic measuring method. The measuring principle is based on the fact that the resistance, which the test material puts up against rotating blades, rotors, screws, etc. in the measuring mixer is made visible. The corresponding torque moves a dynamometer from its zero-position. In accordance with established test conditions a typical plastogram is traced (i.e. torque versus mixing time) for every type of material as shown in Fig. 2.7. At the same time, a stock temperature diagram is recorded. Thus, a direct relation between viscosity and temperature is produced. The torque is measured in Newton-meter (Nm), formerly meterpound (mp) or metergram (mg). The apparent viscosity of the test material can be determined as in rheological measurements. With this device it is possible to create test conditions similar to the processing conditions of mixers, moulds, calenders, extruders and injection moulding machines. It is also possible to determine the influence of stabilisers, plasticisers, lubricants, higher volume loading of powders, catalysts and pigments in the compound (62).

The two-roll mill is also a mixer ideally suited to the

processing of high-viscosity materials. It consists of two-counter rotating differential speed rolls with an adjustable nip and imposes intense shear stresses on the material as it passes the nip. There is little transverse mixing and thus constant operator attention is needed to displace the strip transversely. This process can be partially automated for polymers. A two-roll mill was used by Birchall et al (63) to produce very high solids content mouldable cement pastes.

Two types of extruder are also used for mixing (51): single- and twin-screw extruders. Single-screw devices with a helical screw rotating inside a heated barrel are not efficient mixing devices (64) and are sometimes enhanced by the incorporation of mixing discs, torpedoes or planetary gears into the screw configuration. The total strain imparted to an element of material is strongly dependent on its position and therefore mixing tends to be non-uniform across the screw channel. Unlike the more complex extruders the helical flow behaviour in single-screw machines is well charaterised and machines are well documented in textbooks (51).

Flow in single-screw extruders relies on the adhesion of the material to the barrel wall and it was to overcome this limitation that twin-screw extruders evolved (65). There are four types depending on whether the screws co-rotate or counter-rotate and whether the screws intermesh or not. The first device was an intermeshing co-rotating extruder invented in 1939 and patented in 1949 (66). Considerable variation in screw design is possible to balance pumping and mixing characteristics (67). Intermeshing extruders provide positive displacement pumping unlike single-screw machines and the output per unit time is given by the difference between the theoretical flow rate and the sum of the leakage as follows:

$Q = Q_{th} - Q_L = 2\ m\ N\ V - (Q_f + Q_c + Q_t + Q_s)$ where m is the number of thread starts per screw, V is the volume of the C-shaped channel between the flanks of successive flights and N is the rotation rate. Q_f is the leakage between screw flight and barrel wall, Q_c is the leakage between the screw flight and the other

screw, Q_t is the leakage between the flanks of screw flights and Q_s is the leakage between flanks perpendicular to the plane through the screw axis (65). The leakage paths have a strong influence on residence time in the extruder. Flow characteristics of such extruders have not been well defined and machine development has been largely empirical. As with single-screw devices mixing discs and kneading discs can be incorporated into the screw configuration (51).

Twin-screw extrusion has been used for the preparation of particle-filled polymers (68) for reinforcement, flame retardancy, fabrication of prosthetic materials or incorporation of magnetic or dielectric solids (69). The polymer degradation can be controlled by screw design and is found to be less severe than degradation induced by two-roll milling (69). The degree of dispersive mixing obtained by twin-screw extrusion compounding is greater than that achieved by using a double-blade mixer (20).

2.2.4- Rheological considerations

The rheology of C/M-injection moulding mixtures is governed by the properties of both the binder and the C/M powder (18). In order to understand the system's viscosity, the effect of the C/M powder on the binder's viscosity must be examined (18). This was described in detail in section 2.2.1 of this chapter. As shown by Farris (16) the relative viscosity of the filled polymer system (Σ_r) can be described by $\Sigma_r = (1-V)^{-k}$ ——(13) where V is the volume fraction of solids $=V_p/V_T$, K is a constant which varies according to the particle size distribution of the powder, V_p is the powder volume and V_T is the total volume of the powder plus binder. Fig. 2.5 shows these relationship graphically. Firstly, it can be seen that the mixture viscosity is governed by the binder viscosity, since in equation (1) the binder viscosity is normalised to unity. The second critical observation is that the viscosity is a function of the volume fraction of solids (18). This is critical since this value determines the green (moulded) density. The viscosity is

independent of the particle size distribution below ~ 50 volume % of solids (18). However, it is desirable, and often necessary, to attempt to mould C/M-binder mixtures which have solid contents in the range 60-75 volume %, making the particle size distribution a critical variable. As also shown by Farris (16), by altering the particle size distribution from a sharp, monomodal type distribution to a broad, infinitely modal type distribution, one can increase the solids content without increasing the system's viscosity. Mangels and Williams (46) have verified this relation and phenomenon for silicon powder in a wax binder for volume fractions of o.73-0.79 silicon.

In addition to the particle size distribution, the particle size and surface area of the powder are important variables especially when working with fine, high-surface area powders. Fig. 2.8 shows the effect of surface area on the relative viscosity of a ceramic injection moulding mix at two levels of solid volume loading (18). When working with highly loaded systems, a number of factors come into consideration (18). The binder system must be compatible with the powder,i.e. the binder must completely wet each individual particle. Consequently, surfactants, which act in a manner similar to a deflocculant, must usually be included in the binder formulation. The powders must also achieve the highest packing density so that to utilise the available binder most effectively and also to achieve high moulded and sintered densities. A more spherical powder morphology is desired so that optimum powder packing can be attained. Finally, a uniform distribution of binder and powder is essential and to achieve this high shear mixers must be employed.

C/M injection moulding mixtures exhibit a yield point which must be overcome before the material will flow. The presence of a yield point is due to the presence of an aggregated structure formed by the powder particles (70) and is dependent on the particle shape and packing density (5). Once the material begins to flow, its viscosity is dependent on the temperature and shear rate as shown in Fig. 2.9. This behaviour is also observed in

plastic materials (71). This shear thinning is due to the breakup of the powder agglomerates at the high shear rates, resulting in a complete dispersion of the binder between the powder particles, which lowers the Van der Waals forces between the particles (18). The reduction of these forces results in a lower apparent viscosity. This process is accelerated at higher temperatures which shows the dependency of viscosity on temperature (18). Experience has shown that a good flow during polymer injection moulding requires a viscosity of < 10^4 poise (= 10^3 Pas) with a shear rate (in the gates and mould) in the range 100-1000 s^{-1}, although it can occasionally reach 10000 s^{-1} (13). It is therefore assumed that any binder formulation with a viscosity < 10^4 poise within the indicated shear rate range will be suitable for moulding, and to define the rheological behaviour of such materials plots of viscosity versus shear rate are the most accepted graphical representations which show the dependency of viscosity on shear rate and temperature (72). The viscous flow of such materials is described (13, 72) as follows. (i)- St. Venant where viscosity is inversely proportional to shear rate.

(ii)- Bingham plastic which does not show any flow unless the shear stress reaches a critical unit. The non linearity has been attributed to changes in the network structure and alignment within the network structure of the flowing material as the stresses change. The network structure can support a stress before any material flow can be initiated. This finite stress is known as the yield stress.

(iii)- Pseudoplastic where viscosity decreases continually as shear rate increases.

(iv)- Dilatant where viscosity increases as shear rate increases.

The above flow behaviours can be seen as viscosity flow curves in Fig. 2.10. For a successful injection moulding process, the C/M powder-binder mixture should have either Bingham or pseudoplastic flow characteristics (13, 72).

To obtain the viscosity-shear rate data a capillary rheometer is

usually used which provides the apparent viscosity and apparent shear rate data (13). The viscosity is the ratio of shear stress to shear rate. Mutsuddy (13) also mentioned that the ultimate rheology of filled polymeric systems for injection moulding will be determined by the physical characteristics of the C/M powder being used as filler.

2.2.5- Injection moulding machines

Development of injection moulding machines

C/M injection moulding machines are basically the same as the plastic injection moulding machines (18). However, the injection moulding process (IMP) had its origins in the die-casting techniques (51) invented by Sturges in 1849 (73) for non-ferrous alloys and therefore the designs of the first injection moulding machines for polymers were based upon die-casting methods. The first machine was used to fabricate cellulose nitrate plasticised with camphour and was patented by Hyatt in 1872 (74). In this machine a ram applied pressure to the material in a heated chamber extruding it through a nozzle into a cold mould to produce continuous rod, sheet or tube. The first moulding process used a multi-cavity mould to coat metal parts with celluloid (71). A more detailed account of early work is reported in several texts (75). Uniform heating of the material was a problem in these early ram machines but improvements were achieved by incorporating a spreader into the flow channel patented by Gastrow (76). Many of the characteristics of modern machines appeared in the rapid developments of the 1930's, including early automation made possible by temperature controllers, timers and dosing devices. Better control over injection pressure, mould closing and barrel heating facilitated the fabrication of large components. This in turn gave rise to larger moulding machines, including the large multi-nozzle machines with vertical clamping which appeared in 1936 (51). Serious problems of reproducibility of components remained, and to solve this problem an early automatic machine was patented by Burroughs (77). Thus by 1940 machines had developed to include

hydraulic ram acting in a heated thermostatted cylinder with an internal spreader and injecting into a vertically or horizontally clamped mould with hydraulic and toggle clamping and automatic ejection (51).

By 1944 a machine was available capable of moulding both thermoplastic and thermosetting materials (75). Mould closing and clamping by hydraulic and toggle methods were perfected at this time (78) and a device combining injection and compression moulding was in use (79).

Types of injection moulding machines

Injection moulding machines are characterised by the injection end rather than the clamp geometry and two major types of machine are commonly used: the plunger-type and the reciprocating-screw type injection moulding machine (71).

A typical single-stage plunger-type injection moulding machine is shown in Fig. 2.11. A metered quantity of material enters the heated barrel from the feed hopper and, as the plunger/piston advances, flows over a torpedo or spreader designed to improve heat transfer (80). Such machines suffered from several disadvantages (81). There was little mixing of the molten material, giving rise to inhomogeneity. The pressure at the nozzle could vary considerably from cycle to cycle as the plunger compressed material which ranged from solid granules to viscous fluid. Since viscosity of polymer melts is pressure sensitive, erratic pressure increased the mould filling variability. The torpedo caused a significant pressure drop. The shot size was difficult to meter accurately.

A preplasticising system overcame some of these disadvantages (82). Such machines had twin barrels and in the case of a two-stage plunger device material was plasticised in the first barrel before being fed into the second barrel via a non-return valve (51). The torpedo could then be omitted from the injection barrel. Homogeneity was assisted by passing the material through the inter-connecting nozzle. Shot size was metered by using limit switches on the primary barrel. In screw-plunger machines

the primary plunger was replaced by a rotating screw (51).
The development of the reciprocating screw machine overcame many of the problems of plunger machines (51). The use of a rotating screw to heat and convey material was first introduced in Germany in 1943 (83). A typical reciprocating screw-type injection moulding machine is shown in Fig. 2.12 (51). Adhesion to the barrel wall allows the rotating screw to pump material forward, simultaneously mixing and heating the fluid to achieve uniformity. An adjustable pressure applied to the screw controls the reverse drift of the screw in the barrel and thus the plasticisation of the material. The screw then ceases to rotate and behaves as a plunger, injecting the material into the mould. A check ring or ball valve prevents leakage of material past the end of the screw. The screw remains in the forward position applying a hold pressure to compensate for shrinkage of the material in the cavity. The screw then again rotates recharging the injection chamber while the mould remains closed (51).
The fundamental improvement in the screw machine is the preplasticising action (84) which causes direct Joule heating of the material. High shear rates produce lower viscosities in pseudoplastic fluids. Lower injection and clamp pressures can be used because of the material resulting from non-laminar flow. Degradation problems are less severe because of lower residence times and better heat transfer. This is especially advantageous in the processing of heat-sensitive materials. Finally, screw machines are more efficiently purged as the material is changed (51).
As mentioned earlier both plunger and reciprocating screw-type injection moulding machines used for unfilled polymers are also used for injection moulding of C/M powder-binder mixtures after minor modification (85, 90, 93). Reciprocating screw machines are often favoured (90, 93) as they provide better metering, homogeneity, injection pressure control, reproducibility and lower cycle time. In plunger machines flow moulding is not possible and part size is limited by the maximum volume of the plunger stroke (93). Nevertheless plunger-type machines are

often favoured on the grounds of longer machine life because of less wear (85, 95). They also tend to require less capital investment (95).

Plunger machines can be vertical injection, vertical press type with attainable cavity pressure up to 170 MPa, or of the horizontal type. They are generaly fully microprocessor controlled and equipped with a shuttle table to allow the transfer.

Reciprocating screw machines specifically developed for ceramic injection moulding are also currently marketed (90, 95). These are based on conventional designs and are again fully automated. Some machines contain circuits which permit fine control of injection and hold pressures which is considered essential for ceramic moulding (51).

Wax-based systems tend to have much lower viscosities (< 200 Pas) than high polymer systems and are often injection moulded on plunger machines (85) known as wax-injectors. Such machines vary in size from the small (12000 Kg) horizontally clamped devices to large (300000 Kg) vertical press machines.

For thermoplastic and wax systems direct injection process are used in which the heated suspension is forced into a colder mould under pressure and then subjected to a hold pressure as it solidifies (85, 95). For thermosetting systems, however, transfer moulding is used in which the softened suspension is transferred by a plunger or screw to a heated mould where the resin cross-links (85, 92). In both cases the polymer phase undergoes a shrinkage as it changes state and this can introduce defects (51).

Wear of injection moulding machines

Wear and corrosion of machine parts and tooling is regarded as a problem in ceramics injection moulding (85-86). The barrel, screw, non-return valve, nozzle and mould are areas especially at risk (87). The difference in hardness between ceramic powder particles and metal and cermet parts as can be seen from Table 2.1 is a main factor in abrasive wear (88). A furthur factor in

determining ploughing action is the particle size and size distribution of the ceramic powder (51). Pressure on the material has a pronounced influence on machine wear and this tends to localise the severity of damage (51).

Studies of machine wear caused by filled polymers (89) suggest that material hardness is not a good indicator of wear resistance. Particles produced more severe wear than fibres in the conveying zone. On arrival in the metering zone it is considered that particles would be coated with molten polymer (89).

Japan steel works (90) incorporated corrosion-abrasion resistant screws although the material was not specified. The barrels were lined with a nickel-based iron-chromium boride composite with a hardness of ~ 7.6 GPa. This reduced damage to the mating screw surfaces compared to metallic cylinders. Also barrel wear with a silicon carbide composition was 20 % of that seen on nitrided steel (nitrided barrels and chromium-plated steel screws were subjected to severe wear and enhanced leakage flow between flights and barrel made process control impossible).

Non-return valves of the check ring type have also been subjected to appreciable wear (91). Nozzle and nozzle seat wear has been observed on a carbon steel of hardness 4.7 GPa but was considerably reduced by using a tool steel of hardness 7.5 GPa (51).

Tooling should also be constructed of wear-resistant material and resistance to chipping is also important (86). Thus high carbon-chromium tool steels have been preferred to high wear-resistant but brittle carbide cermets and for the same reason steel-bonded carbide has been rejected (51).

Since 1974 high pressures (35-140 MPa) have been used extensively for ceramic injection moulding (72) and this tends to enhance machine wear. Furthurmore, with incorrectly formulated compositions dilatancy effects can be induced by high material pressures causing separation of fluid from powder (61, 92). These difficulties have led to the use of lower pressures in the range 0.2-0.6 MPa (93). The low-pressure process

originated over 30 years ago in the electronics industry and machines using the same principles are marketed today for ceramic injection moulding (94). In such machines moving parts such as screws or plungers are absent and energy consumption is small (1-3 KW). Dies are generally small and may be constructed from aluminium or wood because of the low pressures (93).
Low viscosities (. 100 Pas) are achieved by using wax-based systems which are mixed in a thermostatted tank incorporating a planetory mixer. Injection of the die is achieved by imposing air pressure on the material in the tank causing it to flow along a feeder pipe into the mould. The method has been used for silicon nitride, silicon carbide and oxide ceramics (93) but it is not clear how shrinkage defects in thick section mouldings were avoided (51).

2.2.6- Moulding cycle

Mutsuddy (72) has defined the moulding cycle as follows:
A moulding cycle is based on time, temperature and pressure. Since moulding is a dynamic process, the various stages usually overlap, and they need to be characterised if analysis and control are to be attempted. The usual mould cycle sequence is as follows: 1- Dead stage. This is the period of time (after the mould closes and the plunger/screw starts forward) before the material starts to flow into the sprue bushing.
2- Mould filling stage. The time during which material flows into the mould and fills the cavity.
3- Pressure build up stage. The time (after the cavity is filled and the material begins to cool) during which pressure in the cavity builds to injection pressure.
4- Packing stage. The time (including the pressure build up period) during which material flows into the cavity at a relatively slow rate. The injection cycle ends with this period and the plunger/screw retracts.
5- Discharge stage. In this stage the material in the gate is still fluid, with zero pressure on the runner side and slightly less than injection pressure in the cavity, the material flow

reverses. Flow rate is determined by either the seal or the follow-up pressure.

6- Cooling stage. In this stage the material in the cavity cools with no flow through the gate in either direction.

Along with a time sequence, it is essential to have the correct temperature and pressure sequence (72). The pressure-temperature functions in moulding processes have been presented as an 'ideal gas' equation: $(P+\pi).(V-W)=RT$ where P is the hydrostatic pressure, V is the specific volume, T is the material temperature and π, W and R are constants for specific moulding materials (72). It can be argued that if the mould temperature is constant in the cavity immediately upon injection, the effective specific volume (V-W) is inversely proportional to the effective applied pressure $(P+\pi)$. Once the gate is frozen, the effective specific volume is constant, and the effective applied pressure drops in proportion to the temperature (72). It is possible to construct a model from this equation and obtain temperatures and pressures for moulding specific material into a fairly simple shape (72).

2.2.7- Injection moulding conditions

It is quite complicated to predict approximately the flow behaviour of ceramic suspensions due to their reduced thermal capacity and increased thermal conductivity which cause rapid cooling in the runner and mould. Furthurmore the yield point behaviour of the suspension changes the flow behaviour at low shear rates (51), and viscosities of suspensions tend to be much higher than those of unfilled polymers (16). For these reasons the correct choice of machine parameters is important if sound mouldings are to be obtained (90).

Peshek (85) has listed several requirements for ceramic moulding as follows: optimisation of pressure, temperature and injection speed is essential. Particular attention to mould temperature and pressure hold times are also very important (61). It is believed that the injection speed has a pronounced effect on ceramic moulding (90) because of the rapid chilling of the melt,

described above. Reliability of temperature control is important with correct choice of thermocouple locations to avoid hot or cold spots. Pressure control mechanisms should be hydraulic and allow repeatable and accurate control over a wide range. Injection pressures are typically in the range 35-140 MPa (93). Internal stresses in moulded ceramic articles can produce internal defects both during solidification in the cavity or shortly after removal (51). This is enhanced by the solidification and cooling of a pocket of fluid trapped in the moulding after the sprue or gate has frozen off. Attempts to solve the problem therefore centre on ways of keeping the sprue molten until the interior of the moulding has completely solidified (51).

Extremely high pressures should compensate for thermal contraction (71) and this approach has been used to produce polyethylene mouldings with net internal compressive stresses (96). However, the pressures used (up to 450 MPa) are impractically high.

Hot runner moulds have been used for moulding plastics (71) and these allow the moulding to solidify completely under the applied hold pressure (97). However, they generally demand very small gates which are unsuitable for ceramic suspensions.

Oscillating hold pressure has been used for both polymer and ceramic mouldings designed to compensate for internal shrinkage (51). This is described in a German patent (98) for a ceramic suspension. The reciprocating screw is bored to receive an oscillating piston activated from the screw drive end of the machine. Another part of the device applies oscillating pressure to the ceramic material in the mould and this oscillation is claimed to enhance pressure transmission.

Oscillating pressure applied to the moulded material in place of a static hold pressure was used by Alan and Bevis (99) to keep the sprue and runners molten during mould cooling and thereby to make 40 X 60 mm thick section mouldings of unfilled polyethylene without sink marks of internal voiding. The oscillating pressure causes viscoelastic heating in the sprue and runners and this

allows the interior of the moulding to be filled, compensating for shrinkage. Continuous monitering of the cavity pressure allows the process to be controlled.
The same technique has been applied to short fibre reinforced thermoplastics (100) and ceramics (51) although the device is subject to wear when used with ceramics.
Defects introduced by entrapped air or adsorbed moisture in ceramic injection moulding mixtures have been overcome by using an injection moulding machine in which the feed reservoir and the mould are held under vacuum by a series of valves, a vacuum pump and vacuum reservoir.
Mangels and Trela (18) reported that plastic moulding results can be analysed in terms of four fundamental variables: material temperature, flow rate or shear rate of the material, the pressure of the material in the cavity and the material's cooling rate. All of these variables related to the material conditions exist in the die cavity. Table 2.2 illustrates how these fundamental variables are affected by selected machine variables (18). From this Table it is obvious that a given machine variable will affect more than one of the fundamental variables simultaneously. Consequently problem analysis involving machine variables alone can often be misleading. Development tooling should be designed to include transient temperature and pressure instrumentation in the die cavity in order to determine the values of the fundamental variables (18).

2.2.8- Mould design

The success of injection moulding is partially determined by mould design efficiency and the quality of the mould construction (72). Consequently, initial consideration should be given to the part (component to be moulded) design before designing its mould. The feasibility of using injection moulding to form a part should be based on factors such as part size and weight, section thickness, shrinkage, tolerances, draft, threads, radii and holes (72). After careful review of all these factors, the actual mould design should be considered in the

light of the following considerations: 1- Best results are achieved if the runner is short in length and circular in shape (diameter can vary). The runner should be placed in the ejector half of the mould.
2- The preferred gate shape is either round or rectangular. Gate size appears to have more influence than shape on the manner in which the cavity is filled. Larger gate sizes appear to be beneficial because, as the gate size is increased, the probability of jetting is reduced by the lower velocity of the material entering the mould, the evidence of knit/weld lines is reduced and cavity filling is rapid, thus preventing the material from freezing prior to completely filling the cavity. In addition, changes in gate location can reduce or eliminate material jetting.
It follows therefore that the gate geometry is one of the major variables affecting the amount of shear encountered during moulding (18), and this is the principal variable affecting the material's viscosity. Gate geometry can also influence other fundamental moulding variables such as the flow rate of the moulding compound into the mould cavity, and through this parameter indirectly controls the cooling rate of the material. The location of the gate relative to the component cavity is equally important in producing high quality articles (18). An improperly placed gate can result in turbulant flow or jetting in the mould cavity resulting in voids and surface blemishes. If the flow rate of the material into the cavity is too low, weld lines will form in the moulded components (18). The thermal conductivity of a ceramic moulding mixture is about ten times that of a plastic, and its specific heat is about two times that of typical plastics. Consequently, unless the cavity is filled rapidly, weld lines will form because the moulding mixture is too cold to knit together to form a homogeneous component. However, a correctly placed gate will result in laminar or plug flow within the cavity, resulting in defect-free components (18).
Fig. 2.13 is the schematic representations showing the effect of

various gating geometries on the resulting material fill patterns in a simple rectangular test bar mould (61, 102, 103). The end gate [Fig. 2.13 (a)] results in the worst flow pattern. The material, when injected at high velocities, produces a turbulant flow pattern, which makes air entrapment (voids) a distinct possibility. Often this flow pattern will result in jetting to the end of the cavity. The backflow pattern may result in knit lines where two flow fronts meet. Unless the material is injected at high rates, the material will cool before it can be compacted and knitted together into a uniform body, resulting in knit lines. Fig. 2.13 (b) is a representation of a side gate, at which the material is injected at high velocity across the cavity into the opposite wall, where a laminar flow pattern develops. Fig. 2.13 (c) shows a special case of the side gate, the fan and top gate. Here the mix is injected from the top of the mould cavity at one end of the test bar. A laminar flow region is immediately formed and continues through the length of the test bar (18).

3- Vent location is most effective when jetting is reduced and the cavity is filled from the gate area through the remainder of the cavity.

4- Filling is more controlled when the material comes into contact with a cavity surface immediately upon entry.

5- When the mixture is injected into the cavity, it takes the path of the least resistance. Consequently, simultaneously using gates of different sizes may not be advisable.

6- Depending upon freezing rate of the material, it may not be desirable, to simultaneously use cavities of different sizes.

7- Material rheological characteristics influence the retention of weld marks and knit lines in the moulded parts.

8- Wear on machine parts and on the mould should be monitered as they may contaminate the moulded parts.

2.2.9- Binder removal techniques

Five techniques of binder removal have been identified (52) and they are as follows:

(1)- Thermal degradation of the organic binder in an inert atmosphere.

(2)- Oxidative degradation.

(3)- Capillary flow into a finer powder.

(4)- Evaporation.

(5)- Solvent extraction.

Thermal degradation

This is the most widely used technique for the removal of organic binders (52). It may involve depolymerisation, in which the carbon-carbon backbone of the molecule is severed, decreasing the molecular weight, or may involve substituent reactions during which side groups are attacked (typified by the stripping of HCl from polyvinyl chloride). The former may occur either by a random process leaving large molecular weight fragments (which occurs for most polyolefins) or by scission at reactive sites yielding mainly monomer but having little initial effect on molecular weight (which occurs for polyoxymethylene). Thermal degradation, however, involves a very slow heating rates and this leads to very long debinding times which could take several weeks for thick and complex articles (61, 110). If the temperature is not accurately controlled, decomposition of the polymer occurs within a narrow temperature range resulting in high degradation product vapour pressures producing swelling and cracking (90). Initially the moulded article may be heated to its softening point fairly rapidly so that the vehicle (binder) becomes fluid (61, 111). An exception is where residual stresses are present in mouldings and a low temperature stress relieving treatment is preferred (110). Subsequently an extremely slow

heating rate (e.g. 2°C/h for a 6 mm thick article) is required at the early stages of decomposition (mostly at - 150-460°C). The rate can be increased (e.g. to - 10°C/h) towards the end of the process when a substantial void volume is present (110).
Vacuum or inert gas atmospheres are required for some polymeric, metallic and ceramic materials during the debinding process so that to prevent the oxidation reactions which cause cracking of the moulded article. Pressures of 7-14 Pa have been found acceptable (110).
A blend of polymers (atactic polypropylene) with different molecular weights has been used in order to broaden the burn-out region (i.e. the critical decomposition region) so that to have an easy and defect free burn-out (112).
It is very important to have no carbon residue (after debinding) particularly for nitrogen ceramics. Similarly ash content of the polymer becomes important in some applications where very low silicate or sodium levels are required and in particular for optical property control.
It is common practice to embed injection moulded articles in a fine powder such as alumina during binder removal (60, 61, 90). The powder bed may perform several functions. It may allow temperature uniformity in the furnace, avoiding surface radiant heating. It may, under certain circumstances, extract fluid from the article by capillary action. It may reduce the steep gas partial pressure gradients at the surface of the moulding. It may also support the moulding in its softened state and thus prevent sagging (90). However, if thermal degradation process is to be carried out in terms of weight loss measurements, then the powder bed is not used since the condensation of polymer degradation products in the powder bed may give errors in weight loss measurements and thus may interfere with process control (110).
Flaw generation during binder removal by thermal degradation can occur early in the cycle (61). When the binder becomes fluid, flaws can be generated by expansion of air compressed into the component during injection moulding. Blistering and cracking of

the components can occur if the temperature is increased too steeply due to rapid evolution of volatiles.

Delamination or internal cracking is a more serious type of burn-out flaw. It is claimed to be independent of the binder removal rate and depends on powder loading and morphology of the powder (61). It can also be related to the use of certain organic binder systems. Control over this type of flaw has been achieved by modifying powder loading levels and by selecting suitable surfactants. The binder is preferentially removed from the surface of mouldings but subsequently, as polymer emerges from the interior, the resulting slight shrinkage generates tensile stresses and causes internal cracks (61). Skin formation is another defect frequently observed. This can produce surface cracks and blistering. This has not been fully explained but may be related to preferential polymer degradation at the surface (52).

Oxidative degradation

This is found (144) to be the most effective binder removal technique for the polyolefine moulded components. Polyolefines, either as waxes or high polymers, have been used extensively as ceramic injection moulding binders (1) and their degradation (115-117), reaction products and catalytic influences (121, 122) have been well documented. Of particular interest is the influence of sample thickness on the oxidation of polyolefines. An effect of thickness caused by oxygen diffusion is found in degradation studies, when sample thickness exceeds 250 μm (122). Not only does the rate of reaction depend on oxygen partial pressure but the nature of the reaction sequence also changes (123). Since most injection moulded articles are much larger than 250 μm the oxygen diffusion step controls the kinetics and the complexity of reaction sequences and hinders the application of known kinetic data to the problem of process control. Thus it was stated that temperature-time schedules have to be modified for changes in size and shape of component as well as minor changes in the binder (114).

Capillary flow into a finer powder

A powder bed (having a particle size equal or less than the injection moulded powder) to extract binder from the component surface by capillary action was used by Peltsman et al (52). They used a low viscosity wax and initiated the capillary extraction process between 50 and 60°C and continued heating to 120°C. Evaporation of the remaining binder continued up to 300°C. However, the same technique may be less effective with high polymers. Its success with mouldings of ultrafine precipitated powders has not yet been demonstrated (52).

Evaporation method

This is another method of binder removal from a green body before sintering or the like wherein the green body is placed in a pressure chamber wherein the pressure is raised to a level above the vapour pressure of the binder in the green body at the ambient temperature within the pressure chamber (124). Where several binders are utilised simultaneously, the pressure within the chamber is maintained higher than the vapour pressure of the lowest of the binders then in the green body at the temperature within the green body. Under these conditions, the binder or binders will turn to a vapour, will follow the normal laws of evaporation and diffusion and diffuse out from the green body into the surrounding environment within the chamber. The binder can subsequently be removed from the chamber in conventional manner (124).

Detailed description of the 'evaporation method'

Referring to Fig. 2.14 (124), a green body, which is formed from particular material and binder in accordance with prior art methods, is placed in a pressure chamber 1 which is filled with an inert gas such as argon, helium, nitrogen or the like via valve 2. The chamber 1 is heated to a predetermined temperature by means of the heater 3 and to a predetermined pressure by means of pressure regulator 4. The pressure within the chamber is designed to be above the vapour pressure of the binder in the

green body 5 at the temperature within the pressure chamber 1. The term pressure relates to the total pressure within the chamber which is represented by the sum of all the partial pressures of the vapours and gases in the chamber 1. At the temperatures and pressures within the chamber 1, the binder within the green body 5 will have a pressure of vapour above zero or of finite value which causes the binder within the green body to leave the green body in a vapour phase to the point where the external pressure of vapour (that in the chamber) is the same as the pressure of vapour within the green body (that of the binder). At this point there would be a dynamic equilibrium between the external (in the chamber) and internal (green body) binder vapour pressure. However, at this point of saturation, the net furthur removal of the binder from the green body into the chamber will be zero.

It is therefore necessary, that the chamber atmosphere continually move from the green body into the atmosphere in other than an equilibrium state. This is accomplished by providing a portion of the pressure chamber which is in a cooled state. Accordingly, there is provided the chamber portion 6 having cooling coils 7 therein wherein binder in the atmosphere is condensed into the condensate collecting region 8, the condensed binder being shown at 9. As this binder is removed from the atmosphere, other binder from the green body 5 can replace it within the atmosphere. The rate of removal of binder from the green body is dependent upon the temperature in the chamber 6 caused by the cooling coils 7. It is necessary that this removal rate not be too great so that internal pressure gradients can be formed in the green body which would tend to cause cracking or rupture as in the prior art systems. In most cases this would not be a concern though it could be a concern in certain isolated situations. The condensate can be removed on line or at the end of a cycle by opening of the pet cock 10 wherein the binder, which is in liquid state or which is maintained in a liquid state, flows through the pet cock into the container 11.

An alternative form of binder removal can be accomplished by means of the valve 12 in the line 13 joining the chamber 1 to the chamber 6 can be controlled, thereby also controlling the amount and rate of binder removal. It is also apparent that the valve 12 can be used in combination with variable setting of the temperature within the chamber 6 caused by the cooling coil 7 to control the rate of binder removal.

In a continuous process, the same apparatus as shown in Fig. 2.14 will be utilised. However, the valve 12 would serve to cut off the chamber portion 6 from the chamber portion 1. In this way, the chamber 1 can now be heated to sintering temperatures whereupon the green body will be sintered in accordance with the prior art techniques. It should be understood that multiple chambers 1 can be coupled via valve 12 to a single cooling chamber 6 and provide the same results as described herein above.

The following example was provided by the inventor (124) of the above invention:

Example

A green body was formed by injection moulding a mixture of nickel powder having particle sizes in the 3-5 micron diameter range and a paraffin binder having a melting point of 56°C. This green body was formed in accordance with standard prior art techniques. The chamber 1 was then filled with argon gas at a pressure of 1000 lbs per square inch (~ 6.9 MPa) at a temperature of . 233°C. The temperature was raised to 233'C from ambient room temperature relatively linearly over a period of 8 hours. This temperature was then maintained within the chamber 1. The cooling chamber 6 was maintained at a temperature of . 21°C by means of the cooling coil 7. Condensate started to collect in the region 9 approximately 2 hours and this condensate continued to collect for 12 hours, whereupon the increase of the quantity of condensate went to zero. The green body 5 was then removed from the pressure chamber 1 and placed in a kiln in an atmosphere of 90 % argon 10 % hydrogen at a

temperature of 1260°C, which was raised from room temperature over a period of - 4 hours in substantially linear manner. This temperature was maintained for - 1 hour at constant temperature whereupon the heater was turned off. The body was permitted to stay in the kiln until the temperature was reduced therein to proper handling temperatures whereupon the part was removed and found to have high integrity and to be free of cracks and flaws. In addition, the outer surface of the part was found to be of superior quality to those parts produced by the prior art solvent extraction techniques due to the maintenance of the integrity of the outer surface layers of the body.

Solvent extraction

This is a method of binder removal from a green (moulded) body before sintering. In this technique the green body is placed in a pressure chamber and it is initially heated to a temperature above the flow point of the binder to liquify the binder and, at this elevated temperature, it will be surrounded by a solvent in the vapour phase and at a temperature slightly above the melting point of the binder (125). The solvent vapour enters the green body slowly and dissolves the binder therein so that excessive stresses are not provided within the body due to binder expansion until binder-solvent ceases to extrude from the body. The body is then placed in a bath of the solvent, the solvent being maintained at a temperature above the flow point of the binder to remove remaining binder from the body. It is desired that the maximum amount of binder be removed during the initial stripping process but that enough binder remain to prevent collapse or cracking of the green body. It is preferably required that the solvent to have a boiling point above the flow point of the binder. The introduction of the solvent in the gaseous space should continue until the chamber (which was originally susbstantially evacuated) begins to show some solvent in the liquid phase. A preferred time period for addition of solvent in the gaseous phase would be that determined by initially evacuating the chamber and then adding the solvent

over a period of one hour in a somewhat linear manner so that the chamber shows a pressure of about 30 inches of mercury at the end of the one hour period. The amount of time required for this step will also depend upon several facts, including the size and geometry of the green body, the paticular solvent utilized, the particular binder utilized, etc. The time required for the removal of the remaining binder in the bath of liquid solvent depends upon wall thickness and geometry of the green body (125) and this can be seen from Fig. 2.15. The green body is then removed from the solvent system and, though substantially free of binder, still includes some binder which may have remained or which may have combined with the solvent and not have been leached from the green body. This remaining binder and solvent, if any, is now removed by a low temperature burn. This involves placing the part in an oven and raising the temperature to a point slightly above the boiling point of the solvent for a period of at least one hour, to remove all remaining solvent from the green body. The temperature is then raised to a temperature of - 110°C for about 1-2 hours to remove any water which may possibly have entered into the green body. The temperature is then raised to the removal temperature of the binder, whether by oxidation, reduction, evaporation, etc., and then the temperature is slowly increased to - 400-500°C for a period of few days. This period will also depend upon the wall size of the body. This slow-temperature burn, if desired, can take place at lower temperatures for delicate parts with the final burn-out taking place during the sintering process. This burn out temperature would always be below the sintering temperature of the green body particles (125).

The above discussion was presented in terms of a single component binder and since the green body has lost some of the adhesive qualities of the leached out binder it becomes more fragile and therefore more difficult to handle. In order to improve the handling characteristics of the leached out green body, the original binder may incorporate a second binder component that is not leached out and thus may provide improved

handling characteristics for the leached green body. It is therefore desirable, under certain conditions, to use a two-component binder (125).

In many cases, it has been found that the leachable portion of the binder may be cottonseed or a soybean oil and the non-leachable portion being polyethylene, in which case the leaching agent may be typically Freon TF. Using these materials the advantage is that the leachable portion of the binder is already in its liquid state at room temperature. The leaching agent for the oil is applied initially in gaseous state and then as a liquid as in the one-component binder system. Therefore, no heating, or only modest heating, if necessary, is required for the binder removal operation. By using a binder and a leaching agent such as these, the leaching process may even take place at room temperature. After the indicated leaching process, the leached green body still contains the second non-leached binder component, and may now be handled more readily, i.e. may be stored, stacked, exposed to furthur shaping processes, etc. This second binder component is of the organic type that decomposes under heat, so that it may be removed during the firing operations. The ratio of binders is preferably such that only sufficient non-leachable binder remains to prevent deformation of the green body (125).

For other applications, it may be desirable to use a three-component binder wherein the two-binder components are each leachable by different solvent. The subsequent firing operation would remove the third binder component. In such a binder system, the first binder component may be polyethylene glycol, polypropane glycol, or polyvinyl alcohol- all of these using water as a solvent. The second binder component may be polystyrene, which may use methylene chloride as a solvent, or may be dioctyl phthalate which uses Freon TF as its solvent. The third binder component may be one of the usual strengthening components such as polyethylene which is decomposed by the firing operation.

Another useful three-component binder may comprise an oil, a wax

and polystyrene.
It is readily apparent that any number of binder compounds can be used, applying the above principles.
The articles provided in accordance with the above disclosed steps have been found to undergo shrinkage of calculable amount and to be relatively free from cracks and the like. Precision articles have been formed from metals, ceramics and cermets and have been found to be reproduceable with substantially high yields (125).
Also, since the binder material is quite expensive relative to many of the particulate materials used in most cases, it is possible to recycle the solvent-binder system remaining and to separate both binder and solvent for re-use (125).

2.2.10- Sintering process

Sintering is one of the most important steps of any fabrication process, since it gives the ceramic body its final properties (104). During this process which is usually carried out at 0.85 of the homologous temperature, thermal densification of the green body takes place. At this temperature there is sufficient atomic mobility. Under the influence of the surface tension, which is the driving force of this process, the green body consisting of a multitude of powder particles with a considerable internal surface, for energy reasons, tend to reduce its internal surface. As a result the precompacted powder particles grow together, which leads to solid state reactions such as recrystallisation and grain growth (104).

Densification, recrystallisation and grain growth occur in the same temperature range. Therefore, a strict control of the sintering conditions (i.e. sintering time and temperature) and of sintering aids are essential in order to achieve a fully dense sintered body. In the coarse of sintering the density increases with the logarithm of time, and the grain size increases with one-third of time (104).

The mechanism of solid-state sintering can be summarised as follows: The driving force for sintering is reduction in surface free energy associated with a decrease of surface area in powder compacts due to removal of solid-vapour interfaces (Kingery 1983). The vapour-pressure difference across a curved interface can enhance evaporation from particle surfaces and condensation at the neck between two particles, particularly for particle diameters of several micrometers or less, such as occur in ceramic fabrication. Although this evaporation-condensation process produces changes in pore shape and joins particles together, the centre-to-centre distance between particles remains constant so that shrinkage and densification do not occur. The driving force for mass transport by solid state processes is shown in Table 2.3 for ceramic powders with low vapour pressure which is the difference in free energy between the neck region and surface of particles. As for the evaporation-condensation pathway, transport from surface to neck

by surface and lattice diffusion does not cause densification. This is produced only by diffusion from the grain boundary between particles and from the bulk lattice. Covalent ceramics such as Si_3N_4 are more difficult to sinter to high density than ionic solids (e.g. Al_2O_3) because of lower atomic mobilities, although difficulties can be overcome by using very fine powders (~ 0.1 μm in diameter), high temperature and high pressures (Popper 1983).

Effect of powder properties, compacting and sintering conditions on density and dimensional change in sintering

Dimensional changes in compacts during sintering are closely related to changes in density (105, 106). In other words changes in green and sintered densities of compacts are primarily due to changes in dimensions (106).

It is well known that compacts shrink rapidly during the early stage of sintering process and the rate of shrinkage slows down with increasing sintering time. The higher the sintering temperature the larger the shrinkage of the compacts (106).

It is also very well known that the higher the compacting pressure the smaller is the shrinkage. In addition to compacting pressure and sintering temperature and time, the properties of the powder from which a compact is pressed, in particular its particle size, have a strong influence upon the dimensional changes during sintering (106). It is reported (107) that the finer the powder the greater will be the shrinkage for a given sintering time. It can therefore be summarised that those compacts with fine powders, pressed at low pressures with low green densities and those sintered for long times at temperatures near the melting point of the powder will exhibit large shrinkages. In most cases large shrinkage values are not desirable because control of the parts dimensions is an important requirement and with large changes in the final dimensions of the part the control becomes difficult and the parts may wrap during sintering (106). It is therefore more desirable to have compacts with high green densities and little dimensional changes during sintering and this is possible by

using powders with high compressibility at high compacting pressures.

It is also very well documented (106) that if the sintering temperature and time cause the growth of the grains (i.e. the powder particles) during sintering then both density and mechanical strength decrease depending upon the extent of the grain growth process. It is therefore important to choose the correct sintering temperature and time for a particular powder so that to prevent excessive grain growth which can also be prevented by the addition of grain growth inhibitors also known as sintering aids.

Effect of sintering upon microstructure

The microstructure of a green powder compact will consist of the original powder particles with their boundaries outlined and the pores in the structure can also be obsreved. Larger powder particles may appear flattened and distorted, the more so the softer the powder and the higher the compacting pressure. If the particles are polycrystalline, grain boundaries within the particles may also be seen (106).

However, when a powder is sintered there is a transition in the structure. The original particle boundaries can no longer be seen. Instead the structure becomes similar to that of the metal in the wrought and annealed condition, except that it contains some pores. In the case of ceramic powders the sintered microstructure will consist of grains, grain boundaries and some pores between and within the grains which is basically the same as that of the wrought and annealed microstructures of metals. It has become quite clear that the establishment of a sintered microstructure is dependent in many cases upon particle size of the powder, the compacting pressure and the purity of the powder in addition to sintering conditions.

Effect of sintering upon mechanical properties

The mechanical properties of sintered compacts are usually determined and discussed as a function of compacting pressure, sintering temperature and time together with the determination

of sintered density as it depends upon processing parameters. From the literature (106) it is quite clear that in parallel with the increase in density with increasing compacting pressure, increasing sintering temperature and increasing sintering time, the mechanical properties, in particular tensile and compressive strengths, also increase. It is also very well known (104, 106) that the strength values for finer and more pure powders are higher than those of coarse and less pure powders and that the mechanical strength increases with increase in sintered density of the compact.

Liquid phase sintering

In liquid phase sintering the composition of the powder is such that one (or more) of the added powders (sintering aids) becomes liquid at one stage during the sintering process. By forming enough liquid at the sintering temperature easy rearrangement of particles take place but not enough to fill in the initial porosity. Subsequent solution and reprecipitation of the solid in the liquid phase allows reshaping of the particles and formation of a dense body (106, 109). From the literature (106, 109) it is clear that there are different types of liquid phase sintering processes: one is the mechanism by which the so-called heavy alloy systems, e.g. tungsten carbibe-(6-10 wt. %) cobalt alloys, are sintered and is referred to as liquid phase sintering by the heavy alloy mechanism and another one is referred to as the transient liquid phase sintering for sintering of, e.g. 90 Cu-10 Sn, Al-Cu and Mg-Si powder mixtures (106).

However, whether we have a solid-state or a liquid-phase sintering process, it is important to know the variables (and their effects) in the sintering process. These variables are: the processing temperature, the time spend at each stage of the process, the particle size and size distribution of the powder, the composition (including the additives) and the processing pressure and atmosphere (where required).

2.2.11- Ceramic injection moulding defects and their causes

The ceramic injection moulding (CIM) process consists of several stages (see section 2.1) at which defects of different types may be introduced (126). These include the process of mixing fine ceramic powders with an organic binder (i.e. mixing defects), the filling of mould cavity and the solidification within the mould cavity (i.e. moulding defects) and during the removal of the organic binders (i.e. debinding defects). The moulding defects described here all originate from thermoplastic polymer or wax organic binder systems which represent the most widely used class of organic binders (1, 51, 126). There are other defects such as microvoiding which may arise in the thermosetting binder systems. The debinding defects described here are those appearing as a result of pyrolysis and not any other extraction techniques.

In this section of chapter two, therefore, the major defects associated with the preparation of ceramic moulding blends, mould filling and solidification and removal of organic binders are covered and their causes are explained.

Defects during the mixing stage

These include undispersed agglomerates, undispersed binder, abrasive contamination, contamination from machinary and atmosphere (126) which will be described individually as follows:

Defects due to undispersed agglomerates

The work of Lange (19, 25, 127) has shown that ceramic fabrication processes must be capable of dispersing agglomerated powders at an early stage. Failure to do so will produce stresses (due to differential shrinkage of agglomerate and matrix) which generate stress limiting defects (25, 127). Large voids between agglomerates may persist during sintering because of stability afforded by a large grain coordination number (19). Edirisinghe and Evans (20) have reported that dispersive mixing of ceramic powder in an organic binder is an essential prerequisite and that low shear double blade mixers are

insufficient for this task. Fig. 2.17 shows the presence of undispersed agglomerates after mixing an alumina powder with a wax binder for 1 h at 160°C in a double blade mixer (20). They also reported that a twin roll mill and a twin screw extruder were capable of dispersing soft agglomerated powders. With one alumina powder a very small population of agglomerates remained after twin screw extrusion at 220-235°C which can be seen in Fig. 2.18.

Defects due to undispersed polymers

It is often the case that organic binder systems are composed of several components (1) with different softening points. For example waxes with softening points in the range 60-80°C are often blended with high polymers with softening point in the range 120-160°C. Thus residual undispersed polymer may result if the temperature profile in the mixing device is insufficient for blending the higher softening point or the higher viscosity component.

Abrasive contamination

The abrasive nature of ceramic moulding blends processed in predominantly steel machinery may result in contamination by iron and other alloying elements which is unacceptable in some applications (126). Abrasive wear is thought to be related to pressure on material which causes the lubricating film of organic material to breakdown. It has been found (128) that wear in a moulding machine is enhanced in regions of the machine where the suspension comes under high local shear stresses. The ploughing action of large angular particles also produce severe wear.

However, the formulation of organic binder plays an important part in the control of abrasion. It was found by Zhang et al (126) that in an alumina-polypropylene blend processed by twin screw extrusion the substitution of stearic acid for some of the polypropylene had a pronounced effect on flow properties and also reduced the iron content considerably during mixing by twin screw extrusion. It is thought that the lubricant plays a

particularly important role in the early stages of mixing before the main binder is fully molten (126).

Contamination from machinary and atmosphere

When the material is removed from a mixing or injection moulding machine the problem of cross contamination is obvious and there is a need for extensive cleaning (126). However, even when the material is not removed, but the machine is shut down, the residue is subjected to a prolonged heat treatment in air as the machine cools. This may leave degraded debris which adheres strongly to the metal wall and is slowly released into the next batch. The use of extensive purging followed by water cooling is therefore desirable as a shutting down schedule. The problem of airborne contaminants is common to all ceramic processing and requires clean room conditions (126).

Moulding defects

These include weld/knit lines, incomplete mould filling, voids caused by adsorbed water, shrinkage voids, shrinkage cracks, demoulding defects, blistering during mould release and contamination from the moulding machine (126) which will be described individually as follows:

Weld lines

Weld lines appear in mouldings when free surfaces of the injected fluid meet inside the cavity at reduced temperatures (126). They present regions of weakness in polymer moulding and discontinuities which persist in the fired body in the case of ceramics. They tend to occur when the melt front splits to overcome an obstacle or where the gate allows jetting into the cavity. Mould design, therefore, plays an important part in the avoidance of weld lines. In general weld/knit lines can be avoided on single gated moulds by side gating the cavity to generate plug flow (10, 61).

Incomplete mould filling

This is a more severe problem with ceramic injection moulding than with polymer fabrication because the low specific heat and high thermal conductivity of ceramics compared with polymers, combined with high volume fractions of ceramic result in high thermal diffusivities for ceramic injection moulding blends (126). Thus cooling is rapid and in cavities with long flow paths the viscosity may increase to a level that inhibits flow before the mould is filled. This is one reason why a low temperature dependence of viscosity is desirable in ceramic moulding blends (129). A number of standard moulding tests are used to quantify mould filling ability of which the spiral flow mould has been used for ceramic suspensions.

Zhang et al (126) found that volume loading of the ceramic powder in a binder system is a critical parameter during moulding of a 62 volume % A16 alumina powder which failed to meet the viscosity criteria for ceramic moulding and increasing the nozzle temperature from 225°C to 240°C caused the degradation of the organic binder and the 62 volume % alumina composition became unmouldable. However, the same powder was successfully moulded at 60 volume % which suggests that ceramic volume loading is a critical parameter and should be optimised for different binder systems.

Voids caused by adsorbed water

Prolonged vacuum drying is generally used prior to processing ceramic blends. Fine powders are capable of adsorbing sufficient water to produce a large void volume at processing temperatures and with this in mind a ceramic moulding machine has been designed to operate under vacuum (130). Nevertheless with a high melting point binder it was possible to combine an alumina powder which had been equilibrated at 100 % RH for several weeks. The feed zone barrel temperature was 180°C and was thus sufficient to dry the powder before encapsulation occured (20).

Shrinkage voids

Shrinkage related defects in ceramic moulding present one of the most troublesome problems (126). If a non-destructive evaluation is not carried out at the moulding stage, either voids or cracks which appear in the final sintered product may be incorrectly diagnosed as originating from the binder removal stage (126). In both events defects have a tendency to appear in thick sections of the moulding. A step wedge component allows the investigation of defects in sections of varying thickness with respect to the sprue and runner dimensions. In static pressure moulding, the sprue solidifies before the centre of the thicker sections. The pressure in the centre of the moulding, initially primed to a level determined by the pressure on the screw or plunger, falls as the fluid solidifies and cools. Should the pressure fall to a level where the liquid components of the blend become unstable with respect to the vapour, the pressure of nucleation sites on the ceramic powder will produce bubbles. Zhang et al (126) observed some voids in the thick sections of a step wedge component prepared from a fine alumina-wax blend. The voids were eliminated by increasing the final stage injection pressure.

Shrinkage cracks

Although high injection pressure may reduce the incidence of voids in moulding it does not necessarily eliminate residual stresses which result from non-uniform solidification, which, in common with foundry processes, is inherent in injection moulding (126). Heat flow to the mould produces successive layers of solidified material from the surface inwards. The resulting stresses can be assessed analytically (131) for simple shapes and this provides guidelines for the intelligent control of the moulding process and also the selection of materials for the suspension (126).

Zhang et al (126) observed some voids which appeared at the centre of silicon nitride four-point test bars moulded with a low hold pressure of 36 MPa. In another attempt the hold pressure was raised to 103 MPa and the voids did not appear. In both case prints of radiographs were used to observe any

defects. In a third attempt the correct choice of pressure and mould temperature allowed a bar to be made without voids or cracks. They also found similar shrinkage cracks in a step wedge component and also in ceramic rotors which were avoided with the use of modulated pressure during solidification in the cavity.

Demoulding (mould ejection) defects

According to Zhang et al (126) three types of defects can occur during ejection of the moulded part from the cavity after solidification: (i)- ejection pin indentation, (ii)- bulk deformation, and (iii)- cracking or fracture. These are associated with adhesion to the mould wall combined with low yield or fracture stress in the material. Adhesion to the mould wall is largely influenced by net thermal contraction of the component, in turn determined by net shrinkage (132) and hence by the extent of packing. The use of proprietory mould release agents reduces friction at the mould wall as does the correct choice of taper, typically 1° or more (126). The flexural strength of ceramic-polymer suspension is low (133) and thus cracking or even complete fracture are possible if proper attention to mould release is not given. Care must be taken to distinguish between cracking associated with thermal contraction and cracking caused by improper mould release.

The presence of indentation marks from ejector pins is associated with either insufficient cooling time in the mould or with low material yield stress (126). This defect should not be confused with surface marks left by even the best machined ejector pins.

A more subtle defect is the slight deformation experienced by the moulded body on ejection. This becomes important for ceramic artefacts with high aspect ratio such as scissor blades or gas turbine blades. Zhang et al (126) measured the linear mould shrinkage from mouldings of silicon powder suspended in polypropylene vehicles with varying proportions of atactic polypropylene (APP). The presence of APP, having ~ 10 % crystallinity measured by differential scanning calorimetry, provided less shrinkage in the mould compared with the isotactic

polypropylene (IPP) having ~ 50 % crystallinity. The elastic modulus of the moulded suspension was decreased by APP addition and deflection was increased.
The consequence of these property changes was that mouldings based on APP were subject to considerable deformation during ejection, and therefore the moulding compositions were not suitable for slender ceramic components. Reducing the APP content of the blend, was effective in overcoming this distortion and some moulded components became acceptable without any distortions (126).

Blistering on mould release

Zhang et al (126) observed this type of defect in their polypropylene based silicon powder mouldings produced at 225°C and a machine failure was followed during which material was resident in the barrel for 30 min. Thermal degradation of the polymer was sufficiently advanced that volatile degradation products were liberated in the surface layer after mould release which resulted blistering of the mouldings. This illustrates the importance of residance time during ceramic moulding which may also affect the subsequent polymer removal stage if polymer degradation mechanisms are thereby advanced (126).

Delayed failure

The absence of shrinkage cracks in the component immediately after moulding is no gaurantee that the body will be free from cracks after reheating to the softening point of the suspension or prolonged storage (126). Many polymers experience time dependent stress rupture, also known as creep rupture, or more obscurely static fatigue. This effect is enhanced by elevated temperatures (134) and by the presence of low molecular weight species (135). The latter are commonly a feature of ceramic moulding compositions (1). Zhang et al (136) found cracks which appeared in a moulded rotor after reheating to 120°C. The component was produced by modulated pressure moulding at an excessive pressure amplitude and in the as-moulded state radiography did not reveal cracks. Prolonged storage at room

temperature was also observed to induce this type of cracking (126).

Contamination from the moulding machine

Zhang et al (126) found coarse steel wear debris in mouldings of alumina test bars containing 62 volume % alumina powder, which appeared dark in a print of a radiograph. The wear debris were due to the jamming of the check ring non-return valve at the screw back stage. The cause of the seizure was a material with unfavourable flow properties (72, 129). It was reported (126) that a loading in excess of 61 volume % was beyond the acceptable limit. This also illustrates the importance of exact filler loading determination, i.e. a change of a few volume percentage has a pronounced influence on rheology.

Defects during the polymer removal stage

These were subdivided (126) as follows: (a)- defects which occur before the softening point of the suspension is reached, (b)- defects which occur immediately after softening point is passed but before the suspension is embrittled by polymer degradation and loss, and (c)- defects which occur in the latter stage when the suspension again behaves in a brittle manner. These defects occuring at different stages are described individually as follows:

Defects appearing before the softening point is reached

Deformation caused by residual stress relaxation

Residual stresses in ceramic mouldings which are 'frozen in' by rapid cooling in low mould temperature conditions may give rise to appreciable deformation when reheated to the region where stress relaxation can occur. Zhang et al (126) observed the distortion of an alumina-polypropylene moulding at the polymer removal stage. Similar mouldings made at higher mould temperatures (40°C and above) did not show this deformation. They also found that identical unfilled polypropylene mouldings made at low mould temperatures (20°C) were distorted in the same way upon release from the mould.

Cracking before the softening point is reached

The appearance of cracks in samples arrested at softening point may be attributed to three causes (126). One type is cracking caused by residual stresses from the moulding operation. Zhang et al (126) observed cracking in 31 mm diameter compression moulded cylinders of composition 60 (volume) % alumina+3 % polypropylene+1 % stearic acid+3 % APP+2 % dibutyl phthalate which was dependent on the rate of reheating to the softening point of 144°C. At the heating rate of 290°C/h cracks occured and these were attributed to thermal shock damage under radiant surface heating conditions. At rates of 2, 5, 10 and 60°C/h cracking was due to the evolution of volatile degradation products which were unable to diffuse through the solid body. At 120°C/h heating rates samples were reproducibly crack free. Thus under suitable conditions of time and temperature it is believed that polymer degradation can produce cracking in the fragile suspension below its softening point (126).

Cracking caused by residual stresses resulting from the moulding operation was seen in the polished section of a rotor moulded with static pressure (126). This cracking was enhanced by reheating the rotor to above its softening point of 144°C at 2°C/min. In another attempt a rotor was made with modulated hold pressure and was free from macroscopic internal cracks after reheating to 150°C (126).

Defects appearing shortly after the softening point is reached

Swelling

Zhang et al (126) observed swelling of a compression moulded cylindrical sample of silicon powder in a polypropylene-silicone oil vehicle heated at 2°C/h to 500°C in air. The swelling of the body was attributed to the evolution of gaseous decomposition products at such a rate that they were unable to diffuse through the bulk. Since swelling/bloating rather than cracking occured, they concluded that deformation occured during a stage when the bulk of the polymer was fluid, i.e. above the softening point

but below the temperature and before the time where polymer thermal degradation and loss had given rise to brittleness.
In another extreme case they found that the component had disintegrated during binder removal in air. The reason being due to the exothermic nature of the reaction which may lead to severe temperature excesses in the component and it is believed that in unfavourable cases combustion may take place (126).

Slumping

The objective in achieving an optimum powder volume loading in powder moulding is to incorporate the maximum possible amount of powder without exceeding viscosity limits (1). Apart from reducing the shrinkage on firing, a high volume loading of powder may also confer upon the molten suspension a high yield stress. During reheating to remove the binder this helps to resist gravitational effects. Thus if insufficient powder is incorporated into the suspension distortion may occur during reheating (137). Some workers (60, 113) have used a powder bed to support the mouldings during reheating and this may have the added advantage of removing some of the binder by capillary flow at the moulding powder-bed interace.

Defects occuring in the latter stages

Cracking caused by thermal degradation of the binder

The identification of cracking in injection moulded bodies during binder removal is not simple (126). In the first place it is necessary to be sure that cracking was not caused by shrinkage stresses either during moulding or subsequently under stress rupture conditions. This may be ascertained in many cases of reheating the moulding to just below its softening point and slowly cooling followed by non-destructive testing (126).
Cracking caused by the release of gaseous decomposition products may occur very early in the process of binder removal during prolonged heating below the softening point or alternatively may occur much later in the heating schedule when the suspension has become embrittled by loss of binder (126).
Cracking has the effect of reducing the component size by

providing fresh surfaces and shortening diffusion distances. Thus swelling/bloating is frequently absent in samples which have cracked at an early stage.

It is also important to know that there are other sources of cracking described below (126) which are not a direct result of the liberation of gaseous products and this emphasises that the diagnosis of cracking in the injection moulding sequence is not facile.

Cracks caused by non-uniform binder removal

The aim of achieving maximum possible filler loading which can be injection moulded is not just to reduce the shrinkage on firing but also to reduce the thickness of the inter-particle binder film which influences shrinkage when the binder is removed (126). Although this shrinkage is low (. 1 % linear) it may be sufficient to introduce cracks in a fragile assembly of particles if it is not uniform. This type of failure was first noted by Quackenbush (61). If the binder is removed from the sections of the moulding at an early stage these regions shrink slightly and become brittle. If the thicker sections of the moulding liberate their binder at a later stage, the shrinkage which they undergo may cause cracking which is not related to the pressure caused by evolution of volatile degradation products (126).

Cracks caused by gravitational effects

Another defect is related to the differing rates of removal of organic binders from thick and thin sections. This was observed by Zhang et al (126) in the blades of an unsupported rotor during binder removal. Cracking was caused by slumping of the periphery of the hub after the binder had been removed from the thinner blades. The only support for the web was the blades acting as the tensile members. Thus slumping of the web is accompanied by brittle fracture of the blades.

Skin effects

Delamination of a surface 'skin' from ceramic moulding has been observed (90, 138) during thermal or oxidation degradation of the binder. This type of defect was also observed by Zhang et al (126) on the surface of compression moulded cubes of four compositions based on polypropylene with silicon powder heated at 2°C/min in nitrogen. The precise cause of the defect is a matter of some contention (126) but preferential removal of the organic phase at the surface and consequent shrinkage is one explanation. The suggestion that the effect results from compositional inhomogeneities arising in the injection moulding process (138) has not been substantiated (126).

Residue

The residue from polymer pyrolysis has been given little attention in published work but may be critical in some applications, notably for electrical and optical components (126). In high temperature ceramics the presence of small amounts of silicates or alkali metals may severely limit mechanical properties (104, 126). In non-carbide ceramics carbon residue may be a problem. The exception is oxide ceramics which are to be fired in air or oxygen. Carbon residue is primarily a function of organic vehicle selection and pyrolysis atmosphere (126).

It is also important to note that there are a number of potential benefits from using residue from the polymer in ceramic moulding (126). The use of silicone oil and resulting silica can be advantageous in some ceramic compositions. Polycarbonsilane has been used as a binder in SiC extrusion (139) and contributes significantly to the final material, probably reducing the shrinkage on binder removal as well as on sintering. There are a range of other polymeric precursors for ceramics used in ceramic-fibre composite processing (140).

Zhang et al (126) concluded that the successful development of the ceramic injection moulding sequence relies on the careful obsevation of defects and the diagnostic isolation of their

causes. Frequently this involves a stepwise experimental procedure in which processes are interrupted before completion.

2.3- General review of injection moulded ceramic, cermet and metallic powders

This section of chapter two is devoted to the review of the most successful injection moulded ceramic, cermet and metallic materials available from the literature. The aim of each subsection is to describe for each powder the available experimental/practical detail of the injection moulding process such as powder and binder properties, moulding and demoulding properties, debinding properties, properties of the sintered parts and sintering conditions where available.

The metal powder injection moulding process is reviewed only for the Rivers process because, as will be seen in the results chapter, this process has been investigated for the 99.5 % alumina ceramic during this work.

The injection moulding of alumina is reviewed in more detail in section 2.4 covering various binder systems available for the injection moulding of alumina ceramics, their advantages and limitations, the sintering conditions for different grades of alumina, mechanical, thermal and electrical properties and also the applications of alumina ceramics.

2.3.1- Injection moulding of silicon nitride

Sintered silicon nitride is among several ceramic materials under consideration for high temperature structural applications such as gas turbine engine blades, nozzle vanes, rotor and stator components, etc. (61). By using ceramic components, e.g. in rocket engine turbines, it will be possible to increase the turbine inlet temperature from ~ 900°C to ~ 1100°C or more so that to achieve greater efficiency (141). Today's rocket engine designs are limited by the properties of nickel base superalloys. One way to operate with an increased turbine inlet temperature is to cool the superalloy component with propellent which are transported as part of the engine. Therefore, there is a strong demand to develop structural ceramics which do not require cooling due to their high-temperature strength (141). The injection moulding technique has now been used for the production of complex shaped structural parts used in high

temperature gas turbine engines (142). Quackenbush et al (61) has described the fabrication of sinterable silicon nitride by injection moulding in the following manner without giving the name of the binder components:

The powder

The silicon nitride powder used for injection moulding was produced by gas-phase reaction resulting in a fine, high-surface area powder with crystalline and amorphous phases. In a ball-milling operation, the Y_2O_3 and Al_2O_3 powders were blended with the silicon nitride as sintering aids. Ceramic compositions of Si_3N_4 + 6 % Y_2O_3 + 2 % Al_2O_3 and Si_3N_4 + 13 % Y_2O_3 + 2 % Al_2O_3 were successfully moulded and sintered to > 98 % density.

The binder

The binder system used for the injection moulding of the turbine blades and test bars had the following approximate composition: major component 80 vol. % of the binder; minor binder component 8 vol. % of the binder; plasticiser 8 vol. % and surfactants 4 vol. % of the binder.

The sintered blades (a single axial turbine blade) and test bars had the following dimensions respectively: - 3.5 cm high with a maximum cross section (in the dovetail) of 1 cm, 6.35 mm X 3.175 mm X 50.8 mm.

Compounding

This was conducted using a torque rheometer which was essentially a dynamometer connected to a mixing head. The head was a temperature controlled chamber that restricted the mix to a confined volume near the mixing blades. The dynamometer portion of the instrument measured the torque required to maintain the mixing blades at a set rpm. The torque data were recorded on a chart recorder which could be used to obtain viscosity information. Torques were generally very high during the initial stages of compounding as the binders wet the ceramic powder (61). As compounding continued, torque values decreased

and eventually reached a steady level. According to Quackenbush et al (61) mixing time was not the controlling variable, and generally, mixing continued until a predetermined torque was reached. In this way ceramic mixtures were reproducible by experiencing the same total work in mixing from batch to batch (61).

An example of mix rheology data obtained by the authors is given in the plot of Fig. 2.19. This type of data is used for the initial comparison of experimental binder systems. One mixing difficulty encountered early was the entrapment of air in the mix while compounding. During injection moulding these small air pockets were compressed to an almost undetectable size by the injection pressures used. During the early stages of thermal binder removal when the temperature rose above the mix flow point, these pockets would re-expand causing massive part disruption. This problem was solved by a separate vacuum deairing step after mixing. The silicon nitride-binder mixture was granulated after deairing into a form suitable for loading into the injection moulding machines.

Injection moulding

The injection moulding machine used was a plunger type injection moulder shown schematically in Fig. 2.20. This was selected over the screw-type machines in order to minimise the contamination problem (61). Iron contamination, however, turned out to be ~ 0.02 % in the milled silicon nitride powder mixture and increased to ~ 0.05 % in the turbine blades after binder removal. It was suggested that the low contamination was a result of binder fluidity and the very fine particle size of the ceramic powder. The authors (61) believed that the use of hardened barrel and plunger assemblies should strongly reduce the amount of wear.

In moulding the turbine blades the gate area was located on the dovetail in an area to be machined. The philosophy used was to make the gate quite large to reduce die wear at the gate, speed mould filling and reduce jetting into the mould.

According to the authors experience of moulding silicon nitride

die wear was minimal since the binder was molten during injection. The only high wear location was at the gates which were highly restricted. The gate enlargement and relocation on the mould solved this problem. The mould used to produce the blades and bars was fabricated out of tool steel but was never hardened (61). The cavities and runners were polished to facilitate part removal.

The authors believed that the major variables in injection moulding are injection speed and pressure, barrel and mould temperatures and holding time. They suggested that parts produced should be inspected so that to select a usable conditions. Refinement of moulding conditions is then made by minor adjustments of the pressures, temperatures and hold times. A major factor, according to the authors, in the injection moulding process was part shrinkage (1.5-2 linear percent) in the mould which was due to the type of binders used and also due to rather low volume loading of the powder. The addition of a large volume loading of the ceramic powder should reduce the shrinkage to 0.4-0.8 % linearly. A high shrinkage value can produce part removal or cracking problems in shapes where the part tends to shrink against and not away from the mould walls (61). The shrinkage problem can be altered through variation in moulding conditions or binder system modifications. Increasing moulding pressure, e.g., causes additional mix to be compressed into the mould cavity during the initial stage of moulding. When the gate freezes this extra material is forced to remain in the cavity reducing the total shrinkage on solidification. The authors found that in this way the moulded bars weighed more but the as-moulded densities were identical for all the bars regardless of the moulding pressure. They also reported that part removal became difficult above 124 MPa injection pressure due to the lower shrinkage.

According to the authors moulding shrinkage problem increases with increasing part cross section. Shrinkage induced stresses can lead to collapsing of the surfaces to form sink marks or the generation of cracks and voids in the last region of the part to solidify. This moulding shrinkage along with the increasing

difficulty in binder removal are the major problem areas to be addressed in moulding parts of large cross section (61).
In the selection of binder systems for moulding silicon nitride it was found by the authors that some binders, particularly certain paraffin-based binder systems, had a tendency to separate from the ceramic within the barrel. As a result an immovable mass of ceramic in the barrel was noted, which was worse at higher moulding pressures and decreased at higher volume fractions of ceramic in the mix. The segregation effect was very binder specific and minor changes in the binder system could reduce or eliminate it (61).

Quality control

This was overemphasised by the authors for every stage of the injection moulding process. Non-destructive evaluation (NDE) was performed after each major process step shown in the boxes of Fig. 2.1. The inspection procedure involved, recording of the part weight, visual and microscopic inspections and radiographic examination to observe the part interior.
The part weight could provide the first indication of a flaw. Small parts from the same mix moulded under identical conditions will usually have weights within a few hundreds of a gram. A high weight may indicate a metallic inclusion, conversely a light weight may reflect the presence of a subsurface void (61). The microscopic visual inspection was used to locate surface connected cracks, regions of pour packing during moulding, general surface finish and rubbing marks which may be indicative of mould backlock (61).
According to the authors radiographic inspection of the as-moulded, debonded and sintered parts was of tremendous benefit in their moulding development program. They were able to eliminate virtually all surface flaws both in the as-moulded and debonded state. Massive internal cracking was also inspected. More than one exposure was recommended for each part and a flaw must be observed on both exposures to be considered real (61). In parts of varying cross section such as the turbine blade, differing exposure conditions was used to highlight the dovetail

in one negative and the airfoil in another. In looking for internal flaws on radiographic negatives the part orientation must be considered (61). Cracks parallel to the direction of the x-ray beam will show clearly, but delaminations or cracks perpendicular to the beam will be faint or invisible. An accurate inspection, therefore, requires exposures at multiple-part orientations.

Radiographic inspection has also been most beneficial in observing flaw generation or enlargement from one process step to the next (61). A second use is to observe differences between binder removal characteristics of various experimental binder systems. In many cases accelerated binder removal cycles can be used to magnify these differences. Inspection of parts after binder removal require somewhat more care in handling than in the other process steps (61).

The limit of resolution for high density metallic inclusions in the turbine blades and test bars was ~ 100 μm. This limit is a function of the radiographic equipment used, film type and part cross section (61). Low density regions, such as pores, provide less contrast and so the flaw detection limit is larger (> 250 μm).

Dimensional checks are valuable in monitoring part shrinkages in moulding, binder removal and sintering (61). In moulding, these checks are used to develop injection parameters minimising shrinkage while maintaining part quality.

The use of density measurements by weight and dimensions and also by the water displacement technique are standard procedures for as-moulded and sintered parts (61).

Binder removal

This was carried out by thermal decomposition and distillation of the binder components. These authors (61) also believed that flaws can be generated early in the binder removal cycle (as the binder becomes fluid) by expansion of air which was compressed into the part during moulding. Another problem at this stage is

part deformation or slumping which can be controlled by imbedding the parts in a sand or setter powder (61). A chromatographic grade of alumina was chosen which provided adequate support and could be cleaned easily for reuse. The parts imbedded in the alumina setter sand, where contained in borosilicate glass vessels.

For both blades and bars a thermal cycle of ~ 150 h (~ 6.25 days) was applied by the authors. Temperature rate increases varied throughout the cycle. The parts were heated rapidly (at ~ 10°C/h) up to the flow point of the binder. The rate was slowed (to ~ 2°C/h) through the binder flow point and during the major portion of the binder removal process. Rates were slowly increased to 10°C/h near the end of the binder removal process (61).

Internal cracking or delamination during binder removal process, according to these authors, was due to a rearrangement of the interior ceramic particles resulting in a denser packing and could not be eliminated by slower binder removal. The surface at this stage is held expanded by the interior until so late in the debinding process that it lacks sufficient liquid binder to supply lubricity for the rearrangement process. As the interior binder is lost, the ceramic particles are pulled into denser packing presumably by capillary forces. This type of cracking was believed (61) to be a kind of relief mechanism depending on powder morphology and powder volume loading. It can also be specific to the type of binder system used (61). For the turbine blades and bars these flaws were controlled by increasing the solids (powder) loading level and changing the type of binder surfactant used (61). Part strength after binder removal was adequate for the handling necessary for inspection and loading into the sintering furnaces.

Sintering and properties of the injection moulded silicon nitride

Dimensional control during sintering is one of the requirements for producing complex-shaped parts. This is particularly difficult in a liquid phase sintered ceramic such as the silicon nitride-yttria-alumina system where extensive particle

rearrangement occurs early in the sintering cycle (61). However, very high tolerances (± 0.05 %) obtained by the authors confirmed that sintered silicon nitride can be produced by the injection moulding process with sufficient dimensional control. A picture of the as-moulded, debonded and sintered axial turbine blade of silicon nitride is shown in Fig. 2.21 which was taken by the authors (61).

Four-point bend tests were conducted at room temperature on sintered silicon nitride test bars with outer and inner spans of 4.06 and 1.78 cm. The average flexural strength was 385.8 MPa with a Weiball modulus of 12. This strength was lower than that of machined sintered silicon nitride samples of similar composition but processed by other fabrication techniques. Room temperature flexural strength for these materials approaches 700 MPa. It was indicated that the lower strength of the injection moulded silicon nitride was due to the presence of the strength-limiting flaws and therefore the processing techniques have to be improved so that to increase the strength to a level that match with pressed and sintered compacts (61). However, the sintered Si_3N_4 turbine blades had roughly equivalent strength to the sintered α-SiC produced by injection moulding (61). The sintered Si_3N_4(+ 6 % Y_2O_3 + 2 % Al_2O_3) with densities > 98 % of theoretical density showed very good resistance to oxidation, i.e. no catasrophic oxidation was found after 300 h at 750, 1000 and 1200°C (61).

Summary

Axial turbine blades and test bars were successfully moulded and sintered to above 98 % of theoretical density. The composition used was Si_3N_4 + 6 % Y_2O_3 + 2 % Al_2O_3. Evaluation of the sintered parts indicated sufficient strength in current quality material to be considered a viable candidate material for turbine applications. Strength testing of non-injection moulded materials indicated potential property improvement with furthur processing modifications. The oxidation resistance of actual injection moulded turbine blades is as low as sintered Si_3N_4-Y_2O_3 produced by other fabrication techniques and showed no

tendency toward catasrophic oxidation (61).

From the above literature it is quite obvious that some experimental detail are missing which can be summarised as follows:

1- The type and name of the binders used for the successful injection moulding of silicon nitride were not specified.

2- The mixing, moulding and sintering conditions were not given.

It is therefore very useful to find the missing informations from other sources and this was provided in the work of Litman et al (143) who experimented with several thermoplastic binders while working with silicon powder. The binders investigated were low and high density polyethylene, polystyrene, polypropylene, nylon, acrylonitrile-butadiene-styrene (ABS), styrene-acrylonitrile (SAN) and polyurethane. Only polypropylene was found suitable. Others were rejected on the basis that their melt viscosity was relatively high at standard processing conditions and increased furthur as filler was added. They also found that loading of the polypropylene was furthur improved by adding hydrogenated peanut oil, which acted as a diluent and lubricant, reducing the viscosity significantly. Litman et al (143) also reported success with a series of low molecular weight polyethylenes and microcrystalline waxes. All of them provided good compounding results and the desired filler loadings could be achieved with any one of the binders. For compounding a silicon nitride powder was used instead of the silicon metal powder which requires nitriding reaction and takes a long time to form a Si_3N_4 powder. An 85 weight % Si_3N_4 + 15 weight % ceria mixture was therefore used for the compounding process. These workers also investigated a mixture of 80 weight % Si metal powder + 20 weight % B_4C mixture and a SiC powder which had particle sizes equal to 325 mesh (- 44 μm). The boron carbide (B_4C) had a density of 2.5 g/cm^3, the SiC had a density of 3.217 g/cm^3, the Si_3N_4 had a density of 3.44 g/cm^3 and the ceria (Ce_2O_3) had a density of 7.3 g/cm^3.

The authors (143) pointed out the following facts: a higher volume loading of the powder will provide less shrinkage, a

higher sintered density and better mechanical properties; since the densities of the powders (ceramic and metallic) are greater than those of the organic binders, a volume percent loading represents an even higher weight percent; as the difference in densities between the powder and the binder increases the degree of difficulty in wetting the powder with the minimum amount of the binder also increases and so does the difficulty in compounding. On this basis they reported that silicon metal powder was easiest to formulate while the Si_3N_4/Ce_2O_3 mixture was the most difficult. Other parameters which also affect loading are the melt properties (viscosity) of the binder and the powder properties (143). Certain problems such as clogging of the injection moulding nozzle and seizing-up of a laboratory extruder were encountered during the initial processing runs which were due to dilatant flow and time dependent (thixotropic) behaviours. A capillary rheometer with capillaries of 20:1 (length:diameter) ratios and greater were used to study the rheological properties. They found that a 70 volume % loading of the Si metal powder resulted in dilatant flow behaviour while at 50 and 60 volume % loadings pseudoplastic flow behaviour was observed. The testing temperature was set at 100'C for all measurements and it was found that the increase in viscosity was non-linear and that a longer capillary (die) length provided a greater pressure drop (as expected). According to Litman et al (143) ceramic injection moulding usually takes place at shear rates of 1000 s^{-1} and greater. The dilatant flow behaviour of the 70/30 powder/binder mixture was believed to be due to a separation of the two phases under an applied load/shear. This was observed when some of the binders actually oozed out of the Instron barrel past the capillary leaving a poor powder-binder mixture behind (143).

The injection moulding of the above silicon nitride- and silicon carbide-binder mixtures was carried out on a plunger type injection moulding machine. The use of a screw-type machine at low rpm tended to bind and pack the compounds with eventual seizing of the screw (143). The mould was a two cavity three plate type hot runner mould fed by a dual nozzle system. A

stripper plate removed the moulded parts. Cooling water at - 27°C was used. The machine settings were as follows:
barrel temperature: rear 260°C, front 288°C
nozzle „ : 260°C
injection pressure: 10000 psi (~ 69 MPa)
clamping: 125 ton maximum
with these moulding conditions the ceramic compounds gave an excellent purging through the nozzle with no difficulty. The mould temperature for best release was found to be 27°C. A heated mould half at 82°C caused sticking on the mandrel and the parts broke on removal. Teflon release agent did not help in the moulding. A carnoba wax applied to the mould halves proved helpful. All shots done on the machine were done manually. The plunger forward time was five seconds while the total cycle time (see section 2.2.6) was 1 min. In the majority of cases short shots charges were obtained. The gates were extremely small (0.04 inch) for their highly filled polymers and the nozzle tip was also very small (0.066 inch). One cavity was closed off so that all the pressure was applied to one cavity of the mould. This gave sufficient pressure to fill the other half. The moulded parts had an excellent surface finish and good detail. The moulded parts were packed into fine alumina powder (Al_2O_3 300 mesh) for the debinding process which took several days. The temperature of the debinding (muffle) furnace was gradually raised from room temperature to - 540°C. The parts were then cooled and placed in a separate sintering furnace. The sintering conditions were not given and this was obtained from another source (144) as follows: for the Si_3N_4 (+yttria + alumina) mixture a sintering temperature of - 1900°C for - 1 h under nitrogen flow was used; for the SiC (+ boron carbide) mixture a sintering temperature of - 2100°C for - 1 h under vacuum (or a protective gas atmosphere) was used.

The above literature review has fulfilled the missing experimental detail for the injection moulding of silicon nitride powder and the following section will cover the injection moulding of silicon carbide in more detail.

2.3.2- Injection moulding of silicon carbide

The rheological properties and processing parameters for the injection moulding of silicon carbide in low molecular weight polyolefin type binders were described in the previous section from the work of Litman et al (143). In another work by Ohnsorg (145) α-SiC having a particle size of 1 micron was mixed with ~ 0.5 parts of B_4C (sufficient to provide ~ 0.5 % by weight boron to SiC) in a ball mill for ~ 24 h. Materials such as carbon, beryllium, nitrogen or boron are used as sintering aids for SiC. The resulting mixture was then placed in a high shear, closed, overlapping sigma blade mixer with ~ 2.04 part of powdered phenolic resin (sufficient to provide ~ 1 % by weight of carbon char). The mixture was steam heated to ~ 120°C during mixing. 27 parts of a mixture comprised of 58 weight % of styrene resin having a molecular weight of between 800-5000, 12 % vegetable oil having a melting point of ~ 55-60°C and 30 % light mineral oil were then added to the mixture and the temperature raised to ~ 150°C. Mixing continued for ~ 1 h. The resulting mixture was cooled, granulated and screened. The screened material was crushed into small pieces and then utilised as feed material for injection moulding. The added sintering aids will react with the ceramic material at the sintering temperature to form a sintered product. The excess carbon (~ 1-1.5 % by weight) is beneficial in reducing the amounts of various oxides and other impurities in the starting ceramic material that otherwise would remain in the finished product (145). The excess carbon can be obtained from char or as residue from an organic material such as epoxy and phenol-formaldehyde resins.

Ohnsorg et al (145) found that plasticised polystyrene was particularly useful as a major binder although other thermoplastic materials such as acrylic, ethyl and hydroxypropyl cellulose, high and low density polyethylene, polybutylene, polysolfone, polyethylene glycol and polyethylene oxide could also be used as binders for the injection moulding of silicon carbide.

The injection moulding operation was carried out by a plunger-type moulding machine. The barrel temperature was maintained at

- 150°C and the mould at room temperature. An injection pressure of 6750 psi (~ 46.5 MPa) was applied with a moulding time of 2 s. The moulded parts were claimed to be full and firm upon ejection and were debonded in a nitrogen atmosphere at a rate of 3.75°C/h to a temperature of - 450°C (i.e. a debinding time of - 115 h up to 450°C). Temperature increments were then raised to - 7.5°C/h and heating continued up to - 800°C [i.e. a total debinding time of 162 h (115 h + 47 h)]. The debonded parts were then sintered in an induction furnace under argon at a sintering temperature of 2160°C for - 1 h. They were heated to 1500°C in - 4 h and then to the sintering temperature at a rate of 300°C/h. The sintered parts were found to be substantially free of exaggerated grain structure. A linear shrinkage of 18 % was found. The sintered density was found to be 3.19 g/cm^3 which is - 99 % of theoretical density.

From Ohnsorg's work (145) it is quite clear that silicon carbide parts can be obtained quite successfully by the injection moulding process. The main obvious limitation, however, was the long debinding time of - 162 h (~ 7 days) due to the use of polystyrene as the major binder. Other properties such as moulding, demoulding and sintering were quite satisfactory (as already described above).

Other important properties of silicon carbide and silicon nitride are given in Table 2.4 which were obtained from reference 144. The following properties are usually required (144) from these ceramic materials used for high temperature applications (e.g. in turbocharged engines):

1- High mechanical resistance up to temperatures above 1100°C.

2- High resistance to oxidation and corrosion.

3- Thermal shock resistance.

It is known (144) that silicon carbide can be distinguished not only by its good resistance to oxidation and corrosion, but also by retaining its room temperature strength to over 1400°C. On the other hand silicon nitride has very good strength at room temperature with excellent thermal shock resistance but its

strength decreases above 1000°C which makes it less favourable than silicon carbide.

2.3.3- Injection moulding of tungsten carbide-6 weight % cobalt

This was investigated very comprehensively over a period of three years by Martyn et al (146) at Loughborough University of Technology. Their investigations included the fundamentals of the injection moulding process as applied to hardmetal (i.e. WC-6 wt. % Co) powder. Later in their programme they produced hardmetal components of near full theoretical density by injection moulding process. A relatively high hardmetal volume fraction mixture with suitable rheological properties for injection moulding was developed using a wax-based binder system. Moulding defects due to incorrect binder system and mould design were discussed and remedies for their prevention were outlined. They found that both the dewaxing heating schedule and atmosphere had a critical effect on the integrity of the sintered structure. Shrinkages and tolerances of the components produced were discussed together with a cost analysis of the components produced by both the conventional die compaction and injection moulding routes.
Details of Martyn's (146) work are as follows:

General

Cold or hot isostatic pressing techniques can be used for the production of complex hardmetal components but these processes are very expensive for mass production (146). Die compaction methods are limited to the production of parts with simple shape and low aspect ratios in order to achieve the necessary uniform density distribution (146). The powder injection moulding (PIM) process does not have these limitations and has the potential of producing net-shaped complex components of uniform density distribution through its hydrostatic nature (146). However, this process has just recently been applied to metal and cemented carbide systems (148, 149), and much of the published literature fail to give the fundamentals of the process which has resulted

a general lack of technical understanding of the PIM process applied to metals, cermets and carbide materials (146). The injection moulding of metal powders was pioneered by Wiech (124, 125, 150) using mixtures of conventional thermoplastics and fine powders. Rivers (151) developed a water-based binder system which provides a more rapid (thus more economic) debinding stage. So far there are very few reported operations of the Rivers process compared to those utilising the Wiech process (146). After Wiech there have been other processes developed each offering improved economics for the debinding stage compared to the original Wiech process (146).

Feedstock formulation

Martyn et al (146) also believed that the most immediate area of investigation was in the formulation and mixing of the hardmetal powder-binder mixture so that to develop suitable rheological characteristics for injection moulding and economic debinding process. The hardmetal powder used in their work was a 94 % WC-6 % Co with the ISO K20 classification. A wax-based binder system was used as the major binder which required a less shear energy for mixing and moulding operations and thus reduced the wear problems caused by the abrasive nature of the hardmetal powder. Martyn pointed out that hardmetals have little tolerance for changes in carbon composition, therefore it is essential that any binder chosen should be completely volatilisable without traces of carboneceous residues. Thermogravimetry was used to identify any detrimental carbon or ash forming resins and to establish the volatilisation kinetics of those found to be favourable.

Mixing

Various mixing procedures were investigated as follows:

(i)- Dry ball milling using the wax in a powder form. A milling period of 24 h was used.

(ii)- Solvent mixing by adding the hardmetal powder to a wax-solvent suspension and agitating using a paddle mixer for a period of 6 h.

(iii)- Shear melt mixing using a closed system Torrance hydraulic paste mixer fitted with a trifoil blade. A 3 h mixing period was used.
(iv)- Intensive shear melt mixing of 30 cm^3 batches of feedstock using a Brabender Plastograph torque rheometer.
It was found that effective mixing was only possible by intensive shear melt mixing which was achieved with the Torrance and Brabender mixers. The mixtures from the solvent mixing operation did not show effective agglomerate dispersion due to lack of intensive shear melt mixing (146).

Moulding and rheology

Rheological analysis showed that powder volume fraction, temperature and shear rate influence the melt viscosity of a system. The mixtures were predominantly pseudoplastic in their behaviour and showed dilatancy only at high volume fractions above a critical shear rate. By increasing the melt temperature it became possible to extend the usable shear rate range of the high volume fraction systems. This had the effect of shifting the critical shear rate to a higher value. These results can be seen from the plots of Figs. 2.22 and 2.23 obtained by Martyn et al (146).
According to Martyn moulding parameters having a direct influence on the process temperature had the greatest effect on the mouldability of the feedstocks. It was found that changes in moulding pressure had no significant effect on the mouldability. This can be seen in Fig. 2.24 for two compositions having different hardmetal volume fraction. The mouldability of various feedstock formulations was quantified in terms of melt flow length achievable within a spiral mould. The 018 and 014 compositions in Fig. 2.24 had volume loadings of 65 and 60 % of the hardmetal powder respectively.

Powder characteristics

This is given in Table 2.5 which was given by Martyn for various hardmetal powders. SEM studies showed that the powders were irregular and angular. All the powders had agglomerations with

the exception of powder D being agglomerated to a lesser degree than the rest. This powder was obtained from a different supplier and was processed by a post milling spray drying process which provided finer particles and higher volume loading (due to its fine high surface area) in comparison to the loading levels of the lower surface area, highly agglomerated powder B. Table 2.5 also shows that the apparent ease of mixing (determined by the time and torque required for mixing) decreased with systems of fine particle size and high degree of agglomeration. Powder reference D was therefore chosen for use in the subsequent feedstocks.

Binder investigations

Montanester waxes were found (146) to have preferential volatilisation kinetics to other binders tested. This was due to their wider temperature range over which volatiles were evolved. These results are shown in Fig. 2.25 which was given in Martyn's paper (146). Rheological analysis on wax-based binder mixtures provided optimisation of the hardmetal powder- binder compositions which are also presented in Fig. 2.25. The wax viscosities were found to be essentially of the same order, being near-newtonian at high shear rates, suggesting that they are of equal wetting ability. However, it was found that the paraffin, polyethylene, and to some extent, the microcrystalline paraffin waxes at high powder volume loadings tended to segregate from feedstock compositions under the influence of shear stress (146). Such findings were also reported by other workers (61, 143) for wax-based binder systems. In montanester and carnoba wax-based binder systems no segregation was observed and only dilatant behaviour at moderate shear rates for high volume loadings was observed (146). Martyn believed that surface chemistry was the main reason for a wax's ability in providing a feedstock having a high volume loading of the powder. This was partly shown by the measured dielectric constants of the materials (see Fig. 2.26), in which the polar, hence more surface active waxes, displayed a greater tendency in promoting such feedstocks than those of lower dielectric constants.

Similar observations have been made by other workers while working with ceramic materials (5). The montanester waxes were found to possess both superior dewaxing and rheological characteristics to other waxes investigated and were therefore used in subsequent formulations by Martyn. The majority of waxes were found to be wholly volatilisable in hydrogen and nitrogen atmospheres (146).

Moulding properties

The high volume fraction feedstocks produced mouldings with higher moulded densities (see Table 2.6) than those normally achievable by using die compaction techniques (146). The moulding shrinkages were found to be negligible within the experimental accuracy of the measuring instruments. In extensive studies conducted by exercising close process control it was found (146) that moulded densities were influenced by injection pressure. In general, moulded densities were proportional to the applied pressure. Too high a pressure was undesirable, since under these conditions, there was a tendency for the mouldings to become overpacked which resulted in their rupture during the ejection process. The pressure causing overpacking was dependent on both temperature and mould geometry. The moulded densities also tended to be inconsistent under such conditions, possibly due to wax segregation taking place under the imposition of the extreme pressure applied (146). However, the use of a low pressure and temperature produced mouldings free of defects and of lower but more consistent moulded densities.

Moulding defects such as density gradients (common in feedstocks of high wax content), remained visually obscure in the green (as-moulded) state but often became obvious as fine cracks on the sectioned surfaces of dewaxed mouldings. Martyn believed that the cracks followed the differential density boundaries which existed within the moulded test bars of 0.5 hardmetal volume fraction.

Martyn reported a more serious problem when single crystalline wax systems were used as major binders, particularly for moulding of high powder volume fractions (e.g. 016 in Table

2.6). Often cracks were visible in sectioned mouldings produced by using the montanester wax (MEW) as a single binder. The observed cracks were mainly in the core regions of the mouldings. This type of defect was thought (146) to arise from a combination of characteristics peculiar to formulation, in particular: (i)- The viscosity of the feedstock, e.g. 016 in Table 2.6, was extremely sensitive to changes in temperature, to the extreme that very little flow resulted in the mould. Thus, short test bars could only be formed within the limits of runner and gate geometries used. It was believed that the material, once ejected, froze almost instantaneously on contact with the cold mould wall causing solidification at the gate region thereby preventing furthur material to enter the moulding core to consolidate any solidification shrinkage.

(ii)- The wax in that composition had pronounced crystalline characteristics and therefore underwent significant volumetric changes due to phase transitions on cooling which can be seen from Fig. 2.27.

Martyn overcame this problem of crystalline shrinkage cracking by using a wax blend and a reduced hardmetal volume fraction, e.g. 018 in Table 2.6. The solidification characteristics of the wax blend can be seen from Fig. 2.27. The 018 composition was found to produce sound, defect-free mouldings. The solidification curves in Fig. 2.27 showed two facts: firstly, the wax blend underwent less crystalline shrinkage than the single MEW and therefore less solidification was required, and secondly, the melting point of the wax blend was obscure extending the temperature over which plastic flow occured. Both factors contributed towards the effective consolidation of moulding cores. Subsequent moulding and dewaxing trials were then conducted using the wax blend with a 0.65 volume fraction of the hardmetal powder.

Moulding defects due to poor design of the cavity feed system were also observed by Martyn. He observed that gate designs promoting a jetting flow regime, ultimately lead to weld lines within the core of the mouldings which converted to cracks during the sintering process. It was therefore found that the

correct design of the mould gate geometry provided a plug flow without any weld lines and the moulded parts were also free from density gradients.

Dewaxing and sintering processes

Martyn's mouldings with powder volume fractions > 0.4 required packing in alumina powder in order to prevent slumping during the early stages of the dewaxing process. The low density polyethylene and reduced wax mouldings were found to be self supporting. The fine alumina powder also helped the dewaxing process by providing a capillary action mechanism (wicking). Attempts for solvent extraction of the wax systems by immersion and gaseous state techniques using various solvents, were not successful. The mouldings were found to disintegrate on prolonged exposure to the various solvents used (146).

Proper dewaxing was therefore carried out by thermal degradation of the wax binder systems. It was found that the dewaxing atmosphere had a critical effect on the sintered microstructure. Inert gases, such as argon, nitrogen, helium and certain mixed hydrogen/nitrogen atmospheres produced gross carbon defects, whereas reducing gases produced sound clean microstructures. However, some residual macro-porosity persisted within the mouldings, which believed to be due to entrapped air within the injected feedstock. The sintered densities were > 99 % of theoretical. Sintered shrinkages were dependent on moulding geometry and injection pressure, but were found to be consistent within each moulded batch. The shrinkage values were typically 14 % linearly, but were not isotropic, possibly due to streamline flow effects, i.e. the anisotropic alignment of the unequiaxed powder particles in the streamline of the melt flow with the major axis preferentially aligning in the flow direction (146).

The sintering conditions were not provided in his paper, but this is given in the results chapter (see chapter four, section 4.7.2).

Cost analysis

The PIM technique requires finer and therefore more expensive powders than the more traditional die compaction technique which uses relatively coarse low cost powders (146). It is therefore very true that a shift towards a finer powder results in a higher powder cost, but it is also very well known that fine powders provide easier mixing and moulding with dewaxing/debinding becoming more difficult (58). The increased reactivity of finer powders is also very useful for sintering but becomes a serious problem where oxygen pick-up is detrimental to product quality. On the other hand a shift towards larger particles results in mixing and moulding difficulties and severe effects on processing equipments, but facilitates the dewaxing process and reduces the powder costs, thereby rendering the PIM technique more competitive with the die compaction technique (58). Fig. 2.28 shows a particle size distribution curve which also summarises the above cost analysis (58).

According to Martyn et al (146) for hardmetals there is no additional premium on the cost of the raw powder as the powder is conventionally already in a fine form, and as the system undergoes liquid phase sintering, densification is no problem providing sufficient volume loading of the powder is used. These advantages, together with high machining costs currently accepted in the production of complex hardmetal components from presintered blocks, justify proposing the PIM process as a competing process to the die compaction methods currently used within that industry (146). Martyn also conducted a tentative costing exercise based on approximate information supplied by the industry and used a costings model proposed by Barrie (153). He concluded that the PIM process can be a competitive alternative to conventional die compaction methods particularly when small relatively slim intricate shaped components are required.

2.3.4- Injection moulding of Ni steel, 316 stainless steel and superalloy by the Rivers process

Rivers process

This process uses a water-soluble binder, i.e. methylcellulose, as the major binder that burns off very rapidly and therefore overcomes the long debinding period of the usual thermoplastic/wax-based (Wiech) binder systems. With the moulded methylcellulose components the binder removal step may not be necessary provided that the moulded parts have been previously oven dried. Another advantage of the Rivers binder system is that there is no limitation on section thickness for the debinding process whereas with the Wiech process this limitation exists and debinding of thick mouldings (> 5 mm thick) is not economical due to the long debinding times (154).

The steps in the Rivers process can be illustrated as follows: Dry blending of the metal or alloy powders with methylcellulose is performed using a simple V-blender. This is followed by a mixing step, during which the water, and additives glycerin and boric acid, are introduced. The use of a sigma mixer to knead these ingredients results in a putty-like compound (154).

During moulding advantage is taken of the fact that methylcellulose is less soluble in hot water than is in cold. The compound prepared in the sigma mixer is fed into the injection cylinder of the moulding machine,and injected, at room temperature. The mould, on the other hand, is held at a higher temperature, so that the injected material partially solidifies by thermal gelation. After ejection from the mould, the parts are oven dried (154).

During the drying stage, the water solvent evaporates, leaving appreciable interconnected porosity, through which the gaseous decomposition products of the organic binder escape, upon subsequent heating.

The sintering atmosphere and temperature cycle are dependent upon the material in question, the size and shape of the starting powder particles, and the required density.

Materials

The Rivers injection moulding (RIM) process has been used with a variety of materials. These range from simple metals, such as iron, copper and nickel, through the various steels (alloy, stainless and tool), to the specialty nickel and cobalt based (super) alloys, designed to resist oxidation, corrosion and wear.

Moulding conditions

Rivers (151) injection moulded a - 325 mesh (< 44 μm) atomised superalloy powder of composition (in weight %): 27-31 Cr + 3.5-5.5 W + 0.9-1.4 C + 3 Ni + 1.5 Si + 3 Fe + 1 Mn + 1.5 Mo + balance Co using a moulding composition (in weight %): 1.5-3.5 % methylcellulose + 0.25-2 % glycerin + 0.1-1 % boric acid + 4-6 % water. The metal powder-binder mixture was then injected (at room temperature) at an injection pressure of ~ 62 MPa into a mould heated to ~ 88°C. The moulded part was dried for a few hours at ~ 105-121°C which then exhibited a transverse rupture strength of ~ 16.5 MPa.

Properties obtained by Rivers process and conventional die compaction process

These are given in Table 2.7. Column A is the average value of three lots of the alloy of - 325 mesh atomised powder conventionally pressed with 3 % polyvinyl alcohol binder and sintered. Column B is an identical powder injection moulded by the Rivers process as described earlier. Rivers (151) moulded a bar 0.75 inch square and 10 inches long with a single injection port located at the centre of the bar. No non-uniformity in sintering shrinkages was experienced, and no blistering or cracking was observed (151).

Injection moulding of Ni steel and 316 stainless steel using the Rivers process

This was carried out by Crook et al (154). The starting powders were the Ni steel (Fe-8Ni-0.5C) prepared from fine carbonyl iron and carbonyl nickel (FN-0705) powders of 5 microns average

particle size, and the 316 stainless steel (Fe-17Cr-12Ni-2.5Mo) prepared from gas atomised powders of a size < 15 microns. These powders were injection moulded using the Rivers binder system with the same moulding and drying conditions (154). The sintering and heat treatment conditions associated with the production of FN-0705 (Ni steel) samples are given in Table 2.8, together with the measured densities, hardness and tensile properties.

The sintering conditions for the 316 stainless steel together with the associated densities are given in Table 2.9.

It was concluded (154) that the use of Rivers process overcame the long debinding time and also the associated problem of thick sections of the Wiech process. It was also found that carbon strongly influences the properties of 316 stainless steel by encouraging the growth of grain boundary carbides. For industrial applications, the carbon level should be controlled to a maximum of 0.03 % by weight in 316 stainless steel. Such control was possible with the Rivers process (154).

2.4- Injection moulding of alumina ceramics

2.4.1- Organic binder systems used for the injection moulding of alumina ceramics

These are given in order of their appearance as follows:

(1)- Howatt, G.N. (US Army), 1945 (155):
Alumina + ethyl cellulose, polystyrene or wax + pine oil or solvent resin.

(2)- Ehlers, R.W. (General Motors Corp.), 1948 (156):
84 finely pulverised ceramic material + 5.8 ethyl cellulose + 5.8 shellac + 4.4 % n-butyl stearate.

(3)- Rogers, E.J. and Mooney, E.L., 1954 (157):
3 parts of a mixture of 88 alumina + 10 tricalcium penta-aluminate and 2 % silica + 0.52 part of polystyrene + 0.11 part of hydrogenated peanut oil + 0.27 part of more volatile oil (volatilising between 51-150°C).

(4)- Moteki Asao, 1960 (158), used the following mix which provided a good mouldability:
alumina powder + 14-16 % polystyrene + 2-4 % stearic acid + 0-2 % diethyl phthalate.

(5)- Ceramic age, 1962 (159):
high purity alumina + normal fluxes + polystyrene resin + a volatile oil + hydrogenated oil.

(6)- Strivens, M.A., 1963 (5, 160):

Material	Function	% by volume
Steatite (ceramic powder)	Filler	63
Epoxy resin	Binder	7.3
Coumarone-indene resin	Diluent	3.2
Phenolformaldehyde resin	Hardner	2.2
Wax	Plasticiser & lubricant	24.3

The above powder-binder mixture was used for the production of ceramic insulating materials by the injection moulding process.

(7)- Burroughs, 1966 (161), Moulding composition for refractory aerospace structural components:

Material	Function	% by wt.
Alumina-electronic grade with -200+300 mesh particles calcined above 900°F (~480°C) prior to mixing	Filler	70-99
Siloxane resin	Organic binder	1-30
PbO	Catalyst to aid curing of the resin	small %
Calcium stearate	Mould release agent	small %

(8)- Herrmann, E.R., 1966 (162), Method of moulding ceramic articles:

Material	Function
Either silica glass, alumina, beryllia, magnesia or mullite	Ceramic fillers
Either naphthalene, paradechloro benzene or camphour	Organic binders
with gum, shellac or silicone resin	Thermosetting binders (to improve the reduction of the binder removal time)

plus a colloidal ceramic, such as alumina or silica, with a particle size of < 0.1 μm to inhibit dilatancy.

The above powder-binder mixture provided an excellent combination of good plastic flow properties for injection

moulding, rapid removal of the organic binders within 12 h or less without distortion, shrinkage or excessive porosity, and also easy burn-out of the thermosetting resin without forming a shell-like layer on the ceramic. The principal application being precision cores for metal castings.

(9)- Newfield et al, 1978 (163):

Material	Volume %	Weight %
Alcoa A-15 Al_2O_3 (calcined, low Na_2O, high purity alumina consisting of 95 % 325 mesh particles)	68.7	87.6
GEM 129 Novaculite SiO_2 (the 129 grade is 99.9 % pure with < 325 mesh particles)	5	3.7
Silicone oil	2.4	0.8
Epon 815 epoxy resin	8.8	3.1
Carnoba wax	15.2	4.8

The carnoba wax, silicone oil and epoxy resin compose the binder-lubricant portion of the body and were combined at 110°C to form a metastable fluid. The silica powder was used as the sintering aid. The ceramic powders (alumina and silica) were added to the organic binder-lubricant and the mass was mixed thoroughly at 110°C.

The above composite mixture becomes plastic when heated above 100°C and will flow under pressure and therefore can be moulded easily (163). The cooled moulded composite has enough strength which allows removal from the mould cavity without fracture. However, due to the brittleness problem, this moulding mixture was most useful for the production of fairly small parts (. 16 cm^3 in volume).

To mould the above mixture it required a reciprocating screw thermoplastic moulding machine because the compound tended to cake in a ram machine. The optimum moulding conditions were as follows:

	Mould	Barrel	Nozzle	Injection
Temp., °C	66	100	125	
Pressure, MPa	—	——	——	4.8
Time, s	40			

The results of the moulding experiment showed that the above mixture had excellent mouldability and firing characteristics. Moulding shrinkage was 0.25 % and firing shrinkage as low as 5 % for 1600°C fired bodies (163).

(10)- Farrow and Conciatori (164) have successfully injection moulded alumina using polyacetal binders. In addition to the ceramic powder and the major binding agent, the mixture may furthur contain small amounts of known materials (- 1-10 %) such as low density polyethylene, atactic polypropylene, ethylene vinyl acetate and waxes (e.g. stearic acid and paraffin wax) which help the binding function (164).
The above binder system provided an easy and defect free burn-out.

(11)- Saito et al (165, 166) have successfully injection moulded several alumina ceramics using atactic polypropylene (APP). They found that it was possible to adjust the thermal decomposition rate (i.e. to broaden the thermal decomposition region) by mixing different fractions of APP having molecular weights of 10000-60000 so that to have an easy and defect free burn-out. It was also reported that an even more effective injection moulding formulation was possible by adding other thermoplastic resins such as high or low density polyethylene, ethylene vinyl acetate, polystyrene or polymethylmethacrylate. Plasticisers, e.g. diethyl, dibutyl, dioctyl and diallyl phthalates, and lubricants, e.g. stearic acid, paraffin wax or ester wax, were

also added. It was pointed out that the use of APP as the major binder is very economical since it is one of the lowest cost polymers on the market and is the amorphous waste product from isotactic polypropylene.

(12)- A mixture of a water-soluble polymer such as polyvinyl alcohol, methylcellulose or gelatin plus an organic substance such as wax, stearic acid or liquid paraffin was used (167) for the injection moulding of alumina (and magnesia) ceramic powders. High quality articles were produced by such binder formulations.

2.4.2- Characteristics and trends of the organic binder systems used for the injection moulding of alumina ceramics

Polystyrene binder system

From the chronological list of organic binder systems given in the previous section it can be seen that the polystyrene binder was used so often as the major binding agent for the injection moulding of alumina ceramics in the 40's, 50's and 60's. The use of polystyrene was believed to be unique, since it provided the free flow of the ceramic mix at normal operating temperatures, mixed evenly, was removable from mould without sticking and was capable of escaping from the moulded part without rupturing it (159). However, this binder could not be used alone in this technique, and best results were obtained when other organic materials with successively higher boiling points were added to the mix. Examples of these materials were light oils (such as animal, vegetable and mineral oil), hydrogenated vegetable oil (such as peanut oil) and synthetic oil (such as a wax). A volatile light oil vaporises at relatively low temperatures (50-170°C) therefore opening up the ceramic part by forming very small pores extended through to the centre of the material. The synthetic oil or wax vaporises next (150-240°C) and escapes through these pores. Finally polystyrene and its decomposition products pass through the existing pores. Polystyrene starts burning at a temperature - 240°C. Debinding times of 100 h or

more (depending upon the thickness of the part) have been reported (159) at very slow heating rates (< 5°C/h for a 6 mm thickness). The final sintered parts have had the standard physical, chemical and electrical properties.

It was therefore realised that a major key to the success of this technique was the opening up of the moulded ceramic part with oils and waxes volatilising in sequence and because of evenly spaced pores throughout the ceramic part, all the polystyrene was removed without deforming, spalling or blistering of the debonded part. The polystyrene resin acted as the major binder and internal lubricant while wax or hydrogenated oil assisted the moulding process as mould and internal lubricants and pore openers and the light oil also acted as a pore opener for the shape (159).

The polystyrene binder system was used for the injection moulding of complex high-alumina ceramic parts used for the electronic and mechanical engineering applications (159).

Silicone resin binder system

By mid 60's as the development of ceramic injection moulding continued, there were new binder systems available for the injection moulding of alumina ceramics. An interesting development was the use of silicone oil as the major binder in the binder mixture. The silicone resin was not fully removed prior to sintering but was converted to silica producing a silicated ceramic body. The use of such binder systems were limited to alumina or other ceramics where the silica content could be tolerated. One practical application was reported by Burroughs and Thornton (161) for the production of refractory aerospace structural alumina components. It was reported that the silicone resin was compatible with the alumina ceramic powder, provided sufficient plasticity for flow during the moulding cycle, was resistant to low and high temperatures, showed inertness and had no unusual surface properties, had good release and antistick properties and provided a low temperature-low pressure (165°C-3000 psi) moulding process. The silicone resin was converted to silica during a presintering process

which involved heating to 510°C over an extended time period to ensure removal of all volatiles prior to conversion to silica. The decomposition rate of the silicone resin was related to the size and thickness of the moulded component. The ideal sintering temperature for a low porosity high strength characteristics was at 1370°C for - 1 to 2 h and then cooling slowly in the furnace to room temperature. It was also suggested that the alumina-silicone binder mixture may be compression or transfer moulded and retain dimensional stability through firing to final part with exceptionally close tolerances (161). The flexural strength of a sintered alumina part with - 9 % porosity was found to be around 17000 psi (~ 120 MPa) at room temperature. Flexural strengths of alumina parts formed by various processes fall into definite categories. A porous 99.5 % alumine body with - 7.5 % porosity has a flexural strength varying between 10000-22000 psi (~ 70-155 MPa). The flexural strength of the low pressure-low temperature formed alumina falls into this category (161). Among refractory oxides, sintered alumina has the highest fracture strength (161).

Thermosetting binder systems

Epoxy resin was one of the early thermosetting binders used for the injection moulding of alumina ceramics (160), but it could not be used alone and was usually mixed with a thermoplastic and a plasticiser so that to obtain the main requirements of the moulding formulations (i.e. low viscosity in the softened state, low addition to metal parts and suitable removal properties). Among the known thermosetting resins there are none which could satisfy all the moulding requirements simultaneously (160). It is therefore necessary to dilute the thermosetting resin with a thermoplastic resin so that the concentration of polymerisable nuclei may be controlled and the flow properties made less sensitive to changes in the degree of polymerisation in its early stages. In addition, by using a thermoplastic resin of lower softening range than that of the thermosetting resin, the working range of temperature for mixing and moulding may be increased and the distillation characteristics improved (160).

It is also necessary to use a plasticiser so that a sufficiently low viscosity in the softened state and a low adhesion to metal parts are obtained. The plasticiser can be a wax or oil or mixture thereof, which acts as a blending agent for the two resins, reduces the viscosity by virtue of its low melting point, gives good release properties from metal surfaces and improves the distillation characteristics.

Examples of epoxide thermosetting resins are: araldite, epikote types 1001 and 1004 resins which may be used alternatively with other types of resins that cause alloying or cross-linking, e.g. the epikote resins may be alloyed with thermoplastic phenolic resins of the Novolac type; thermosetting phenolic resin of the Resol type may be used as the hardenable component of the binder (160).

Examples of thermoplastic non-reacting types of resins are coumarone-indene resins, e.g. epok resin C640 (softening point 85-100°C) which may be used as modifiers to control the rate of hardening of the hardenable component of the binder, coumarone-styrene resin (melting point 110°C) and naphthalene-formaldehyde resins marketed under the Trade name of claromene resin (melting point 80-120°C).

Examples of waxes are, e.g. beeswax or any wax of similar composition to beeswax may be used, e.g. wax 365 which is a synthetic substitute for beeswax (160).

Butyl stearate or glyceryl monostearate are also added to the mixture which act like a wax or oil.

Mixing of the binder components with the alumina powder is carried out at 120-130°C for . 15 to 20 min to form a satisfactory mixture.

According to the author (160) the following compositions can be moulded and taken through to the final firing stage without distortion or spoilage of the moulded part:

	Material	% by weight
(1)-	Milled alumina	85-86
	Epok resin C640	5-7
	Araldite resin type I	3.3-4
	Wax 365	3-4
	Butyl stearate	1.3-2
(2)-	Milled alumina	85-86
	Epikote resin type 1004	5-7
	Bakelite resin R.5363	2
	Epok resin C640	2
	Wax 365	3
	Butyl stearate	1.5-2
(3)-	Milled alumina	85-86
	Epikote resin type 1001	6
	Bakelite resin R.5468	1.5
	Epok resin C640	2.9
	Wax 365	4.6

(4)- As in (1) but with the wax 365 and butyl stearate replaced by an equivalent weight of glyceryl monostearate.

(5)- As in (4) but with the araldite resin replaced by bakelite resin R.5368.

Curing

The moulded parts are heated to cure the thermosetting constituent of the moulding compound. The parts may be placed in an oven at the moulding temperature (- 140°C) and the temperature raised at - 15°C/h to a peak curing temperature (≤ 220°C) and held there for a period sufficient to cure its thermosetting constituent (160). In general it is preferred to embed the parts in fused alumina powder. This ensures that all surfaces are adequately supported whatever the shape. There is a small loss of volatile matter during curing and embedding ensures a uniform loss per unit area over all surfaces (160).

Low pressure distillation or solvent extraction

The greater part of the binding media is removed from the moulded parts by low pressure distillation or by solvent extraction; both of these processes being examples of chemical separation by fractionation, which is based on differential properties of the components being separated, e.g. vapour pressure for distillation, solubility for solvent extraction. It is preferred to remove ~ 90-95 % and recover the maximum material for re-use. The remaining fraction consists of a carbonaceous residue which is burnt-off in the early part of the final firing.

For low pressure distillation, the parts may be embedded in granular alumina and then placed in a vacuum chamber provided with internal heaters and thermocouples. The chamber is pumped down to ~ 2-5 mm Hg and the temperature increased gradually depending on the shape and section of the moulded parts. The total distillation time has been 8 h for small parts and as long as 20 h for larger parts. The critical temperature range is between 200 to 250°C, since in this range both the araldite type and the bakelite type of resin tend to foam and the overall rate of distillation is high. A temperature rise of ~ 10°C/h is considered to be safe in this range, provided excessive temperature gradients are not allowed to develop in the moulding (160).

In the solvent extraction process, the formed parts are subjected, with or without prior heat treatment, to exraction by means of a suitable solvent or solvent vapour to remove the major part of the binding medium and finally fired by the usual ceramic or powder metallurgical methods.

At least two components must be used as the binding agents, and one of them being insoluble or only slightly soluble in the extraction solvent at the time of extraction, and the remainder being soluble. Organic binding media as described in the previous examples (examples 1-5) may be used.

Suitable solvents are: acetone, amyl acetone, methyl ethyl

ketone, carbon tetrachloride and trichloroethylene.
However, the components of the binding agent may consist of only thermoplastic binders and plasticisers and therefore excluding the thermosetting binders which require a heat-hardening step in the process.
Suitable thermoplastic binders are: epok C.460 which is a coumarone-indene type of thermoplastic resin and claromene resin (melting point 80-120°C) which is a naphthalene-formaldehyde thermoplastic resin (168).
The plasticiser comprises one or more waxes or wax-like substances and should be soluble or dispersible in the solvent liquid or its vapour, and the thermoplastic binder should be insoluble or non-dispersible therein, or partially soluble or partially dispersible therein, or should dissolve or disperse therein at a much slower rate than does the plasticiser, so that all or a major part of the binder remains after the plasticiser has been extracted. The extraction time must be closely related to the solubility properties of the binder being used, and to the degree of extraction required of the plasticiser (168).
Suitable solvent liquids are: n-butyl chloride, petroleom ethers, acetone, amyl acetate, methyl ethyl ketone, carbon tetrachloride, trichloroethylene and industrial methylated spirits (168).
The extraction may be carried out by placing the parts in a cage and immersing them in the boiling solvent, or running hot solvent or solvent vapour over the parts stacked in a suitable container. After extraction the parts may be simply air dried or oven dried for a short period (- 15 min) to remove residual solvent before firing (168).
It is believed that the relatively insoluble part of the binding vehicle is strong enough to give the parts adequate coherence and mechanical strength to prevent deformation cracks and blistering in processing etc. or breakage due to handling.

The advantages of the solvent extraction process over the low pressure distillation process may be summarised as follows (168):

(i)- The removal of the binding media is faster and requires less expensive and more easily maintained plant.

(ii)- The major part of the binding vehicle is recovered and can be re-used.

(iii)- Defects in treated parts are easily detected, facilitating rejections before they enter the firing stage.

(vi)- After vacuum distillation, the parts are too friable for satisfactory machining, whereas after solvent extraction, the parts are still workable and there is less tendency to clogging of the tools. However, machining can be carried out prior to vacuum distillation but after the hardening of the thermosets and this tends to clog the tools.

(v)- After solvent extraction, the parts have relatively higher mechanical strength and therefore can be handled more easily.

The following examples were moulded using thermoplastic binders and plasticisers and then the binders were removed satisfactorily by solvent extraction (168):

	Material	% by weight
(1)-	Steatite (calcined and ground ceramic powder based primarily on a high purity talc with minor addition of fluxes)	83.7
	Epok resin C460	7.1
	Wax 360 or 365	9.2
(2)-	Steatite	83.4
	Claromene resin (M.Pt. 80-120°C)	7.5
	Wax 360 or 365	9.1

The moulded parts were extracted with industrial methylated spirits in a soxhelt extractor, the percentage extract reaching

a maximum value corresponding with the wax content in period of 8-12 h. This extraction time was for the parts weighing ~ 3.5 gram in example 1. The extraction time was 12 h for parts in the form of discs ~ 25 mm diameter and ~ 3 mm thickness in example 2. The extracted parts were satisfactorily fired in each case.

Firing

The firing (or sintering) schedule for the high purity alumina parts may be as follows (168):

After an initial burning off period of ~ 1 h at a temperature between 400 and 600°C, the temperature may be raised to 1200°C in ~ 2 h. From 1200°C to the peak 1750-1800°C, the heating rate should not exceed 200°C/h as all the shrinkage takes place in this range. The peak temperature is maintained for ~ 1 h and the furnace may then be allowed to cool overnight or may be force cooled in a few hours.

The above ceramic process has been applied to a number of other ceramic bodies such as high alumina fluxed body, soft porcelain body, rutile body, kaoline, flint, alkaline earths and wollastonite body as well as the high purity alumina powder (168).

Polyacetal binder system

This was invented by Farrow and Conciatori (164) for the injection moulding of alumina and other ceramic materials such as zirconia, silica, silicon nitride, silicon carbide, silicon, ferrite and mixtures thereof. According to the inventors this binder system has the following properties (164):

(i)- It provides an easy and defect-free burn-out. This is because polyacetals depolymerise through unzipping of the polymer chain and therefore heating causes a uniform evolution of volatiles which remove the polyacetal binding agent without causing disruptions in the structure that might otherwise lead to defects or weak spots in the moulded article. Additionally, the volatile material is a clean-burning fuel that does not leave any undesirable or difficult-to-remove residue.

Furthurmore, the volatiles resulting from the depolymerisation of the polyacetal are generally not toxic and can be released with little or no treatment.

(ii)- The polyacetal binding agent may also comprise small amounts (1-10 %) of other binding materials such as low density polyethylene, atactic polypropylene, ethylene vinyl acetate and waxes (e.g. stearic acid and paraffin wax) which serve an additional binding function.

(iii)- In addition to the ceramic powder, the major polyacetal binding agent and the minor binding agents, the ceramic-binder mixture may furthur contain conventional amounts of wetting agents (0.5-2 % by weight), plasticisers (1-10 % by weight) and other types of processing aids which are added to the composition to obtain a suitable rheological system for moulding.

Suitable wetting agents or surfactants include lignite, mineral oil and low molecular weight waxes which promote addition between the ceramic powder and the binding agent, thereby reducing the degree of agglomeration.

Typical plasticisers include waxes, silicones, alkyl phthalates, polyalkylene (e.g. polyethylene) glycoles and linear saturated polyesters which decrease the viscosity of the mixture to promote mixing.

Mould release agents (0.05-1 % by weight) prevent addition to the mould wall thereby facilitating removal of the shaped article from the mould. Typical mould release agents include silicones and various phthalates and amides such as Acrawax C (a fatty acid amide).

The amount of the polyacetal binder in the ceramic-binder composition can be from 20 to 30 % by weight of the total mixture. This binding agent also serves to maintain the integrity of the shaped article prior to sintering (164).

The polyacetal binding agent employed is available under the Registered Trade Mark 'Celcon'.

Mixing

Mixing of the alumina ceramic powder (1 micron average diameter), the polyacetal binding agent and any additives was performed with a two σ-blade hot mixer rotated at 40 rpm at a temperature of 200°C for ~ 30 min. The ceramic powder was added in the mixer after melting and mixing of the binding agents. The polyacetal binder had a melting point of ~ 165°C and thus mixing at 200°C should provide a homogeneous mixture.

According to the authors (164) the resulting mixture should have a viscosity < 100 Pas at a shear rate of 1000 s^{-1} at a temperature of 100-300°C.

Injection moulding

The mixture composition is preferably extruded and then chopped into pieces (1-7 mm) which is then fed into a hooper feeder of a conventional injection moulding machine. The extrusion may be performed with a twin-screw extruder operating at a die temperature in the range 190-220°C and a pressure in the range 3000-14000 KPa. The chopped composition may then be heated to a temperature 175-200°C and injected at a pressure 3500-7000 KPa into a relatively cold mould (20-70°C) where the composition hardens. Pressure is maintained on the composition until hardening is achieved. Typically, this requires 20-60 s (164).

Debinding (binder removal)

The moulded article is gradually heated with a heating rate depending on the amount and type of components in the composition and the shape and size of the article. A typical rate of heating will range from 5 to 20°C/h until a temperature range 20-300°C is reached. The selected temperature may then be maintained for 0.5-2 h.

Sintering

The sintering cycle for the high purity alumina involves heating the debonded article to 1800°C at a rate of 200°C/h and to achieve a full sintering the article is maintained at 1800°C for

- 0.5-2 h. Sintering is usually carried out in air and the sintered article will have a volumetric reduction (shrinkage) of - 15 % (164).

The following example was provided by the above inventors (164): 20 g of polyacetal (composed of 50 parts of trioxane and 50 parts of dioxolane having a melting point of 140-150°C) was charged into a mixer at - 200°C. Sigma blades of the mixer were rotated at 40 rpm while 75-85 g of alumina powder (1 micron average diameter) was added. After - 15 min the mixture was removed from the mixer and was extruded under pressure at - 200°C. The shaped article was placed in a furnace and heated to 300°C in - 30 min, which removed most of the binder. Upon sintering at 1800°C, an acceptable sintered article was obtained (164).

Atactic polypropylene binder system

This has been one of the most successful binder systems during the last 10 years invented by Saito et al (165) and used widely in Japan and USA for the injection moulding of ceramic components such as alumina, porcelain, silica, piezoelectric, titania and zirconia.

The inventors discovered that atactic polypropylene (APP) rendered the mix sufficiently fluid (even when added in a smaller amount than the prior art binder systems) for injection moulding and that allowed the thermal decomposition rate to be freely adjusted by mixing different fractions of APP having molecular weights in the range 5000-120000. In other words it was possible to broaden the critical decomposition region by mixing different fractions of APP having different molecular weights and this was very useful for an easy and defect-free burn-out. According to the inventors an even more effective injection moulding composition was possible by adding other thermoplastic binders such as ethylene vinyl acetate (EVA) copolymer, polystyrene, polymethacrylate and polyolefins such as polyethylene and polypropylene (excluding the atactic type). Plasticisers and lubricants were also added. The plasticisers

included diethyl, dibutyl, dioctyl or diallyl phthalate. The lubricants included stearic acid, paraffin wax and ester wax. It was found that these plasticisers and lubricants had good solubility in the APP binder and therefore addition of any said plasticisers and lubricants increased the fluidity of the injection moulding composition and decreased the requirement of a binder by that extent. It was also shown that all the said plasticisers and lubricants commenced decomposition and evaporation at a lower temperature than the APP binder and therefore addition of any of these additives enables the heating weight loss (decomposition rate) of the moulding composition to be easily controlled.

It was shown (165) that APP has a far higher wettability (or contact angle) to an alumina substrate than other binders such as low and medium density polyethylene, EVA copolymer (containing 30 % vinyl acetate) and polystyrene. This, therefore, proved that the APP fully acts as a binder for raw material of ceramics in a smaller amount and at a lower temperature than other binders which can be seen clearly from Fig. 2.29. The curves A, B, C, D, E, F and G respectively represent APP having a molecular weight of 10000-20000, APP having an average molecular weight of 60000, low density polyethylene, EVA copolymer (with 30 % vinyl acetate), medium density polyethylene and polystyrene.

Ceramic-binder composition

The authors stated that a proper amount of binder is essential in order to obtain a good moulded article free from defects, and this was given as follows:

8-30 parts by weight of APP + 3-15 parts by weight of a thermoplastic binder + 5 parts by weight of a plasticiser or lubricant and 10 parts by weight at maximum when both types of additives are used + 100 parts by weight of raw ceramic material.

Debinding (binder removal)

It was suggested that for the removal of the organic binders, the moulded part should be heated up from room temperature to a level ranging from 100-140°C in . 2 h and then heating the part to 340-380°C in increments of 3-10°C/h. The debonded part is finally sintered to provide a ceramic product.

The following examples were provided by the inventors (165) so that their findings are more fully understood:

Example 1

An injection moulding composition H was prepared according to this invention by adding a mixture of 10 parts by weight of APP having a density of 0.9 g/cm^3 and an average M. wt. of 60000 and 3.8 parts by weight of APP having a density of 0.86 g/cm^3 and a M. wt. of 10000-20000 to 100 parts by weight of raw alumina powder (60 % of which being . 5 microns in diameter) for porcelain containing 84.6 % Al_2O_3 + 3.6 % $CaCO_3$ + 9.1 % gairome clay (a kind of kaoline) + 2.7 % Cr_2O_3 , having a density of 3.7 g/cm^3.

A prior art injection moulding composition I was prepared by adding a mixture of 15 parts (all by weight) of polystyrene having a density of 1.04 g/cm^3, 4.9 parts of stearic acid having a density of 0.847 g/cm^3 and 2.4 parts of diethyl phthalate (DEP) having a density of 1.121 g/cm^3 to 100 parts of alumina powder having the same composition as described above.

A spiral flow test was made of both compositions H and I by injecting them into a spiral flow mould at temperatures of 140, 160 and 180°C under various pressures at 30, 40 and 60 Kg/cm^2 to determine the spiral flow lengths of each composition. Throughout the test a 1/2 ounce injection moulder was used with the mould temperature set at 15-20°C and the nozzle inner diameter set at 2.5 mm.

The results of the test are shown in Fig. 2.30. Referring to this Figure, the characters H and I represent compositions H and I of this invention. The numbers 1, 2 and 3 suffixed to said characters denote the injection moulding temperatures of 140,

160 and 180°C. As apparent from this Figure, the prior art composition I showed a much shorter spiral flow length than composition H of this invention, though containing a larger amount of organic substances and suggesting therefore that the prior art composition I has a lower thermal fluidity than composition H of this invention.

Example 2

An injection moulding composition was prepared by adding a mixture of 10.2 parts (all by weight) of APP having a M. wt. of 10000-20000 to 100 parts of raw material of ceramics containing 93 % alumina, 5 % talc, 2 % clay, having a density of 3.8 g/cm^3. The mixture was then crushed into smaller sizes of - 3 mm long after kneaded at 170-180°C.

The resulting mixture was injection moulded into a flat plate 3 mm thick, 25 mm wide and 100 mm long with the moulding temperature set at 140-180°C and the injection pressure at 800-1200 Kg/cm^2. The flat moulded plate was heated from 70 to 350°C in increments of 3-4°C/h for the decomposition and evaporation of the organic binders contained therein. The debonded plate was finally sintered at 1600°C to provide an alumina porcelain ceramic. The porcelain ceramic was determined to have a density of 3.6 g/cm^3 which was very similar to a porcelain plate press moulded from the same composition as described above.

The same result was obtained when the above injection moulding composition was furthur mixed with 2 parts (all by weight) of stearic acid as a lubricant and 1 part of diethyl phthalate as a plasticiser (165).

Composite binder system

A composite organic binder system, comprising an incompatible mixture of a water-soluble polymer and a sparingly water-soluble organic substance dispersed in emulsion form, has been used in powder moulding processes (167). It is claimed that such formulations gave rise to high quality powder moulded articles.

The ceramic powders used were alumina or magnesia. The water-soluble polymer was polyvinyl alcohol, methylcellulose or gelatin and the sparingly water-soluble organic substance was wax, stearic acid or liquid paraffin.

The effective amount of the mixture of a water-soluble polymer and a sparingly water-soluble organic substance was in the range 0.2-20 % by weight based on the weight of the inorganic powder. For a homogeneous moulded body and the ease of handling in moulding operation, it is most preferable to keep the amount of addition within the range 0.5-10 % by weight based on the inorganic powder. The proportion of the sparingly water-soluble organic substance should be 5 % or more, preferably 10 % or more, most preferably 20 % by weight or more. The proportion of the water-soluble polymer should be at least 10 %, preferably 20 % by weight or more.

The mixing of the powder with the composite organic binder is carried out by rotating blades, ball milling, ultrasonic mixing or the like. The composite binder is blended with the powder and the blend is mixed with a solvent, e.g. water, or alternatively, the binder components are dissolved or dispersed in water each independently or as a mixture and the resulting aqueous solution or emulsion is mixed with the powder (167). It is also possible to add a surface active agent, ph regulator or the like.

The granulation of the mixture is done most effectively by fluidized or spray drying.

The moulding of the granules is accomplished by use of moulding equipments employed in the dry moulding of the powdered materials. Such equipments include mechanical and hydraulic presses with metallic mould and isostatic presses with rubber mould. With respect to homogeneity of texture of the moulded body and releasability from the mould, the advantage of the present binder is fully manifested in moulding a tubular object by using the isostatic press (167).

The present composite binder is effectively applicable to carbides such as SiC, TiC, WC, TaC, HfC, ZrC and B_4C ; nitrides such as Si_3N_4, AlN, BN and TiN and borides such as TiB_2, ZrB_2 and LaB_6.

The present composite binder is used most advantageously in the manufacture of translucent, insulating, semiconductor, piezoelectric, magnetic and opto-electronic materials. Furthur, the present composite binder is advantageously used in the manufacture of translucent materials from the powders of Al_2O_3, MgO, Y_2O_3 or $Pb_{1-x}La_xZr_{1-y}Ti_yO_3$ (x = 0 to 1, y = 0 to 1). It is particularly effective for the manufacture of translucent materials from Al_2O_3 (167).

The present binder manifests its effectiveness with a powder of 20 μm or below, particularly 5 μm or below, in average particle size. Although effectively applicable to a superfine powder of 0.01 μm or below.

The following examples were provided by the inventors (167) so that to illustrate their invention in more detail. However, according to them, the invention is not limited thereto. In these examples all percentages are by weight unless otherwise indicated.

Example 1

As the water-soluble polymer, there were used a 10 % aqueous solution of polyvinyl alcohol (PVA), a 3 % aqueous solution of methylcellulose, a 5 % aqueous solution of gelatin. As the sparingly water-soluble organic substance, there were used a wax emulsion, a stearic acid emulsion and liquid paraffin. As the inorganic powder, there was used a high purity alumina (99.99 %, having a 0.5 μm average particle size). Magnesium oxide (0.1 %) was also added as the sintering aid for alumina. The alumina powder together with the sintering aid was mixed with water to an alumina concentration of 40 % and milled in a ball mill for 10 h. To the slurry was added a composite binder of the composition given in Table 2.10; the amounts added were 2 % of the water-soluble polymer and 1 % of the sparingly water-soluble organic substance (3 % in total), each in terms of solids, except for liquid paraffin. The resulting slurry was granulated by spray drying at 180°C. All the granules were in the form of nearly spherical bead having good flow properties. The granules

were moulded by means of an isostatict press into a tubular specimen of 10 mm inner diameter X 150 mm length X 2 mm wall thickness. The mouldability of each granulate was very good and the moulded body was easily released from the mould without any adhesion. The strength of the moulded body was sufficient enough for machining. The moulded tubular body was externally ground to a wall thichness of 1 mm and presintered in air at 1000°C. On subsequent sintering in vacuum at 1750°C the specimen showed good translucency as can be seen from Table 2.10. Properties of the moulded and sintered alumina specimens obtained by various binder systems are shown in the same Table (Table 2.10). As is apparent from this Table all the alumina specimens prepared by the use of composite binders showed superiority in mouldability and in physical properties of the sintered products.

Comparative example 1

The procedure of example 1 was repeated, except that 3 % (based on alumina powder) of a water-soluble polymer was used alone in place of the composite binder. The water-soluble polymers used were the same as those used in example 1. The results of evaluation for the mouldability of the granulates and physical properties of sintered specimens were as shown in Table 2.10.

Comparative example 2

The procedure of example 1 was repeated, except that 3 % (based on alumina powder) of sparingly water-soluble substance was used alone in place of the composite binder. The mouldability of granulates and the physical properties of sintered specimens were evaluated. The sparingly water-soluble substances employed were the same as those used in example 1. The granulates obtained were inferior in flow properties and were difficult to handle. Upon moulding a tubular body, the mandrel, used as the core, sticked so firmly to the wall of the moulded tube that the moulded tube could not be removed. By use of a release agent, the moulded tubular body could be released from the mould. However, owing to insufficient strength, the moulded body was broken upon external machining and the intended specimen was not

obtained. The results of these evaluations were as shown in Table 2.10.

Other organic binder systems

A U.S. patent (162) describes the use of an organic binder having a high solid state vapour pressure. The patent defines this type of organic binder as being solid at normal room temperature but having a melting point of ~ 200°C and a vapour pressure of at least 1 mm within the temperature range 20-200°C. Examples of such organic binders are naphthalene, paradichlorobenzene and camphour. These binders reduced the time required for debinding and also substantially reduced the shrinkage (to ~ 1 % maximum linear shrinkage) associated with debinding. This binder system was used with ceramic powders such as alumina, silica glass, berylia, magnesia, mullite, petalite, silica and spodumene. The principal application being precision cores for metal castings. However, serious difficulties were encountered in injecting this basic combination as the sole batch composition (162). This difficulty was due to the 'bleeding' or flow of the organic binder substantially alone leaving a ceramic-rich mixture behind which does not possess enough plastic flow properties for subsequent injection. It was therefore found necessary to add either a thermosetting resin or a colloidal ceramic powder (having a particle size substantially < 1 μm) or combinations of the two materials to prevent bleeding. The thermosetting resin can be either shellac or silicone resins. Gum shellac was found particularly useful. The addition of such thermosetting resins furthur improved the reduction of the binder removal time. The colloidal ceramic may be the same ceramic material as the major ceramic powder or a different one according to the properties desired in the article to be formed. The mixing was performed in a hot mixer by melting the organic binders and then adding the ceramic powder to the melted binders. In this way a homogeneous mixture is obtained. However, the mixing should be carried out in a closed container because of the exceptionally high vapour pressure of camphour. The resulting mixture is fed into the barrel of a conventional

ceramic injection moulder, heated (above the melting point to ~ 150-200°C) to make it fluid with a good flow, and then injected (under pressures of 50-70 MPa) into a conventional mould having the desired cavity (162).

The following ceramic-binder composition (162) provided an excellent combination of good plastic flow properties for injection moulding without detrimental bleeding, rapid burn-out of the binders within 12 h or less and easy burn-out of the thermosetting resin without forming a shell-like layer on the ceramic:

(a)- 10 % to less than 32 % by weight of solid organic binder having a high solid state vapour pressure,

(b)- at least one material effective to prevent 'bleeding' during injection selected from the group consisting of: 1- colloidal ceramic having a particle size substantially < 0.1 μm in an effective amount up to 4 %; 2- thermosetting resin in an effective amount up to 8 %,

(c)- major ceramic powder having a particle size not less than 1 micron being the remainder, and wherein the sum of organic binder plus thermosetting resin is 18 to 32 %.

The injected composition is solidified in the air cooled mould, then removed and heated to 70°C to drive off naphthalene. The time required for this step varies from 3 to 12 h for body thickness varying from 3 to 13 mm respectively. If a thermosetting resin such as gum shellac is included within the mixture then after driving off the naphthalene the body is heated relatively slowly (~ 100°C/h) to ~ 400°C to completely set or polymerise the gum shellac. Finally, the body is fired to sinter the ceramic material into a coherent body. For silica, the sintering process may be carried out at 1125°C for 2 h.

It was believed (162) that the substantial absence of shrinkage in the moulded articles was related to the fact that the organic binder remained solid during the initial burn-out (that of naphthalene) and this does not happen with the thermoplastic binder systems where the body becomes fluid during the debinding process.

The above invention, however, has the following drawbacks (165): application of a sublimable substance such as naphthalene restricts the conditions in which the raw components should be mixed and later subjected to injection moulding; the moulded mass is generally so brittle and therefore utmost care in handling is required; and treatment of naphthalene sublimated during removal of a binder raises different problems.

Ethylene vinyl acetate (EVA) copolymer

In the present literature the EVA copolymer (with ~ 30 % vinyl acetate) has only been used for formulation, mixing and rheological investigations. Mutsuddy (13) used a low molecular weight (~ 3500) EVA copolymer with a melt index of 200 and a density of 0.92 g/cm^3 to investigate the influence of powder characteristics on the rheology of ceramic injection moulding mixtures. A bimodal alumina powder (1-3 μm and 13-20 μm) and two commercial oxides (A16-SG alumina and a type C zirconia) were used by Mutsuddy for comparison. The results indicated that filler loading can be improved with powders having a wide particle size distribution, while the loading of ceramic powders with a 5 μm upper size limit was influenced by the extent of agglomeration. It was also reported that even with an ideal spherical shape, free from agglomerates, a powder with a narrow particle size distribution will fall short of maximum filler loading. Mutsuddy (13) stated that a shear rate of ~ 100 s^{-1} approximates injection moulding conditions and viscosity is very much dependent on both temperature and shear rate. The maximum achievable filler loading (into the EVA copolymer) with A16-SG alumina ultrafine powder (0.62 μm average particle size) was limited to ~ 65 volume percent which was lower than that with the bimodal alumina providing ~ 78 % volume loading. The A16-SG alumina is a low-soda, high-purity (99.9 %) ultrafine powder which is produced by the Bayer process and then ground by special milling to the ultimate particle size.

In other works (164) the EVA copolymer has been used as a minor binder to provide better flow and higher volume loading.

No furthur usage of this binder could be found in the present literature.

However, it was found during this work that the EVA copolymer could not be used as a major binder due to its crumbling and cracking problems during the debinding process (see chapter four, section 4.1.1-Debinding results).

2.4.3- Limitations and disadvantages of the available binder systems according to the present literature

Polystyrene binder system

As described in the previous section, the polystyrene binder system, i.e. a mixture of polystyrene + light oil + beeswax (or similar waxes), was considered (159) as a major processing breakthrough among the prior art injection moulding ceramic-binder mixtures. However, when this binder system is used in large amount, the light oil tends to coagulate during injection moulding (165). Furthur, since the light oil and polystyrene resin jointly occupy a large volume, the moulded mass is likely to decrease in density after removal of the binders. This process is also unadapted for the injection moulding of, for example, fine powders of clay (as well as the alumina powder) due to a large requirement of oil (165). Another major limitation (159) with this binder system is the long debinding time which may take a week for thin sections (< 5 mm thick) and several weeks for thick sections (. 10-20 mm thick).

Another known polystyrene binder system uses diethyl phthalate instead of oil and this is indeed well usable with raw powders of ceramics having a high tap density, but is unsuitable for raw ceramic powders having a low tap density (particularly very fine powders) which require a considerable amount of binder which is difficult to remove (165).

As will be seen in the results chapter (chapter four, section 4.1.2), due to rather low volume loading of the alumina powder into the polystyrene binder system, rather low as-moulded and sintered densities were obtained which all together make this binder system economically and technically not viable.

Polyolefin binder systems

Polyolefins such as polyethylene, polypropylene or polybutene were first used in the USA (137) for the injection moulding of ceramic powders including alumina. In this case, however, the binder had to be added in a large amount which gave rise to problems in its removal and also caused the moulded mass to have a low density after removal of the binder, thus making it difficult to control the dimensional change of the moulded mass when sintered (165). In addition, removal of a large amount of the binder gives rise to the deformation of the moulded mass as well as a low sintered density (1, 146).

Thermosetting binder systems

As also described in the previous section, thermosetting resins such as epoxy or phenolic resins are used as major binders in the ceramic-binder composition so that to prevent the thermal deformation of the moulded mass when a binder is removed therefrom. However, application of such thermosetting resins is unsuitable for the injection moulding of minute raw powders of ceramics, because a large amount of such resins have to be added as in the case of ordinary thermoplastic resins (165). Moreover, it is impossible to recover and regenerate scraps such as those remaining in sprue, sprue runner or sprue lock after injection moulding. Therefore this process gives rise to a prominent loss of powders of ceramics and consequently is unadapted to be applied to expensive raw material of ceramics, failing to attain quantity production (165).

2.4.4- Sintering of alumina ceramics

Typical sintering temperatures for the most common alumina grades are as follows (169): 88 % alumina 1440-1500°C, 95 % alumina 1520-1600°C and 99.8 % alumina 1750°C. It can therefore be realised that the sintering temperature depends on the alumina grade and, as stated in section 2.2.10, on grain size distribution, surface energy and on the additives to the (alumina) ceramic powder. The sintering time, particularly the heating rate during the heating-up period, should be adapted to the size and thickness of the body to be sintered (104). However, as shown in Fig. 2.31, the density grows linearly, according to the densification process during sintering, until it reaches saturation, representing the final density. A furthur increase in the sintering time does not improve either the density or the mechanical properties, on the contrary, it promotes grain growth which reduces the mechanical strength. For this reason the sintering process should be stopped as soon as the final density is obtained (104). Fig. 2.32 shows a typical sintering cycle used for achieving saturation density in medium-sized parts with a diameter of ~ 50 mm. Larger parts require a longer sintering time, particularly a longer heating-up period. Smaller parts can be heated up more quickly, allowing a much shorter sintering time.

Alumina ceramics allow sintering in every atmosphere (104). For economic reasons, the sintering process is normally carried out in air. Hydrogen or high vacuum are applied if special properties such as light transmission are required. The use of inert gases is of no practical value (104).

For die compacted alumina powders, the sintering shrinkage may be in the order of ~ 20 % in volume, within a tolerance of ~ 1 %. The shrinkage rate depends on the precompaction. Higher precompaction means lower shrinkage, and conversely. Non-uniform compaction leads to different shrinkage and consequently to warping, cracking or to the development of internal stresses. The same results occur if the temperature distribution during sintering is not uniform. Therefore, a uniform precompaction as well as a strict control of the temperature distribution during

sintering, is necessary in order to obtain uniform production (104).

During sintering all contacts between alumina ceramic parts and other materials must be prevented in order to avoid reactions, which take place intensively at the peak temperature. Therefore, all components of the furnace as well as the base plates have to be made out of the same materials, usually out of porous high alumina ceramics (104).

Magnesium oxide (MgO) is the main additive to the alumina powder which promotes densification and inhibits grain growth. Other additives such as silica (SiO_2) and calcia (CaO) are added as sintering aids to lower the sintering temperature and reduce the sintering time. However, it is found (104) that both silica and calcia impurities inhibit densification and promote grain growth and this effect should be avoided because it leads to low strength and poor wear resistance.

2.4.5- Mechanical, thermal and electrical properties of alumina ceramics

Mechanical properties

Aluminium oxide stands out due to its beneficial properties such as high hardness, high wear resistance, low coefficient of friction, high resistance to corrosion by practically all chemical reagents, a very high resistance to high-temperature corrosion in air, thermodynamic stability, i.e. the absence of phase transformations within the entire temperature range of solid state, and the fact that the material retains its strength at very high temperatures (~ 1500-1700°C). Its unfavourable properties are also well known: it has a low strength as compared with the theoretical strength and with the strength of metallic alloys, the large statistical spread of its strength values, its great brittleness, i.e. the complete absence of plastic deformation until ~ 1200°C, its low toughness and hence large susceptibility to thermal and mechanical shock loading, and the phenomenon of time-dependent strength. Due to these detrimental properties, the use of aluminium oxide in some

engineering applications, like that of many other structural ceramics, is still limited (104).

It is well known that the strength of ceramics is controlled mainly by two important variables: fracture energy and flaw size. This can be seen quite clearly from the 'Griffith equation of strength' as follows:

$\sigma = 1/y\ (2\delta_I\ E/a)^{½}$

where σ is the strength, δ_I is the fracture energy per unit area necessary to initiate failure, E is the young's modulus, a is the flaw size and y is a dimensionless constant which depends on the flaw size-sample size ratio. Both parameters (δ_I and a) depend strongly on the microstructure (104).

Some characteristic mechanical properties of aluminium oxide (or alumina) ceramics is given in Table 2.11. This Table demonstrates the influence of composition of two typical aluminas on their mechanical properties. Addition of silicates generally result in a decrease in mechanical strength, particularly at elevated temperatures, because they are mainly present as a glassy phase at the grain boundaries. They thus facilitate grain boundary sliding and hence contribute to plastic flow. On the other hand, magnesium oxide, leads to an increase in the mechanical strength by accelerating the sintering process and inhibiting discontinuous grain growth.
The variation of the properties with composition can be explained by differences in the microstructure. Fig. 2.33 shows the microstructure of alumina ceramics with additions of 10 % silicates (104). The alumina grains which have relatively sharp edges, are embedded in a glassy silicate phase. They do not change their shape during sintering, which is an indication of low sintering temperatures. The silicate phase controls the strength properties. As the weakest link in the chain of load bearing microstructural features within the sintered body, it is the reason for the considerably lower mechanical strength of silicate-containing alumina ceramics (104).

In cases of wear or corrosion attack the silicate binder, which has lower hardness, lower wear resistance and less chemical stability, is erroded or dissolved, leaving behind isolated alumina grains that lose their adherence. This leads to a strength loss of the whole mechanically attacked surface (104). In contrast to this, the microstructure of a high-purity alumina ceramic grade with an addition of ~ 0.25 % MgO shows an essentially single-phase material consisting of equiaxed grains sintered together directly which can be seen in Fig. 2.34. The absence of the silicate binder results in a considerable increase in wear and corrosion resistance as well as an improvement of the mechanical strength (104). The surface grains which are shown in Fig. 2.34 have rounded edges due to the effect of surface tension during sintering, which is an indication of high sintering temperatures. When exposed to mechanical loads, fracture occurs at considerably higher stresses compared to the silicate-bonded alumina ceramic. As observed in many cases, the fracture is transcrystalline if the microstructure is coarse grained and intercrystalline if the microstructure is fine grained (104). It is also very well known that even a slight increase in grain size results in a significant decrease in the compressive strength (104).

Thermal and electrical properties

These are given in Table 2.12 for the same alumina compositions as in Table 2.11. With respect to the electrical/electronic applications, the silicate binder also influences the properties. Due to the presence of the interconnected glassy phase a decrease of volume resistivity and dielectric strength and a considerable increase in the ionic conductivity of the system occur (104).

The absence of the silicate binder, however, results in a considerable increase in volume resistivity and dielectric strength with a considerable decrease in the ionic conductivity which can be seen from Table 2.12.

The applications in the field of electronic require an insulating material with relatively high mechanical strength for

rectifier housings, with high volume resistivity at elevated temperatures, and with low dielectric losses for transmitter tubes, with high density resulting in an increased thermal conductivity and in an excellent polishability for microelectronics, and with translucency for discharge lamps. Most of these requirements can be met only by a high-purity alumina ceramic quality (104). A silicate content can only be tolerated if electrical resistance and dielectric properties are not specified, since it reduces both volume resistivity and dielectric strength and increases the dielectric losses (104).

With respect to the thermal properties, the silicate binder increases the thermal conductivity which can be related to the increase in the ionic conductivity of the alumina-silicate bonded material (104).

2.4.6- Applications of alumina ceramics

Electronics/electrical and mechanical engineering are the main application fields of high alumina ceramics. In recent years medical and armour applications have become of growing importance. Thermal and chemical applications are of minor importance compared to the electronics and mechanical engineering applications (104). The alumina content of high alumina ceramic grades being used in the application fields described here ranges from 95 to 99.9 % Al_2O_3. The lower grades have a silicate binder, the higher grades (above 99 %) considered here as high-purity alumina ceramics, have only small additions of MgO.

Electronic applications

The first important practical application of high alumina ceramics in the field of electronics was the production of spark-plug insulators. They were initially produced by the injection moulding process which was replaced later by the isostatic compaction process as a more effective and more efficient forming method. However, the spark-plug insulator was made from ceramic materials containing - 94 % alumina. Other

insulating materials such as propellers used in high power engines (e.g. racing cars) or in airplanes require a higher alumina content and this is a rather small portion of the production (104).
Other applications in this field are as follows: components and housings for electron tubes, e.g. high frequency transmitter tubes, housings for rectifier tubes and thyristors, electrical terminals and bushings as feedthroughs for ultrahigh vacuum furnaces, vacuum chambers for particle accelerators, etc.; sodium vapour discharge lamps with tubes of translucent high-purity alumina ceramics for a lamp power from 100 to 400 W; electronic circuits, i.e. high alumina substrates for thin film technique, and the multilayer packages consisting of alternating layers of ceramics and metal, etc. (104).

Mechanical engineering applications
Most of the applications in this field require a material with a considerable resistance to abrasive wear, adhesive wear, erosive wear and fatigue wear. Because of their extreme hardness, high alumina ceramics are well suited to meet these requirements. However, it has been considered that wear resistance cannot be described as an isolated material property and therefore, high hardness, while necessary, is not sufficient for the suitability of a material exposed to extreme abrasion. The behaviour of the material depends on the existing operating conditions. A number of elementary wear processes, each of which depending on physical properties, contribute to the totally observed wear (104).
Other requirements in this field are: strength at high temperatures, corrosion resistance and dimensional stability. Most of these requirements are met by the use of high alumina ceramics (104).
One of the large-scale applications for high alumina ceramic parts in this field is thread guides for textile machines. These include: deviation elements, stretch pins and thread brakes which have a rather complex shape and the injection moulding process is a suitable technique for economical mass production

of these alumina ceramic materials. Step cones, capstans, pulleys, rollers and other wire drawing elements made of high alumina ceramics have also proved quite adequate in this field for many years (104).

In the paper manufacturing the efficiency and economy has improved considerably during the last 30 years by the application of high alumina ceramics. The development of paper machines has taken place in two steps: (1)- replacement of dynamic dewatering elements as table rolls by stationary elements; (2)- increasing wear resistance of stationary elements by the replacement of high density polyethylene and wood by high alumina ceramics (104). The use of high alumina ceramics in paper machines has provided the following advantages: 1- improved productivity by higher machine speed and reduced down-time; 2- reduction of production cost by increasing the lifetime of the wire and felt as well as energy savings; and 3- improvement of the paper quality.

Bearings such as seal rings, sleeve bearings, plain bearings, pump parts and plungers are a typical example of a combined exposure to corrosion and wear. In this special case, ceramic materials, particularly high alumina ceramics, meet these requirements to a much greater extent than metals. Therefore, ceramic bearings are preferably applied to pumps for chemically aggressive fluids, see water, dirty water as well as to high pressure pumps. The main field of application, however, are in pumps for central heatings. Within this group, mechanical seals with seal rings made of high alumina ceramics have gained increasing importance for their longer lifetime, lower leakage losses and absence of maintenance (104).

High-purity, high-density, fine grain (< 5 μm) alumina ceramics have been used as cutting tools for the machining of metals. Cutting tools require high wear resistance, high mechanical strength at elevated temperatures and good impact strength. To fulfill these requirements, high-purity alumina with only small

additions of MgO (as a grain-growth inhibitor) has been used. Additions of TiC and ZrO_2 have also turned out to be successful in improving the thermal shock resistance (by increasing thermal conductivity) and toughness of alumina respectively (104).

Medical applications

Due to their good mechanical strength, high wear and corrosion resistance, the high-purity alumina ceramics are being used in this field primarily as bone and joint replacement, dental implants as well as in the field of maxillary and oral surgery (104, 169).

Armour applications

Due to their extreme theoretical strength (~ 100000 MN/m^2) and their low specific weight, hard materials such as oxide ceramics or carbides, particularly high alumina ceramics and boron carbide are potential materials for light-weight effective armour facing (104).

Other applications

Due to their outstanding resistance to elevated temperatures as well as to corrosion, high alumina ceramics were considered long ago for thermal applications as super refractories and for chemical applications such as laboratory and metallurgical equipment.

The applications described here require neither a high-strength nor a high-abrasion resistance. Therefore, there is no particular necessity for a very high density and a small grain size; only a high purity is desirable so that to obtain good temperature endurance and chemical stability (104).

Tubes for high temperature furnaces (1200-1400°C) are one of the most frequent applications of the as-described high purity alumina ceramics. High alumina protective tubes for thermocouples and pyrometers as well as crucibles, trays, dishes and boats for high temperature uses can generally be exposed to temperatures up to 1800°C.

Besides the thermal and chemical applications described here, high alumina ceramics are used for grinding equipment such as grinding balls, grinding cases, mortars and pestles (104).

2.5- Introduction to the present work

It is quite clear from the literature review relating to the injection moulding of alumina that even in cases where successful overall results have been claimed, few details of individual stages have been given for all the process stages (see Fig. 2.1). There is therefore no clear pattern of the routes and optimisation conditions used. Furthermore there is no information which relates physical or mechanical properties of injection moulded bodies to processing conditions.

The missing information can be summarised as follows, and from this the need to provide the basic information throughout all stages of the process (see Fig. 2.1) becomes apparent.

1- Binder properties.

For most organic binders only scattered and incomplete general properties such as melting and softening points, molecular weights, melt flow index and some other physical, chemical and mechanical properties are available. Other important properties such as thermophysical (e.g. thermogravimetric analysis or burning properties) and viscosities are not available and therefore have to be investigated. These properties are very important for the debinding and moulding processes and therefore have to be evaluated for every binder used in the ceramic-binder mixture.

2- Powder-binder compositions.

Except in the cases of a few workers (161, 163 and 168) who gave the exact compositions, no other information is available about the optimum powder-binder compositions. It is therefore necessary to optimise the composition for each powder-binder mixture so that to obtain the maximum/best possible properties such as moulded and sintered densities.

3- Powder-binder mixing conditions and properties.

There is very little and very incomplete information about the exact mixing conditions (temperature, time and speed), mixing properties (e.g. amount of torque during mixing and adhesion

properties) and physical properties of the resulting mixtures. These properties need to be investigated so that to determine the best mixing conditions for a homogeneous powder-binder mixture.

4- Rheological characteristics.

This is one of the most important and vital information basis necessary for successful injection moulding process and little precise information is available for any of the alumina-binder mixtures which has been moulded successfully. This property has to be investigated for each alumina-binder mixture and for different binder systems.

5- Debinding conditions and properties.

A successful debinding process is the most difficult and crucial stage of the injection moulding process and therefore has to be carried out very carefully and accurately (with the correct heating rates, temperatures and times) for each binder system. There is almost no exact debinding details and properties for any binder system used for the injection moulding of alumina ceramics and therefore these have to be optimised experimentally for each available binder system.

6- Sintering conditions.

Most of the available sintering conditions (i.e. heating rate, temperature and time) are those for compacted alumina ceramics and these conditions may not be necessarily valid for injection moulded aluminas. It is therefore necessary to optimise the sintering conditions for the injection moulded alumina ceramics so that to achieve the optimum properties such as physical, mechanical, chemical, thermal and electrical properties, etc.

The overall objective of the present work is the systematic development of an injection moulding process system for the preparation of high density alumina with mechanical and thermal properties which at least match those of alumina obtained by other routes (e.g. by compaction methods). A furthur objective

within the programme has been to reduce the time required for debinding and hence processing costs.

Because of the lack of detail in previously published work one of the objectives of the present work (i.e. the first stage) has been to obtain complete experimental/practical detail for each stage of the injection moulding of alumina ceramics which, in other words, means the fulfillment of the above missing informations. This was achieved by re-evaluation of the most successful binder systems (such as polystyrene and atactic polypropylene, etc.) available from the literature for the injection moulding of alumina ceramics. After the completion of this stage it was possible to see the optimum properties provided by each binder system which is an original work since this is not available in the present literature. The optimum properties for each binder system includes: the maximum possible volume loading of the alumina powder, mixing, moulding and demouling properties, debinding properties and times, as-moulded and sintered densities. This original re-evaluation process also revealed the advantages and limitations of each binder system and therefore it became possible to choose the best binder system and where possible to make compromises.

The other major objectives of the present work (second stage) have been to obtain better properties such as higher volume loading of the alumina powder which should result in higher moulded and sintered densities and hence better mechanical properties, shorter debinding times, better moulding and demoulding properties and shorter (moulding) cycle time than those provided by the re-evaluated binder systems. These objectives were achieved by developing two new binder systems, one based on thermoplastic-wax and the other one based on water-soluble polymers. A volume loading of 70 % of the alumina powder was achieved with the newly developed thermoplastic-wax based binder system resulting in sintered densities of 98.5 % (theoretical) with bend and compressive strengths comparable to those of the compacted alumina ceramics and higher than those of

the present injection moulded aluminas. The newly developed water-based binder system also provided a higher volume loading (56 % maximum) of the alumina powder than the existing water-soluble (methylcellulose) binder system resulting in (higher) sintered densities of 96 % (theoretical) with bend and compressive strengths comparable to those of the compacted aluminas. This binder system provided much better moulding and demoulding properties with shorter moulding and debinding cycle times than the existing water-soluble (methylcellulose/Rivers) binder system. Thermal conductivities of the alumina ceramics obtained using the newly developed binder systems were measured for the first time during this work and these results were quite similar (if not marginally better) to those of the compacted aluminas having similar chemical compositions.

The new binder systems were also used quite successfully (during the third/final stage of this work) for the injection moulding of other powders such as zirconia, silicon nitride, silicon carbide, tungsten carbide-6 weight % cobalt and iron-2 weight % nickel. For these powders, optimum properties such as composition, mixing, moulding, demouling and debinding were fully evaluated which showed quite satisfactory results. Other properties such as sintered densities were obtained when the required sintering temperature was not above 1800°C due to furnace limitations.

The experimental details of the above results are given in chapter three followed by the results and their interpretation in chapter four.

Table 2.1- A Comparison of Hardness Values for Typical Ceramics and Some Wear-resistant Materials.

	Hardness (GPa)
Ceramics	
Zirconia	14
Sialon	20
Alumina	22
Silicon nitride	25
Silicon carbide	33
Wear-resistant metals and cermets	
Carbon tool steels	8·5
High-speed steels	9·0
Nitrided steels	10·0
Tungsten carbide—16% cobalt	11·5
Tungsten carbide—6% cobalt	15·5

FUNDAMENTAL VARIABLE	*MACHINE VARIABLE*
• MATERIAL TEMPERATURE	• MELT TEMPERATURE • INJECTION PRESSURE • PLUNGER VELOCITY • MOLD GEOMETRY • MOLD TEMPERATURE
• FLOW RATE (SHEAR RATE)	• PLUNGER VELOCITY • MOLD GEOMETRY • INJECTION PRESSURE
• CAVITY PRESSURE	• INJECTION PRESSURE • MELT TEMPERATURE • PLUNGER VELOCITY • MOLD GEOMETRY
• COOLING RATE	• MELT TEMPERATURE • MOLD TEMPERATURE

Table 2.2- Relation of fundamental injection moulding variables to plunger machine variables.

Table 2.3- *Alternative pathways for mass transport during sintering (Kingery et al., 1976).*

Transport pathway	Mass source	Mass sink
Vapour transport	Surface	Neck
Surface diffusion	Surface	Neck
Lattice diffusion	Surface	Neck
Boundary diffusion	Grain boundary	Neck
Lattice diffusion	Grain boundary	Neck
Lattice diffusion	Dislocations	Neck

Table 2.4- Mechanical and thermal properties of SiC and Si_3N_4.

	SiC	Si_3N_4
Flexural strength (M Pa) at room temperature	400	750
Young's modulus (G Pa) at room temperature	420	290
Thermal expansion coefficient (K^{-1})	$4.2X10^{-6}$	$3.4X10^{-6}$
Heat conductivity (W/mK)	100	30

Table 2.5-

Characteristics of Various 94% Tungsten Carbide - 6% Cobalt Powders Investigated.

Powder Reference	Average Particle Size (μm)	Distribution (μm)	Specific Surface Area (cm^2/g)	Relative Density		Mixing Characteristics at 130°C				Qualitive Assessment of mixing
				Apparent	Tap	Volume Loading %	Steady State Torque (mg)	Time to steady state (mins)	Total mixing time (mins)	
A	2.04	< 1-20	1967	0.245	0.406	65	110	17	28	Moderate
B	1.61	< 1-16	2490	0.218	0.400	63	180	14	44	Difficult
C	1.85	< 1-16	2160	0.250	0.412	65	80	12	26	Easy
D	1.5	< 1-8	4210	0.189	0.340	65	130	10	30	Easy
E	~ 0.5	Submicron	~8000	0.217	0.355	62	220	15	55	Difficult

Feedstock Reference	% Volume Hardmetal	% Volume binder & type	Theoretical Density g/cc.
016	69	31 Montan ester wax	10.625
014	60	40 "	9.378
LD5	60	23 LDPE 250 MFI. 17 WAX BLEND	9.346
018	65	35 WAX BLEND	10.046

Table 2.6- Formulations with suitable rheological properties.

Table 2.8- **Process Parameters and Properties for P/M Fe-8Ni-0.5C Alloy Steel.**

Sintering			Heat Treatment			Density		Tensile Properties		
Atmosphere	Time	Temperature	Atmosphere	Time	Temperature	(% of Theoretical)	Hardness	Yield	Ultimate	Elongation
Hydrogen	1 hr	2050°F	Argon	1/2 hr (oil quench) +	1550°F	90.9	38 HRC (38 HRC)	— (110ksi)	138 ksi (140ksi)	0.7% (1.0%)
			Argon	1 hr (air cool)	500°F					
Vacuum	2 hr	2500°F	As above			94.3	45 HRC (40 HRC)	— (130ksi)	178 ksi (168ksi)	1.3% (1.5%)

( ) above indicates the ASM Handbook value for press & sinter at same density.

Table 2.7- Properties obtained by the Rivers process.

	A	B
Green Density, %	68.0	65.0
Sintered Density, %	98.7	99.5
Sintered Hardness, Rc	38-39	41-43
Ult. Strength, psi	141,333	146,500
Elongation, %	2.6	2.5

Table 2.9- Vacuum Sintering Cycles for P/M 316 Stainless Steels of Various Carbon Levels and Resulting Densities.

Carbon Level (wt%)	Sintering			Density (% of Theoretical)
	Atmosphere	Time	Temperature	
0.03	Vacuum	2 hr	2500°F	96.0
0.11	Vacuum	2 hr	2485°F	96.1
0.20	Vacuum	2 hr	2475°F	97.5

Table 2.10-

Relationship between the binder composition and the moldability of granulate and the physical properties of sintered article.

	Sample No.	Water-soluble organic binder	Sparingly water-soluble organic binder	Moldability			Physical props. of sintered body	
				Homogeneity	Strength of molded body	Releasability	Density (%)	Light transmittance (%)
Example 1	1	Polyvinyl alcohol	Wax	◎	◎	◎	99.8	30
	2	,, ,,	Stearic acid	◎	◎	◎	99.7	29
	3	,, ,,	Liquid paraffin	◎	O	O	99.8	30
	4	Methylcellulose	Wax	◎	O	O	99.7	29
	5	,,	Stearic acid	◎	O	O	99.6	27
	6	,,	Liquid paraffin	◎	O	O	99.7	29
	7	Gelatin	Wax	◎	O	O	99.7	28
	8	,,	Stearic acid	◎	O	O	99.6	26
	9	,,	Liquid paraffin	◎	O	O	99.6	27
Comp. Example 1	10	Polyvinyl alcohol	–	X	◎	◎	99.4	13
	11	Methylcellulose	–	X	◎	O	99.4	12
	12	Gelatin	–	X	◎	O	99.4	12
Comp. Example 2	13	–	Wax	◎	X	X	Not measured due to molding failure	
	14	–	Stearic acid	◎	X	X		
	15	–	Liquid paraffin	◎	X	X		

Note: ◎, O and X mean excellent, good and poor, respectively.

Table 2.11- Mechanical properties data for typical alumina ceramics.

Property	Unit	99.7% alumina + 0.25% MgO	97% alumina + silicates
Average grain size	µm	4	10
Density	g/cm^3	3.9	3.7
Residual porosity	%	0.2	7.2
Leak rate	mbl/s	$< 10^{-12}$	$< 10^{-12}$
Compressive strength			
at 20°C	MN/m^2	5000	3000
at 1000°C	MN/m^2	2000	600
Flexural strength			
at 20°C	MN/m^2	500	300
at 1000°C	MN/m^2	400	200
		Polycrystal-line alumina	
Hardness			
at 20°C	Kg/mm^2	~ 2100	
at 1000°C	"	~ 320	
Young's modulus			
at room temp. and 0 % porosity	GN/m^2	386-411	
Shear modulus			
at room temp. and 0 % porosity	GN/m^2	160-166	
Fracture toughness, K_{IC}, at room temp., grain size 3-30 µm	$MN/m^{3/2}$	3.8-5.1	
Poisson's Ratio, v		0.23-0.27	

Table 2.12- Electrical and thermal properties of typical alumina ceramics.

Electrical properties	Unit	99.7% alumina + 0.25% MgO	97% alumina + silicates
Volume resistivity			
at 100°C	Ω cm	10^{14}	10^{13}
at 500°C	Ω cm	10^{12}	10^{11}
at 1000°C	Ω cm	10^{7}	10^{6}
Dielectric strength			
at 20°C	KV/mm	30	18
Loss coefficient (tan δ) at 20°C and 400 mega cycles	---	$1X10^{-4}$	$14X10^{-4}$
Thermal properties			
Thermal conductivity	W/mK	20	38
Thermal expansion	1/K		
between 0-300°C		$6.7X10^{-6}$	The same as 99.7% alumina + 0.25% MgO
0-500°C		$7.3X10^{-6}$	
0-1100°C		$9.5X10^{-6}$	

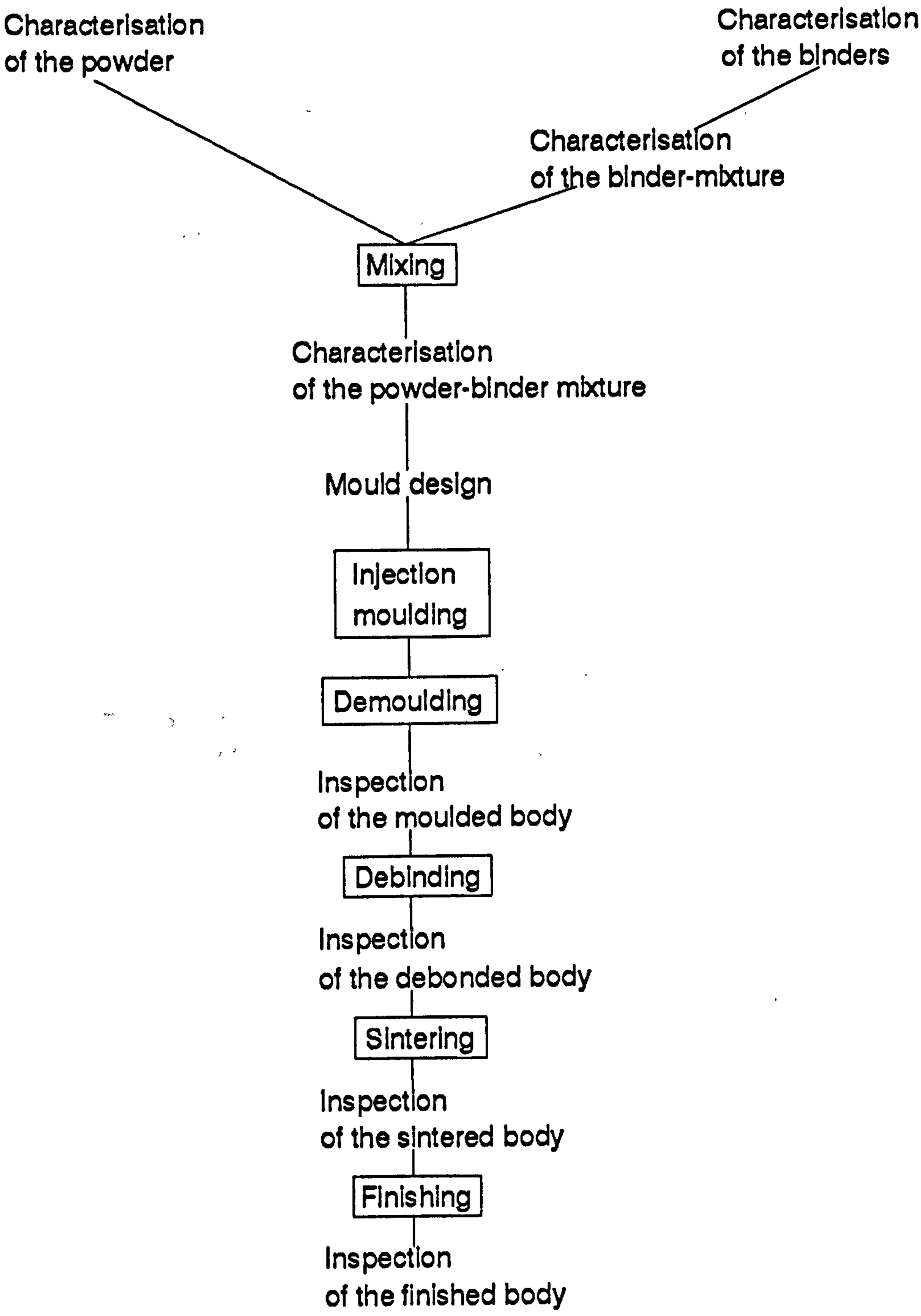

Figure 2.1- Process flow chart illustrating the individual stages of a complete ceramic/metallic injection moulding process.

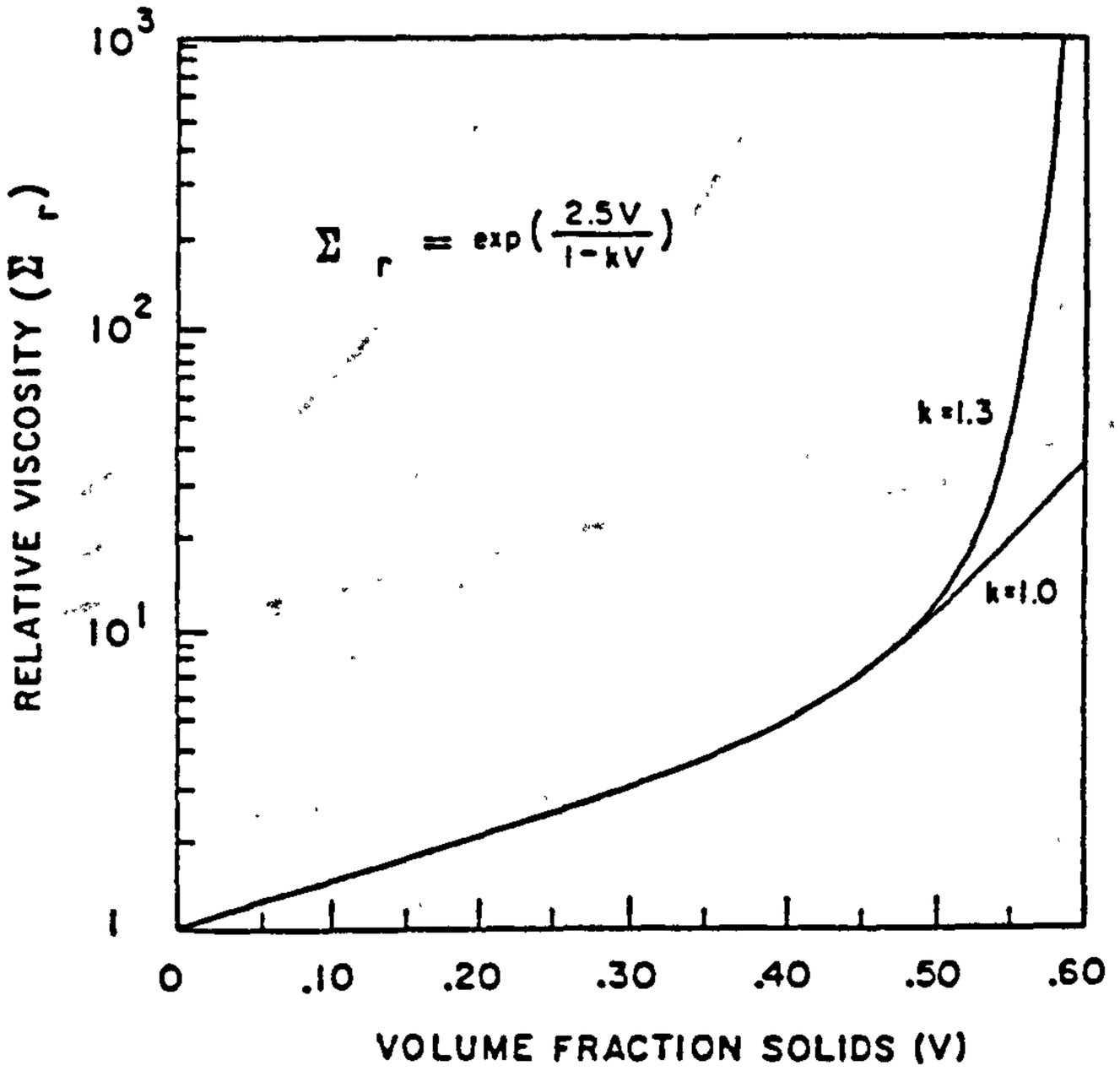

Figure 2.2- Relative viscosity as a function of volume fraction of monodispersed spheres in an organic suspension; after Farris.

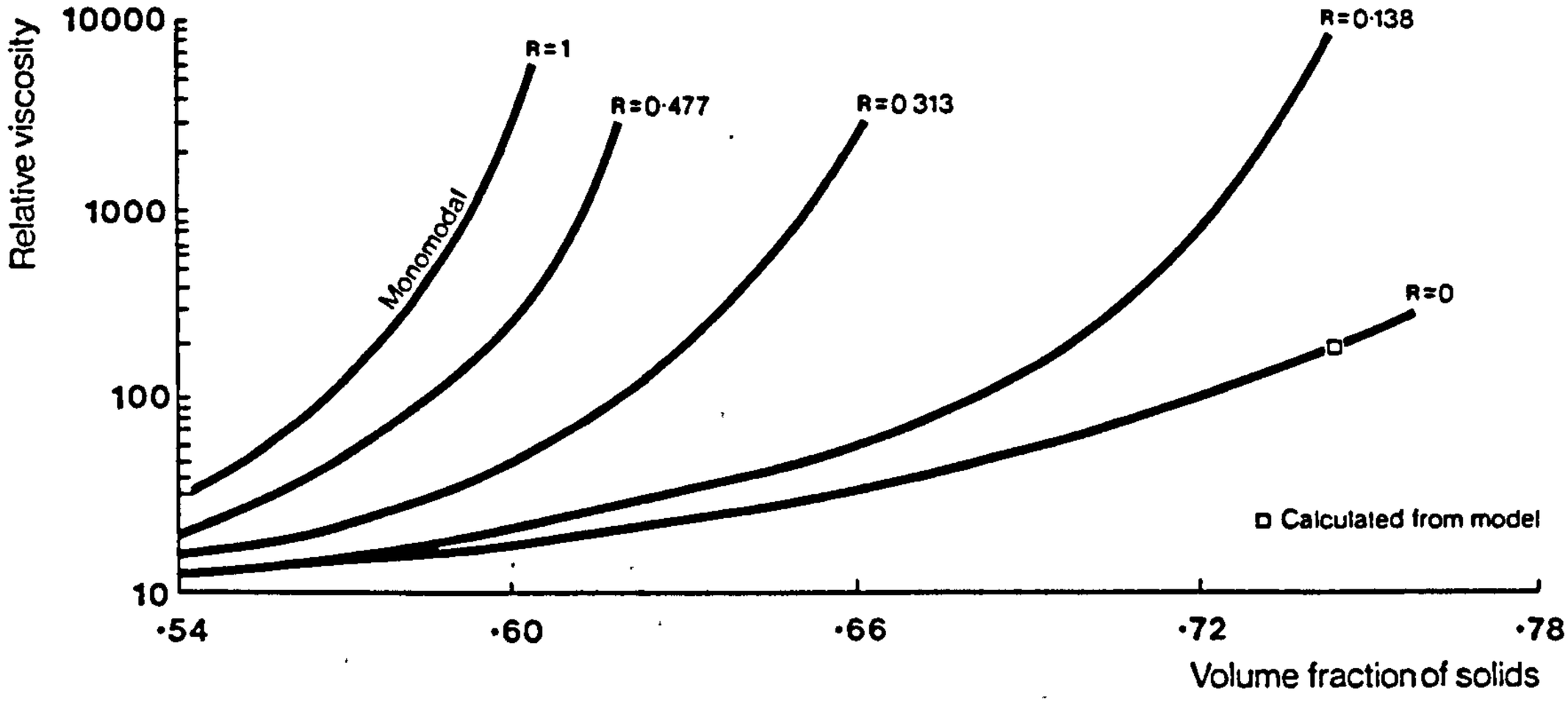

Figure 2.3- Calculated and measured viscosities of monomodal and bimodal suspensions; after Farris. R = (mean fine particle size)/(mean coarse particle size).

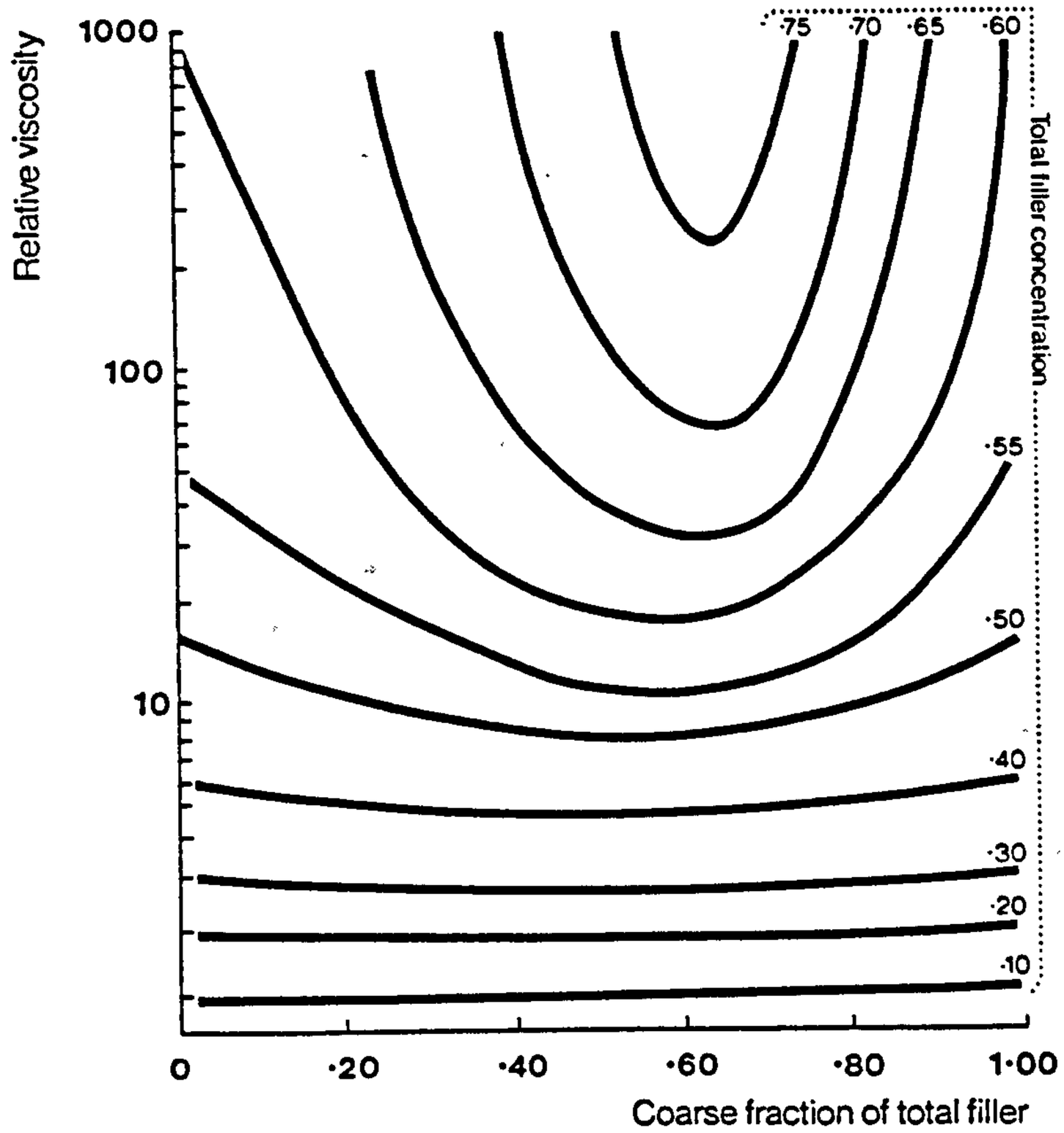

Figure 2.4- Comparison of calculated viscosity for bimodal suspension for various blend ratios and concentrations; after Farris.

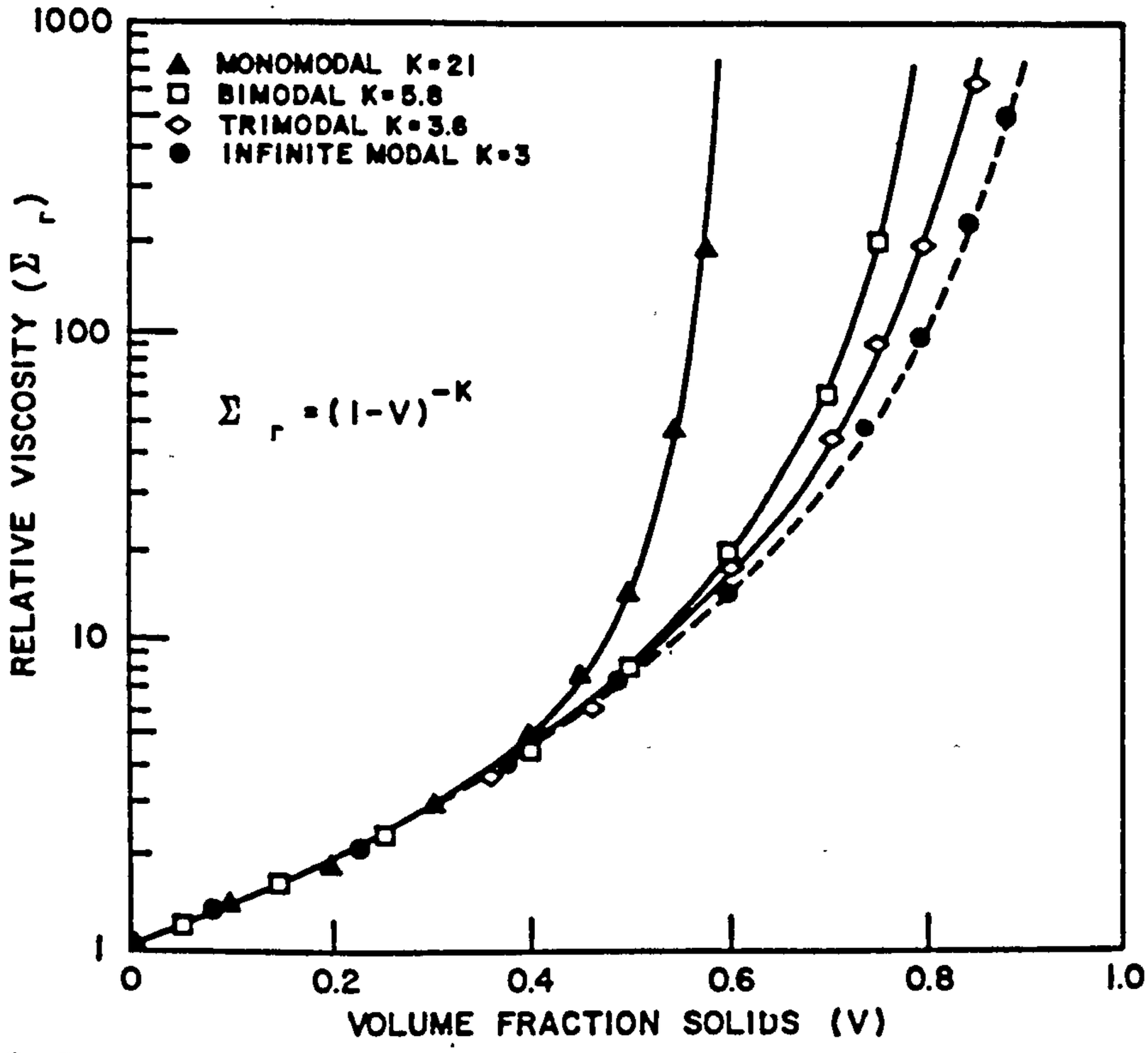

Figure 2.5- Comparison of calculated relative viscosity for the best multimodal system; after Farris.

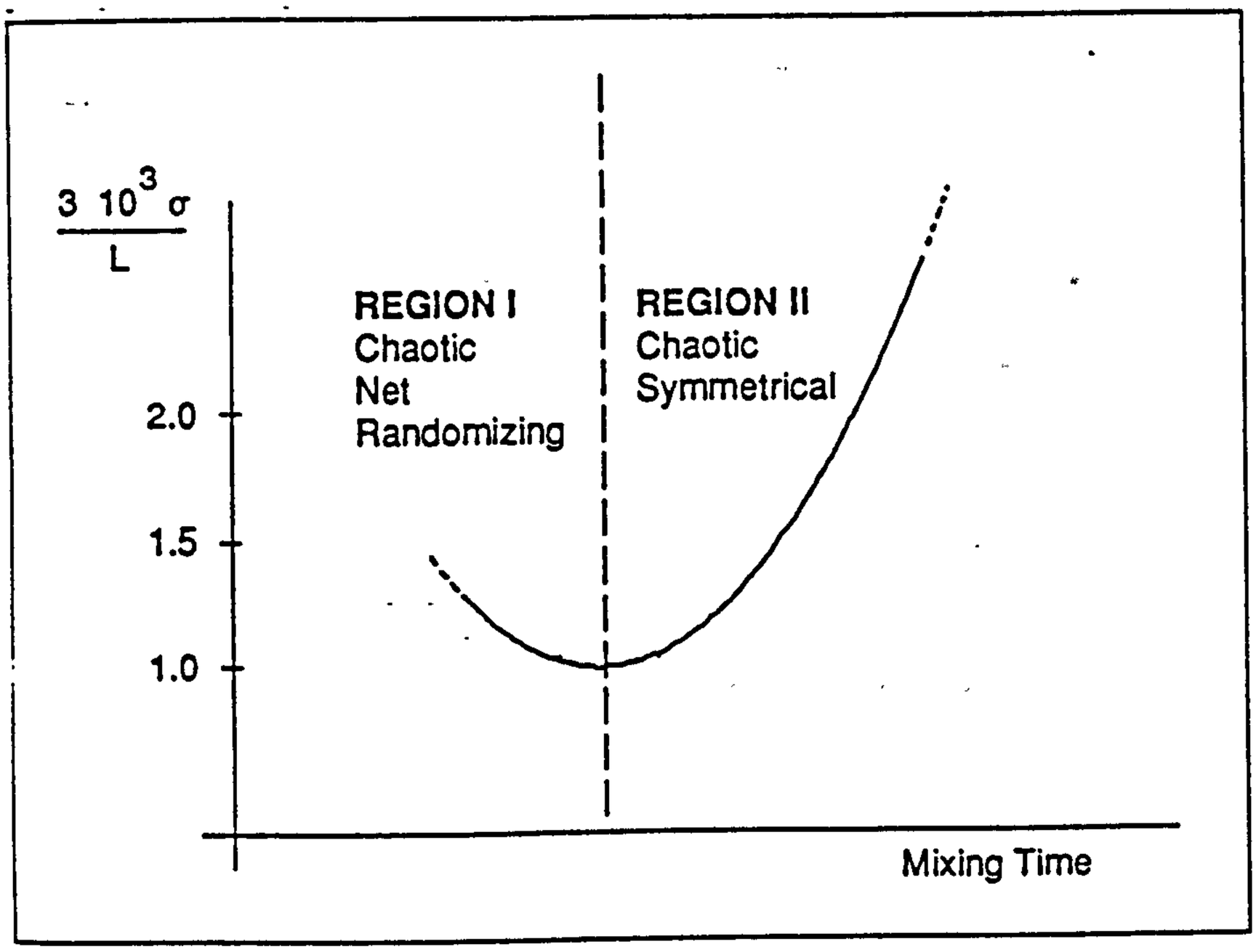

Figure 2.6- *Time-dependency of the mixing operation.*

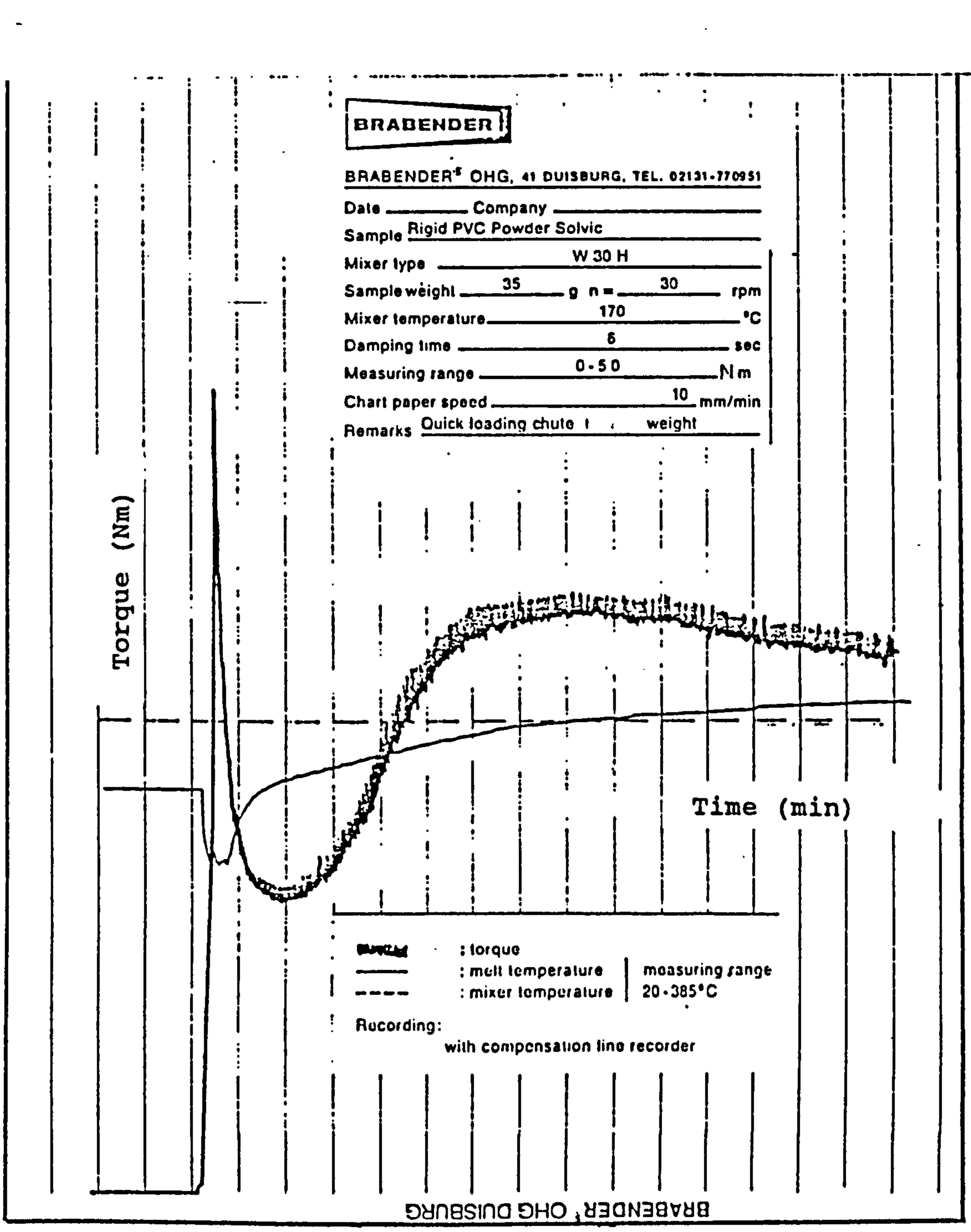

Figure 2.7- Graph of torque versus mixing time from the Brabender mixing device.

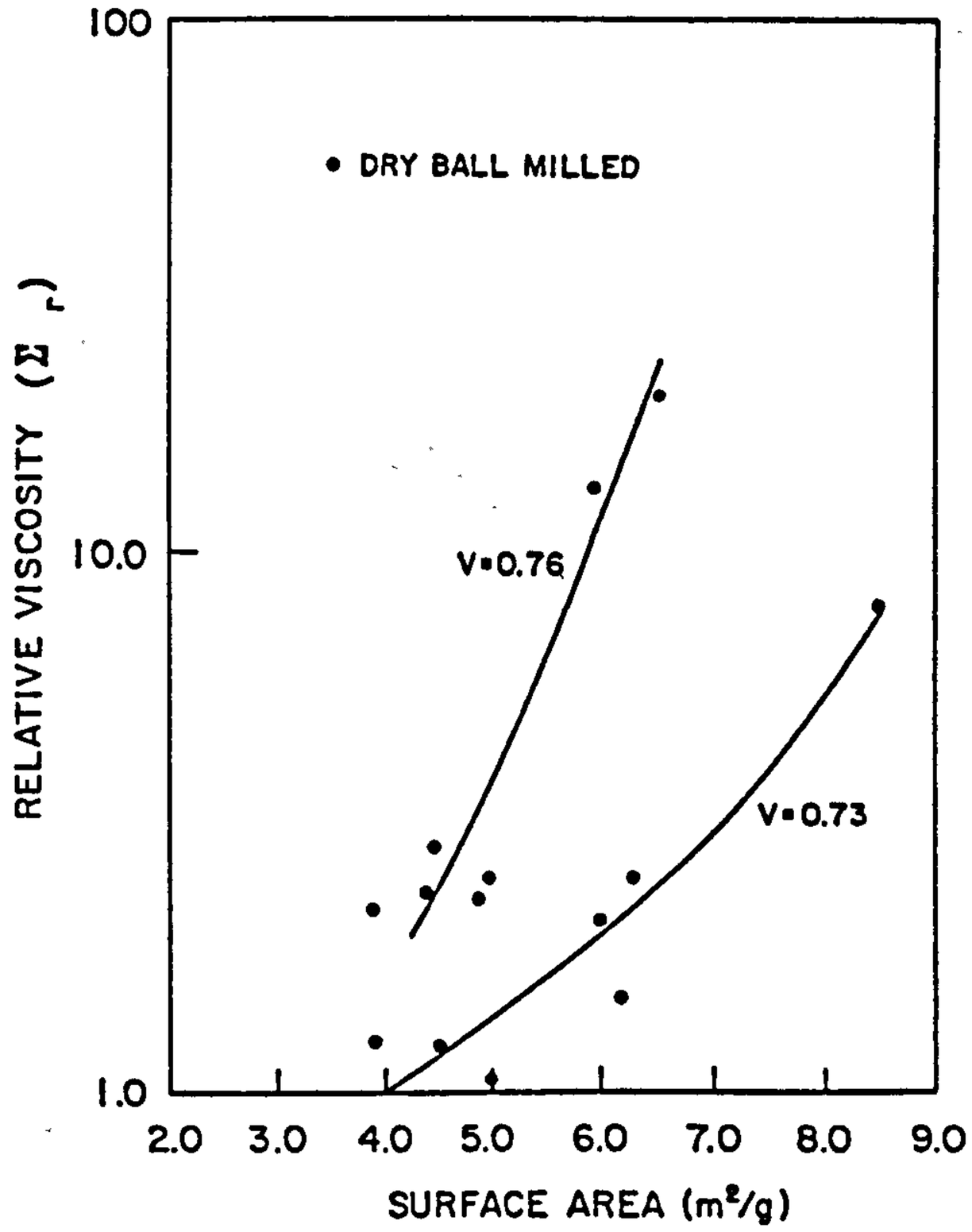

Figure 2.8- Effect of surface area on the relative viscosity of a ceramic-injection-molding mix at two volume fraction solids.

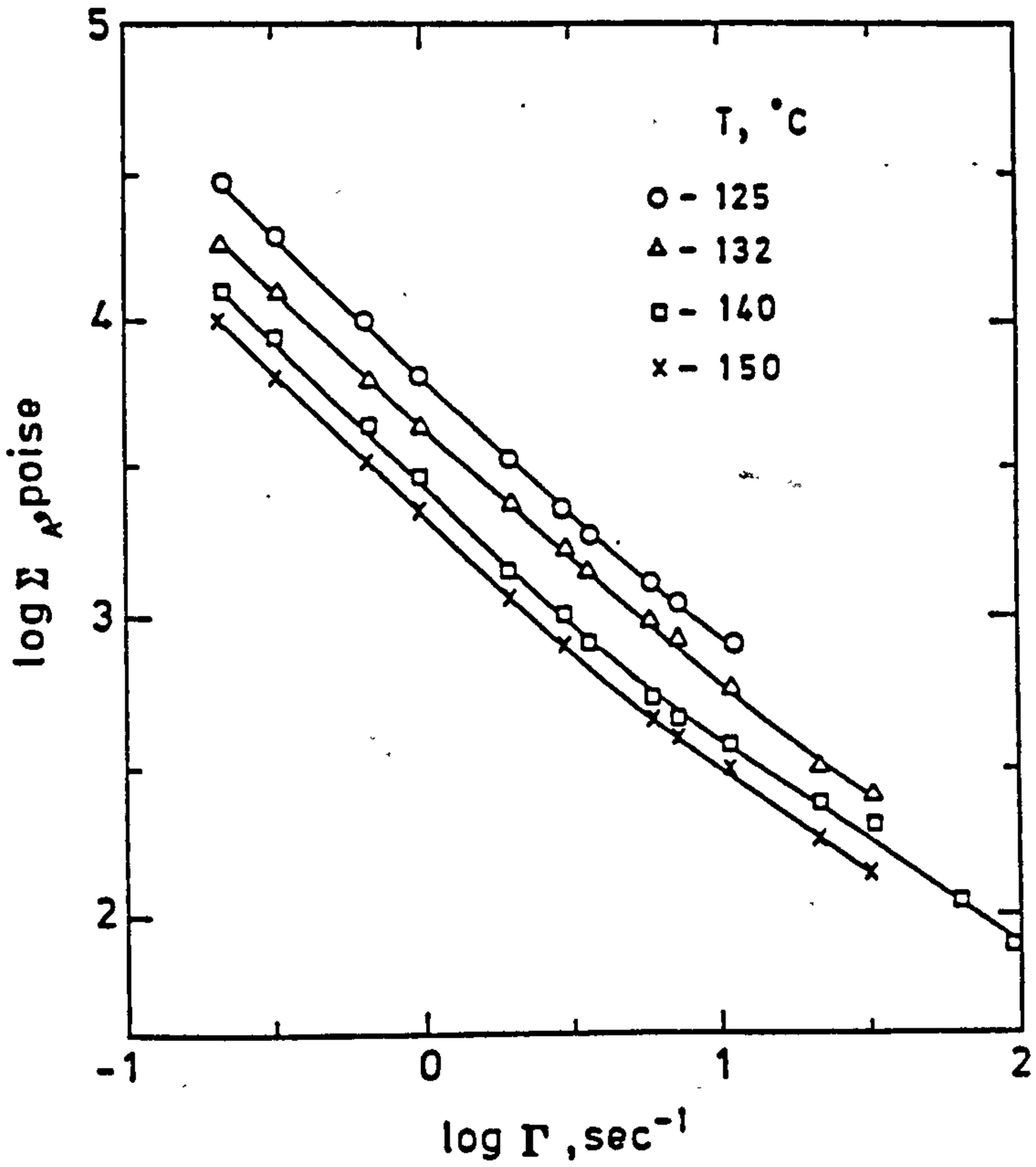

Figure 2.9- Dependence of apparent viscosity on shear rate at different temperatures for ceramic-filled material.

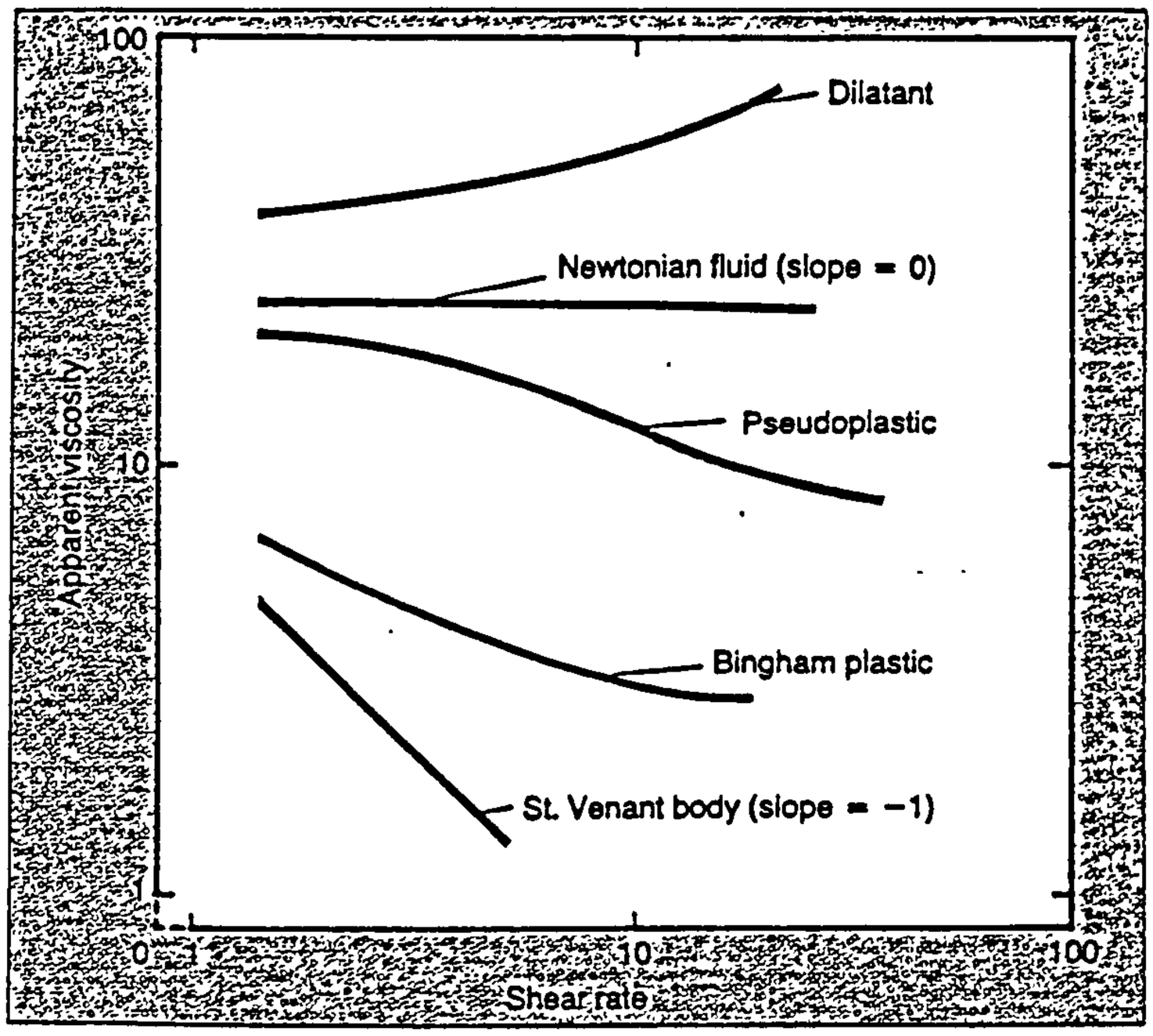

Figure 2.10- Graph of apparent viscosity versus shear rate showing different types of flow behaviour for polymeric materials.

In the development of a binder for ceramic injection molding, correct flow properties are essential if the molding process is to be successful. The graph shows the relationship of the four flow behavior categories. Ceramic binder combinations with either Bingham or pseudoplastic flow characteristics have been most successful.

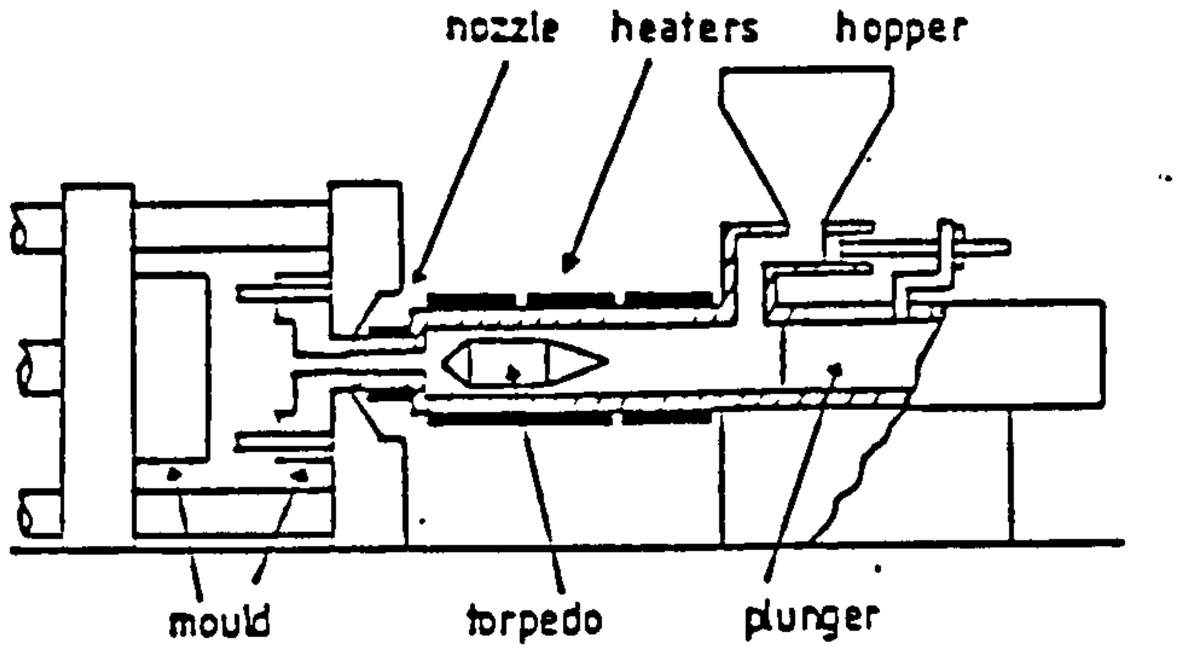

Figure 2.11- Plunger-type injection moulding machine.

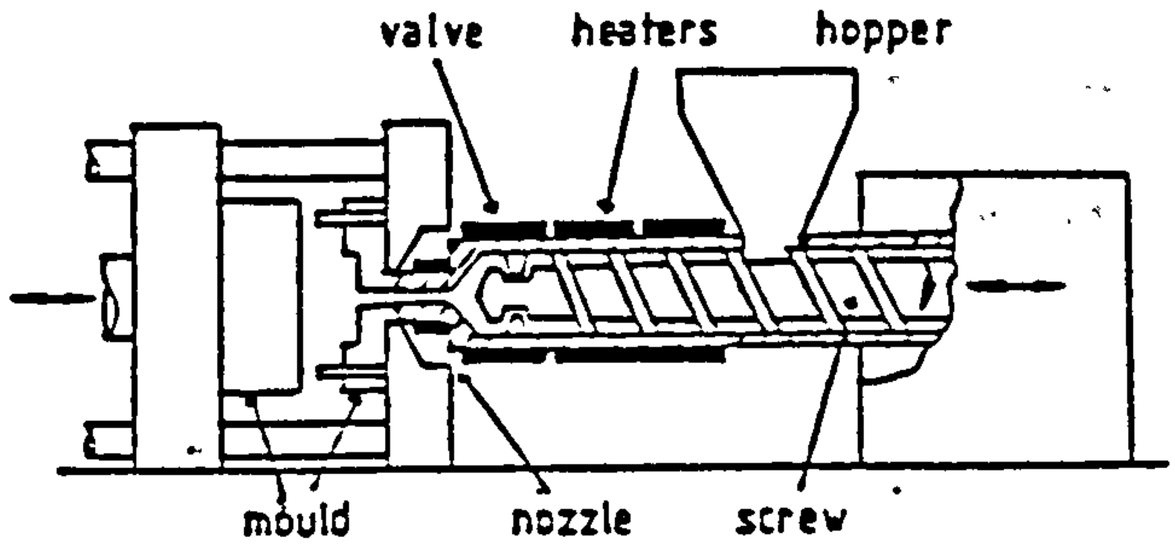

Figure 2.12- Reciprocating screw-type injection moulding machine.

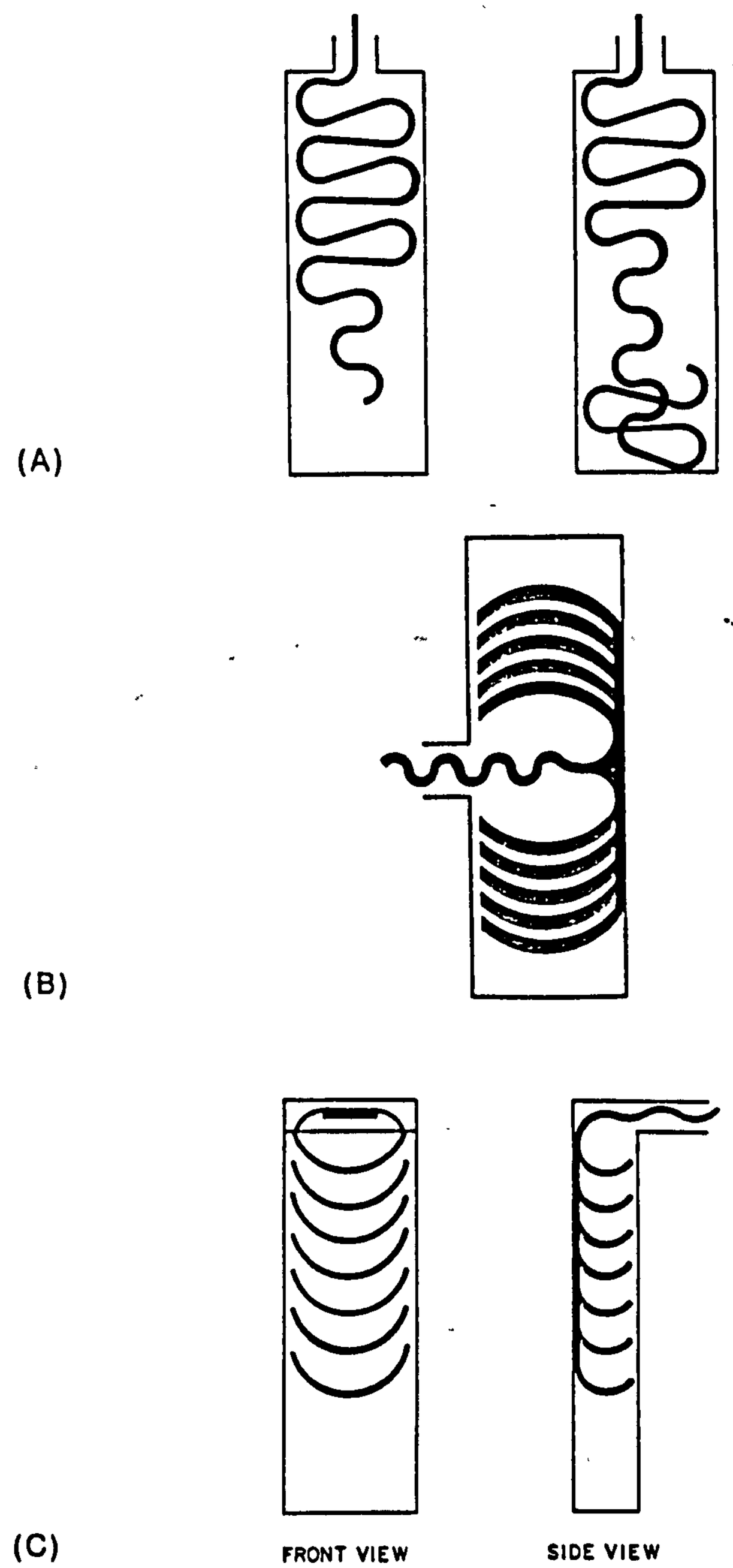

Figure 2.13- Schematic representation of flow into a rectangular test bar cavity using (*A*) an end gate, (*B*) a side gate, and (*C*) a fan, top gate.

Figure 2.14- Schematic diagram of apparatus used for binder extraction by 'evaporation method'; (124).

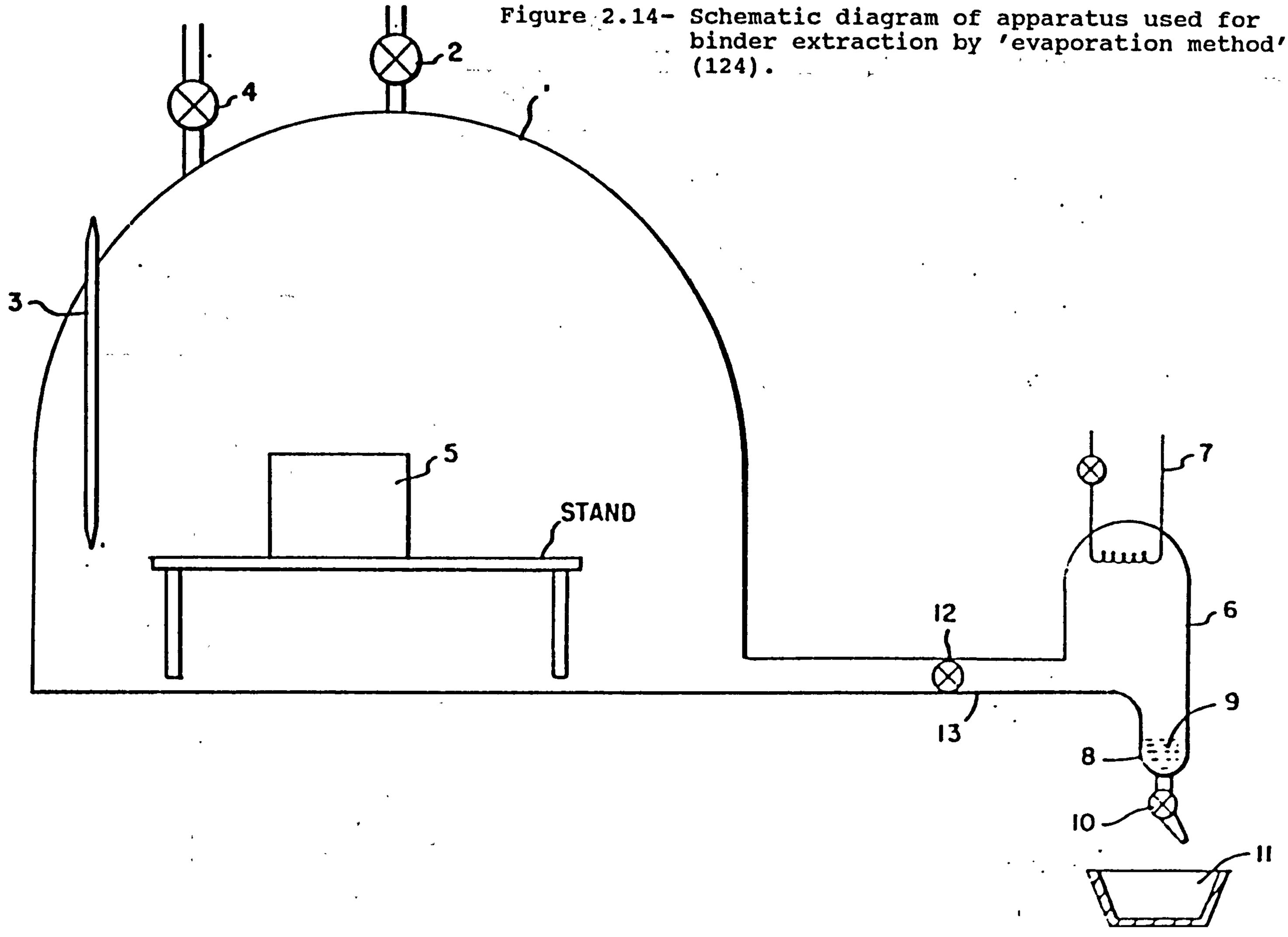

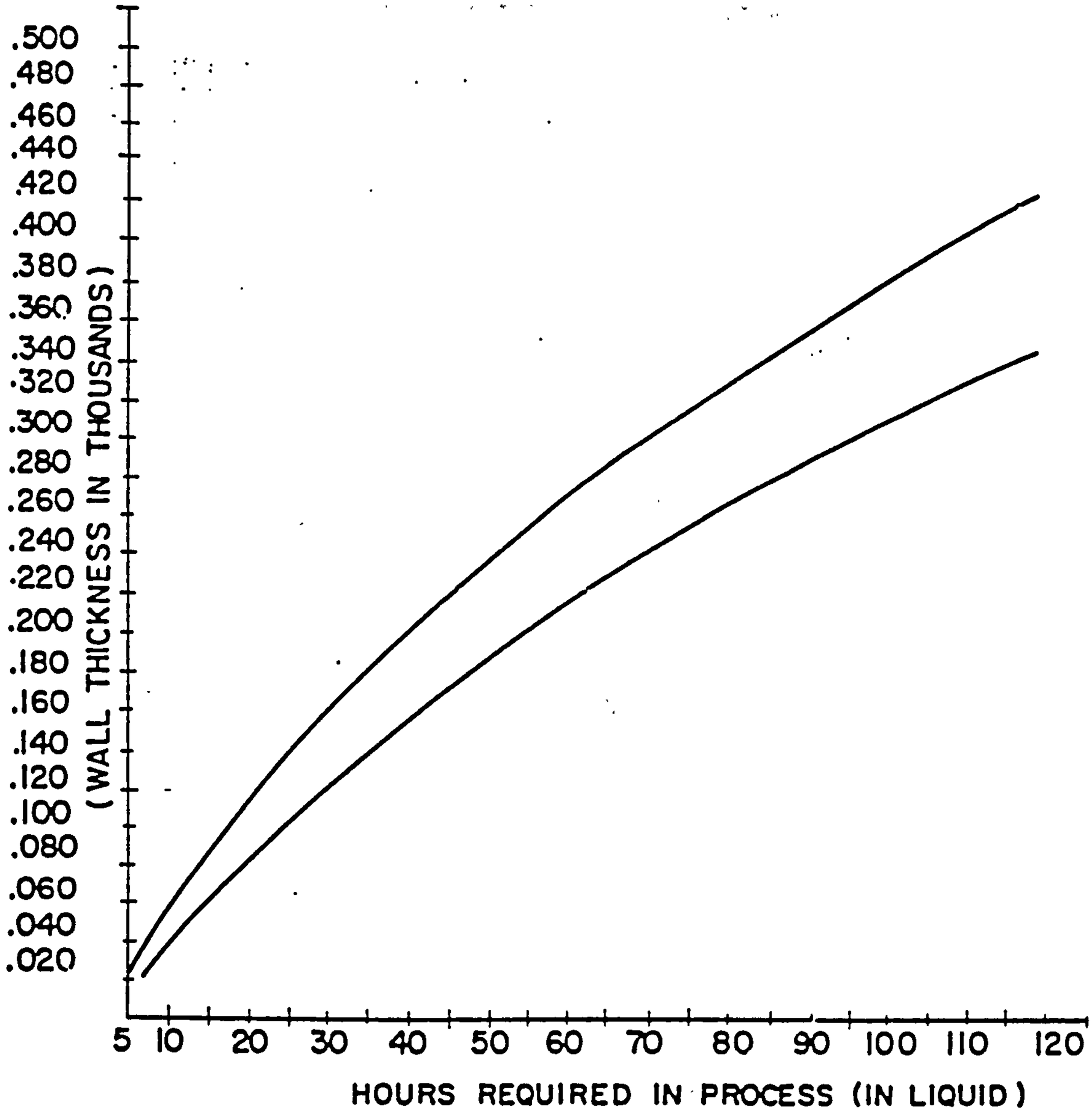

Figure 2.15- Graph of processing time in liquid solvent as a function of wall thickness of the green body.

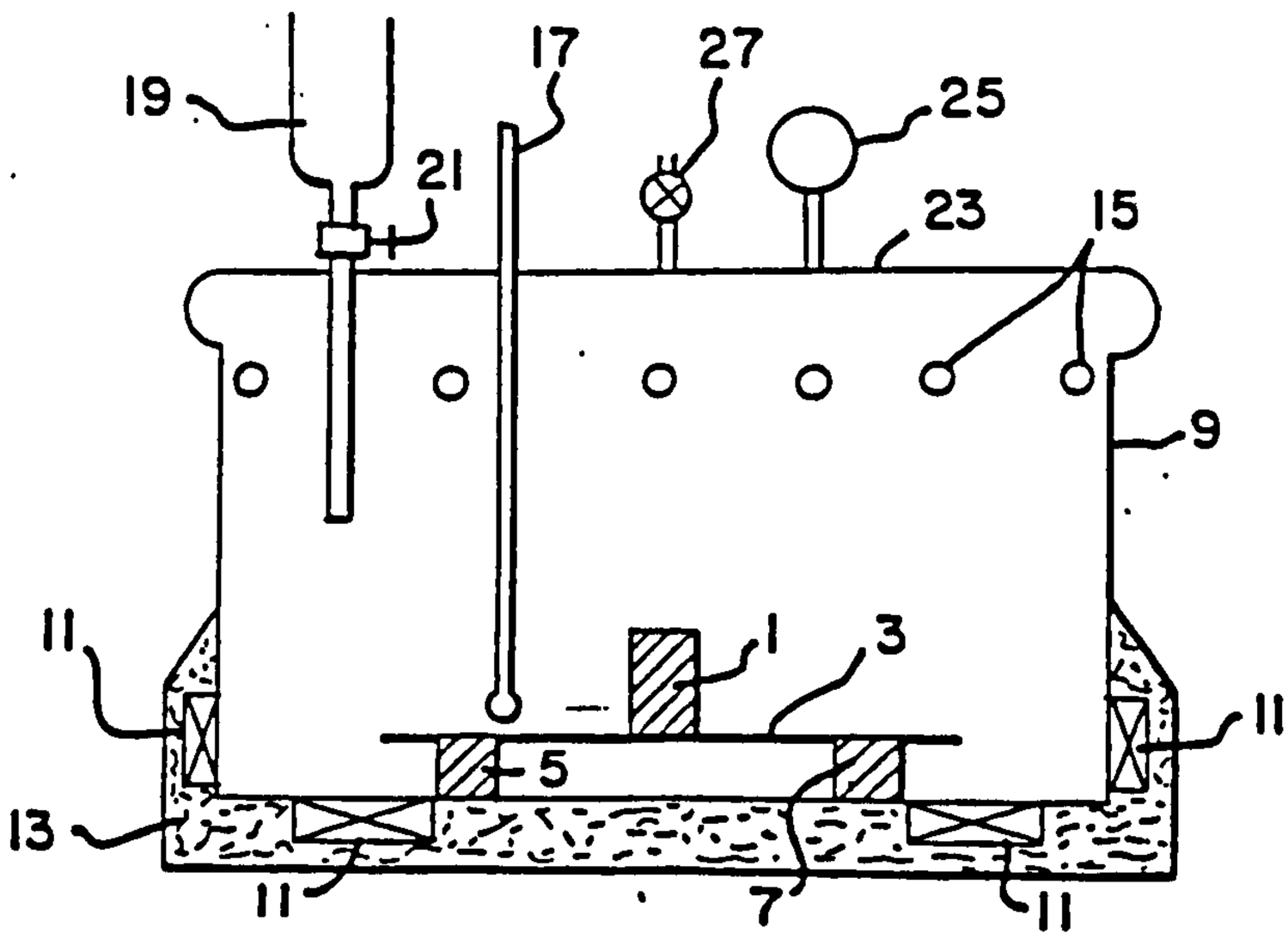

Figure 2.16- Schematic diagram of apparatus used for binder removal by 'solvent extraction'.

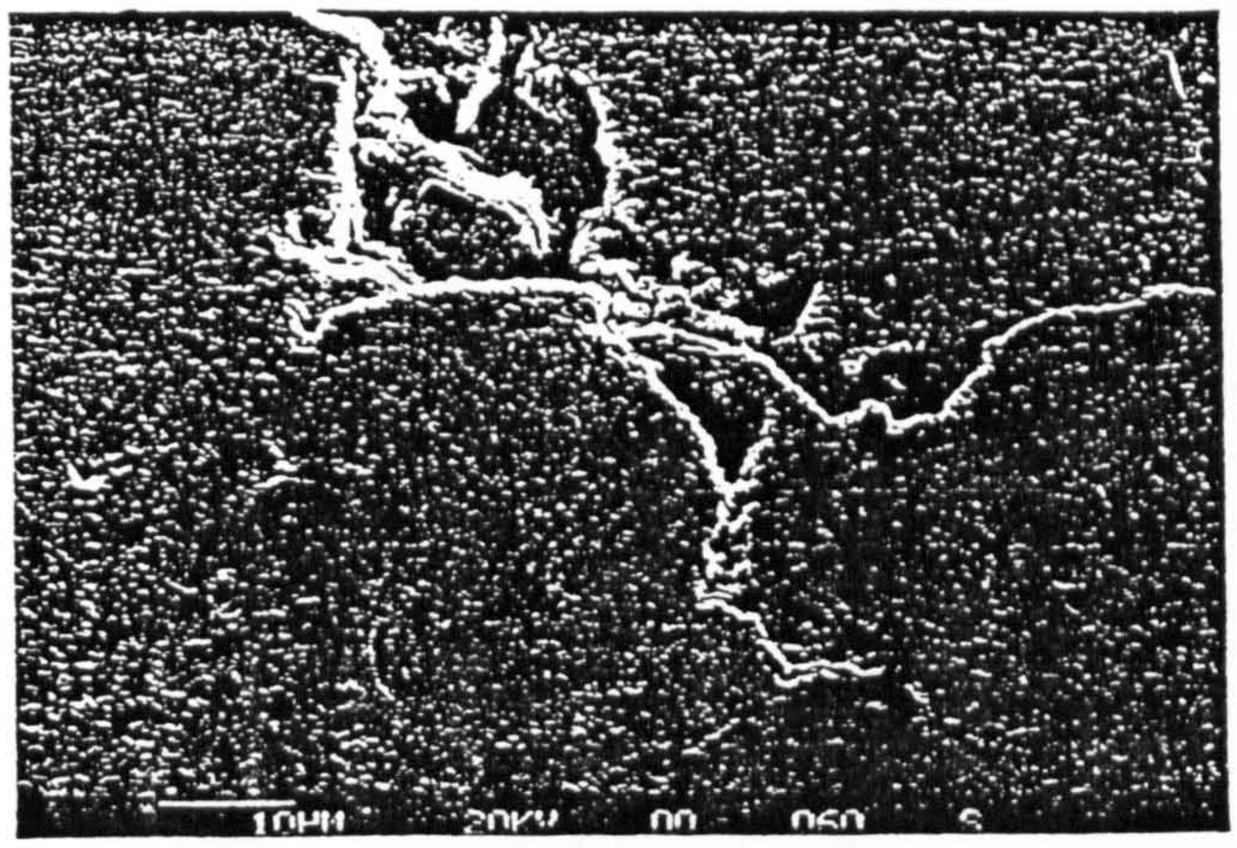

Figure 2.17- Polished section of an alumina composition produced in a double blade mixer at 160 °C for 1 hour using a wax based binder. The wax was removed by slow heating in air and the ceramic was fired at 1200 °C for 30 minutes to confer sufficient strength for polishing.

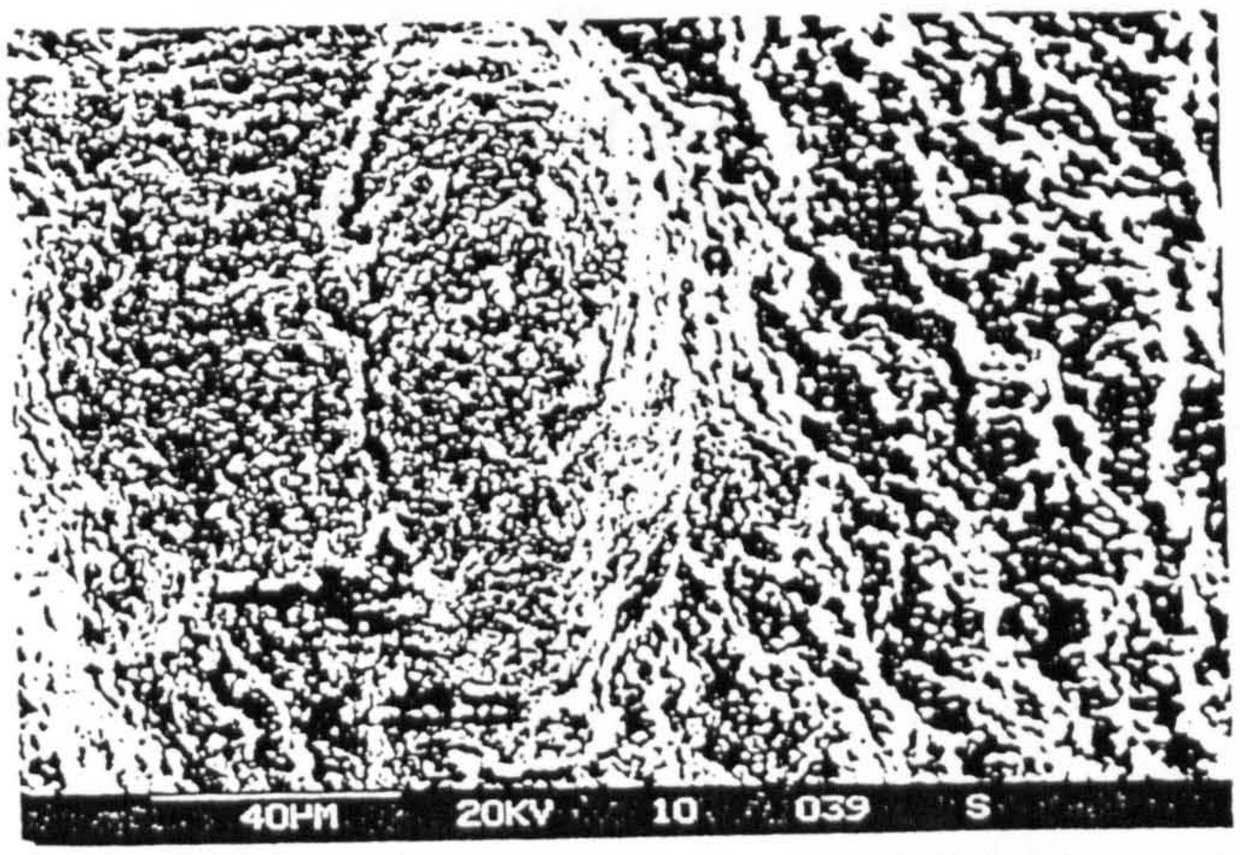

Figure 2.18- Fracture surface of a compounded alumina blend (Composition 6L) after removal of the polypropylene binder. The micrograph shows an atypical agglomerate undispersed by high shear mixing.

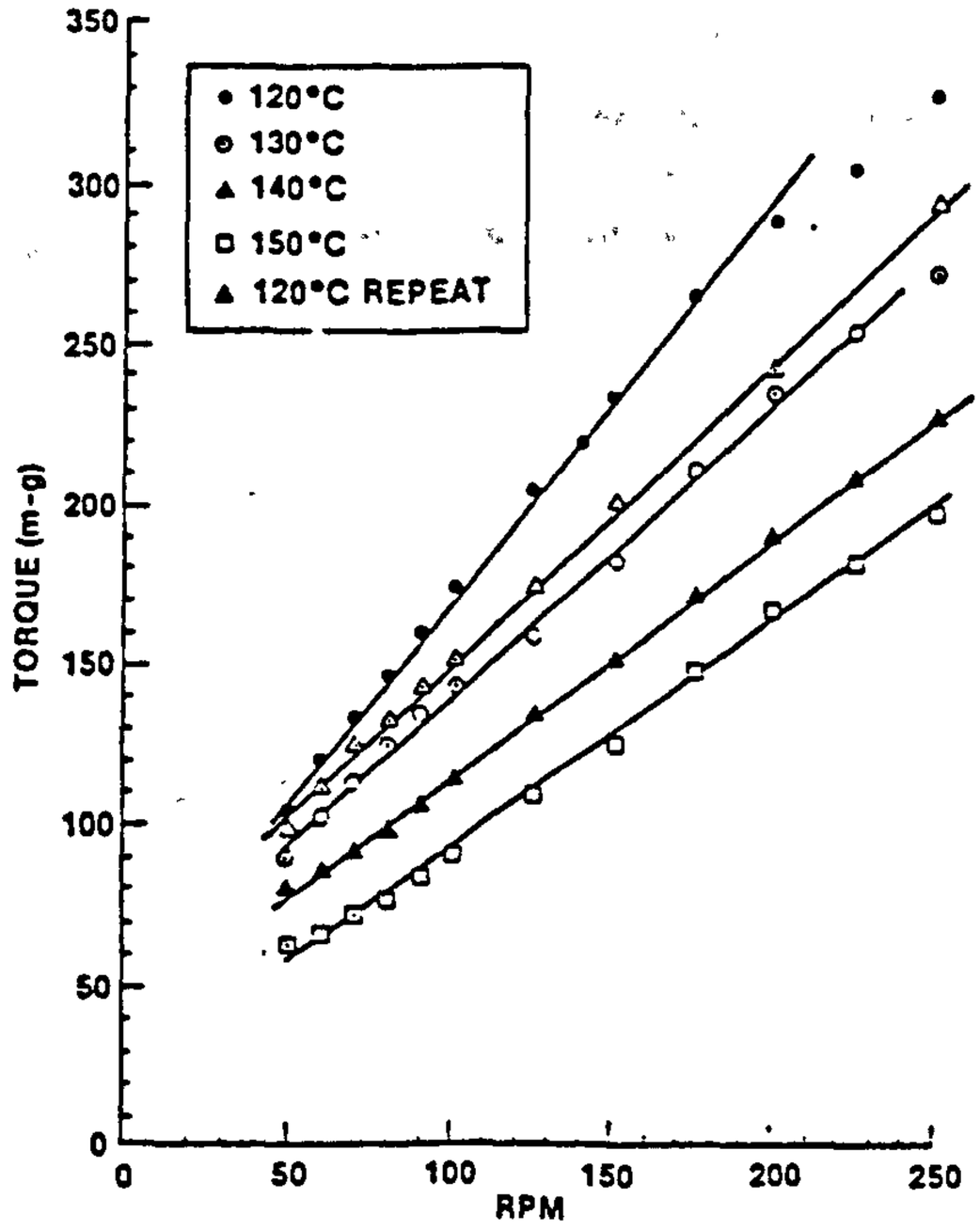

Figure 2.19- Example of data mix rheology generated by torque rheometer mixer.

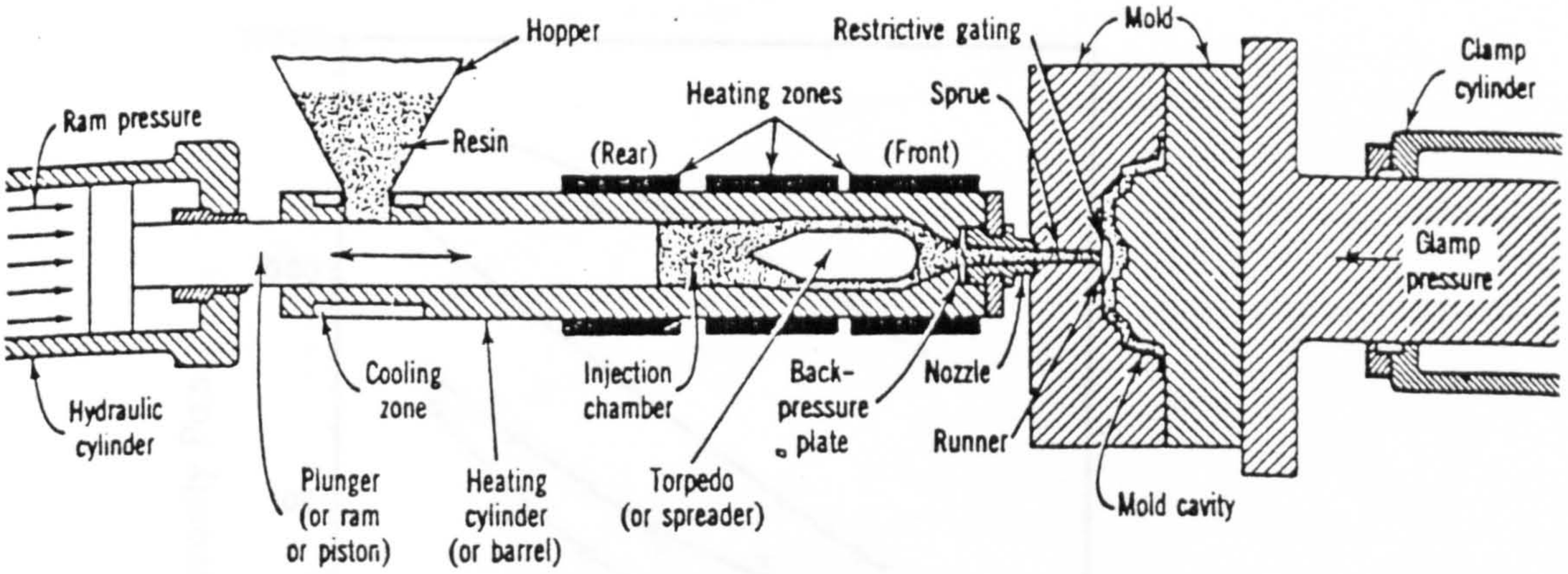

Figure 2.20- Cross section of plunger-type injection molding machine.

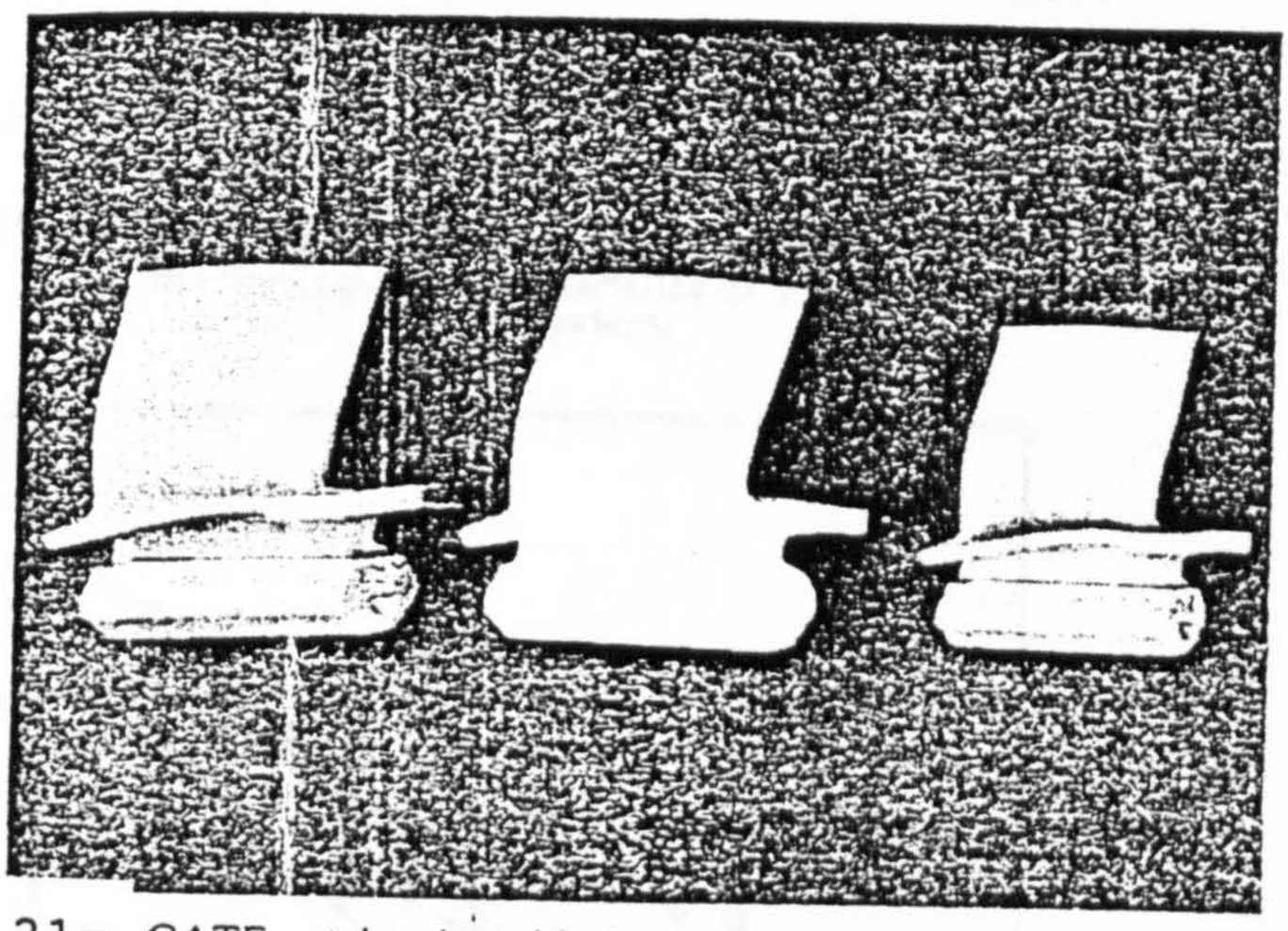

Figure 2.21- CATE axial turbine blades of Si_3N_4. From left to right: as injection molded; with binder removed; after sintering. The sintered blade is about 3.5 cm high.

Figure 2.22- Rheological characteristics of a 0.6 volume fraction formulation produced by various mixing techniques.

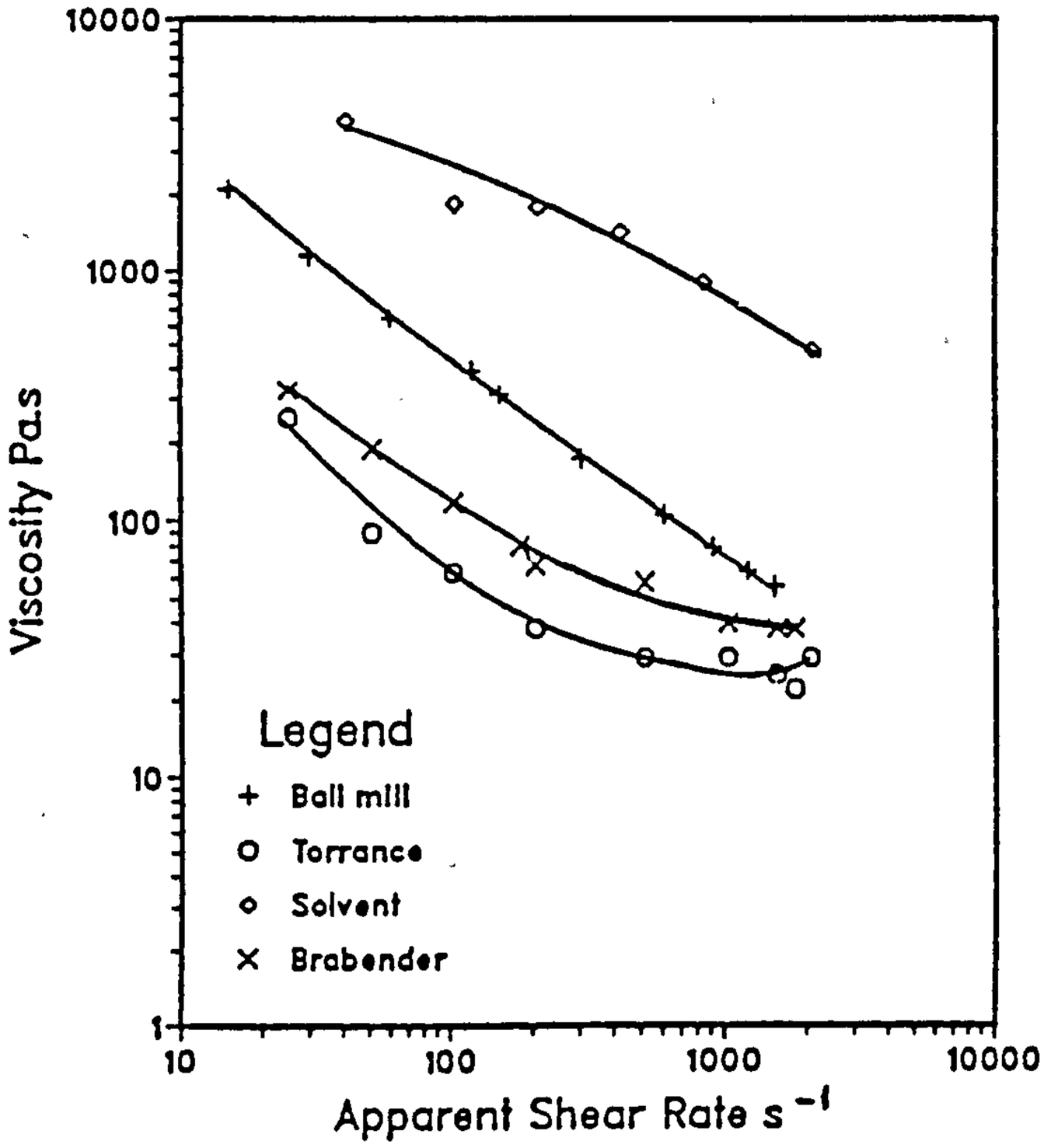

Figure 2.23- Effect of hardmetal volume loading on the rheological characteristics of a waxed based system.

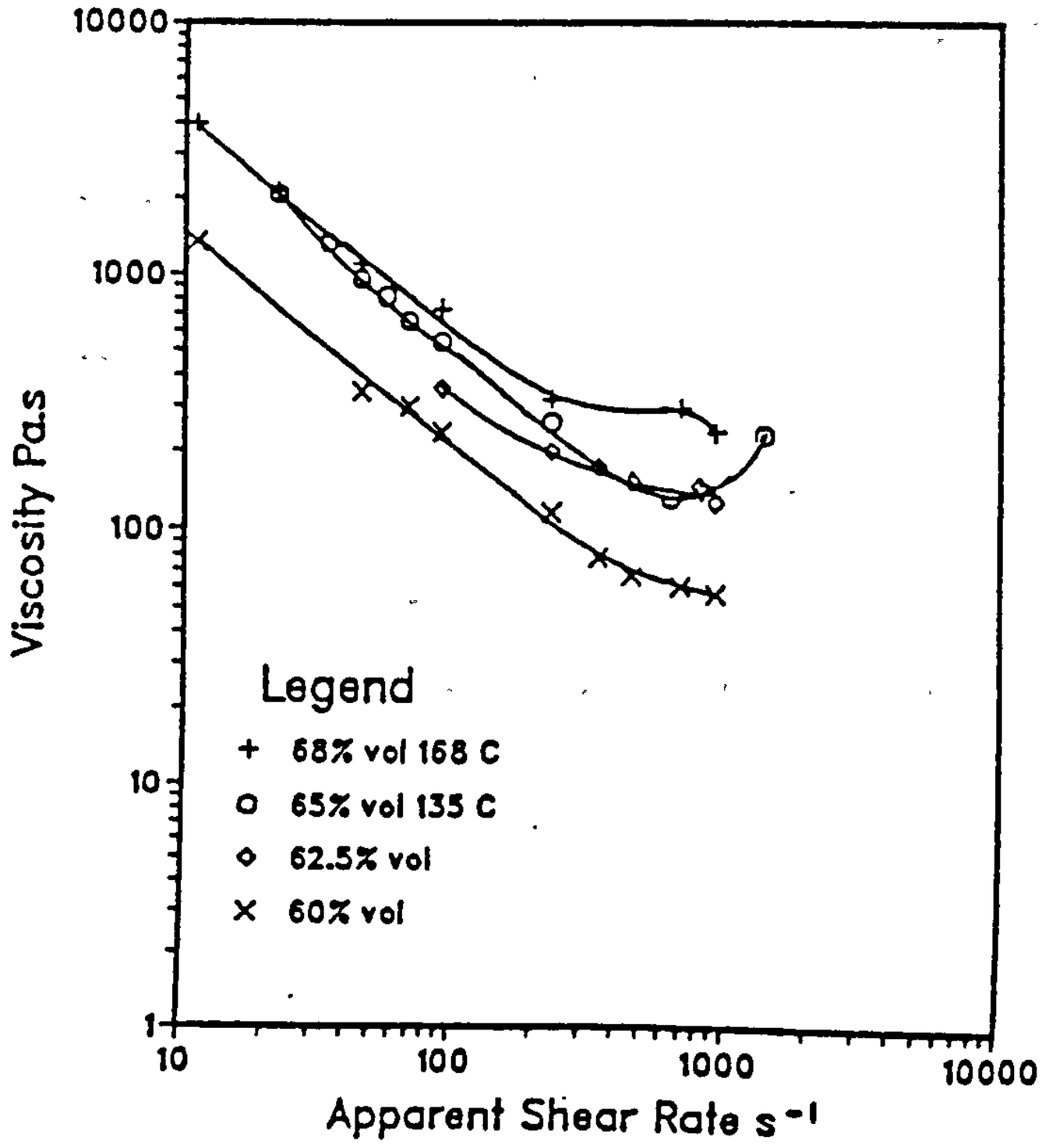

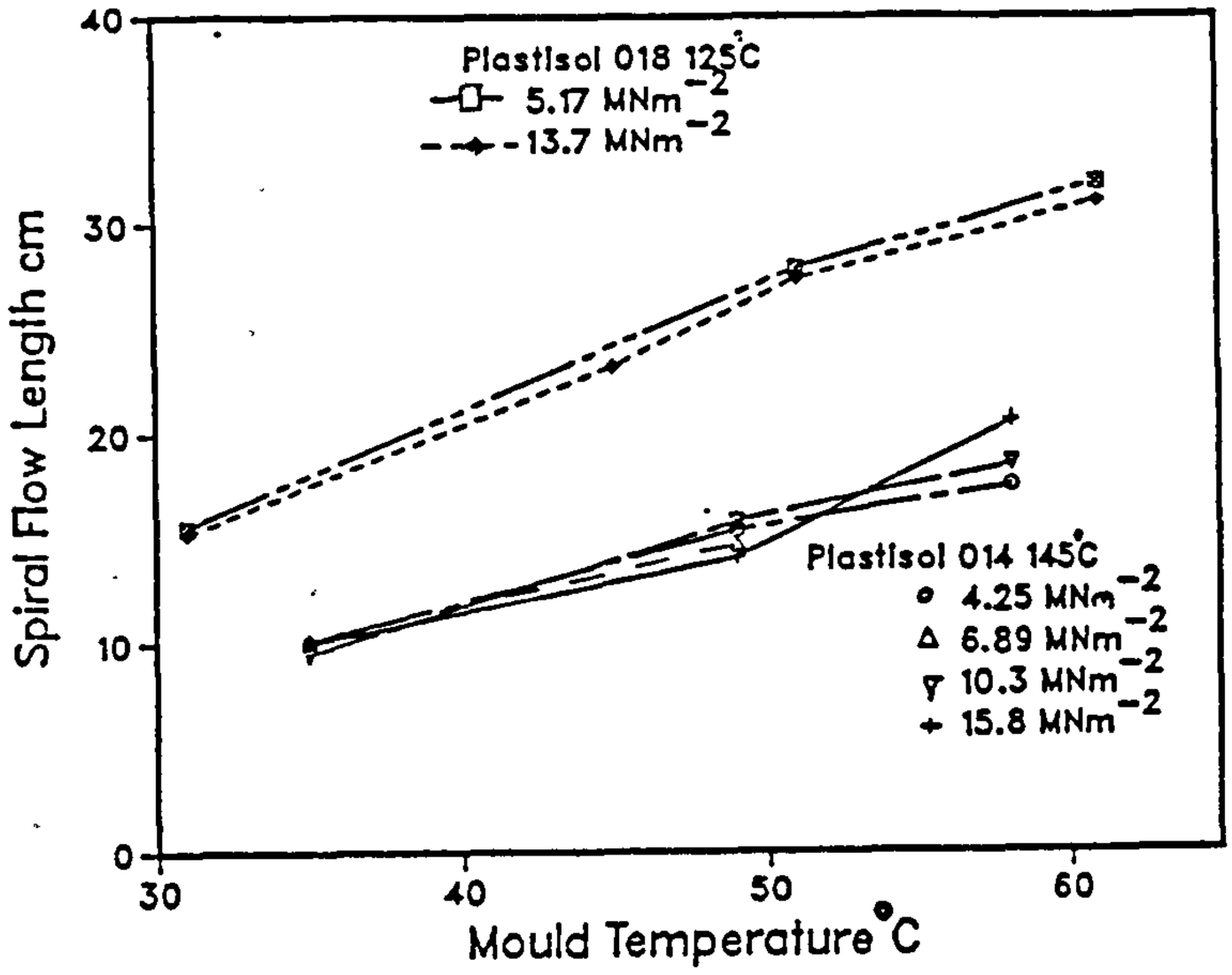

Figure 2.24- Spiral mould flow data for two formulations of different hardmetal volume fraction.

Figure 2.25- Thermograms of various wax types investigated.

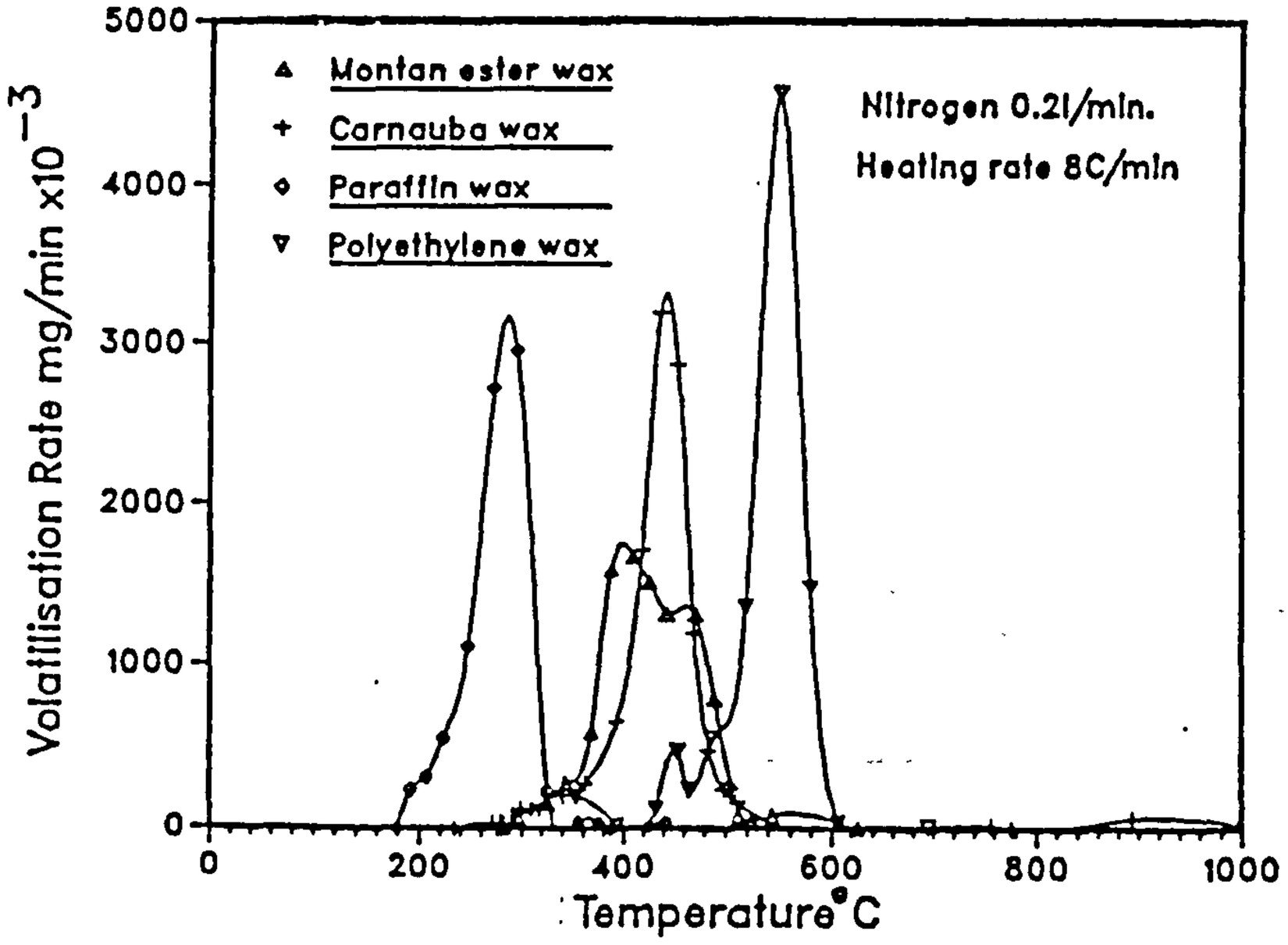

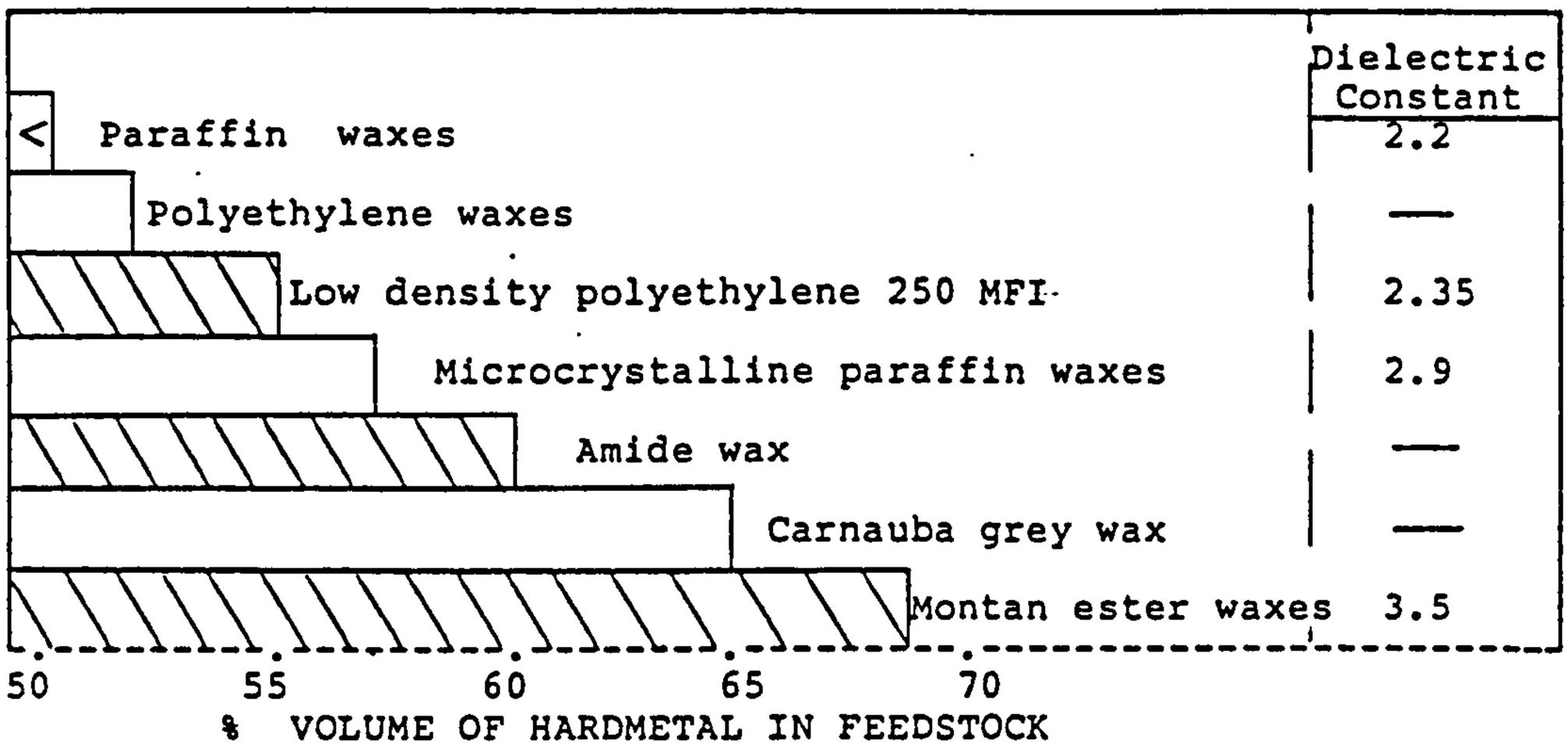

Figure 2.26-Comparison of various polymers and waxes in forming high volume loading feedstocks with satisfactory rheological characteristics in the shear rate range 10^2 - $10^3 s^{-1}$.

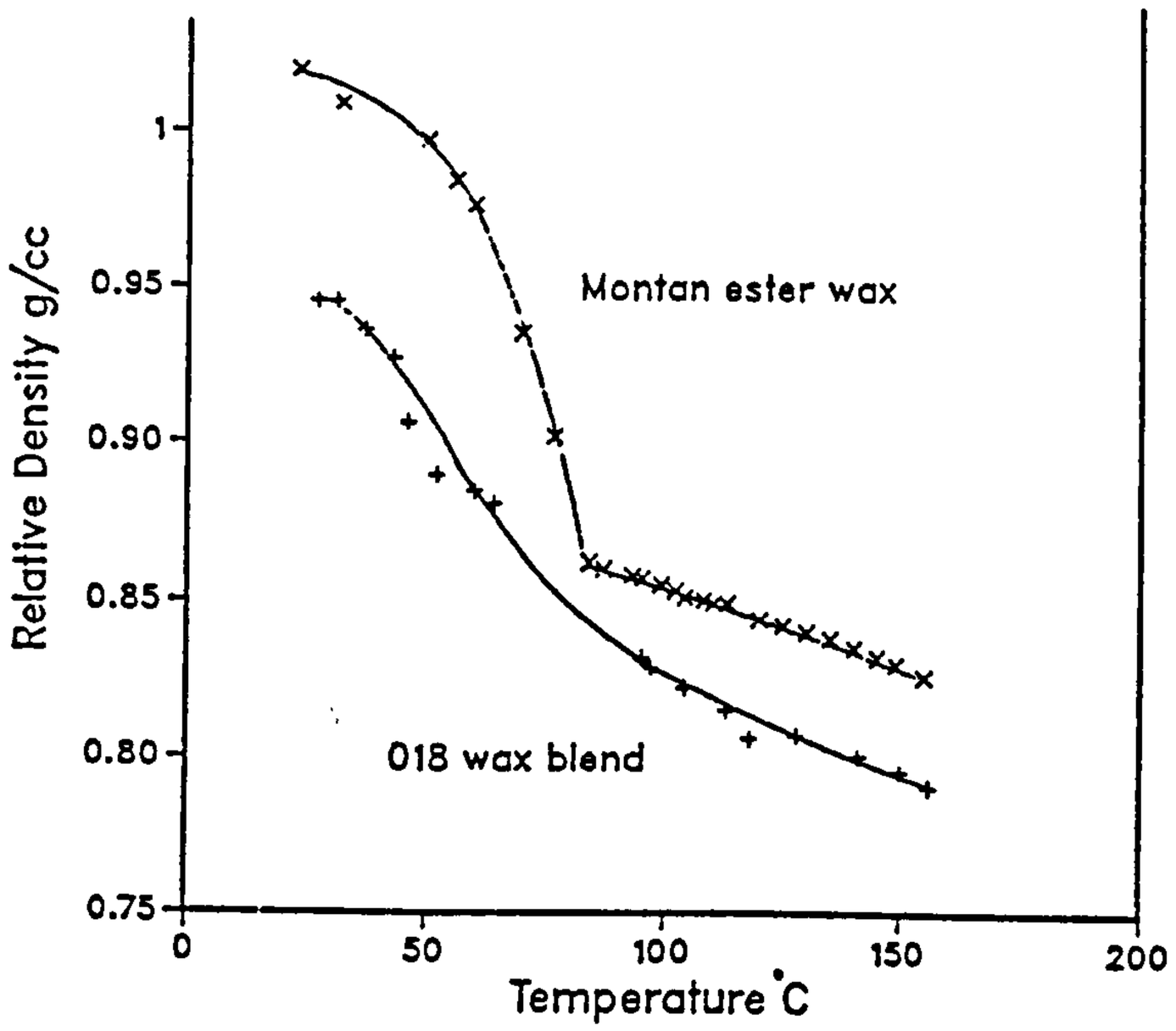

Figure 2.27-Solidification densification of wax systems.

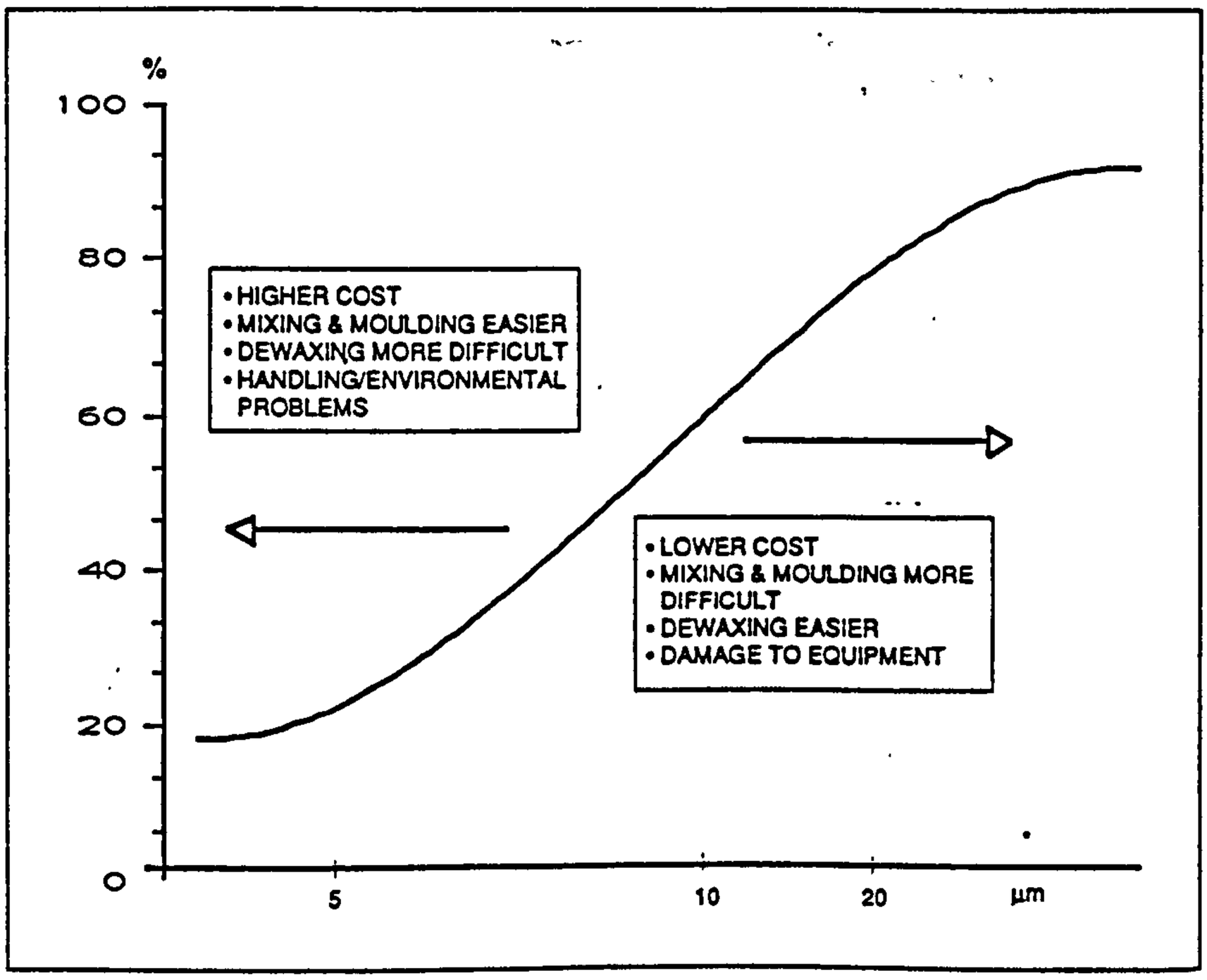

Figure 2.28- *Particle size distribution curve.*

Figure 2.29-
CONTACT ANGLE OF RESIN TO ALUMINA SUBSTRATE CORRESPONDING TO VARIATIONS IN THE TEMPERATURE OF THE RESIN.

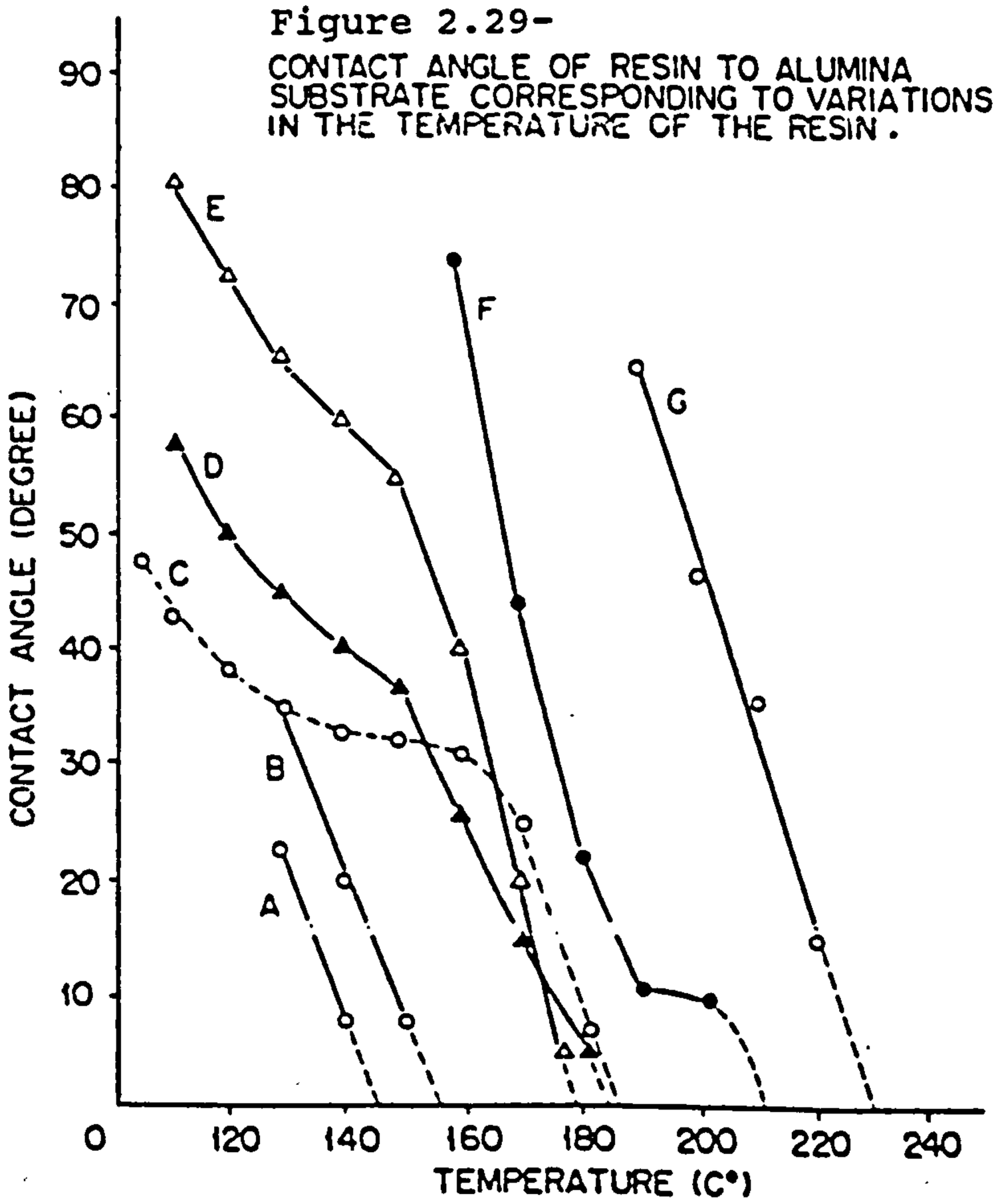

Figure 2.30- RELATIONSHIPS OF THE SPIRAL FLOW LENGTH TO THE PRESSURE AND TEMPERATURE OF INJECTION MOLDING.

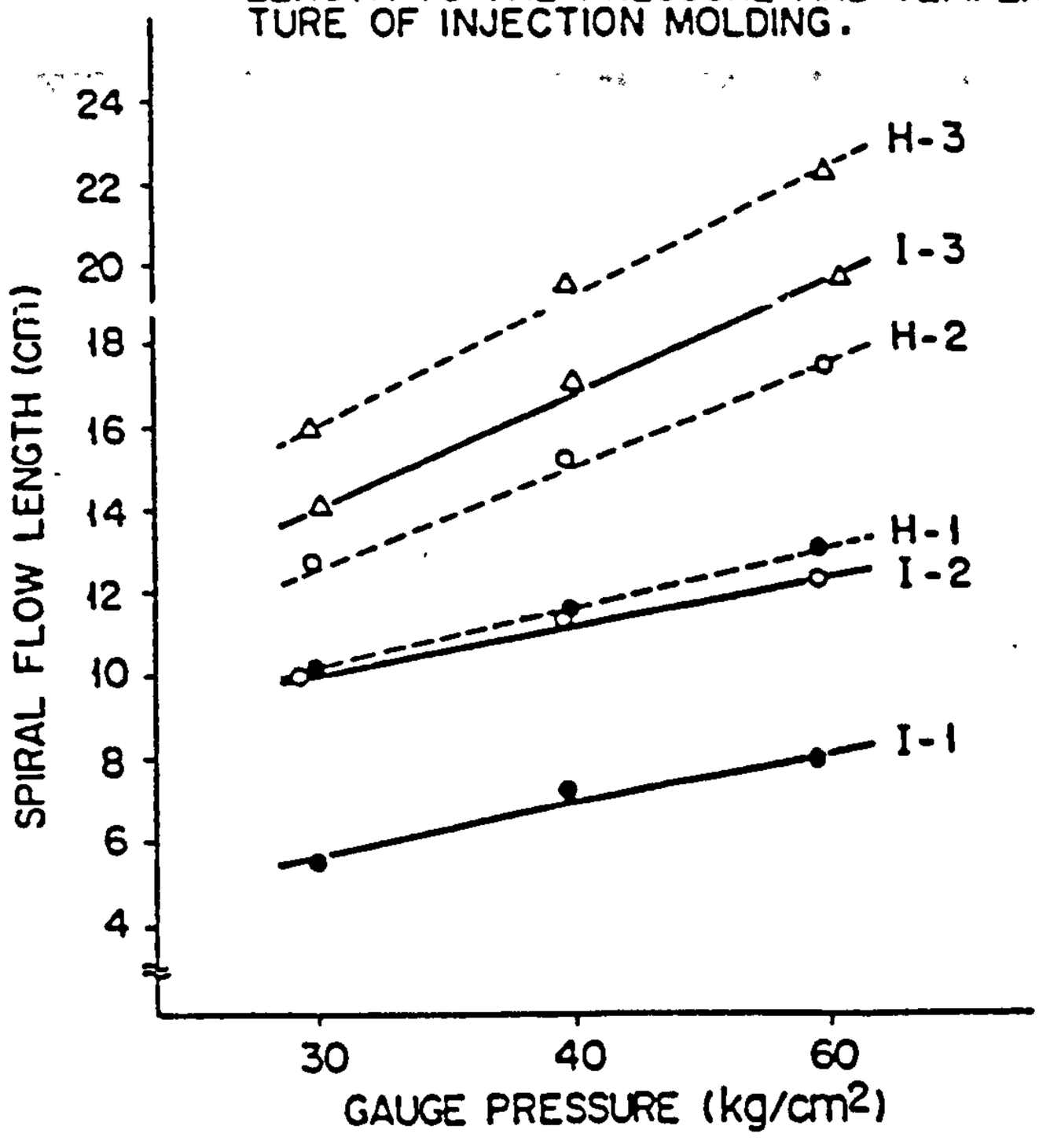

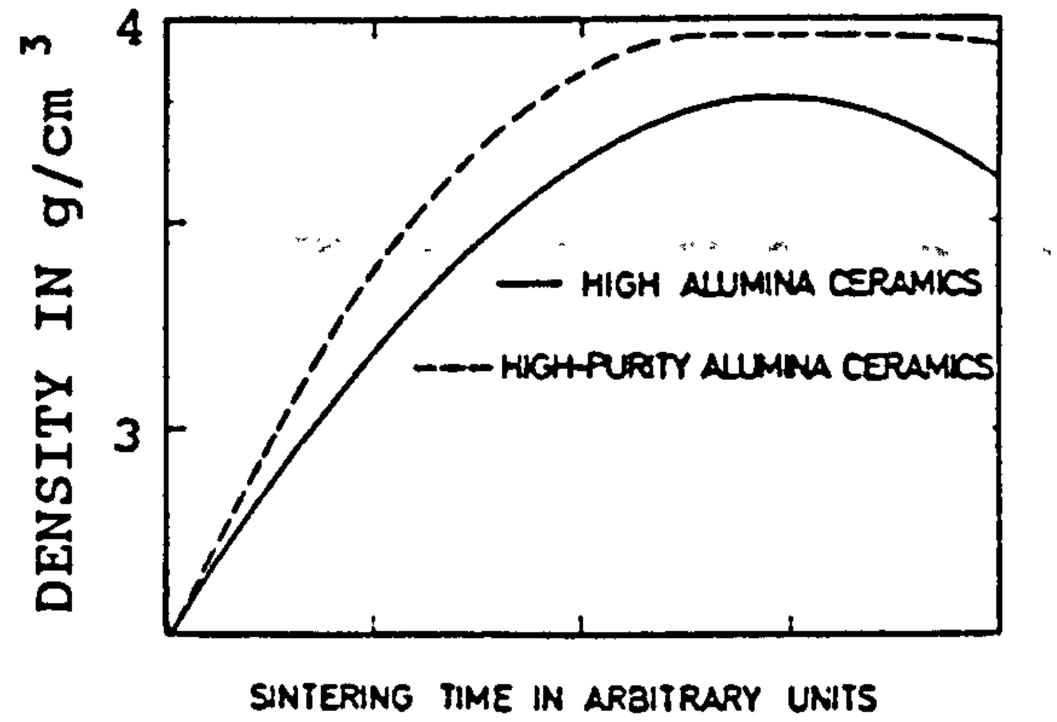

Figure 2.31- Development of the density of alumina ceramics during sintering.

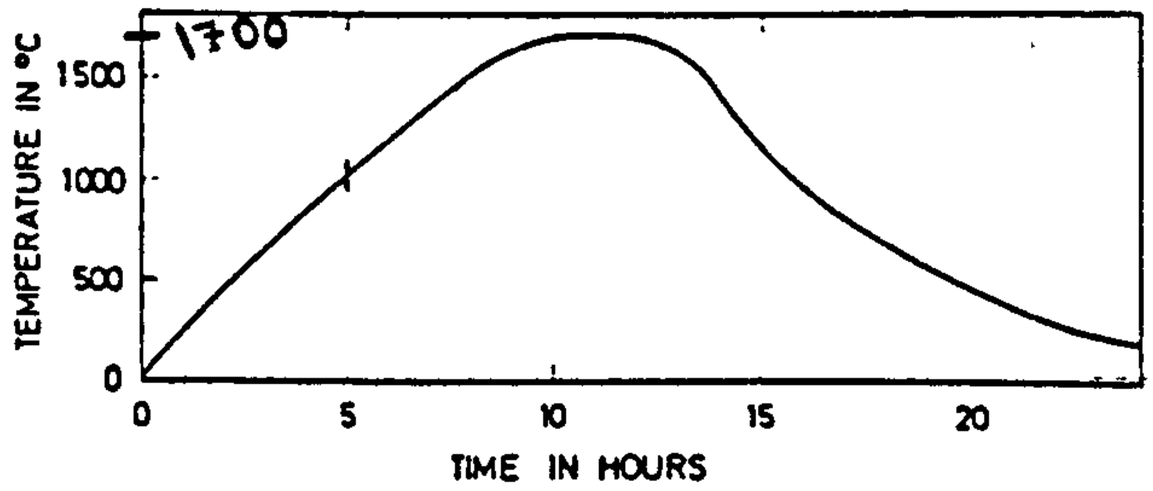

Figure 2.32- Sintering cycle for medium sized parts.

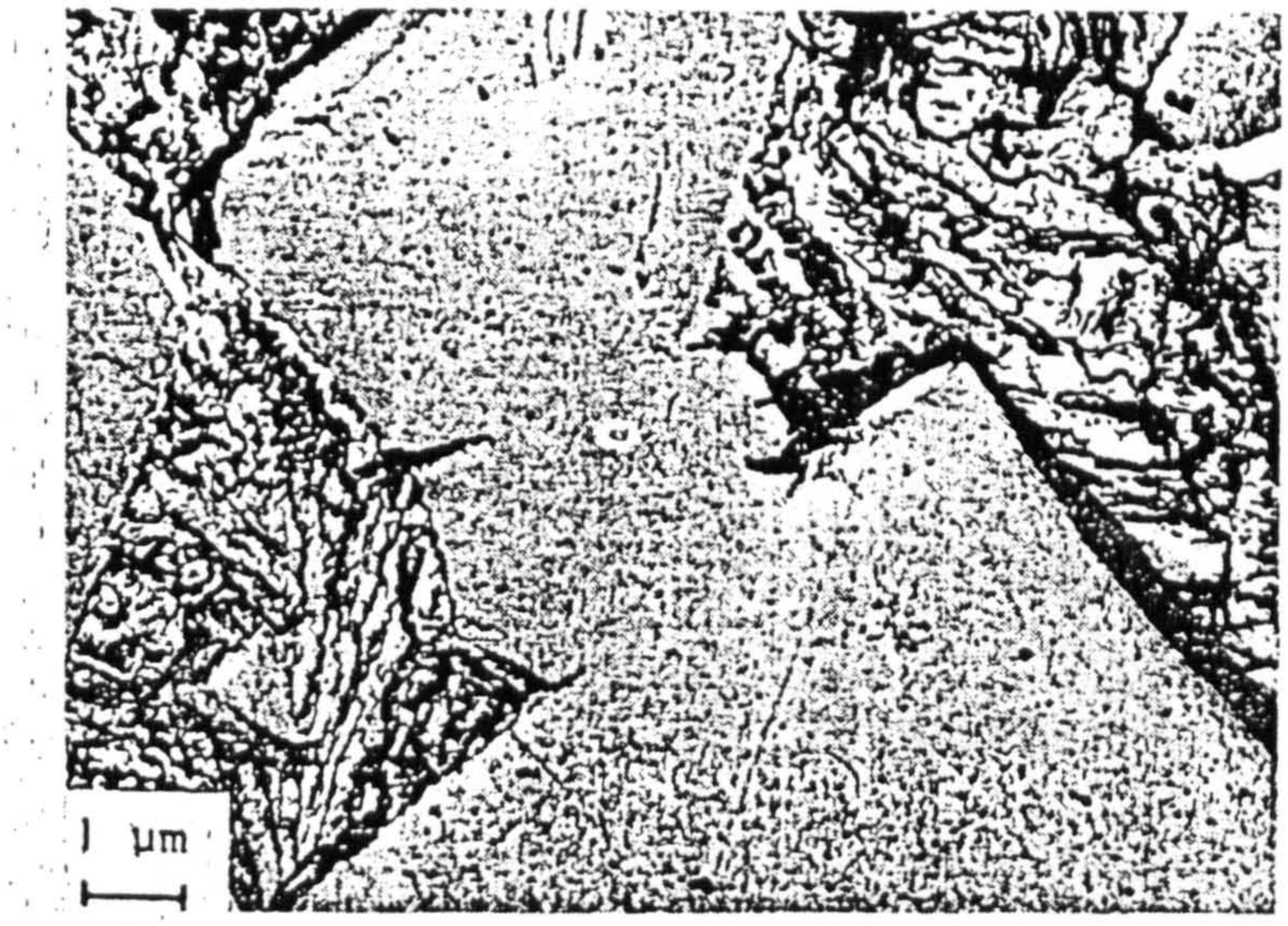

Figure 2.33- Microstructure of alumina ceramics with additions of 10% silicates.

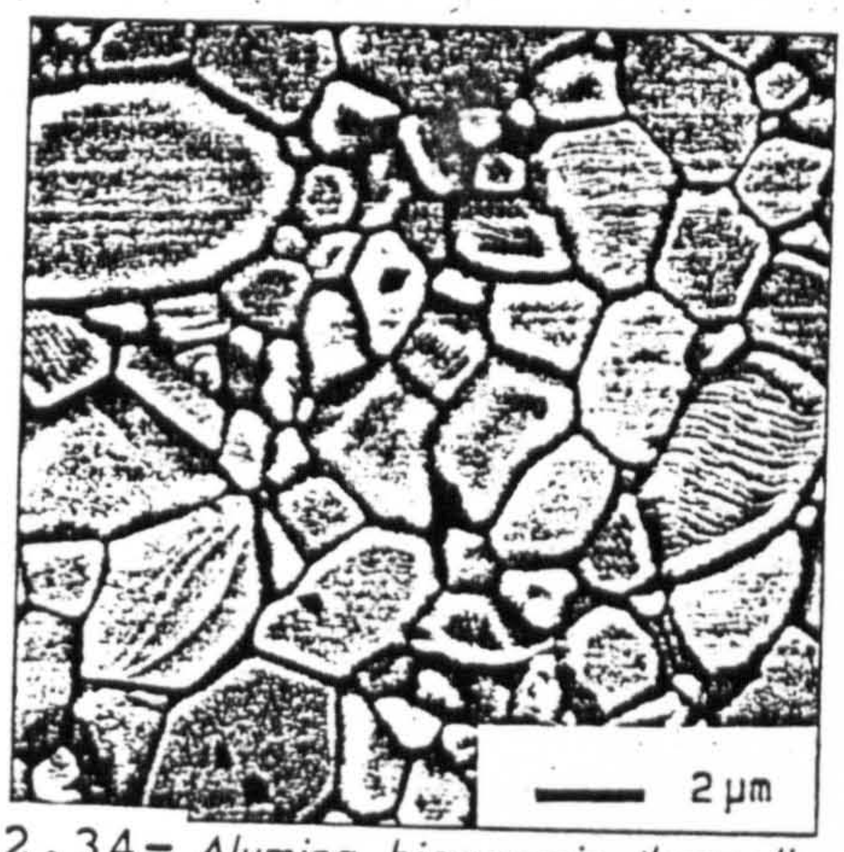

Figure 2.34- *Alumina bioceramic thermally etched at 1500°C for 2 h (SEM).*

CHAPTER THREE

CHAPTER THREE

3- EXPERIMENTAL

This chapter is devoted to materials and equipment used during this research work. The first part of this chapter covers all the powders (ceramic and metallic) and organic materials with their relevant properties. The second part covers the equipment and procedures used for the experimental work.

3.1- Materials used and their properties

3.1.1- Powders and their properties

This section of chapter three covers all the ceramic, nitride, carbide, cermet and metallic powders with their physical and chemical properties relevant to this work.

3.1.1.1- Aluminium oxide

The 99.5 % aluminium oxide (or alumina, Al_2O_3) powder was supplied by BA Chemicals Ltd., Buckinghamshire under the Trade name BACO RA7 and had the following properties given by the supplier.

BACO RA7 is a white, crystalline, medium-soda aluminium oxide which has been finely milled. When properly used it does not constitute a risk to health nor does it carry any fire or explosion hazard. It is recommended that masks are worn when any dusty mixing processes are carried out since fine particles of dust may cause irritation to the breathing passages.

Chemical analysis (%)

Al_2O_3	99.5
Na_2O	0.18
SiO_2	0.07
Fe_2O_3	0.02
CaO	0.03
Loss on ignition	0.2

Physical properties

Average particle size (μm)	1.4
Particle size distribution (μm)	0.1-10
Specific surface area (m^2/g)	3
Particle shape	Near spherical with some agglomeration
Bulk density (g/cm^3)	
Tamped	1.58
Untamped	1.1
Full density (g/cm^3)	3.87
Water absorption value (g/100g)	15

See Fig. 3.1 at the end of this chapter for a typical particle size distribution curve provided by the supplier.

3.1.1.2- Zirconium oxide

The 99.9 % zirconium oxide (or zirconia, ZrO_2) powder was obtained from Aldrich Chemical Company Ltd., Dorset and had the following properties.

Physical properties

Average particle size (μm)	4.2
Particle size distribution (μm)	0.1-20
Specific surface area (m^2/g)	8.5
Particle shape	Near spherical
Colour	Grey/white
Full density (g/cm^3)	5.8
Safety	Irritant

See Fig. 3.2 for the particle size distribution curve obtained during this work using the Malvern particle sizer.

3.1.1.3- Silicon nitride

The silicon nitride powder (predominantly ß-phase) was obtained from Aldrich Chemical Company Ltd., Dorset and had the following properties.

(see next page)

Physical properties

Average particle size (μm)	9.5
Particle size distribution (μm)	0.5-55
Specific surface area (m^2/g)	22
Particle shape	Near spherical
Tap density (g/cm^3)	1.2
Full density (g/cm^3)	3.2
Colour	Grey/green
Safety	Irritant

See Fig. 3.3 for the particle size distribution curve obtained during this work using the Malvern particle sizer.

3.1.1.4- Silicon carbide

The silicon carbide powder was also obtained from the Aldrich Chemical Company Ltd., Dorset and had the following properties.

Physical properties

Average particle size (μm)	52
Particle size distribution (μm)	10-100
Specific surface area (m^2/g)	31
Particle shape	Mostly plate-like
Tap density (g/cm^3)	1.8
Full density (g/cm^3)	3.2
Colour	Black

See Fig. 3.4 for the particle size distribution curve obtained during this work using the Malvern particle sizer.

3.1.1.5- Tungsten carbide-6 weight % cobalt

The tungsten carbide-6 weight % cobalt (or hardmetal/cermet, WC-6 wt. % Co) powder was supplied by Sandvik Hard Materials Ltd., Coventry and had the following properties given by the supplier.

Physical properties

Average particle size (μm)	1.2
Particle size distribution (μm)	sub.-16
Specific surface area (m^2/g)	0.43
Particle shape	Plate/needle like

Tap density (g/cm^3)	6.87
Full density (g/cm^3)	14.95
Colour	Black

3.1.1.6- Iron-2 weight % nickel

The iron-2 weight % nickel (Fe-2 wt. % Ni) powder was a mixture of 70 weight % pure iron (gas atomised-Osprey Metals Ltd.) + 28 weight % pure iron (carbonyl-Poudmet) + 2 weight % nickel (SP4-Inco) and had the following properties given by the supplier.

Physical properties

Average particle size (μm)	10
Particle size distribution (μm)	1-46
Specific surface area (m^2/g)	9
Particle shape	Almost spherical
Tap density (g/cm^3)	2.4
Full density (g/cm^3)	7.88
Colour	Brown/red

3.1.1.7- Silicon dioxide

The 99 % silicon dioxide (or silica, SiO_2) powder was supplied by the British Industrial Sands Ltd., Ipstones and had the following properties obtained during this work.

Physical properties

Average particle size (μm)	18
Particle size distribution (μm)	0.1-100
Specific surface area (m^2/g)	0.3147
Particle shape	Near spherical
Full density (g/cm^3)	2.6
Colour	White

See Fig. 3.5 for the particle size distribution curve obtained during this work using the Malvern particle sizer.

3.1.1.8- Calcium oxide

The 99.9 % calcium oxide (or calcia, CaO) powder was supplied by the FSA Chemicals, Loughborough and had the following properties obtained during this work.

Physical properties

Average particle size (μm)	24.3
Particle size distribution (μm)	5-100
Specific surface area (m^2/g)	0.087
Particle shape	Near spherical
Full density (g/cm^3)	3.3
Colour	White
Safety	Irritant

See Fig. 3.6 for the particle size distribution curve obtained during this work using the Malvern particle sizer.

3.1.1.9- Magnesium oxide

The 99 % plus magnesium oxide (or magnesia, MgO, calcined) powder was obtained from Aldrich Chemical Company Ltd., Dorset and had the following properties.

Physical properties

Average particle size (μm)	14.6
Particle size distribution (μm)	sub.-44
Specific surface area (m^2/g)	0.13
Particle shape	Near spherical
Full density (g/cm^3)	3.58
Colour	White

3.1.1.10- Chromium oxide

The 99 % plus chromium oxide (Cr_2O_3, fused) powder was obtained from Aldrich Chemical Company Ltd., Dorset and had the following properties.

(see next page)

Physical properties

Average particle size (μm)	4.5
Particle size distribution (μm)	0.1-40
Specific surface area (m^2/g)	0.6817
Particle shape	Near spherical
Full density (g/cm^3)	5.21
Colour	Green
Safety	Irritant

See Fig. 3.7 for the particle size distribution curve obtained during this work using the Malvern particle sizer.

3.1.1.11- Yttrium oxide

The 99.99 % yttrium oxide (or yttria, Y_2O_3) powder was obtained from Aldrich Chemical Company Ltd., Dorset and had the following properties.

Physical properties

Average particle size (μm)	10
Particle size distribution (μm)	0.1-30
Specific surface area (m^2/g)	0.16
Particle shape	Near spherical
Full density (g/cm^3)	5.01
Colour	White

3.1.2- Organic materials

This section of chapter three covers all of the organic materials used during this research work. Due to the large number of properties for the organic materials it is intended to give only those properties of each material which are relevant to this work. Note also that the burning properties (thermogravimetric behaviour or analysis) of the lubricants, plasticisers, thermoplastic and wax binders are given in the Results Chapter (Chapter four of this thesis).

3.1.2.1- Ethylene vinyl acetate (EVA) copolymer

This material was obtained from Aldrich Chemical Company Ltd., Dorset and had the following properties.

Vinyl acetate content (%)	25
Molecular weight	-4000
Density (g/cm^3)	0.93
Melt flow index	350
T_g (glass transition temperature, °C)	- 28
Physical form	Beads

This EVA copolymer is atactic (amorphous) and it is used as a major binder during this work.

3.1.2.2- Polystyrene

This polystyrene was an easy flow grade (1810) and it was supplied by Atochem-UK Ltd., Stalybridge, Cheshire and had the following general properties given by the supplier.

Molecular weight	10000-50000
Density (g/cm^3)	1.04
Melt flow index (200°C 5 Kg load)	20
Vicat softening temperature (1 Kg load, °C)	87
Physical form	Beads

This material is used as a major binder during this work.

3.1.2.3- Polyacetal copolymer

The polyacetal copolymer (also referred to as polyoxymethylene) with the Trade name Kemetal-Grade M90 was supplied by Hoechst Celanese Plastics Ltd., Watford and had the following properties given by the supplier.

Molecular weight	>100000
Density (g/cm^3)	1.41
Burn rate (1 mm thickness, mm/min)	24
Physical form	Beads

This material is used as a major binder during this work.

3.1.2.4- Atactic polypropylene (APP)

Two atactic polypropylenes having different molecular weights were obtained from APP Ltd., UK Branch with the following properties obtained by a polymer analyst in RAPRA Thechnology Ltd., Shrewsbury.

Material	Average molecular weight	Density (g/cm^3)	Physical form
APP	10600	0.86	Solid block
APP	60400	0.9	Solid block

The atactic polypropylene is a by-product of the stereoregular polypropylene and being amorphous does not have a sharp melting point and melts over a temperature range of 110-140°C. This material is quite soft and rubbery and has a softening temperature below 0°C. It is used as a major binder during this work.

3.1.2.5- Methylcellulose (water-soluble polymer)

The methylcellulose was the Methocel 20-223 obtained from the Dow Chemical Co., UK Branch and had the following general properties given by the supplier.

The Methocel is a Trademark used by the Dow Chemical Co. and it

is a cellulose ether product. Aqueous solutions of this methylcellulose polymer gel upon heating, are pseudoplastic and surface active. These gels are completely reversible, i.e. they liquify upon cooling. The methylcellulose is produced by methylating cellulose (wood pulp or cotton linters) with methyl chloride in the presence of caustic soda (NaOH). The nominal viscosities in 2 weight % aqueous solution at 20°C for weight average molecular weights ranging from 20000 to 800000 are 5 to 100000 m Pa s respectively. Methylcellulose dissolves in water at room temperature. The incipient gelation temperature of a 2 % aqueous solution of Methocel 20-223 having nominal viscosity of 100 m Pa s at a shear rate of 86 per second when heated at 0.25°C/min is about 48-50°C. However, the gelation temperature decreases in the presence of additives which may compete with the polymer for water. Depending on the molecular weight, concentration and temperature, gels in a wide variation of strengths, viscosities and rheological behaviours can be achieved which make these polymers useful as binders in various ceramic processes. In extrusion and injection moulding of ceramic bodies, thermal gelation of methylcellulose after extrusion and injection provides the high wet strength required for fabrication of extremely complicated shapes. The methylcellulose, by thermal gelation, inhibits binder migration during drying and this gives uniform green strength in the article. Binder migration can be a problem in many other processes, such as tape or slip casting and granulation. Methylcellulose offers a solution to this problem while providing desired plasticity, viscosity and flow characteristics achievable by proper choice of molecular weight and concentration.

It is important to have a clear burn-out of any organic binder in ceramic materials, since residues of ash and carbon can adversely affect critical properties of the ceramic. Methylcellulose and its chemical modifications are carbohydrate and non-ionic in structure. These products contain no sodium as a major component of chemical structure and in this respect differ from carboxymethylcellulose which is a polyelectrolyte

type of polymer.
The thermogravimetric analysis (TGA results) obtained at a heating rate of 10°C/min is shown in Fig. 3.8 at the end of this chapter. This is for oxidising (air) and inert (nitrogen containing less than 5 ppm oxygen) atmospheres. In an inert atmosphere, there was an initial weight loss of ~ 5 % due to vapourisation of water. The methylcellulose lost no more weight until ~ 280°C where it went into a sharp pyrolytic degradation and lost another 82 % of weight before reaching 410°C. Above 410°C there was a gradual loss of another 2 % until ~ 800°C where approximately 10 % carbon residue remained. The addition of 10 % carbon monoxide to create a reducing atmosphere did not alter the shape of the curve for this inert atmosphere. The TGA in air shows an initial weight loss of ~ 3 % followed by no furthur loss until a sharp oxidative as well as pyrolytic degradation and an additional weight loss of ~ 72 %, took place between 250°C and 350°C. Above 350°C furthur oxidative degradation, producing 99 to 100 % weight loss at 500°C, took place indicating combustion of the carbon residues to carbon dioxide. Thus for temperatures up to 900°C, complete burn-out of methylcellulose products may require the presence of some oxygen (see reference 175).
A wide variety of compounds can be generated during pyrolysis of methylcellulose. The type and extent depend on all the variables of furnace operation. Some of the pyrolysis products of methylcellulose are potentially hazardous, but not significantly more so than gases generated in other ceramic firings. Secondary combustion of exhaust gases may be desirable if gas odors are a problem (175).

3.1.2.6- Polyethylene glycol

This material was obtained from Aldrich Chemical Company Ltd., Dorset and had the following properties given by the supplier.
(see next page)

Average molecular weight	8000
Viscosity at 100°C (Centistokes)	800
T_m (melting temperature, °C)	62
Density (g/cm^3)	1.2
Physical form	Powder

This material is a crystalline, synthetic water-soluble polymer and is used as a major binder during this work.

3.1.2.7- Montanester wax

This material was obtained from Hoechst UK Ltd., Halifax with the Trade name Hoechst-Wachs E and had the following properties given by the supplier.

Molecular weight	250-550
Viscosity at 100°C (m Pa s)	. 30
Density (g/cm^3)	1.01-1.03
Colour	Pale yellowish
Physical form	Flakes of size 125-500 µm

This material is used as a major binder during this work.

3.1.2.8- Paraffin wax

This material was obtained from FSA Chemicals, Loughborough and had the following properties.

Molecular weight	. 300-500
Melting point (°C)	56-61
Kinematic viscosity at 100°C (Centistokes)	3.6-4
Density (g/cm^3)	0.89
Physical form	Solid block
Colour	White

This material is used as a minor binder during this work.

3.1.2.9- Carnoba wax

This material was available in the Department and had the following general properties. (see next page)

Molecular weight	- 400-600
Melting point (°C)	- 80
Density (g/cm^3)	0.9
Physical form	Solid block
Colour	White

This material is used as a minor binder during this work. From the literature (146) it is found that carnoba wax is often used as a major or minor binder. It has excellent wetting properties that allow plastic flow in low binder concentrations. However, if unmodified, it does not provide the physical strength required for removing parts from the moulds (146). Early modifiers included other waxes and low molecular weight polyethylene. They were compatible, but they had adverse effects on wetting and flow, and contributed very little to strength. To reduce the brittleness and improve the toughness of the carnoba wax a less compatible additive that could disrupt crystallinity and provide plasticisation is required (146). Carnoba waxes consist of long chain, primary alcohols and are considered essentially nonpolar, despite the polar terminal functional groups (176).

3.1.2.10- Microcrystalline wax

This material was also available in the Department with a Trade name Multiwax W-445 and had the following properties.

Molecular weight	- 500-800
Melting point (°C)	78.3
Viscosity at 100°C (Centistokes)	- 8
Density (g/cm^3)	0.9
Physical form	Solid block
Colour	White

This material is used as a minor binder during this work. These waxes are known as microcrystalline because their relatively small crystals give an amorphous appearance to the waxes in solid state. Microcrystalline waxes vary considerably in composition and properties, in contrast to paraffin wax.

Generally, microcrystalline waxes consist of branched-chain hydrocarbons and naphthenic hydrocarbons as well as some straight-chain molecules, depending on the particular wax. This wax has moderate chemical reactivity to paraffin wax (176). On the other hand paraffin waxes are basically mixtures of saturated straight-chain hydrocarbons. These paraffin waxes are soluble in non-polar organic solvents such as benzene, chloroform, carbon tetrachloride and naphtha and insoluble in polar solvents such as water and methanol. They have generally lower melting, lower molecular weights and lower viscosities when liquid than microcrystalline waxes. In the solid state, they exist in the form of large, distinct crystals, in contrast to the microscopic crystals of microcrystalline waxes (176).

3.1.2.11- Stearic acid

The 99 % plus stearic acid was obtained from Aldrich Chemical Company Ltd., Dorset and had the following properties.

Molecular weight	284.5
Melting point (°C)	67-69
Boiling point (°C)	183-184
Density (g/cm^3)	0.847
Physical form	Flakes
Colour	Yellow

This material is used as a lubricant during this work.

3.1.2.12- Diethyl phthalate

This material was obtained from Aldrich Chemical Company Ltd., Dorset and had the following properties.

Molecular weight	122
Melting point	Liquid
Boiling point (°C)	296
Density (g/cm^3)	1.118
Colourless	

This material is used as a plasticiser during this work.
Plasticisers and lubricants are often used for the injection

moulding of ceramics. A plasticiser enters into the intermolecular void of the polymer and reduces the intermolecular condensing forces. Furthur, a plasticiser acts as a lubricant and increases the fluidity and softness of the polymer. Therefore, plasticisers should be those which do not easily separate out from the polymer and generally have relatively high boiling points (1). However, for ceramic-binder mixtures, a high boiling point plasticiser is not necessary and a plasticiser which can volatilise out before the polymer decomposition is preferred.

3.1.2.13- Liquid paraffin

This material was obtained from FSA-Chemicals, Loughborough with its Grade Technical-CAS 8012-95-1 and had the following properties.

Molecular weight	- 200
Melting point	Liquid
Boiling point (°C)	- 300
Density (g/cm^3)	0.88
Colourless	

This material is used mainly as a plasticiser during this work, but it was found that this material provided both excellent plasticity and lubricity particularly for alumina powders.

3.1.2.14- Polyisobutylene

This material came from the Exxon Chemical Company, USA, with the Trade name VISTANEX and had the following properties given by the manufacturer.

Viscosity average molecular weight (Staudinger)	
for LM-MS (*1) grade	8700-10000
for LM-MH (*2) grade	10000-11700
for MM (*3) grades	64000-135000
Viscosity average molecular weight (Flory)	
for LM-MS grade	40000
for LM-MH grade	50000

for MM grades 990000-2100000

Density (g/cm^3, all grades) 0.92
Colour White to pale yellow

This material is used as a minor amorphous binder in order to reduce the crystallinity and shrinkage of the montanester wax so as to prevent the shrinkage cracking problem of the moulded samples.
VISTANEX polyisobutylenes are highly paraffinic hydrocarbon polymers, composed of long-straight chain molecules having terminal unsaturation only. Because of this molecular structure they are relatively inert and resistant to chemical or oxidative attack, but are soluble in hydrocarbon solvents. VISTANEX is light coloured, odorless, tasteless and nontoxic. They are classified into two groups according to molecular weight range: the LM (low molecular weight) grades are clear, very viscous tacky semi-solids (which were used during this work) and the MM (medium molecular weight) grades which are tough rubbery solids. The LM grades of VISTANEX blend readily with oils, waxes, solvents and with other polymers. They can be handled and processed like other viscous tacky materials using heavy-duty mixers such as those made by Baker Perkins and Bramley machinery. VISTANEX LM will soften substantially with temperature. A Brookfield viscosity of 10 Centipoise at - 100°F (~38°C) decreasing to 0.05 Centipoise at 350°F (~177°C) has been obtained by the supplier.
VISTANEX like other elastomers, breaks down and depolymerises when severely kneaded or milled in contact with air or oxygen. This means that, e.g. the molecular weight will decrease from - 0.16 (Staudinger) to - 0.05 after 24 h mastication in a Banbury mixer at 140°C.
The LM and MM grades of VISTANEX can be compounded easily with fillers, plasticisers, other polymers, waxes and other materials. VISTANEX should be the matrix to which other materials are added since it is more viscous at compounding temperatures than wax and other materials commonly blended with

VISTANEX. Addition should be slow and as the mix approaches the consistency of the material being added, the rate of addition can be increased.

Good processability and release are obtained by using plasticisers of limited compatibility such as ester like tricresyl phosphate or triethylene glycol diethylhexoate.

VISTANEX polyisobutylenes are highly resistant to penetration by water vapour and gases, and are often added to other polymers to reduce their permeability. The higher the molecular weight of the polyisobutylene the lower its permeability.

VISTANEX polyisobutylenes are very stable polymers under normal conditions of use, but they can be degraded or depolymerised by heat, mechanical shear, radiation and some chemicals such as organic peroxides. The thermal depolymerisation of VISTANEX polyisobutylene (TGA results) will be illustrated in chapter four.

During processing, VISTANEX is subject to simultaneous degradation by oxidation, heat and mechanical shear. Oxidation is apparently the most active of these since inclusion of stabilisers in both VISTANEX LM and VISTANEX MM will prevent molecular weight degradation for a long time even at high temperatures and under severe mechanical working. Certain organic peroxides such as ditertiary-butyl peroxide accelerate the depolymerisation of VISTANEX.

Depolymerisation can be retarded or prevented by use of stabilisers such as PARABAR 441 BHT and commercial grades of VISTANEX MM contain very small quantities of this antioxidant added during manufacture. Due to this property the MM grade of VISTANEX polyisobutylene was not used during this work and instead the LM grade was used which did not contain any antioxidant and therefore should depolymerise easily by heat in air during the debinding process.

(*1)= Low molecular weight-medium soft; (*2)= Low molecular weight-medium hard (used during this work); (*3)= Medium molecular weight

3.1.2.15- Polyvinyl alcohol (water-soluble polymer)

The 100 % hydrolyzed polyvinyl alcohol was obtained from Aldrich Chemical Company Ltd., Dorset and had the following properties given by the supplier.

Molecular weight	106000-110000
T_g (°C)	99
T_m (°C)	256
Density (g/cm^3)	1.4
Physical form	Powder
Colour	White

This water-soluble polymer is used as a major binder during this work. Its burning characteristic is very similar to that of water-soluble methylcellulose (see Fig. 3.8).

In spite of the hygroscopicity of polyvinyl alcohol (PVA) it has a very slow rate of solution in water at room temperature or slightly above. Yet PVA dissolves in water readily enough at temperatures of 70°C or more, and as the temperature is increaed it dissolves more rapidly. The T_g of PVA in contact with excess water is readily reduced to below room temperature, through diffusion of water into the glassy phase. The solubility of PVA in water depends on its degree of polymerisation and degree of hydrolysis. Due to having many hydroxyl groups PVA has a high affinity to water. However, with strong hydrogen bonding between the intra and intermolecular hydroxyl groups its solubility in water is restricted. On the other hand, the residual acetate groups in partly hydrolysed PVA are essentially hydrophobic and weaken the hydrogen bonding of adjoining hydroxyl groups. The presence of an adequate amount of these acetate groups increases the water solubility, e.g. an 80 % hydrolysed PVA has a higher solubility than a 88 % hydrolysed PVA at low temperatures, but solubility increases as temperature rises above 40°C for the 88 % hydrolysed PVA, and decreases for the 80 % hydrolysed PVA due to a decrease in the temperature of phase separation.

Up to 10 % PVA (of high degree of hydrolysis) aqueous solutions are found to undergo viscosity increases with time, depending on the storage conditions. This viscosity change can be influenced

by the addition of organic and/or inorganic materials. Organic additives include solvents that are soluble in water (i.e. alcohols). The addition of methanol, acetone, ethylene glycol and dimethylsulphoxide reduces the viscosity stability, but some organic additives, such as isopropanol and n-propanol, show some viscosity-stabilising effect, depending on the amount added, although the effect varries with the conditions. Others such as isobutanol, n-butanol, pyridine, cyclohexanone, cyclohexanol and phenol, have a marked viscosity-stabilising effect.

Aqueous solutions of PVA form a thermal-reversible gel upon cooling to low temperatures, i.e. by heating to - 70°C to dissolve the PVA in water and then cooling the solution to - 5°C to form a gel. The rate of gelation depends upon solution concentration, pressure and temperature. In order to produce gels of sufficient rigidity it will often require long periods typically 40-50 h.

The ease with which PVA gels in solution is strongly dependent on the content of residual acetate groups, i.e. the lower the acetate content the higher the gelling of PVA in solution. It follows therefore that the bulky acetate groups have the adverse effect on the microcrystalline formation and development as the gel ages at room temperature.

However, aqueous solutions of PVA also form stiffer gels with the help of a gelling agent that forms hydrogen-bonded crosslinks in addition to the microcrystalline framework of the ordinary gel. Various organic reagents having phenolic hydroxyl, aromatic primary and secondary amino, and sulphonate groups are found useful in this connection. Systems involving such compounds as polyhydric phenols, naphthylsalicylamide, salicyclic acid diamide, benzidine, and congo red are other examples in this regard.

From 0.5-5 % of the reagent may be added to aqueous solutions containing - 3-20 % of PVA. For example, the addition of - 2 % (dye) Congo Red to a 5 % solution of PVA causes the formation of a gel at room temperatures and converts the gel to a fluid at temperatures above 40°C. Organic compounds which form colourless, thermally reversible gels include resorcinol, catechol,

phloroglucinol, salicylanilide, gallic acid, and 2, 4-dihydroxybenzoic acid (see reference 180).

From the above discussion it is therefore possible to produce rigid gels very quickly by mixing a hot solution of fully hydrolysed PVA with a gelling agent such as resorcinol (which is a phenolic hydroxyl) which will cause the solution to gel rapidly on cooling to about ambient temperatutes. This is very useful as an alternative water-soluble (PVA) binder system to the existing methylcellulose (Rivers) water-soluble binder system for the injection moulding of ceramic/metallic powders as will be seen in chapter four.

3.1.2.16- Resorcinol

The 99 % resorcinol reagent was obtained from Aldrich Chemical Company Ltd., Dorset and had the following properties given by the supplier.

Melting point (°C)	110-113
Boiling point (°C/16 mm)	178
Physical form	Powder
Colour	White
Safety	Toxic irritant

This material is used as a gelling agent for the water-soluble PVA binder system.

3.2- Equipments and procedures

This section of chapter three describes the equipment and the procedures used during this research work. It is intended to describe only those practical and theoretical procedures which are related to this work.

3.2.1- Powder characterisation

This includes average particle size, particle size distribution, particle shape, specific surface area, surface chemistry (e.g. oxide films), dispersion, wettability and surface tension forces. The rheology, apparent and tap densities of ceramic and metallic powders are influenced by these parametric variables (1-7).

During this work average particle size, particle size distribution and specific surface area were determined by using the Malvern particle sizer. These parameters were determined only when they were not given by their suppliers. The Malvern particle sizer uses the laser diffraction technique which is shown schematically in Fig. 3.9 at the end of this chapter. As can be seen from this figure a point He/Ne laser source is expanded using optics to obtain parallel laser beam. Upon hitting a particle suspended in liquid, a component of the beam diffracts at an angle θ. The smaller the particle the larger the angle θ. The diffracted light is focussed (using a Fourier transform lens) on to a series of concentric semi circular detectors. Each detector detects light scattered over a small range of angles, i.e. a small range of particle size. A light scatter distribution is produced. This, however, does not correlate directly with size distribution due to Fraunhofer diffraction, i.e. for a single particle light scatter may be as in Fig. 3.10, and not as one would expect as in Fig. 3.11.

Light scatter distribution must be resolved for all component particles. This is done by regression analysis of light scatter data using a PC software package. This is shown in Fig. 3.12 along with the Malvern instrument.

The particle shapes were determined from SEM pictures of the powders.

No attempts were made to study the surface chemistry, dispersion, wettability and surface tension properties of the powder paricles prior to the injection moulding process. These properties will become obvious during the powder-binder formulations, mixing and sintering stages of the injection moulding process.

3.2.2- Mixing processes

Two mixing devices were used during this work. One was a double cone mixer used for the blending of different powders and the other one was the Brabender Plastograph used for the mixing of the powders with the organic materials. These are described as follows:

Double cone mixer

This is the most common type of mixing equipment used for the mixing of different metallic and ceramic powders (106) which is shown schematically in Fig. 3.13. The important consideration in mixing is that the powder must not fall freely through the air during any stage of mixing because this will always cause segregation (106). For this reason the cylindrical parts of double cone mixers are kept short and one blade is positioned across the diameter of the cylinder in one of the cones as shown in Fig. 3.13.

Brabender Plastograph

This is a recording torque rheometer used for testing and mixing thermoplastics, thermosets, elastomers and many other plastifiable materials as well as filled polymers such as the ceramic/metallic-binder mixtures (62).

By using various measuring heads many different tests can be carried out. For example, by employing measuring heads such as mixing head, extruders, etc., production process like mixing, extruding, etc. can be simulated on a laboratory scale followed

by measurements. Other processes include kneading, masticating, calendering, etc.

The Brabender torque rheometer plastograph functions according to a practice related dynamic measuring method. The measuring principle is based on the fact that the resistance, which the test material puts up against rotating blades, rotors, screws, etc., in the measuring mixer or extruder is made visible. The corresponding torque moves a dynamometer from its zero position. In accordance with established test conditions a typical plastogram (see Figs. 2.7 or 4.1 in chapters two and four) is traced (i.e. torque versus time) for every type of material. The torque is measured in meter gram (mg). The apparent viscosity of test material can also be evaluated rheologically.

Parameters, which influence the viscosity of the material under test, such as temperatures of the measuring heads and shear rate, can be varied over a wide range. Therefore, it is possible to create test conditions similar to the processing conditions of mixers, moulds, calenders, extruders and injection moulding machines. Whenever the influence of the test conditions on the test material is known, the processing conditions on production machines can be adjusted quickly and reliably.

The influence of stabilizers, plasticisers, lubricants, fillers, catalyts and pigments in the compound on the processability can be determined using the Brabender Plastograph.

The picture of this device used during this work can be seen in Fig. 3.14. The mixing head was a roller mixer of approximately 30 cc volume which was heated by four heating elements (two for each part). The rotor blades of the mixing head were rotating in opposite directions at different speeds providing an excellent mixing effect. Other technical data for this device were as follows according to the technical data sheet provided by the manufacturer.

(see next page)

Dynamometer= DC motor with gear drive, oscillating in bearings
Power output= 1.1 KW (1.5 hp)
Torque= max. 10000 mg (=100 NM) independent of speed
Speed= 5-150 rpm
Total measuring range= 0 ... 10000 mg (=0 ... 100 NM)
Accuracy= Better than ± 1 % of the respective measuring range
Damping= Hydraulic, infinitely variable
Recording= Laterally mounted mechanical continuous line recorder

Power supply permissible voltage= 220 V single-phase
50 ... 60 cps, max. 17.5 A
tolerance -5% + 10%

Dimensions= 600X650X1000 mm
Weight= . 155 Kg

Mixing procedure using the Brabender Plastograph

The mixing procedure used during this work is as follows. For the thermoplastic/wax binder systems the mixing head was firstly heated up to the melting temperature of the binder and then the binder was added to the heated mixing chamber/head. Before adding the ceramic/meatllic powder the organic materials were mixed for . 5-10 min so as to have a homogeneous binder mixture after which the powders were added gradually and slowly so that to allow enough time for the mixture to settle while mixing continued. After reaching the steady state torque (see Fig. 4.1 at the end of chapter four) the mixing was stopped and the mixture was removed from the chamber.

In the case of the water-soluble methylcellulose binder system mixing was done at room temperature since methylcellulose dissolves in water at room temperature and gels upon heating.

In the case of the water-soluble polyvinyl alcohol (PVA) binder system mixing was carried out at 72°C since PVA does not dissolve in water at room temperature and therefore the PVA-powder mixtures were prepared in a heated mixing chamber. The mixtures were removed from the mixing chamber while still hot so as to

avoid the complete gelation at ambient temperatures.
The water-based binder-powder mixtures were usually moulded or tested (e.g. for rheology) immediately after mixing to avoid water losses, alternatively they were stored in a humidity cabinet with more than 90 % humidity.
Note that the exact mixing conditions (temperature, time and speed) for each binder system used during this work are given in the Results Chapter (Chapter four of this thesis).

3.2.3- Rheological measurements

In order to study the rheological behaviour, i.e. viscosity versus shear rate relationship, of the ceramic/metallic powder-binder mixtures two extrusion rheometers were used during this research work. One was the Davenport and the other one was an Instron extrusion rheometer (Model numbers = 3211) shown schematically in Fig. 3.15. Note that the viscosity-shear rate results does not depend on the type of rheometer used.

Procedures and viscosity-shear rate calculations using the Davenport/Instron extrusion rheometers

The powder-binder mixtures were loaded into the preheated barrel of the rheometer (at specific temperatures) and extruded through a die (of length L and diameter d) as shown schematically in Fig. 3.15. The actual temperatures selected were, in some measure, related to the barrel/nozzle temperatures of the injection moulding machines. However, in some cases, attempts were made to assess the effect of temperature on flow by extruding the mixtures at different temperatures. The viscosities and shear rates were obtained by using capillary dies of diameters 1-3 mm and of length 20 mm. These viscosities and shear rates are much higher than those expected during the injection moulding process due to the larger nozzle diameter (=4 mm) of the moulding machines used during this work. The diameter of the capillary dies were chosen smaller than that of the nozzle purposely so as to ensure that the correct flow behaviour is obtained within the barrel and through the nozzle of the injection moulding machines. The correct flow behaviour for ceramic/metallic powder-binder mixtures is the pseudoplastic flow (72) which can be obtained by having the correct powder-binder formulation/composition. The type of flow behaviour is determined from the viscosity-shear rate relatioship after the rheological analysis. This is obtained for each powder-binder mixture used during this work and can be seen in the Results Chapter.

Note that with the Davenport extrusion rheometer pressure variations were recorded from an inbuilt pressure transducer and

with the Instron rheometer pressure variations were read directly from the machine. By measuring the volumetric throughput and knowing the die dimensions, it was possible to calculate shear stress, shear rate and viscosity over a wide range of flow conditions using the following relationships:

Using "viscosity = shear stress/shear rate"

where shear stress, $\tau = (p_2 - p_1)\ r\ /\ 2L = pr\ /\ 2L$ (Pa)

shear rate, $\Gamma = 4Q\ /\ \pi\ r^3$ (s^{-1})

p = pressure = force / csa of the barrel

r = radius of the die

L = length of the die

Q = volumetric throughput = $\pi/4\ .\ D^2\ .\ V$

D = diameter of the barrel

V = velocity through the die = $v_r/60\ .\ (D/d)^2$

v_r = ram velocity

d = diameter of the die

Therefore, shear rate, $\Gamma = 1/15r\ .\ v_r\ .\ (D/d)^2$

and viscosity, $\Sigma = \tau\ /\ \Gamma$ (Pa s) ————(1)

(see Fig. 3.15 for the schematic diagram of the above viscosity-shear rate calculations)

Equation (1) is normally used for Newtonian flow behaviour, where τ is directly proportional to Γ (i.e. $\tau=\Sigma\Gamma$). For systems such as polymer melts and ceramic/metallic powder-binder mixture, flow behaviour deviates from the above in several ways, as illustrated in Fig. 3.16. For these non-Newtonian regimes of flow, i.e. pseudoplastic and dilatant, the viscosity is no longer a constant and takes on an instanteneous value for each value of shear rate and is known as the apparent viscosity Σ_A. In this case shear stress, $\tau=k\Gamma^n$ ————(2), where n is the material's 'flow index' and k is an empirical constant. Equation (2) is known as the 'power law' equation (15).
Ideally, this power law should reduce to a linear relationship

in a log-log plot of τ versus Γ, known as the materials flow curve with a constant gradient n. In practice, however, ceramic/metallic powder-binder mixtures do not produce flow curves that exhibit linear relationships over wide ranges of shear rate. Thus, a correction factor, (3n+1)/4n, has been developed (15) for the power law equation, which has proved to give a better fit to experimental data. Thus correction of non-Newtonian flow behaviour is determined by evaluating the gradient n from the material's flow curve in narrow regions of shear rate where it approximates to a straight line, and this is then utilised to determine the true wall shear rate, Γ_{TW} where $\Gamma_{TW} = 3n+1/4n \; . \; 4Q/\pi r^3$.

Hence, corrected apparent viscosity is given as

$\Sigma_A = \tau_A \; / \; \Gamma_A$ or $\Sigma_{TA} = \tau_{TW} \; / \; \Gamma_{TW}$ ——(3)

where τ_{TW} is the true wall shear stress given as

$\tau_{TW} = (p_2 - p_1)/2(L+er)$

where $(p_2 - p_1)$ is the pressure drop along an equivalent die of length L and of radius r, and e is an end correction factor. The e factor is determined by plotting ram pressure p versus L/2r and extrapolating to zero pressure, as shown in Fig. 3.17. However, it is found (15) that for dies of length >15 mm the end correction factor e is quite small and can be ignored. For this reason the e values were not determined during this work and only graphs of apparent viscosity versus apparent shear rate were plotted (as will be seen in chapter four). This is a more usual way of showing the viscosity-shear rate relationship (as shown by many workers, see references 13, 14, 15 and 146) and therefore the apparent graphs of viscosity versus shear rate (during this work) were plotted using the following equations:

apparent viscosity, $\Sigma_A = \tau_A \; / \; \Gamma_A$ (Pa s)

where τ_A = apparent shear stress = pr / 2L (Pa)

and Γ_A = apparent shear rate = $1/15r \; . \; v_r \; . \; (D/d)^2$ (1/s)

with p=force/csa of the barrel, r=die radius, L=die length, v_r=ram velocity, D=barrel diameter and d=die diameter as also shown schematically in Fig. 3.15.

3.2.4- Injection moulding process

This was carried out by using two different injection moulding machines. One was a small plunger type compressed air (PTCA) injection moulder (Model No. = SP 1-01-6) and the other one was the Fox and Offord plunger type injection moulder (Model No. = U1211, 1037/1064).

Plunger type compressed air (PTCA) injection moulder

This machine is shown both schematically and with its real picture in Figs. 3.18 and 3.19 respectively. This machine was used for moulding rectangular samples of size 35 mm X 12 mm X 5 mm as shown in Fig. 3.20 along with the mould used with this machine. The PTCA injection moulder had the following specifications:

Model = SP 1-01-6

Max. injection pressure = 80 lb/in^2 ~ 0.55 MN/m^2

Fox and Offord plunger type injection moulder

This machine is shown both schematically and with its real picture in Figs. 3.21 and 3.22 respectively. This machine was used for moulding rectangular and test bar samples of size 62 mm X 12 mm X 6 mm and 187 mm X 12 mm X 3 mm respectively as shown in Fig. 3.23 along with the mould used with this machine. The Fox and Offord injection moulder had the following specifications:

Model = Fox and Offord, U1211, 1037/1064

Max. injection pressure = 2000 lb/in^2 ~ 13.8 MN/m^2

Max. pressure of the press = 2000 lb/in^2 ~ 13.8 MN/m^2

Moulding procedure

This was very similar for both injection moulding machines. The only difference was that the PTCA moulder operated vertically by compressed air at very low pressure whereas the Fox and Offord moulder operated horizontally by hydraulics at moderate pressure.

Before filling the barrel with the ceramic/metallic powder-binder mixture the barrel was heated up to the moulding

temperature using the heating bands around the barrel. The barrel was then filled through the hopper allowing ~ 10 min for the material to reach the barrel temperature prior to moulding. The mould temperature depended on the type of binder used. For the thermoplastic/wax binder systems and also for the water-based polyvinyl alcohol binder system the mould was used at room temperature whereas for the water-based methylcellulose (Rivers) binder system the mould was heated to 72°C to cause gelling of the moulded samples. The Rivers binder system was moulded at room temperature whereas the other binder systems were moulded at their melt (in case of the thermoplastic/wax binder systems) and solution (in case of the PVA binder system) temperatures. Note that the exact mouling conditions (temperature and injection pressure) for each moulded powder-binder sample will be given in the Results Chapter.

3.2.5- Thermogravimetric analysis (TGA)

This was carried out by using the TGA machine shown schematically in Fig. 3.24. This machine was used for determining the burning characteristics of the organic materials used during this work. The TGA data were then used to determine the thermal ramping cycle for the debinding (binder removal) process.

Two TGA data graphs could be obtained: one showing the % weight loss and the other one showing the % rate of weight loss both against temperature. These are shown schematically in Fig. 3.25.

Procedure

The TGA machine could be run under air or an inert atmosphere at a constant heating rate. A sample of maximum weight 5 mg is placed inside a small crucible which is then placed inside the furnace as shown schematically in Fig. 3.24. Before heating the furnace (using the temperature controller) the microbalance is balanced against air or an inert gas going through the furnace. After setting up the microbalance for the desired range the furnace is then heated up to the set temperature of the controller (Eurotherm 815) with the chosen heating rate. As the

temperature rises weight losses and rate of weight losses (both against temperature) are recorded graphically by a chart recorder. The recorded data are then used to plot the graphs of % weight loss versus temperature (to obtain the TGA data curves) for each organic material. These graphs are given in the Results Chapter for each organic material used during this research work. The TGA data curves obtained from the graphs of % rate of weight loss versus temperature always showed the same shape, i.e. the maximum rate of weight loss always occured in the middle of the critical decomposition range for all the organic materials/binders used during this work. These TGA data curves are shown schematically in Fig. 3.25 at the end of this chapter.

3.2.6- Debinding process

This was carried out by using two different types of furnaces. One was a bench type air circulating oven which was run by a Eurotherm 821P digital temperature controller and used for the debinding of the moulded alumina and zirconia samples. The other one was a tube furnace which was run under a controlled atmosphere (depending on the type of material) by a Eurotherm 818P digital temperature controller and used for the debinding of the other moulded samples such as silicon nitride, silicon carbide, tungsten carbide-6 weight % cobalt and iron-2 weight % nickel.

The 821P digital temperature controller

This is a digital programmable temperature controller with an eight step thermal ramping cycle. Each step has three functions: rate of heating (in °C/h), temperature level (in °C) and dwell (or hold time, in h) which can set according to the desired thermal ramping cycle. This controller is capable of increasing the heating rate by 0.1°C/h which might be needed for very slow burnings.

The 818P digital temperature controller

This controller is the same as the 821P controller except that the 818P is capable of increasing the heating rate only by 1°C/h.

By using the above 8-step programmable temperature controllers it was possible to obtain excellent debinding results which is considered (1,2) to be the most critical and important result for the injection moulding of ceramic/metallic powders.

3.2.7- Sintering process

This was carried out by using two different type of furnaces. One was a high-temperature high-vacuum furnace used for the sintering of alumina and zirconia samples and the other one was a tube furnace used for the sintering of other samples (under an inert gas or vacuum) such as silicon nitride, silicon carbide, tungsten carbide-6 weight % cobalt and iron-2 weight % nickel.

The high-temperature high-vacuum furnace

This was a Torvac tungsten element high-temperature high-vacuum furnace which could provide a maximum temperature of 1800°C under a vacuum of . 1 X 10^{-9} atmosphere (~1 X 10^{-6} mmHg). The high vacuum was provided by a rotary and a diffusion pump and the heating up process could be carried out at a constant heating rate by using a Eurotherm 818P temperature controller. This furnace was used for the sintering of 99.5 % alumina and zirconia samples which required sintering temperatures between 1700-1800°C.

The tube furnace

This was a high-temperature tube furnace providing a maximum temperature of 1700°C under an inert atmosphere or a vacuum of 1 X 10^{-3} atmosphere (~1 mmHg) obtainable using an ordinary pump. This furnace was also run by a 818P temperature controller which has already been described. This furnace was used for the sintering of samples such as silicon nitride and silicon carbide which required inert atmospheres.

Note that the exact sintering conditions (temperature, time and

atmosphere) used for each material during this work will be given in the Results Chapter.

3.2.8- Mechanical testing

Four-point bend tests and compression/crushing tests were carried out on sintered alumina samples (obtained by the injection moulding process during this work) using an Instron testing machine (Model = MT 0110). Testing procedures, bend and compressive strengths calculations were as follows:

Four-point bend strength test procedure and calculation

All tests were carried out in air at room temperature at a crosshead speed of 0.1 mm/min with a 4-point test rig having an outer span of length 35 mm and an inner span of length 19 mm. These testing conditions have also been used by other workers such as Mutsuddy (173) to determine the bend/flexural stregths of injection moulded ceramic materials. The bend/flexural strength was calculated using the following equation:

$$\sigma_f = 3\ p_f\ a\ /\ b\ h^2$$

where σ_f = flexural/bend strength (N/m^2)

p_f = force required to break the test piece (N)

a = as shown in Fig. 3.26 (mm)

b = width (mm)

h = thickness (mm)

This test is shown schematically in Fig. 3.26.

Compressive strength test procedure and calculation

All tests were carried out in air at room temperature at a crosshead speed of 0.1 mm/min on sintered alumina samples (obtained by the injection moulding process during this work) of size 6 mm X 5 mm. The compressive/crushing strength was calculated using the following equation:

(see next page)

Compressive strength = F_{max} / csa of the test piece over which the load is applied

where F_{max} = maximum load at which crushing took place

csa = length X width

This test is shown schematically in Fig. 3.27.

3.2.9- Thermal conductivity measurements

The "flash method" was used to measure the thermal diffusivity of the sintered alumina samples obtained during this work by the injection moulding process using the best binder systems (see chapter four-section 4.3). The thermal diffusivity values were then used to calculate the thermal conductivities using the following equation: th. conductivity = th. diffusivity X density of the sintered samples X specific heat capacity at constant pressure.

In the "flash method" the front face of a small disc shaped sample (. 20 mm dia and < 10 mm thick) is subjected to a very short burst of radiant energy. The source of the radiant energy was a xenon lamp and irridiation times were of the order of one millisecond or less. The resulting temperature rise of the rear surface of the sample was recorded on a oscilloscope screen and the thermal diffusivity values were calculated from the recorded temperature rise-versus-time graph (as shown below schematically) by using the following equation:

th. diffusivity = $0.1388\ L^2 / t_{½}$

where L = sample thickness

$t_{½}$ = time from the initiation of the pulse until the rare face temperature rise reaches half of its maximum value as shown below

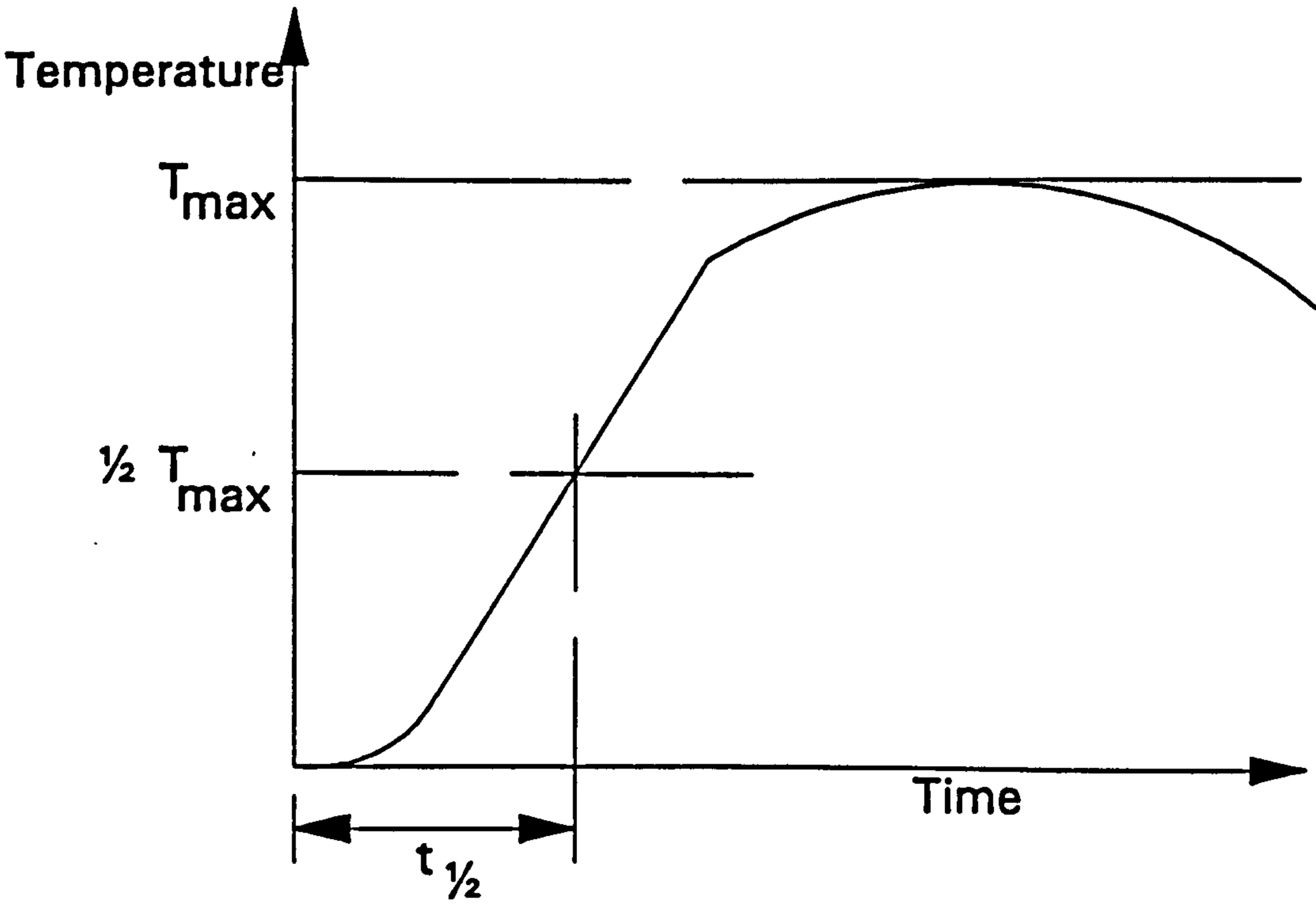

The specific heat capacities (C_p) of the sintered alumina samples were measured by using differential scanning calorimetry (DSC). A constant C_p value of 1.037 J/g°C was obtained at a temperature of 260°C for all the sintered alumina grades.

3.2.10- Compaction process

Cold-dry compaction of different grades of alumina (88 %, 95 % and 99.5 %) was carried out using a rectangular 32 mm X 6.4 mm double-acting steel die without lubrication. All the compactions were carried out at a crosshead speed of 1 mm/min at compaction pressures of 30-200 MN/m^2 by using an Instron testing machine (Model = MT 0110). The load-deflection curves were recorded and showed very similar positions and shapes.

Selected compacts were sintered and sintered densities were determined (by dimensional and weight measurements) for comparison with those of the injection moulded alumina samples having the same chemical compositions.

3.2.11- Optical and scanning electron microscope (SEM, Cambridge Stereo Scan 360) examinations

These were carried out in order to study the macro and microstructures of the ceramic/metallic powder-binder mixtures, moulded, debonded, sintered and fractured sintered surfaces. Some of these studies which are not shown in the results chapter were as follows:

Structure of ceramic/metallic powder-binder mixtures

It is very important to have a homogeneous powder-binder mixture so as to produce uniform properties such as uniform as-moulded (green) and sintered structures and hence uniform mechanical properties. Fig. 3.28 shows a typical SEM photomicrograph of a fairly uniform ceramic powder-binder mixture which was observed throughout this work for each powder-binder mixture. This photomicrograph shows the microstructure of a 70 vol. % alumina (99.5 % grade)+30 vol. % atactic polypropylene mixture. A fairly uniform mixture of the alumina powder covered by the atactic polypropylene binder can be seen from this photomicrograph. A dark patch/hole can also be seen which might be due to the entrapped air.

Structure of debonded samples

A typical debonded microstructure is shown in Fig. 3.29 which was observed throughout this work after debinding (binder removal) of the moulded samples. As can be seen there are a lot of voids (dark areas) between the powder particles (alumina powder in this case) which are created during the burning of the binders (atactic polypropylene binder as in Fig. 3.28). These voids will cause the debonded samples to be physically weak and therefore these samples must be handled with care. However, these voids will disappear during the sintering process as the body densifies.

It is very important to have a defect-free debinding process, i.e. there should be no macro/micro-cracks, no blistering, no swelling and no layers of voids (no delamination) after the debinding process. Such defects, if present, cannot be removed during the sintering process and will cause structural damage and hence low mechanical strength. A typical debinding defect is the occurrence of macro/micro-cracks due to high heating rates. This type of defect can be seen in Fig. 3.30 which is the cross section of a debonded sample showing horizontal and vertical macro-cracks.

Mould filling defects

One type of defect observed during this work was the presence of layers of voids (delamination) in few of the moulded samples as showm in Fig. 3.31. This type of defect may take place during the mould filling stage or during the solidification in the cavity (51). It is believed that this type of defect may be due to inhomogeneity created during the mixing or moulding stages. It is therefore very important to create a homogeneous mixing and moulding processes so as to prevent the formation of such defects which may cause structural damage in the sintered body as can be seen in Fig. 3.31.

Another type of mould filling defect observed during this work was the jetting of the highly loaded binder mixtures as shown in Fig. 3.32. It is found (13, 146) that the fluidity of ceramic/metallic-binder mixtures becomes limited when large

loadings of powder are incorporated and may show a greater tendency to jet into the mould cavity producing a coil and resulting weld lines within the moulding. Weld lines are regions of weakness and may persist as defects in the fired material (126). This type of jetting flow may be avoided by increasing the mould temperature as was the case with the 88 % and 95 % moulded alumina-atactic polypropylene samples during this work which will be described in detail in the Results Chapter. However, higher mould temperatures are limited by the need to eject the mouldings without distortion.

Note that jetting flow due to improper mould/gate design did not take place during this work. This was because all the mouldings were performed using two moulds which had the proper gate position and design as shown in Figs. 3.20 and 3.23.

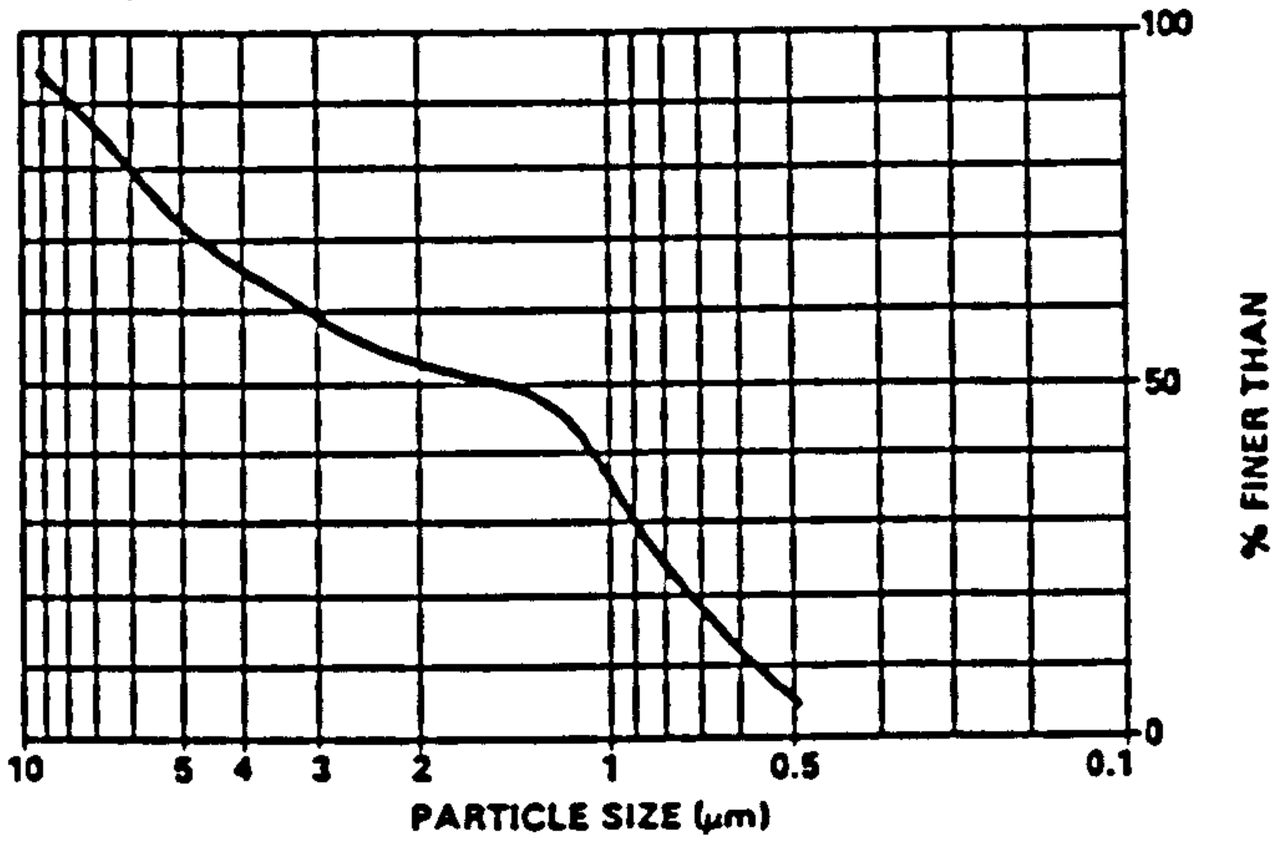

Figure 3.1- Particle size distribution curve for the 99.5 % aluminium oxide (BACO RA7) powder.

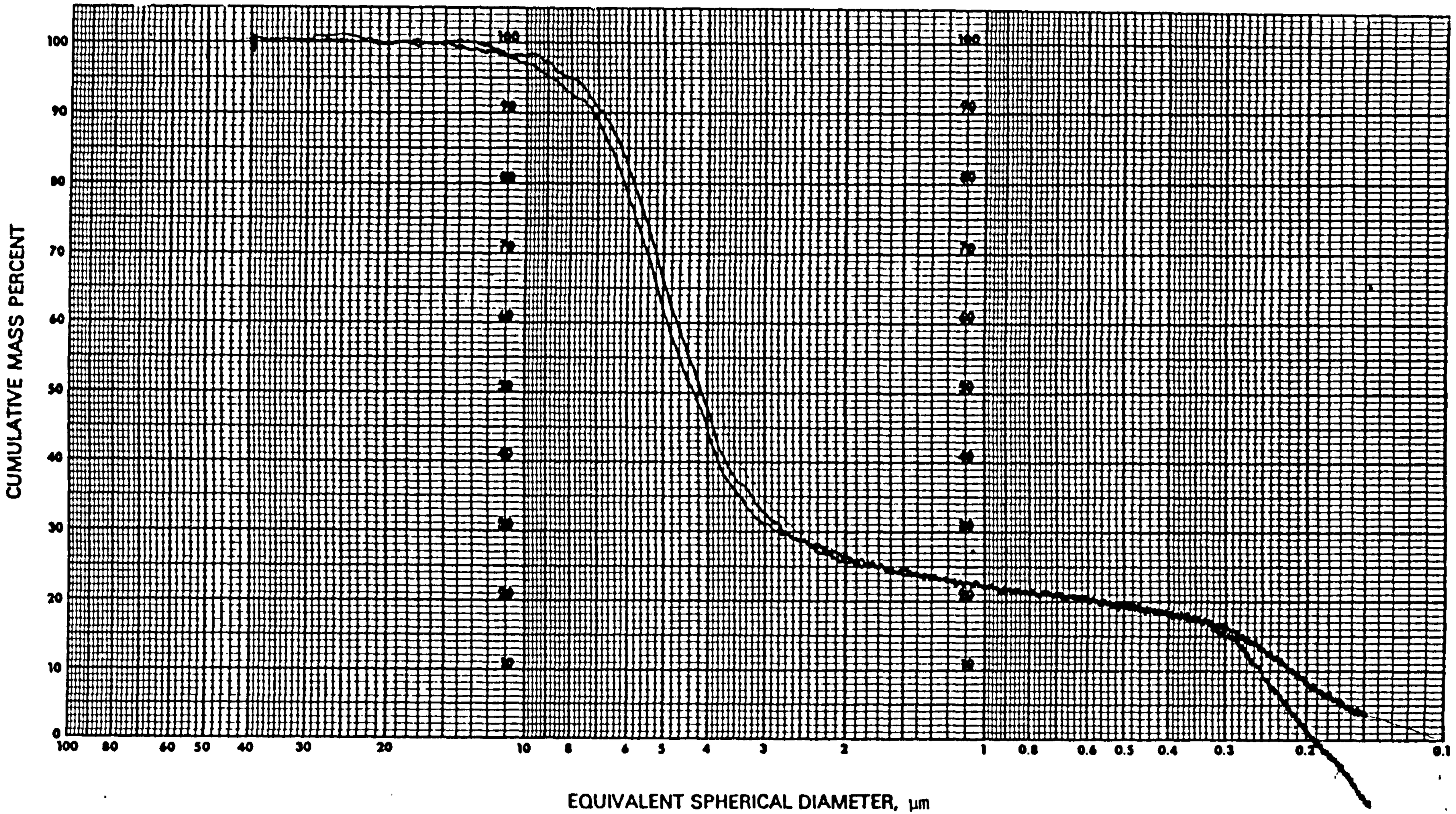

Figure 3.2- Particle size distribution curve for the zirconium oxide powder.

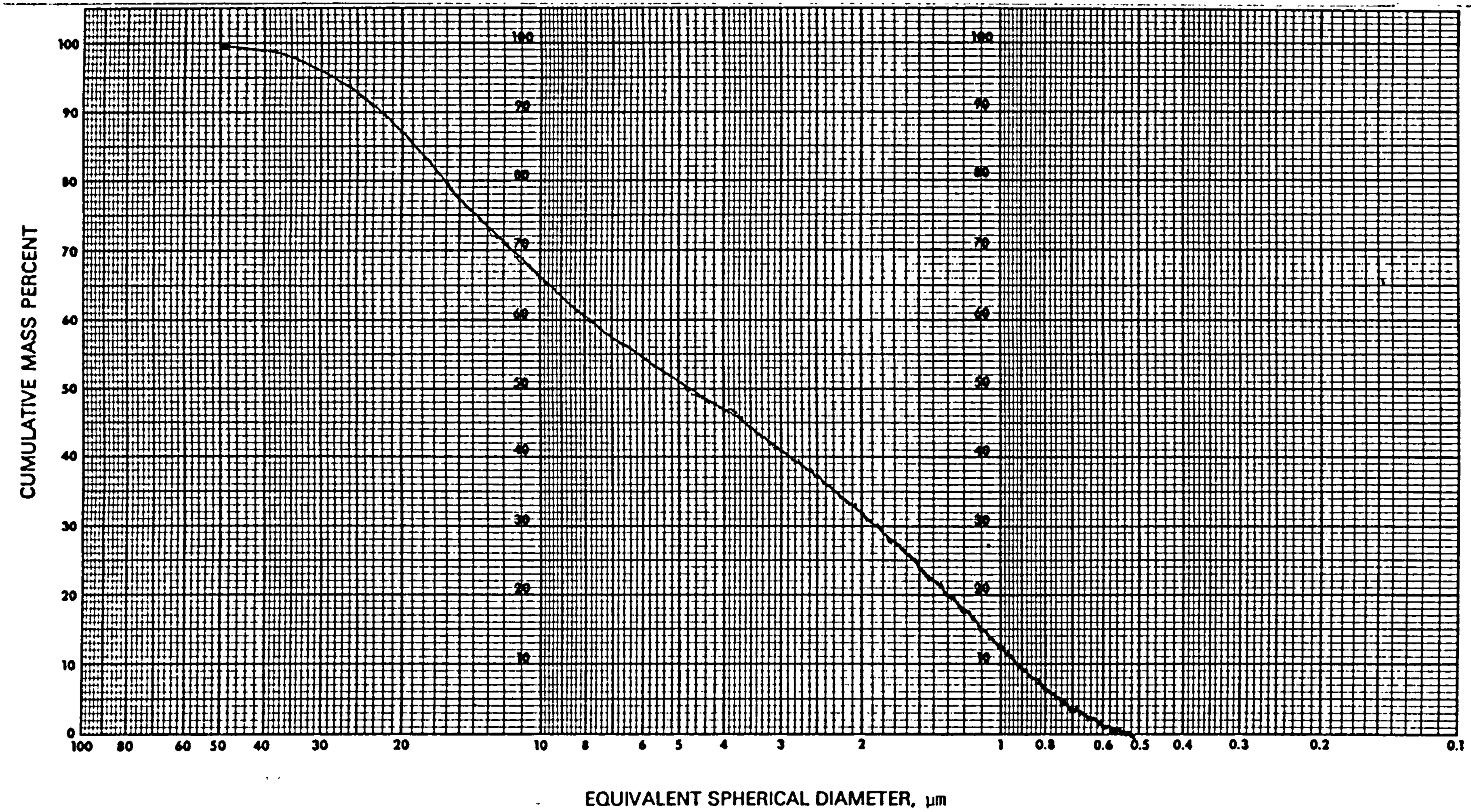

Figure 3.3- Particle size distribution curve for the silicon nitride powder.

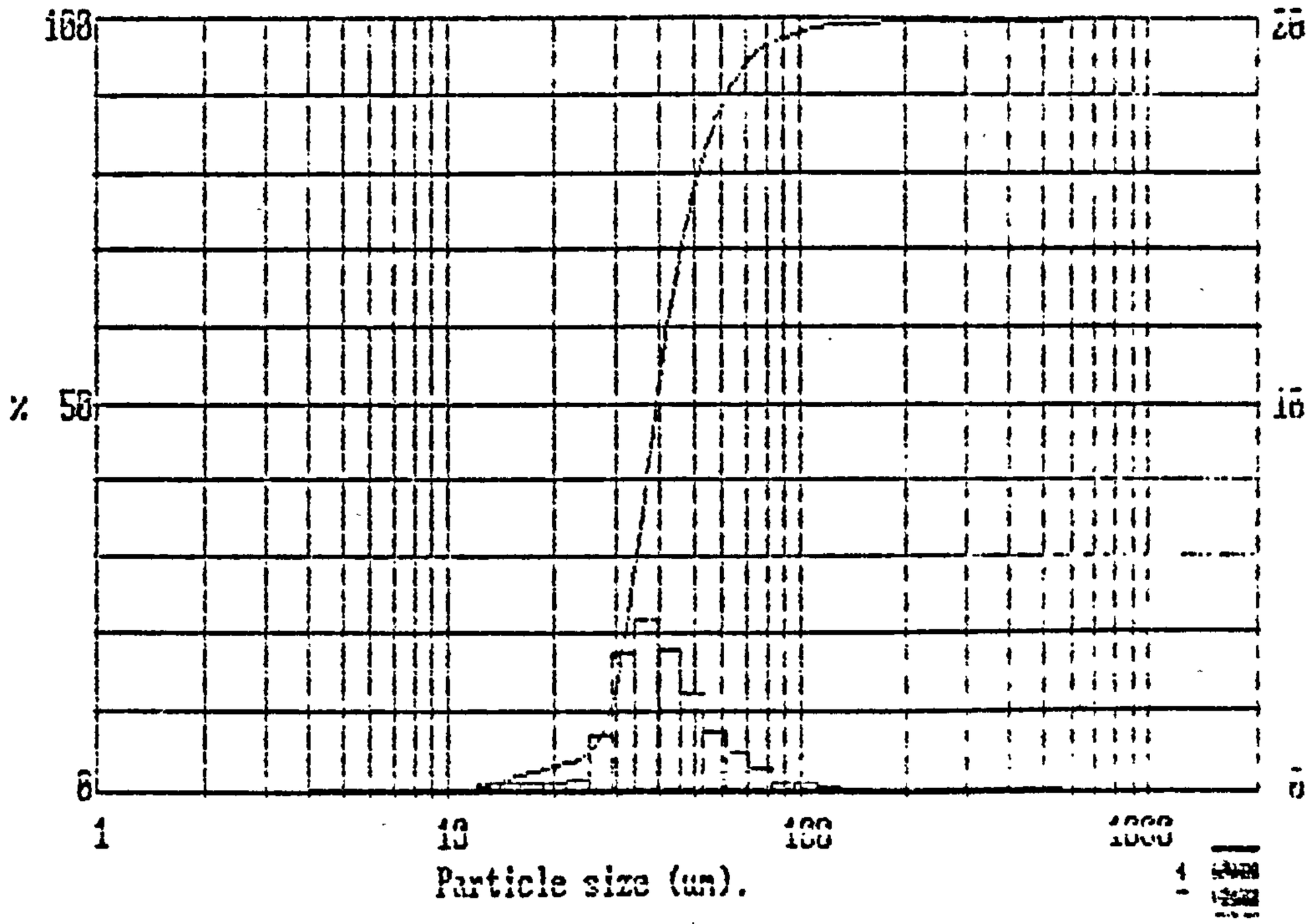

Figure 3.4- Particle size distribution curve for the silicon carbide powder.

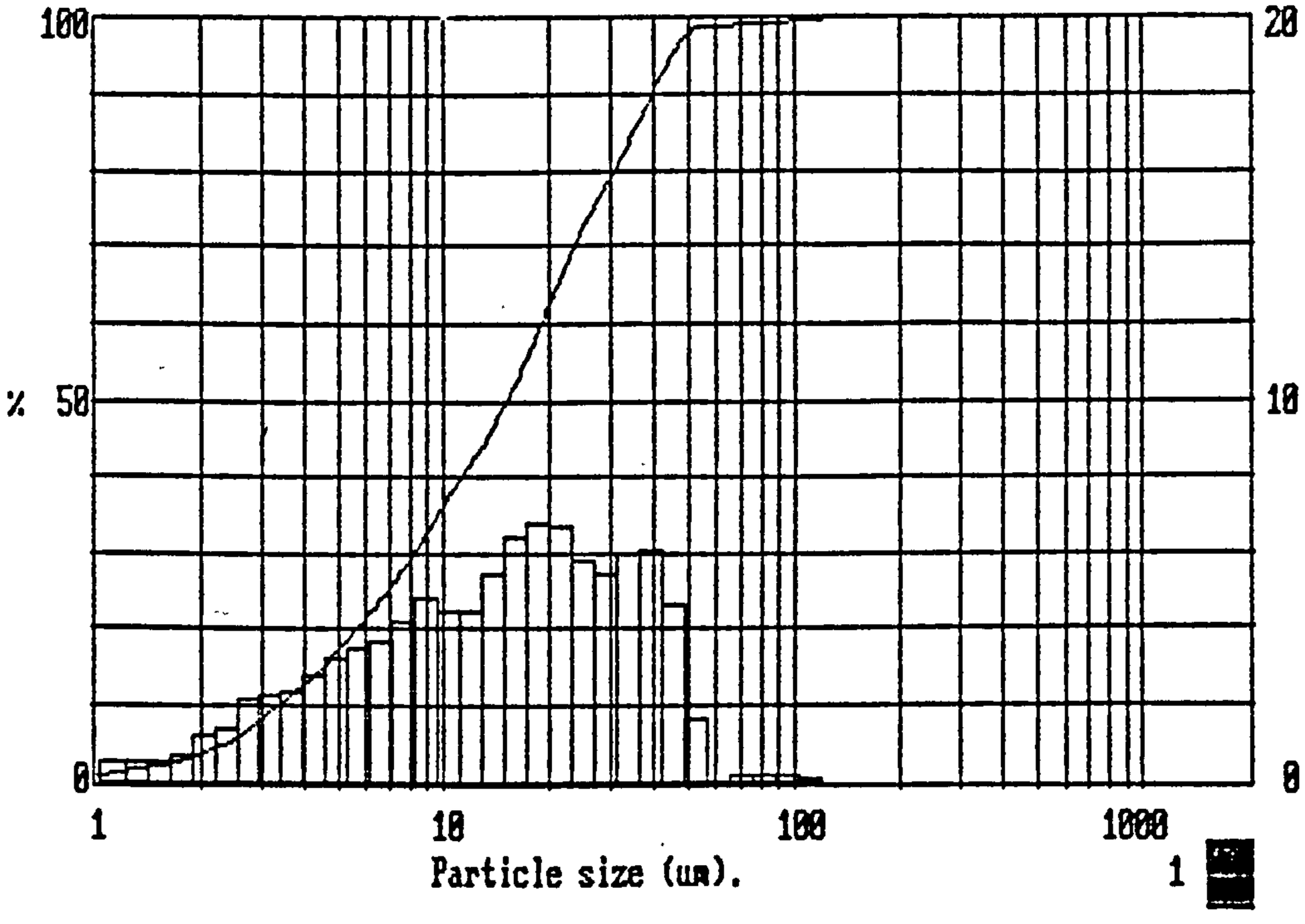

Figure 3.5- Particle size distribution curve for the silicon dioxide (SiO_2) powder.

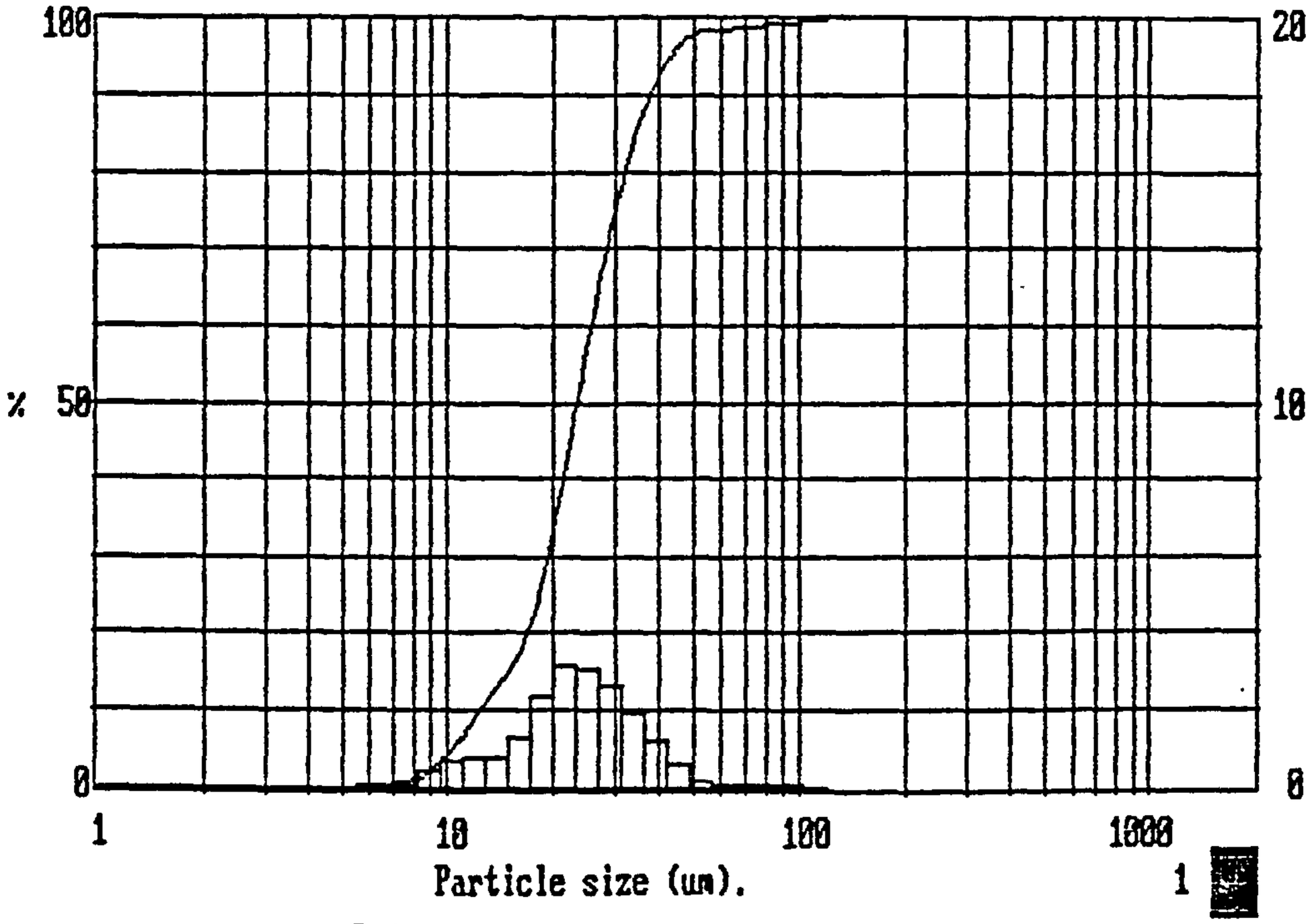

Figure 3.6- Particle size distribution curve for the calcium oxide (CaO) powder.

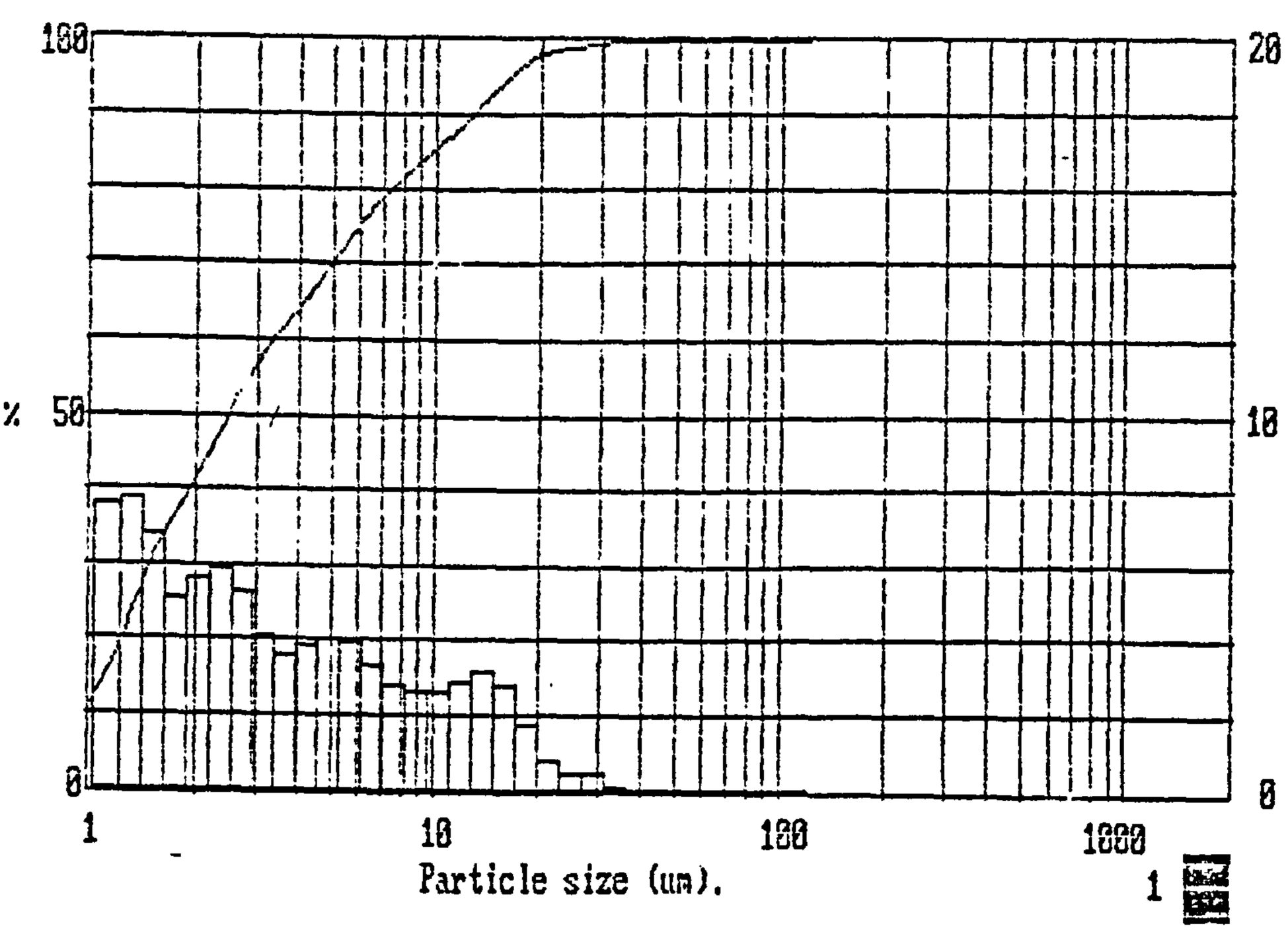

Figure 3.7- Particle size distribution curve for the chromium oxide (Cr_2O_3) powder.

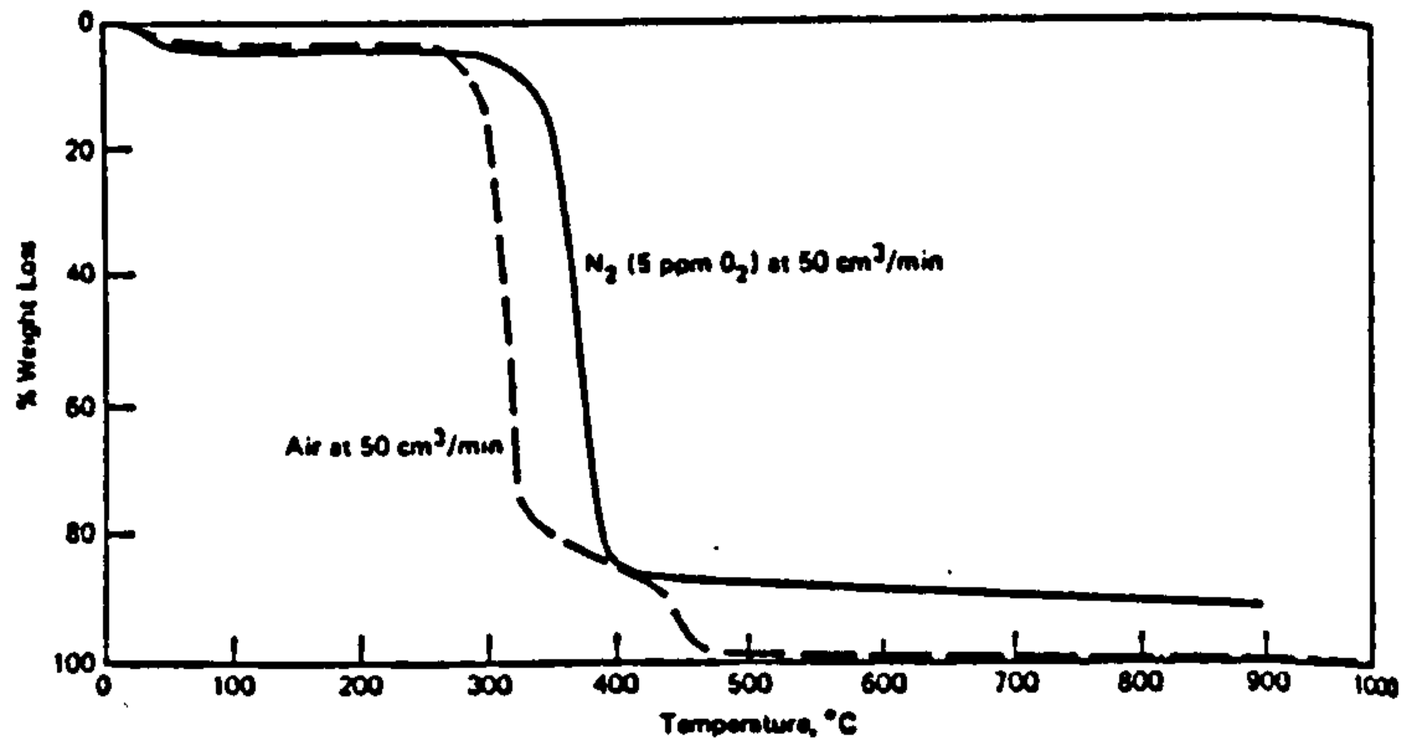

Figure 3.8- TGA data at 10°C/min for methylcellulose.

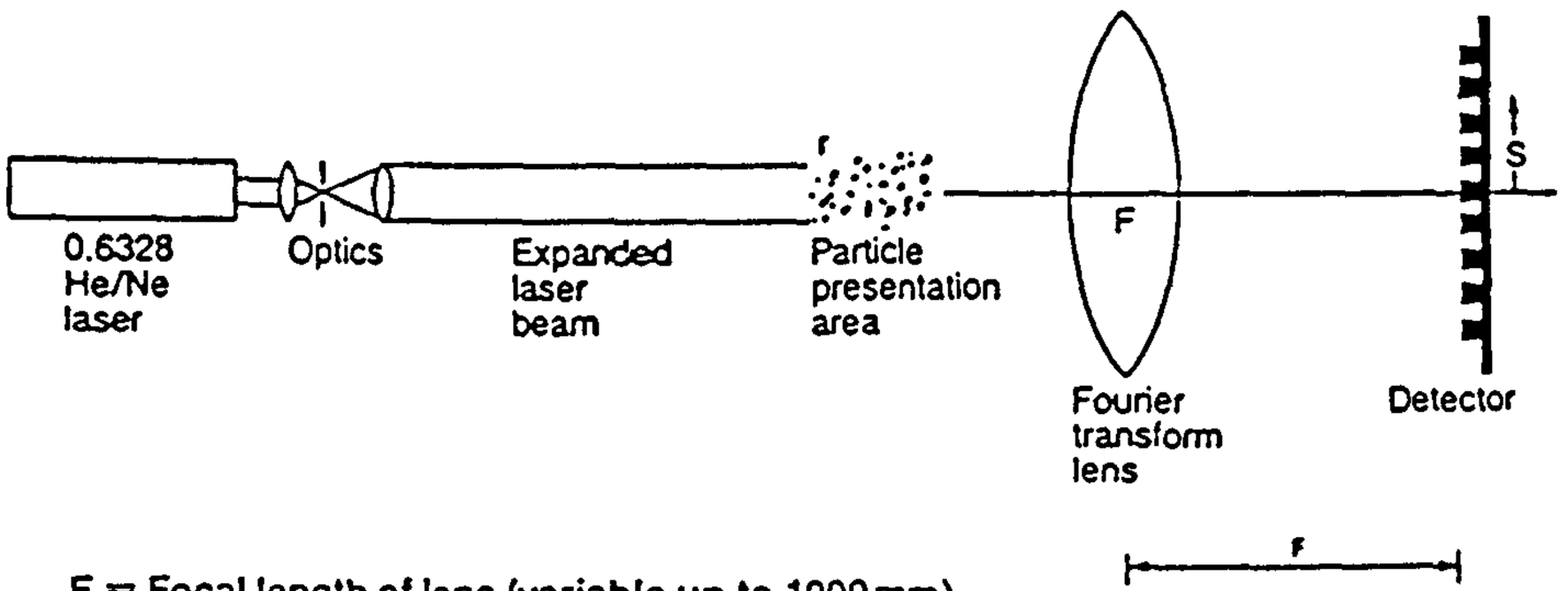

Figure 3.9- Schematic diagram of the Malvern (-Laser diffraction) Particle sizer.

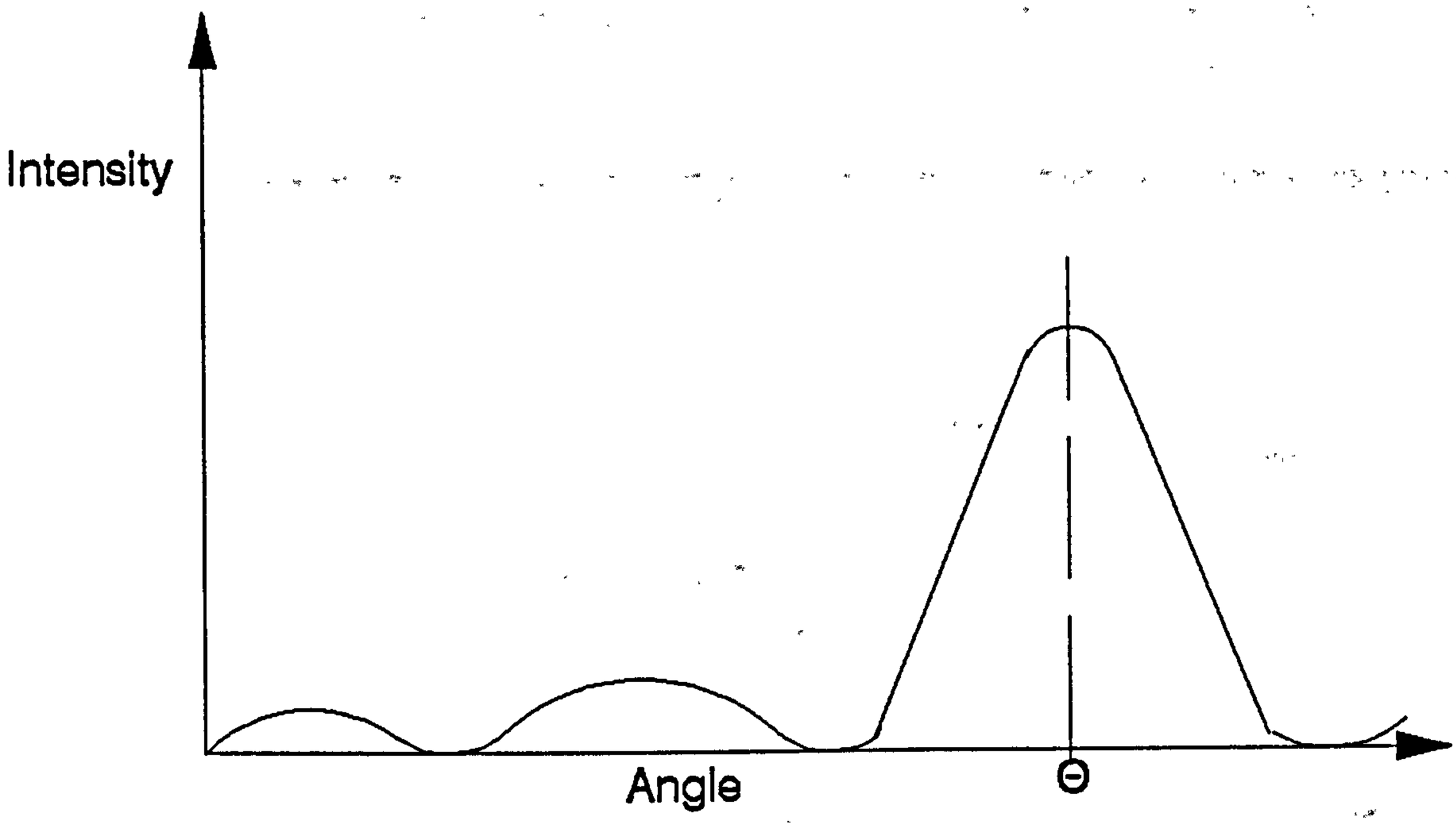

Figure 3.10- Fraunhofer diffraction pattern for circular aperture or disc.

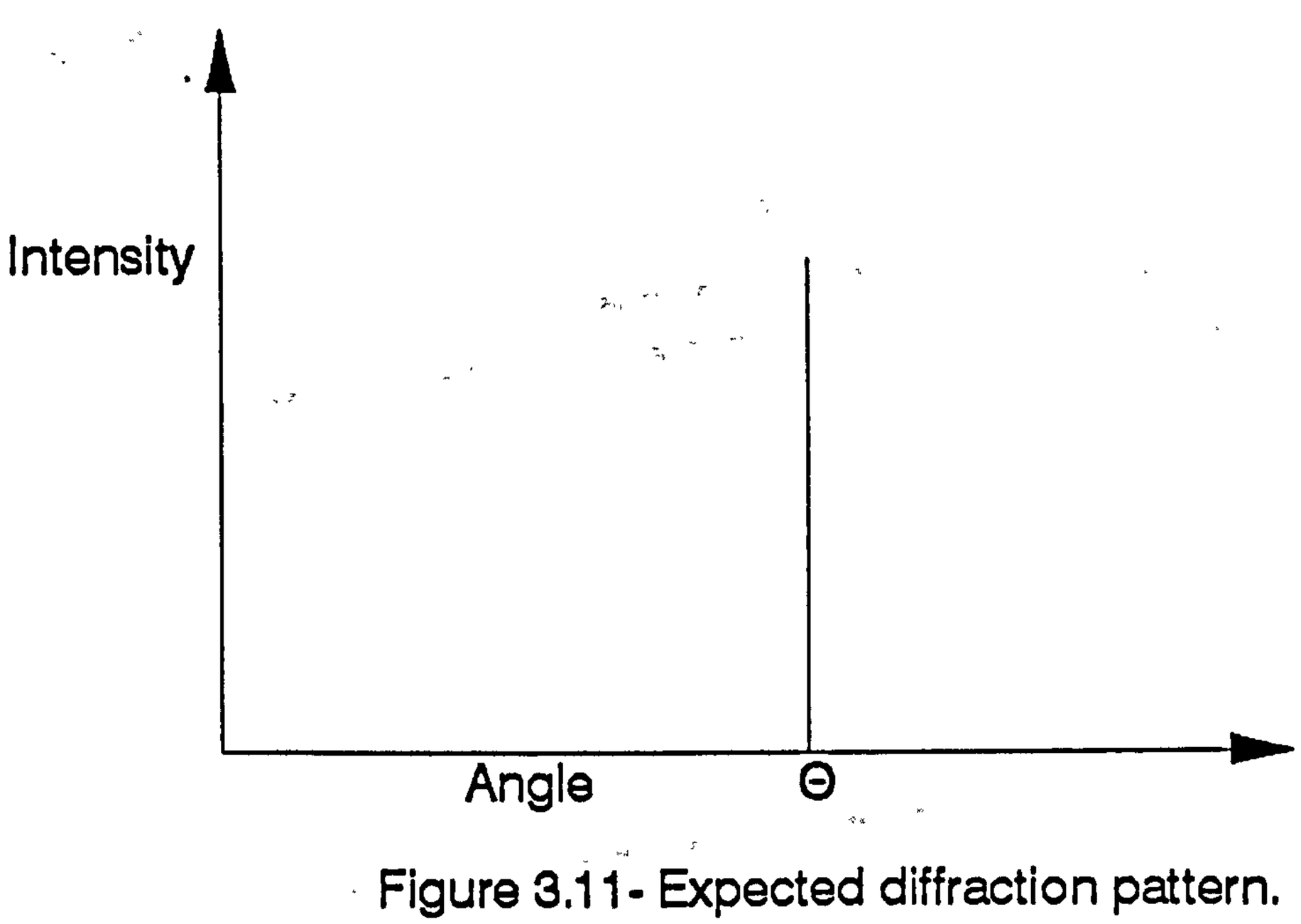

Figure 3.11- Expected diffraction pattern.

Figure 3.12- Malvern particle sizer showing a typical particle size distribution curve on the screen.

Automatic particle size analysis with Malvern SERIES 2600c

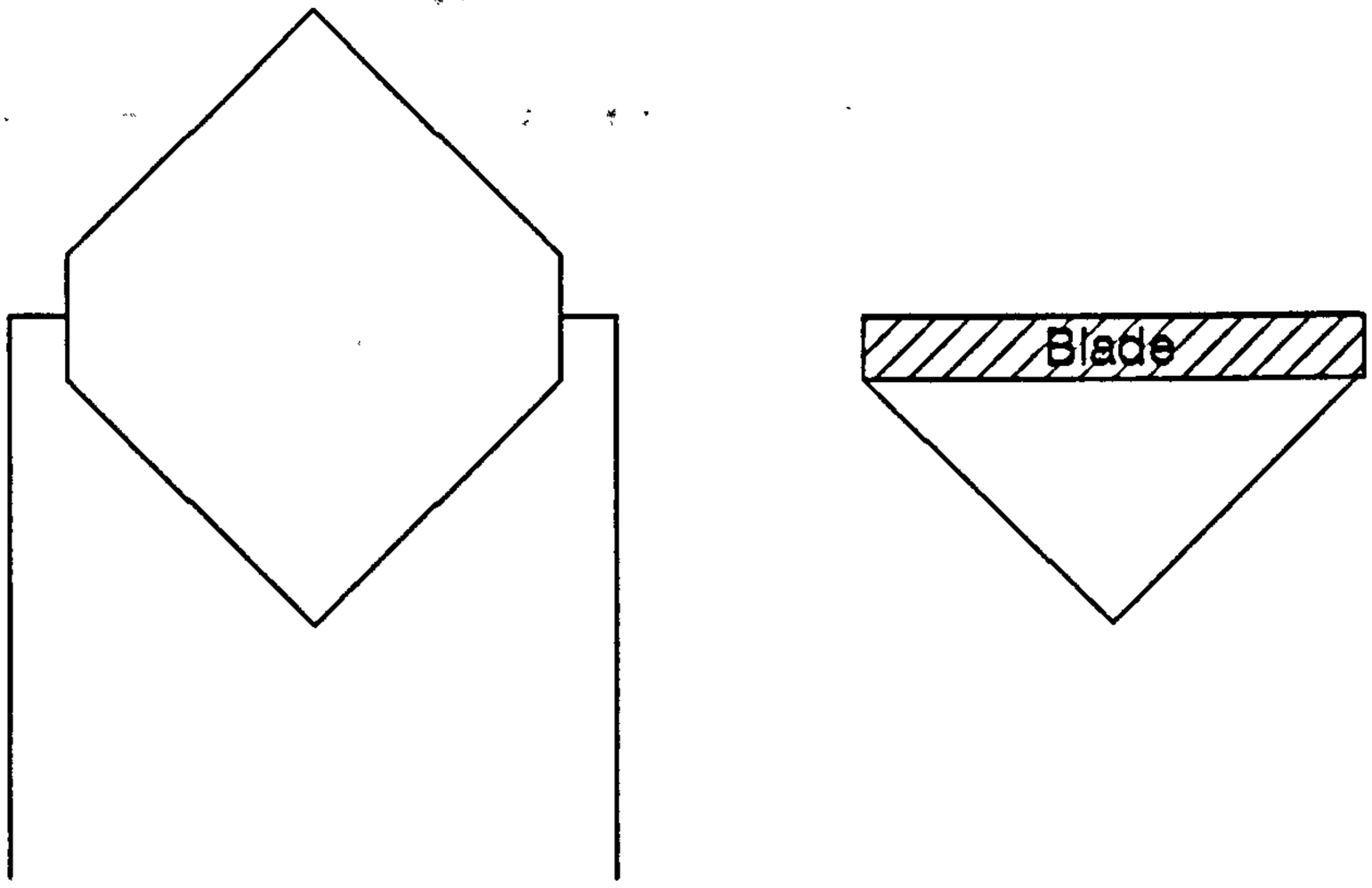

Figure 3.13- Schematic diagram of the double cone mixer.

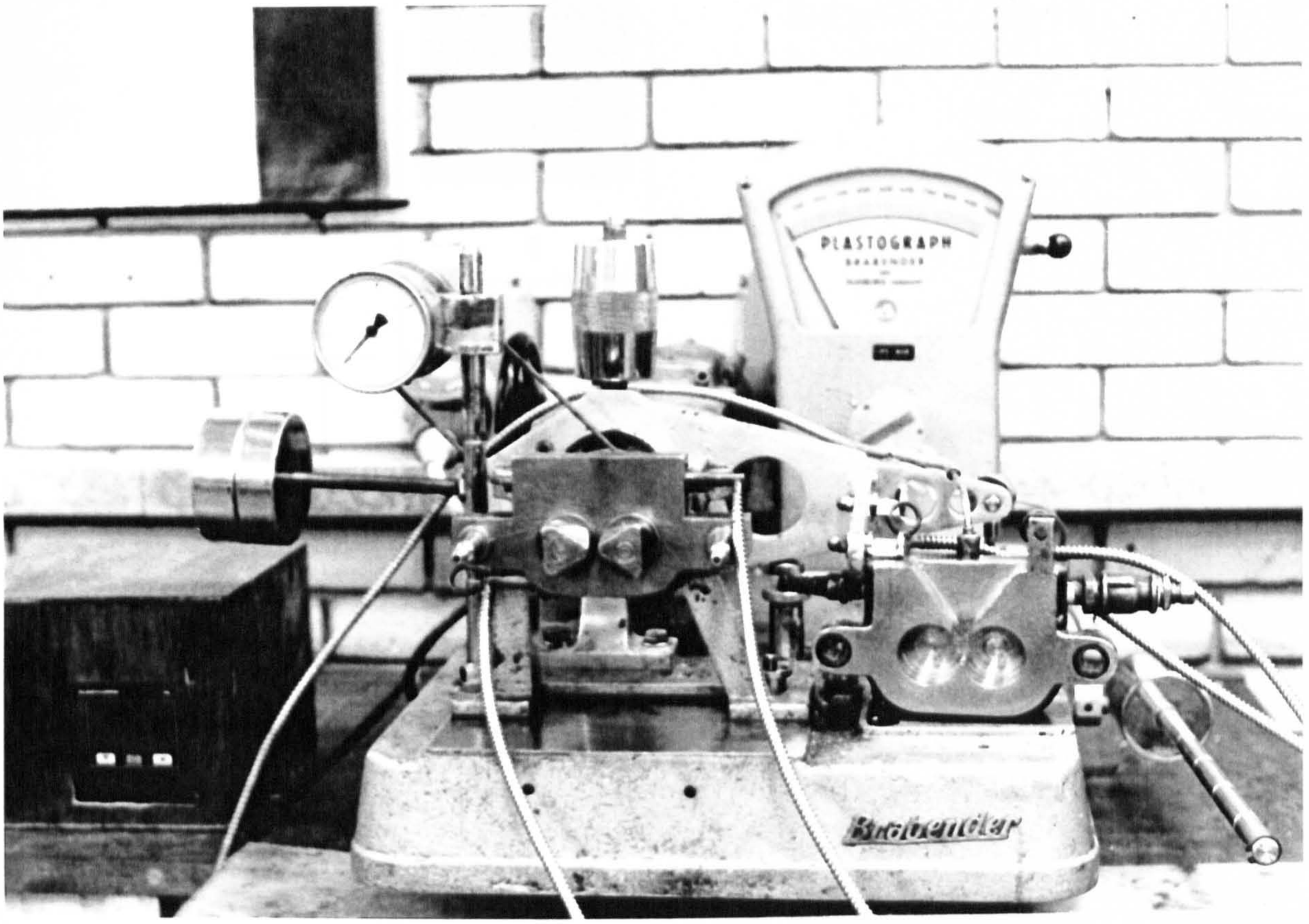

Figure 3.14- Picture of the Brabender Plastograph used during this work for the mixing of ceramic/metallic powders with the organic materials.

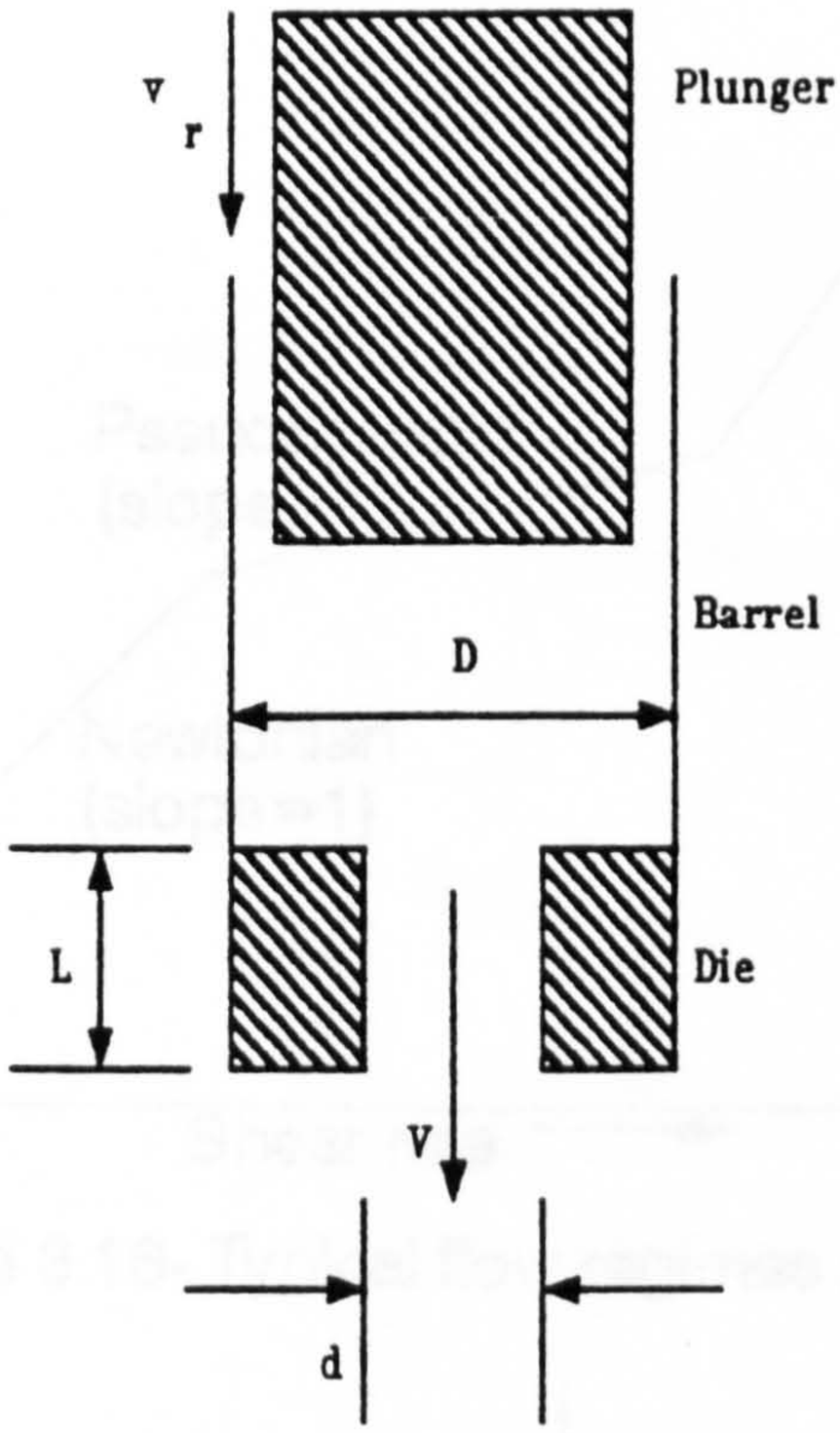

Figure 3.15 – Schematic diagram of the Davenport/Instron extrusion rheometer.

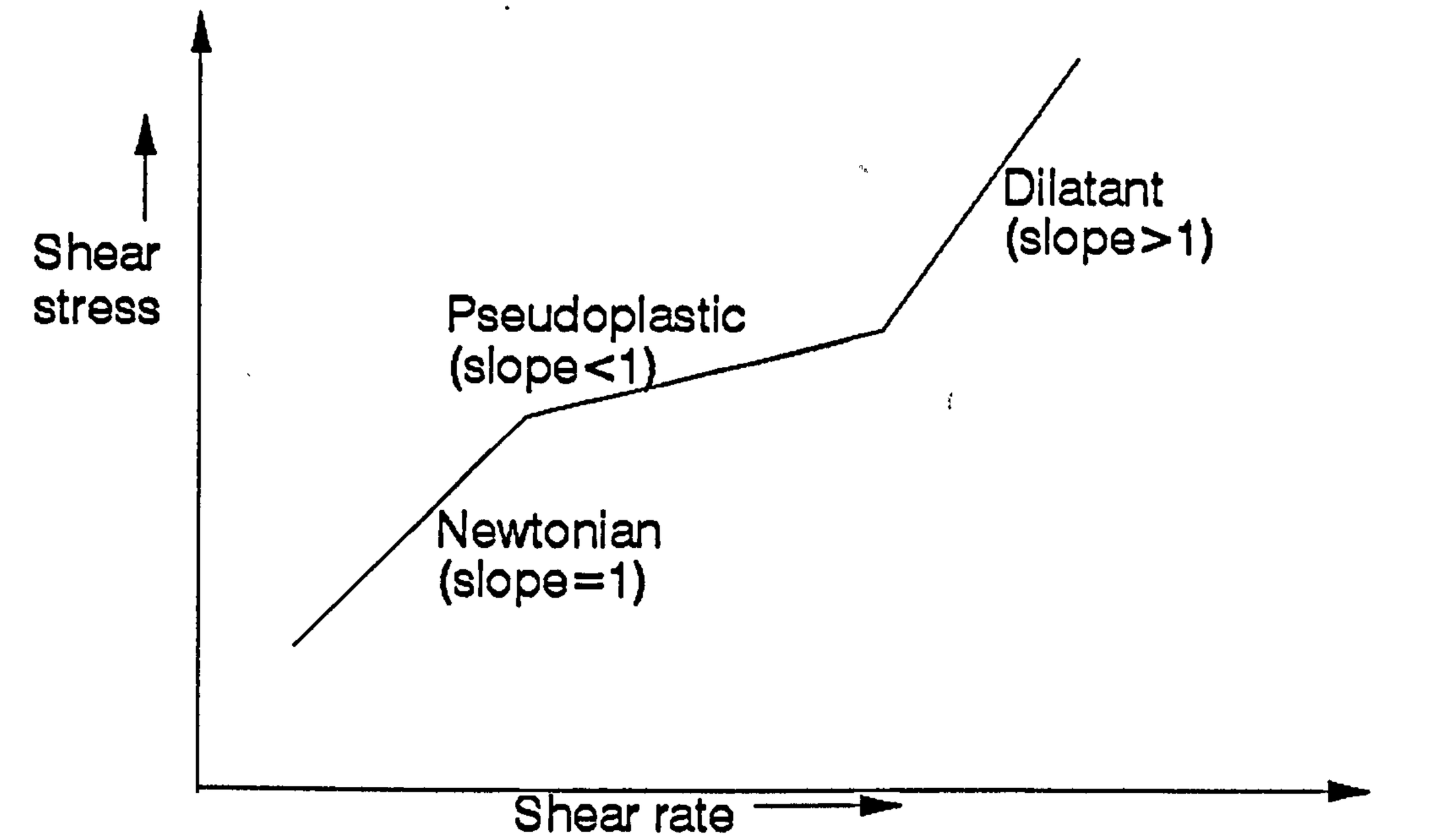

Figure 3.16- Typical flow regimes in rheological behaviour.

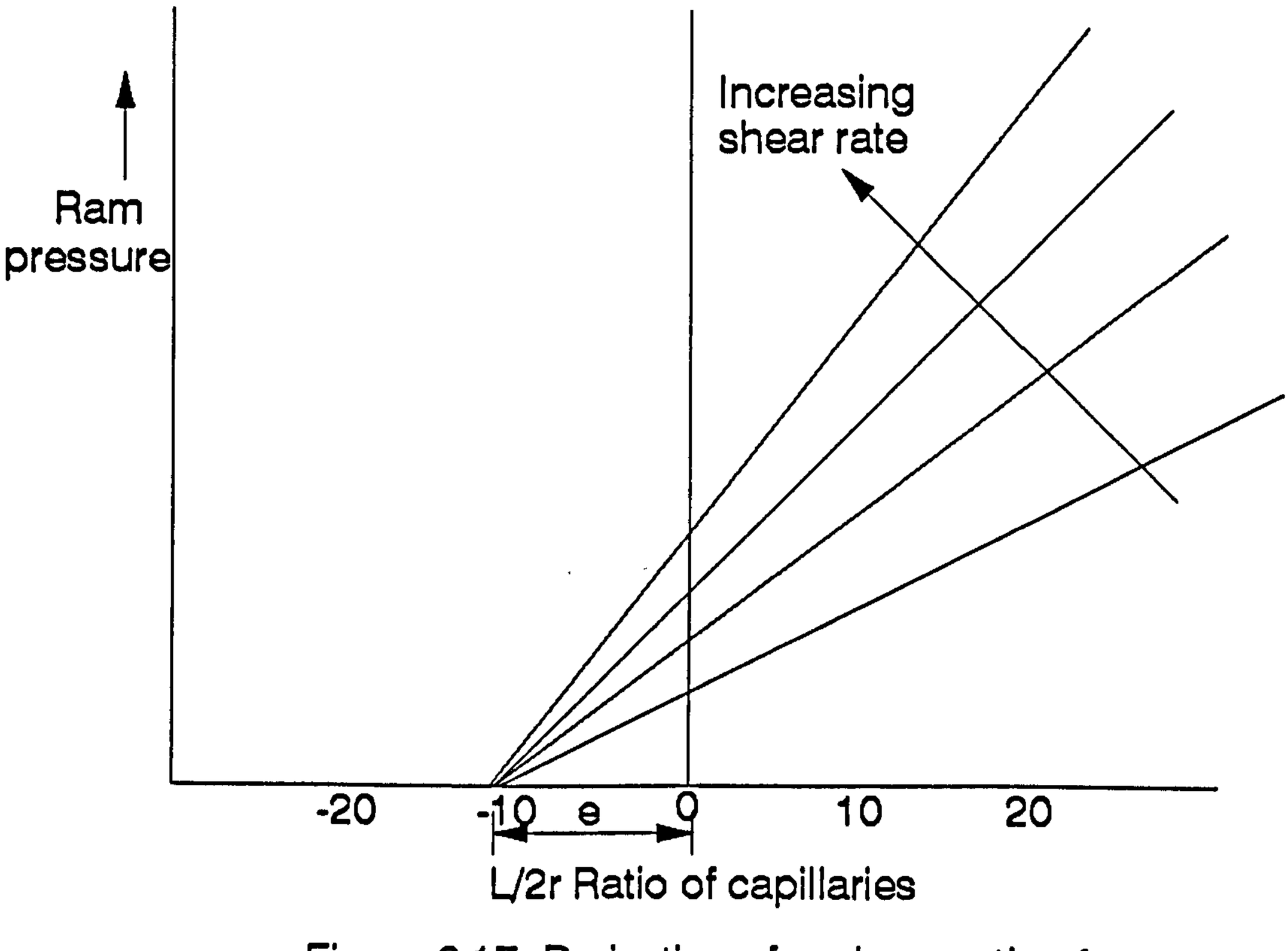

Figure 3.17- Derivation of end correction factor e for determination of true wall shear stress.

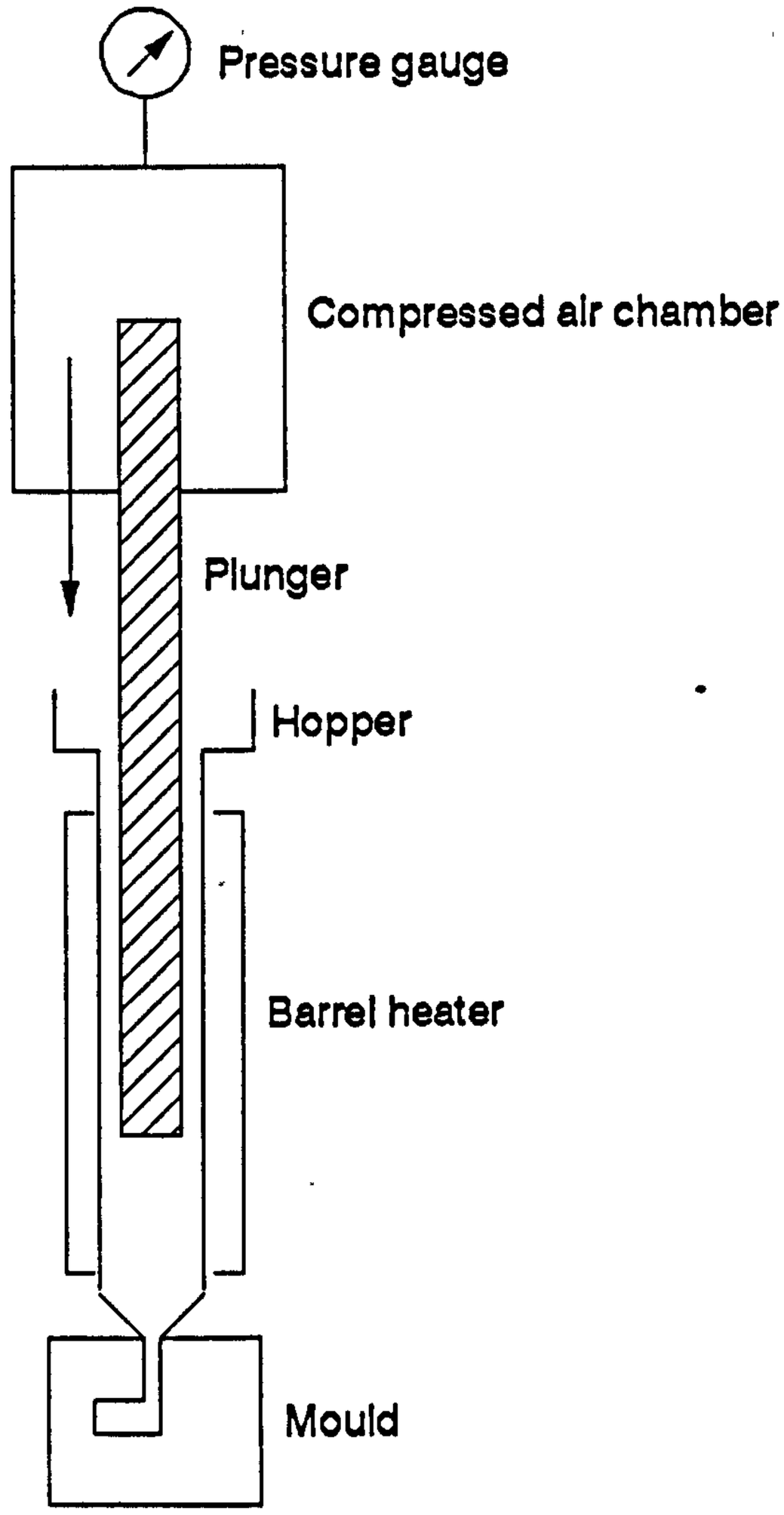

Figure 3.18- Schematic diagram of the plunger type compressed air (PTCA) injection moulder.

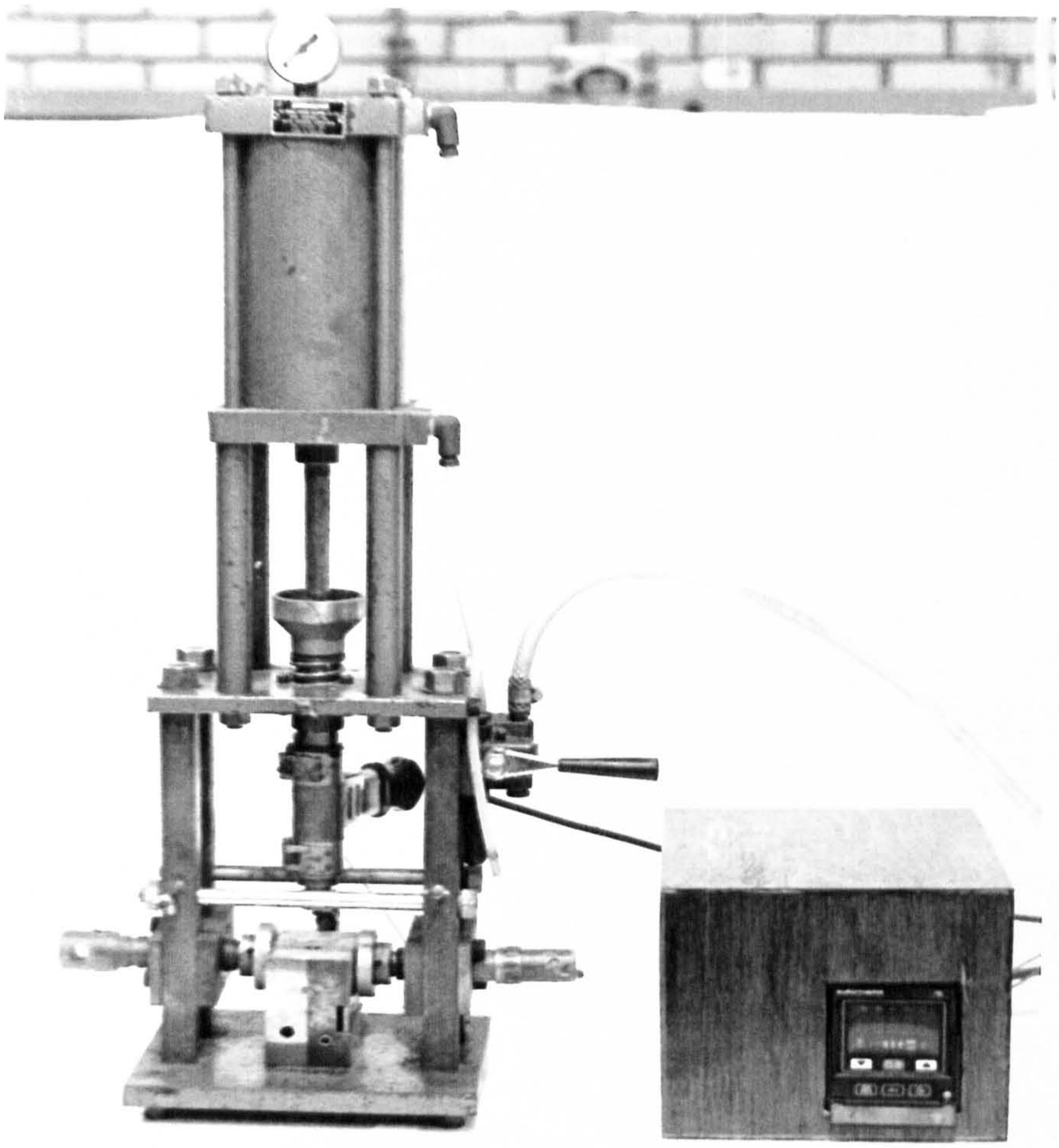

Figure 3.19- Picture of the small plunger type compressed air (PTCA) injection moulding machine.

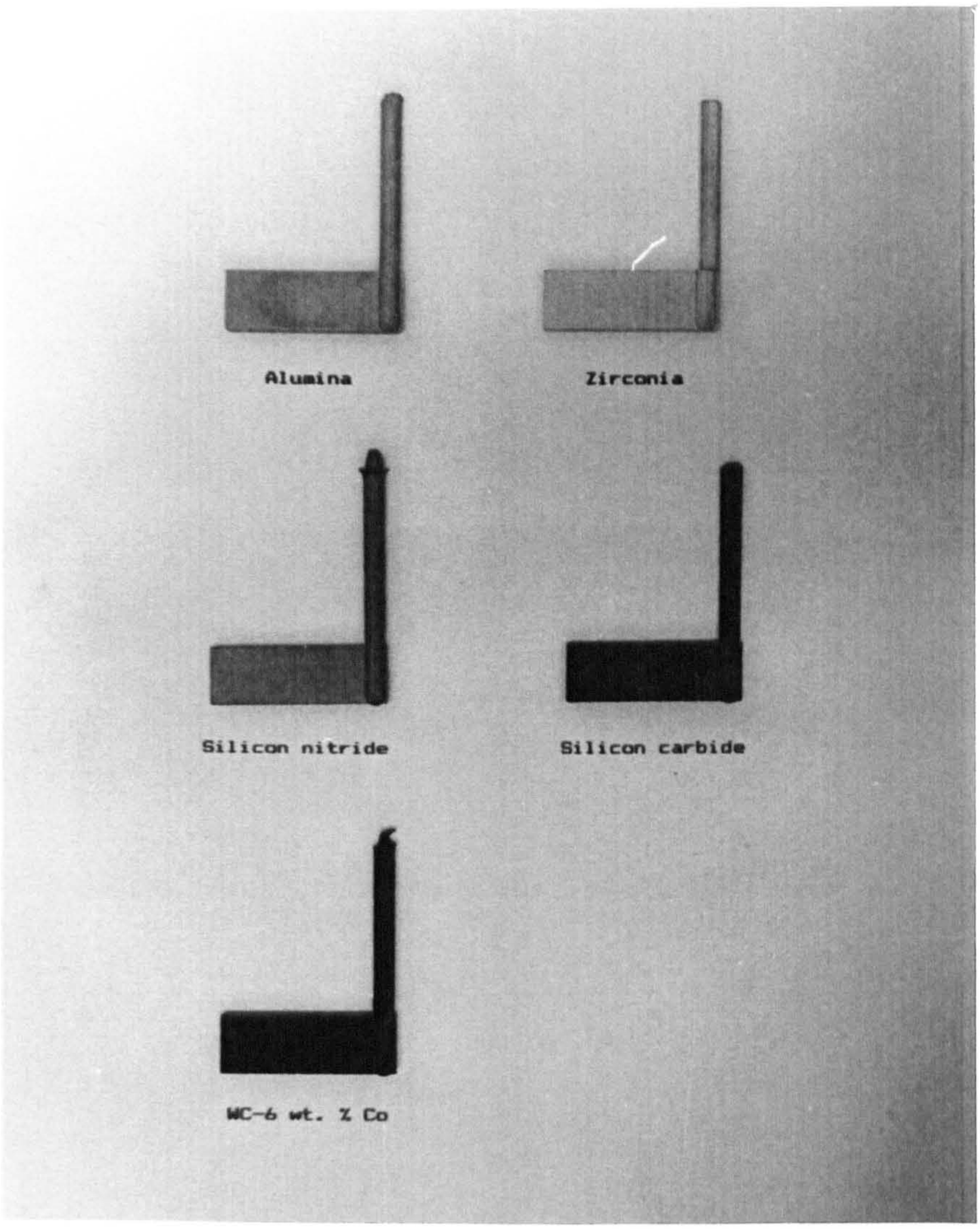

Figure 3.20- (a) Injection moulded rectangular samples of size 35 mm X 12 mm X 5 mm using the PTCA moulder;

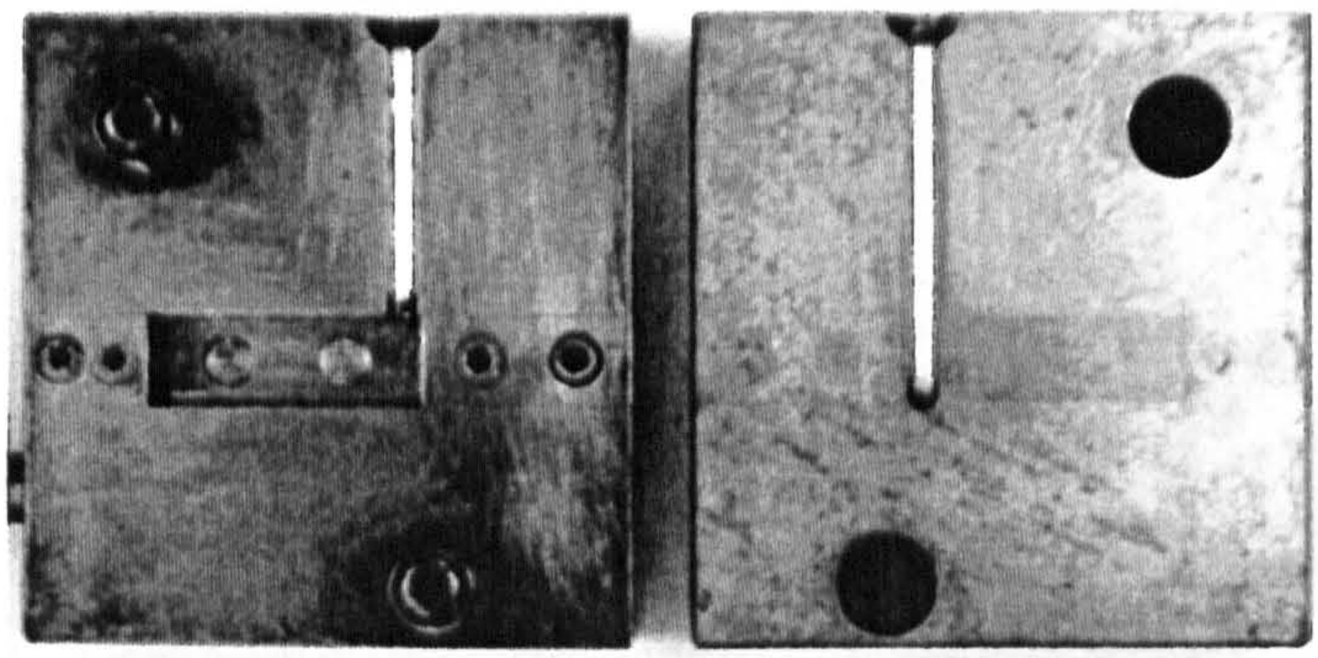

Figure 3.20- (b) Picture of the mould used for the moulding of the samples in Fig. 3.20- (a).

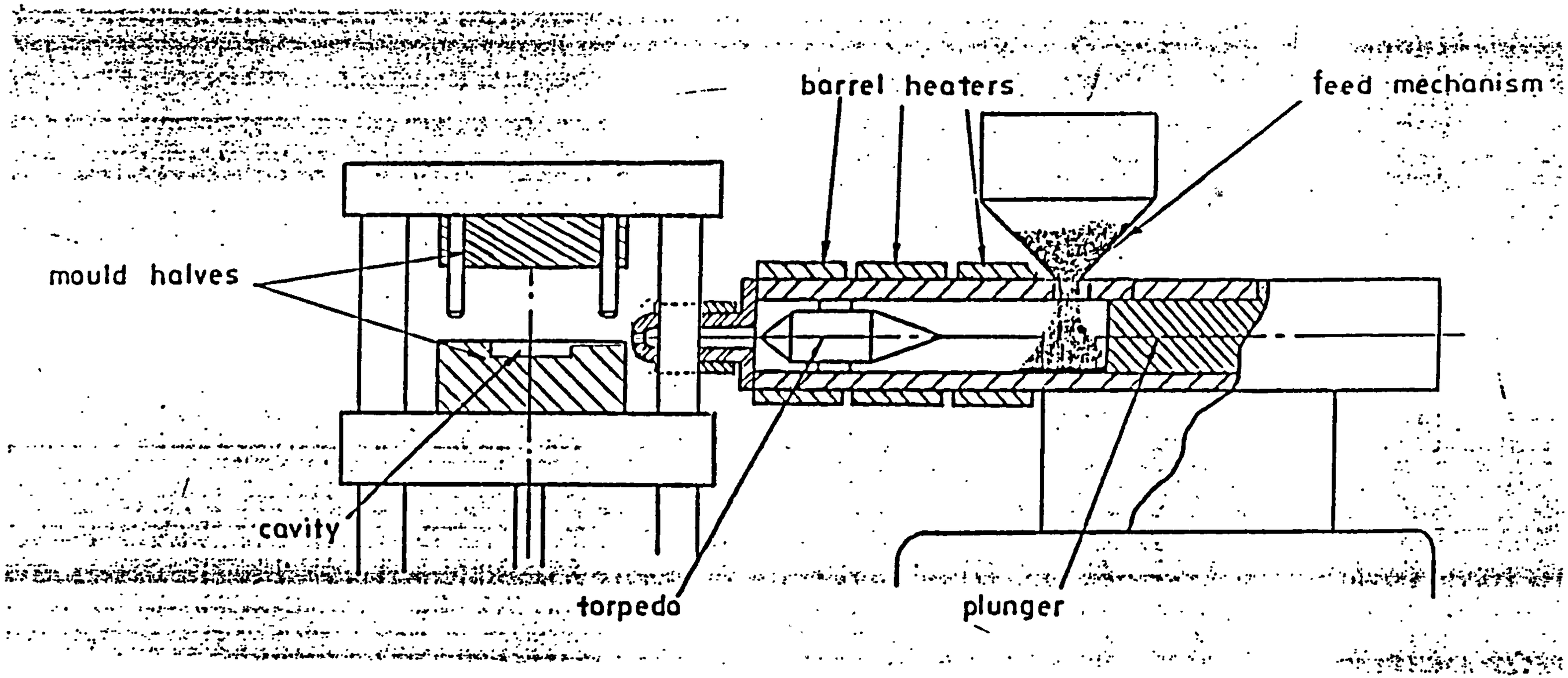

Figure 3.21- Schematic diagram of the Fox and Offord plunger type injection moulding machine used for mouldings of simple geometries.

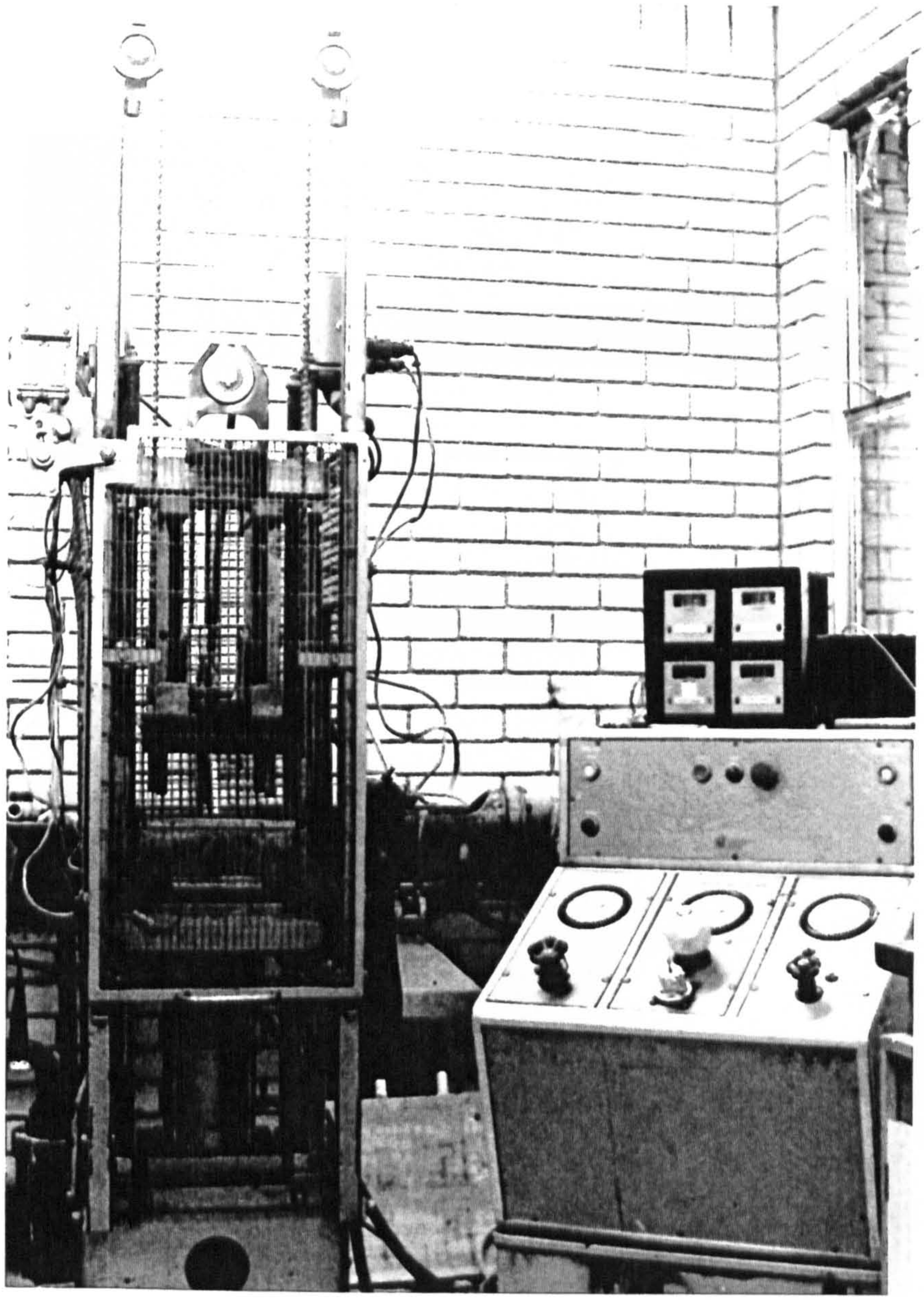

Figure 3.22- Picture of the Fox and Offord plunger type injection moulding machine used for the moulding of simple geometries.

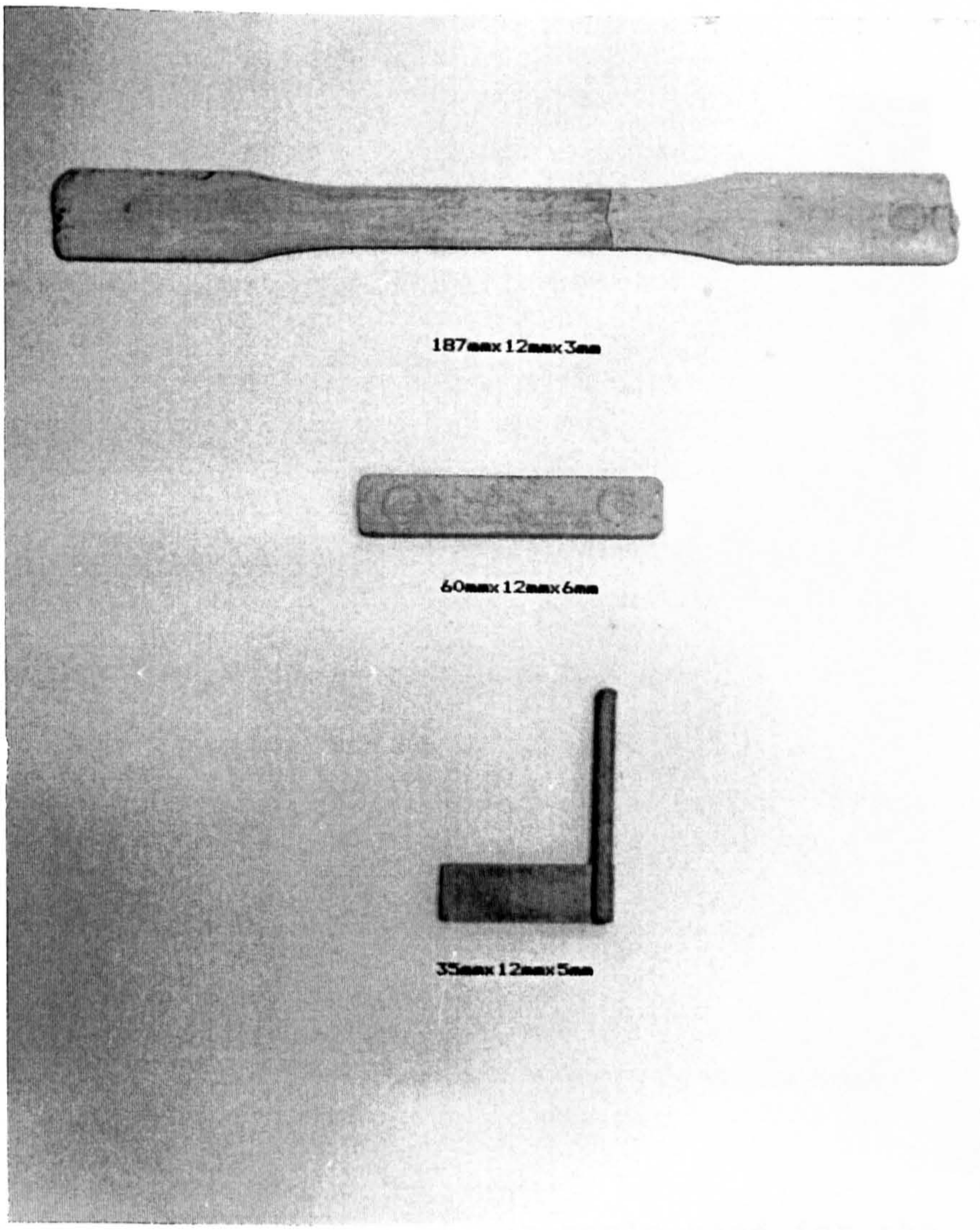

Figure 3.23- (a) Injection moulded samples of size 187 mm X 12 mm X 3 mm and 62 mm X 12 mm X 6 mm using the Fox and Offord injection moulder;

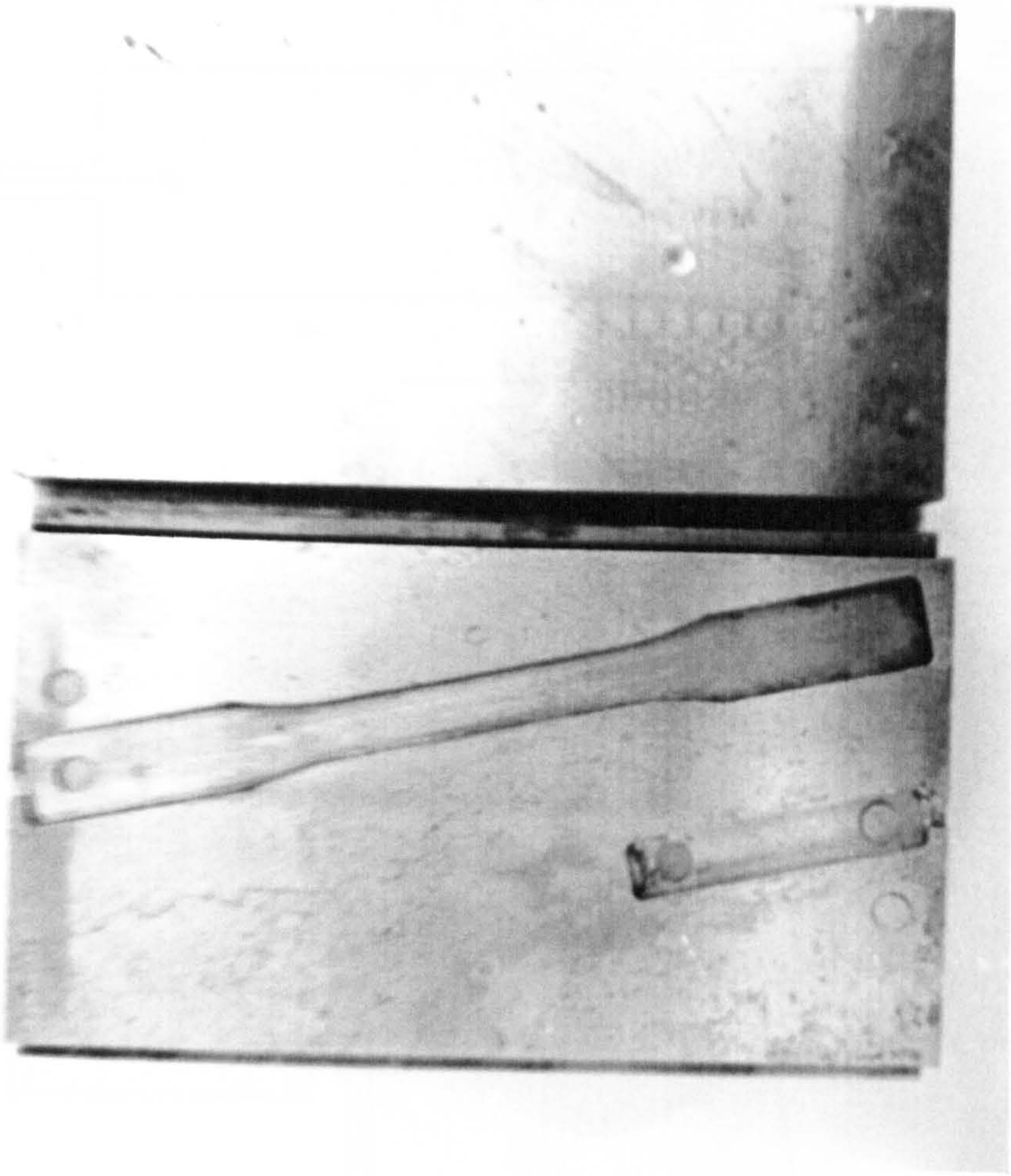

Figure 3.23- (b) Picture of the mould used for the moulding of the samples in Fig. 3.23- (a).

Figure 3.24- Schematic diagram of the thermogravimetric analysis (TGA) machine.

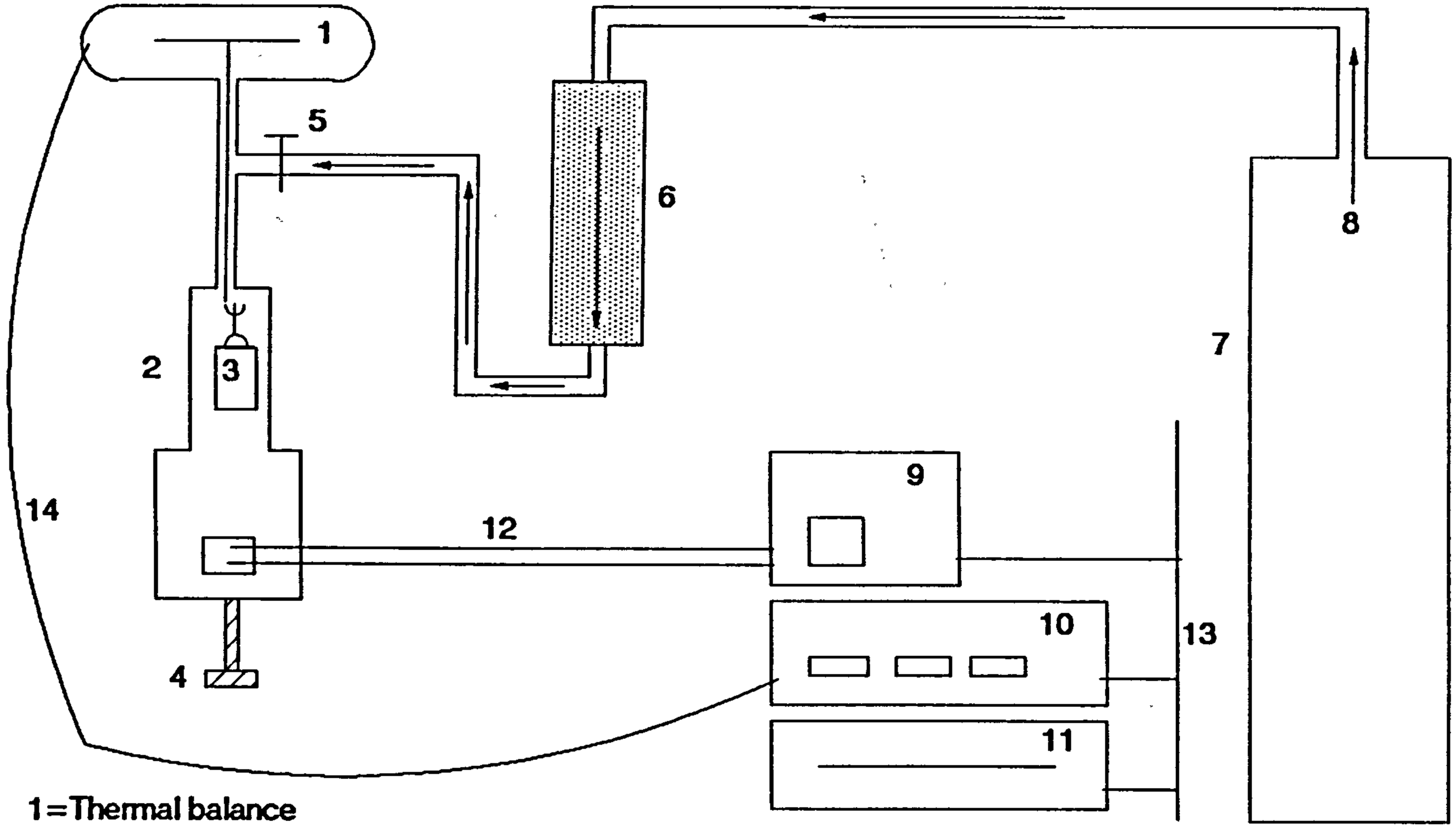

1=Thermal balance
2=Furnace
3=Crucible
4=Screw
5=Valve
6=Deoxidiser column
7=Gas cylinder
8=Gas inlet
9=Temperature controller
10=Micro balance
11=Chart recorder
12=Thermocouple
13=Connections between 9,10 & 11
14=Connection between 1 & 10

Figure 3.25- Schematic graphs of % weight loss and % rate of weight loss versus temperature obtainable from the TGA machine

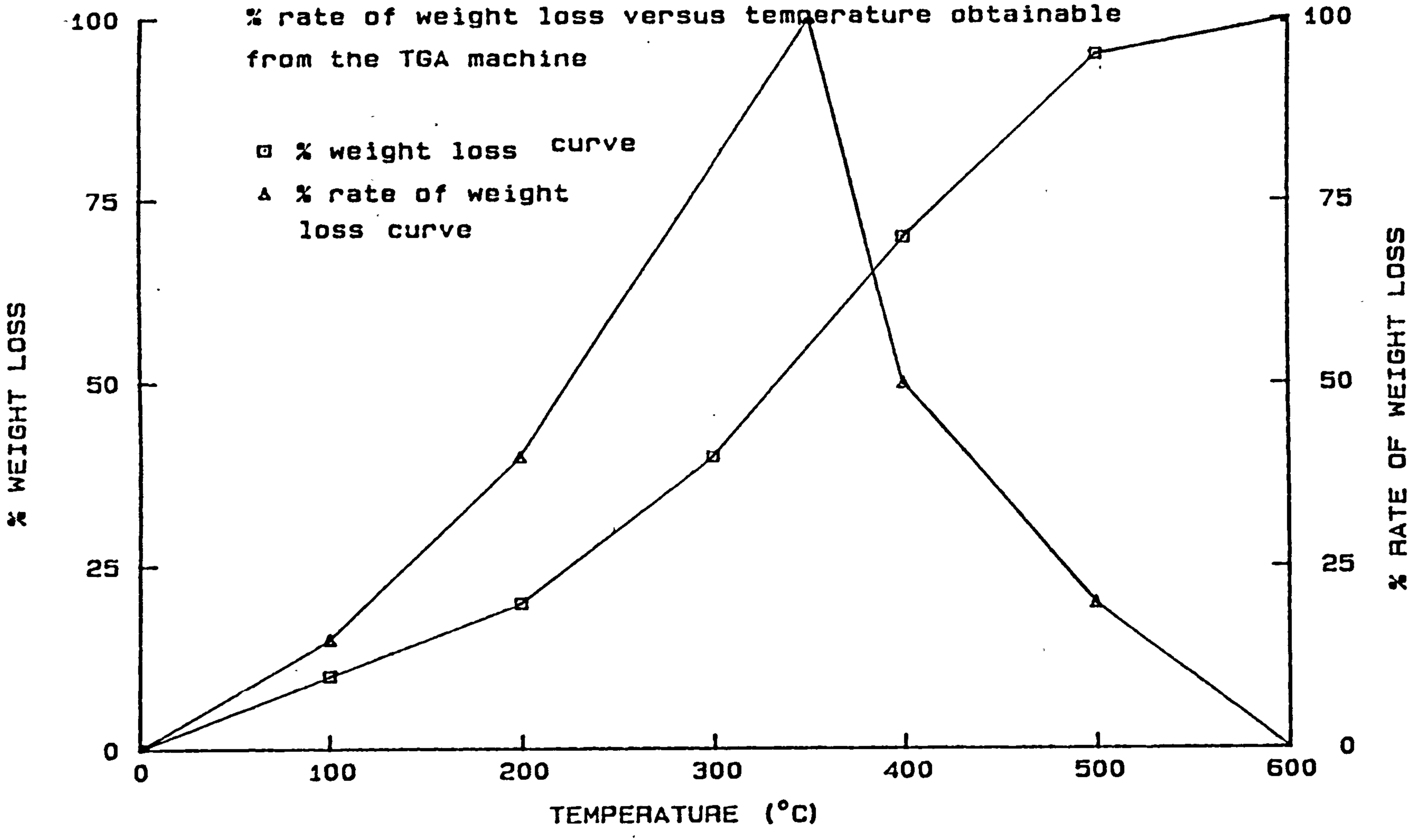

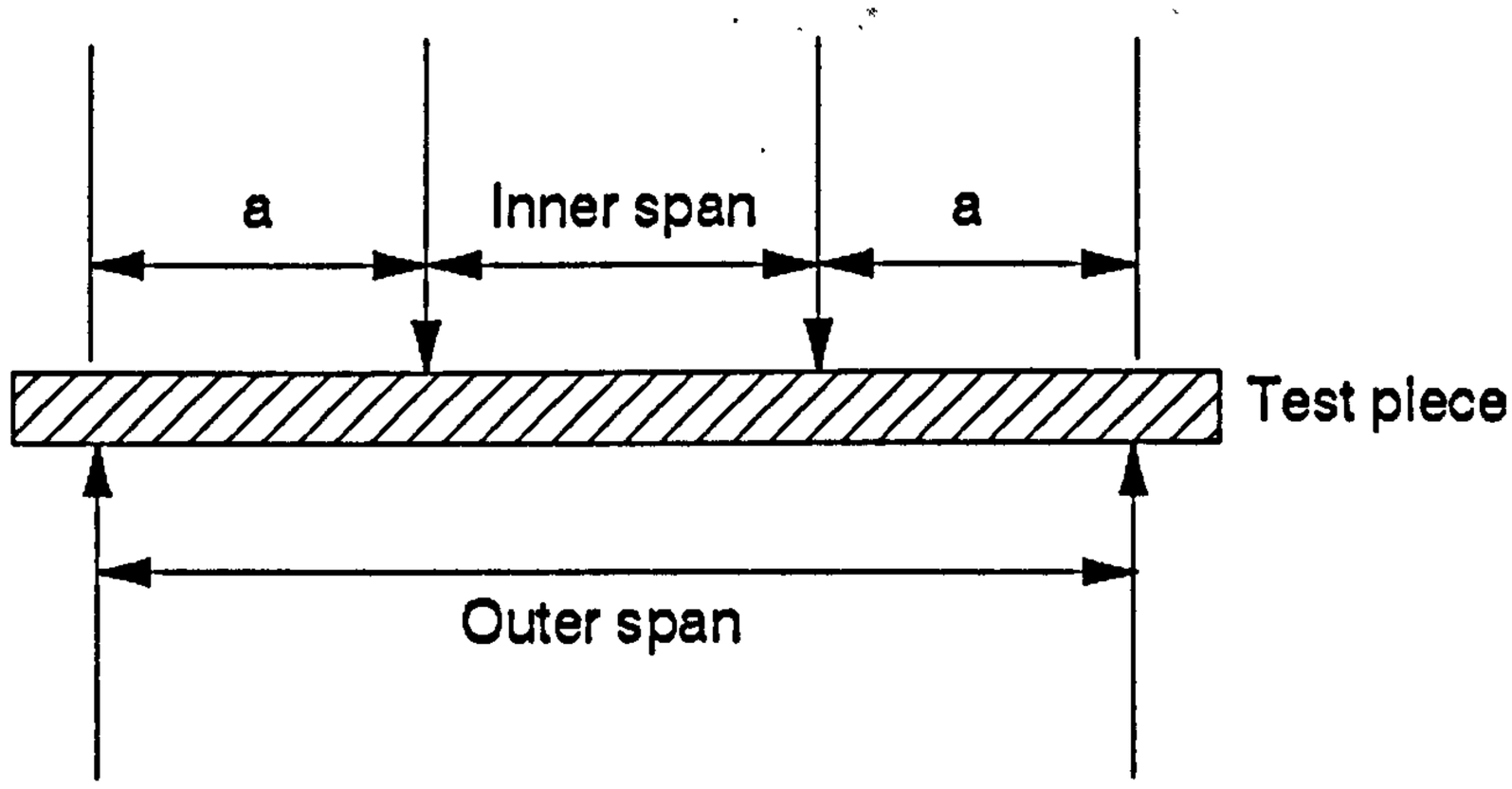

Figure 3.26- Schematic diagram of the 4-point test rig.

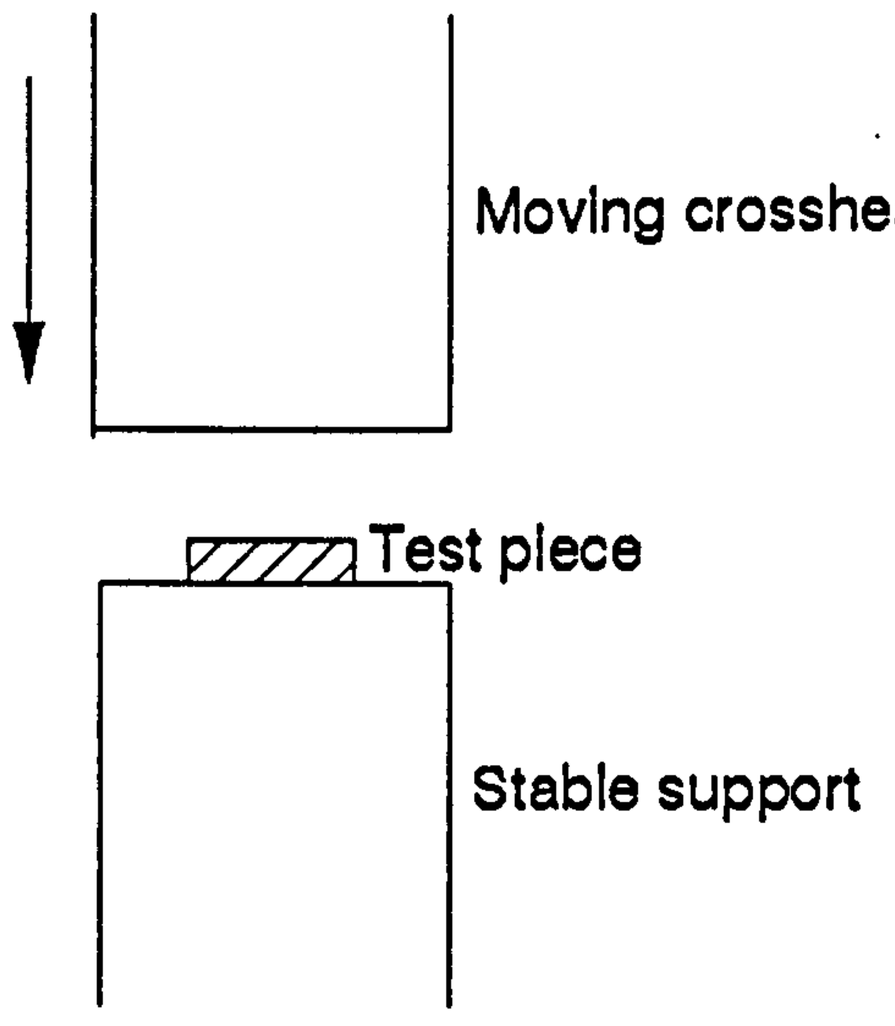

Figure 3.27- Schematic diagram of the compressive test.

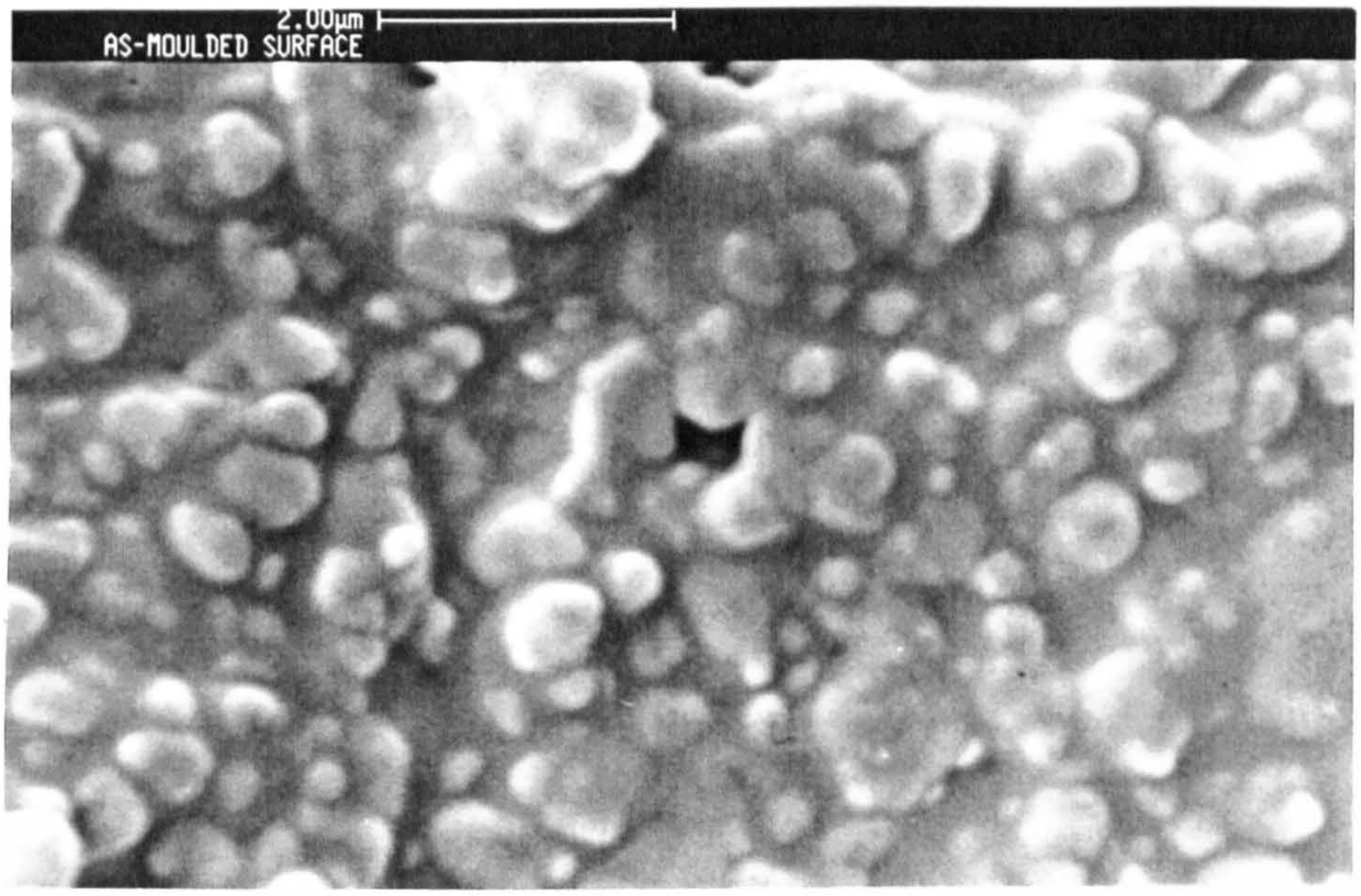

Figure 3.28- SEM photomicrograph showing a typical microstructure of a ceramic powder-binder mixture.

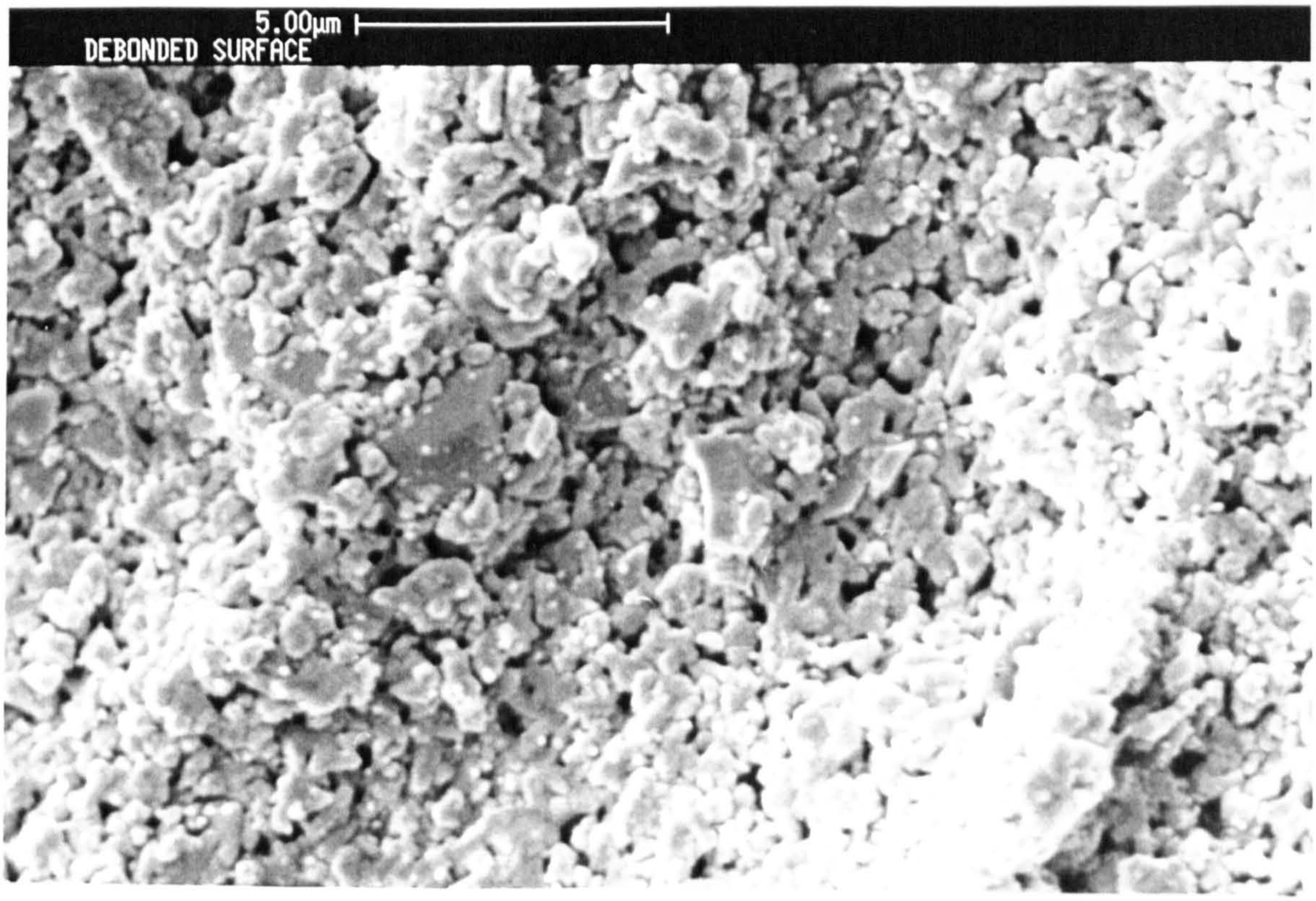

Figure 3.29- SEM photomicrograph showing a typical microstructure of a debonded body.

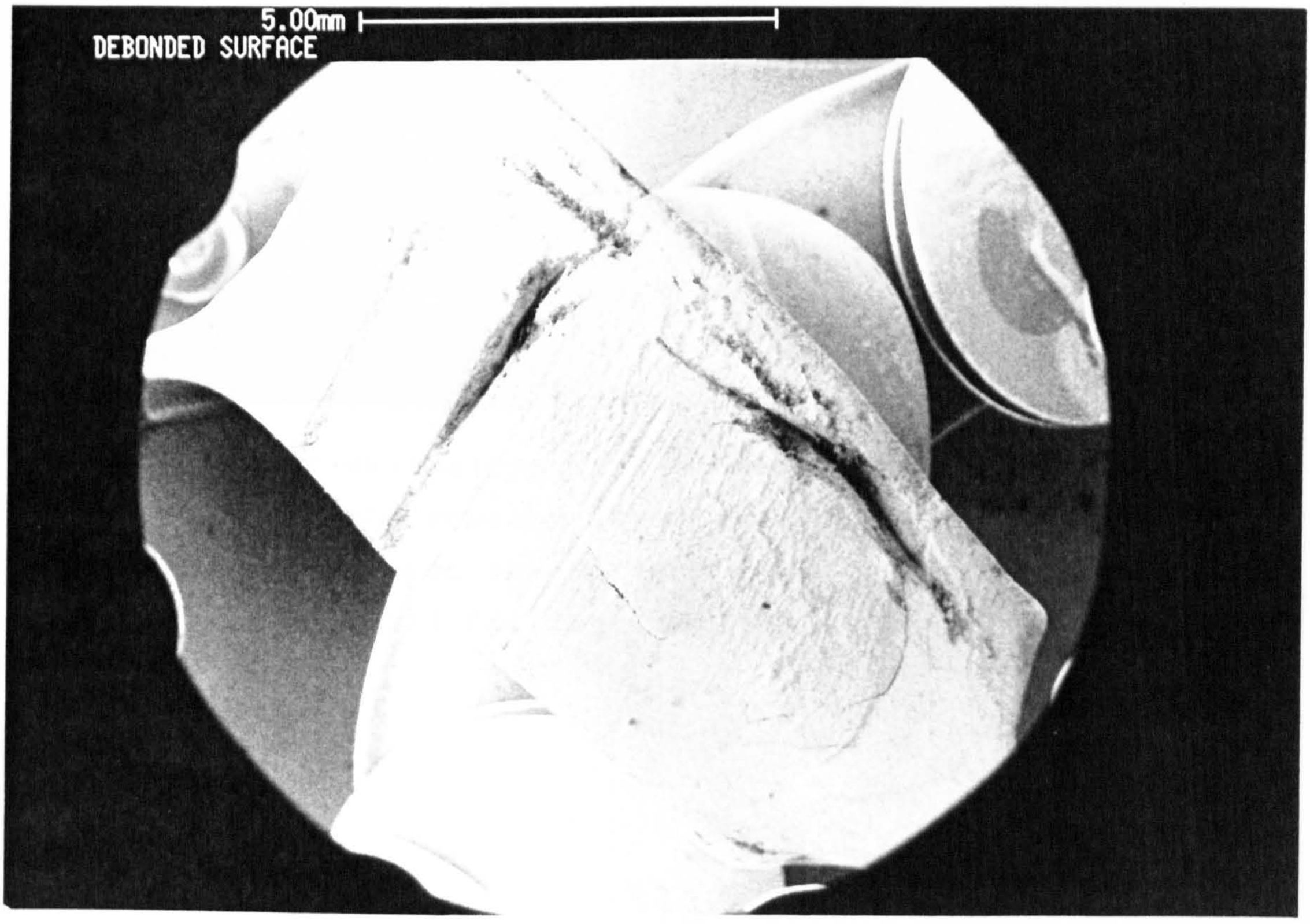

Figure 3.30- SEM photomicrograph showing macro-cracks within a debonded body.

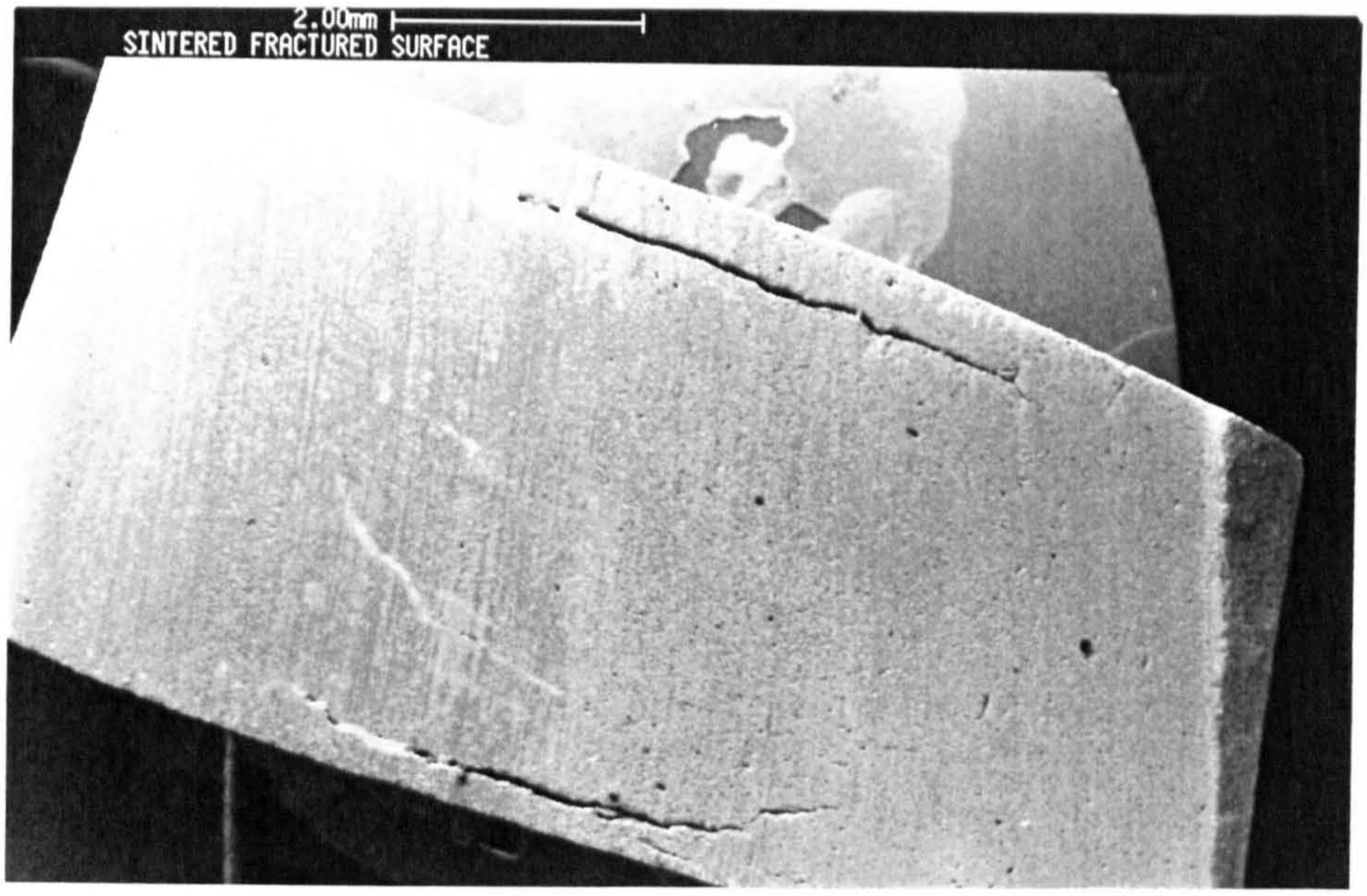

Figure 3.31- SEM photomicrograph of a sintered fractured surface showing layers of voids (delamination) near the surface which appeared during the mould filling stage.

Figure 3.32- Optical photograph of a moulded 88 % alumina-atactic polypropylene sample showing jetting flow due to limited fluidity.

CHAPTER FOUR

CHAPTER FOUR

4- RESULTS AND THEIR INTERPRETATION

This chapter is devoted to the experimental/practical results obtained during this research programme. These results are interpreted for each stage of the injection moulding process and also for the mechanical, microstructural and thermal properties of the injection moulded alumina ceramics obtained during this work.

This chapter is divided, mainly, into five sections. Section 4.1 covers the properties of the re-evaluated (existing) binder systems used for the injection moulding of alumina ceramics. Section 4.2 covers the properties of the newly developed (during this work) binder systems used for the injection moulding of alumina ceramics. Section 4.3 gives the mechanical, microstructural and thermal properties of the alumina ceramics obtained during this work by the injection moulding process using the best re-evaluated binder system and the newly developed binder systems during this work. Sections 4.4 and 4.5 cover the results obtained for the injection moulding of other powders using the newly developed binder systems during this work.

A summary of the results (properties) for each section is also given at the end of each section. Related Tables and Graphs (Figures) are given at the end of this chapter.

4.1- The re-evaluation of binder systems for which some successes have been claimed in the literature

The objectives of the first part of this research work was to re-evaluate the properties of some of the most popular binder systems used for the injectiom moulding of alumina ceramics. As will be seen the binder systems have been studied in variable detail depending upon initial findings. In most cases composition and mixing processing, rheology, thermogravimetric analysis, moulding, debinding and sintering properties were studied. These initial investigations were carried out to evaluate the advantages and disadvantages of the binder systems studied and by using this knowledge to develop new binder systems with improved properties which is the objective of the second part of this work.

From the literature it was concluded that there are two main groups of binder systems and the whole powder injection moulding industry uses one or other of these systems. One group uses the usual thermoplastics and waxes and is referred to as the Wiech process. The other group is based on water-soluble polymers which is known as the Rivers process. These processes are named after their respective inventers.

The first part of chapter four was started by using the binder systems based on the Wiech process and ended by using the Rivers binder system. The binder systems are listed in a manner that shows improvements in their properties.

4.1.1- Ethylene vinyl acetate (EVA) binder system

Preliminary trials were carried out to gain an overview of the system from mixing through rheology, thermogravimetric analysis, moulding trials and debinding. No sintering trials were carried out due to the lack of promise of the system.

Composition and mixing results

The mixture of a typical composition as shown in Table 4.1 was prepared using the Brabender plastograph at 50 rpm and 160°C for 1 h. The mixture produced was soft and rubbery and tended to stick to the sides of the mixing chamber above 60°C . On cooling down to room temperature it was possible to remove it from the mixing chamber.

The softness and rubbery behaviour of the mixture was due to the presence of 25 % acetate in the EVA binder. The higher the acetate content the more rubbery the EVA copolymer and vice versa. It is known that the higher the acetate content the more amorphous (less crystalline) the EVA copolymer.

Torque rersults

A steady state torque of 280 mg was observed during the mixing process from the Brabender plastograph. This torque can be recorded graphically as shown schematically in Figure 4.1 by using the Brabender chart recorder.

Note that this torque is related to the amount of shearing taking place during mixing inside the mixing chamber and can be used to calculate viscosity. It is therefore an important result and there is a critical steady state torque above which moulding cannot be carried out, i.e. the binder mixture is too viscous to be moulded.

Viscosity results

The apparent viscosity was determined as a function of apparent shear rate for the above mixture and the results are shown in Fig. 4.2. The relationship indicates typical pseudoplastic behaviour of this system. Note that at a shear rate of 300 s^{-1} the viscosity is approximately 400 Pas which is a low value at 160°C and therefore it is possible to reduce the barrel/nozzle temperature to reduce the sticking problem during moulding.

The viscosity results were obtained by using the Davenport rheometer with a barrel of diameter 19 mm at 160°C and a die of diameter 1.5 mm and of length 15 mm.

Thermogravimetric analysis (TGA results)

The alumina-EVA binder mixture was subjected to thermogravimetric analysis and the results are summarised in Fig. 4.3. Here the weight losses are shown as a function of temperature for different heating rates. From the TGA curves it is clear that there is a wide burning zone with two clear decomposition stages. It is likely that the first stage which occurs at temperatures in the range 250-410°C corresponds to the breakdown of the vinyl acetate side groups, whereas the second stage at 410-500°C corresponds to the breakdown of tha main ethylene chain.

Injection moulding results

Preliminary injection moulding trials were made using the Fox and Offord injection moulder under the conditions given in Table 4.2. Rectangular samples of size 62 mm X 12 mm X 6 mm were moulded for density measurements and debinding trials. A mould release agent was sprayed on the tops and bottoms of the mould prior to injection because of the tendency of the samples to stick. The moulded samples showed no obvious defects.

Note that the moulded samples throughout this work showed very small moulding shrinkages of about < 0.01 % which is negligible and due to this reason there will be no moulding shrinkage results throughout this work.

As-moulded (green) density

The average green density of five samples was 2.60 $g.cm^{-3}$ which is less than the theoretical density of 2.79 $g.cm^{-3}$. The average measurerd value is 93.5 % of the theoretical value.

Note that the green and sintered density values throughout this work were very consistent (for each binder system) and there were no variations in these results up to two decimal points (±0.00 %) which is the usual way of showing the density values. However, for each binder system, the green and sintered densities of five samples (in each case) were determined (by weight and size measurements) and the average density values are given without showing any variations.

Debinding results

Attempts were made to debind the moulded samples at heating rates of ≤5°C/h, i.e. much less than the heating rates in the TGA work. It was found that cracking and crumbling of the samples took place during the second decomposition stage at 350-450°C.

Due to the cracking and crumbling of the samples no sintering trials were carried out.

Summary

Overall the EVA binder system did not show great promise as being suitable for the injection moulding of the alumina powder due to the relatively low volume loading of the alumina powder and the unsatisfactory debinding behaviour.

4.1.2- polystyrene binder system

Composition and mixing results

The compositions shown in table 4.3 were mixed using the Brabender plastograph at 50 rpm and 150°C for 45 min for each composition.

It was found that at room temperature compositions 1 and 2 were quite plastic and easily granulated (crushed into small pieces) whereas composition 3 provided a less plastic and a better granulating properties . Composition 4 was very tough and could not be granulated easily and as can be seen from Table 4.3 it produced a very high torque during mixing which may cause seizure during injection moulding and a dialatant flow behaviour above a certain shear rate.

The above compositions provided no sticking problems during and after mixing which was due to the adequate amount of diethyl phthalate and stearic acid as plasticiser and lubricant respectively.

Viscosity results

These are shown in the plot of Fig. 4.4. From this it can be seen that compositions 1, 2, and 3 have produced typical pseudoplastic viscosity curves whereas composition 4 with a 65 % volume loading of alumina powder has shown a dilatant flow behaviour which is not suitable for injection moulding. This is due to having insufficient polymer to carry the ceramic-binder mixture through the injection system. From these results it can be concluded that composition 3 with the highest possible volume loading of 62 % alumina powder is the most suitable alumina-polystyrene formulation for injection moulding. This composition was therefore chosen for moulding, debinding and sintering

investigations. From the viscosity curve for composition 3 it can be seen that fairly low viscosities have been obtained at this temperature (150°C) which suggests that it is possible to mould this composition at a lower barrel/nozzle temperature (< 150°C). The above viscosity results were obtained by using the Davenport rheometer with a barrel of diameter 19 mm at 150°C and a die of diameter 3 mm and length 20 mm.

Thermogravimetric analysis (TGA results)

The results are shown in Fig. 4.5 for stearic acid (S. A.), diethyl phthalate (D.E.P.) and alumina-polystyrene-SA-DEP binder mixture. Note that all the TGA results during this work were determined for the optimised (most suitable) composition (e.g. composition 3 in this section). As can be seen from the TGA curves the stearic acid burns out first creating some pores within the sample. Diethyl phthalate comes off next causing more pores which promotes the burn out of the polystyrene. According to the TGA curve for the alumina-PS (polystyrene) binder mixture the actual critical temperature range for the removal of the binders is between 300 and 480°C . This leads to the use of few ramps and dwell times in this temperature range during the debinding process in order to have a defect-free product.

Injection moulding results

Rectangular samples of size 62 mm X 12 mm X 6 mm were moulded using the Fox and Offord injection moulder with moulding conditions given in table 4.4.

It is worth noting that the mould temperature was increased to 50°C in order to prevent incomplete filling of the mould cavity which took place at room temperature. The moulded samples showed no obvious moulding defects and were removed from the mould

without any problems.

Since the moulding operation above yielded promising results an attempt was made to mould test bars of the size shown in Fig. 4.6 with 3 mm thickness. This attempt was not completely successful, due to incomplete cavity filling, with this binder system using the same moulding conditions (see Table 4.4.). Increasing the barrel and nozzle temperatures to 160°C did not lead to complete cavity filing. However, the maximum moulded length was about 143 mm which provided samples with 3 mm thickness for the debinding process.

As-moulded (green) density

The average green density of five samples was 2.65 $g.cm^{-3}$ which is less than the theoretical green density 2.80 $g.cm^{-3}$. The average measured value is 94.5 % of the theoretical density which is slightly higher than that for the alumina-EVA binder mixture. This is mainly due to the higher volume loading of the alumina powder into the polystyrene binder system.

Debinding results

For the 6 mm thick samples of size 62 X 12 X 6 mm^3 the shortest debinding time was 180 h (≈7.5 days) with the optimised debinding cycle given in Table 4.5.

Note that the optimised debinding cycle for each binder system was achieved over a period of one to two months after trying several debinding programmes in order to obtain the ideal heating rate, temperature level and dwell time for each ramp. The optimised cycle provided the shortest possible debinding without any debinding defects, i.e. no cracks, no blistering and no swelling. Detail of the optimisation process is as follows: The optimisation process for each binder system started

by considering the TGA results and then programming the thermal ramping cycle using eight ramps. Each ramp had three variables, i.e. heating rate, temperature level and dwell/hold time which varried accordingly. Each variable was set at a reasonable value and optimised (usually) for three different stages of the debinding process. The first stage was below the softening point of each binder (typically < 200°C) during which higher heating rates (≤ 10°C/h) were used with 2-3 ramps providing shorter debinding times. The second stage was the critical decomposition zone (≈ 230-470°C) where the actual burning of the majer binder took place and therefore slower heating rates and longer hold times with 3-4 ramps were required. This stage was the longest stage of the debinding process. In the third stage it was possible to increase the heating rates due to the presence of more open channels of voids which also required fewer ramps (1-2) and hence shorter debinding times.

Debinding was also carried out for 3 mm thick samples to compare the debinding time with that of the 6 mm thick samples. After optimisation it was found that the shortest debinding time for the 3 mm thick samples of size 40 X 19 X 3 mm^3 and 40 X 12 X 3 mm^3 was 125 h which is about 65 h less than the debinding time for the 6 mm thick samples. The debinding cycle for the 3 mm thick samples is given in Table 4.6.

From the weight loss measurements after debinding it was found that more than 99 % of the organic binders had been removed from both the 3 mm and 6 mm thick samples.

Sintering results

The debonded alumina samples were sintered at 1750°C for 2.5 h under a vacuum of 6.5 X 10^{-9} atmosphere. The samples were heated up to the sintering temperature at a rate of 300°C/h.

The sintered samples were furnace cooled within 5 h, i.e. cooled to about room temperature and then removed from the furnace.
The as mentioned sintering cycle was achieved after optimising the sintering temperature and time. The optimisation details for the sintering process are as follows. The debonded samples were heated up to their typical sintering temperature, e.g. to 1750°C for the 99.5 % alumina grades, and held at this temperature for different periods of 1, 2, 2.5, 3, 4, 5, and 6 h. The sintered densities were measured after each period and it was found that, e.g. for the 99.5 % alumina grades, there was no change in the sintered densities after 2.5 h and therefore this was the optimised sintering time. For the lower grades of alumina the sintering temperature were also optimised since there was no clear information in the literature. The optimised sintering temperatures were obtainbed by sintering each grade at different temperatures for a constant period of 2 h. The sintered densities were measured and it was found that sintering temperatures of 1650 and 1580°C provided the highest densities for the 95 % and 88 % alumina grades respectively. The sintering times were then optimised as before and it was found that ther was no change in the sintered densities after a period of 3 h for both alumina grades (95 % and 88 %) and therefore the 3 h period was chosen as their optimised sintering time.

The average sintered density (for the 99.5 % alumina grade) of five samples was 3.67 $g.cm^{-3}$ which is 95 % of the theoretical density 3.87 $g.cm^{-3}$. A linear shrinkage of 15 % of the total volume was found for each sintered sample.

Summary

The polystyrene binder system provided very long debinding times of 180 and 125 h for the 6 mm and 3 mm thick mouldings respectively. Due to relatively high viscosities with a maximum possible volume loading of 62 % of the alumina powder only medium sized mouldings of 62 X 12 X 6 mm^3 and 143 X 12 X 3 mm^3 (see Fig. 4.4) could be prepared. However, with this volume loading green and sintered densities of 94.5 % and 95 % of their respective theoretical values were achieved.

No further improvement in density seemed likely.

4.1.3- Polyacetal binder system

Composition and mixing results

The compositions in Table 4.7 were mixed using the Brabender plastograph at 50 rpm and 180°C for 1 h in each case. Torques of 255, 315 and 420 mg were observed for compositions 1, 2 and 3 respectively. It was found that all the resulting mixtures were quite tough and granulated with difficulty. There were no sticking problems during and after mixing.

Viscosity results

These are shown in the plots of Figs. 4.7 and 4.8 for two different 20 mm dies of diameter 3 mm and 1.5 mm respectively. The capillary dies were used with a Davenport rheometer having a barrel of diameter 20 mm.

From these Figures it can be seen that compositions 1 and 2 show typical pseudoplastic flow behaviour which is essential for injection moulding. Composition 3 with a volume loading of 59.5 % shows dilatant flow behaviour above a certain shear rate which is not suitable for injection moulding. These plots also show that the smaller the die diameter the higher the shear rates and that there is a critical shear rate above which dilatant flow takes place. The dilatant flow takes place because there is not enough organic binder at the critical shear rate to carry the powder through and eventually there will be a seizure as the shear rate increases within the die or at the tip of the nozzle.

These data therefore suggested that composition 2 with a maximum possible volume loading of 56.8 % alumina powder has the most suitable flow properties and was therefore chosen for moulding, debinding and sintering investigations.

Thermogravimetric analysis (TGA results)

TGA data for atactic polypropylene (APP, molecular weight=10,600 and density = 0.86 $g.cm^{-3}$) and low density polyethylene (LDPE) is shown in Fig. 4.9. The TGA curve for LDPE shows that this (minor) binder burns in a narrow temperature range at about 380-460°C whereas the APP binder burns in a wider temperature range at about 260-420°C. It follows therefore that in terms of easy debinding the APP binder burns out more easily (than the LDPE binder) over a wide decomposition zone whereas the LDPE burns faster within a narrow critical zone. The decomposition zone for any binder depends on different factors and the most important one is the molecular weight. Most waxes, e.g. polyethylene wax, have low molecular weights and thus have less carbon backbone to break which means faster burning and a narrower decomposition zone. For an organic material, e.g. APP, with higher molecular weights it takes longer to burn due to higher carbon backbones to be broken.

The TGA data for the alumina (99.5 % Grade)-polyacetal binder mixture at different heating rates are shown in Fig. 4.10. The TGA curves show that the actual decomposition zone is at 280-420°C and that at about 440°C almost 100 % weight loss has been achieved.

Injection moulding results

Rectangular samples of size 62 mm X 12 mm X 6 mm were moulded using the Fox and Offord injection moulder with the conditions given in Table 4.8.

The moulded samples were rigid and there were no demoulding problems and no moulding defects.

Another attempt was made to mould longer samples of size 187 mm X

12 mm X 3 mm with the same moulding conditions as in Table 4.8. This attempt was not completely successful due to incomplete cavity filling and only samples of size 73 mm X 12 mm X 3 mm were obtained. By increasing the mould temperature to 56°C so that to increase the amount of flow within the mould cavity only moulded samples of size 87 mm X 12 mm X 3 mm were obtained.

As-moulded (green) density

The average green density of five samples was 2.52 $g.cm^{-3}$ which is 92 % of the theoretical density 2.74 $g.cm^{-3}$. This is a relatively low green density which is due to the low volume loading of the alumina powder into the polyacetal binder system.

Debinding results

The shortest debinding time for the 6 mm thick samples of size 62 X 12 X 6 mm^3 was 129 h with the optimised debinding cycle given in Table 4.9.

Sintering results

The debonded alumina samples were sintered at 1750°C for 2.5 h under a vacuum of 6 X 10^{-9} atmosphere. The samples were heated up at a rate of 300°C/h. The sintered samples were furnace cooled to room temperature within 5 h.

The average sintered density of five samples was 3.62 $g.cm^{-3}$ which is 93.5 % of the theoretical density 3.87 $g.cm^{-3}$. A linear shrinkage of 16 % of the total volume was obtained for each sintered sample.

Summary

The polyacetal binder system provided a debinding time of 129 h for the 6 mm thick samples of size 62 X 12 X 6 mm^3 which is 51 h shorter than that of the polystyrene binder system. A maximum possible volume loading of 56.8 % alumina powder was provided by the polyacetal binder system which resulted in green and sintered densities of 92 % and 93.5 % of their respective theoretical densities. Both the amount of volume loading and the obtained densities are lower than those obtained for the polystyrene binder system.

4.1.4- Atactic polypropylene (APP) binder system

This section is divided into three parts. The first part is devoted to the injection moulding of 99.5 % alumina powder using a single APP binder with a molecular weight of 10,600. The second part is devoted to the injection moulding of 99.5 % alumina powder using a mixture of two atactic polypropylenes (APP mixture) having two different molecular weights of 10,600 and 60,400. The third part is devoted to the injection moulding of 88 % and 95 % alumina powders using the APP mixture.

The first part of the work described was carried out in order to investigate the flow characteristics of the system, the volume loading which could be achieved, the moulding and demoulding properties and the debinding characteristics of the lower molecular weight APP. It was then intended to use the results of these investigations to reduce the debinding time by using the APP mixture. Finally it was hoped to determine whether any improvements could be achieved in the sintering properties by moulding lower grades of alumina powder using the APP mixture.

4.1.4. (a)- The single APP binder system

Composition and mixing results

The compositions given in Table 4.10 were mixed using the Brabender plastograph at 50 rpm and 150°C for 40 min in each case.

Torques of 270, 315 and 395 mg were recorded for compositions 1, 2 and 3 respectively. It was found that all the alumina-APP mixtures granulated quite easily and provided no sticking problems during or after mixing.

Viscosity results

These are shown in the plots in Figs. 4.11 and 4.12. From Fig. 4.11 it can be seen that compositions 1 and 2 show pseudoplastic flow behaviour whereas composition 3 shows dilatant flow behaviour above a shear rate of 360 s^{-1}. The dilatent flow behaviour of composition 3 is probably due to the high volume loading of the alumina powder into the APP binder system and therefore this composition cannot be used for moulding. Composition 2 with a maximum possible volume loading of 64 % of the alumina powder was chosen as the most suitable formulation for moulding, debinding and sintering investigations.

For this system the most suitable temperature range for moulding was determined and the results can be seen in Fig. 4.12. This shows that as the extrusion temperature decreases the viscosity increases, i.e. can see the temperature dependency of viscosity. From these results it is clear that in order to have a defect-free moulding the right moulding temperature has to be chosen so that to provide the correct flow behaviour. The viscosity curves in Fig. 4.12 therefore suggest that it is quite safe to mould within the temperature range 90-120°C since the pseudoplastic flow behaviour is observed for each temperature throughout the extrusion process. However, as the temperature decreases the viscosity increases which means the amount of flow within the mould cavity will decrease and therefore it is necessary to choose the right temperature for the right amount of flow.

The above viscosity results were obtained using the Davenport rheometer with a barrel of diameter 19 mm and a die of diameter 1 mm and of 20 mm length.

Thermogravimetric analysis (TGA results)

The results are shown in Fig. 4.13 for the alumina (99.5 % Grade)-APP binder mixture at different heating rates. The TGA curves show that the critical temperature range is at 280-480°C and that the APP binder has a wide decomposition zone which is helpful in obtaining easy and defect-free burn-out.

Injection moulding results

Rectangular samples of size given in Table 4.11 were moulded using the Fox and Offord injection moulder with the conditions given in Table 4.12.

From Table 4.11 it can be seen that it was possible to mould longer samples due to the higher fluidity of the APP binder system even at a lower moulding temperature whereas this was not possible with the polystyrene and polyacetal binder systems. The moulded samples were demoulded quite easily and there were no handling problems and no obvious defects. So far the APP binder system has provided the best flow and moulding properties and also the highest volume loading of the alumina powder compared to the previous binder systems. In this case it was worthwhile therefore to proceed with further investigations.

Debinding results

For the 3 mm thick samples of size 40 X 19 X 3 mm^3 and 40 X 12 X 3 mm^3 the shortest debinding time was 105 h with the optimised debinding cycle given in Table 4.13. For the 6 mm thick samples of size 62 X 12 X 6 mm^3 the shortest debinding time was 129 h which is the same as the 6 mm thick debonded alumina-polyacetal samples with the same debinding cycle (see Table 4.9).

As-moulded (green) density

The average green density of five samples was 2.67 $g.cm^{-3}$ which is 95.5 % of the theoretical density 2.80 $g.cm^{-3}$. This is the highest green density so far which is due to the highest volume loading of the alumina powder into the APP binder system.

Sintering results

The debonded samples were sintered at 1750°C for 2.5 h under a vacuum of 6.6 X 10^{-9} atmosphere. A heating rate of 300°C/h was applied. The sintered samples were furnace cooled to room temperature over a period of 5 h after which they were removed from the furnace.

The average sintered density of five samples was 3.71 $g.cm^{-3}$ which is 96 % of the theoretical density 3.87 $g.cm^{-3}$. This is the highest sintered density so far achieved.

A linear shrinkage of 11.5 % of the total volume was obtained for each sintered sample.

Summary

The APP binder system provided the highest volume loading of 64 % of the alumina powder which resulted in the highest green and sintered densities of 95.5 % and 96 % of their theoretical values respectively so far. This binder system also provided the longest moulded samples of size 187 mm X 12 mm X 3 mm which was not possible with the previous binder systems. Debinding periods of 105 and 130 h were obtained for the 3 mm and 6 mm thick samples respectively.

4.1.4. (b)- The atactic polypropylyne (APP) binder system with the APP being a 60/40 mixture of two different molecular weights

It was discovered by Saito et al (165) that by mixing different fractions of atactic polypropylene having molecular weights of 5000-120000 the thermal decomposition rate can be freely adjusted. This also broadens the critical decomposition region which is very useful for an easy and defect-free burn-out. A wider decomposition range allows higher heating rates which provides shorter debinding periods. It was suggested that for the removal of the organic binders, the moulded samples should be heated from room temperature to a level between 100-140°C in about 2 h and then to 340-380°C in increments of 3-10°C/h. This part of the work was carried out in order to investigate the claims of Saito et al (165) and therefore to obtain more detailed experimental information concerning the mixing, moulding, debinding and sintering processes.

Composition and mixing results

From the work in the previous section it was found that composition 2 in Table 4.10 provided the highest possible volume loading of 64 % for the alumina powder into the APP binder system and therefore the same composition was used throughout this section except that the APP binder was a mixture of 60 % by weight of an APP having a density of 0.9 $g.cm^{-3}$ and an average molecular weight of 60400 and 40 % by weight of another APP (i.e. the same APP as in the previous section) having a density of 0.86 $g.cm^{-3}$ and an average molecular weight of 10600. The Brabender plastograph was used with the same mixing conditions as in the previous section. A slightly higher torque of 325 mg was observed for the 60/40 APP binder mixture which was due to the presence of

a higher molecular weight APP causing higher shearing within the mixing chamber. There were no sticking problems during and after mixing and the mixture granulated quite easily.

Viscosity results

These are summarised in Fig. 4.14. As can be seen from the viscosity curve a typical pseudoplastic flow behaviour was obtained with slightly higher viscosities at 120°C as compared to the viscosities obtained at the same temperature for the alumina-APP binder system of composition 2 in the previous section. This viscosity rise is due to the presence of the higher molecular weight APP. Due to the viscosity rise it is necessary to increase the extrusion and moulding temperatures so that to increase fluidity during the extrusion and moulding processes.
The above viscosity results were obtained by using the Davenport rheometer with the same barrel and die as in the previous section.

Thermogravimetric analysis (TGA results)

The results of the investigations are shown in Fig. 4.15 for the two APP with different molecular weights and also for the 60/40 APP mixture.

From the TGA curves it can be seen that the APP with a higher molecular weight of 60400 decomposes rapidly in the range 280-400°C and the APP with a molecular weight of 10600 decomposes in the range 320-460°C. For an easy and defect-free burn-out a wide decomposition zone at a slow burning rate is more desirable and this can be observed from the TGA curve for the 60/40 APP mixture. This curve shows a very wide decomposition zone at 240-460°C with an almost linear decomposition rate.

Injection moulding results

The same rectangular samples as in Table 4.11 (see previous section) were moulded using the Fox and Offord injection moulder with the conditions given in Table 4.14.

As can be seen from Table 4.14 the barrel and nozzle temperatures were increased so as to provide good fluidity for the alumina-60/40 APP binder mixture during injection moulding. The moulded samples were quite rigid and therefore were demoulded without any problems. No obvious moulding defects were found in cut sections of the samples.

Debinding results

The debinding cycle was programmed according to the TGA results for the 60/40 APP mixture (Fig. 4.15). After optimisation, the shortest debinding time for the 3 mm thick samples of size 40 X 19 X 3 mm^3 and 40 X 12 X 3 mm^3 was 78 h with the optimised debinding cycle given in Table 4.15.

For the 6 mm thick samples of size 62 X 12 X 6 mm^3 the shortest debinding time was 107 h with the optimised debinding cycle given in Table 4.16.

As-moulded (green) and sintered densities

The average moulded density of five samples was 2.67 $g.cm^{-3}$ which is 95.5 % of the theoretical moulded density 2.8 $g.cm^{-3}$. The average sintered density of five samples was 3.71 $g.cm^{-3}$ which is 96 % of the theoretical density 3.87 $g.cm^{-3}$. The sintering conditions were the same as the previous section. A linear shrinkage of 11.5 % of the total volume was obtained for each sintered sample.

The above results show no changes in the moulded and sintered density values to those obtained in the previous section.

Summary

The 60/40 APP binder system provided debinding times of 78 h and 107 h for the 3 mm and 6 mm thick moulded samples respectively. These are the shortest debinding times so far achieved. A maximum possible volume loading of 64 % of the alumina powder provided as-moulded and sintered densities of 95.5 % and 96 % of their theoretical values respectively.

Overall in terms of mixing, volume loading, fluidity, rheology, moulding, demoulding, thermogravimetric analysis, debinding time, green and sintered densities the 60/40 APP binder system has provided the best results so far.

4.1.4. (c)- Injection moulding of 88 % and 95 % alumina powders using the 60/40 APP binder system

Compositions of the alumina powders

These are given in Table 4.17. Each composition was dry blended for 3 h using a double cone mixer.

Particle size analysis for the 88 % and 95 % alumina powders

Particle size analysis for the 88 % and 95 % alumina grades was carried out during this work using the Malvern particle sizer. The results are given in Table 4.18. The particle size analysis for the 99.5 % alumina grade was carried out by the supplier (BA Chemicals).

From Table 4.18 it can be seen that the 88 % and the 95 % alumina powders have a wide range of particle size distribution (0.1-100 μm) which means that their tap densities will be higher than that of the 99.5 % alumina powder with a narrow particle size distribution (0.1-10 μm). A higher tap density means higher green and sintered densities for the compacted and injection moulded samples.

Tap densities of the 88 %, 95 % and 99.5 % alumina powders

The tap density for each composition/alumina grade is given in Table 4.19.

As expected from the wider particle size distribution range for the 88 % and 95 % alumina powders (see Table 4.18) higher tap densities were obtained for each composition as compared with the 99.5 % alumina powder. This is due to the more efficient filling (for the 88 % and 95 % alumina powder) of the empty spaces between large particles by smaller particles.

Composition and mixing results

The composition given in Table 4.20 was chosen (as in the previous section) for the injection moulding of the 88 % and 95 % alumina powders. Each composition was mixed by using the Brabender plastograph at 50 rpm and 150°C for 40 min. Both compositions provided an easy mix and a rather soft mixture at room temperature which granulated easily. There were no sticking problems during or after mixing. A torque of 330 mg was observed for each composition during the steady state period. The 88 % alumina-60/40 APP mixture looked more green (due to the presence of more Cr_2O_3 which is green in colour) than the 95 % alumina-60/40 APP mixture.

Viscosity results

The results are summarised in Figs. 4.16 and 4.17 for the 88 and 95 % alumina-60/40 APP binder mixtures respectively. Both Figures show that viscosity is temperature dependent, i.e. as temperature increases viscosity decreases and vice versa. Both Figures also show that the 64 vol. % alumina (88 % & 95 % grades) + 28 vol. % 60/40 APP mixture + 4.5 vol. % DEP+ 3.5 vol.% SA composition has behaved pseudoplastically and therefore it is a suitable composition for injection moulding different grades of alumina ceramic.

The above viscosity results for the the 88 % alumina-60/40 APP binder mixture were obtained by using the Davenport extrusion rheometer with a barrel of dia 19 mm and a die of dia 1mm and of length 20 mm. The viscosity results for the 95 % alumina-60/40 APP binder mixture were determined using the Davenport rheometer with a barrel of dia 10 mm and a die of dia 1 mm and of length 20 mm.

Thermogravimetric analysis (TGA results)

This is shown in the plot of Fig. 4.18. Both alumina grades were subjected to the same heating rate of 10°C/min and the TGA data was the same for each grade and therefore only one TGA curve is plotted in this Figure. The TGA curve shows a wide decomposition zone at 280-540°C which is very useful for an easy and defect-free burn-out. Stearic acid is the first (minor) binder to come out and diethyl phthalate is the next (minor) binder to burn out and both will create internal channels of pores which will help the 60/40 APP binder to come off easier as the last major binder.

Detemination of moulding conditions and the results of the moulding studies for the lower grade 88 % and 95 % alumina-60/40 APP binder mixtures

By comparing the viscosity curves at 130°C for each alumina grade (see Figs. 4.14, 4.16 and 4.17) it can be seen that the 99.5 % alumina-60/40 APP binder mixture has provided lower viscosities than both 88 % and 95 % alumina-60/40 APP binder mixtures. For example, at a shear rate of 400 s^{-1} the 99.5 % alumina grade has a viscosity of 108 Pas whereas the 88 % and the 95 % alumina grades have viscosities of 270 and 130 Pas respectively. These relatively higher viscosities for the 88 % and 95 % alumina 60/40 APP binder mixtures suggest that the lower grade alumina ceramics should be injected at a higher barrel/nozzle temperature than the high grade 99.5 % alumina-60/40 APP binder mixture. From the viscosity curves it can also be seen that the 95 % alumina-60/40 APP binder mixture has provided lower viscosities than the 88 % alumina-60/40 APP binder mixture, e.g. at a shear rate of 300 s^{-1} viscosities of 160 and 350 Pas at a temperature of 130°C are obtained for the 95 % and 88 % alumina grades respectively. This also suggests that the 88

% alumina-60/40 APP binder mixture should be injected at a higher barrel/nozzle temperature than the 95 % alumina grade so that to achieve similar flows in each case.

By considering the viscosity results, rectangular samples of size given in Table 4.22 were moulded using the Fox and Offord injection moulder with the conditions given in Table 4.21. As can be seen from Table 4.21 higher barrel/nozzle temperatures were used for both 95 % and 88 % alumina-60/40 APP binder mixtures due to their higher viscosities than the 99.5 % alumina-60/40 APP binder mixture. From this Table it can also be seen that the 88 % alumina-60/40 APP binder mixture was moulded at a higher barrel/nozzle temperature than the 95 % grade due to its higher viscosities than the 95 % grade.

From the dimentions of the moulded samples in Table 4.22 it can be seen that it was not possible to mould samples with 187 mm length due to insufficient flow within the mould cavity. This incomplete mould filling did not take place with the 99.5 % alumina-60/40 APP binder mixture which was due to its lower viscosities providing higher fluidity.

Another attempt was made in order to obtain longer moulded samples by increasing the mould temperature to 56°C and at this mould temperature only samples of size 62 mm X 12 mm X 6 mm and 68 mm X 12 mm X 3 mm were obtained for both 88 % and 95 % alumina-60/40 APP binder mixtures.

As-moulded (green) densities

These are tabulated in Table 4.23 along with the theoretical densities for all three grades of alumina-60/40 APP moulded samples.

As can be seen from the % theoretical densities in Table 4.23 the

88 % and 95 % alumina-60/40 APP moulded samples have provided higher green/moulded densities than the 99.5 % alumina-60/40 APP moulded samples which is due to their higher tap densities.

Debinding results

The optimised debinding times for the 88 % and 95 % alumina-60/40 APP samples were the same as those for the 99.5 % alumina-60/40 APP samples except that the low-grade (moulded) samples were debonded completely at a higher temperature of 520°C with the debinding cycles given in Tables 4.24 and 4.25 for the 3 and 6 mm thick samples respctively.

Sintering results

After optimisation of the sintering temperture and time the debonded 88 % and 95 % alumina samples were sintered at 1580°C and 1650°C respectively for 3 h. The samples were heated in air at a rate of 260°C/h up to the sintering temperature and then furnace cooled to room temperature within 7 h. The sintered densities and shrinkage values are given in Table 4.26. As can be seen from the % theoretical densities in Table 4.26 slightly higher sintered densities have been obtained for the 88 % and 95 % alumina grades which is due to their higher tap and green densities than the 99.5 % alumina grade.

4.1.5- Methylcellulose (water-soluble) binder system

This part of the research was carried out in order to investigate the Rivers binder system (Rbs) for the injection moulding of alumina powder. This binder system was originally used by Rivers (151) for the injection moulding of a high performance superalloy. A green density of 65 % and a sintered density of 99.5 % of their respective theoretical values were obtained using this binder system for the superalloy. The Rbs consisted of methylcellulose as the major binder, water as the solvent, glycerin and boric acid as modifiers (i.e. as plasticisers and lubricants/mould release).

Composition and mixing results

The compositions given in Table 4.27 were mixed at room temperature for 30 min in each case by using the Brabender plastograph at 50 rpm. The methylcellulose, glycerin and boric acid are soluble in water at room temperature and methylcellulose gels upon heating and therefore mixing and rheological analysis are carried out at about room temperature. The details of the compositions investigated are presented in Table 4.27.

Torques of 282, 328 and 460 mg were observed for compositions 1, 2 and 3 respectively. It was found that the mixtures were losing water even at room temperature and therefore had to be moulded or tested for rheology immediately after mixing. An alternative way to prevent water loss was to keep the mixtures in a humidity cabinet with more than 90 % humidity.

Viscosity results

The results are shown in Fig. 4.19. As can be seen from the viscosity curves for compositions 1 and 2 the pseudoplastic flow behaviour has taken place throughout the extrusion process. This

flow behaviour was not followed in the case of composition 3 which exhibited dilatant flow behaviour from a very early stage, i.e. the binder mixture shows dilatant flow above a shear rate of 266 s^{-1} and eventually composition 3 could not be extruded above a shear rate of 2670 s^{-1}.

The above viscosity results suggest that composition 2 with the highest possible volume loading of 55 % is the most suitable alumina-methylcellulose binder mixture for moulding, debinding and sintering investigations.

The above viscosity results were obtained by using the Instron rheometer with a barrel of dia 10 mm and a die of dia 1 mm and of 20 mm length.

Injection moulding results

Rectangular samples of size 35 mm X 12 mm X 5 mm were moulded using the small plunger type compressed air (PTCA) moulder with the moulding conditions given in Table 4.28.

The chosen composition was quite mouldable but there were adhesion and distortion problems during the demoulding process. Adhesion of the mouldings to the walls of the mould cavity was prevented by spraying a silicon-based mould release agent on to the mould prior to the moulding operation. The distortion (or bending) problem (which was due to the mouldings being not strong enough to resist the injection forces during the demoulding process) could not be prevented even after allowing a 5 min gelation time at 72°C.

Debinding results

The moulded samples were firstly dried at 80°C in an air circulating oven for 10 h and then debonded in air without any debinding defects with the optimised debinding cycle given in

Table 4.29. The total debinding time was about 20 h (10 h for drying at 80°C and 10 h for the thermal ramping cycle given in Table 4.29). The total % weight loss for each sample after drying was about 80 % of the total weight and that after debinding was more than 98 %.

As-moulded (green) density

The avearge green density of five moulded samples was 2.27 $g.cm^{-3}$ which is 88 % of the theoretical value 2.58 $g.cm^{-3}$. This is the lowest green density so far which is due to the low volume loading of the alumina powder into the water-soluble methylcellulose binder system.

Sintering results

The debonded samples were sintered at 1750°C for 2.5 h under a vacuum of 6.6 X 10^{-9} atmosphere. A heating rate of 300°C/h was applied. The sintered samples were furnace cooled to room temperature within 5 h.

The average sintered density of five samples was 3.56 $g.cm^{-3}$ which is 92 % of the theoretical value 3.87 $g.cm^{-3}$. A linear shrinkage of 18 % of the total volume was obtained for each sintered sample.

Another attempt was made to improve the sintered density by sintering at a higher temperature for a longer time. In this case after optimisation of the sintering cycle the debonded samples were sintered at 1800°C for 3.5 h under the same vacuum and heating rate. The average sintered density of five samples was increased to 3.63 $g.cm^{-3}$ which is 94 % of the theoretical value 3.87 $g.cm^{-3}$. A linear shrinkage of 18 % of the total volume was obtained for each sintered sample.

Summary

The water-soluble methylcellulose binder system (i.e. Rbs) provided the lowest volume loading of 55 % of the alumina powder which resulted in the lowest green and sintered densities of 88 % and 92 % of their theoretical values respectively.

By sintering at a higher temperature for a longer period a sintered density of 94 % of the theoretical value was obtained. However, this binder system provided the shortest debinding time of 20 h for a 5 mm thick sample of size 35 X 12 X 5 mm^3 although there were distortion problems during the demoulding process. Adhesion of the samples to the mould was prevented by the use of a mould release agent. A cycle time of 5 min was necessary for complete gelation within the mould cavity at 72°C.

4.1.6- Comparison between compacted and injection moulded alumina samples

This part of the work was carried out in order to compare the sintered densities of the compacted alumina samples with those of the injection moulded samples having the same physical and chemical powder properties.

Compaction and sintering results for the 88 %, 95 % and 99.5 % alumina grades

The alumina powders were compacted in a rectangular 32 mm X 6.4 mm double-acting steel die without lubrication. Four gram quantities of powder were cold pressed at pressures in the range 30-200 MN/m^2 using the Instron testing machine at a crosshead speed of 1 mm/min. The load-deflection curves were recorded and it was found that the position and shape of the curves were different when the die was used with lubrication (by a 10 % stearic acid solution), indicating that the results are sensitive to die-wall friction. Selected samples were sintered and sintered densities are given in Table 4.30 for each alumina grade. The compacted 99.5 % alumina samples were sintered at 1750°C for 2.5 h under a vacuum of 6.6×10^{-9} atmosphere and a heating rate of 300°C/h. The compacted 95 % alumina samples were sintered at 1650°C for 2 h in air with a heating rate of 260°C/h and the compacted 88 % alumina samples were sintered at 1550°C for 2 h in air with a heating rate of 260°C/h. The as-mentioned sintering cycles were optimised for each alumina grade (as described in section 4.1.2).

As can be seen from the above sintering cycles the compacted alumina samples were sintered with the same sintering conditions, time and temperatures as the injection moulded alumina samples so that to be able to compare the sintered densities in each case.

It can be seen from Table 4.30 that by increasing the compaction pressure the sintered density for each alumina grade increases. It is quite obvious that most of this densification results from a decrease in the amount of porosity. It has also been found that other factors such as agglomeration have an influence on the amount of densification, e.g. it has been reported (20) that as the amount of aggregates decrease (e.g. by increasing the compaction pressure or by deagglomeration) the tapped, pressed and sintered densities increase.

Comparison between sintered densities of the compacted and injection moulded alumina samples

By comparing Tables 4.26 and 4.30 it can be seen that only the compacted samples at 200 MN/m^2 have higher sintered densities than the injection moulded samples and this is because the compaction pressure has a strong effect on the final density.

Summary

It was found in this work that by increasing the compaction pressure from 30 to 200 MN/m^2 the sintered densities were increased from 90 % to 99 % of their theoretical values which proves that the compaction pressure has a marked effect on the final density.

The comparison of the sintered densities between the compacted and injection moulded alumina samples showed that only the compacted alumina samples at 200 MN/m^2 had higher sintered densities than the injection moulded samples at an injection/moulding pressure of 13.8 MN/m^2.

As will be seen in section 4.2 similar sintered densities are obtained for the injection moulded 99.5 % alumina samples with an injection pressure of 0.55 MN/m^2 which suggests that the

injection/moulding pressure has very small effect on the final sintered density and the only effective way to increase the moulded and sintered densities is by increasing the amount of volume loading of the alumina powder (as already observed during this section).

4.1.7- Summary

A summary of the results obtained during the first part (section 4.1) of this research work is given in Tables 4.31, 4.32 and 4.33. As can be seen from Table 4.31 the 60/40 APP binder system has provided the best properties amongst the thermoplastic binder systems and showed the following features: the highest volume loading of 64 % of the alumina powder;
the shortest debinding times of 78 and 107 h for the 3 mm and 6 mm thick samples respectively;
the longest moulded samples of size 187 X 12 X 3 mm^3 ; and excellent mixing, moulding and demoulding properties.

The water-soluble methylcellulose binder system (i.e. the Rivers binder system) provided a very short debinding time of 20 h for the 5 mm thick samples but rather low green and sintered densities of 88 % and 94 % of their theoretical values respectively. A cycle time of 5 min was necessary to allow complete gelation after which there were still distortion problems during the demoulding process.

From Table 4.32 it can be seen that tap density (i.e. particle size distribution, particle shape, surface area, etc.) has some effect on green and sintered densities. The higher the tap density the higher the green and sintered densities of the alumina powder. On the other hand the higher tap densities of the 88 % and 95 % alumina powder mixtures caused higher viscosities which resulted in smaller moulded samples (due to insufficient flow) than the 99.5 % alumina-60/40 APP moulded samples.

Table 4.33 shows that compaction pressure has a marked effect on the sintered density, i.e. as the compaction pressure increases

so does the sintered density of the alumina powder. This Table also shows that only the samples compacted at 200 MN/m^2 have higher sintered densities than the injection moulded samples which proves that compaction pressure has a strong effect on the final sintered density.

Table 4.33 also shows quite clearly that the only effective way to increase the (green and) sintered density for an injection moulded sample is by increasing the amount of volume loading of the (alumina) powder.

4.2- Development of new (and original) binder systems during this work for the injection moulding of alumina and other powders

This section of chapter four is devoted to the new binder systems developed during this work in order to obtain better properties such as higher volume loading (resulting in higher sintered density) for both thermoplastic/wax- and water-based binder systems and also better moulding and demoulding properties for water-based binder systems.

The newly developed binder systems are described and presented in a manner that shows improvements in their properties and therefore this section ends with two differently based binder systems which provided much better properties than the existing (re-evaluated) binder systems. These two new binder systems are the montanester wax + polyisobutylene + liquid paraffin binder system which is a mixture of wax + thermoplastic and provided the highest volume loading of the alumina powder (resulting in the highest as-moulded and sintered densities) amongst all the binder systems used during this work. The other newly developed binder system is the water-based polyvinyl alcohol binder system which provided higher volume loading of the alumina powder (resulting in higher as-moulded and sintered densities) than the water-based methylcellulose (Rivers) binder system without any demoulding problems.

4.2.1- Polyethylene glycol (PEG)-atactic polypropylene (APP)-liquid paraffin (LP) binder system

Composition and mixing results

The compositions given in Table 4.34 were mixed using the Brabender plastograph at 50 rpm and 150°C for 45 min in each case.

Torques of 290, 310 and 380 mg were observed during the steady state mixing stage (see Fig. 4.1) for compositions 1, 2 and 3 respectively.

It was found that each mixture/composition was quite tough at room temperature which was due to the crystallisation (and hence toughening) of the PEG during the cooling stage. For the same reason each composition was granulated (broken into small pieces) with difficulty. However, each composition provided an easy mix without any sticking problems during or after mixing which was due to the presence of liquid paraffin as an excellent plasticiser and lubricant.

Viscosity results

These are shown in the plots of Figs. 4.20 and 4.21. From the viscosity curves it can be seen that compositions 1 and 2 have shown pseudoplastic flow behaviour whereas composition 3 has shown dilatant flow behaviour which is not suitable for injection moulding of ceramic (and metallic) powders. The dilatant flow behaviour takes place above a certain shear rate causing the viscosity of the material to increase which will eventually cause seizure within the extruding/injecting barrel. The viscosity rise is due to the lack of enough organic material to carry the powder-binder mixture in a pseudoplastic flow behaviour through the die/nozzle of the rheometer/moulder. Due to this reason composition 3 cannot be used for the injection moulding process and instead composition 2 (showing pseudoplasticity) with a maximum possible volume loading of 62 % of the alumina powder mixture can be used as the best (optimised) alumina-PEG-APP-LP composition.

Fig. 4.21 shows the temperature dependency of viscosity for

composition 2. This Figure also shows quite clearly that composition 2 has behaved pseudoplastically at temperatures 80-120°C and therefore this means that it is possible to mould this composition within this temperature range without the risk of dilatancy.

The above viscosity results were obtained using the Instron rheometer with a barrel of diameter 10 mm and a die of dia 1 mm and of 20 mm length.

Thermogravimetric analysis (TGA results)

This is shown in the plot of Fig. 4.22 for the polyethylene glycol (PEG) binder and also for the alumina-PEG-APP-LP binder mixture. The TGA curve for the PEG binder shows that this material has a critical decomposition range at ~ 280-420°C and burns almost completely at 450°C. On the other hand the TGA curve for the PEG-APP-LP binder mixture shows a wider decomposition zone at ~ 280-520°C which is quite useful for an easy and defect-free debinding process. It is quite obvious that the LP burns out first at ~ 300°C and PEG comes off next creating some pores for the burning of the APP binder which burns completely at ~ 520°C.

Injection moulding results

Rectangular samples of size 35 mm X 12 mm X 5 mm were injection moulded using the small plunger type compressed air (PTCA) moulder with the moulding conditions given in Table 4.35.

There were no moulding and no demoulding problems and the moulded samples were very rigid with very good handling properties. There were no obvious moulding defects and the cross section examinations at different areas also showed no moulding defects.

As-moulded (green) density

The average green density of five moulded samples was 2.63 g/cm^3 which is 95 % of the theoretical moulded density 2.77 g/cm^3.

Comparing the average % theoretical green densities of the

alumina-PEG and the alumina-polystyrene (see section 4.1.2) moulded samples having the same volume loadings of 62 % solid alumina powder it can be seen that the alumina-PEG moulded samples show higher average moulded density (only 0.5 %) with an injection pressure of 0.55 MN/m^2 which is less than 13.8 MN/m^2 used for the moulding of the alumina-polystyrene samples and this comparison shows that the injection/moulding pressure has very small effect on the as-moulded density. The higher as-moulded density of the alumina-PEG samples is most probably due to the higher tap density of the alumina + silica + calcia powder mixture than that of the as-recieved 99.5 % alumina powder used as ceramic powder fillers for the PEG and polystyrene binder systems respectively and also due to the slightly higher density of the PEG binder than the polystyrene binder.

Debinding results

The shortest possible debinding time for the 5 mm thick moulded samples was 170 h (~ 7 days) with the optimised debinding cycle given in Table 4.36.

Sintering results

After optimisation of the sintering temperature and time the debonded alumina (+ silica + calcia) samples were sintered at 1700'C for 2 h under a vacuum of 6.5 X 10^{-9} atmosphere with a heating rate of 300°C/h. The sintered samples were furnace cooled to room temperature within 5 h.

The average sintered density of five samples was 3.57 g/cm^3 which is 96 % of the theoretical density 3.72 g/cm^3. This shows slight improvement (1 %) over the sintered alumina-polystyrene samples which is due to the higher as-moulded density of the alumina (+ silica + calcia)-PEG samples.

A linear shrinkage of 12 % of the total volume was obtained for each sintered sample.

Summary

The PEG-APP-LP binder mixture provided a maximum possible volume loading of 62 % of the alumina powder mixture with green and sintered densities of 95 and 96 % of their theoretical densities respectively. A debinding time of 170 h for the 5 mm thick samples of size 35 X 12 X 5 mm^3 was obtained which is 10 h less than that of the 6 mm thick alumina-polystyrene samples of size 62 X 12 X 6 mm^3.

The alumina (+ silica + calcia)-PEG samples were moulded at a lower injection pressure of 0.55 MN/m^2 resulting in a higher average green density of 95 % (of the theoretical density) in comparison to the alumina-polystyrene samples which were moulded at a higher injection pressure of 13.8 MN/m^2 but resulting in slightly lower average green density of 94.5 % (of the theoretical density) suggesting that the injection/moulding pressure has very small effect on the as-moulded (and sintered) density.

4.2.2- Montanester wax (MEW) binder system

This part of the work was carried out in order to study the mixing, volume loading, rheology, moulding, demoulding and debinding properties of the MEW when mixed with alumina powder as a single binder.

Composition and mixing results

The compositions given in Table 4.37 were mixed using the Brabender plastograph at 50 rpm and 90°C for 45 min in each case. As can be seen from this Table there were no needs for the addition of a plasticiser and a lubricant due to the self-plasticisation and self-lubrication properties of the MEW. From this Table it can also be seen that the MEW has provided a volume loading of > 70 % of the alumina powder mixture which was due to the excellent flow properties of this wax binder during the mixing process. There were no sticking problems during or after mixing. The resulting mixtures were quite brittle which was due to the recrystallisation (after cooling) and high crystallinity of the MEW.

Steady state torques of 260, 305 and 380 mg were observed during the mixing period for compositions 1, 2 and 3 respectively.

Viscosity results

This is shown in the plot of Fig. 4.23. From the viscosity curves it can be seen that compositions 1 and 2 have behaved pseudoplastically throughout the extrusion process whereas composition 3 has shown the dilatant flow behaviour above a shear rate of ~ 260 s^{-1}. It follows therefore that composition 2 with a maximum possible volume loading of 70 % of the alumina powder mixture has the most suitable flow properties and it was therefore chosen as the optimised composition for the moulding process.

The above viscosity results were obtained using the Instron rheometer with a barrel of 10 mm dia at 90°C and a die of 1 mm dia and 20 mm length.

Thermogravimetric analysis (TGA results)

This is given in the plot of Fig. 4.24 for the alumina (+ silica + calcia)-MEW binder mixture. The TGA data curve shows that the MEW binder has a wide decomposition range at 400-640°C with an almost linear (or constant) burning rate and that this binder burns completely (100 % weight loss) at ~ 650°C.

From the TGA results it can be concluded that the moulded MEW samples can be heated up quite rapidly up to ~ 400°C and then debonded quite moderately over a short period with few ramps and dwells within the critical decomposition zone. The actual heating rates will depend on the burning characteristics of the MEW and on the thickness of the moulded samples.

Injection moulding results

Attempts were made to mould samples of size 35 mm X 12 mm X 5 mm by using the PTCA moulder with the moulding conditions given in Table 4.38. Due to shrinkage cracking within the mould cavity it was not possible to obtain the 35 mm length and only randomly moulded samples of size 20, 15 and 10 mm X 12 mm X 5 mm were obtained by cutting/grinding the unwanted areas.

Except the shrinkage cracking problem there were no other muolding problems and the moulded samples showed no obvious and no internal defects.

As-moulded (green) density

The average green density of five samples was 2.89 g/cm^3 which is 97.3 % of the theoretical green density 2.97 g/cm^3. This is the highest as-moulded density so far which is due also to the highest volume loading of 70 % of the alumina powder mixture. This increase in green density should provide higher sintered density which should in turn provide better mechanical properties.

Debinding results

The shortest possible debinding time for the 5 mm thick samples of size 20, 15 or 10 X 12 X 5 mm^3 was 36 h with the optimised

debinding cycle given in Table 4.37. This is the shortest debinding time so far which was predicted from the TGA results for the MEW.

Sintering results

The debonded alumina (+ silica + calcia) samples were sintered as in the previous section (section 4.2.1) at 1700°C for 2 h under a vacuum of 6.5 X 10^{-9} atmosphere with a heating rate of 300°C/h. The sintered samples were furnace cooled to room temperature within 5 h.

The average sintered density of five samples was 3.65 g/cm^3 which is 98.2 % of the theoretical sintered density 3.72 g/cm^3. This is the highest sintered density so far which is due to the highest volume loading of 70 % of the alumina powder mixture. A linear shrinkage of 10.5 % of the total volume was obtained for each sintered sample which is the lowest sintering shrinkage so far (due to the same reason).

Summary

The single MEW binder system provided the highest volume loading of 70 % of the alumina powder mixture which resulted in the highest as-moulded and sintered densities of 97.3 and 98.2 % of their respective theoretical densities. This binder provided an easy mix without the use of a plasticiser or a lubricant. However, due to shrinkage cracking within the mould cavity only random moulded samples of size 20, 15 and 10 X 12 X 5 mm^3 could be obtained. An optimised debinding time of 36 h was obtained for the moulded samples which is the shortest debinding time amongst the thermoplastic/wax binder systems used during this research work.

4.2.3- Montanester wax (MEW) + microcrystalline wax (MW) and MEW + carnoba wax (CW) + paraffin wax (PW) binder systems

These MEW-based binder systems were formulated in the hope of reducing the crystallinity of the MEW so that to prevent the shrinkage cracking of the mouldings.

In this section the composition optimisation was not carried out and instead the 70/30 (powder/binder) volume % loading was used for each binder system. No viscosity results were obtained and only the torque values were recorded during the mixing process which should provide adequate information about the flow behaviour of the mixtures by considering the experience gained from the previous torque results.

Composition and mixing results

The compositions given in Table 4.40 were mixed using the Brabender plastograph at 50 rpm and 90°C for 45 min in each case. Each composition provided an easy mixing process without any sticking problems during or after the mixing process. There were no needs for the addition of a plasticiser or a lubricant. Steady state torques of 307 and 310 mg were observed for binder mixtures 1 and 2 respectively. However, the resulting mixtures were still quite brittle and granulated with difficulty suggesting that they were still quite crystalline which may cause shrinkage cracking of the moulded samples.

Comparing the torque values obtained during this section for binder mixtures 1 and 2 with that of the alumina-MEW binder mixture (= 305 mg) and also with those obtained in section 4.1 it becomes quite clear that the torque values are very similar suggesting that binder mixtures 1 and 2 in this section should be quite mouldable without showing any dilatancy.

Thermogravimetric analysis (TGA results)

These are shown in Fig. 4.25 for the microcrystalline wax (MW), carnoba wax (CW) and paraffin wax (PW) binders and also for the alumina + MEW + MW and the alumina + MEW + CW + PW binder

mixtures. From the TGA data curves it can be seen that the MW and PW have very similar burninig characteristics, i.e. they have a very narrow decomposition range at - 100-300°C with high decomposition rates. The TGA curve for the CW shows that this binder has a wider decomposition range at - 200-450°C with a slower decomposition rate than those of the MW and PW binders. These curves, therefore, show that all these waxes come off before the major binder (MEW) creating some pores for the easier burning of the MEW which comes off between - 400 and 640°C.

Injection moulding results

Attempts were made to mould samples of size 35 mm X 12 mm X 5 mm with both binder mixtures by using the PTCA moulder with the same moulding conditions as in Table 4.38. Both binder mixtures provided complete filling of the mould cavity but causing the same type of shrinkage cracking problems due to the high crystallinity of the binder systems. Due to this problem only moulded samples of size 20, 15 and 10 mm X 12 mm X 5 mm could be prepared by cutting/grinding the unwanted areas.

From the moulding results of the last two sections (4.2.2 and 4.2.3) it can be concluded that purely wax binder systems having high crystallinity and high shrinkage are not suitable for the injection moulding of alumina (and most likely for other oxide ceramics with low thermal conductivities) powders. In other words the MEW-based binder system for the moulding of alumina powders has to be a mixture of MEW and an organic material which can reduce the crystallinity of the MEW considerably so that to prevent the shrinkage cracking problem.

Debinding results

The shortest possible debinding time for the 5 mm thick moulded alumina-MW samples of size 20, 15 or 10 X 12 X 5 mm^3 was 90 h with the optimised debinding cycle given in Table 4.41. The shortest possible debinding time for the 5 mm thick moulded alumina-CW-PW samples of size 20, 15 or 10 X 12 X 5 mm^3 was 50 h which is 40 h less than that of the above alumina-MW samples.

The optimised debinding cycle for the 50 h period is given in Table 4.42.

As-moulded (green) and sintered densities

The average green and sintered densities of five samples (in each case) were 97.3 and 98.2 % of their respective theoretical values (= 2.97 and 3.72 g/cm^3) for each binder mixture. These values are the same as those obtained for the optimised alumina-MEW binder mixture (see composition 2 in Table 4.37). A linear shrinkage of 10.5 % of the total volume was obtained for each sintered sample. Note that the sintering condition was the same as that in the previous sections (see sections 4.2.2 or 4.2.1-sintering results).

Summary

From the moulding results it became quite clear that purely wax-based binder systems having high crystallinity and high shrinkage are not suitable for the injection moulding of alumina powders because of shrinkage cracking of the moulded samples within the mould cavity. However, due to excellent properties (see summary in section 4.2.2) of the MEW as a major binder it is possible to reduce its high crystallinity and high shrinkage by adding an amorphous polymer so that to prevent the shrinkage cracking problem and therefore obtain sound mouldings with high green densities, etc. as will be shown in the next two sections.

The MEW + MW and MEW + CW + PW binder systems provided very good flow properties with the 70 volume % loading of the alumina powder mixture. Debinding times of 90 and 50 h were obtained for the 5 mm thick samples of size 20, 15 or 10 X 12 X 5 mm^3 using the MEW-MW and the MEW-CW-PW binder systems respectively. Green and sintered densities of 97.3 and 98.2 % of their respective theoretical values were obtained for both binder mixtures.

4.2.4- Montanester wax (MEW) + atactic polypropylene (APP) + liquid paraffin (LP) binder system

In order to reduce the crystallinity and shrinkage of the MEW so that to prevent the shrinkage cracking problem the amorphous APP binder (density = 0.86 g/cm^3, M.wt. = 10600) was added to the MEW. However, this binder formulation may provide lower volume loading of the alumina powder and longer debinding time than those provided by the single MEW binder system due to the addition of the APP as a minor binder.

Composition and mixing results

The compositions given in Table 4.43 were mixed using the Brabender plastograph at 50 rpm and 130°C for 45 min in each case.

These compositions provided an easy mix without sticking problems which was due to the presence of liquid paraffin as an excellent plasticiser and lubricant.

Steady state torques of 272, 304 and 396 mg were observed for compositions 1, 2 and 3 respectively. The resulting mixtures were less brittle and granulated with less difficulty than the previous MEW binder mixtures. This was due to the presence of the APP which is quite soft and rubbery and therefore provided a softer mixture with the MEW which is quite brittle and tough.

Viscosity results

These are shown in Figs. 4.26, 4.27, 4.28 and 4.29. From Figs. 4.26, 4.27 and 4.28 it can be seen that compositions 1 and 2 show pseudoplastic flow behaviour at all extruding temperatures and composition 3 with a 70 % volume loading of the alumina powder mixture shows dilatant flow above certain shear rates at all the extruding temperatures. These results therefore suggest that composition 3 is not suitable for injection mouling due to its dilatant flow behaviour and instead composition 2 with a maximum possible volume loading of 68 % of the alumina powder mixture has the most suitable flow behaviour and was therefore chosen as the optimised composition for the injection moulding

process.

Fig. 4.29 shows the temperature dependency of viscosity for composition 2. The viscosity curves in this Figure also show that it is quite safe to mould composition 2 at temperatures between 90 and 110°C which is due to the pseudoplastic flow behaviour of this composition at this temperature range. However, the moulding temperature will influence the amount of flow within the mould cavity and therefore a correct moulding temperature is essential for complete filling of the mould cavity.

The above viscosity results were obtained by using the Instron rheometer with a barrel of 10 mm dia and a die of 1 mm dia and 20 mm length.

Thermogravimetric analysis (TGA results)

The TGA data for the alumina (+ silica + calcia)-MEW-APP-LP binder mixture is shown in Fig. 4.30. The TGA data curve for this binder mixture shows a wide decomposition zone at . 300-620°C. This curve also shows that . 70 weight % of the organic binders come off at a narrow temperature zone between 480 and 600°C which requires slower heating rates and may result in longer debinding times.

Injection moulding results

Rectangular samples of size 35 mm X 12 mm X 5 mm were moulded (without any shrinkage cracking problems) using the PTCA moulder with the moulding conditions given in Table 4.44.

The moulded samples showed no obvious moulding defects and the cross section examination of the moulded samples at different areas showed that more than 98 % of the moulded samples were free from internal moulding defects. The major moulding defect was the presence of macro/micro voids (10-1000 μm) due to probably entrapped air or inhomogeneity during the mixing and moulding processes.

As-moulded (green) density

The average moulded density of five samples was 2.78 g/cm^3 which is 96.4 % of the theoretical moulded density 2.89 g/cm^3. This is also a very high as-moulded density which is due to the high volume loading of the alumina powder mixture into the MEW-APP-LP binder system.

Debinding results

The shortest possible debinding time for the 5 mm thick samples of size 35 X 12 X 5 mm^3 was 136 h (~ 5.6 days) with the optimised debinding cycle given in Table 4.45.

As predicted from the TGA data curve the debinding time using the MEW-APP-LP binder system is longer than that of the single MEW binder system which is due to the addition of the APP binder to the MEW. It may be possible to replace the APP binder with another amorphous binder so that to obtain shorter debinding times as will be seen in the next section.

Sintering results

The debonded alumina (+ silica + calcia) samples were sintered at 1700°C for 2 h under a vacuum of 6.5 X 10^{-9} atmosphere with a heating rate of 300°C/h. The sintered samples were furnace cooled to room temperature over a period of 5 h.

The average sintered density of five samples was 3.62 g/cm^3 which is 97.3 % of the theoretical density 3.72 g/cm^3. This is also a high sintered density which is due to the high volume loading of the alumina powder mixture.

A linear shrinkage of 11 % of the total volume was obtained for each sintered sample.

Summary

The MEW-APP-LP binder system provided a maximum volume loading of 68 % of the alumina powder mixture which resulted in green and sintered densities of 96.4 and 97.3 % of their respective theoretical values. The APP addition prevented the shrinkage cracking problem but reduced the amount of volume loading of the

alumina powder mixture from 70 (for single MEW) to 68 % and also increased the debinding time from 36 (for single MEW) to 136 h (for 5 mm thick samples of size 35 X 12 X 5 mm^3).
However, it is possible to reduce the debinding time and also increase the volume loading of the alumina powder by replacing the APP binder with another amorphous binder as will be shown in the next section.

4.2.5- Montanester wax (MEW) + polyisobutylene (PIB) + liquid paraffin (LP) binder system

In order to reduce the debinding time and increase the volume loading of the alumina powder the APP binder was replaced by PIB. The PIB is another amorphous binder (see chapter three-section 3.1.2. for more detail) and should therefore reduce the crystallinity and shrinkage of the MEW which in turn prevents the shrinkage cracking problem. The PIB addition increased the alumina volume loading from 68 to 70 % and reduced the debinding time from 136 to 104 h as will be seen in more detail during this section

Composition and mixing results

The compositions given in Table 4.46 were mixed using the Brabender plastograph at 50 rpm and 120°C for 45 min in each case.
These compositions mixed very well without any sticking problems during or after mixing which was due to the presence of liquid paraffin as an excellent and compatible plasticiser and lubricant.
Steady state torques of 280, 322 and 388 mg were observed for compositions 1, 2 and 3 respectively. The resulting mixtures were quite soft and granulated easily which was due to the presence of PIB being very soft and very rubbery. From the torque results and the past experience it can be predicted that composition 3 with a 72 % volume loading of the 99.5 % alumina powder may show dilatant flow behaviour above a critical shear rate which is due to the lack of enough binder to carry the

feedstock through the extruding/moulding die/nozzle without showing a viscosity rise as shear rate increases.

Viscosity results

These are shown in Figs. 4.31-4.36. From Fig. 4.31 it can be seen that composition 3 with a 72 % volume loading of the alumina powder has shown dilatant flow behaviour above a shear rate of ~ 260 s^{-1} at all the extruding temperatures. This type of flow behaviour was also predicted from the torque result for composition 3. The viscosity results for composition 3 therefore suggest that this composition is not suitable for injection moulding due to the risk of dilatancy which may cause seizure within the barrel of the injection moulder. The viscosity curves in Fig. 4.32 show that composition 2 with a 70 % volume loading of the alumina powder has behaved pseudoplastically at all the extruding temperatures. These results therefore suggest that composition 2 with a maximum possible volume loading of 70 % alumina powder is the most suitable composition for injection moulding and was therefore chosen as the optimised composition. Figs. 4.32-4.33 show the temperature dependency of viscosity and Fig. 4.32 suggests that it is quite safe (without risk of dilatancy) to mould composition 2 at temperatures between 80 and 120°C depending on the amount of flow required within the mould cavity.

Figs. 4.34-4.36 show that by increasing the amount of volume loading of the alumina powder from 68 to 72 % the viscosity of the powder-binder mixtures increases and that there is a limit to the amount of any powder into an organic binder system. This limit can be determined by rheological studies as found for composition 3 which showed dilatancy in Figs. 4.34-4.36 at different extruding temperatures.

The above viscosity results were obtained using the Instron rheometer with a barrel of 10 mm dia and a die of 1 mm dia and 20 mm length.

Thermogravimetric analysis (TGA results)

This is given in Fig. 4.37 for the polyisobutylene (PIB) and the optimised alumina-MEW-PIB-LP binder mixture. The TGA curve for the PIB binder shows a critical decomposition zone at 280-450°C and that for the MEW-PIB-LP binder mixture is at 320-540°C. From these TGA curves it can be realised that LP and PIB come off first creating some pores prior to the complete burning of the MEW.

The TGA results also show that the PIB binder has changed the burning characteristics of the MEW by lowering its critical decomposition zone from . 400-640°C (see Fig. 4.24) to . 320-540°C. This change did not take place with the addition of the APP binder to the MEW which resulted in a long debinding period for the MEW-APP-LP binder system (see section 4.2.4). It follows therefore that by having a lower burning zone for the MEW-PIB-LP binder system and complete burning of the PIB at . 460°C it is believed that the debinding time will be less than that of the MEW-APP-LP binder system.

Injection moulding results

Rectangular samples of size given in Table 4.47 were moulded (without any shrinkage cracking problems) by using the Fox and Offord injection moulder with the moulding conditions given in Table 4.48. The PTCA moulder was also used for the moulding of rectangular samples of size 35 mm X 12 mm X 5 mm with the moulding conditions given in Table 4.48.

The moulded samples were very rigid resulting in good demoulding and good handling properties. There were no obvious moulding defects (i.e. no sink marks, no swelling and no cracks) and the cross section examinations showed that more than 99 % of the moulded samples were free from moulding defects and only one sample (out of a batch of 12 moulded samples) showed some macro and micro voids which were probably due to the entrapped air during the mixing or moulding operations.

As-moulded (green) density

The average moulded density of five samples for each injection pressure was 2.91 g/cm^3 which is 97.35 % of the theoretical moulded density 2.99 g/cm^3. This is the highest as-moulded density obtained during this research work which is due to the highest volume loading of 70 % of the alumina powder into the MEW-PIB-LP binder system.

As can be seen from the above average densities the injection/moulding pressure had no effect on the moulded densities and this effect has already been mentioned in section 4.1.6.

Debinding results

For the 3 mm thick samples of size 40 X 19 X 3 and 40 X 12 X 3 mm^3 the shortest possible debinding time was 80 h (~ 3.3 days) with the optimised debinding cycle given in Table 4.49.

For the 5 mm thick samples of size 35 X 12 X 5 mm^3 the shortest possible debinding time was 104 h (~ 4.3 days) with the optimised debinding cycle given in Table 4.50.

For the 6 mm thick samples of size 62 X 12 X 6 mm^3 the shortest possible debinding time was 112 h (~ 4.6 days) with the optimised debinding cycle given in Table 4.51.

Comparing the debinding times for the 5 mm thick samples it can be seen that the debinding time obtained with the MEW-PIB-LP binder system is 32 h (~ 1.3 days) less than that obtained with the MEW-APP-LP binder system which was predicted from the TGA results in Fig. 4.37.

Sintering results

The debonded alumina (99.5 % grade) samples were sintered at 1750°C for 2.5 h under a vacuum of 6.5 X 10^{-9} atmosphere with a heating rate of 300°C/h. The sintered samples were furnace cooled to room temperature over a period of 5 h.

The average sintered density of five samples was 3.81 g/cm^3 which is 98.5 % of the theoretical sintered density 3.87 g/cm^3. This is the highest sintered density obtained during this research

work which is due to the highest voulme loading of 70 % of the alumina powder into the MEW-PIB-LP binder system.
A linear shrinkage of 10.2 % of the total volume was obtained for each sintered sample.

Summary

The MEW-PIB-LP binder system provided the highest possible volume loading of 70 % of the (99.5 %) alumina powder which resulted in the highest moulded and sintered densities of 97.35 and 98.5 % of their respective theoretical values. These are the highest moulded and sintered densities obtained during this research work by the injection moulding process. The sintered densities obtained by the compaction process during this work (see Table 4.33) at 200 MN/m^2 are the same as those obtained by the injection moulding process using the MEW-PIB-LP binder system which suggests that it is possible to obtain very similar densities by the injection moulding process to those of the compacted powders provided that a high volume loading of powder is incorporated into the binder system as seen during this section.
Debinding times of 80, 104 and 112 h were obtained for 3, 5 and 6 mm thick samples respectively. These are very close to those obtained by the 60/40 APP binder system (see Table 4.31) which provided the shortest debinding times for the 3 and 6 mm thick samples amongst all the thermoplastic binder systems used during this work.
Overall the MEW-PIB-LP binder system provided the best properties amongst all the thermoplastic/wax binder systems used during this work for the injection moulding of alumina powder and therefore this binder system was the last thermoplatic-wax based binder system developed during this research work.

4.2.6- Polyvinyl alcohol + gelling agent + liquid paraffin + water (water-based PVA) binder system

This part of the work was carried out in order to find an alternative water-based binder system to the water-based methylcellulose (Rivers) binder system without the limitations (disadvantages) of the Rivers process for the injection moulding of alumina (and other) powders.

As already explained in chapter three (see section 3.1.2.) it is known that aqueous solutions of polyvinyl alcohol (PVA) form a thermal-reversible gel upon cooling to low temperatures (. 5°C after . 45 h). It is also known (180) that it is possible to produce rigid gels very quickly at room temperature by mixing a heated solution of fully hydrolysed PVA with a gelling agent that forms hydrogen-bonded crosslinks in addition to the microcrystalline framework of the ordinary gel. Various reagents/gelling agents such as (dye) congo red, resorcinol, etc have been found to provide such gels at room temperature when added to aqueous PVA solutions. From 0.5-5 % of the reagent may be added to aqueous solutions containing . 3-20 % of PVA. Note that PVA dissolves readily in water at temperatures of 70°C or more.

By using the above findings the water-based PVA binder system was developed for the first time during this work for the injection moulding of alumina (and other) powders with much better moulding and demoulding properties, higher alumina volume loading and hence higher sintered density than those provided by the water-based methylcellulose (Rivers) binder system as will be seen in detail during this section.

Composition and mixing results

The compositions given in Table 4.52 were mixed using the Brabender plastograph at 50 rpm and 72°C for 20 min in each case.

Steady state torques of 300, 320 and 396 mg were observed for compositions 1, 2 and 3 respectively. There were no sticking problems during or after mixing and the mixtures granulated quite easily. Due to the loss of water even at room temperature

the mixtures were tested (e.g. for rheology) and moulded immediately after mixing or otherwise they were stored in a humidity cabinet with more than 90 % humidity for later use.
It was noticed that the mixtures were quite fluid during the mixing process and gelled quickly upon cooling to room temperature. This thermally-reversible gelling characteristic of these mixtures is very useful for the moulding process to produce rigid moulded samples.

Viscosity results

These are shown in Fig. 4.38. From the viscosity curves in this Figure it can be seen that compositions 1 and 2 show pseudoplastic flow behaviour during the entire extrusion process whereas composition 3 shows dilatant flow very early (above a shear rate of ~ 80 s^{-1}) during the extrusion process and this composition eventually caused seizure within the rheometer above a shear rate of 800 s^{-1}. These results therefore suggest that composition 3 with a 57 % volume loading of the (99.5 %) alumina powder cannot be used for the injection moulding process and instead composition 2 with a 56 % alumina volume loading was chosen as the most suitable (optimised) composition for the moulding process.
The above viscosity results were obtained by using the Instron rheometer with a barrel of 10 mm dia and a die of 1 mm dia and 20 mm length.

Injection moulding results

Rectangular samples of size 35 mm X 12 mm X 5 mm and 62 mm X 12 mm X 6 mm were moulded using the PTCA and the Fox and Offord injection moulding machines respectively with their moulding conditions given in Table 4.53.
The moulded PVA samples were quite rigid and there were no adhesion and no distortion problems during the demoulding process. After each moulding it was noticed that there was an expulsion of the solvent (being a mixture of PVA + gelling agent + liquid paraffin + water) between the moulded sample and the

walls of the mould cavity which acted as a mould release agent and therefore prevented the adhesion of the moulded samples. The moulded samples showed no obvious moulding defects and the cross section examinations also showed that more than 98 % of the moulded samples were free from internal moulding defects. The observed defects were macro and micro voids probably due to the entrapped air during mixing or moulding operations.

As-moulded (green) density

The average moulded density of five samples was 2.42 g/cm^3 which is 91.5 % of the theoretical moulded density 2.64 g/cm^3. This is higher than that obtained with the water-based methylcellulose (Rivers) binder system. This higher moulded density of the alumina-PVA samples is due to the higher volume loading of the alumina powder (by 1 %, than that provided by the Rivers binder system) into the newly developed water-based PVA binder system.

Debinding results

The moulded alumina-PVA samples of size 35 X 12 X 5 and 62 X 12 X 6 mm^3 were debonded over a period of 12 h with the optimised debinding cycle given in Table 4.54. This is the shortest debinding time obtained during this research work. The total % weight loss after debinding was more than 98.5 % of the original weight of the organic binders. No measure of the carbon residues were possible but it is believed that between . 0.1-0.5 % by weight of carbon might be left as residue after debinding.

Sintering results

The debonded 99.5 % alumina samples were sintered at 1800°C for 3.5 h under a vacuum of 6.5 X 10^{-9} atmosphere with a heating rate of 300°C/h. The sintered samples were furnace cooled to room temperature over a period of 5 h. Note that the as-mentioned (optimised) sintering cycle is the same as that used for the sintering of water-based methylcellulose debonded samples.
The average sintered density of five samples was 3.71 g/cm^3 which is 96 % of the theoretical sintered density 3.87 g/cm^3. This is

higher than that obtained for the debonded 99.5 % alumina-methylcellulose samples which is due to the higher volume loading of the alumina powder incorporated into the newly developed water-based PVA binder system.
A linear shrinkage of 17 % of the total volume was obtained for each sintered sample.

Summary

The newly developed water-based PVA binder system provided the shortest debinding time of 12 h during this work for the 5 and 6 mm thick samples of size 35 X 12 X 5 and 62 X 12 X 6 mm^3 respectively. This binder system provided a volume loading of 56 % of the alumina powder which resulted in moulded and sintered densities of 91.5 and 96 % of their respective theoretical values. The moulded PVA samples were quite rigid and there were no adhesion and no distortion problems during the demoulding process. A cycle time of less than 1 min was allowed for the complete gelation process within the mould cavity at room temperature.
Overall the water-based PVA binder system provided much better moulding and demoulding properties, higher volume loading of the alumina powder (resulting in higher moulded and sintered densities) and much shorter cycle time than those provided by the water-based methylcellulose (Rivers) binder system (which caused adhesion and distortion problems during the demoulding process).

4.2.7- Summary

A summary of the results obtained during the second part (section 4.2) of this research work is given in Table 4.55 at the end of this chapter. From this Table it can be seen that the newly developed MEW-PIB-LP binder system has provided the highest as-moulded and sintered densities with a 70 % volume loading of the alumina powder which are the highest values obtained during this work. This Table also shows that this binder system provided very similar debinding times to those obtained with the 60/40 APP binder system which provided the shortest debinding times amongst the thermoplastic binder systems used during this work. The MEW-PIB-LP binder system also provided excellent flow, moulding and demoulding properties which make this binder system superior to the existing (re-evaluated) thermoplastic/wax based binder systems.

Table 4.55 also shows that the newly developed water-based PVA binder system has provided the shortest debinding times for the 5 and 6 mm thick samples during this work. This binder system provided a higher volume loading of the alumina powder which resulted in higher moulded and sintered densities than those obtained with the water-based methylcellulose (Rivers) binder system. The water-based PVA binder system also provided much better moulding (with a moulding cycle of < 1 min) and demoulding (without any adhesion or distortion problems) properties than those provided by the water-based methylcellulose binder system (which caused adhesion and distortion of the moulded samples even with a moulding cycle of 5 min).

From these results (Table 4.55) it can be realised that a compromise is needed depending on the property requirements, i.e. for a very high sintered density, short cycle time but rather long debinding time the MEW-PIB-LP binder system can be used and when only a high sintered density but very short debinding time is required then the water-based PVA binder system should be used.

4.3- Mechanical properties of the sintered alumina samples obtained during this work by the injection moulding process

Flexural and compressive strengths of the sintered alumina samples obtained during this work by the injection moulding process using the best binder systems (i.e. the MEW-PIB-LP, 60/40 APP and the water-based PVA binder systems) were determined for comparison with those obtained by other workers for the injection moulded and compacted alumina ceramics.

4.3.1.1- Flexural strength results

The flexural (or bend) strengths were determined by four-point bend tests using an Instron testing machine. All tests were carried out in air at room temperature at a loading rate (crosshead speed) of 0.1 mm/min with an outer span of length 35 mm and inner span of length 19 mm. The flexural strength was calculated by using the equation: $\sigma_f = 3p_f a / bh^2$ which has already been described in chapter three (see section 3.2.8).

The flexural/bend strength results are given in Table 4.56 which are the average values of five tested samples in each case. From this Table it can be seen that the 99.5 % alumina with a sintered density of 98.5 % of its theoretical value (obtained using the MEW-PIB-LP binder system) has provided the highest bend strength which is due to its highest sintered density amongst the 99.5 % alumina grades.

Table 4.56 also shows that the higher the purity and also the higher the density of the alumina samples the higher the flexural strength and vice versa which is the well known trend for ceramic materials.

4.3.1.2- Compressive strength results

Crushing tests were carried out in order to calculate the compressive strength values using the following equation: compressive (or crushing) strength = F_{max} / csa of the test piece over which the load is applied. Note that this equation has already been described in chapter three (see section 3.2.8).

All tests were carried out by using an Instron testing machine at room temperature and a loading rate (crosshead speed) of o.1 mm/min with samples of size 6 mm X 5 mm.

The compressive strength results are given in Table 4.57 which are the average values of five tested samples. From this Table it can be seen that the same 99.5 % alumina with a 98.5 % sintered density has provided the highest compressive strength which is due to its highest density amongst the 99.5 % alumina grades. This highest density value was obtained only with the MEW-PIB-LP binder system which also provided the highest volume loading of 70 % of the 99.5 % alumina powder.

From this Table it can be understood that the compressive strength is more strongly effected by impurity and density variations than flexural strength. However, it is quite clear that the higher the purity and also the higher the density of the alumina ceramic the higher the compressive strength and vice versa. It follows therefore that in order to have a high compressive strength a high level of purity and density is essential.

4.3.2- Microstructure of sintered and fractured-sintered alumina samples obtained during this work by the injection moulding process

Both optical and scanning electron microscopes were used to study the microstructure of the sintered alumina samples obtained during this work by the injection moulding process using the best binder systems (see 4.3). Fig. 4.39.(a) is an optical photomicrograph of the as-sintered surface of the 99.5 % alumina sample obtained by the injection moulding process using the MEW-PIB-LP binder system. The grain size was measured on the photomicrograph by linear intercept technique. The average sintered grain size on this photomicrograph is 12.3 μm which means that a significant grain growth has taken place during sintering at 1750°C for 2.5 h since the average particle size of the as-received powder was only 1.4 μm. This photomicrograph shows quite clearly some variations in grain

size and some pores located both at the grain boudaries and within the grains. Fig. 4.39.(b) is a typical SEM picture of the same sintered 99.5 % alumina sample as in Fig. 4.39.(a) showing the rounded grains of alumina (due to a high sintering temperature) and the voids between the grains.

Fig. 4.40 shows SEM pictures of the fractured surfaces of the same sintered 99.5 % alumina sample as in Fig. 4.38. These photomicrographs show typical ceramic brittle fracture surfaces, i.e. can see the grain structure, the voids and some grain pullouts of a smooth brittle fractured surface. The large pores at the fracture surface of the specimen might be the fracture origin.

Fig. 4.41 is an optical photomicrograph of the as-sintered surface of the 99.5 % alumina sample obtained by the injection moulding process using the water-based PVA binder system. The average grain size on this photomicrograph is 23 μm (measured by the linear intercept method) which also means that a significant grain growth has taken place during sintering at 1800°C for 3.5 h. This photomicrograph also shows the grain size variation and some pores at the grain boundaries and within the grains. The SEM examination of the sintered and fractured samples showed very similar microstructures to those in Figs. 4.39 and 4.40.

Fig. 4.42 is an optical photomicrograph of the as-sintered surface of the 95 % alumina sample obtained by the injection moulding process using the 60/40 APP binder system. The average grain size (measured by the linear intercept method) on this photomicrograph is 19 μm which shows some grain growth during sintering at 1650°C for 3 h since the average as-blended grain size was 14 μm. However, the average sintered grain size for the 95 % alumina sample is lower than that of the 99.5 % alumina (sintered at 1800°C for 3.5 h) which shows the effect of sintering temperature on the grain structure of sintered ceramic materials. Fig. 4.42 shows a large variation in grain size (due to the large grain size distribution of the as-blended powder mixture) and more pores (due to lower sintered density of 96.5 %) than those of Fig. 4.41. The white phases in micro 4.42 show

the presence of the glassy silica and calcia added to the alumina powder as sintering aids.

The SEM examination of the sintered and fractured 95 % alumina samples showed similar microstructures to those of the 99.5 % alumina samples (see Figs. 4.39 and 4.40).

Fig. 4.43 is an optical photomicrograph of the as-sintered surface of the 88 % alumina sample obtained by the injection moulding process using the 60/40 APP binder system. The average grain size (measured by the linear intercept method) on this photomicrograph is 26 μm which shows that some grain growth has taken place during sintering at 1580°C for 3 h. However, compared to the 99.5 % (sintered) alumina the grain growth of the 88 % (sintered) alumina is not significant which is due to the much lower sintering temperature for the 88 % alumina grade. Fig. 4.43 also shows a very large variation in grain size which is due to the wide grain size distribution of the as-blended powder. The white glassy phases of silica and calcia are much more visible and are covering the alumina phase. The alumina grains appear to have sharp edges which are embedded in the glassy phase. The sharp edge alumina phase is an indication of the low sintering temperature for the low grade 88 % alumina ceramic (104). The change in the shape of the alumina grains is due to the effects of surface tension at the sintering temperature (104).

The SEM examination of the sintered and fractured 88 % alumina samples showed very similar microstructures to those of the 99.5 and 95 % alumina samples (see Figs. 4.39 and 4.40).

4.3.3- Thermal properties of the sintered alumina samples obtained by the injection moulding process during this work

Thermal conductivities of the sintered alumina samples obtained by the injection moulding process using the best binder systems (see 4.3) were determined (for the first time during this work) by measuring the thermal diffusivity of each sintered sample using the "flash method" as described in chapter three (see section 3.2.9) and then using the equation: "th. conductivity = th. diffusivity X density X specific heat capacity at a constant pressure" to calculate the thermal conductivity values as described in chapter three (see section 3.2.9).

Thermal conductivity results

These are given in Table 4.58 along with the measured thermal diffusivities, specific heat capacity (C_p at 260°C) and sintered densities for each alumina grade. From this Table it can be seen that both thermal conductivity and thermal diffusivity are strongly effected by density variations, i.e. both parameters decrease as density decreases and vice versa. This effect can be seen quite clearly from the 99.5 % alumina samples with different densities. Table 4.58 also shows that both thermal conductivity and diffusivity decrease as purity of the alumina sample decreases. This property change can also be seen quite clearly from the 99.5, 95 and 88 % alumina samples.

4.4- Injection moulding of other powders using the MEW-PIB-LP binder system

This part of the research work was carried out in order to investigate the properties of the newly developed MEW-PIB-LP binder system with other oxide and non-oxide ceramic powders and also with metallic powders. These investigations should therefore provide adequate experimental results to find out whether this binder system can also be used successfully for the injection moulding of other powders as well as the alumina powder which is the main powder investigated during this work.

4.4.1- Zirconia

This is another oxide ceramic powder which is injection moulded (most probably for the first time during this work) using the MEW-PIB-LP binder system.

Composition and mixing results

The compositions given in Table 4.59 were mixed using the Brabender plastograph at 50 rpm and 120°C for 45 min in each case. These compositions provided easy mixing without any sticking problems during or after mixing. The resulting mixtures were quite soft and granulated easily. The softness of the mixtures was due to the presence of the PIB binder which is very soft and rubbery.

Steady state torques of 290, 330 and 394 mg were observed for compositions 1, 2 and 3 respectively. From the past experience it can be realised that composition 3 may cause dilatant flow during extrusion/moulding considering its high torque value which is also related to viscosity/shear rate parameters.

Viscosity results

These can be seen from the plots of apparent viscosity versus apparent shear rate (as in sections 4.1 and 4.2) in Figs. 4.44 and 4.45. From the viscosity curves in both Figures it can be seen quite clearly that composition 3 with a 67 % volume loading of the zirconia powder mixture shows dilatant flow above shear

rates of - 80 and 260 s^{-1} at extrusion temperatures of 100 and 120°C respectively. These Figures also show very clearly that compositions 1 and 2 behave pseudoplastically throughout the extrusion process (at all shear rates) at temperatures of 100 and 120°C. These results therefore suggest that composition 2 with a maximum possible volume loading of 65 % of the zirconia powder mixture has the most suitable formulation (due to its correct flow behaviour) and therefore it was chosen as the optimised composition for the moulding process.

The above viscosity results were obtained by using the Instron extrusion rheometer with a barrel of 10 mm dia and a die of 1 mm dia and 20 mm length.

Thermogravimetric analysis (TGA results)

The results of the analysis is given in Fig. 4.46. The TGA curve shows very similar results to that of the alumina-MEW-PIB-LP binder mixture (see Fig. 4.37). From this curve it is clear that the zirconia-MEW-PIB-LP binder mixture has a wide decomposition zone at 360-520°C which is quite useful for an easy and defect-free burn out. This data therefore suggests that few ramps with slow heating rates are required at temperatures between 420 and 500°C so that to avoid defects such as swelling and cracks during the debinding process.

Injection moulding results

Rectangular samples of size 35 mm X 12 mm X 5 mm were moulded quite successfully using the small plunger type compressed air (PTCA) moulder with the moulding conditions given in Table 4.60. The moulded samples were quite rigid and therefore there were no demoulding and no handling problems. There were no obvious moulding defects and the cross section examinations showed that only two of the moulded samples (out of a batch of twelve) had few macro and micro voids probably due to the entrapped air during mixing or moulding operations.

As-moulded (green) density

The average moulded density of five samples was 3.88 g/cm^3 which is 96 % of the theoretical moulded density 4.05 g/cm^3. This is a very satisfactory moulded density which is due to the high volume loading of the zirconia powder mixture into the MEW-PIB-LP binder system.

Debinding results

The shortest possible debinding time for the 5 mm thick samples of size 35 X 12 X 5 mm^3 was 110 h (4.5 days) with the optimised debinding cycle given in Table 4.61.

Sintering results

The debonded zirconia (+ MgO) samples were sintered at 1700°C for 2 h under a vacuum of 6.5 X 10^{-9} atmosphere (a typical sintering conditions). The samples were heated up at a rate of 300°C/h and the sintered samples were furnace cooled to room temperature over a period of 5 h.

The average sintered density of five samples was 5.59 g/cm^3 which is 96.5 % of the theoretical density 5.8 g/cm^3. This is a satisfactory sintered density which may be improved by the optimisation of the sintering conditions. A linear shrinkage of 20 % of the total volume was obtained for each sintered sample.

Summary

The MEW-PIB-LP binder system provided a maximum possible volume loading of 65 % of the zirconia powder mixture which resulted in high moulded and sintered densities of 96 and 96.5 % of their respective theoretical values. A debinding time of 110 h was obtained for the 5 mm thick samples of size 35 X 12 X 5 mm^3. From the above results it can be concluded that the newly developed MEW-PIB-LP binder system can be used quite successfully for the injection moulding of zirconia powder.

4.4.2- Silicon nitride

After the successful injection moulding of oxide ceramic powders (alumina and zirconia) using the MEW-PIB-LP binder system the next powder to be injection moulded using this binder system was chosen from the nitrides, i.e. silicon nitride was the next powder.

Composition and mixing results

The compositions given in Table 4.62 were mixed using the Brabender plastograph at 50 rpm and 120°C for 45 min in each case. These compositions provided easy mixing without any sticking problems during or after mixing. The resulting mixtures were quite soft and granulated easily.

Steady state torques of 285, 320 and 386 mg were observed for compositions 1, 2 and 3 respectively.

Viscosity results

These results are shown in the plots of Figs. 4.47 and 4.48 for different extrusion temperatures. From the viscosity curves in both Figures it can be seen that composition 3 with a 67 % volume loading of the silicon nitride powder mixture shows dilatant flow above shear rates of . 80 and 260 s^{-1} at extrusion temperatures of 100 and 120°C respectively. These Figures also show that compositions 1 and 2 have behaved pseudoplastically throughout the extrusion process (at all shear rates) at both temperatures. These results therefore suggest that composition 2 with a maximum possible volume loading of 65 % of the silicon nitride powder mixture has the most suitable flow behaviour and it was therefore chosen as the optimised composition for the injection moulding process.

The above viscosity results were obtained by using the Instron rheometer with a barrel of 10 mm dia and a die of 1 mm dia and 20 mm length.

Thermogravimetric analysis (TGA results)

The TGA result for the silicon nitride (+yttria + alumina)-MEW-PIB-LP binder mixture was the same as that of the zirconia (+ magnesia)-MEW-PIB-LP binder mixture (see Fig. 4.46) and therefore it is not shown in this section.

Injection moulding results

Rectangular samples of size 35 mm X 12 mm X 5 mm were moulded using the PTCA moulder with the moulding conditions given in Table 4.63.

The moulded samples were very rigid and had excellent demoulding and handling properties. There were no obvious moulding defects and the cross section examinations showed that more than 99 % of the moulded samples were free from internal moulding defects and only one sample (out of a batch of 12 moulded samples) showed some macro voids probably due to the entrapped air or inhomogeneity during the mixing and moulding operations.

As-moulded (green) density

The average moulded density of five samples was 2.38 g/cm^3 which is 96.5 % of the theoretical moulded density 2.47 g/cm^3. This is a high moulded density which is due to the high volume loading of the silicon nitride powder mixture into the MEW-PIB-LP binder system.

Debinding results

The moulded silicon nitride (+ yttria + alumina) samples were debonded in air using the air circulating oven (as in previous debinding processes) without any oxidation problems (Edax* analysis showed no sign of oxidation products). The shortest possible debinding time for the 5 mm thick samples of size 35 X 12 X 5 mm^3 was 110 h (~ 4.5 days) with the same optimised debinding cycle given in Table 4.63.

* Energy dispersive and x-ray chemical analysis

Sintering results

The debonded silicon nitride (+ yttria + alumina) samples were sintered at 1750°C for 3 h under nitrogen (to prevent oxidation). The samples were heated up at a rate of 300°C/h and the sintered samples were furnace cooled to room temperature over a period of 5 h.

The average sintered density of five samples was 2.97 g/cm^3 which is 93 % of the theoretical density 3.2 g/cm^3.

A linear shrinkage of 11 % of the total volume was obtained for each sintered sample.

It is strongly believed that a higher sintering temperature (. 1900°C which was not possible during this work due to furnace limitations) should result in a higher sintered density (> 93 %) with powder volume loadings of > 60 %.

Summary

The newly developed MEW-PIB-LP binder system provided a maximum possible volume loading of 65 % of the silicon nitride powder mixture which resulted in a high moulded density of 96.5 % of the theoretical moulded density. A rather low sintered density of 93 % of the theoretical density was obtained which was due to the rather low sintering temperature of 1750°C. It should have been possible to obtain a higher sintered density (> 93 %) by sintering at a higher temperature (. 1900°C) but this was not possible during this work due to furnace limitations. This binder system provided an easy mixing and moulding operations without any problems. The moulded silicon nitride samples were very rigid and there were no demoulding and no handling problems. More than 99 % of the moulded samples showed no moulding defects. A debinding time of 110 h was obtained for the 5 mm thick samples of size 35 X 12 X 5 mm^3.

From the above results it can be concluded that the MEW-PIB-LP binder system is a very suitable binder system for the injection moulding of silicon nitride powder.

4.4.3- Silicon carbide

The next powder to be injection moulded using the MEW-PIB-LP binder system was chosen from carbides, i.e. silicon carbide was the next powder.

Composition and mixing results

The compositions given in Table 4.64 were mixed in the usual way using the Brabender plastograph at 50 rpm and 120°C for 45 min in each case. These compositions mixed quite easily without any sticking problems during or after mixing. The resulting mixtures were quite soft and granulated without difficulties.
Steady state torques of 295, 335 and 400 mg were observed for compositions 1, 2 and 3 respectively. From the past experience it can be understood that composition 3 with a torque of 400 mg will show dilatant flow above a critical shear rate which may eventually cause seizure within the extruding/moulding barrel.

Viscosity results

These are shown in the plots of Figs. 4.49 and 4.50. From the viscosity curves in both Figures it can be seen that composition 3 shows dilatant flow above shear rates of . 80 and 260 s^{-1} at extrusion temperatures of 100 and 120°C respectively. This type of flow behaviour for composition 3 was also predicted by its high torque value. Figs. 4.49 and 4.50 also show that compositions 1 and 2 behave pseudoplastically throughout the extrusion process (at all shear rates) at both temperatures. From these results it can be seen that composition 2 with a maximum possible volume loading of 60 % of the silicon carbide powder has the most suitable flow and formulation and it was therefore chosen as the optimised composition for the injection moulding process. The above viscosity results were obtained using the Instron rheometer with a barrel of 10 mm dia and a die of 1 mm dia and 20 mm length.

Thermogravimetric analysis (TGA results)

This is given in the plot of Fig. 4.51 for the silicon carbide (+ B_4C)-MEW-PIB-LP binder mixture. The TGA curve shows a critical decomposition zone at 380-500°C which requires few ramps and slow heating rates. This data curve also shows a complete burn out at a temperature of 510°C which is lower than that of the previous data (see section 4.6.2). This is due to the presence of higher amount of polyisobutylene (PIB) which has lowered the decomposition zone of the montanester wax (MEW) binder and may result in shorter debinding time.

Injection moulding results

Rectangular samples of size 35 mm X 12 mm X 5 mm were moulded quite successfully using the PTCA moulder with the moulding conditions given in Table 4.65.

A silicon based mould release agent was sprayed on the mould prior to mouling so that to prevent sticking of the moulded samples during the demoulding process. The moulded samples were quite rigid and therefore there were no distortion and no handling problems. The moulded samples showed no obvious defects and the cross section examinations showed no internal moulding defects.

Debinding results

The moulded silicon carbide samples could not be debonded in air due to oxidation and crumbling of the samples. Debinding was therefore carried out successfully under argon without any debinding defects (i.e. no cracks and no swelling). The shortest possible debinding time for the 5 mm thick samples of size 35 X 12 X 5 mm^3 was 106 h with the optimised debinding cycle given in Table 4.60. This is 4 h less than that obtained by the silicon nitride-MEW-PIB-LP binder mixture which was predicted by TGA results.

As-moulded (green) density

The average moulded density of five samples was 2.17 g/cm^3 which is 95 % of the theoretical moulded density 2.29 g/cm^3. This is a satisfactory (and typical) result which is due to the (typical) 60 % volume loading of the silicon carbide powder into the MEW-PIB-LP binder system.

Due to furnace limitations no sintering results were obtained. A sintering temperature of ~ 2000°C under an inert atmosphere is usually required for the sintering of silicon carbide which was not possible to obtain during this work.

Summary

The MEW-PIB-LP binder system provided a maximum possible volume loading of 60 % of the silicon carbide powder which resulted in an average moulded density of 95 % of the theoretical value. Similar amount of volume loading has also been achieved by another worker (41) which resulted in a sintered density of > 95 % of the theoretical density after sintering at 2100°C for 1 h under argon. The moulded silicon carbide samples were very rigid and there were no demoulding and no handling problems except that a mould release agent was used to prevent sticking of the moulded samples during the demoulding process. No obvious moulding defects were found and there were no internal moulding defects. A debinding time of 106 h was obtained for the 5 mm thick samples of size 35 X 12 X 5 mm^3.

Overall the newly developed MEW-PIB-LP binder system provided a satisfactory mixing, moulding, demoulding, debinding and geen density results for the silicon carbide powder.

4.4.4- Tungsten carbide-6 weight % cobalt

This powder was the last powder to be injection moulded using the MEW-PIB-LP binder system. The WC-6 wt. % Co is also known as hardmetal which is a ceramic and metallic mixture, i.e. a cermet.

Composition and mixing results

The compositions given in Table 4.67 were mixed using the Brabender plastograph at 50 rpm and 120°C for 45 min in each case. These compositions provided easy mixing without any sticking problems during or after mixing. The resulting mixtures were soft and granulated easily.

Steady state torques of 292, 333 and 397 mg were observed for compositions 1, 2 and 3 respectively. Considering the past experience it can be realised that composition 3 with a high torque value of 397 mg will show dilatant flow behaviour which is not suitable for ceramic/metallic injection moulding.

Viscosity results

These are given in the plots of Figs. 4.52 and 4.53. From the viscosity curves in both Figures it can be seen that composition 3 shows dilatancy above shear rates of . 260 and 800 s^{-1} at extrusion temperatures of 100 and 120°C respectively. This type of flow behaviour was also predicted from the high torque value of composition 3. These Figures also show that compositions 1 and 2 behave pseudoplastically throughout the extrusion process (at all shear rates) at both temperatures. These results therefore suggest that composition 2 with a maximum possible volume loading of 65 % of the hardmetal powder has the most suitable flow and formulation and it was therefore chosen as the optimised composition for the injection moulding process.

The above viscosity results were obtained using the Instron rheometer with a barrel of 10 mm dia and a die of 1 mm dia and 20 mm length.

Thermogravimetric analysis (TGA results)

This is given in the plot of Fig. 4.54 for the hardmetal-MEW-PIB-LP binder mixture. The TGA data curve shows a wider decomposition zone at 420-580°C than that of the previous binder mixture (see section 4.6.3). This is due to the lower content of the PIB and higher amount of MEW which resulted in a wider decomposition zone which may then provide a shorter debinding time.

Injection moulding results

Rectangular samples of size 35 mm X 12 mm X 5 mm were moulded quite successfully using the PTCA moulder with the moulding conditions given in Table 4.65.

The moulded samples were quite rigid and there were no sticking problems which provided excellent demoulding and handling properties. There were no obvious moulding defects and the cross section examinations showed no internal moulding defects.

Comparing the PIB content of composition 2 for the silicon nitride, silicon carbide and the hardmetal (see Tables 4.62, 4.64 and 4.67 respectively) it can be seen that in the case of the hardmetal powder it was possible to reduce the amount of the PIB binder (which may result in shorter debinding time). The reason for this reduction is that the hardmetal (powder) is more conductive than both silicon nitride and silicon carbide (powders) and therefore the moulded hardmetal allows an easier heat loss than the less conductive materials and this also reduces the risk of shrinkage cracking with the MEW (due to the less insulating property of the moulded hardmetal).

As-moulded (green) density

The average moulded density of five samples was 8.88 g/cm^3 which is 91 % of the theoretical moulded density 9.76 g/cm^3. This is the lowest moulded density in this part (4.6) which is most likely due to the hardmetal powder characteristics. According to the supplier the hardmetal powder particles were irregularly shaped (needle/plate-like) and had a distribution of sub-16 μm

with an average particle size of 1.2 μm. These properties caused a very low tap density of 35 % of the theoretical density which all together caused a rather low moulded density.

Debinding results

The moulded hardmetal samples could not be debonded in air due to oxidation reactions causing cracking, swelling and crumbling. Debinding was therefore carried out successfully under nitrogen to prevent the oxidation problems. The shortest possible debinding time for the 5 mm thick samples of size 35 X 12 X 5 mm^3 was 100 h which is lower than that obtained for the zirconia, silicon nitride and silicon carbide samples. This was expected due to reduction in the PIB content. The optimised debinding cycle for the 100 h period is given in Table 4.68.

Sintering results

The debonded hardmetal samples were sintered at 1450°C for 1 h under a vacuum of 1.3 X 10^{-3} atmosphere (a typical sintering conditions). The samples were heated up at a rate of 240°C/h and the sintered samples were furnace cooled to room temperature over a period of 3.5 h. The as-mentioned sintering process was carried out in a tube furnace.

The average sintered density of five samples was 14.2 g/cm^3 which is 95 % of the theoretical density 14.95 g/cm^3. This is a satisfactory (typical) sintered density which may be improved by optimisation of the sintering conditions.

A linear shrinkage of 12 % of the total volume was obtained for each sintered sample.

Summary

The MEW-PIB-LP binder system provided a maximum possible volume loading of 65 % of the hardmetal powder which resulted in moulded and sintered densities of 91 and 95 % of their respective theoretical values. The moulded samples were quite rigid and therefore provided excellent demoulding and handling properties. The moulded samples showed no moulding defects. A

debinding time of 100 h was obtained for the 5 mm thick samples of size 35 X 12 X 5 mm^3.

Overall the newly developed MEW-PIB-LP binder system provided a quite satisfactory mixing, moulding, demoulding, debinding, green and sintered density results for the hardmetal powder.

4.4.5- Summary

A summary of the results obtained during this part (4.4) of the research work is given in Table 4.69. This Table shows that quite satisfactory results have been obtained for the injection moulded powders using the MEW-PIB-LP binder system. Comparing the amount of volume loading of each powder with those obtained by other workers using different binder systems it was found that the MEW-PIB-LP binder system provided higher volume loading in case of the silicon nitride and the hardmetal powders and very similar amount in case of the silicon carbide powder.

The zirconia powder was injection moulded quite successfully for the first time during this work using the newly developed MEW-PIB-LP binder system.

From the above results it can therefore be concluded that the newly developed MEW-PIB-LP binder system can be used quite successfully for the injection moulding of oxide powders as well as nitrides, carbides and cermets.

4.5- Injection moulding of other powders using the water-based PVA binder system

This part of the work was carried out in order to study the properties of the newly developed PVA water-based binder system (i.e. polyvinyl alcohol + gelling agent + liquid paraffin + water) with other powders other than alumina. These studies should provide adequate experimental results so that to find out whether this binder system can also be used successfully for the injection moulding of other powders.

4.5.1- Silicon nitride

The next powder (after alumina) to be injection moulded using the water-based PVA binder system was silicon nitride.

Composition and mixing results

The compositions given in Table 4.70 were mixed in the usual way using the Brabender plastograph at 50 rpm and 72°C for 20 min in each case. These compositions were mixed without any problems and there were no sticking problems during or after mixing. The resulting mixtures were tested for rheology or moulded immediately after mixing so that to avoid water losses. They were otherwise stored in a humidity cabinet with more than 90 % humidity.

Steady state torques of 300, 330 and 400 mg were observed for compositions 1, 2 and 3 respectively. From the past experience it can be predicted that composition 3 with a high torque of 400 mg will show dilatant flow after a critical shear rate and that it may eventually cause seizure within the extruding/moulding barrel.

Viscosity results

These can be seen from the plot of Fig. 4.55. The viscosity curves in this Figure show that compositions 1 and 2 behave pseudoplastically throughout the extrusion process whereas composition 3 shows dilatant flow above a shear rate of . 260 s^{-1} which was also predicted by its high torque value. These results

therefore suggest that composition 2 has the most suitable flow and formulation and it was therefore chosen as the optimised composition for the injection moulding process.
The above viscosity results were obtained using the Instron rheometer with a barrel of 10 mm dia and a die of 1 mm dia and 20 mm length.
Comparing the water-based PVA viscosity values with those of the thermoplastic-wax based MEW-PIB-LP binder system it can be realised that the water-based PVA viscosities are generally higher than those of the thermoplastic-wax based MEW-PIB-LP binder system.

Injection moulding results

Rectangular samples of size 35 mm X 12 mm X 5 mm were moulded quite successfully using the PTCA moulder with the moulding conditions given in Table 4.71.
A 45 s cycle time was allowed for the complete gelation of the moulded samples within the mould cavity. The moulded samples were demoulded (ejected) without any distortion problems and there were no adhesion problems during demoulding which was due to the solvent expulsion (acting as a mould lubricant) during the moulding process. Due to the rigidity of the mouldings there were no handling problems. The moulded samples showed no obvious and no internal moulding defects.

Debinding results

The moulded silicon nitride-PVA samples were debonded under argon so that to prevent the oxidation problems. Edax chemical analysis showed no sign of oxidation of the debonded samples. This is because silicon nitride starts oxidising (in air) above - 600°C (174) and if there is no air and no water present (below this temperature) thus there will be no oxidation. The water in the moulded samples evaporates at - 100°C and debinding took place under an inert atmosphere (argon) which meant no oxidation reactions.
A debinding time of 12 h was obtained for the 5 mm thick samples

of size 35 X 12 X 5 mm^3 with the optimised debinding cycle given in Table 4.72.
The total % weight loss after debinding was > 96 %. No measure of the carbon residue was possible. However, it is believed that some % of carbon might be present as residue.

Sintering results

The debonded samples were sintered at 1750°C for 2.5 h under argon with a heating rate of 300°C/h. The sintered samples were furnace cooled to room temperature over a period of 5 h.
The average sintered density of five samples was 2.96 g/cm^3 which is 92.5 % of the theoretical density 3.2 g/cm^3. A higher sintered density would require a higher sintering temperature (. 1900°C for silicon nitride) which was not possible to obtain during this work due to furnace limitations.
A linear shrinkage of 9 % of the total volume was obtained for each sintered sample.

Summary

The water-based PVA binder system provided quite satisfactory mixing, moulding and demoulding properties. A cycle time of 45 s was allowed for each moulding and the moulded samples were free from moulding defects. A debinding time of 12 h for the 5 mm thick samples of size 35 X 12 X 5 mm^3 was obtained. A maximum possible volume loading of 51 % of the silicon nitride powder mixture was achieved with this binder system. A sintered density of 92.5 % of the theoretical density was obtained by sintering at 1750°C for 2.5 h under argon. This value can be increased by sintering at a higher temperature. A linear shrinkage of 9 % of the total volume was obtained for each sintered sample.
It can therefore be concluded that the newly developed water-based PVA binder system can be used quite successfully for the injection moulding of silicon nitride powder.

4.5.2- Tungsten carbide-6 weight % cobalt

After alumina and silicon nitride powders the next powder to be injection moulded using the water-based PVA binder system was the hardmetal powder which is a cermet (WC + 6 wt. % Co).

Composition and mixing results

The compositions given in Table 4.73 were mixed using the Brabender plastograph at 50 rpm and 72°C for 20 min in each case. These compositions mixed very well and there were no sticking problems during or after mixing. The resulting mixtures were tested for rheology or moulded immediately after mixing so that to avoid water losses. They were otherwise stored in a humidity cabinet with more than 90 % humidity.

Steady state torques of 305, 335 and 405 mg were observed for compositions 1, 2 and 3 respectively. From the past experience it can be predicted that composition 3 with a high torque value will show dilatant flow above a critical shear rate and this type of flow is not suitable for ceramic/metallic injection moulding.

Viscosity results

These are shown in the plot of Fig. 4.56. From the viscosity curves for compositions 1 and 2 it is clear that both compositions behave pseudoplastically throughout the extrusion process (at all shear rates) whereas the viscosity curve for composition 3 shows dilatant flow above a shear rate of 800 s^{-1} which suggests that composition 3 with a 47 % volume loading of the hardmetal powder is not suitable for the injection moulding process and this was also predicted from its high torque value. The viscosity results therefore suggest that composition 2 has the most suitable formulation and it was therefore chosen as the optimised composition for the injection moulding process.

The above viscosity results were obtained using the Instron rheometer with a barrel of 10 mm dia and a die of 1 mm dia and 20 mm length.

Injection moulding results

Rectangular samples of size 35 mm X 12 mm X 5 mm were moulded quite successfully using the PTCA moulder with the same moulding conditions given in Table 4.73.

A 40 s cycle time was allowed for the complete gellation of the moulded samples. The moulded samples were quite rigid and therefore there were no demoulding and no handling problems. There were no adhesion problems which was due to solvent expulsion during the moulding process. The moulded samples showed no obvious and no internal moulding defects.

Debinding results

The moulded samples were debonded under nitrogen without any debinding defects. The shortest possible debinding time for the 5 mm thick samples of size 35 X 12 X 5 mm^3 was 7 h with the optimised debinding cycle given in Table 4.74.

The total % weight loss after debinding was > 95 %. It is believed that some carbon residue is present within the debonded samples which could not be removed due to the inert atmosphere of the debinding process.

Sintering results

The debonded hardmetal samples were sintered at 1450°C for 1 h under a vacuum of 1.3 X 10^{-3} atmosphere with a heating rate of 240°C/h. The sintered samples were furnace cooled to room temperature over a period of 3 h. The as-mentioned sintering process took place in a tube furnace.

The average sintered density of five samples was 14.57 g/cm^3 which is 97.5 % of the theoretical sintered density 14.95 g/cm^3. This is a high sintered density which is due to the correct sintering conditions. A linear shrinkage of 13.5 % of the total volume was obtained for each sintered sample.

Summary

The newly developed water-based PVA binder system provided a very satisfactory mixing, moulding, demoulding, debinding and sintering properties. A cycle time of 40 s was allowed for each moulding. A debinding time of 7 h was obtained for the 5 mm thick samples of size 35 X 12 X 5 mm^3. A maximum possible volume loading of 46 % hardmetal powder was obtained with this binder system. A high sintered density of 97.5 % of the theoretical value with a linear shrinkage of 13.5 % of the total volume were obtained after sintering at 1450°C for 1 h.

From the above results it can be concluded quite clearly that the newly developed water-based PVA binder system can be used quite successfully for the injection moulding of hardmetal (WC-6 wt. % Co) powders.

4.5.3- Iron-2 weight % nickel

This is a metallic powder mixture to be injection moulded as the last powder using the water-based PVA binder system.

Composition and mixing results

The compositions given in Table 4.75 were mixed using the Brabender plastograph at 50 rpm and 72°C for 20 min in each case. These compositions were mixed without any problems. The resulting mixtures were tested for rheology or moulded immediately after mixing so that to avoid water losses even at room temperature. The mixtures were otherwise stored in a humidity cabinet with more than 90 % humidity for later usage. Steady state torques of 300, 332 and 403 mg were observed for compositions 1, 2 and 3 respectively. From the past experience it can be predicted that composition 3 with a high torque value will show dilatant flow above a critical shear rate and this may cause seizure within the extruding/moulding barrel.

Viscosity results

These are given in the plot of Fig. 4.57. From the viscosity curves for compositions 1 and 2 it is quite clear that both

compositions show pseudoplastic flow behaviour throughout the extrusion process (at all shear rates) whereas the viscosity curve for composition 3 shows dilatant flow above a shear rate of 800 s^{-1}. These results therefore suggest that composition 2 with a 56 % volume loading of the iron powder mixture has the most suitable flow and formulation and it was therefore chosen as the optimised composition for the injection moulding process. The above viscosity results were obtained using the Instron rheometer with a barrel of 10 mm dia and a die of 1 mm dia and 20 mm length.

Injection moulding results

Rectangular samples of size 35 mm X 12 mm X 5 mm were moulded quite successfully using the PTCA moulder with the same moulding conditions given in Table 4.71.

A 50 s cycle time was allowed for each moulding. The moulded samples were quite rigid and thus demoulded without any distortion problems. There were no adhesion problems during the demoulding process. The mouldings showed no obvious and no internal moulding defects.

Debinding and sintering results

The moulded samples were debonded under nitrogen at a heating rate of 115°C/h up to 850°C and then heated up to 1335°C for sintering under the same atmosphere and held at this temperature for 6 h. The sintered samples were furnace cooled to room temperature over a period of 3 h. The debinding and sintering processes were carried out in a tube furnace.

The average sintered density of five samples was 7.44 g/cm^3 which is 94.5 % of the theoretical sintered density 7.88 g/cm^3. A higher sintered density may be possible by optimisation of the sintering conditions.

A linear shrinkage of 12.5 % of the total volume was obtained for each sintered sample.

Summary

The newly developed water-based PVA binder system provided a quite satisfactory mixing, moulding, demoulding, debinding and sintering properties for the iron-2 weight % nickel powder. A cycle time of 50 s was allowed for each moulding. The moulded samples were free from moulding defects. A debinding time of 7.2 h was obtained for the 5 mm thick samples of size 35 X 12 X 5 mm^3. A maximum possible volume loading of 56 % of the iron powder mixture was obtained with this binder system. A sintered density of 94.5 % of the theoretical density was obtained after sintering at 1335°C for 6 h. A higher sintered density may be obtained by optimisation of the sintering conditions. A linear shrinkage of 12.5 % of the total volume was obtained for each sintered sample.

From the above results it can therefore be concluded quite clearly that the newly developed water-based PVA binder system can be used quite successfully for the injection moulding of metallic iron-(2 weight %) nickel powders.

4.5.4- Summary

A summary of the results obtained during this part (4.5) is given in Table 4.76. This Table shows that quite satisfactory mixing, moulding, cycle time, demoulding and debinding results have been obtained for the injection moulded powders using the newly developed water-based PVA binder system. This binder system provided high sintered densities for the alumina, hardmetal and the iron-2 weight % nickel powders. A higher sintered density would have been possible for the silicon nitride powder if sintered at a higher temperature (e.g. at 1900°C for 2 h under argon).

From the above results it can be concluded that the newly developed water-based PVA binder system can be used quite successfully for the injection moulding of oxide, nitride, carbide and metallic powders. This binder system can therefore be used as an alternative binder system to the water-based methylcellulose (Rivers) binder system which provided lower sintered density with long moulding cycle, adhesion and distortion problems for the moulded alumina samples (see 4.1.5).

4.6- Effect of tap density (or powder characteristics) on the amount of volume loading of powders into the newly developed binder systems during this work

The ceramic/metallic powder characteristics has a considerable influence on the maximum ceramic/metallic volume loading that can be incorporated into an organic phase (Farris 1968). Farris (16) has shown that it is possible to increase the amount of a powder in a suspension without increasing the viscosity of the suspension. This was possible by increasing the difference in mean particle size between coarse and fine fractions. He showed that the volume loading of powders can be increased by . 17 % in a mix containing 75 % coarse and 25 % fines by progressively decreasing the size ratio, R = mean fine particle size / mean coarse particle size (see chapter two-Fig. 2.3).

It is also known (35) that in order to have a maximum packing density (which results in maximum green density) the powder should have a broad particle size distribution without an excessive concentration of particles in any narrow particle size range. This means that a high tap density is required which also depends on the powder characteristics such as size, size distribution, shape and flow.

However, it was found during this work that if an ideal particle size distribution (as described by Farris) does not exist then the higher the tap density the more the amount of the organic binder needed to injection mould that powder which means the lower the volume loading of that powder. This result can be seen from Tables 4.77 and 4.78. The most obvious trend in both Tables is that the lower the % tap density the higher the % volume loading of the powder into the newly developed binder systems and vice versa. The inconsistency in these Tables is due to the variation in average particle size, particle size distribution, particle shape and surface area of the powders used during this work. These variations can be seen from Table 4.79.

Table 4.1- Details of the trial composition for the alumina (99.5% grade)-EVA binder mixture

Material	Composition (volume %)	Function
Alumina	59.5	Ceramic powder filler
EVA	35	Major binder
DEP(1)	3.17	Plastisizer
SA(2)	2.3	Lubricant

(1) Diethyl phthalate, (2) Stearic acid

Table 4.2- Injection moulding conditions for the alumina (99.5% grade)-EVA binder mixturey

Temperature (°C)			Injection pressure (MN/m^2)
Barrel	Nozzle	Mould	
130	130	23	13.8

Table 4.3- 99.5% alumina-polystyrene compositions

	Vol. % alumina	Vol. % PS(3)	Vol.% DEP	Vol.% SA	Torque (mg)
Composition 1	56	35	6	3	250
Composition 2	60	32	5	3	285
Composition 3	62	30	5	3	325
Composition 4	65	27	5	3	400

(3) Polystyrene

Table 4.4- Injection moulding conditions for the 62 vol.% alumina-30% PS- 5% DEP-3% SA binder mixture

Temperature (°C)			Injection pressure (MN/m^2)
Barrel	Nozzle	Mould	
125	130	23	13.8

Table 4.5- Debinding cycle for the moulded 99.5% alumina-polystyrene samples of size 62X12X6 mm^3

	R *1	R 2	R 3	R 4	R 5	R 6	R 7	R 8
Heating rate (°C/h)	10	3.5	3	2.5	2	1.5	2	2.5
Temperature level (°C)	100	160	240	320	380	420	450	500
Dwell (hold time, h)	0.1	0.5	0.5	1	1	2	1	1

* Ramp

Table 4.6- Debinding cycle for the moulded 99.5% alumina-polystyrene samples of size 40X19X3 mm^3 and 40X12X3 mm^3

	R 1	R 2	R 3	R 4	R 5	R 6	R 7	R 8
Heating rate (°C/h)	13	5	4	3.5	3	2.5	3	4
Temperature level (°C)	100	160	240	320	380	420	450	500
Dwell (hold time, h)	0.1	0.5	0.5	1	1	2	1	1

Table 4.7- 99.5% alumina-polyacetal compositions

Material	Comp.* 1 (vol. %)	Comp. 2 (vol. %)	Comp. 3 (vol. %)	Function
Alumina	50	56.8	59.5	Ceramic filler powder
PA(4)	32.7	29.26	27.5	Major binder
APP(5)	5.12	2.75	2.9	Minor binder
LDPE(6)	2.56	2.97	2.6	Minor binder
EVA(7)	2.56	2.97	2.3	Minor binder
SA	2.56	2.92	2.5	Lubricant
DEP	5.12	2.28	2.7	Plasticiser

(4) Polyacetal, (5) Atactic polypropylene,
(6) Low density polyethylene, (7) Ethylene vinyl acetate
* Composition

Table 4.8- Injection moulding conditions for the 99.5% alumina-polyacetal binder mixture

Temperature (°C)			Injection pressure (MN/m^2)
Barrel	Nozzle	Mould	
180	180	23	13.8

Table 4.9- Debinding cycle for the moulded 99.5% alumina-polyacetal samples of size 62X12X6 mm^3

	R 1	R 2	R 3	R 4	R 5	R 6	R 7	R 8
Heating rate (°C/h)	40	5	3.75	2.75	2.2	2	2.2	10
Temperature level (°C)	120	150	250	310	350	400	440	470
Dwell (hold time, h)	0.1	0.5	1	1	1.5	2	1	1

Table 4.10- 99.5% alumina-atactic polypropylene compositions

Material	Comp. 1 (vol. %)	Comp. 2 (vol. %)	Comp. 3 (vol. %)	Function
Alumina	60	64	66	Ceramic powder filler
APP (density =0.86 g/cm^3, M.wt.*=10600)	30	28	26	Major binder
SA	4	3.5	4	Lubricant
DEP	6	4.5	4	Plasticiser

* Molecular weight

Table 4.11- Dimensions of the moulded 99.5% alumina-APP-SA-DEP samples

	Sample 1	Sample 2	Sample 3	Sample 4
Length (mm)	187	62	40	40
Width (mm)	12	12	19	12
Thickness (mm)	3	6	3	3

Table 4.12- Injection moulding conditions for the 99.5% alumina-APP-SA-DEP binder mixture

Temperature (°C)			Injection pressure (MN/m ^{2})
Barrel	Nozzle	Mould	
110	110	23	13.8

Table 4.13- Debinding cycle for the moulded 99.5% alumina-APP-SA-DEP samples of size 40X19X3 mm^3 and 40X12X3 mm^3

	R 1	R 2	R 3	R 4	R 5	R 6	R 7	R 8
Heating rate (°C/h)	41	5.25	4.25	3.75	3.2	3	3	5
Temperature level (°C)	120	190	250	300	340	380	450	480
Dwell (hold time, h)	0.1	0.5	1	1	1	1	1	1

Table 4.14- Injection moulding conditions for the 99.5% alumina-60/40 APP-SA-DEP binder mixture

Temperature (°C)			Injection pressure (MN/m ^{2})
Barrel	Nozzle	Mould	
120	125	23	13.8

Table 4.15- Debinding cycle for the moulded 99.5% alumina-60/40 APP-SA-DEP samples of size 40X19X3 mm^3 and 40X12X3 mm^3

	R 1	R 2	R 3	R 4	R 5	R 6	R 7	R 8
Heating rate (°C/h)	43	6.75	5.25	4.75	4	3.25	4	4.6
Temperature level (°C)	130	180	230	280	345	380	430	485
Dwell (hold time, h)	0.1	1	1	1	1	2	1	1

Table 4.16- Debinding cycle for the moulded 99.5% alumina-60/40 APP-SA-DEP samples of size 62X12X6 mm^3

	R 1	R 2	R 3	R 4	R 5	R 6	R 7	R 8
Heating rate (°C/h)	32	5.75	4.5	4	3	2.25	3.25	4.5
Temperature level (°C)	130	180	230	280	345	380	430	485
Dwell (hold time, h)	0.1	1	1	1	1	1	1	1

Table 4.17- Compositions of the 88% and 99.5% alumina powders

Material	88% alumina (wt. %)	95% alumina (wt. %)	Function
Al_2O_3	88	95	Major ceramic powder
SiO_2	7	3	Sintering aid
CaO	2	0.5	Sintering aid
MgO	1.5	1	Sintering aid
Cr_2O_3	1.5	0.5	Sintering aid

Table 4.18- Particle size analysis results for the 88%, 95% and 99.5% alumina powders

Composition	Average particle size (μm)	Particle size distribution (μm)
88% alumina	23	0.1-100
95% alumina	14	0.1-100
99.5% alumina	1.4	0.1-10

Table 4.19- Tap densities for the 88%, 95% and 99.5% alumina powders

Composition	Tap density (g/cm^3)
88% alumina	1.79
95% alumina	1.72
99.5% alumina	1.58

Table 4.20- The 60/40 APP-SA-DEP composition for the injection moulding of the 88% and 95% alumina powders

Material	Composition (vol.%)	Function
60/40 APP mixture	28	Major binder
SA	4.5	Plasticiser
DEP	3.5	Lubricant
88% or 95% alumina powder	64	Ceramic powder filler

Table 4.21- Injection moulding conditions for the 88% and 95% alumina-60/40 APP-SA-DEP binder mixtures

	Temperature (°C)			Injection pressure (MN/m^2)
	Barrel	Nozzle	Mould	
88% alumina-60/40 APP-SA-DEP b.m.*	160	160	23	13.8
95% alumina-60/40 APP-SA-DEP b.m.	150	150	23	13.8

* Binder mixture

Table 4.22- Dimensions of the moulded 88% and 95% alumina-60/40 APP-SA-DEP samples

	Sample 1	Sample 2	Sample 3
Length (mm)	45	40	40
Width (mm)	12	19	12
Thickness (mm)	6	3	3

Table 4.23- Green and theoretical densities of the moulded 88%, 95% and 99.5% alumina-60/40 APP-SA-DEP samples

	Theoretical density (g/cm^3)	Green density (g/cm^3)	% theoretical density
88% alumina-60/40 APP-SA-DEP b.m.	2.61	2.52	96.8
95% alumina-60/40 APP-SA-DEP b.m.	2.7	2.6	96.5
99.5% alumina-60/40 APP-SA-DEP b.m.	2.8	2.67	95.5

Table 4.24- Debinding cycle for the moulded 88% and 95% alumina-60/40 APP-SA-DEP samples of size 40X19X3 mm^3 and 40X12X3 mm^3

	R 1	R 2	R 3	R 4	R 5	R 6	R 7	R 8
Heating rate (°C/h)	43	7.25	6.25	5.5	4.75	4	4.5	8
Temperature level (°C)	130	200	240	290	355	400	450	520
Dwell (hold time, h)	0.1	1	1	1	1	1	2	0.5

Table 4.25- Debinding cycle for the moulded 88% and 95% alumina-60/40 APP-SA-DEP samples of size 45X12X6 mm^3

	R 1	R 2	R 3	R 4	R 5	R 6	R 7	R 8
Heating rate (°C/h)	31	7	5.5	5	4	3	2.5	3.5
Temperature level (°C)	130	200	240	290	355	400	450	520
Dwell (hold time, h)	0.1	1	1	1	1	1	2	0.5

Table 4.26- Sintered densities and shrinkage results for the injection moulded 88%, 95% and 99.5% alumina samples

	Theoretical density (g/cm^3)	Sintered density (g/cm^3)	% th.* density	% shrinkage by volume
88% alumina	3.56	3.45	97	12
95% alumina	3.70	3.57	96.5	12
99.5% alumina	3.87	3.71	96	11.5

* Theoretical

Table 4.27- 99.5% alumina-methylcellulose compositions

Material	Comp. 1 (vol.%)	Comp. 2 (vol.%)	Comp. 3 (vol.%)	Function
Alumina	52	55	56.5	Ceramic powder filler
Methylcellulose (methocel 20-223)	11	10	8.5	Major binder
Glycerin	4	3.5	3	Plasticiser and lubricant
Boric acid	1	1	1	Plasticiser and lubricant
Water	32	30.5	31	Solvent (8)

(8) To dissolve and uniformly disperse the binders

Table 4.28- Injection moulding conditions for the 99.5% alumina-methylcellulose binder mixture

Temperature (°C)			Injection pressure (MN/m^2)
Barrel	Nozzle	Mould	
23	23	72	0.55

Table 4.29- Debinding cycle for the moulded 99.5% alumina-methylcellulose samples of size 35X12X5 mm^3

	R 1	R 2	R 3	R 4	R 5
Heating rate (°C/h)	200	40	210	100	500
Temperature level (°C)	85	110	160	380	850
Dwell (hold time, h)	1	2	0.5	1	1

Table 4.30- Sintered densities of the compacted 88%, 95% and 99.5% alumina samples at different compaction pressures

Alumina grade	Compaction pressure (MN/m^2)	Theoretical density (g/cm^3)	Sintered density (g/cm^3)	% theoretical density
88%	30	3.53	3.17	90
	60		3.24	92
	100		3.35	95
	150		3.42	97
	200		3.50	99
95%	60	3.70	3.36	91
	100		3.50	94.5
	150		3.58	97
	200		3.66	99
99.5%	100	3.87	3.63	94
	150		3.71	96
	200		3.82	98.5

Table 4.31- Properties of the injection moulded 99.5% alumina ceramic using the re-evaluated thermoplastic and water-soluble binder systems

Binder system	% max. possible volume loading of alumina powder	As-moulded (green) density (% th.)	Sintered density (% th.)	Shrinkage (% total vol.)	Debinding time (h, 6 mm thick)
EVA	——	93.5 (for 59.5 vol. % alumina powder)	——	——	——
Polystyrene	62	94.5	95	15	180
Polyacetal	56.8	92	93.5	16	129
APP (density= 0.86, M.wt.= 10600)	64	95.5	96	11.5	129
60/40 APP mixture	64	95.5	96	11.5	107
Water-soluble methylcellulose (Rivers process)	55	88	94	18	20 (5 mm thick)

Table 4.31 continued

Binder system	Debinding time (h, 3 mm thick)	Longest possible moulded sample (mmXmmX mm)	Mixing, moulding and demoulding props.	Moulding temp. (°C, B/N*)	% vol of the major binder in the opt. comp.
EVA	——	——	Sticking problems during demoulding and after mixing	130	——
Polystyrene	125	143X12X3	Good	130	30
Polyacetal			Fairly good	180	29.26
APP (density= 0.86, M.wt.= 10600)	105	187X12X3	very good	110	28
60/40 APP mixture	78	187X12X3	very good	125	28
Water-soluble methylcellulose (Rivers process)			Adhesion and distortion problems during demoulding, long cycle time (~5 min)	23	10

* Barrel/Nozzle

Table 4.32- Properties of the injection moulded 88%, 95% and 99.5% alumina using the 60/40 APP binder system

Alumina grade	Average particle size (μm)	Particle size distribution (μm)	Tap density (g/cm^3)	Th. as-moulded density (g/cm^3)	Th. sintered density (g/cm^3)
88%	23	0.1-100	1.79	2.61	3.56
95%	14	0.1-100	1.72	2.7	3.7
99.5%	1.4	0.1-10	1.58	2.8	3.87

Table 4.32 continued

Alumina grade	As-moulded density (% th.)	Sintered density (% th.)	Moulding temp. (°C, B/N)	Longest possible moulded sample (mmXmmX mm)	Viscosity (Pa s) at a shear rate of 400 s^{-1} and a temp. of 130°C
88%	96.8	97	160	68X12X3	270
95%	96.5	96.5	150	68X12X3	130
99.5%	95.5	96	125	187X12X3	108

Table 4.33- Sintered densities of compacted and injection moulded 88%, 95% and 99.5% alumina samples

Alumina grade	Injection moulded (using the 60/40 APP b.s.*) sintered density (% th.)	Compacted sintered density (% th.) at different compaction pressures of 30, 60, 100, 150 and 200 MN/m^2 respectively				
88%	97	90	92	95	97	99
95%	96.5		91	94.5	97	99
99.5%	96			94	96	98.5

* Binder system

Table 4.34- Alumina (+silica+calcia)-polyethylene glycol compositions

Material	Comp. 1 (vol.%)	Comp.2 (vol.%)	Comp.3 (vol.%)	Function
Al_2O_3	57.5	58.5	60	Ceramic powder filler
SiO_2	1.5	2	2.5	Sintering aid
CaO	1	1.5	1.5	Sintering aid
PEG (9)	24	23	21	Major binder (11)
APP (density =0.86, M.wt. =10600	11	10	10	Minor binder (12)
LP (10)	5	5	5	Plasticiser and lubricant

(9) Polyethylene glycol, (10) Liquid paraffin
(11) To provide good moulding, handelling and shorter debinding time, (12) To provide good flow and high filler loading

Table 4.35- Injection moulding conditions for the alumina (+silica+calcia)-polyethylene glycol binder mixture

Temperature (°C)			Injection pressure (MN/m^2)
Barrel	Nozzle	Mould	
135	135	23	0.55

Table 4.36- Debinding cycle for the moulded alumina (+silica+ calcia)-polyethylene glycol samples of size 35X12X5 mm^3

	R 1	R 2	R 3	R 4	R 5	R 6	R 7	R 8
Heating rate (°C/h)	15	8	7	3	1.5	1.5	1.5	2
Temperature level (°C)	125	220	300	340	380	430	490	540
Dwell (hold time, h)	0.1	0.5	1	1	1	1	1	0.5

Table 4.37- Alumina (+silica+calcia)-montanester wax compositions

Material	Comp. 1	Comp. 2	Comp. 3	Function
Al_2O_3	62	66	67.5	Major ceramic powder filler
SiO_2	2	2.5	3	Sintering aid
CaO	1	1.5	1.5	Sintering aid
MEW (13)	35	30	28	Major binder (also acting as plasticiser & lubricant)

(13) Montanester wax

Table 4.38- Injection moulding conditions for the alumina (+ silica+calcia)-montanester wax binder mixture

Temperature (°C)			Injection pressure (MN/m^2)
Barrel	Nozzle	Mould	
100	100	23	0.55

Table 4.39- Debinding cycle for the moulded alumina (+silica+ calcia)-montanester wax samples of size 20, 15 or 10X12X5 mm^3

	R 1	R 2	R 3	R 4	R 5
Heating rate (°C/h)	40	20	10	7	10
Temperature level (°C)	300	400	450	520	600
Dwell (hold time, h)	1	1	1	1	1

Table 4.40- Compositions of the alumina (+silica+calcia)+ montanester wax+microcrystalline wax and alumina (+silica+calcia)+montanester wax+ carnoba wax+paraffin wax binder mixtures

Material	b.m.* 1 (vol.%)	b.m. 2 (vol.%)	Function
Al_2O_3	66	66	Major ceramic powder filler
SiO_2	2.5	2.5	Sintering aid
CaO	1.5	1.5	Sintering aid
Montanester wax	20	18	Major binder
Microcrystalline wax	10	——	Minor binder to reduce the crystallinity of the montanester wax
Carnoba wax	——	6	"
Paraffin wax	——	6	"

* Binder mixture

Table 4.41- Debinding cycle for the moulded alumina (+silica+ calcia)+montanester wax+microcrystalline wax samples of size 20, 15 or 10X12X5 mm^3

	R 1	R 2	R 3	R 4	R 5	R 6	R 7
Heating rate (°C/h)	13	6.5	4.5	4.5	5.5	8	12
Temperature level (°C)	110	260	320	360	420	500	620
Dwell (hold time, h)	1	1	1	1	1	1	1

Table 4.42- Debinding cycle for the moulded alumina (+silica+ calcia)+montanester wax+carnoba wax+paraffin wax samples of size 20, 15 or 10X12X5 mm^3

	R 1	R 2	R 3	R 4	R 5	R 6	R 7
Heating rate (°C/h)	30	7	7	7	10	20	30
Temperature level (°C)	150	250	320	360	420	500	600
Dwell (hold time, h)	0.1	2	1	1	1	1	1

Table 4.43- Alumina (+silica+calcia)-MEW-APP-LP compositions

Material	Comp. 1 (vol.%)	Comp. 2 (vol.%)	Comp. 3 (vol.%)	Function
Al_2O_3	62	64	65.5	Major ceramic powder filler
SiO_2	2	2.5	3	Sintering aid
CaO	1	1.5	1.5	Sintering aid
MEW	22	20	19	Major binder
APP	13	10	9	Minor bider
LP (14)	2	2	2	Minor binder

(14) Liquid paraffin

Table 4.44- Injection moulding conditions for the moulded alumina (+silica+calcia)-MEW-APP-LP samples of size 35X12X5 mm^3

Temperature (°C)			Injection pressure (MN/m^2)
Barrel	Nozzle	Mould	
130	130	23	0.55

Table 4.45- Debinding cycle for the moulded alumina (+silica+calcia)-MEW-APP-LP samples of size 35X12X5 mm^3

	R 1	R 2	R 3	R 4	R 5	R 6	R 7	R 8
Heating rate (°C/h)	13	6	5	4.5	3.5	3	3	4
Temperature level (°C)	140	280	330	370	420	470	530	620
Dwell (hold time, h)	0.1	0.5	1	1	1.5	1.5	1	1

Table 4.46- 99.5% alumina-montanester wax (MEW)-polyisobutylene (PIB)-liquid paraffin (LP) compositions

Material	Comp. 1 (vol.%)	Comp. 2 (vol.%)	Comp. 3 (vol.%)	Function
Alumina	68	70	72	Ceramic powder filler
MEW	17	16	15	Major binder
PIB	9	8	7	Minor binder (to reduce the crystallinity of the MEW)
LP	6	6	6	Plasticiser and lubricant

Table 4.47- Dimensions of the moulded 99.5% alumina-MEW-PIB-LP samples using the Fox and Offord and the plunger type compressed air (PTCA) moulding machines

Dimensions	Sample 1	Sample 2	Sample 3
Length (mm)	62	40	40
Width (mm)	12	19	12
Thickness (mm)	6	3	3

Table 4.48- Injection moulding conditions for the moulded 99.5% alumina-MEW-PIB-LP samples

Temperature (°C)			Injection pressure (MN/m^2)	
Barrel	Nozzle	Mould	PTCA moulder	Fox & Offord moulder
130	130	23	0.55	13.8

Table 4.49- Debinding cycle for the 3 mm thick moulded 99.5% alumina-MEW-PIB-LP samples of size 40X19X3 mm^3 and 40X12X3 mm^3

	R 1	R 2	R 3	R 4	R 5	R 6	R 7	R 8
Heating rate (°C/h)	12	5.5	4.5	4.5	5	6	7	8.25
Temperature level (°C)	110	150	210	250	290	350	420	530
Dwell (hold time, h)	0.5	0.5	0.5	1	1	1	1	1

Table 4.50- Debinding cycle for the 5 mm thick moulded 99.5% alumina-MEW-PIB-LP samples of size 35X12X5 mm^3

	R 1	R 2	R 3	R 4	R 5	R 6	R 7	R 8
Heating rate (°C/h)	10	4.5	3.5	3.5	3	4.25	5.25	7.5
Temperature level (°C)	110	150	210	250	290	350	420	530
Dwell (hold time, h)	0.5	0.5	0.5	0.5	1	1	1	1

Table 4.51- Debinding cycle for the 6 mm thick moulded 99.5% alumina-MEW-PIB-LP samples of size 62X12X6 mm^3

	R 1	R 2	R 3	R 4	R 5	R 6	R 7	R 8
Heating rate (°C/h)	9.25	4.25	3.25	3.25	2.8	4.2	5.2	7.3
Temperature level (°C)	110	150	210	250	290	350	420	530
Dwell (hold time, h)	0.5	0.5	0.5	0.5	1	1	1	1

Table 4.52- 99.5% alumina-polyvinyl alcohol-gelling agent-liquid paraffin-water compositions

Material	Comp. 1 (vol.%)	Comp. 2 (vol.%)	Comp. 3 (vol.%)	Function
Alumina	53	56	57	Ceramic powder filler
PVA (15)	6.5	6	5.5	Major binder (98% hydrolysed, water-based)
Resorcinol	4.5	4	3.5	Gelling agent
Liquid paraffin	33	31	31	Plasticiser and lubricant
Water	3	3	3	Solvent

(15) Polyvinyl alcohol

Table 4.53- Injection moulding conditions for the moulded 99.5% alumina-PVA-gelling agent-LP-water samples

Temperature (°C)			Injection pressure (MN/m^2)	
Barrel	Nozzle	Mould	PTCA moulder	Fox & Offord moulder
72	72	23	0.55	13.8

Table 4.54- Debinding cycle for the moulded 99.5% alumina-PVA-gelling agent-LP-water samples of size 35X12X5 mm^3 and 62X12X6 mm^3

	R 1	R 2	R 3	R 4	R 5
Heating rate (°C/h)	210	45	220	110	520
Temperature level (°C)	80	110	160	380	850
Dwell (hold time, h)	2	2	1	2	1

Table 4.55- Properties of the injection moulded 99.5% and other alumina ceramics using the new binder systems developed during this work

Binder system	% max. possible vol. loading of 99.5% Al_2O_3 or other alumina powder mixture	As-moulded (green) density (% th.)	Sintered density (% th.)	Shrinkage (% total volume)
PEG-APP-LP (16)	62 (Al_2O_3 + SiO_2 +CaO)	95	96	12
MEW	70 (Al_2O_3 + SiO_2 +CaO)	97.3	98.2	10.5
MEW-MW (17)	70 (Al_2O_3 + SiO_2 +CaO)	97.3	98.2	10.5
MEW-CW-PW (18)	70 (Al_2O_3 + SiO_2 +CaO)	97.3	98.2	10.5
MEW-APP-LP	68 (Al_2O_3 + SiO_2 +CaO)	96.4	97.3	11
MEW-PIB-LP	70 (99.5% Al_2O_3)	97.35	98.5	10.2
PVA-Gelling agent-LP-water	56 (99.5% Al_2O_3)	91.5	96	17

(16) Polyethylene glycol-atactic polypropylene-liquid paraffin; (17) Montanester wax-microcrystalline wax; (18) Montanester wax-carnoba wax-paraffin wax

Table 4.55 continued

Binder system	Debinding time (h, for 6, 5 & 3 mm thick samples respectively)			Mixing, moulding and demoulding properties
PEG-APP-LP		170		Good mixing & no sticking problems; good flow props.; moulded easily at 135°C; very rigid mouldings & no demoulding problems;
MEW		36		Good mixing & no sticking problems; good flow props.; shrinkage cracking within the mould cavity due to high crystallinity; very brittle mouldings of small size 10, 15 & 20X12X5 mm^3; moulded easily at 100°C;
MEW-MW		90		The same as MEW binder system
MEW-CW-PW		50		The same as MEW binder system
MEW-APP-LP		136		Good mixing & no sticking problems; very good flow props.; no shrinkage cracking problems; good demoulding & handling props.; moulded easily at 130°C with small/ medium/large size mouldings;
MEW-PIB-LP	112	104	80	Good mixing & no sticking problems; excellent flow props.; no shrinkage cracking problems; good demoulding & handling props.; moulded easily at 130°C with small/ medium/large size mouldings;
PVA-Gelling agent-LP-water	12	12		Good mixing & no sticking problems; good flow props.; quite rigid mouldings; no distortion & no adhesion problems during the demoulding process; a cycle time of < 1 min was required for the complete gelation of the moulded samples within the mould cavity; moulded easily at 72°C;

Table 4.56- Flexural/bend strength of the sintered alumina samples obtained by the injection moulding process (using the best binder systems) during this work

Binder system	Alumina grade (%)	Sintered density (% th.)	4-point flexural/bend strength (MN/m^2)
60/40 APP mixture	88 95 99.5	97 96.5 96	312 ± 38 348 ± 40.5 367 ± 43
Water-based PVA	99.5	96	360 ± 46
MEW-PIB-LP	99.5	98.5	401 ± 39

Table 4.57- Compressive strength of the sintered alumina samples obtained by the injection moulding process (using the best binder systems) during this work

Binder system	Alumina grade (%)	Sintered density (% th.)	Compressive/crushing strength (MN/m^2)
60/40 APP mixture	88 95 99.5	97 96.5 96	2405 ± 110 2910 ± 107 4101 ± 101
Water-based PVA	99.5	96	4000 ± 119
MEW-PIB-LP	99.5	98.5	4400 ± 85.5

Table 4.58- Thermal conductivity of the sintered alumina samples obtained by the injection moulding process (using the best binder systems) during this work

Binder system	Alumina grade (%)	Sintered density (g/cm^3)	c_p at 260°C (J/g°C)	Th. diff., α (19) (mm^2/s)	Th. cond., k (20) (KW/m°C)
60/40 APP mixture	88 95 99.5	3.45 3.57 3.71	1.037 1.037 1.037	3.68 4.43 5.48	13.2 16.4 21.1
Water-based PVA	99.5	3.71	1.037	5.4	20.8
MEW-PIB-LP	99.5	3.81	1.037	5.89	23.3

(19) Thermal diffusivity; (20) Thermal conductivity

Table 4.59- Compositions of the zirconia (+MgO)-MEW-PIB-LP binder mixtures

Material	Comp. 1 (vol.%)	Comp. 2 (vol.%)	Comp. 3 (vol.%)	Function
ZrO_2	61	61.3	62.5	Major ceramic powder filler
MgO	2	3.7	4.5	Sintering aid
MEW	19	18	17	Major binder
PIB	10	9	9	Minor binder
LP	8	8	7	Plasticiser and lubricant

Table 4.60- Injection moulding conditions for the moulded zirconia (+MgO)-MEW-PIB-LP samples

Temperature (°C)			Injection pressure (MN/m^2)
Barrel	Nozzle	Mould	
130	130	23	0.55

Table 4.61- Debinding cycle for the moulded zirconia (+MgO)-MEW-PIB-LP samples of size 35X12X5 mm^3

	R 1	R 2	R 3	R 4	R 5	R 6	R 7	R 8
Heating rate (°C/h)	8	4.5	4	3.5	3	3.5	4.5	6.7
Temperature level (°C)	115	155	210	250	290	350	430	520
Dwell (hold time, h)	0.1	0.5	0.5	0.5	1	1	1	1

Table 4.62- Compositions of the silicon nitride ($+Y_2O_3+Al_2O_3$)-MEW-PIB-LP binder mixtures

Material	Comp. 1	Comp. 2	Comp. 3	Function
Si_3N_4	60	61	62	Major nitride powder filler
Y_2O_3	2	2.7	3.2	Sintering aid
Al_2O_3	1	1.3	1.8	Sintering aid
MEW	13	12	11	Major binder
PIB	16.5	16	15	Minor binder
LP	7.5	7	7	Plasticiser and lubricant

Table 4.63- Injection moulding conditions for the moulded silicon nitride ($+Y_2O_3+Al_2O_3$)-MEW-PIB-LP samples

Temperature (°C)			Injection pressure (MN/m^2)
Barrel	Nozzle	Mould	
130	130	23	0.55

Table 4.64- Compositions of the silicon carbide ($+B_4C$)-MEW-PIB-LP binder mixtures

Material	Comp. 1 (vol.%)	Comp. 2 (vol.%)	Comp. 3 (vol.%)	Function
SiC (+1 wt. % B_4C)	58.5	60	61	Main carbide powder filler (+sintering aid)
MEW	15	14	13.5	Binder
PIB	17.5	17	16.5	Binder
LP	9	9	9	Plasticiser and lubricant

Table 4.65- Injection moulding conditions for the moulded silicon carbide (+B_4C)-MEW-PIB-LP samples

Temperature (°C)			Injection pressure (MN/m^2)
Barrel	Nozzle	Mould	
130	130	23	0.55

Table 4.66- Debinding cycle for the moulded silicon carbide (+B_4C)-MEW-PIB-LP samples of size 35X12X5 mm^3

	R 1	R 2	R 3	R 4	R 5	R 6	R 7	R 8
Heating rate (°C/h)	8	4.5	4.25	3.75	3.5	4	4.5	6.7
Temperature level (°C)	115	155	220	260	300	350	430	510
Dwell (hold time, h)	0.1	0.5	0.5	0.5	1	1	1	1

Table 4.67- Compositions of the tungsten carbide+6 wt.% cobalt -MEW-PIB-LP binder mixtures

Material	Comp. 1 (vol.%)	Comp. 2 (vol.%)	Comp. 3 (vol.%)	Function
WC (+6 wt.% Co)	63	65	66	Hardmetal powder filler
MEW	19	18	17.5	Major binder
PIB	13	12	11.5	Minor binder
LP	5	5	5	Plasticiser and lubricant

Table 4.68- Debinding cycle for the moulded tungsten carbide (+6 wt.% cobalt)-MEW-PIB-LP samples of size 35X12X5 mm^3

	R 1	R 2	R 3	R 4	R 5	R 6	R 7	R 8
Heating rate (°C/h)	14	11	8	6	3	3.5	4	6
Temperature level (°C)	120	180	260	330	400	450	510	580
Dwell (hold time, h)	0.5	0.5	0.5	1	2	1	1	1

Table 4.69- Properties of the injection moulded zirconia, silicon nitride, silicon carbide and tungsten carbide-6 wt.% cobalt powders using the newly developed MEW-PIB-LP binder system

Powder	% max. possible volume loading	As-moulded (green) density (% th.)	Sintered density (% th.)	Shrinkage (% total volume)
Zirconia (+MgO)	65	96	96.5	20
Silicon nitride (+Y_2O_3+Al_2O_3)	65	96.5	93	11
Silicon carbide (B_4C)	60	95	—	—
Tungsten carbide-6 wt.% cobalt	65	91	95	12

Table 4.69 continued

Powder	Debinding time (h, for 5 mm thick samples)	Mixing,moulding and de-moulding properties
Zirconia (+MgO)	110	Good mixing & no sticking problems;good flow props.; moulded easily at 130°C; very rigid mouldings & no demoulding & no handling problems;
Silicon nitride (+Y_2O_3+Al_2O_3)	110	The same as zirconia except that a mould release agent was used to prevent adhesion during the demoulding process
Silicon carbide (+B_4C)	106	The same as zirconia
Tungsten carbide-6 wt.% cobalt	100	The same as zirconia

Table 4.70- Compositions of the silicon nitride (+Y_2O_3 +Al_2O_3)-PVA-gelling agent-LP-water binder mixtures

Material	Comp. 1 (vol.%)	Comp. 2 (vol.%)	Comp. 3 (vol.%)	Function
Si_3N_4	47	48	49	Major nitride powder filler
Y_2O_3	1.3	2	2	Sintering aid
Al_2O_3	0.7	1	1	Sintering aid
PVA	7	6	5.5	Major binder
Resorcinol	3	3	2.5	Gelling agent
LP	2	1.5	1.5	Plasticiser and lubricant
Water	39	38.5	38.5	Solvent

Table 4.71- Injection moulding conditions for the moulded silicon nitride (+Y_2O_3+Al_2O_3)-PVA-gelling agent-LP-water samples

Temperature (°C)			Injection pressure (MN/m^2)
Barrel	Nozzle	Mould	
72	72	23	0.55

Table 4.72- Debinding cycle for the 5 mm thick moulded silicon nitride (+Y_2O_3+Al_2O_3)-PVA-gelling agent-LP-water samples of size 35X12X5 mm^3

	R 1	R 2	R 3	R 4	R 5
Heating rate (°C/h)	210	45	220	110	520
Temperature level (°C)	80	110	160	380	850
Dwell (hold time, h)	2	2	1	2	1

Table 4.73- Compositions of the tungsten carbide-6 wt.% cobalt-PVA-gelling agent-LP-water binder mixtures

Material	Comp. 1 (vol.%)	Comp. 2 (vol.%)	Comp. 3 (vol.%)	Function
WC-6 wt.% Co	44	46	47	Hardmetal/cermet powder filler
PVA	8	7	6.5	Major binder
Resorcinol	4	3.5	3	Gelling agent
LP	2.5	2	2	Plasticiser and lubricant
Water	41.5	41.5	41.5	Solvent

Table 4.74- Debinding cycle for the 5 mm thick moulded tungsten carbide-6 wt.% cobalt-PVA-gelling agent-LP-water samples of size 35X12X5 mm^3

	R 1	R 2	R 3	R 4	R 5
Heating rate (°C/h)	100	120	200	350	600
Temperature level (°C)	90	110	300	500	860
Dwell (hold time, h)	1	1	0.5	0.5	1

Table 4.75- Compositions of the iron-2 wt.% nickel-PVA-gelling agent-LP-water binder mixtures

Material	Comp. 1 (vol.%)	Comp. 2 (vol.%)	Comp. 3 (vol.%)	Function
Fe-2 wt.% Ni	54	56	57	Metallic powder filler
PVA	6	5	4.5	Major binder
Resorcinol	4.5	4	3.5	Gelling agent
LP	1.5	1	1	Plasticiser and lubricant
Water	34	34	34	Solvent

Table 4.76- Properties of the injection moulded silicon nitride, tungsten carbide-6 wt.% cobalt and iron-2 wt.% nickel using the PVA-gelling agent-LP-water (PVA) binder system

Powder	% max. possible volume loading	Sintered density (% th.)	Shrinkage (% total volume)
Silicon nitride ($+Y_2O_3+Al_2O_3$)	51	92.5	9
Tungsten carbide-6 wt.% cobalt	46	97.5	13.5
Iron-2 wt.% nickel	56	94.5	12.5

Table 4.76 continued

Powder	Debinding time (h, for the 5 mm thick samples)	Mixing, moulding and demoulding properties
Silicon nitride ($+Y_2O_3+Al_2O_3$)	12	Quite satisfactory (no mixing, no moulding and no demoulding problems); no moulding defects; no oxidation problems after debinding; a cycle time of 45 s was used for each moulding;
Tungsten carbide-6 wt.% cobalt	7	The same as silicon nitride except that a cycle time of 40 s was used for each moulding
Iron-2 wt.% nickel	7.2	The same as silicon nitride except that a cycle time of 50 s was used for each moulding

Table 4.77- Tap densities and the amount of volume loading of powders in the MEW-PIB-LP binder system

Powder	Density (g/cm^3)	Tap density (g/cm^3)	% tap density	% max. possible volume loading
99.5% alumina	3.87	1.5	38.78	70
Zirconia (+MgO)	5.8	2.5	43	65
Silicon nitride ($+Y_2O_3+Al_2O_3$)	3.2	1.2	37.5	65
Silicon carbide ($+B_4C$)	3.2	1.8	56.25	60
Tungsten carbide-6 wt.% cobalt	14.95	6.87	46	65

Table 4.78- Tap densities and the amount of volume loading of powders in the water-based PVA binder system

Powder	Density (g/cm^3)	Tap density (g/cm^3)	% tap density	% max. possible volume loading
99.5% alumina	3.87	1.5	38.75	56
Silicon nitride ($+Y_2O_3+Al_2O_3$)	3.2	1.2	37.5	51
Tungsten carbide-6 wt.% cobalt	14.95	6.87	46	46
Iron-2 wt.% nickel	7.88	2.4	30.45	56

Table 4.79- Characteristic properties of the powders used during this work

Powder	Average particle size (μm)	Particle size distribution (μm)	Surface area (m^2/g)	Particle shape
99.5% alumina	1.4	0.1-10	3	Near spherical
Zirconia (+MgO)	4.2	0.1-20	8.5	"
Silicon nitride (+Y_2O_3+Al_2O_3)	4.8	0.5-55	22	"
Silicon carbide (+B_4C)	52	10-100	31	Mostly plate-like
Tungsten carbide-6 wt.% cobalt	1.2	sub.-16	13.5	Plate/ needle like
Iron-2 wt.% nickel	10	1-46	9	Almost spherical

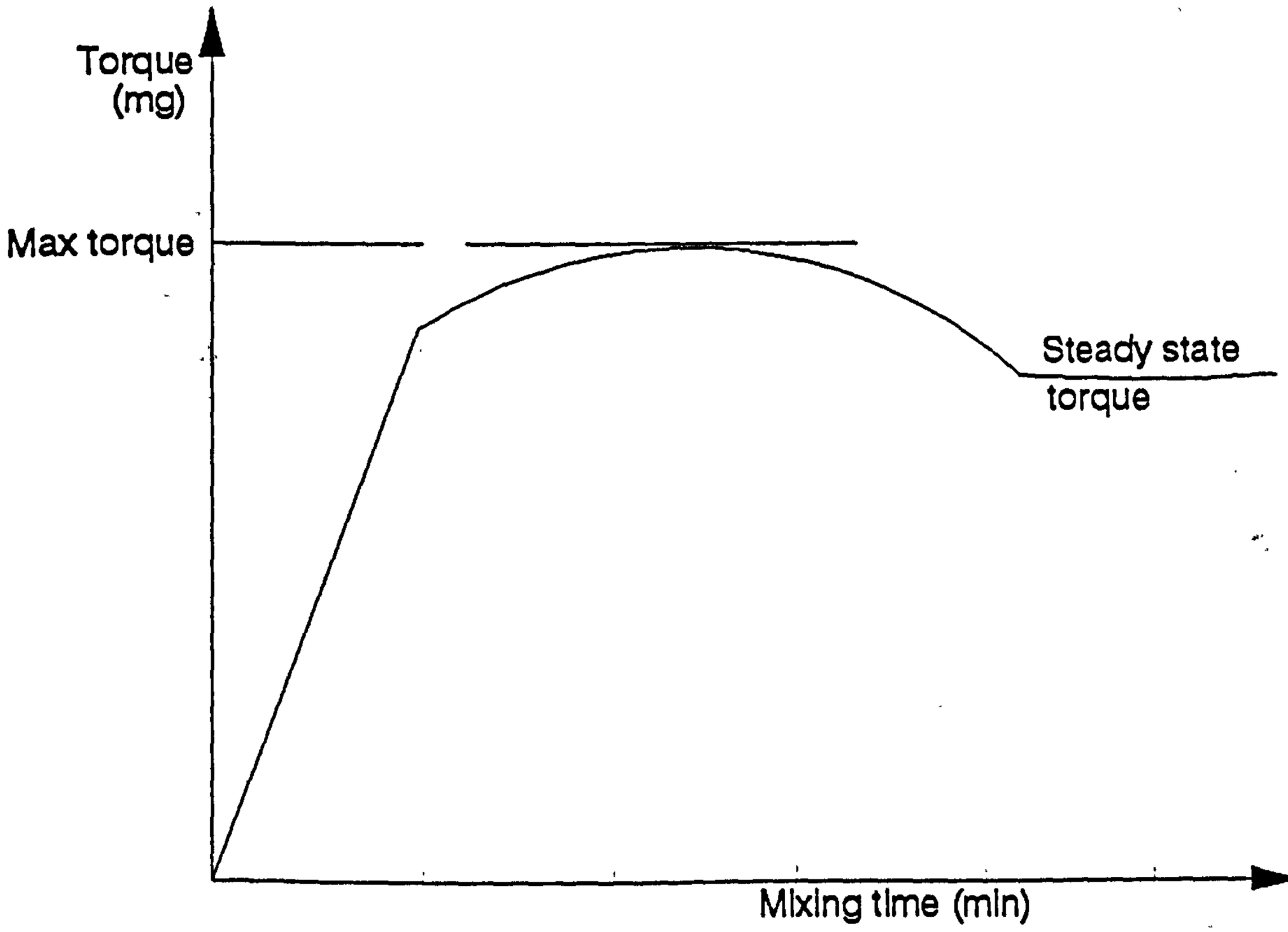

Figure 4.1- Schematic graph of torque against time from the Brabender mixing device.

Figure 4.2- Apparent viscosity versus apparent shear rate for the alumina (99.5% G) -EVA b.m. at 160 °c.

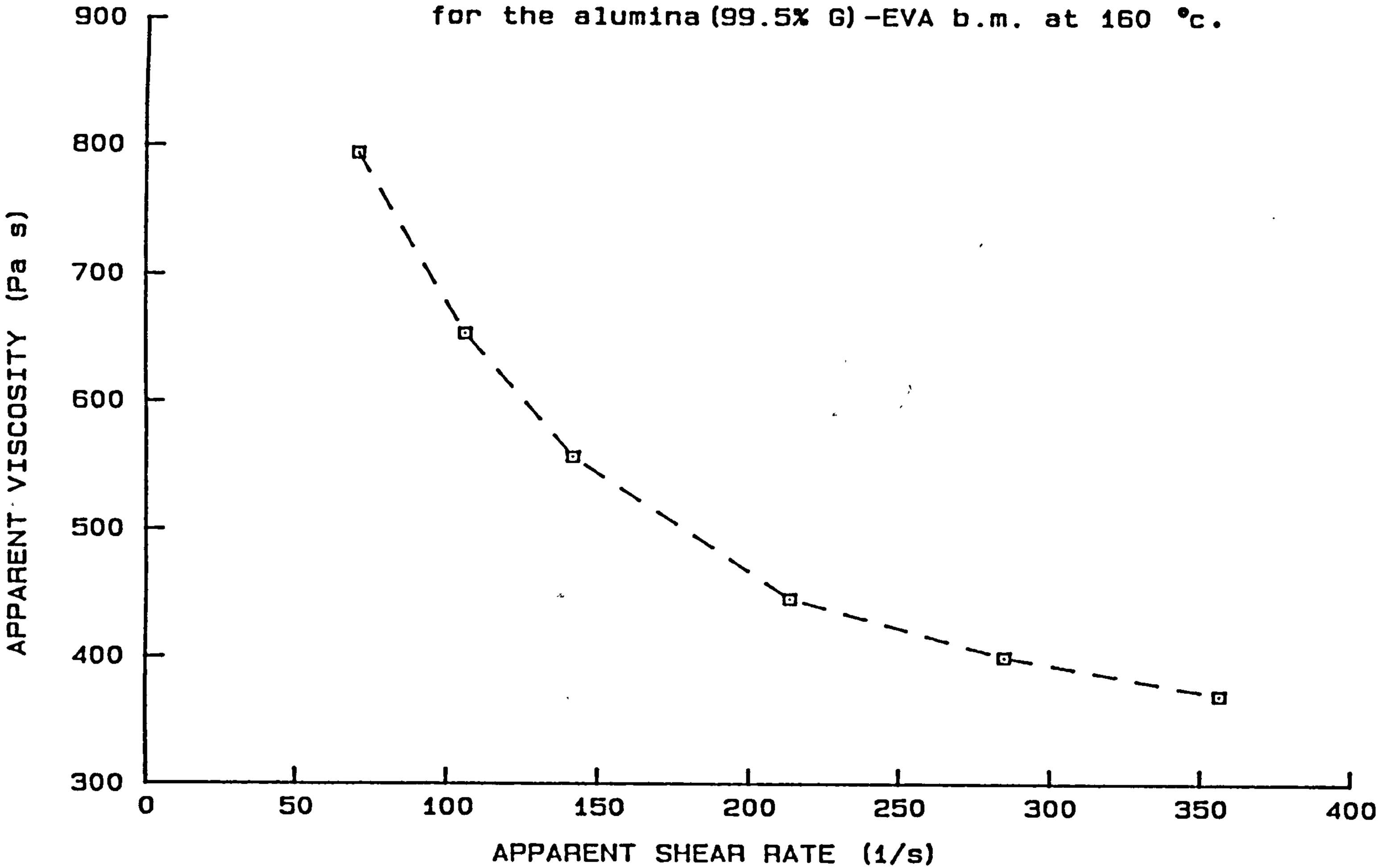

Figure 4.3- TGA data for the alumina (99.5% G) -EVA b.m. at different heating rates.

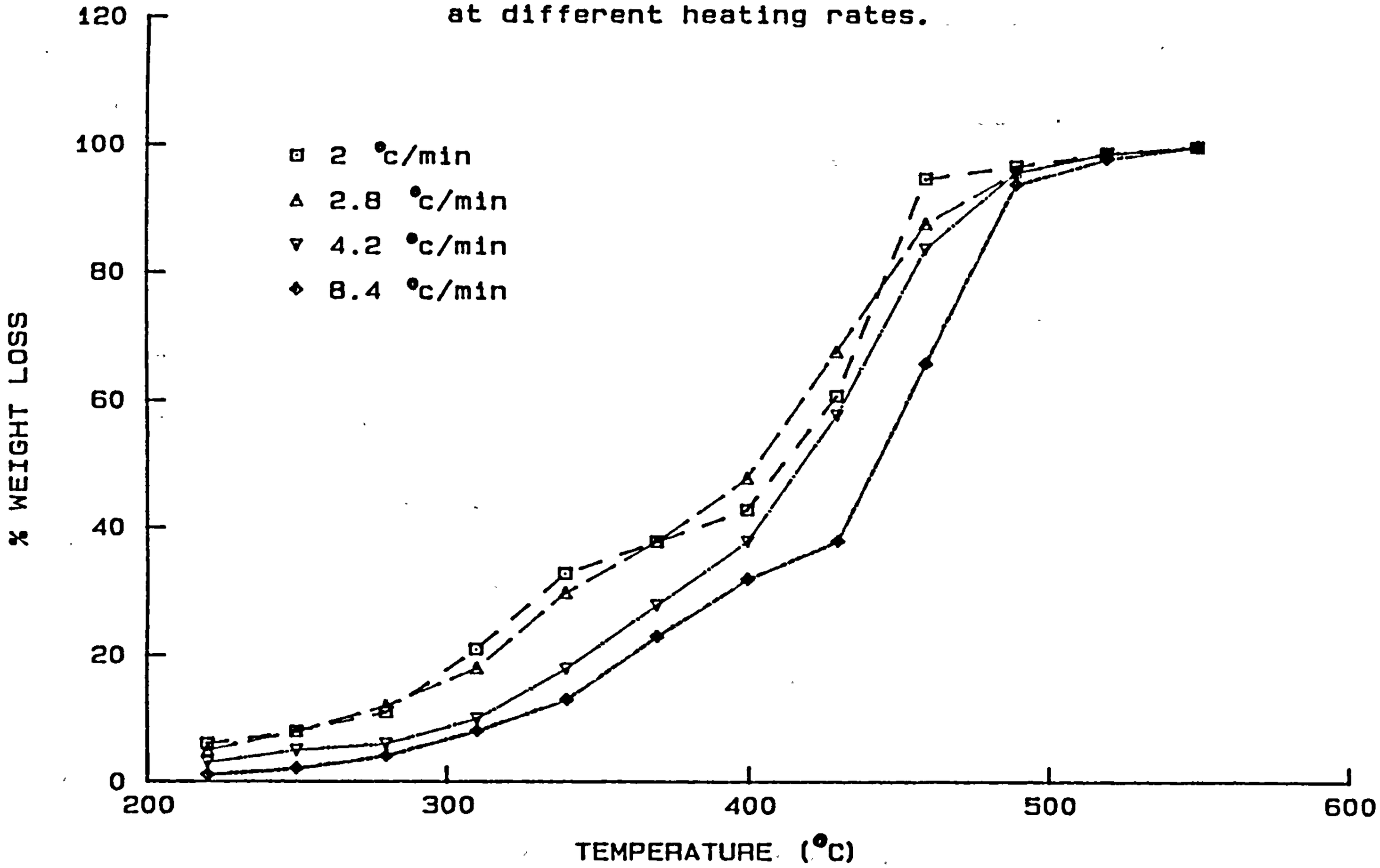

Figure 4.4- Apparent viscosity versus apparent shear rate for the alumina-PS b.m. at 150 °c.

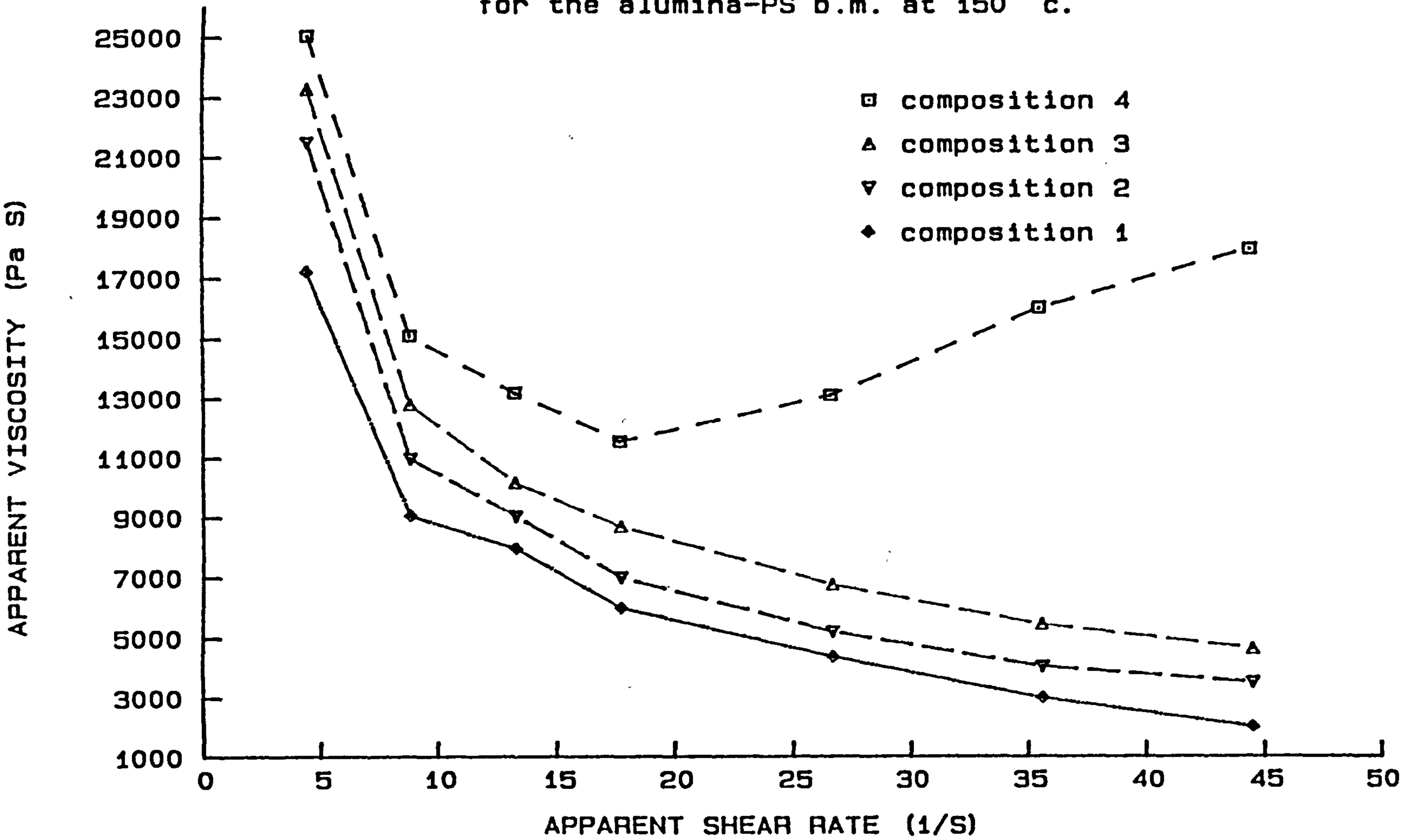

Figure 4.5- TGA data at 4.2 °c/min for S.A. , D.E.P. & alumina-PS-DEP-SA b.m..

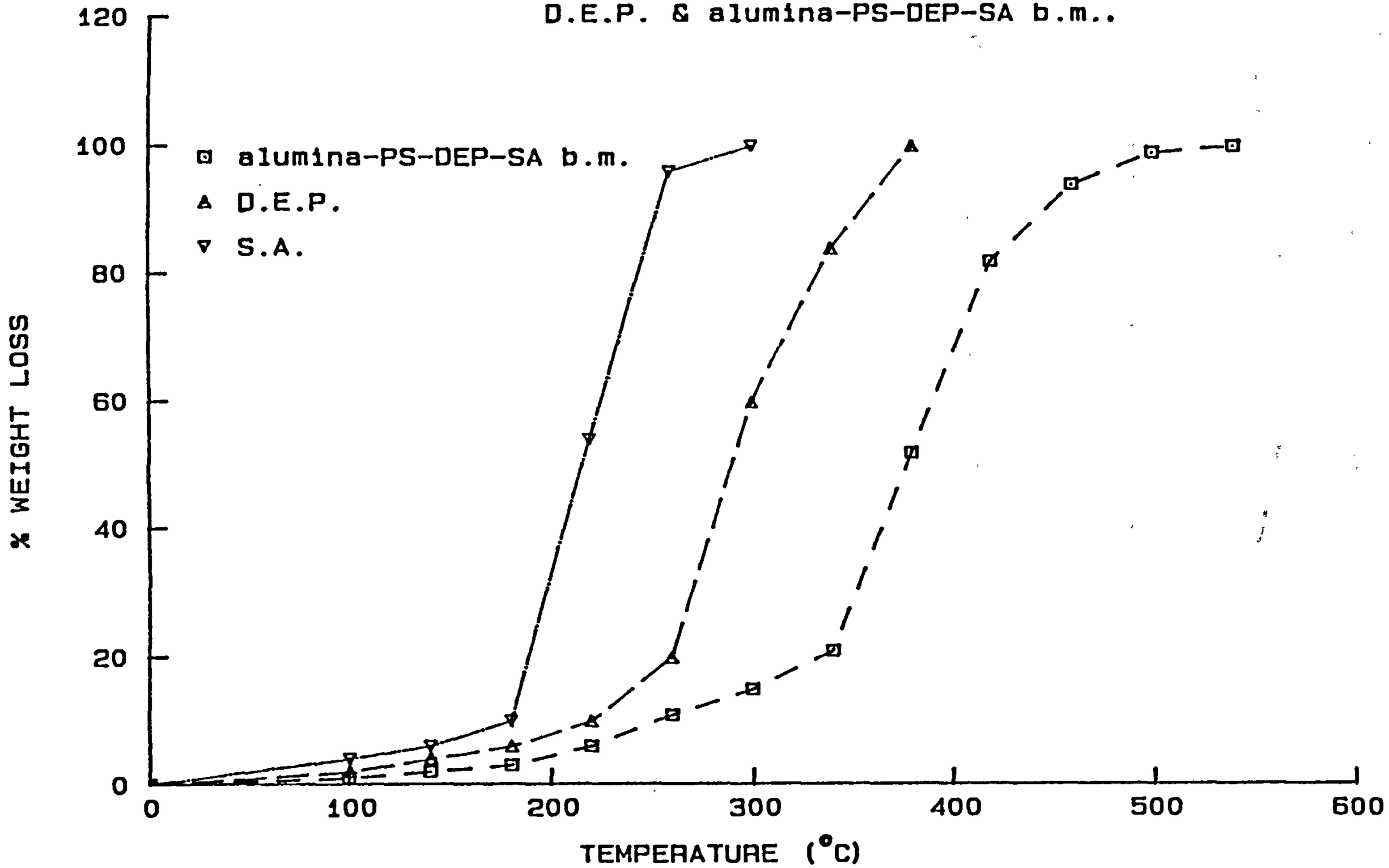

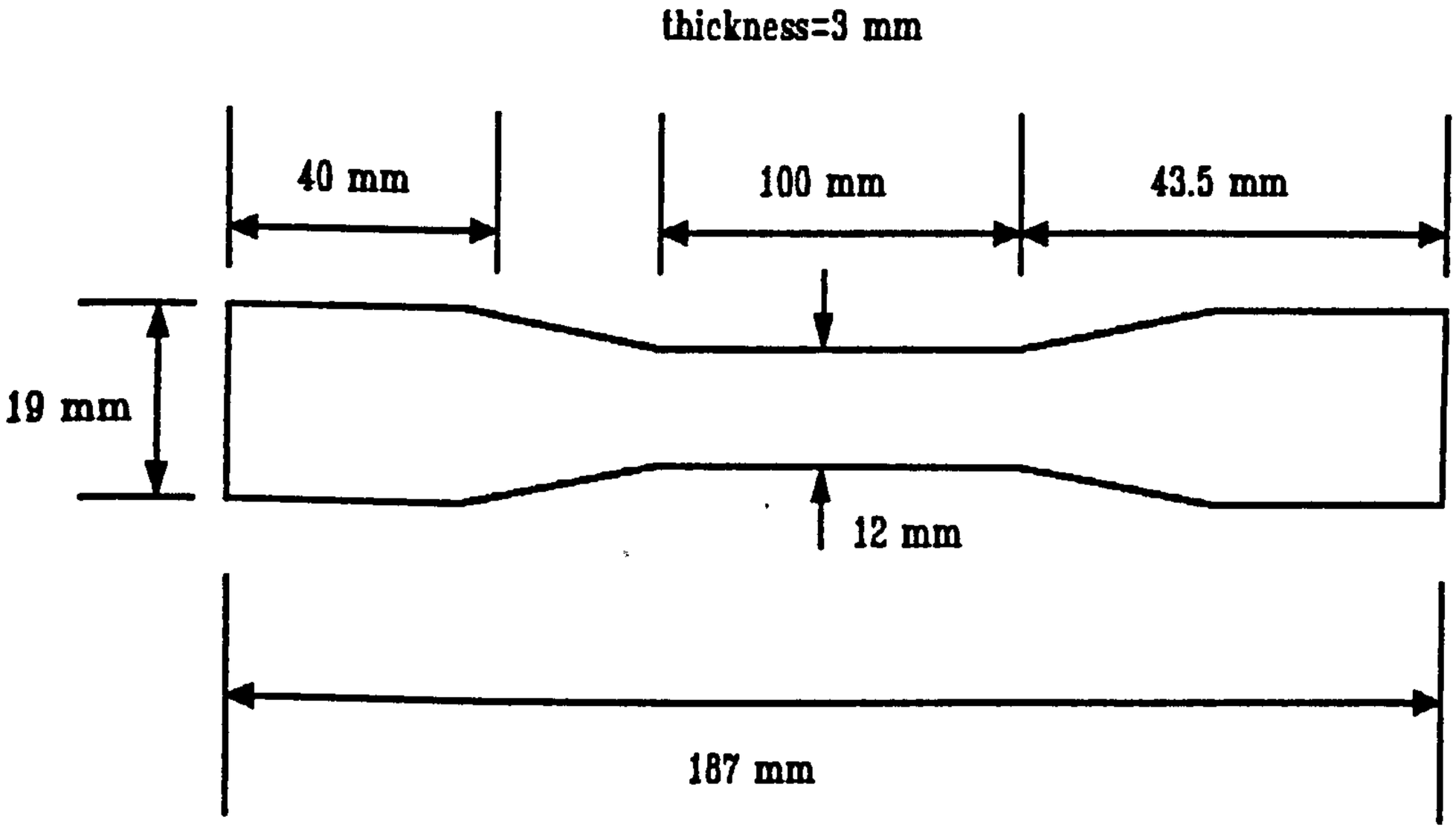

Figure 4.6- Test bar of size 187mmX12mmX3mm.

Figure 4.7- Apparent viscosity versus apparent shear rate for the alumina(99.5% G)-PA b.m. at 180 °c; d=3 mm.

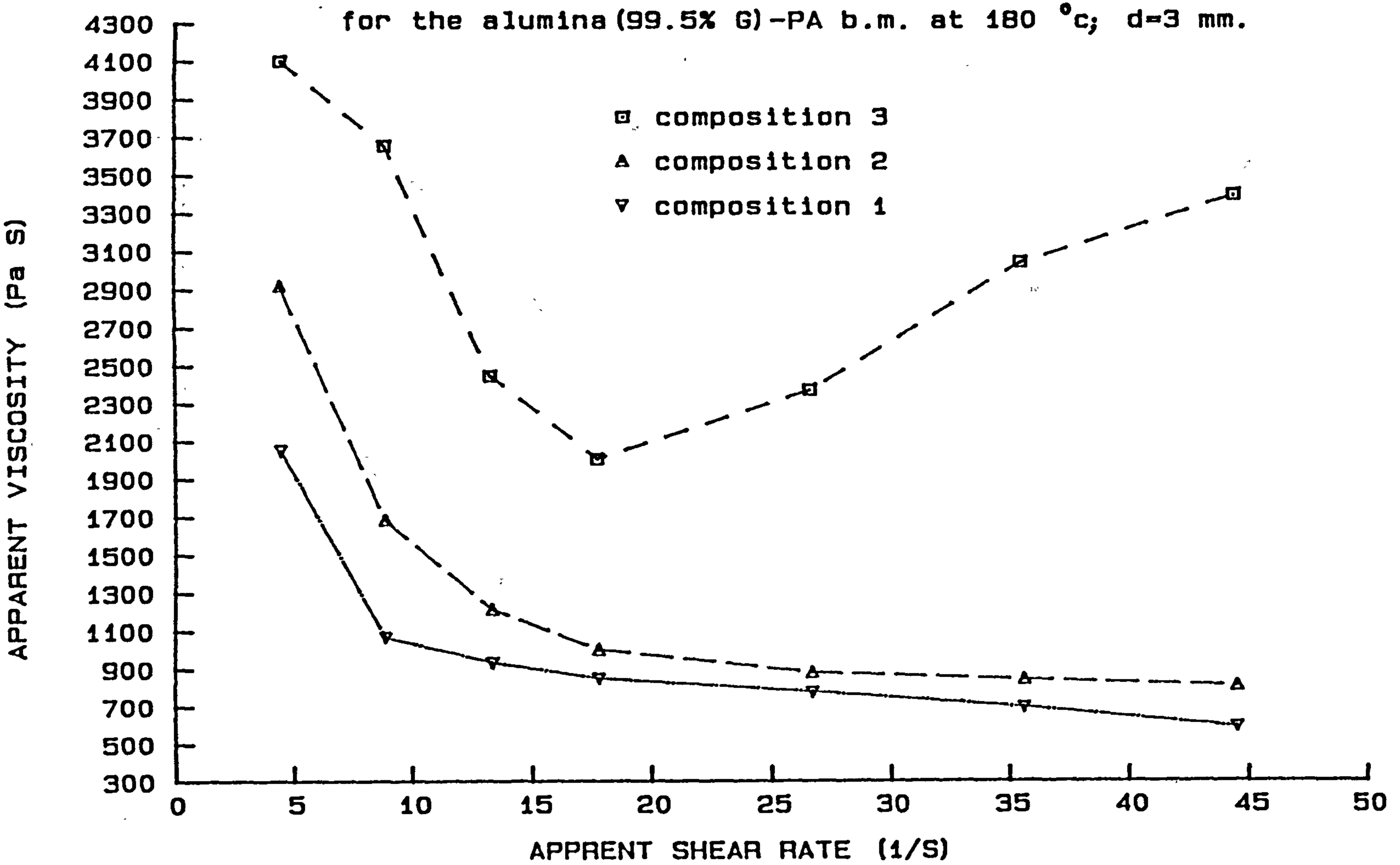

Figure 4.8- Apparent viscosity versus apparent shear rate for the alumina (99.5% G) -PA b.m. at 180 °c; d=1.5 mm.

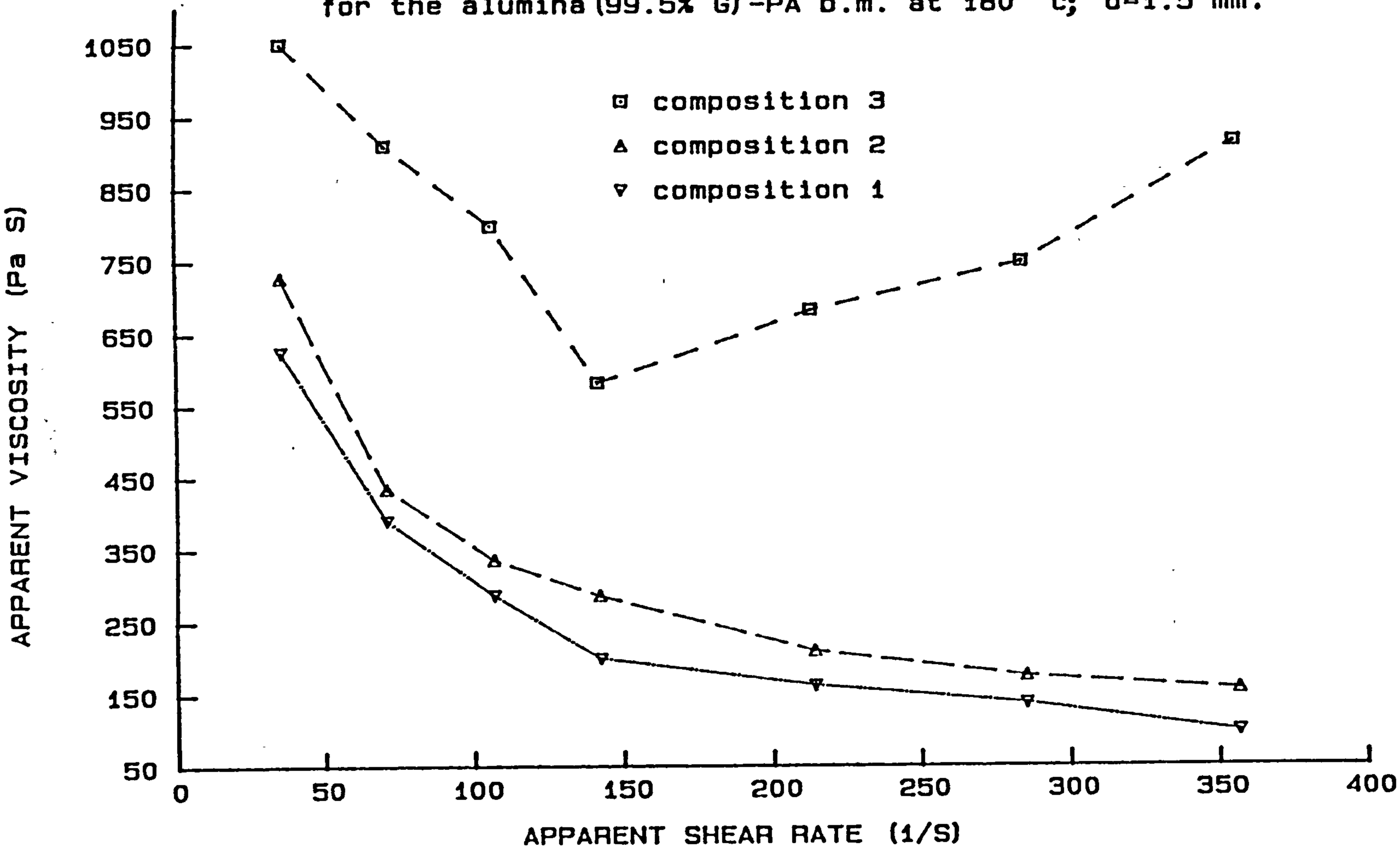

Figure 4.9- TGA data at 4.2 °c/min for the APP & LDPE binders.

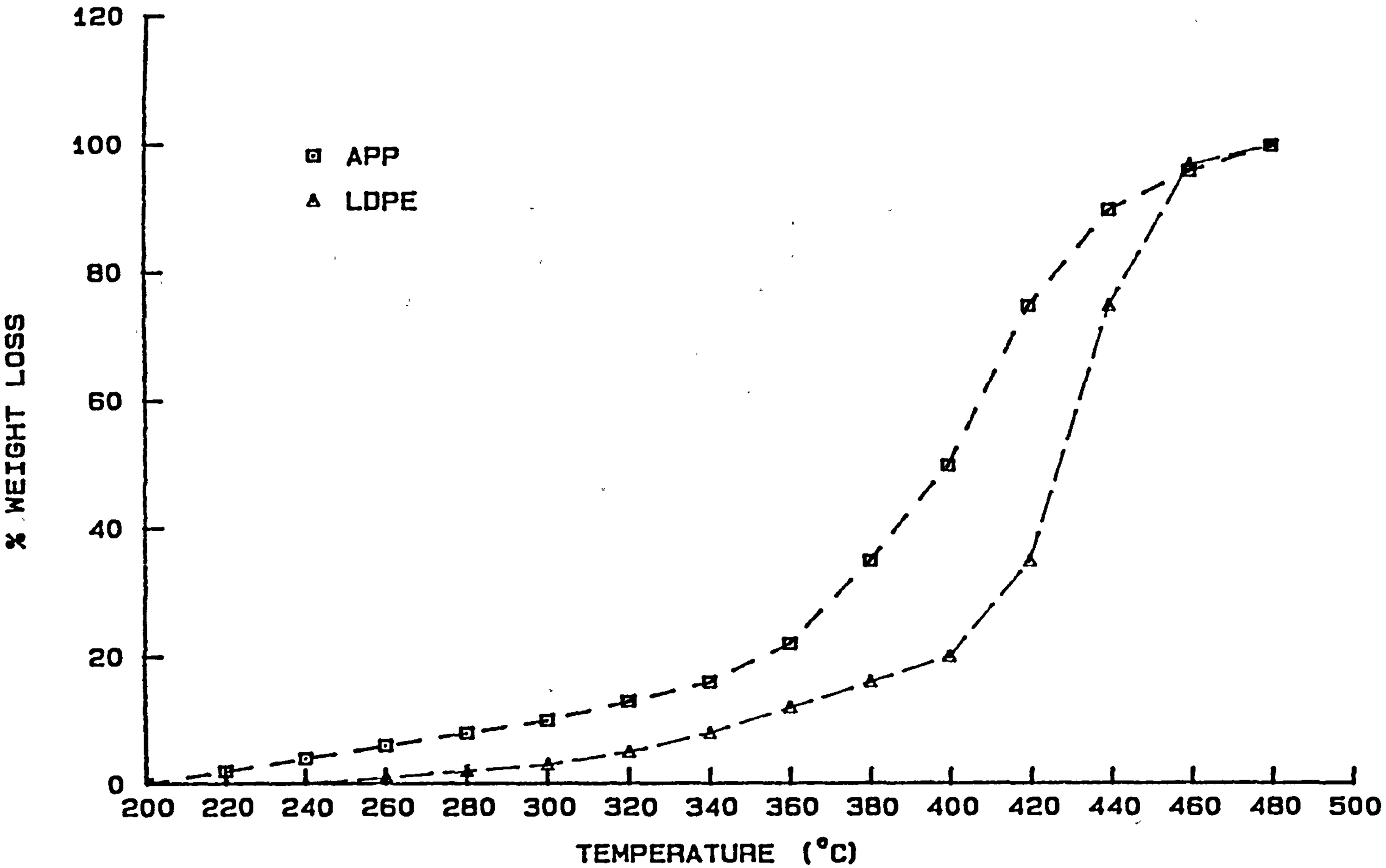

Figure 4.10- TGA data for the alumina(99.5% G)-PA-APP-LDPE-EVA-DEP-SA b.m. at different heating rates.

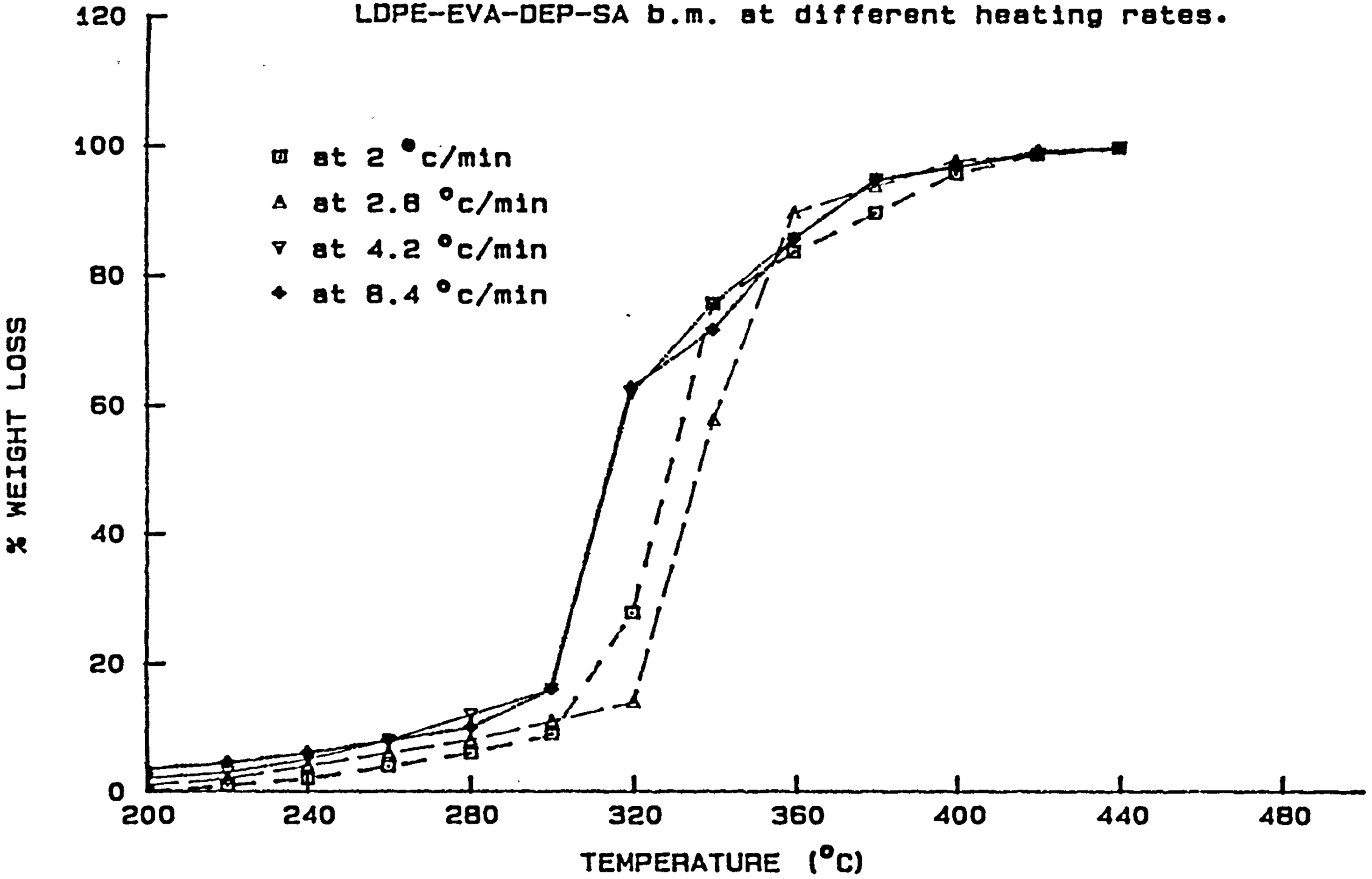

Figure 4.11- Apparent viscosity versus apparent shear rate for the alumina (99.5% G) -APP b.m. at 120 °c.

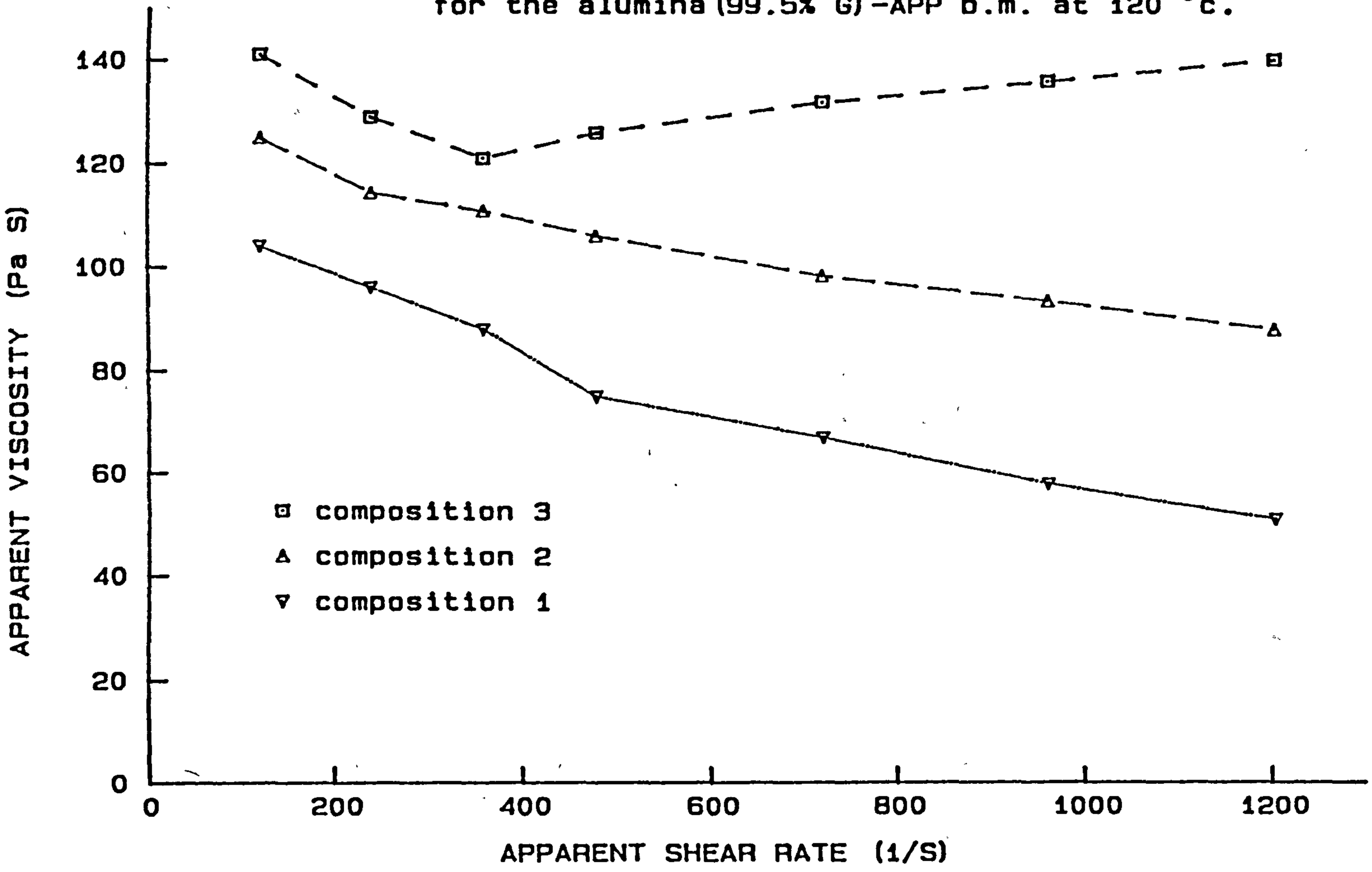

Figure 4.12- Apparent viscosity versus apparent shear rate for composition 2 at different temperatures.

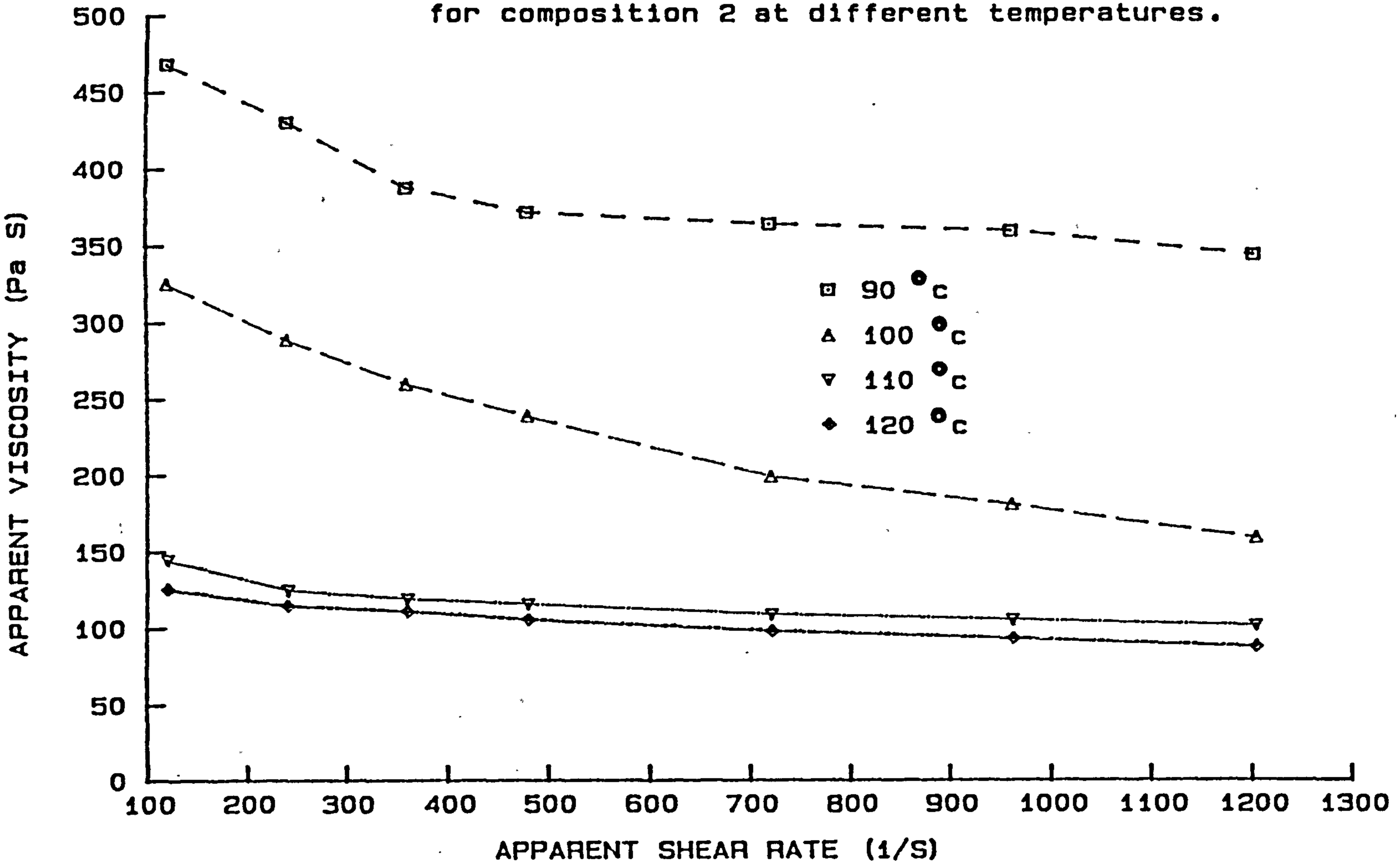

Figure 4.13- TGA data for the alumina (99.5% G) -APP-SA-DEP b.m. at different heating rates.

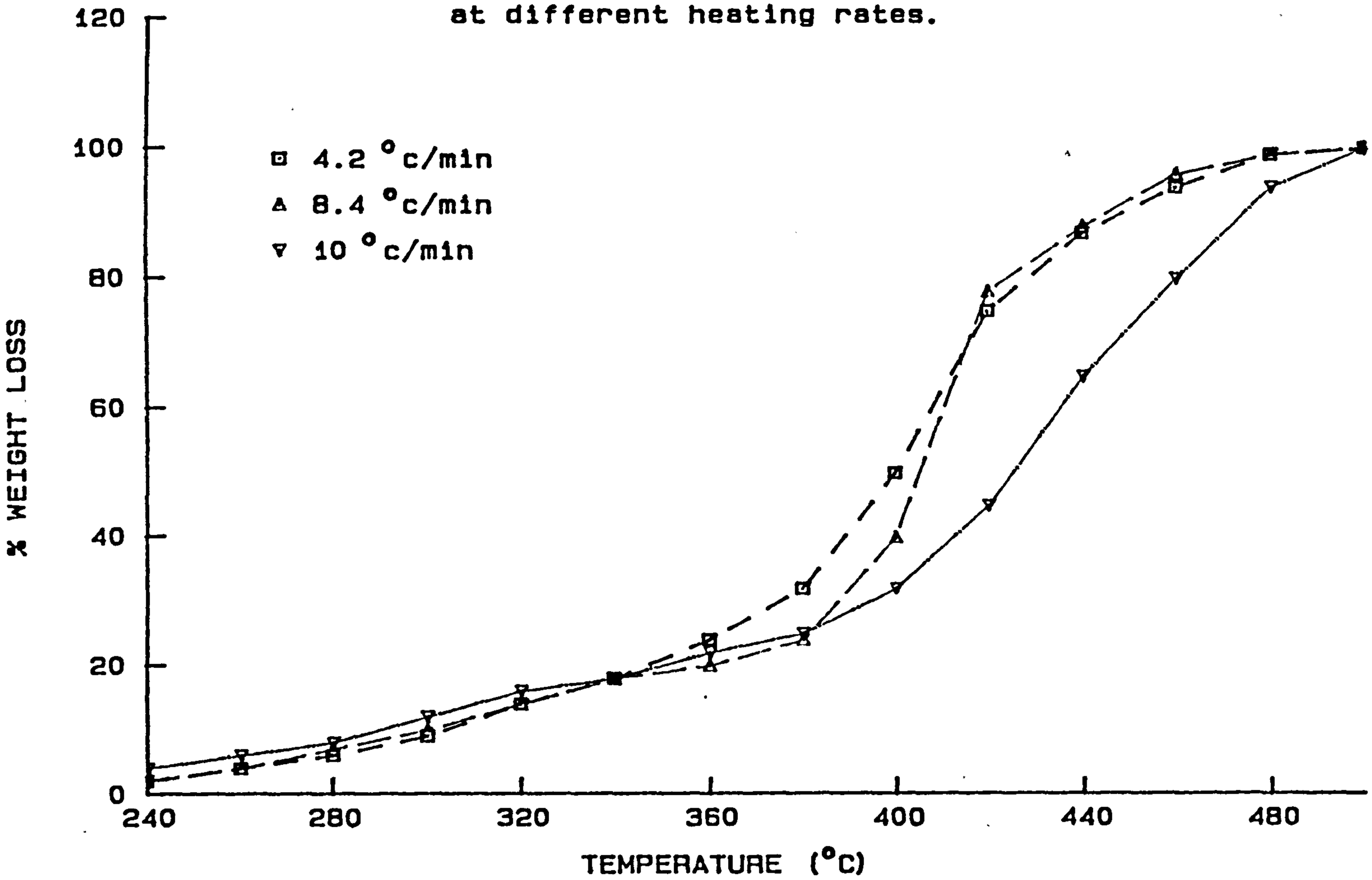

Figure 4.14- Apparent viscosity versus apparent shear rate for the alumina(99.5% G)-60/40 APP mixture b.m..

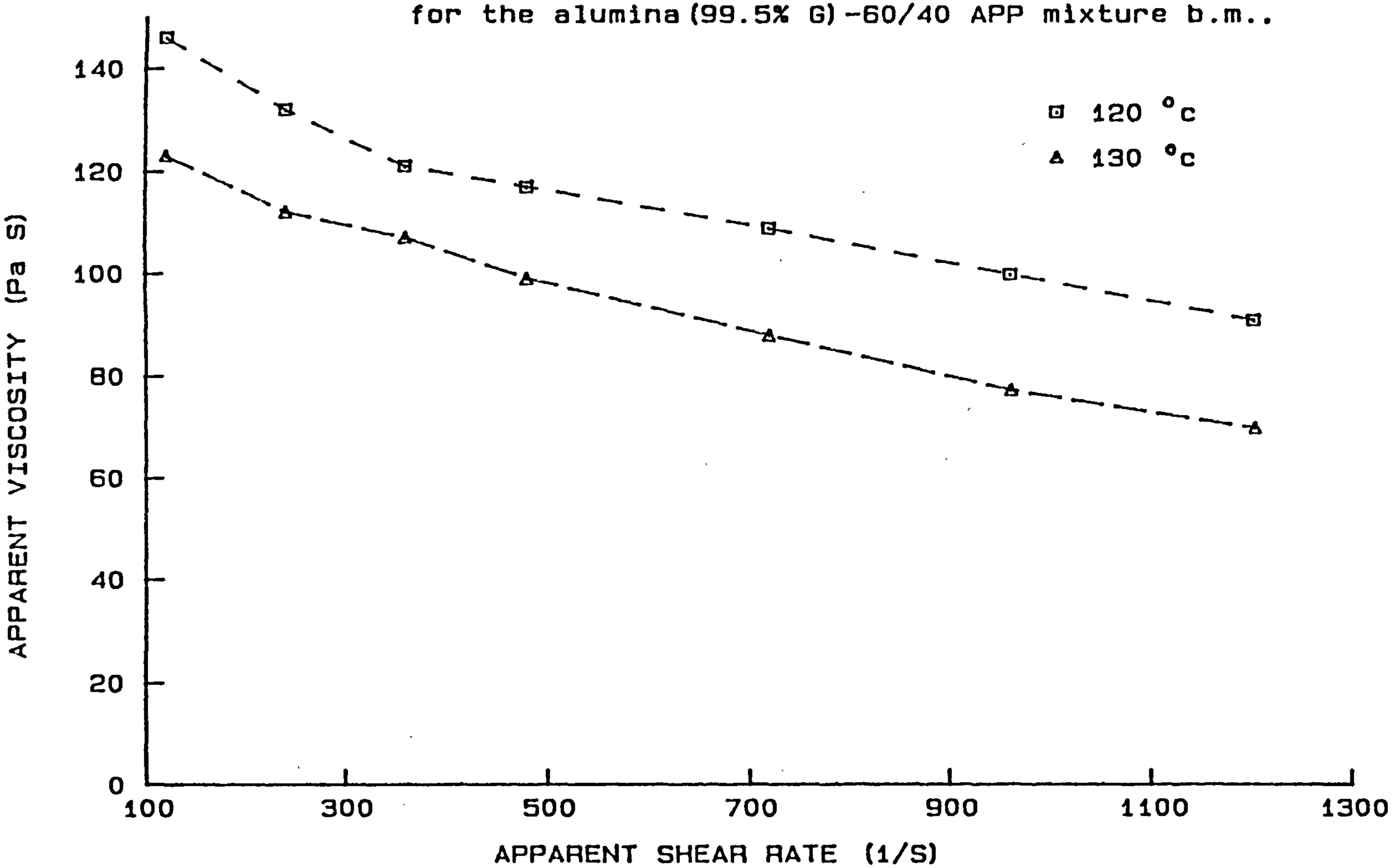

Figure 4.15- TGA data at 4.2 °c/min for the APP binders.

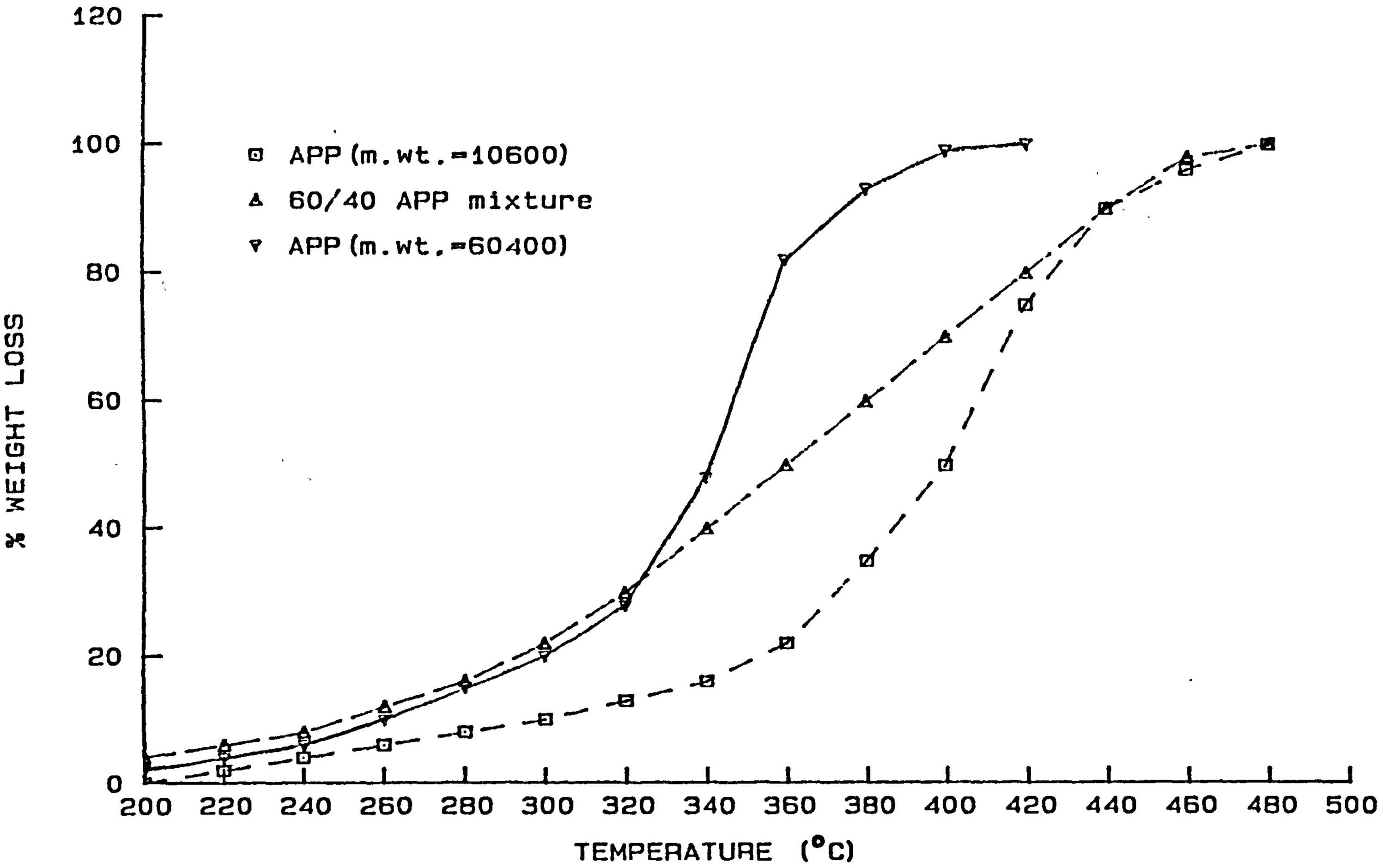

Figure 4.16- Apparent viscosity versus apparent shear rate for the 88% alumina-60/40 APP b.m. at different temparatures.

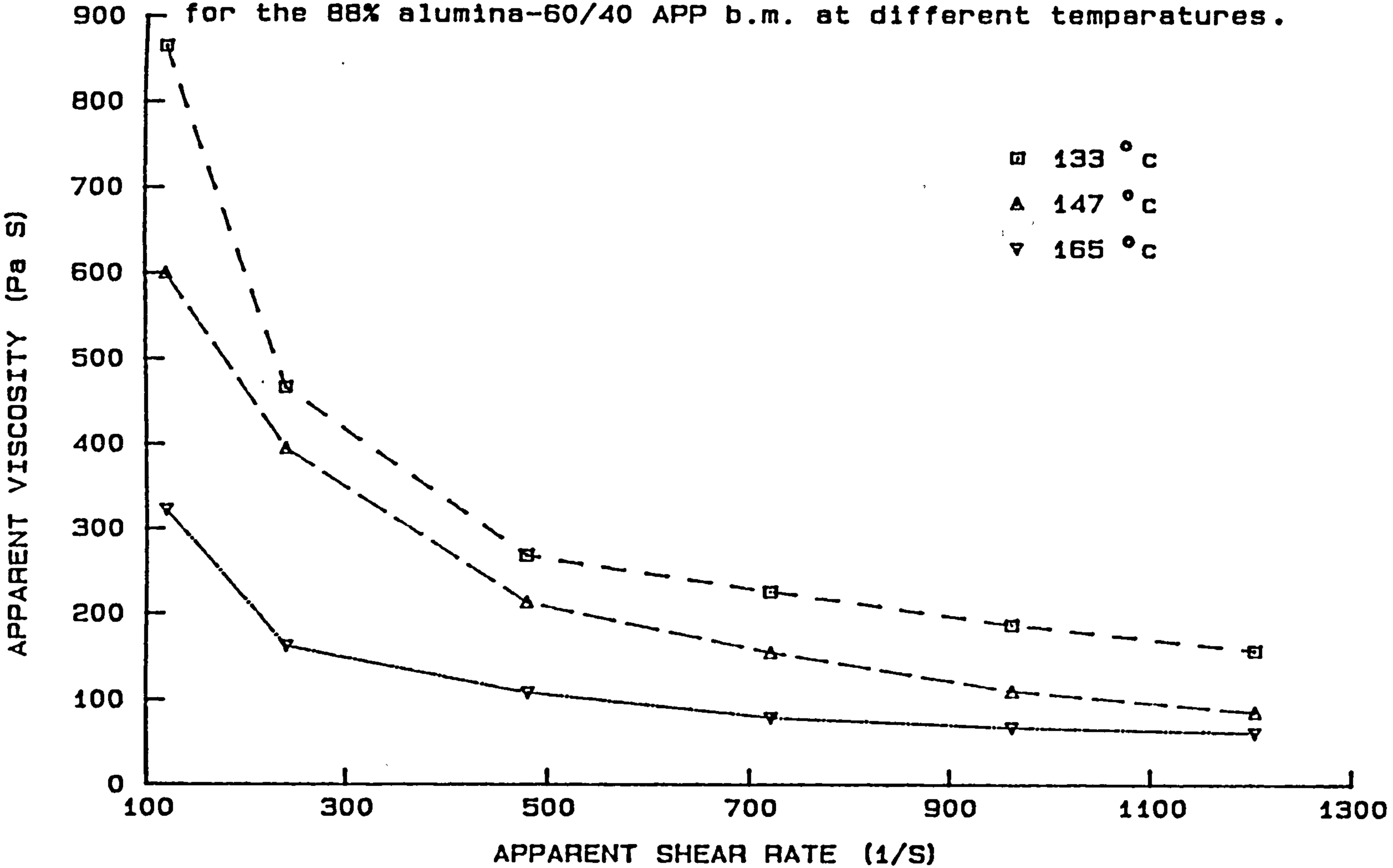

Figure 4.17- Apparent viscosity versus apparent shear rate for the 95% alumina-60/40 APP b.m. at different temperatures.

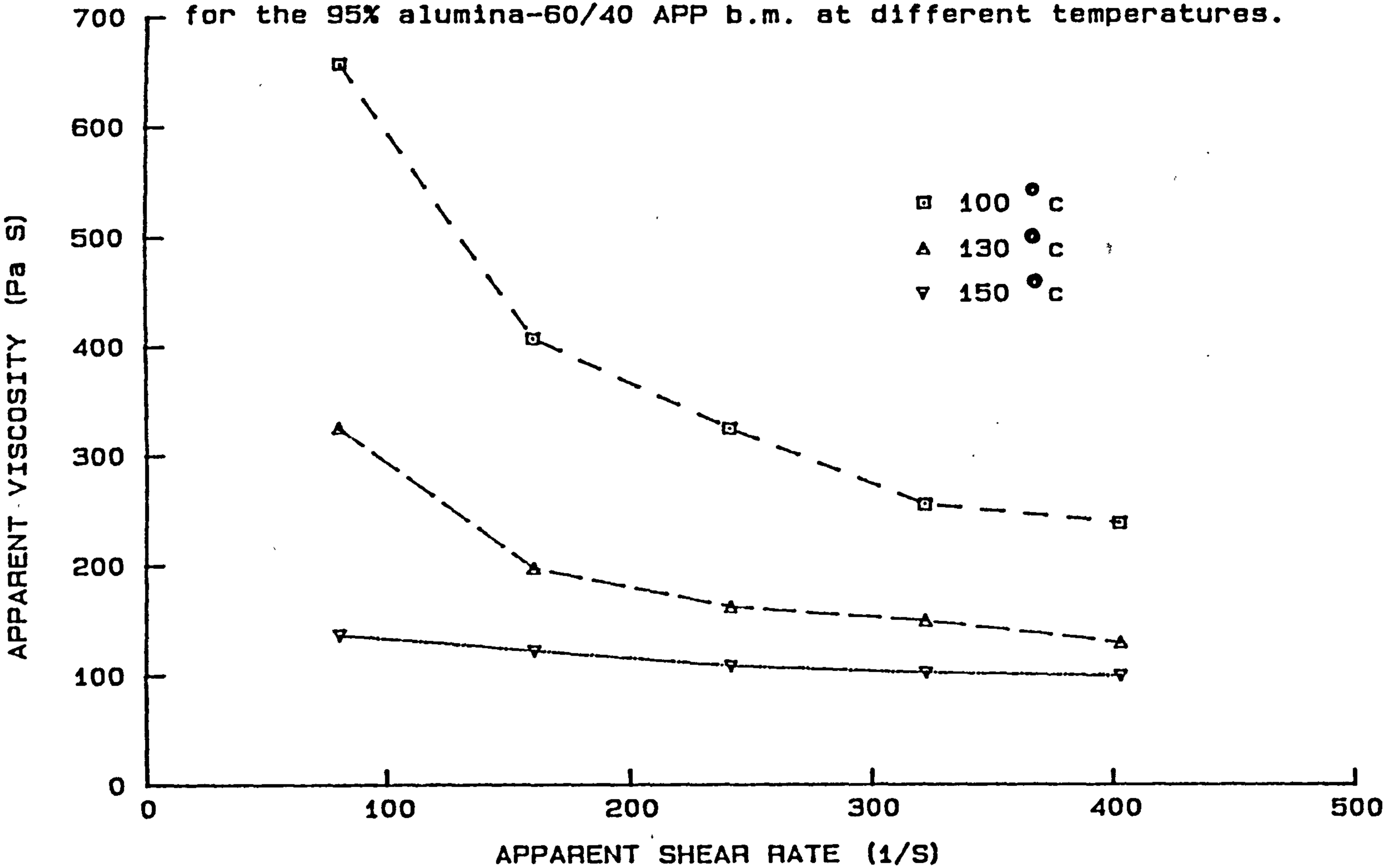

Figure 4.18- TGA data at 10 °c/min for the 88% & 95% alumina-60/40 APP binder mixtures.

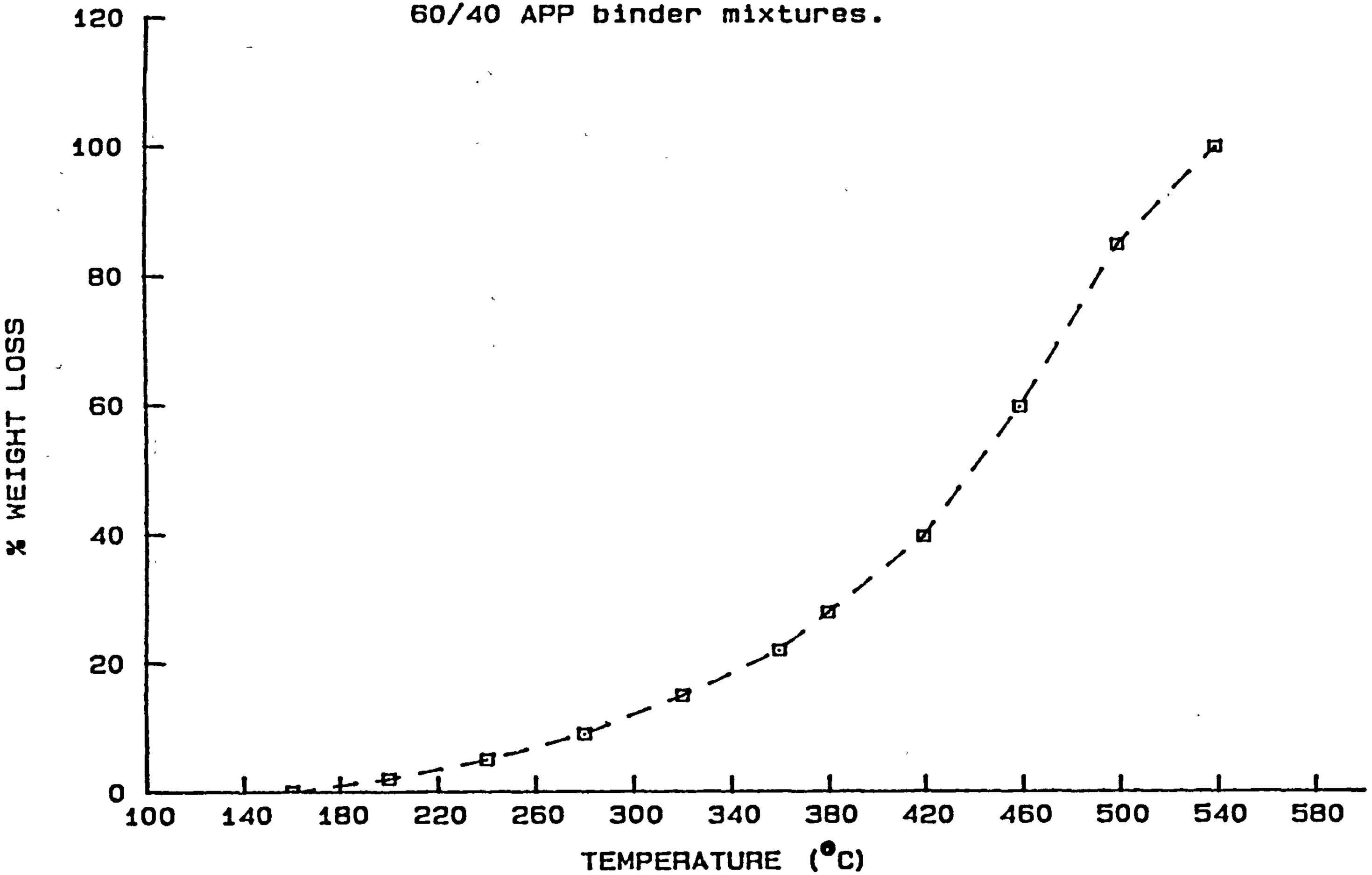

Figure 4.19- Apparent viscosity versus apparent shear rate for the alumina (99.5% G) -methylcellulose b.m. at 23 °c.

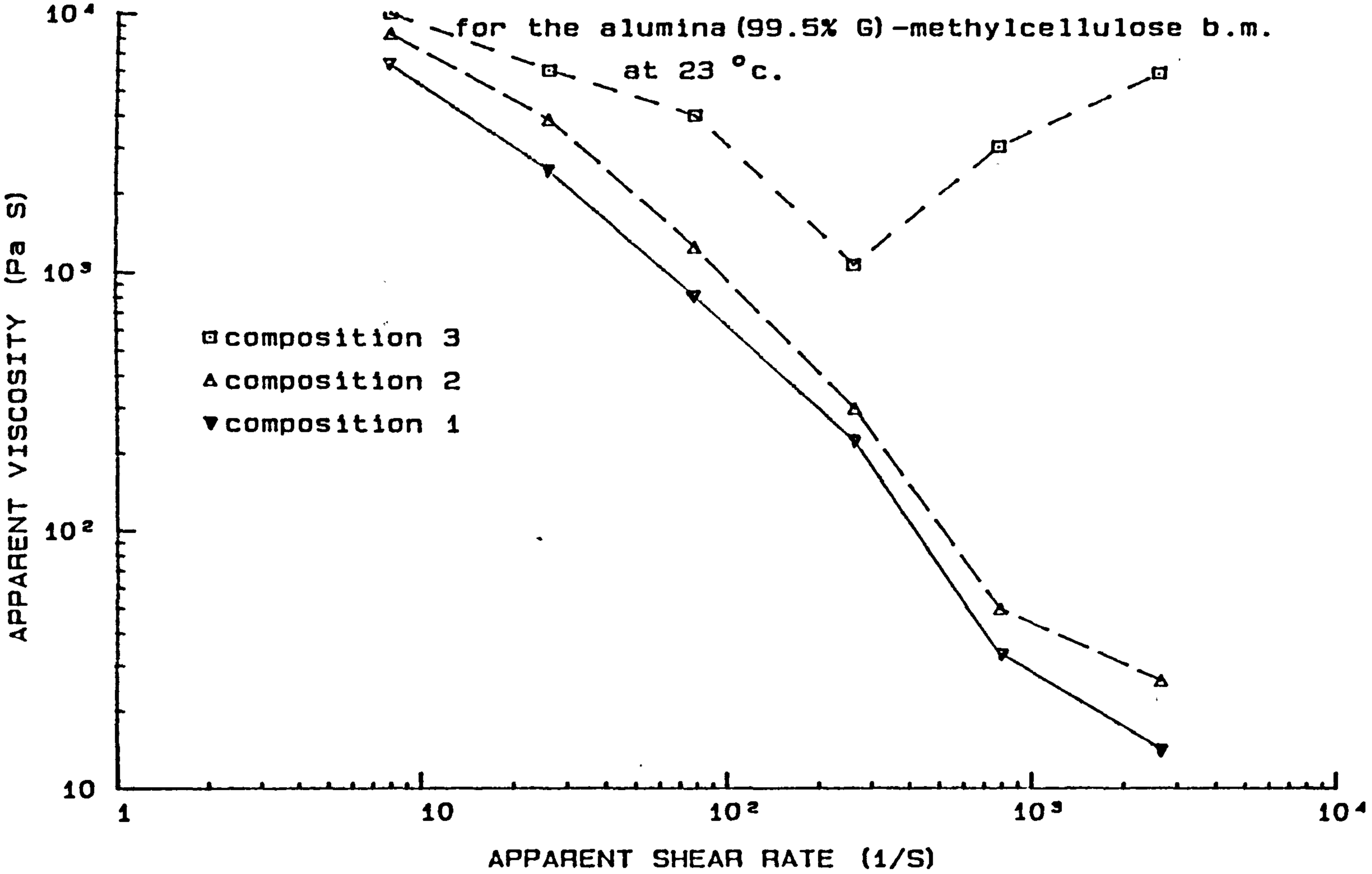

Figure 4.20- Apparent viscosity versus apparent shear rate for the alumina (+SiO2+CaO) -PEG b.s. at 120 °c.

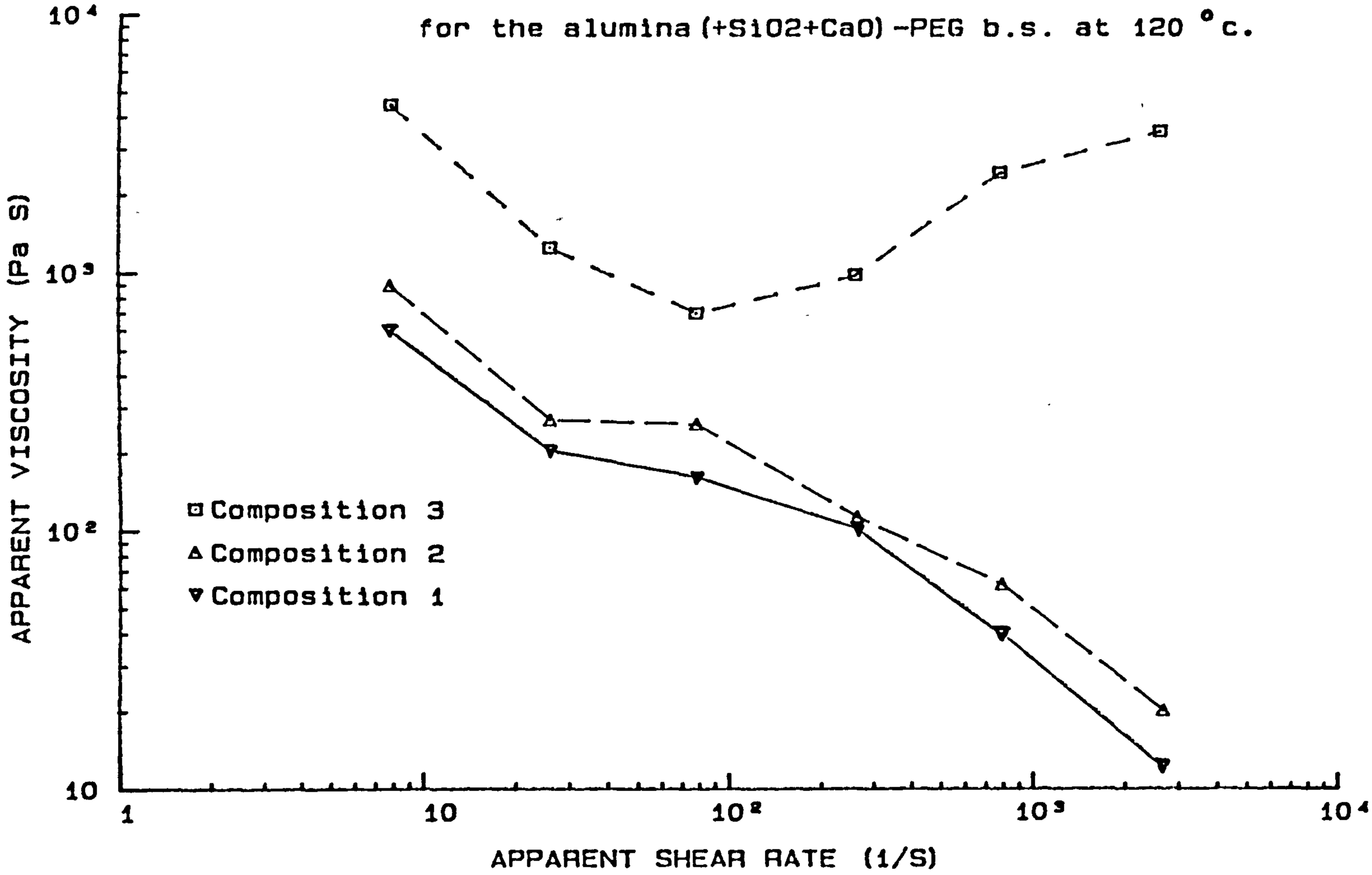

Figure 4.21- Apparent viscosity versus apparent shear rate for composition 2 at different temperatures.

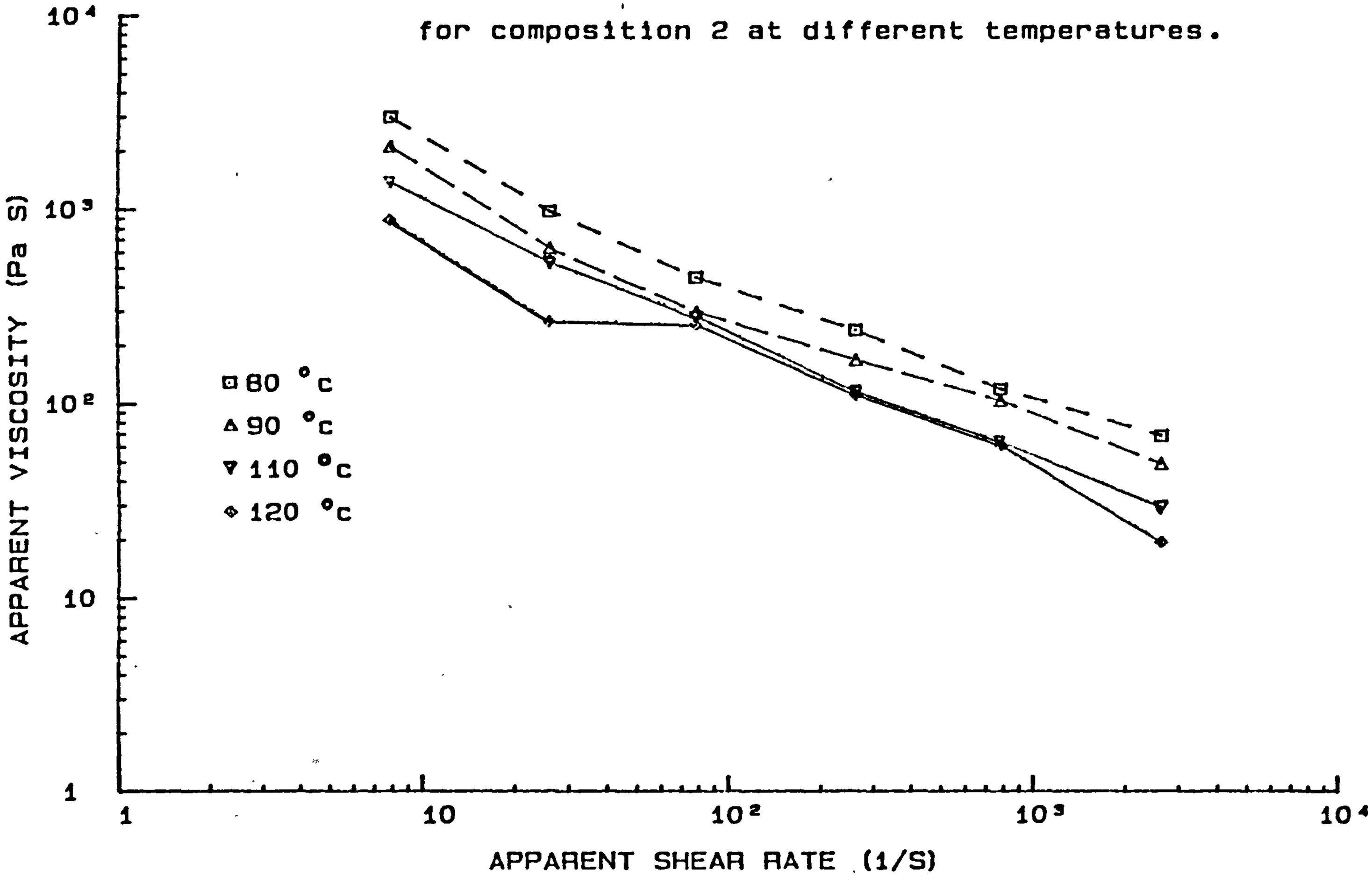

Figure 4.22- TGA data at 10 °c/min for the polyethylene glycol binder & the alumina(+SiO2+CaO)-PEG-APP-LP b.m..

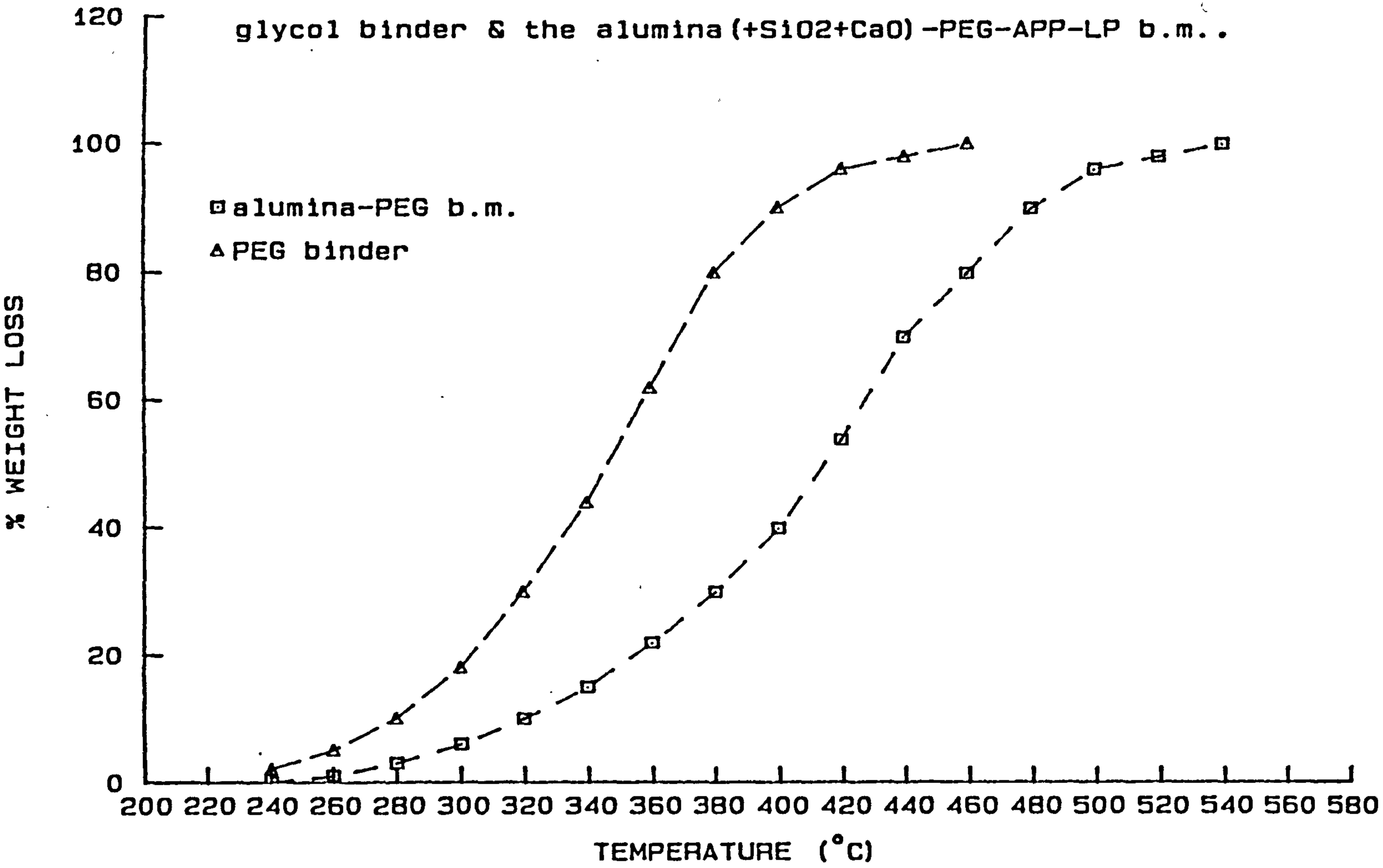

Figure 4.23- Apparent viscosity versus apparent shear rate for the alumina (+SiO2+CaO) -MEW b.m. at 90 °c.

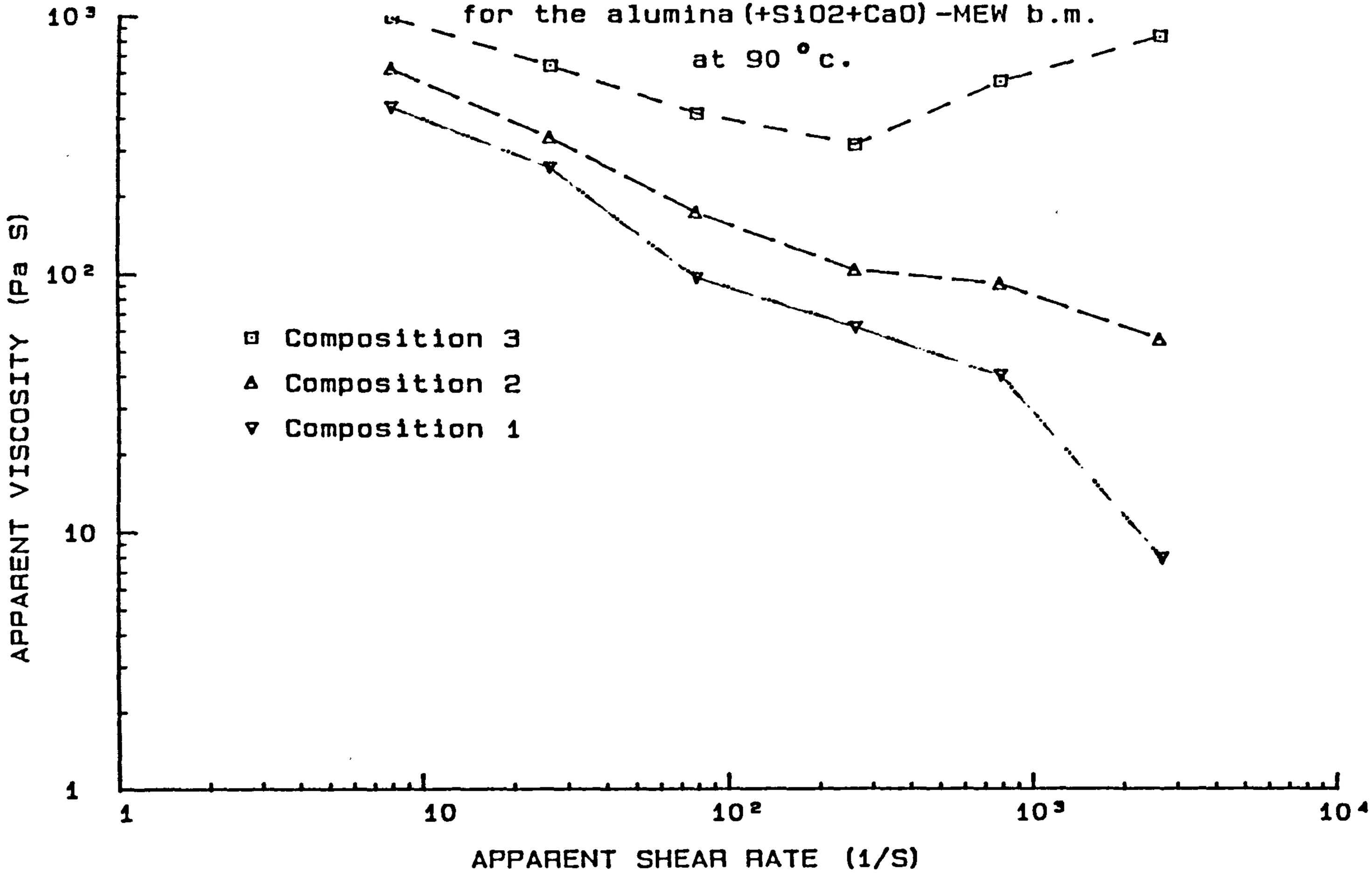

Figure 4.24- TGA data at 10 °c/min for the alumina (+SiO2+CaO) -MEW b.m..

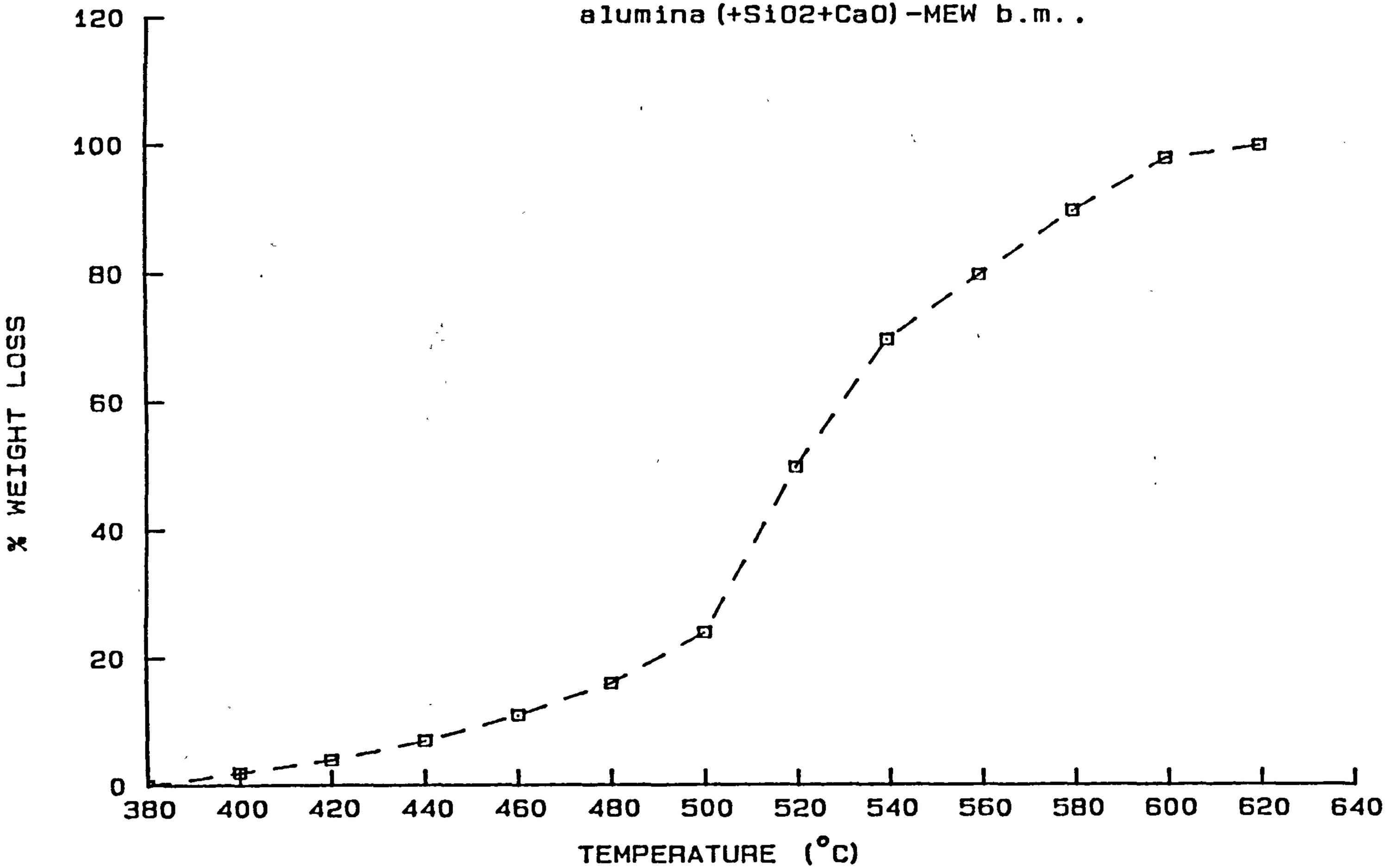

Figure 4.25- TGA data at 10 °c/min for M.W., P.W., C.W., alumina (+SiO2+CaO) +MEW+MW & alumina (+SiO2+CaO) +MEW+CW+PW .

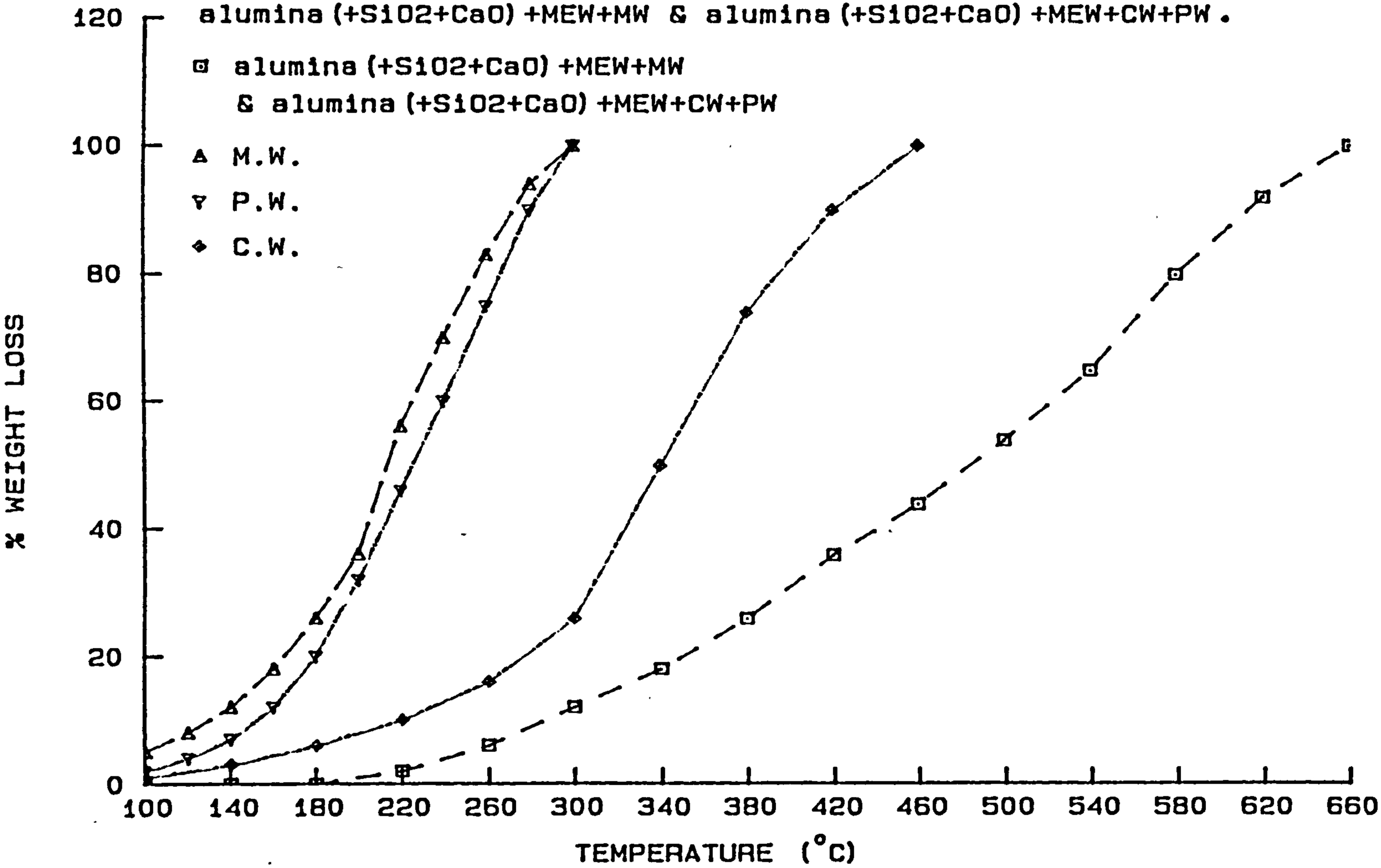

Figure 4.26- Apparent viscosity versus apparent shear rate for the alumina (+SiO2+CaO) -MEW-APP-LP b.m. at 90 °c.

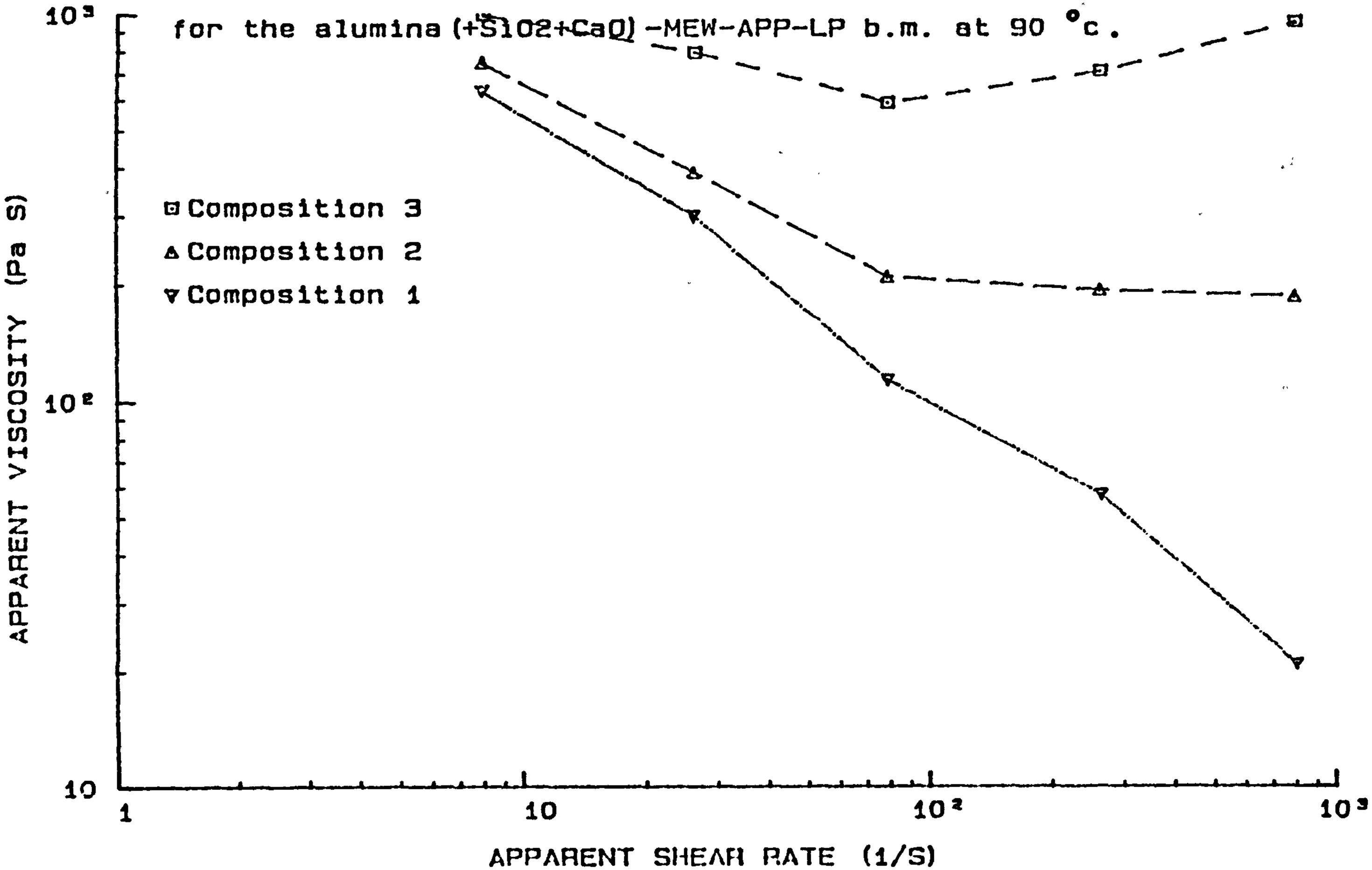

Figure 4.27- Apparent viscosity versus apparent shear rate for the alumina (+SiO2+CaO) -MEW-APP-LP b.m. at 100 °c.

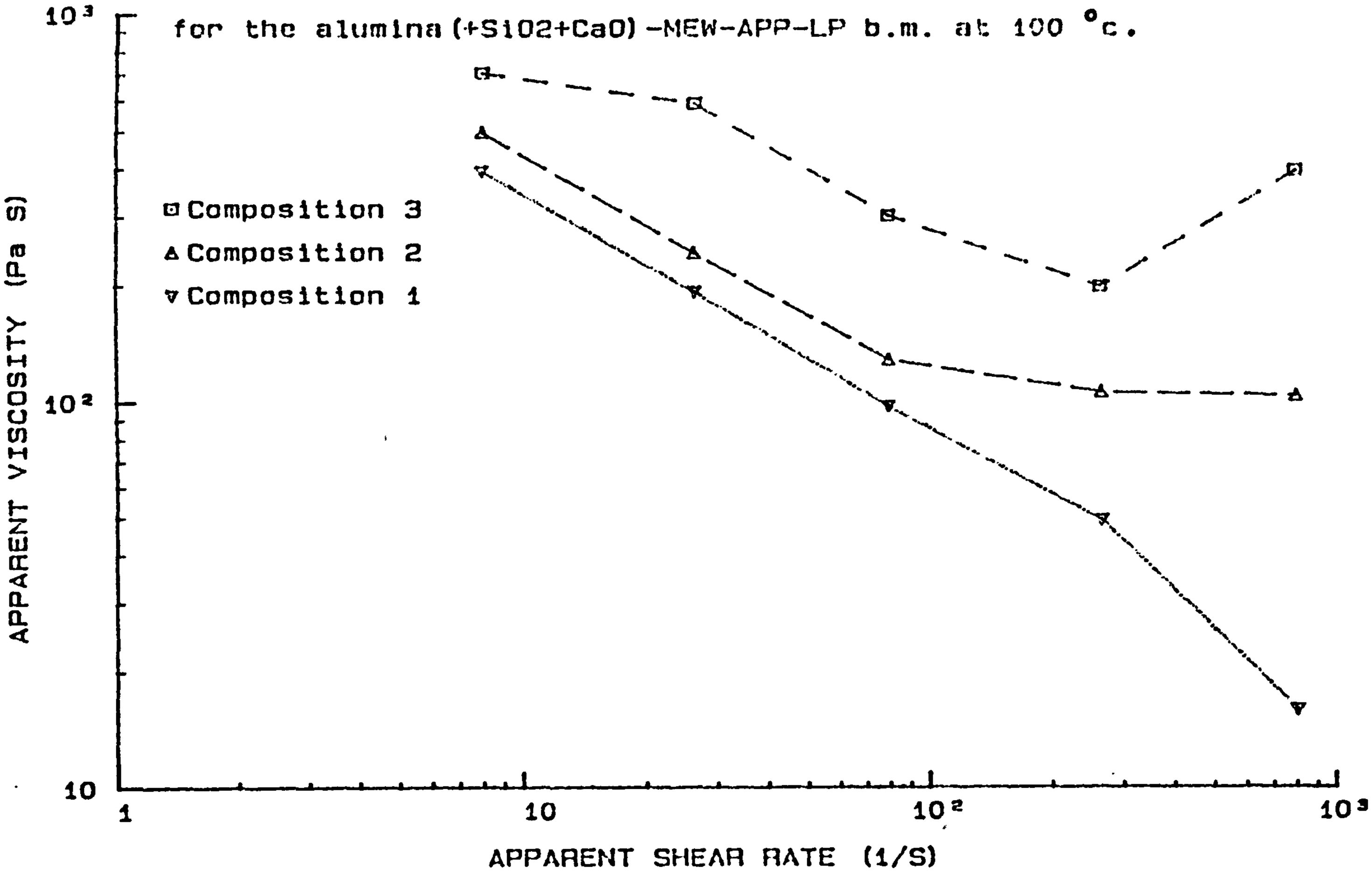

Figure 4.28- Apparent viscosity versus apparent shear rate for the alumina (+SiO2+CaO) -MEW-APP-LP b.m. at 110 °c.

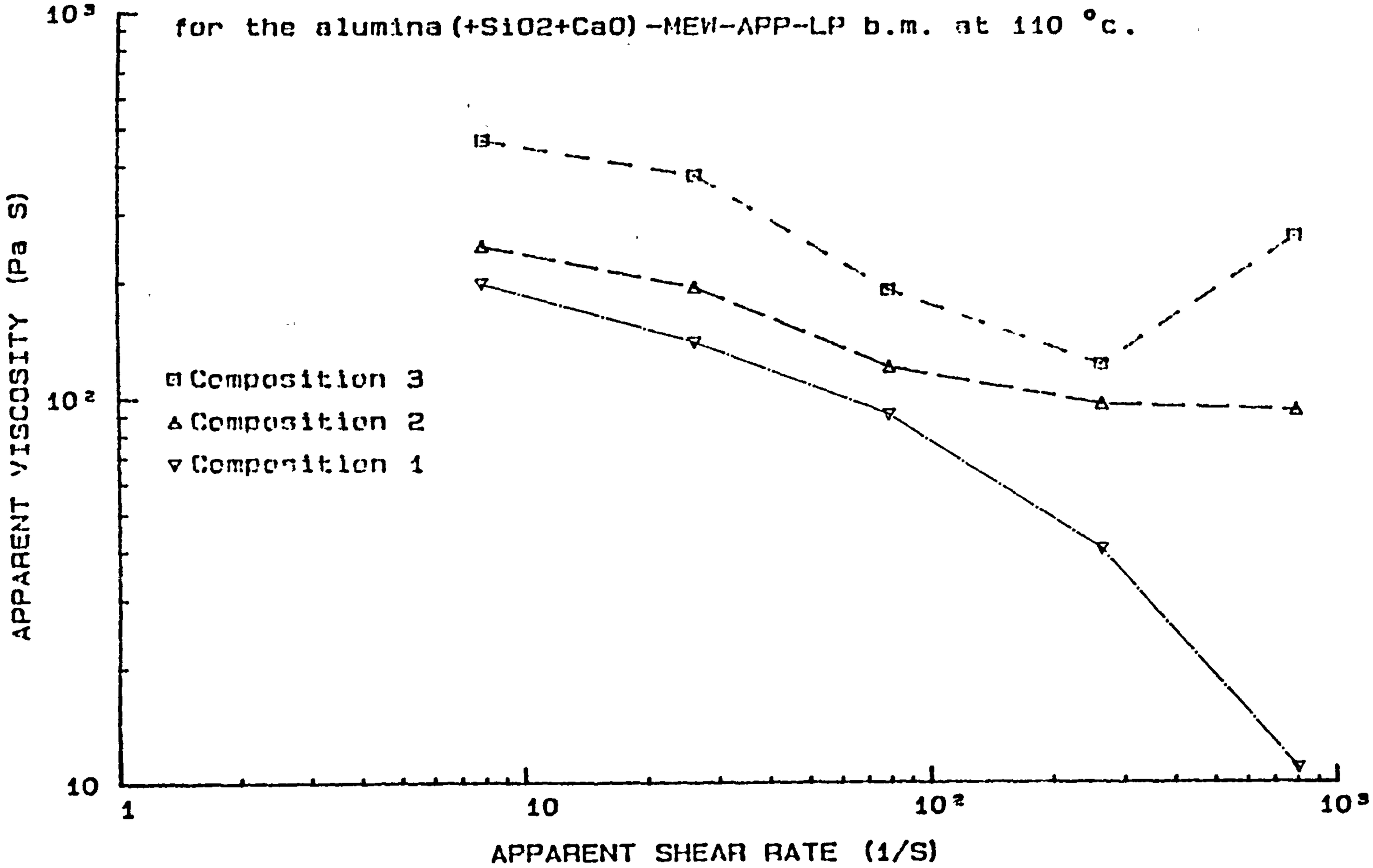

Figure 4.29- Apparent viscosity versus apparent shear rate for composition 2 at different temperatures.

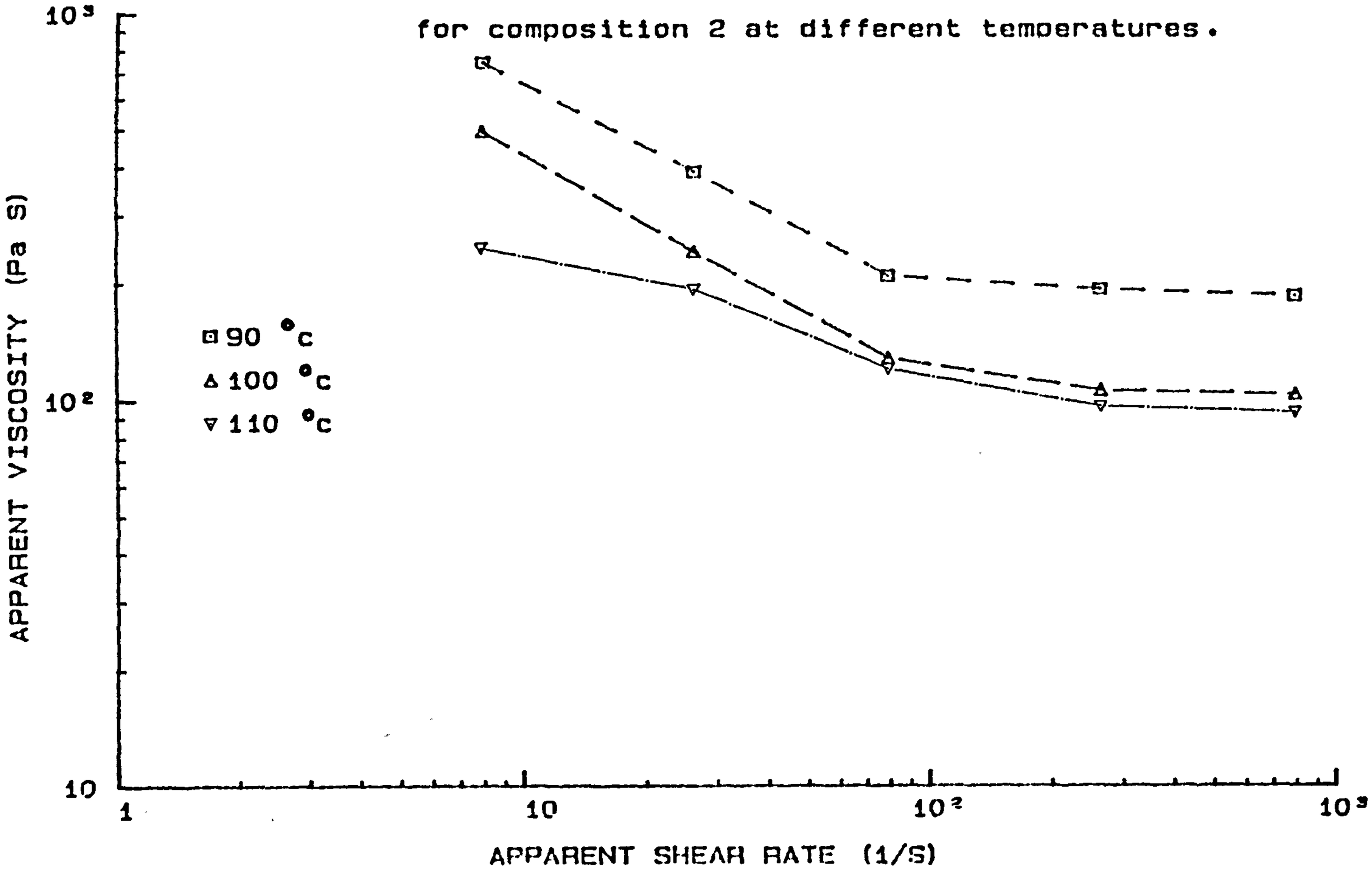

Figure 4.30- TGA data at 10 °c/min for the alumina (+SiO2+CaO) -MEW-APP-LP b.m..

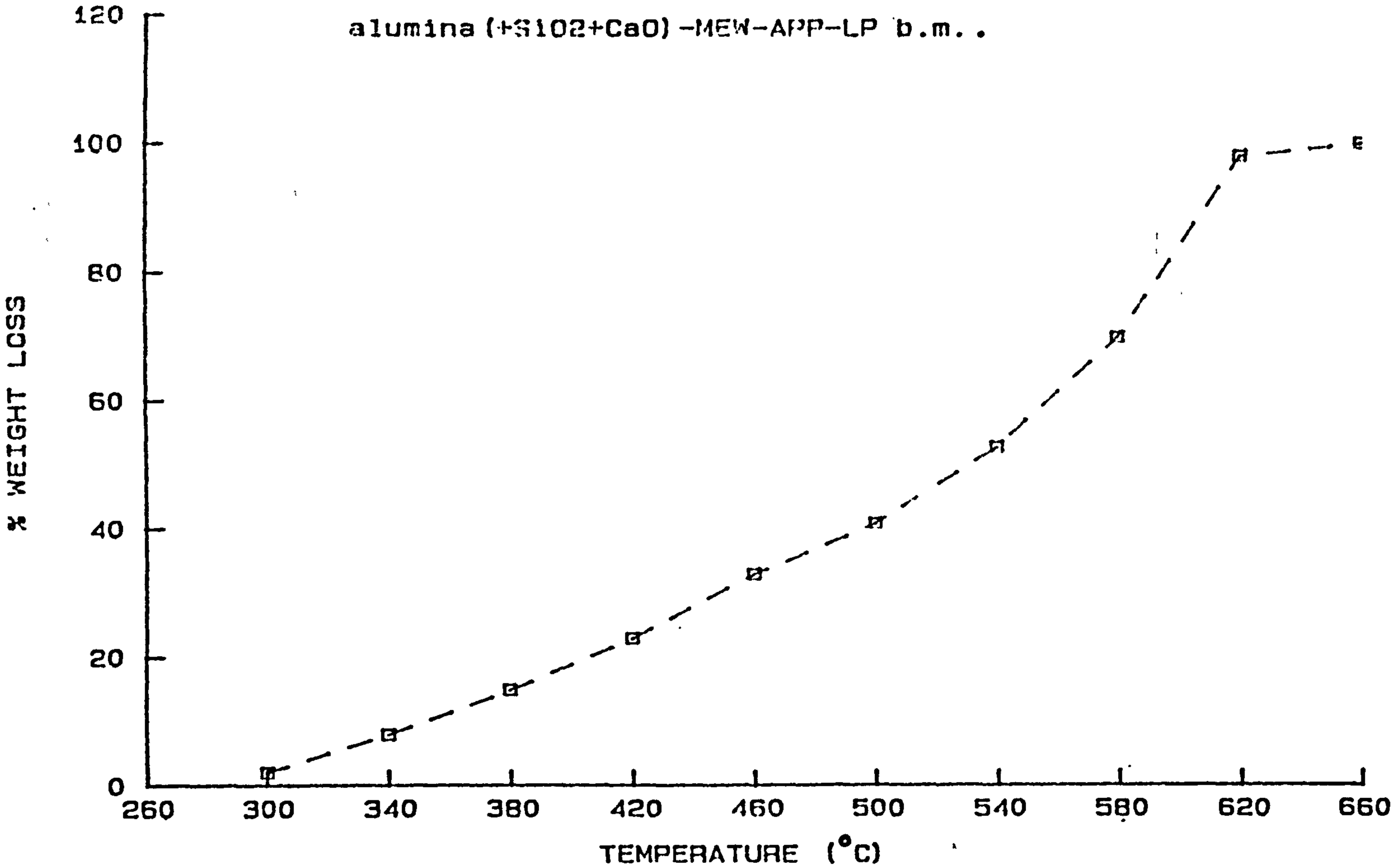

Figure 4.31- Apparent viscosity versus apparent shear rate for composition 3 at different temperatures.

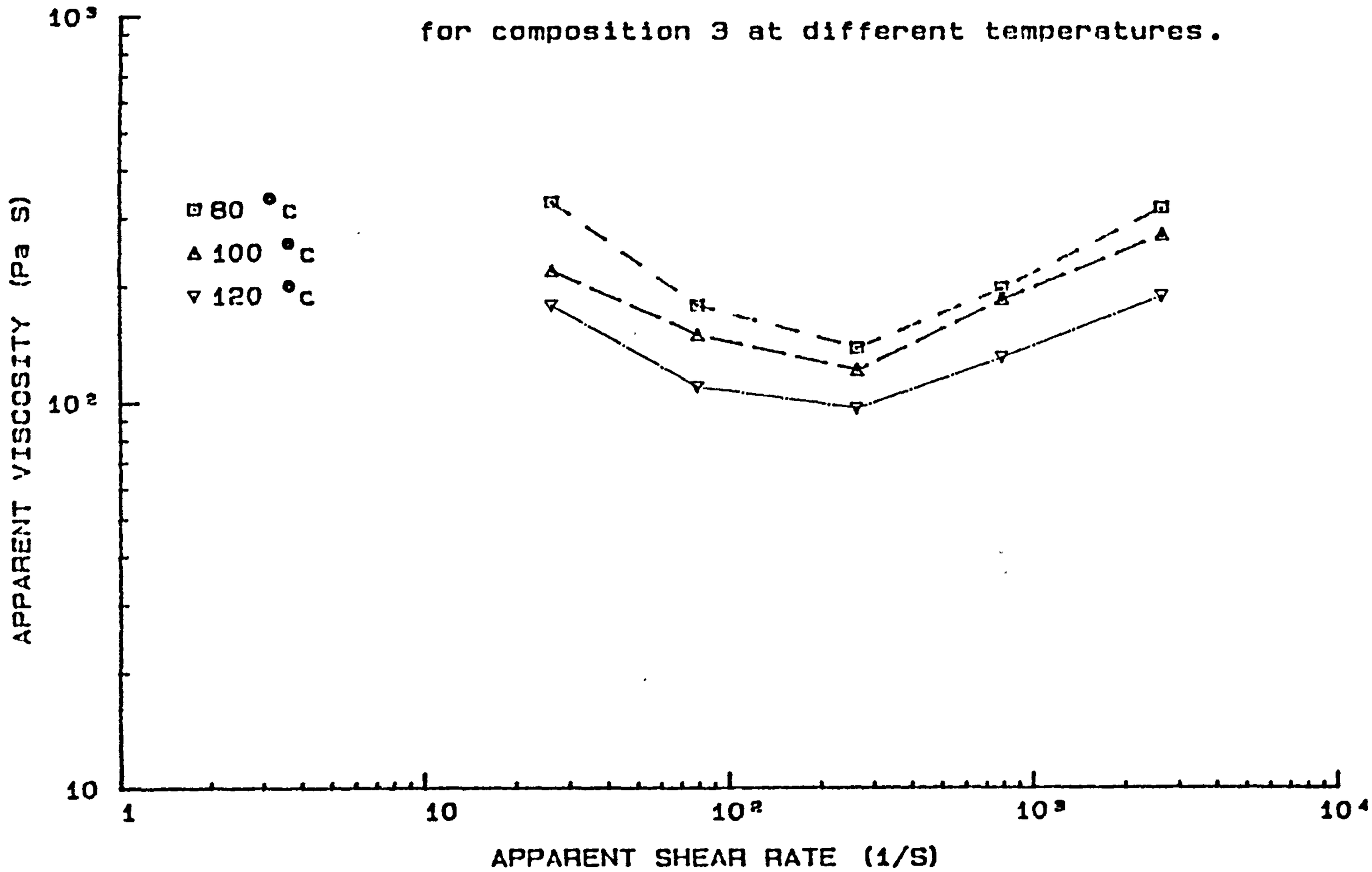

Figure 4.32- Apparent viscosity versus apparent shear rate for composition 2 at different temperatures.

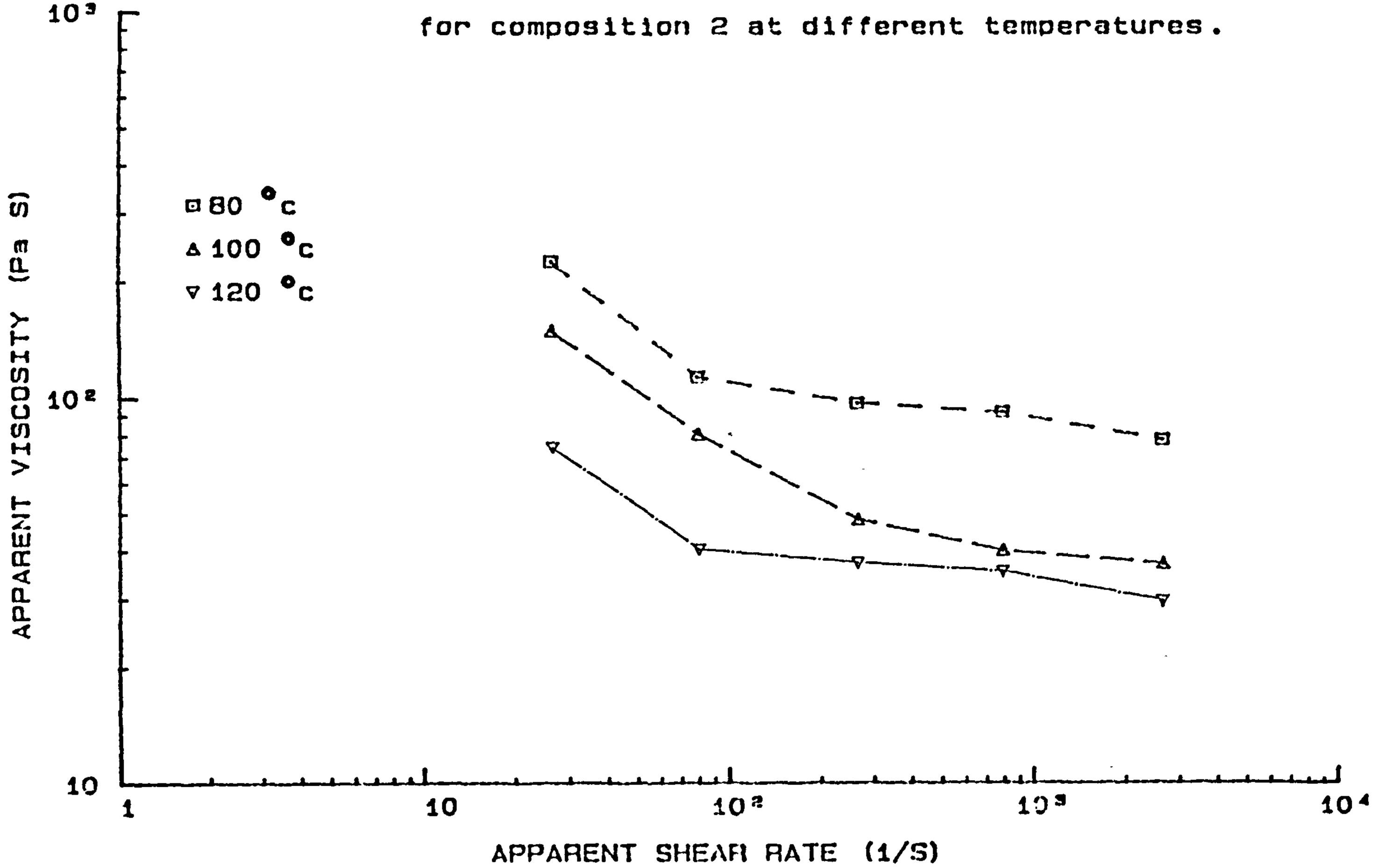

Figure 4.33- Apparent viscosity versus apparent shear rate for composition 1 at different temperatures.

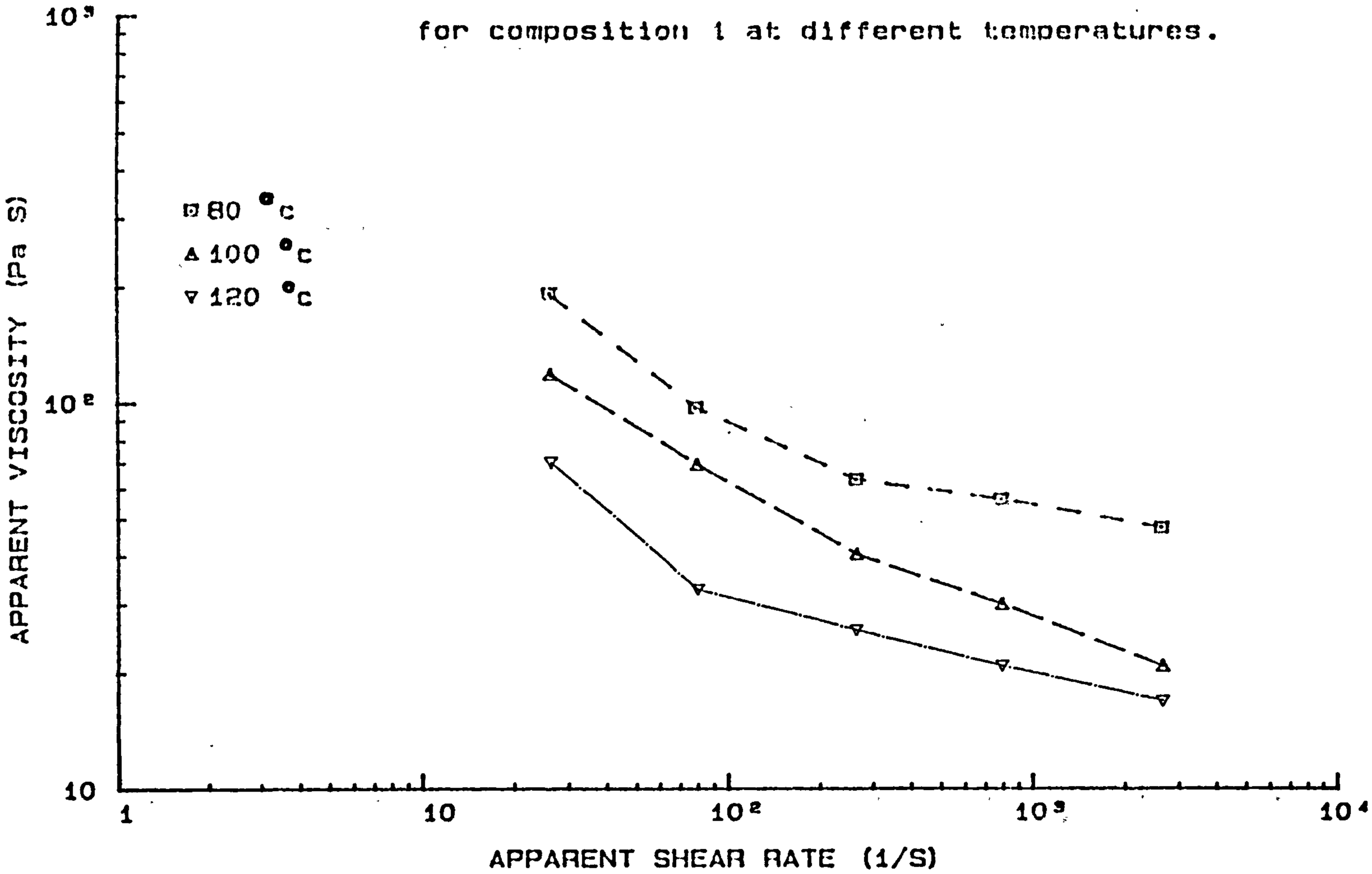

Figure 4.34- Apparent viscosity versus apparent shear rate for compositions 1, 2 & 3 at 80 °c.

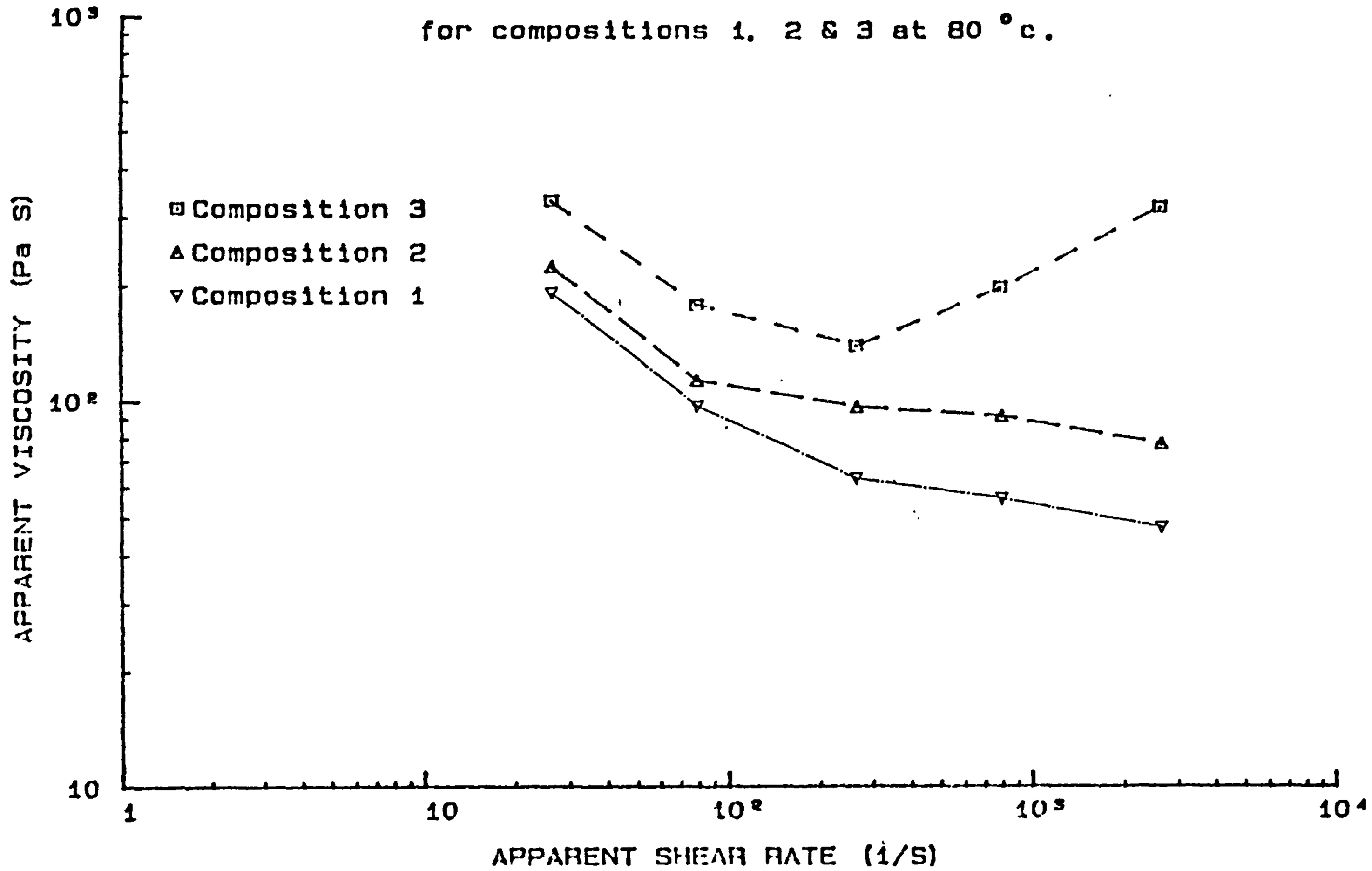

Figure 4.35- Apparent viscosity versus apparent shear rate for compositions 1, 2 & 3 at 100 °c.

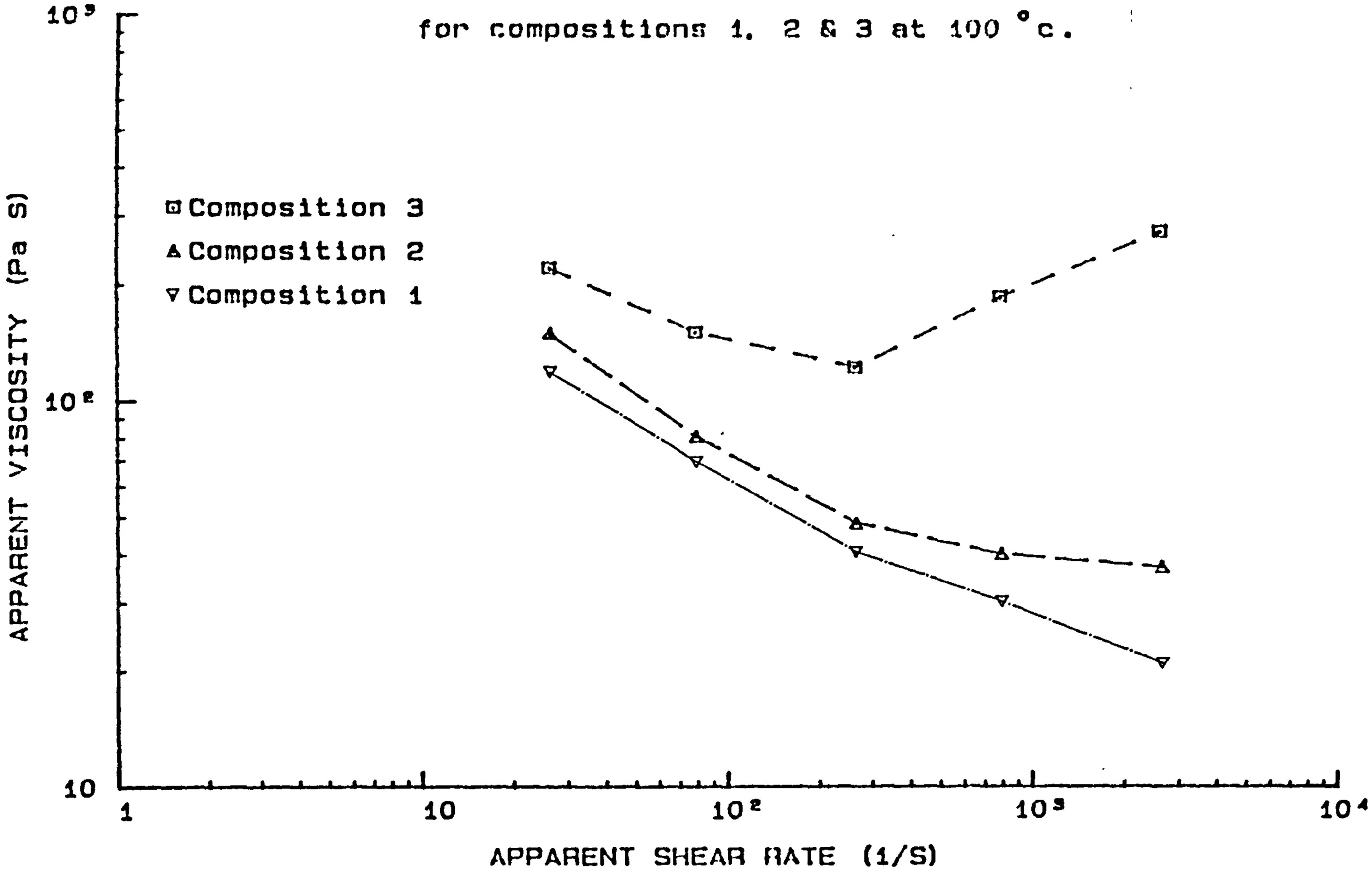

Figure 4.36- Apparent viscosity versus apparent shear rate for compositions 1, 2 & 3 at 120 °c.

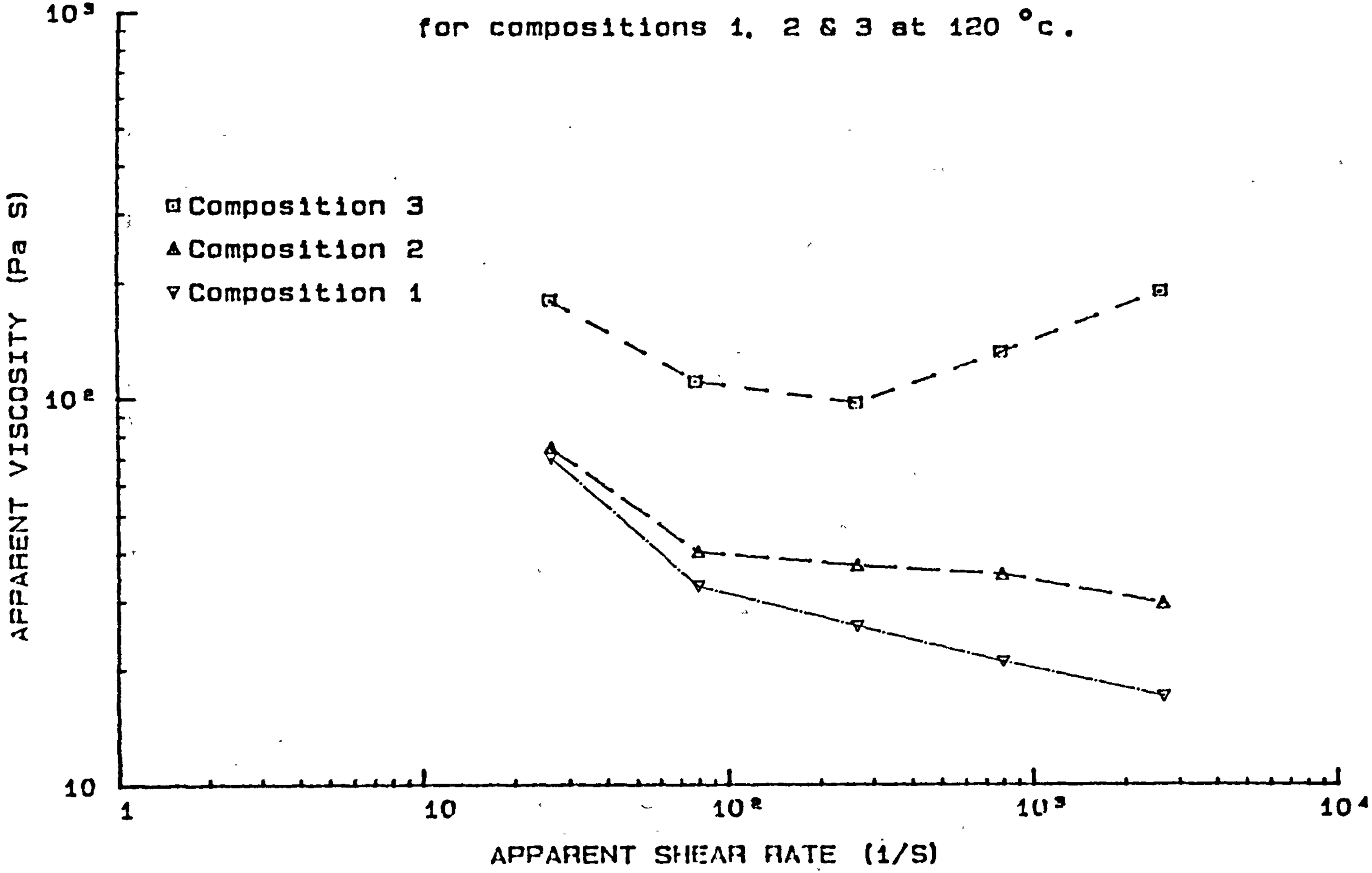

Figure 4.37- TGA data at 10 °c/min for the
PIB binder & alumina (99.5% Grade) -MEW-PIB-LP b.m..

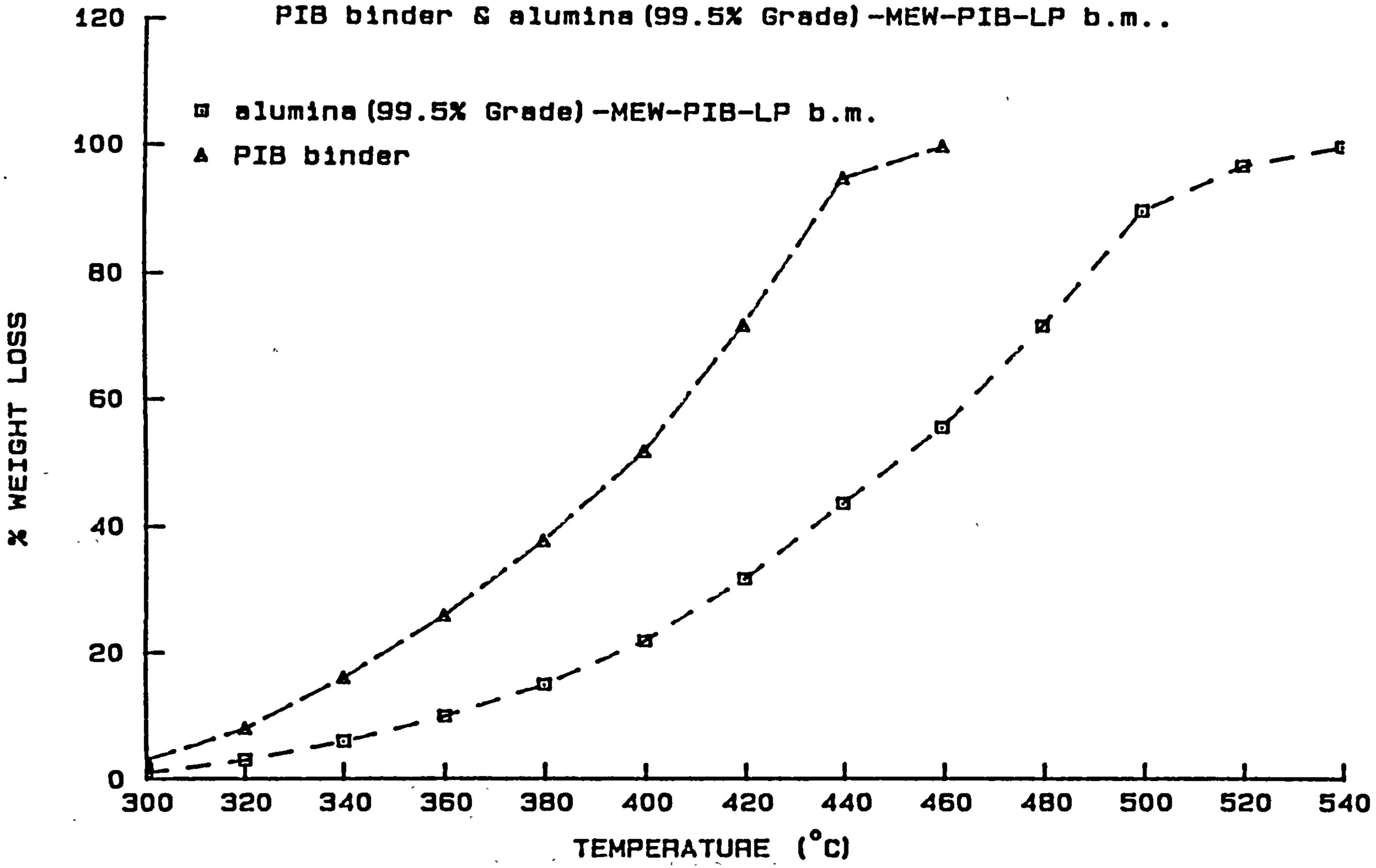

Figure 4.38- Apparent viscosity versus apparent shear rate for the alumina (99.5% Grade) -PVA b.s. at 72°C.

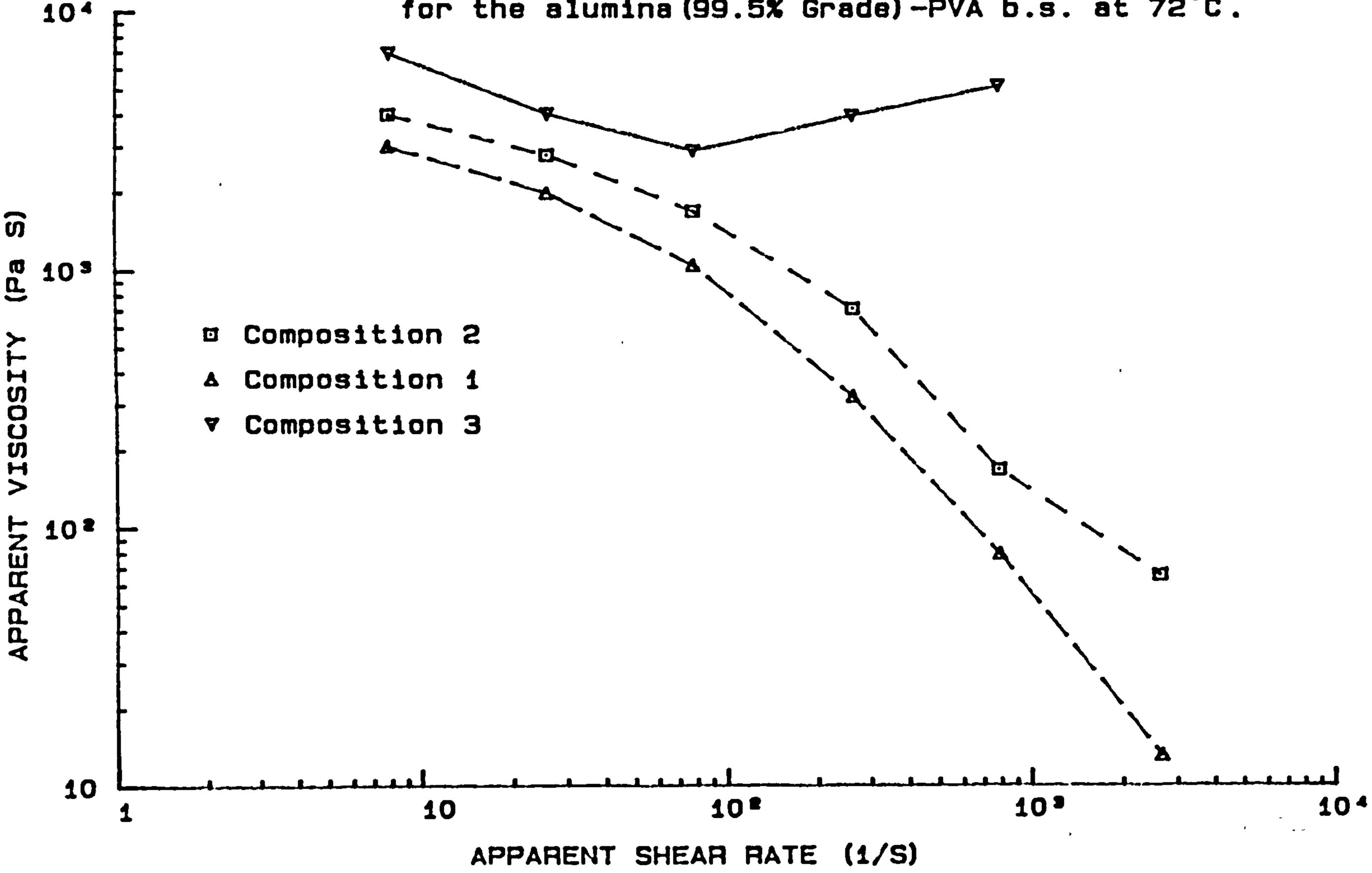

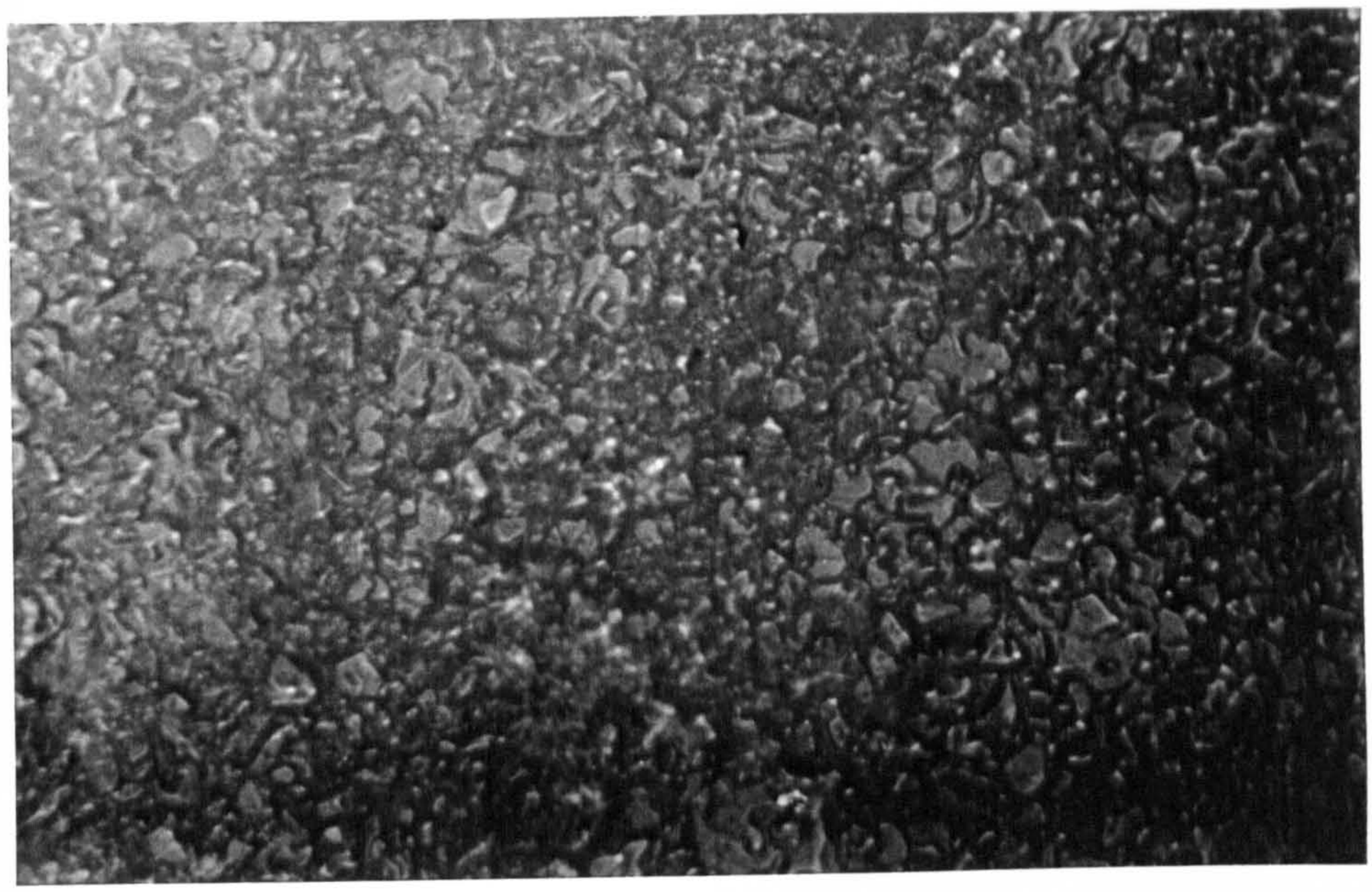

(a)

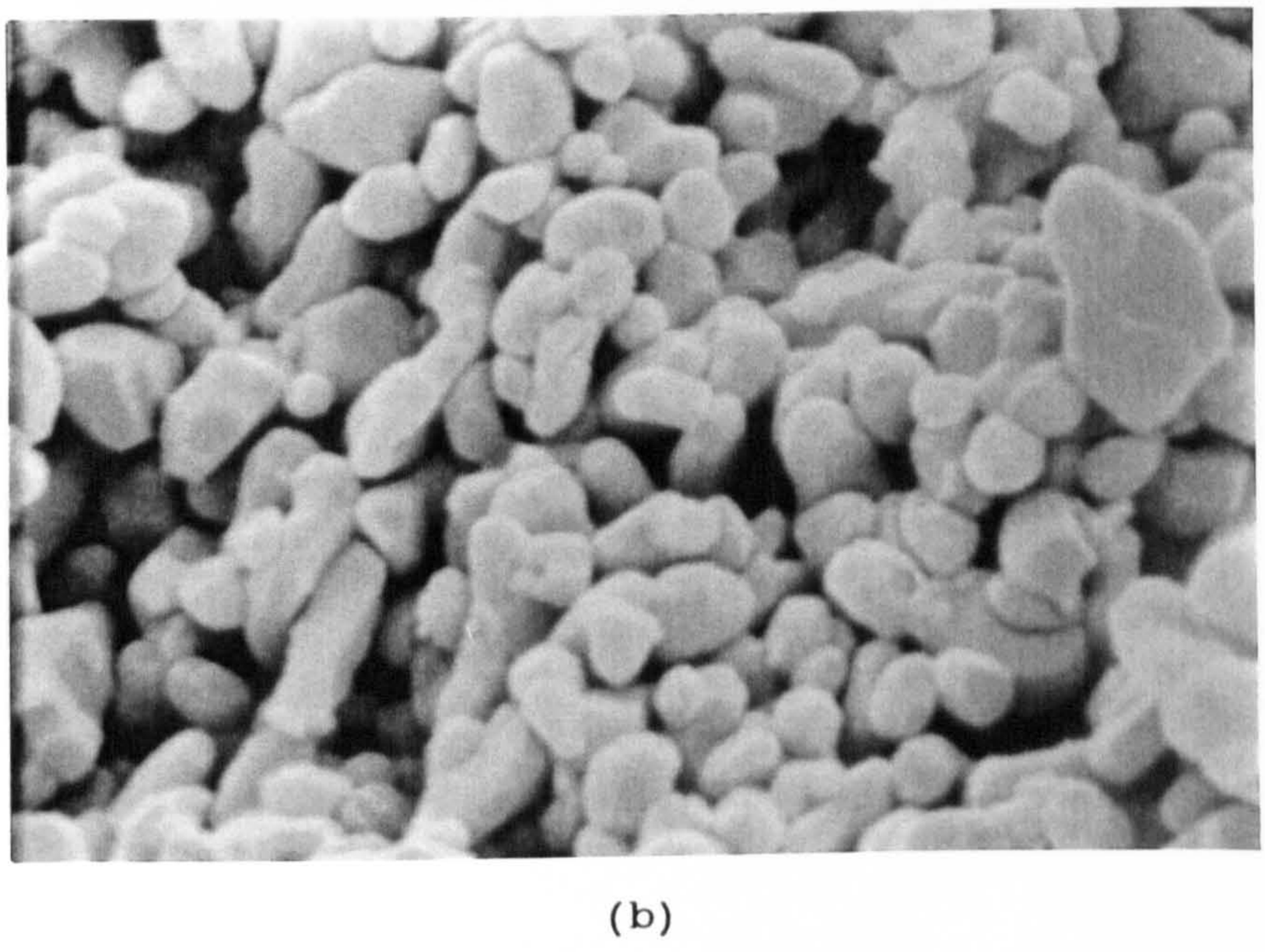

(b)

Figure 4.39- (a) Optical photograph of the as-sintered surface (sintered at 1750°C for 2.5 h) of the 99.5 % alumina; magnification X 1600;
(b) SEM photograph of the sintered 99.5 % alumina (as in photograph (a)); magnification X 2000.

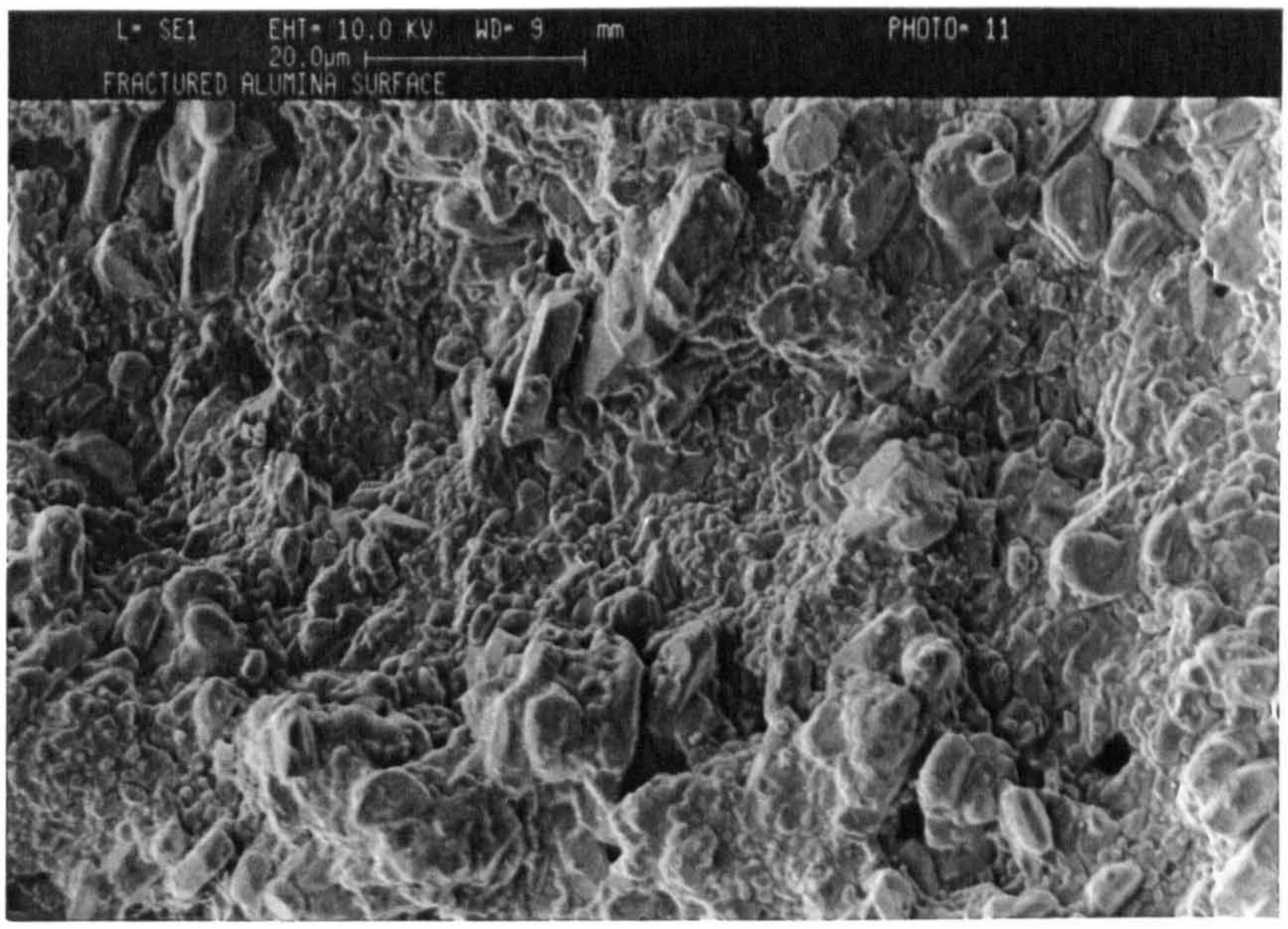

(a)

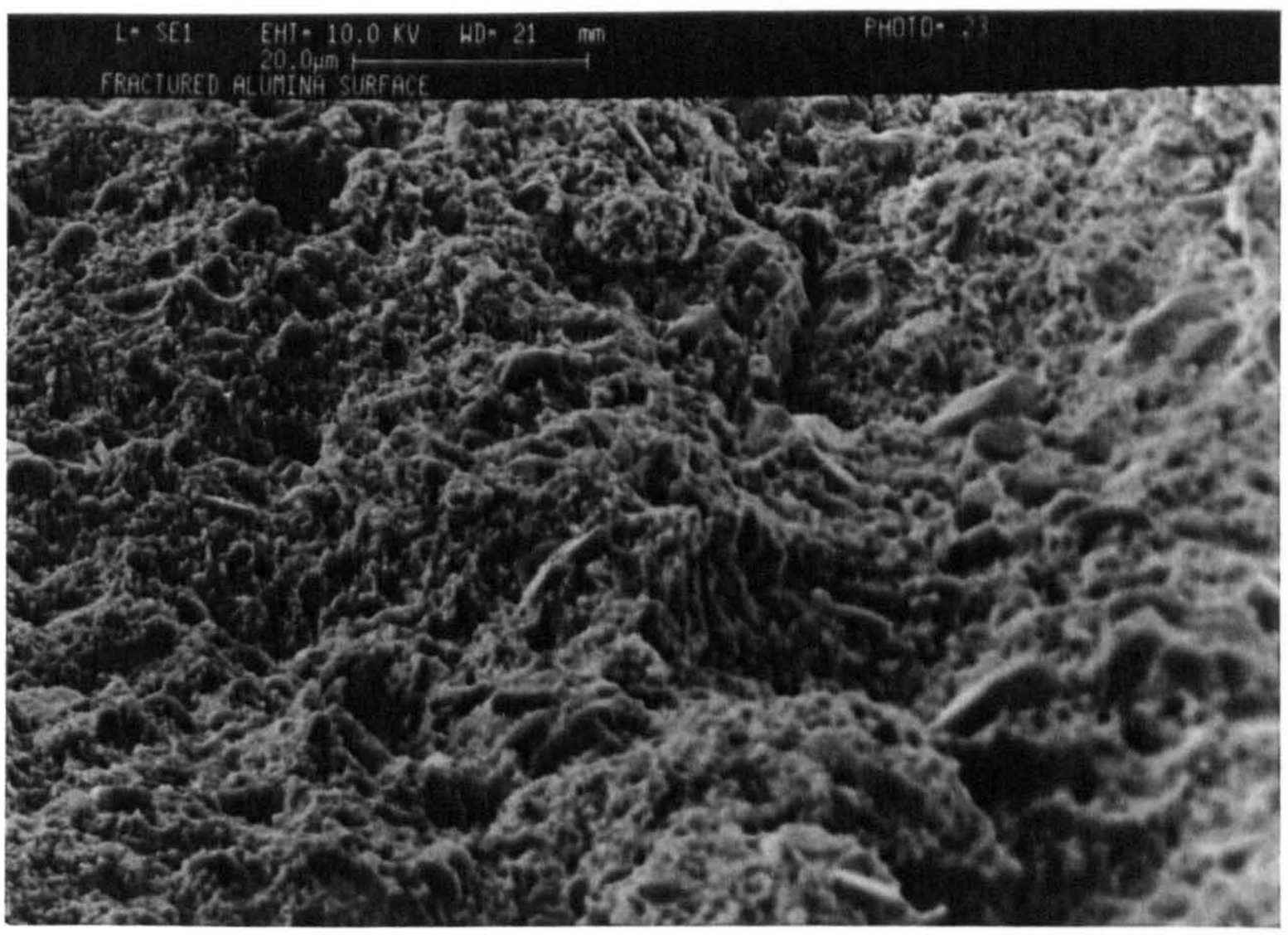

(b)

Figure 4.40- (a) and (b) SEM photographs of the fractured surfaces of the sintered 99.5 % alumina (as in Fig. 4.39).

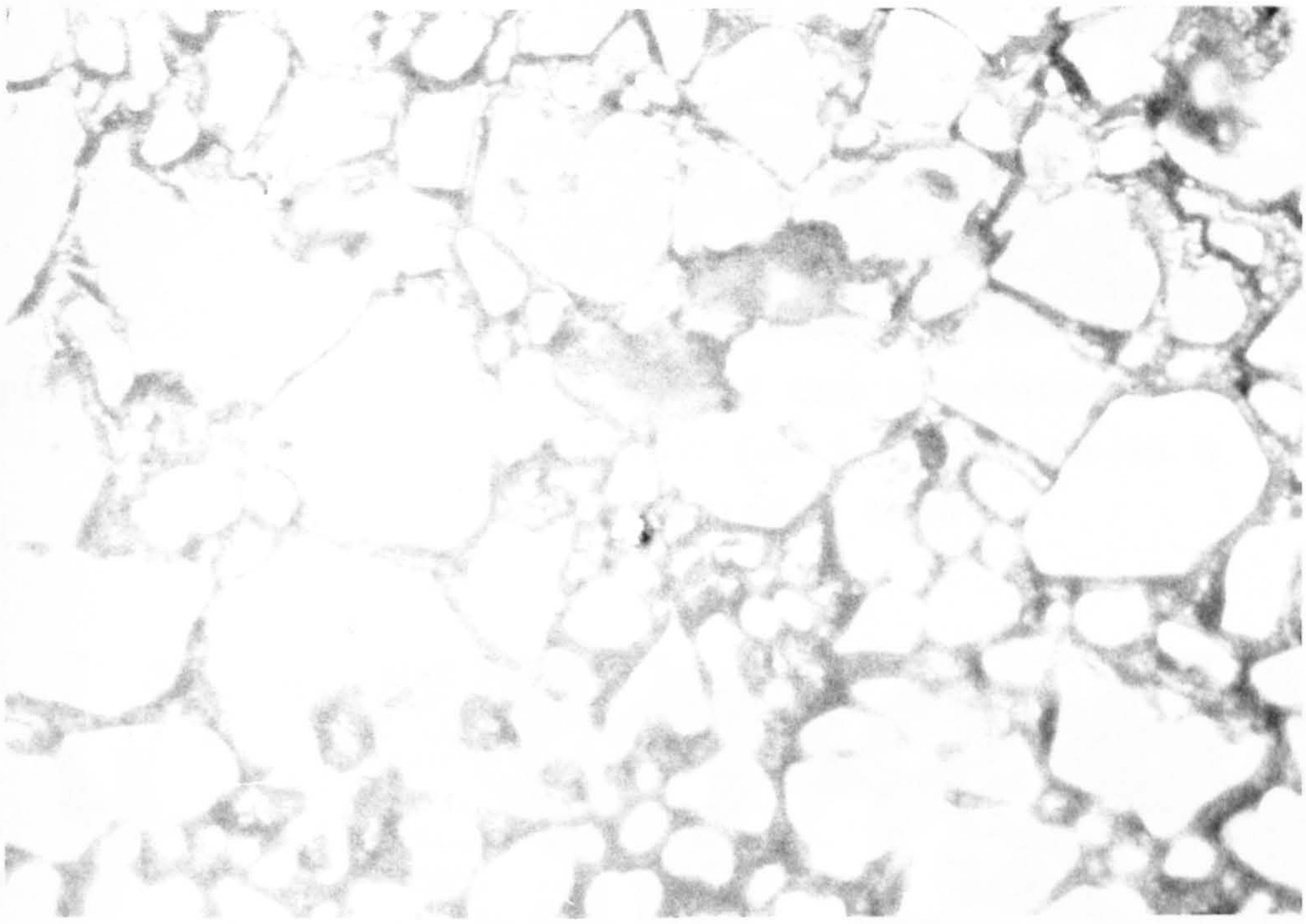

Figure 4.41- Optical photograph of the as-sintered surface (sintered at 1800°C for 3.5 h) of the 99.5 % alumina; magnification X 1600.

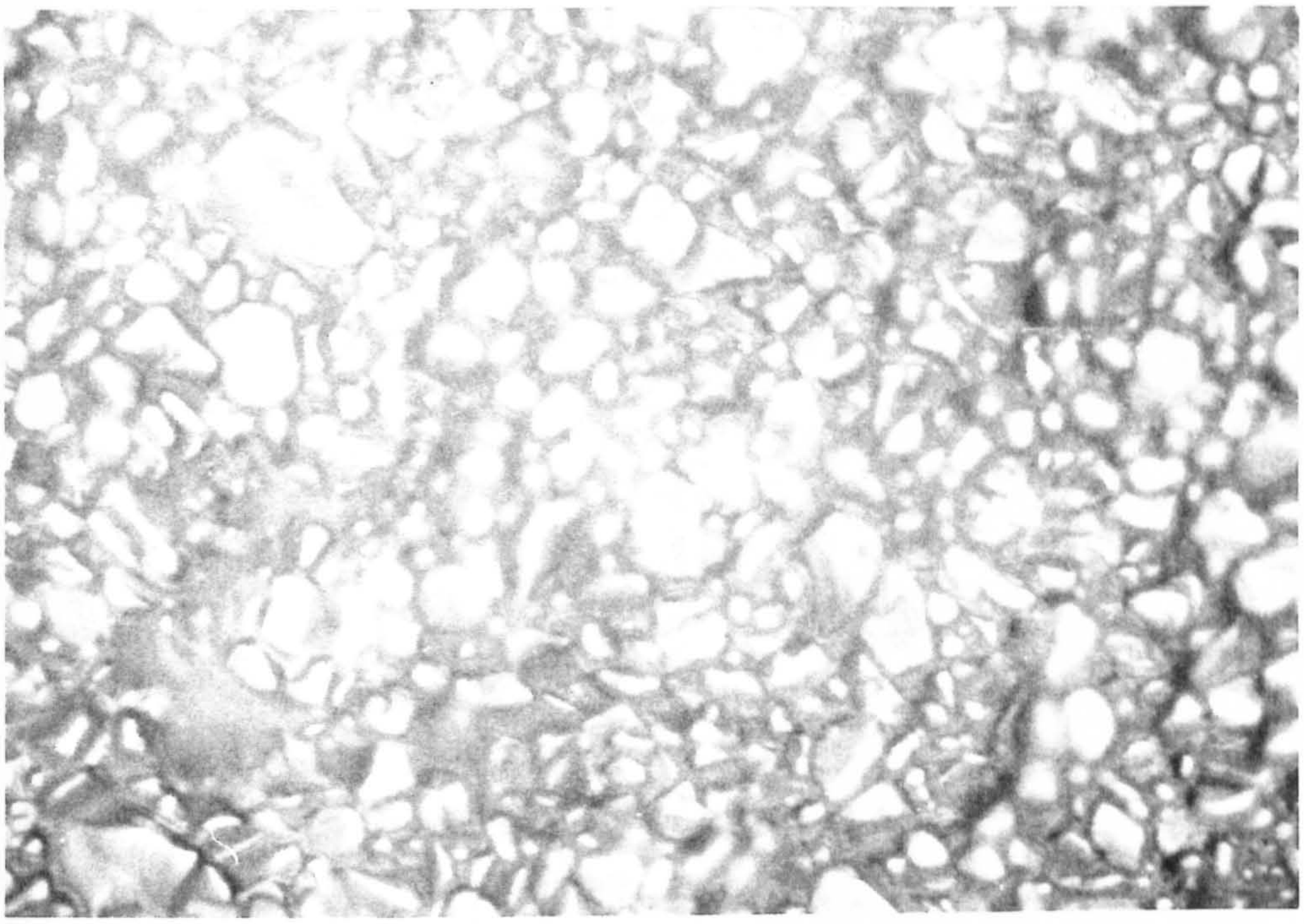

Figure 4.42- Optical photograph of the as-sintered surface (sintered at 1650°C for 3 h) of the 95 % alumina; magnification X 1600.

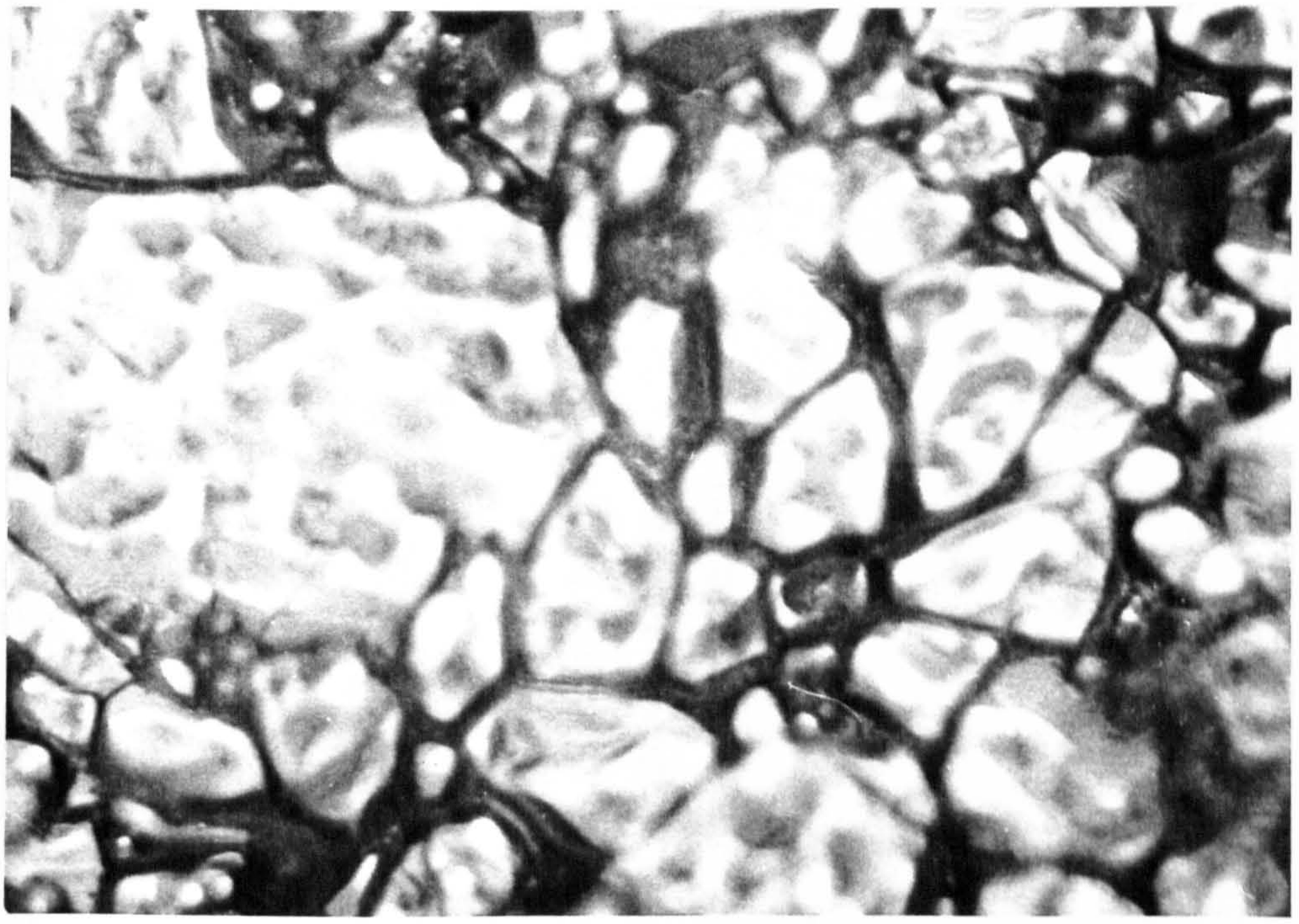

Figure 4.43- Optical photograph of the as-sintered surface (sintered at 1580°C for 3 h) of the 88 % alumina; magnification X 1600.

Figure 4.44- Apparent viscosity versus apparent shear rate for the zirconia(+MgO)-MEW-PIB-LP b.m. at 100°C.

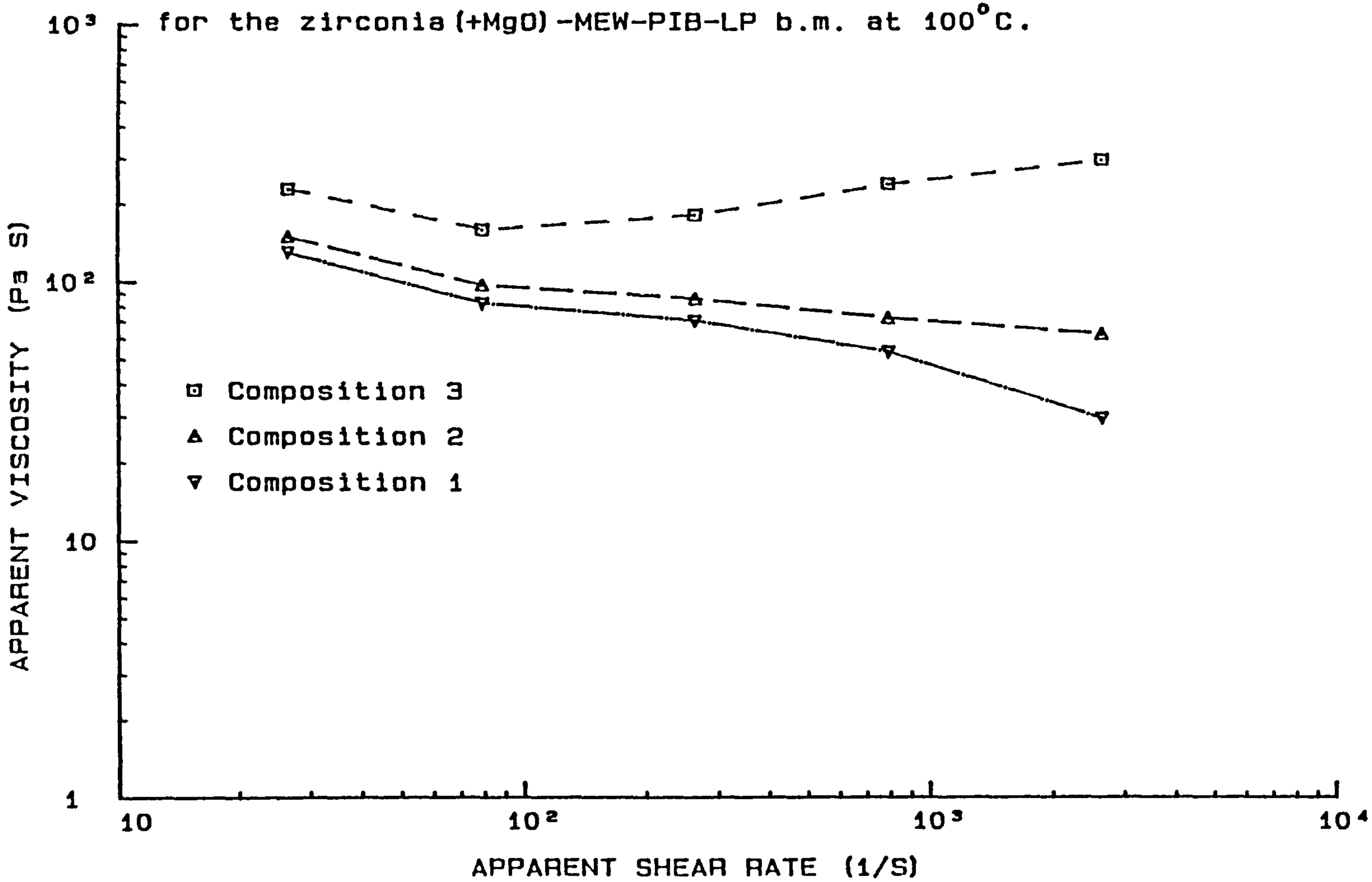

Figure 4.45- Apparent viscosity versus apparent shear rate for the zirconia (+MgO) -MEW-PIB-LP b.m. at 120°C.

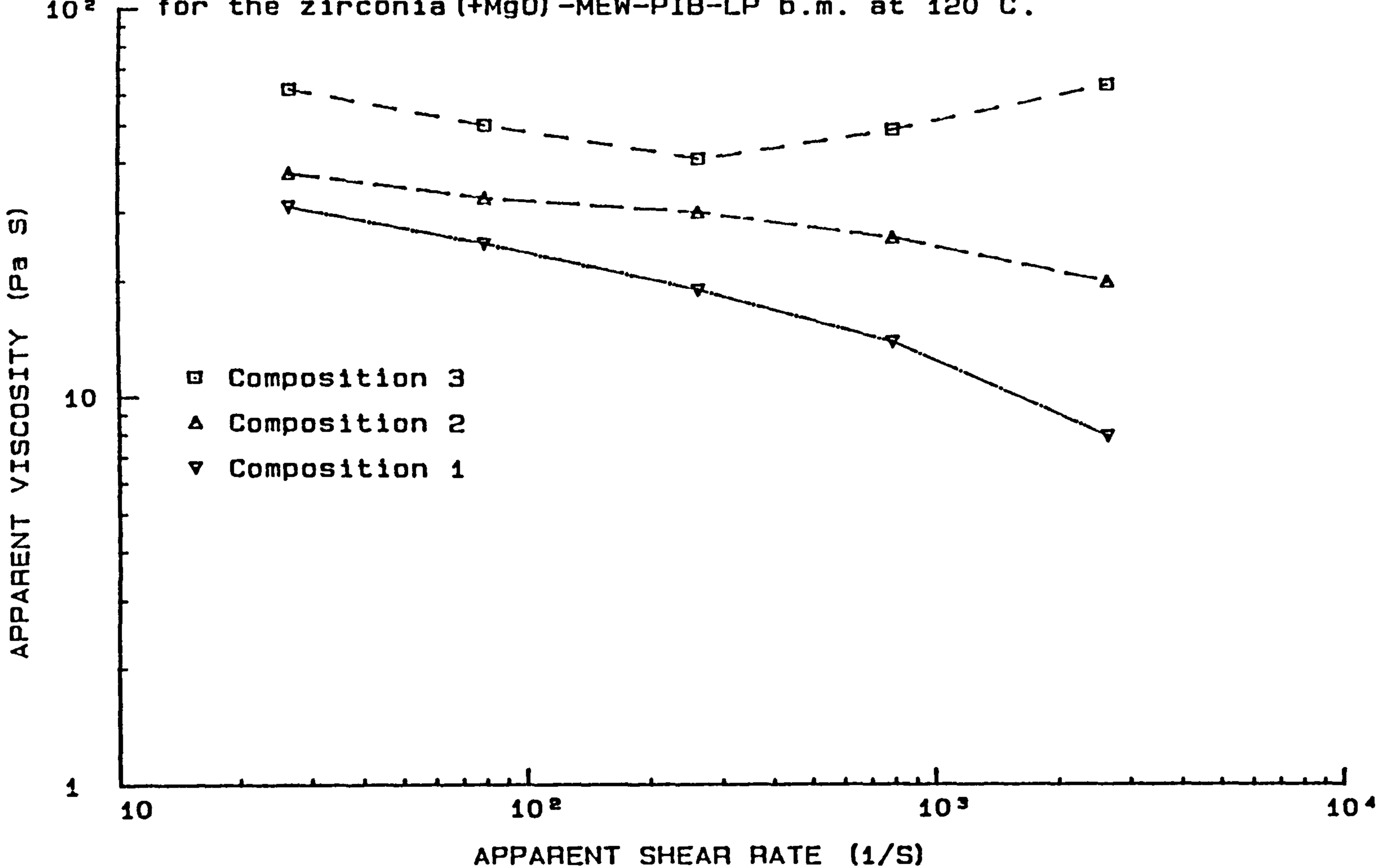

Figure 4.46- TGA data at 10 °c/min for the zirconia (+MgO) -MEW-PIB-LP b.m..

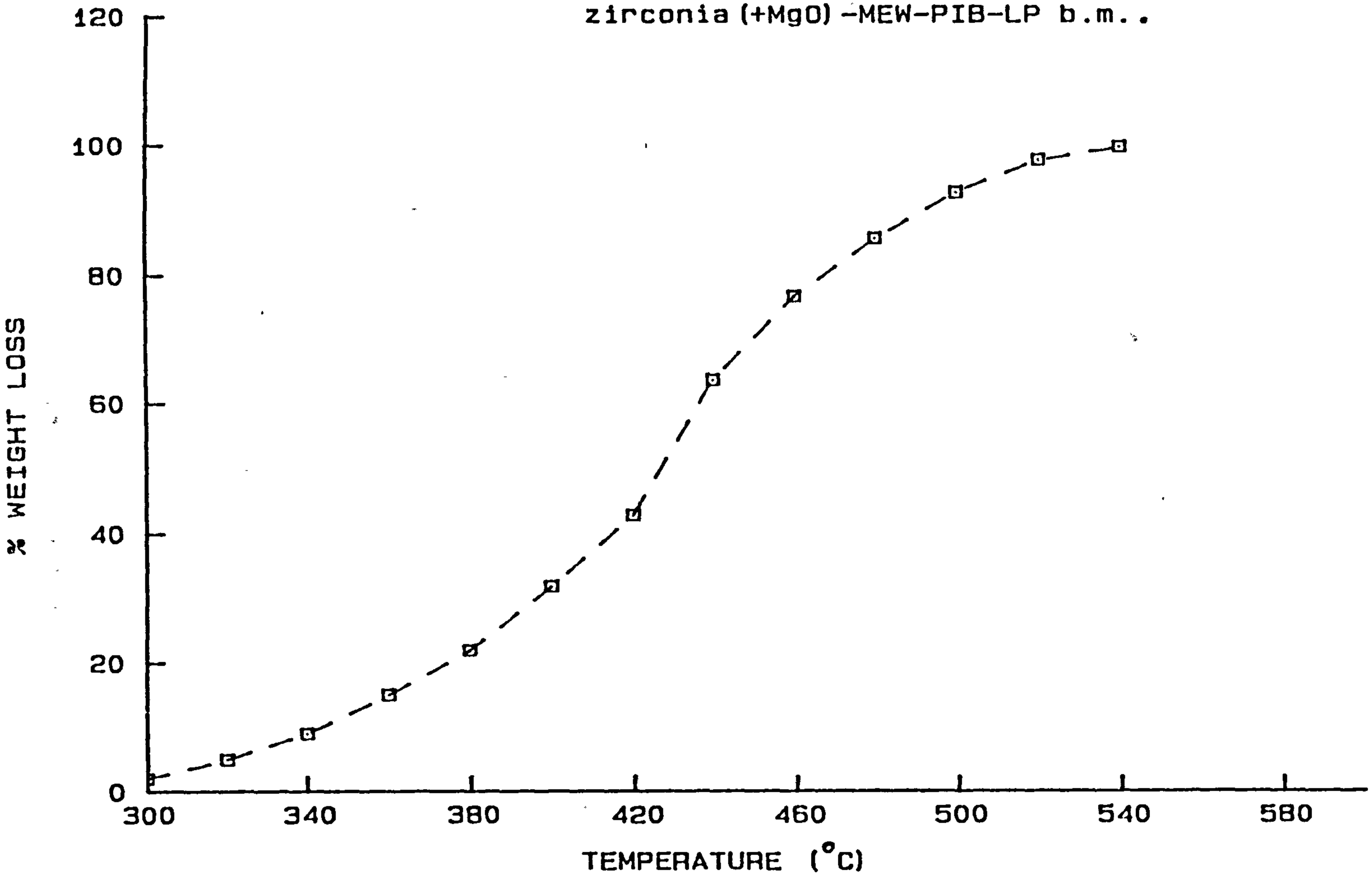

Figure 4.47- Apparent viscosity versus apparent shear rate for the S13N4 (+Y2O3+Al2O3) -MEW-PIB-LP b.m. at 100°C.

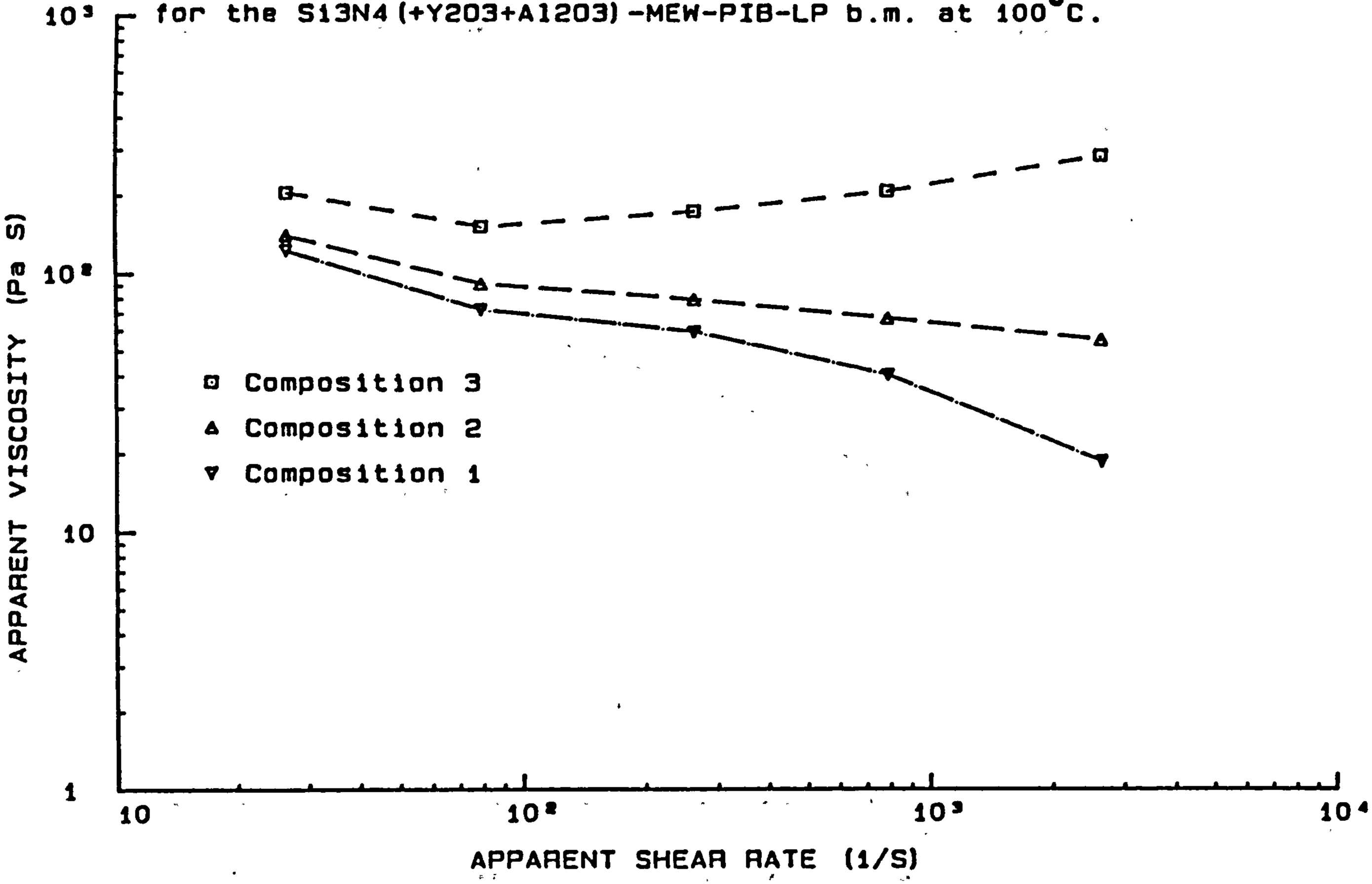

Figure 4.48- Apparent viscosity versus apparent shear rate for the Si3N4 (+Y2O3+Al2O3) -MEW-PIB-LP b.m. at 120°C.

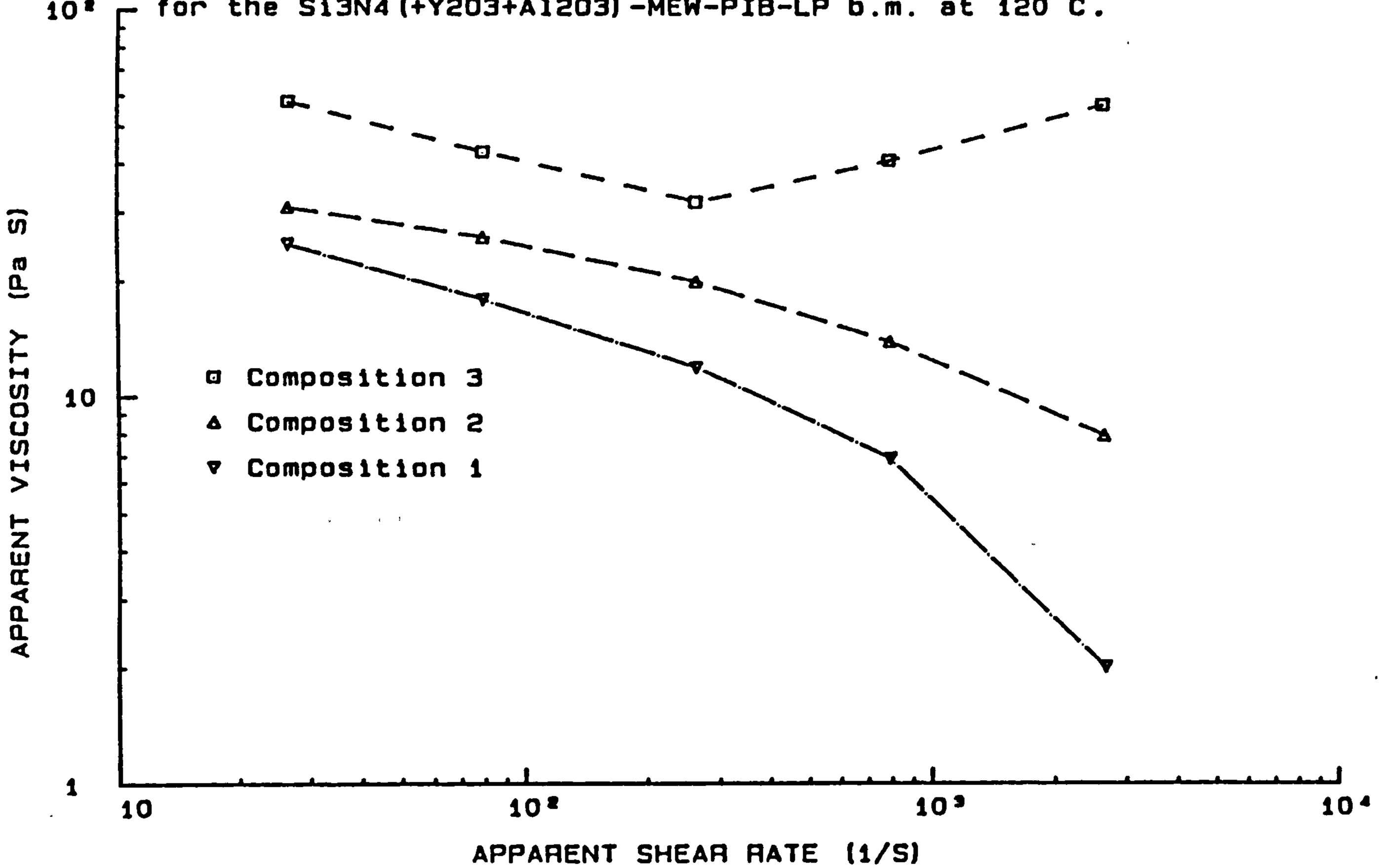

Figure 4.49- Apparent viscosity versus apparent shear rate for the SiC(+B4C)-MEW-PIB-LP b.m. at 100°C.

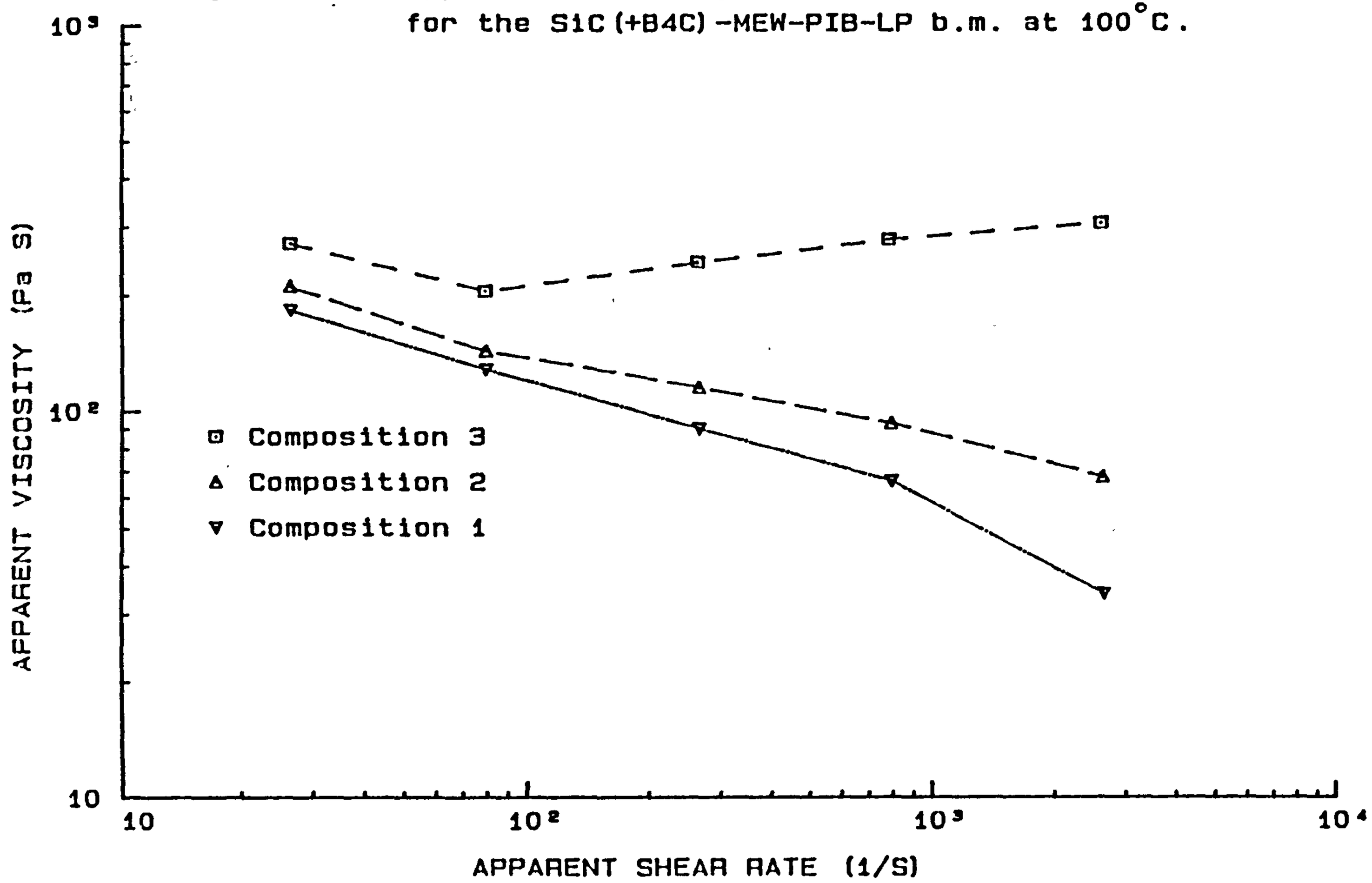

Figure 4.50- Apparent viscosity versus apparent shear rate for the SiC(+B4C)-MEW-PIB-LP b.m. at 120°C.

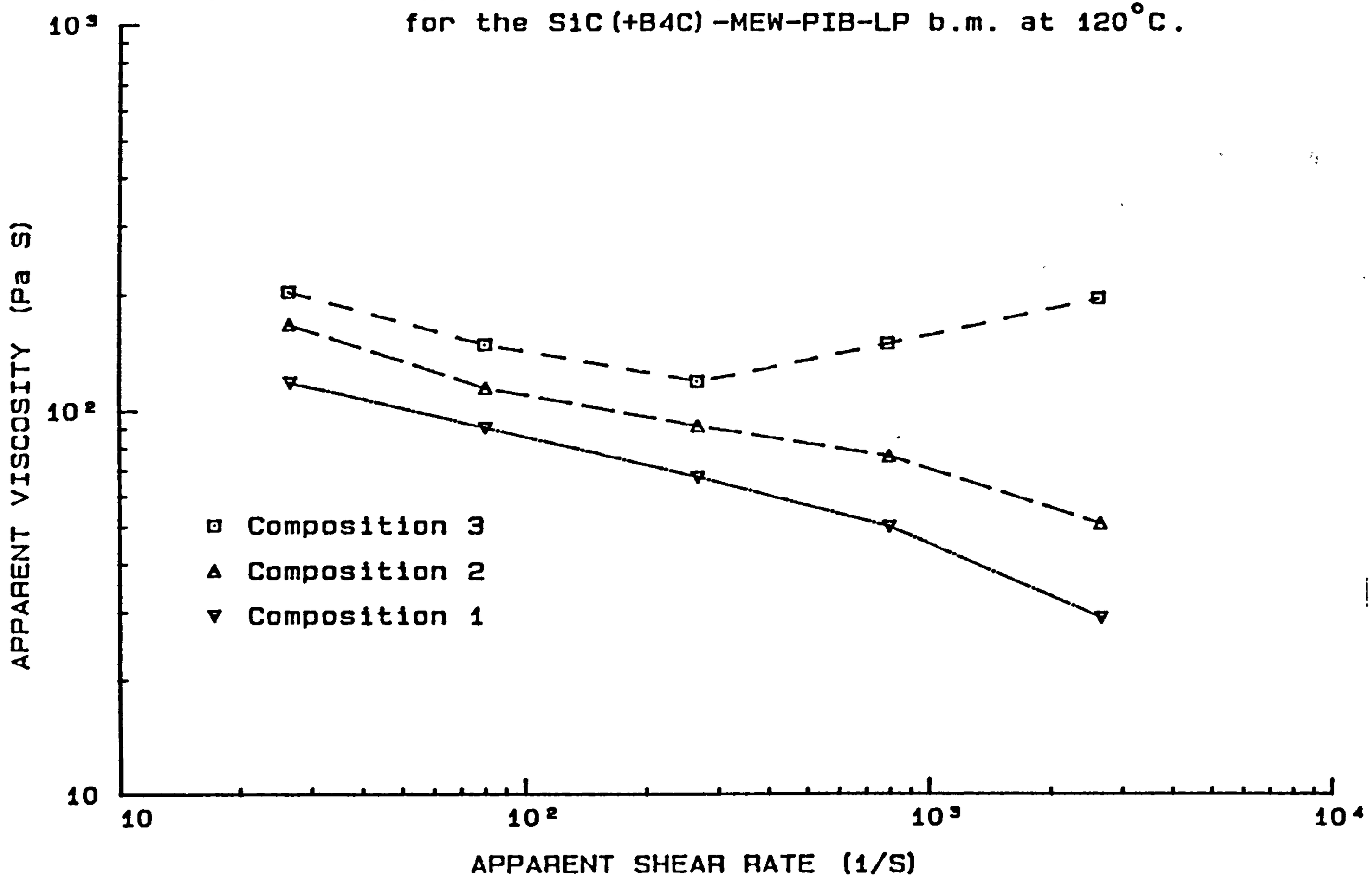

Figure 4.51- TGA data at 10 °c/min for the SiC(+B4C)-MEW-PIB-LP b.m..

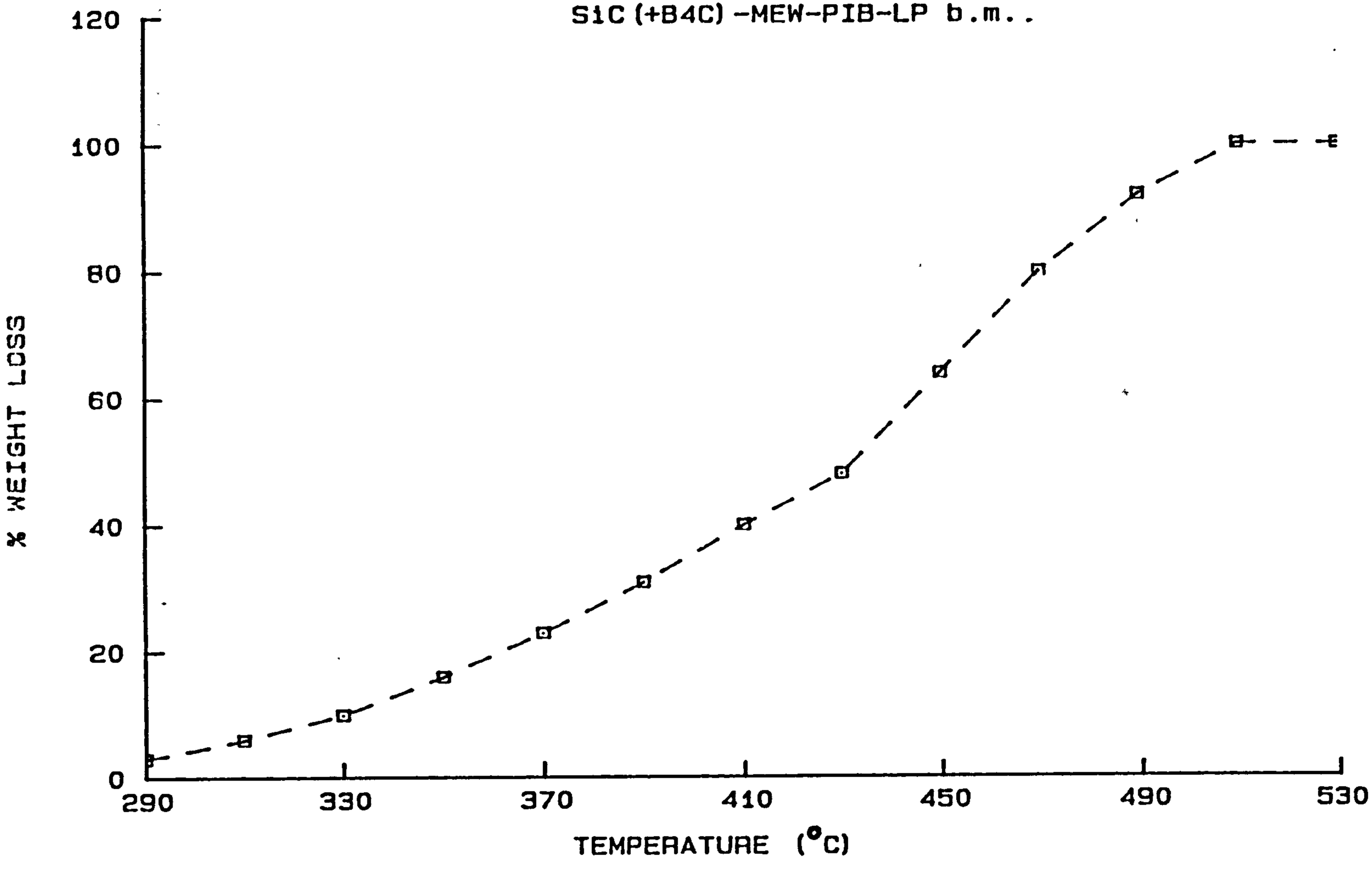

Figure 4.52- Apparent viscosity versus apparent shear rate for the WC-6wt.% Co-MEW-PIB-LP b.m. at 100°C.

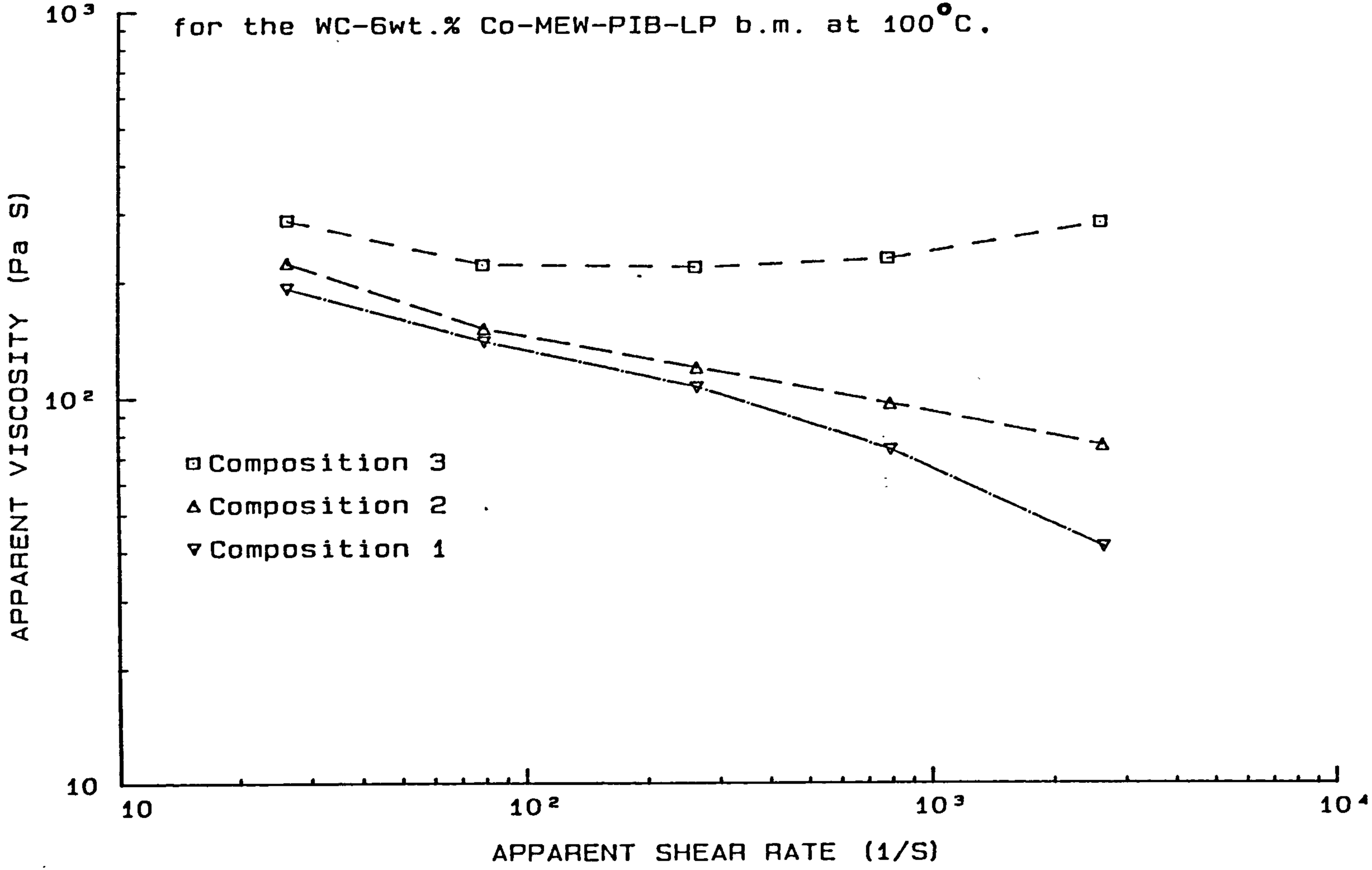

Figure 4.53- Apparent viscosity versus apparent shear rate for the WC-6wt.% Co-MEW-PIB-LP b.m. at 120°C.

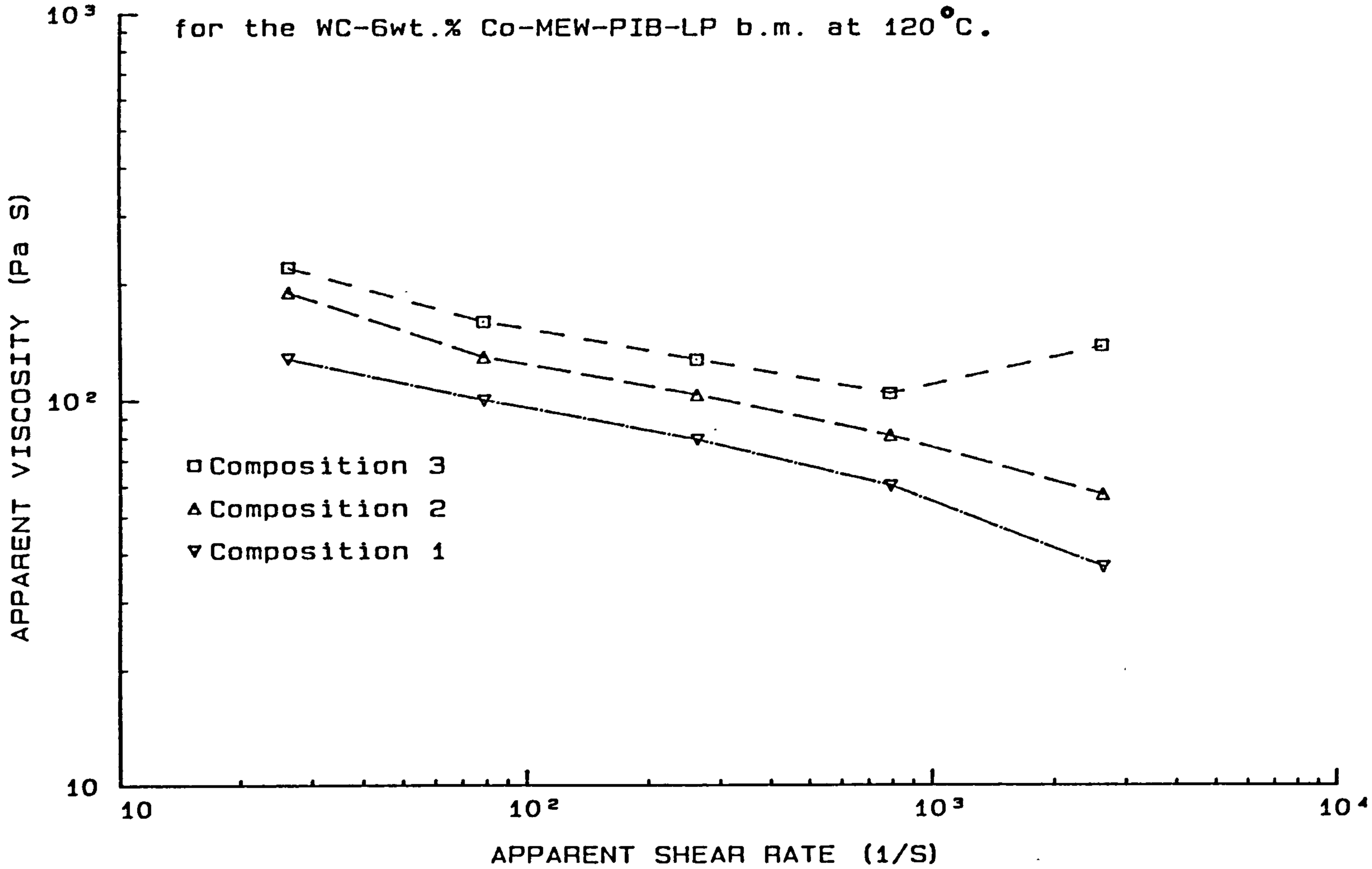

Figure 4.54- TGA data at 10 °c/min for the WC-6wt.% Co-MEW-PIB-LP b.m..

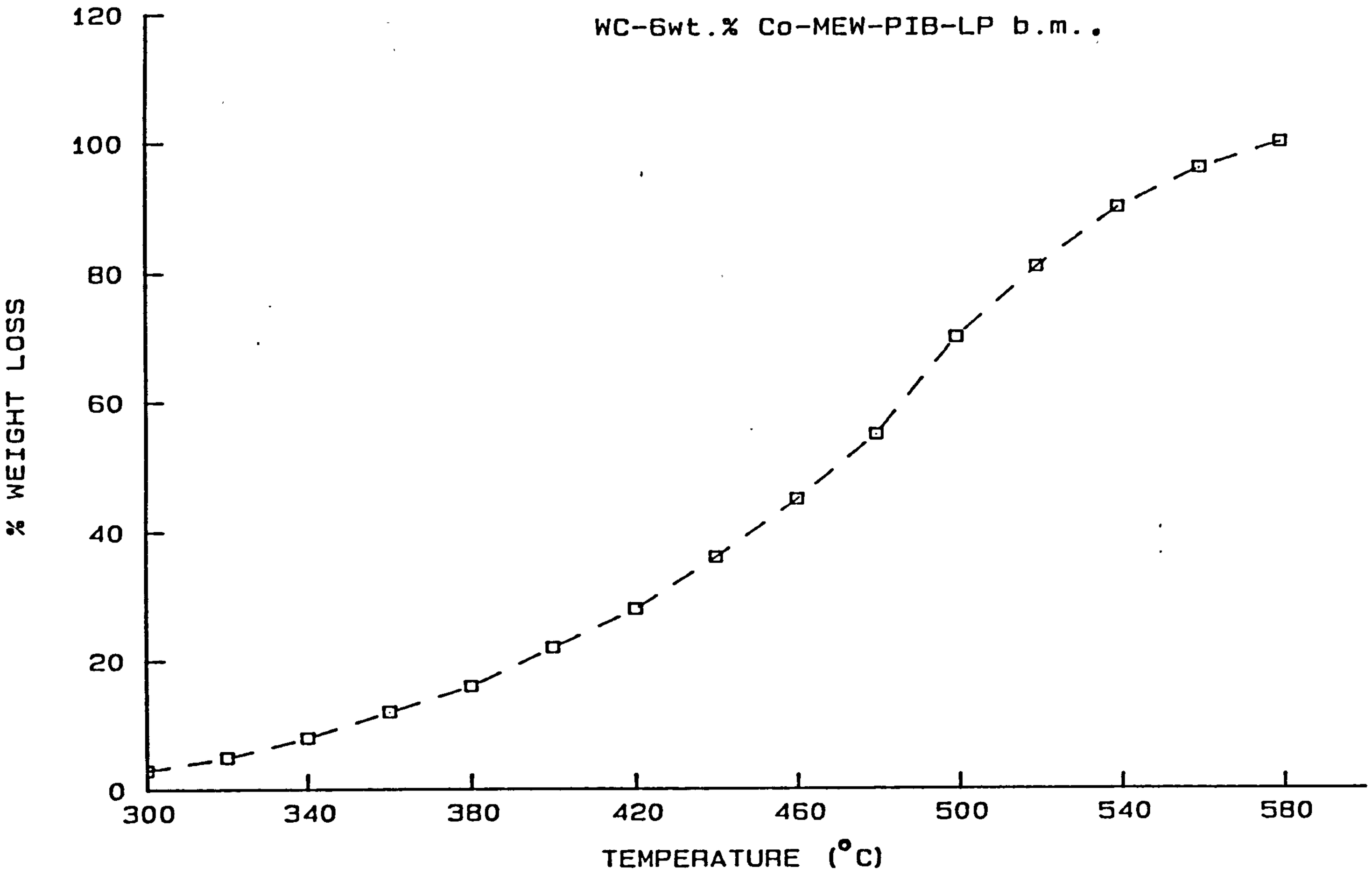

Figure 4.55- Apparent viscosity versus apparent shear rate for the Si3N4 (+Y2O3+Al2O3) -PVA-Gelling agent-LP-Water b.m. at 73°C.

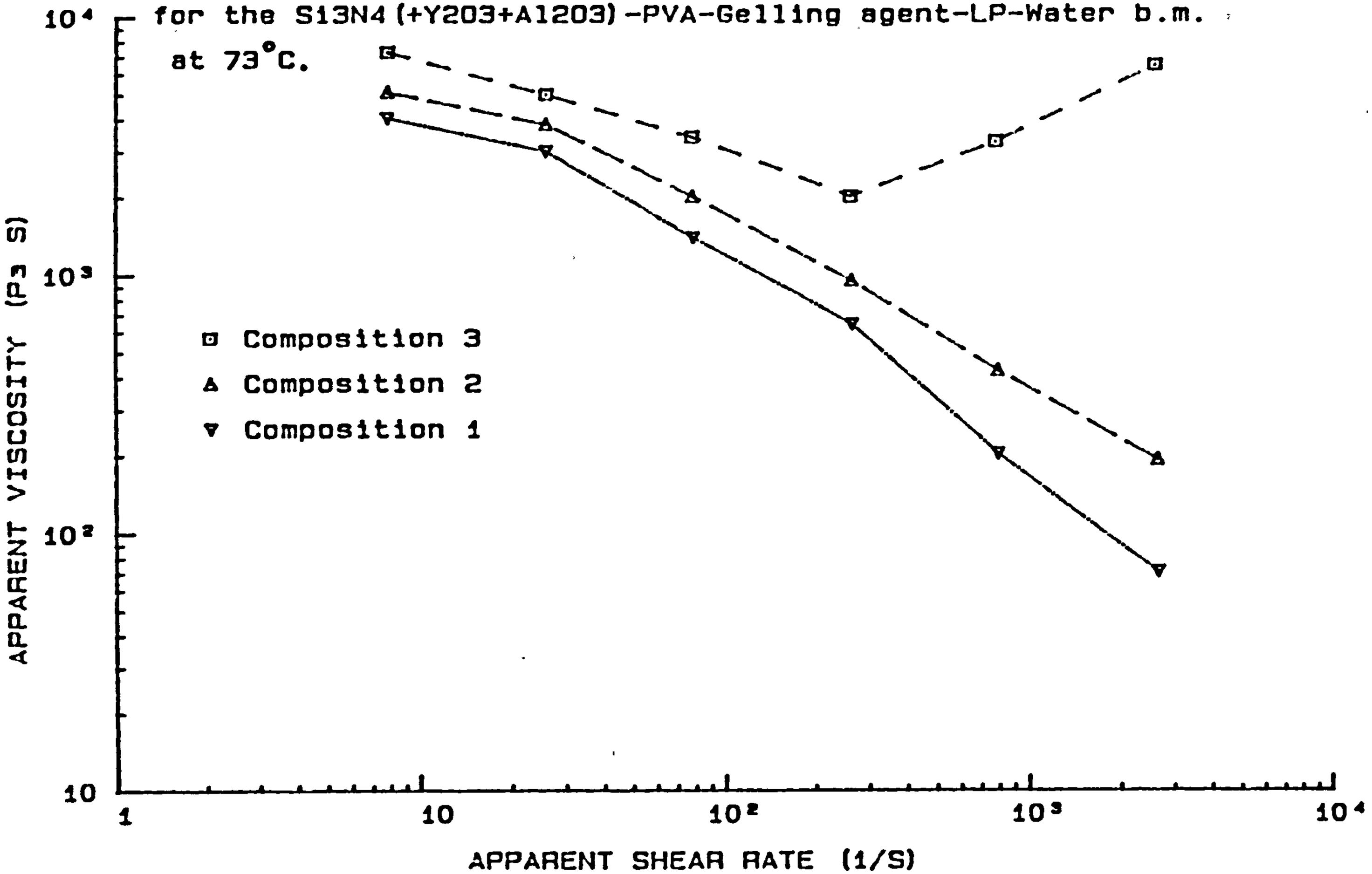

Figure 4.56- Apparent viscosity versus apparent shear rate for the WC-6wt.% Co-PVA-Gelling agent-LP-Water b.m. at 73°C.

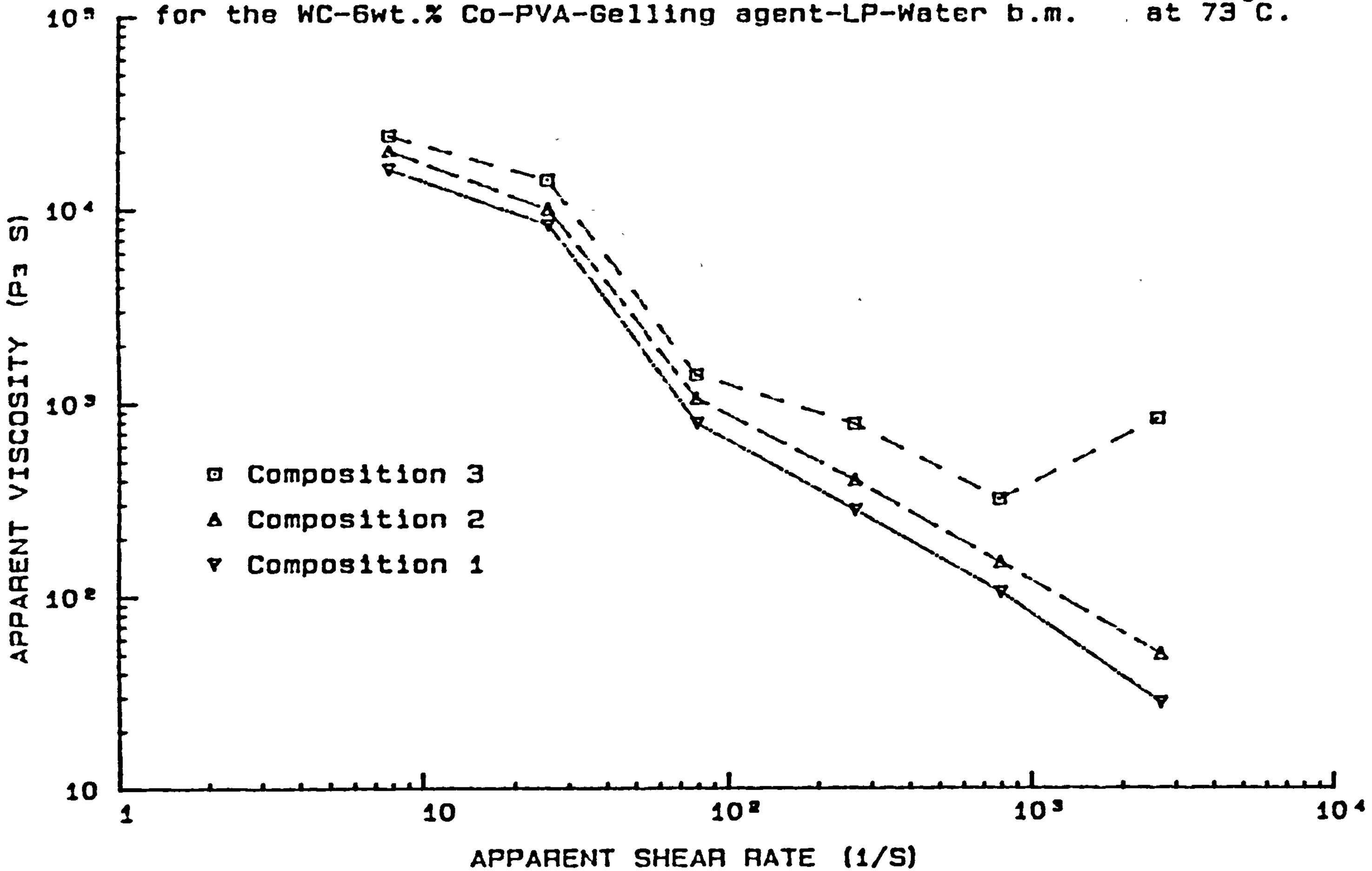

Figure 4.57- Apparent viscosity versus apparent shear rate for the Fe-2wt.% Ni-PVA-Gelling agent-LP-Water b.m. at 73°C.

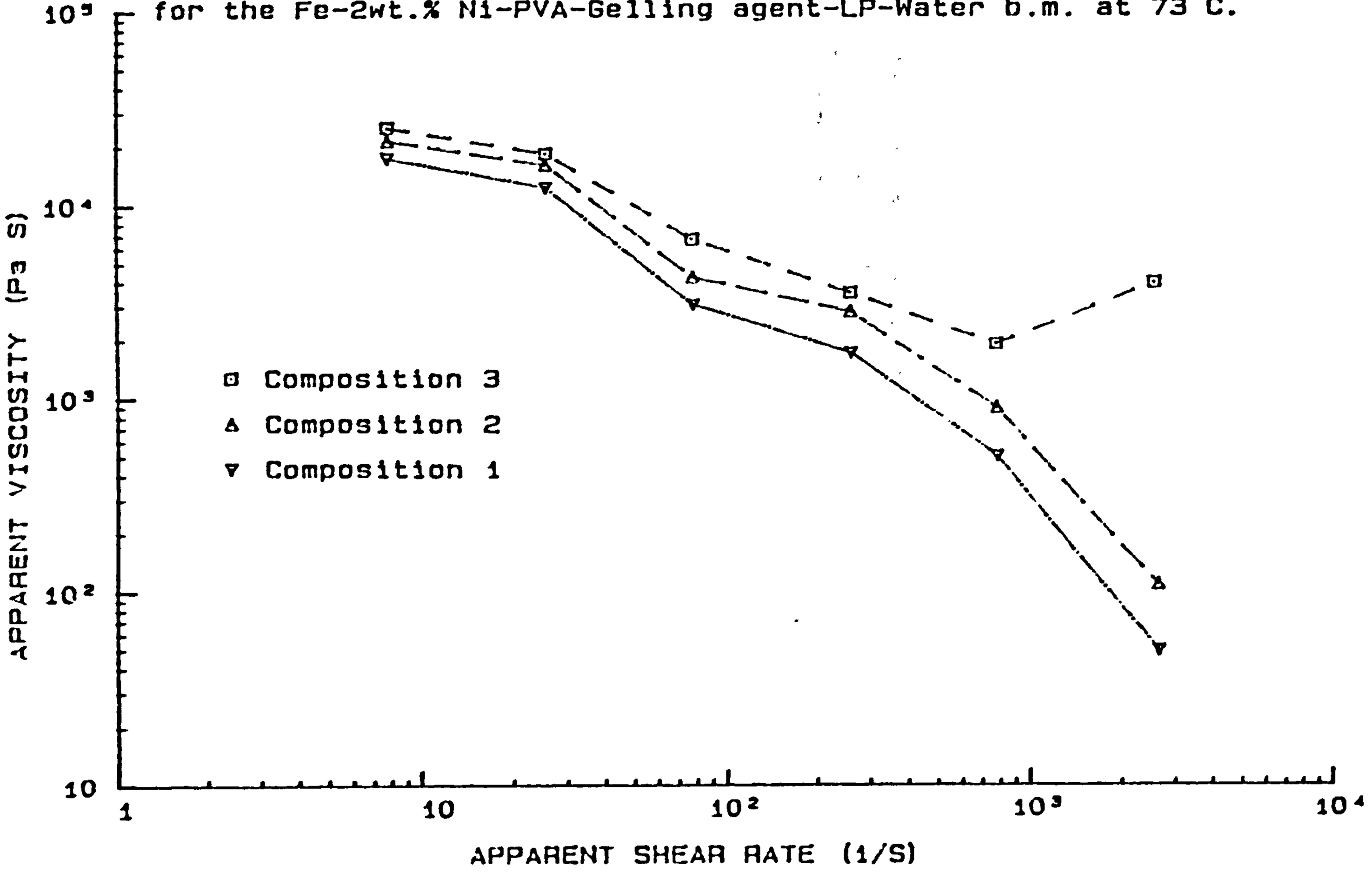

CHAPTER FIVE

CHAPTER FIVE

5- DISCUSSION

In the previous chapter (chapter four) the experimental results and relevant interpretation of the results were given for each stage of the injection moulding process (IMP) for each alumina and other powder-binder mixtures. In this chapter the properties obtained for each stage of the IMP will be discussed in detail for each re-evaluated binder system and also for the new binder systems developed during this work. These properties are compared among the re-evaluated binder systems and also with those of the newly developed binder systems and the present literature where available. The main properties discussed and compared are the critical properties such as amount of volume loading of powder, rheology, debinding, green and sintered densities which are of major concern in the injection moulding of ceramic/metallic materials. Other properties such as mixing, moulding and demoulding are also discussed and compared between the thermoplastic/wax and those of the water-soluble polymers. The mechanical and thermal properties of the injection moulded alumina ceramics obtained during this work are also discussed and compared with those of the present literature for the injection moulded and compacted alumina ceramics having similar chemical compositions.

5.1- Properties of the re-evaluated thermoplastic binder systems

A summary of the % maximum possible volume loadings, as-moulded (green) and sintered densities, debinding times and other results such as shrinkage values, mixing, moulding and demoulding properties were given in Table 4.31 for the re-evaluated binder systems at the end of chapter four. From this Table it is quite clear that all the above mentioned properties have been evaluated fully for each binder system with the exception of the ethylene vinyl acetate (EVA) binder system which could not be evaluated fully due to its cracking and crumbling problems during the debinding process. This Table also shows that the 60/40 atactic polypropylene (APP) binder system has provided the best properties in comparison with the other re-evaluated thermoplastic binder systems. These best properties and possible reasoning for their occurrence are as follows.

1- The highest possible volume loading of 64 % of the 99.5 % alumina powder which was due to the highest fluidity and wettability of the APP binder in comparison with the other binders [Saito et al (165)]. For the same reason a smaller amount of 60/40 APP binder at a lower moulding temperature than other thermoplastic binders was used (see Table 4.31). Due also to the highest fluidity of the APP binder the longest moulded samples of size 187 mm X 12 mm X 3 mm were only obtained using this binder system.

2- The highest as-moulded and sintered densities of 95.5 and 96 % of their respective theoretical values which was due to the highest volume loading of the alumina powder into the 60/40 APP binder system which also resulted the lowest shrinkage of 11.5 % by volume during the sintering process. Very similar results have been reported by many other workers (1, 5, 17, 18, 146, 170) and they all concluded that the powder volume loading into a polymer suspension should be as high as possible so that to obtain high as-moulded and sintered densities, reduce shrinkage

and slumping during binder removal, improve handling and mechanical strength after binder removal and also reduce shrinkage and distortion during sintering.

3- The shortest debinding times of 78 and 107 h for the moulded samples of 3 mm and 6 mm thickness respectively. This was due to the higher heating rates applied during the decomposition/burning of the 60/40 APP binder system which can be seen from Tables 4.15 and 4.16 and comparing them with Tables 4.6, 4.9 and 4.13 (see chapter four) for the polystyrene, polyacetal and the single APP debinding cycles. As found during this work and also reported by Saito et al (165) the APP can have its heating weight loss freely adjusted by mixing correct amounts of a type of relatively low molecular weight (. 60 weight %) and a type of relatively high molecular weight (. 40 weight %). This causes the broadening of the decomposition zone which is essential for a defect free and quick burn-out. Fig. 4.15 (see chapter four) showed the burning characteristics of the APP with different molecular weights and that of the 60/40 APP mixture. From this Figure it can be seen that the TGA curves for the APP binders with 10600 and 60400 molecular weights show rapid decomposition over a relatively narrow temperature range at . 260-380°C and . 320-460°C respectively. On the other hand the TGA curve for the 60/40 APP mixture shows that this binder mixture has decomposed and evaporated slowly and almost linearly over a wide temperature range at . 240-460°C which is more suitable for a defect-free and shorter debinding process. This wider decomposition zone resulting easier burning was the main reason for the shortest debinding times (i.e. higher heating rates) provided by the 60/40 APP binder system. In contrast to this binder system the TGA curves for the EVA, polystyrene and polyacetal binder systems (see Figs. 4.3, 4.5 and 4.10 respectively) showed narrower decomposition zones at respectively . 320-400 and 430-510°C (for the EVA), 350-480°C (for the polystyrene) and 300-420°C (for the polyacetal) which caused longer debinding times due to lower heating rates. The cracking and crumbling of the moulded EVA samples during the

second decomposition stage of the debinding process was most probably due to the very rapid decomposition and evaporation of the main ethylene chain which can be even worse for thicker and larger moulded samples. The other main reason could be due to fast nonuniform decomposition taking place at two stages having similar high decomposition rates.

4- The most suitable rheological properties which resulted the 60/40 APP mixture to carry the highest volume loading of 64 % of the 99.5 % alumina powder without showing any dilatant flow behaviour (see Fig. 4.14 in chapter four). The optimised 99.5 % alumina-60/40 APP composition showed a very low viscosity of . 80 Pas at a shear rate of . 1300 s^{-1} at a temperature of 120°C (see Fig. 4.14) in comparison to that of the other thermoplastic binder systems. The polystyrene and polyacetal binder systems showed dilatancy above volume loadings of 62 and 56.8 % of the 99.5 % alumina powder which took place above very low shear rates of . 20 s^{-1} (at 150°C) and . 20 s^{-1} (at 180°C) with viscosities of >11000 and >2000 Pas respectively (see Figs. 4.4 and 4.7 in chapter four). The dilatant flow behaviour is obtained when the critical shear rate for a particular powder-binder mixture is exceeded (15, 17, 143) and during this type of flow interparticle contact develops due to lack of enough binder which will eventually cause seizure at some stage within the extruding/injecting barrel. This type of flow must therefore be avoided. It follows therefore that the polystyrene and polyacetal binder systems have shown less favourable flow behaviour (due to their higher viscosities) and lower volume loadings than those of the 60/40 APP binder system.

5- In terms of mixing the 60/40 APP binder system provided the easiest mixing due to its lowest torque value of 320 mg (see Table 5.3) during the steady state mixing stage (see Fig. 4.1) and this binder system caused no sticking problems during or after mixing which was due to the presence of diethyl phthalate (DEP) and stearic acid (SA) as excellent and compatible plasticiser and lubricant respectively. The SEM examination of

the optimised 99.5 % alumina-60/40 APP-SA-DEP binder mixture showed a highly homogeneous mixture (see Fig. 3.28 in chapter three). The optimised polystyrene and polyacetal binder mixtures showed higher steady state torques of 325 and 335 mg respectively (see Table 5.3) besides their higher mixing temperatures (150°C and 180°C for polystyrene and polyacetal respectively) than that of the 60/40 APP (145°C) binder system. The polystyrene and polyacetal binder systems caused no sticking problems during or after mixing. In terms of granulation the 60/40 APP binder system provided much easier granulation than both the polystyrene and polyacetal binder systems which was due to the softness and more rubbery state of the APP binder.

6- The 60/40 APP binder system provided lower moulding temperature and longer moulded samples than both the polystyrene and polyacetal binder systems (see Table 4.31) which was due to the higher fluidity and lower viscosities of the 60/40 APP binder system (which carried a higher volume loading of the 99.5 % alumina powder). The demoulding and handling properties of all three binder mixtures were quite satisfactory with very short moulding cycles (< 30 s) which is expected from thermoplastic/wax-based binder systems. Generally, more than 90 % (i.e. ≤ 2 samples out of a batch of 20 samples) of the moulded samples showed no moulding defects, i.e. no macro/micro-cracking, no sink marks, no swelling and no delamination. Most of the moulding defects were macro/micro voids (. 100-1000 μm) possibly due to entrapped air or inhomogeneity during the mixing or moulding operations.

Overall assessment of the re-evaluated thermoplastic binder systems

From the above discussion and the work during section 4.1 and the lack of experimental/practical details in the reviewed literature it is clear that some original work related to the injection moulding of alumina powder has also been carried out during the first part of this research work. However, besides the originality and the properties provided by the 60/40 APP binder system the overall assessment was that there were still some needs for improvements in vital areas such as higher sintered densities so that to obtain better mechanical properties. This was possible only by increasing the amount of volume loading of the alumina powder (to > 64 %) into a new binder system. This was one of the main objectives of the second part of this research programme which resulted in the development of a new thermoplastic-wax based binder system which provided a higher volume loading of 70 % (maximum) of the alumina powder and hence a higher sintered density (98.5 % theoretical) resulting in better mechanical properties as will be seen in section 5.7 of this chapter.

5.2- Properties of the re-evaluated water-based methylcellulose (Rivers) binder system in comparison to those of the thermoplastic/wax-based binder systems

These are given in Table 4.31 along with those of the re-evaluated thermoplastic binder systems.

From the existing literature related to the use of different binder systems for the injection moulding of ceramic/metallic powders it can be concluded that there are mainly two groups of binder systems. One group uses the usual thermoplastic/wax binders which is referred to as the Wiech process (125) and the other group is based on the water-soluble polymers which is referred to as the Rivers process (151). According to the present literature (1, 2, 51, 146) and also from the experimental results during the first part (section 4.1-chapter four) of this research work it is quite clear that both groups of binder systems have some advantages and some disadvantages (limitations) which can be summarised as follows: the Wiech process (the use of thermoplastics/waxes) provides rigid mouldings in relatively short moulding cycles (< 30 s), but as seen during the first part of this work and also by other workers (125, 150), it is clear that such binders require considerable debinding times (typically > 40 h) depending upon the thickness of the moulded part to be debonded. Due to this reason, only thin section mouldings are economically viable. In contrast the Rivers process (the use of water-soluble polymers such as methylcellulose) has the advantage of rapid debinding periods (typically < 20 h) as obtained during this work for the 5 mm thick samples (see Table 4.31). This, therefore, makes the production of thick mouldings economically viable. However, the Rivers process requires long cycle times (≥ 5 min as experienced during this work, see Table 4.31), suffers from mould adhesion and distortion problems during the demoulding process (as observed during this work). The methylcellulose (Rivers) binder system also provided a relatiely low sintered density of 94 % of

the theoretical value (= 3.87 g/cm^3) which was due to the relatively low volume loading of (55 % maximum) the alumina powder into this binder system. According to other reports (171) this binder system may also cause premature gelation of the composition during the moulding process because of exothermic reactions between active particulates and water in the binder. It follows therefore that a binder system which can provide the favourable properties of both the Wiech and the Rivers processes could significantly improve the powder injection moulding technology and for this purpose a new water-based binder system was also developed during the second part of this research work.

The second part of this research programme was therefore concentrated on developing two new binder systems based on thermoplastic-wax and water-soluble polymers which could provide powders (mainly alumina) to be injection moulded with rigid mouldings so that to withstand demoulding and handling, with shorter moulding cycles and debinding times and also with higher volume loadings of the powder for higher as-moulded and sintered densities.

5.3- Properties of the injection moulded 88 %, 95 % and 99.5 % alumina grades using the 60/40 APP binder system in comparison with those of the compacted alumina samples at different compaction pressures having the same compositions

A summary of the results obtained for the injection moulded 88 %, 95 % and 99.5 % alumina samples using the 60/40 APP binder system was given in Table 4.32 at the end of chapter four. From this Table it can be seen that tap density, i.e. particle size, particle size distribution, particle shape and surface area, has some effect on the as-moulded and sintered densities. It can be seen that the higher the tap density the higher the as-moulded and sintered densities of the alumina samples which is due to the higher packing efficiency of the alumina powder with a higher tap density. This Table also shows that the lower alumina grades with higher tap densities have caused higher viscosities which resulted in shorter mouldings even at a higher moulding temperatures (see Table 4.32). From this Table it is therefore clear that the 99.5 % alumina grade with a lower tap density provided a longer moulding (187 mm long, 3 mm thick) at a lower moulding temperature but with slightly lower green and sintered densities than those of the 88 % and 95 % alumina grades which resulted in shorter mouldings (68 mm long, 3 mm thick) due to their higher tap densities and higher viscosities. These results therefore suggest that there is a need for compromise between higher densities and size of the mouldings for a powder with different tap densities.

Table 4.33 shows a comparison between the sintered densities of the injection moulded and compacted 88 %, 95 % and 99.5 % alumina samples. It can be seen that only the compacted samples at 200 MN/m^2 have higher sintered densities than the injection moulded samples. This suggests that injection/moulding pressure has a very small effect on the (green and) sintered density and

the only effective way to increase the (green and) sintered density for an injection moulded sample is by increasing the amount of volume loading of the powder and this can be seen quite clearly from Table 4.31 and also from the as-moulded (green) and sintered density values in part two (see sections 4.2.1-4.2.6) for alumina samples injection moulded at a much lower moulding pressure of 0.55 MN/m^2 having similar or higher density results than those in part one (see sections 4.1.1-4.1.4) injection moulded at a higher moulding pressure of 13.8 MN/m^2 but producing similar or lower density results which were due to mainly lower volume loadings of the alumina powder. Table 4.33 also shows that compaction pressure has a marked effect on the final sintered density of the compacted samples, i.e. it can be seen quite clearly that as the compaction pressure increases from 30 to 200 MN/m^2 the sintered densiy increases from 90 to 99 % of the theoretical value (= 3.87 g/cm^3). Similar results have been reported (172) for the increase in green density of compacted alumina powder as the compaction pressure was increased from 34.5 to 103.4 MN/m^2 which resulted an increase in green density from 38 to 41 % of the theoretical green density. It was also reported (172) that agglomeration has a strong influence on the flow properties, pressed and fired densities of a ceramic body and that hard agglomerates cause low density and microstructural defects, and therefore control of the state of agglomeration is one of the most important aspects of ceramic processing. In the same paper (172) it was also reported that the aggregates were being crushed during compaction and increasing the compaction pressure progressively decreased the population of aggregates but did not eliminate the aggregates below a certain size (< 10-15 μm) suggesting that only large aggregates were being crushed. It was noted that pressing crushes the aggregates essentially into individual particulates, rather than shifting the aggregate size distribution to smaller sizes in a uniform way. Examination of the microstructure of the sintered compacts showed that the 34.5 MN/m^2 sintered compact had more pores and aggregates than the 103.4 MN/m^2 sintered compact which had a tighter structure with smaller aggregates. It was

therefore concluded that the density achieved at any pressure is markedly influenced by the aggregates, i.e. as the amount of the aggregate increases the tap, pressed and sintered densities decreases and vice versa (172).

5.4- Properties of the injection moulded 99.5 % alumina ceramic using the newly developed thermoplastic-wax based binder system in comparison to those of the injection moulded 99.5 % alumina ceramic using the re-evaluated 60/40 APP binder system

A summary of the properties obtained during the second part of this research work was given in Table 4.55 at the end of chapter four. During this part of the work two new binder systems were developed. One was a thermoplastic-wax and the other one was a water-based binder system both of which provided better properties than the existing/re-evaluated binder systems. The newly developed thermoplastic-wax, i.e. the polyisobutylene + montanester wax + liquid paraffin (PIB-MEW-LP), binder system provided a maximum possible volume loading of 70 % of the 99.5 % alumina powder which resulted in as-moulded and sintered densities of 97.35 % and 98.5 % of their respective theoretical values (see Table 4.55). These values are higher than those obtained by the 60/40 APP binder system which provided the best properties amongst the re-evaluated thermoplastic binder systems (see Table 4.31) as discussed in section 5.1 of this chapter. The PIB-MEW-LP binder system provided debinding times of 80, 104 and 112 h for 3, 5 and 6 mm thick samples respectively which are very similar to those obtained by the 60/40 APP binder system (see Table 4.31). Note that the 60/40 APP binder system provided debinding times of 78 and 107 h for 3 and 6 mm thick samples which are the shortest debinding times obtained during this work amongst all the thermoplastic/wax based binder systems. Other properties of the newly developed PIB-MEW-LP binder system such as mixing, moulding, flow, demoulding, moulding cycle and handling were very similar to those of the 60/40 APP binder system except that a more rigid mouldings were obtained due to

the presence of the montanester wax (MEW) which recrystallised after moulding within the mould and therefore provided a tougher moulding than the 60/40 APP binder system which was non-crystalline (amorphous) and less tough.

Comparing the sintered densities of the injection moulded 99.5 % alumina samples using the new PIB-MEW-LP binder system with those of the compacted 99.5 % alumina samples at a compaction pressure of 200 MN/m^2 (see Table 4.33) it can be seen that both fabrication techniques have produced the same sintered density of 98.5 % of the theoretical density (= 3.87 g/cm^3) which suggests that it is therefore possible to produce very similar densities (and hence other properties) by the injection moulding technique provided that a high volume loading of the ceramic/metallic powder is incorporated into the binder system prior to moulding.

It can therefore be seen that the newly developed PIB-MEW-LP binder system has provided the highest as-moulded and sintered densities amongst all the thermoplastic/wax binder systems used during this research work and in fact amongst all the present binder systems available for the injection moulding of alumina ceramics. This new binder system also provided the lowest shrinkage value of 10.5 % of the total volume amongst all the binder systems used during this work which was due to its highest volume loading of the alumina powder.

Considering the rheological properties of the 99.5 % alumina-PIB-MEW-LP binder mixture it can be seen from Fig. 4.35 that the optimised composition (see Table 4.46-composition 2) has viscosities varying between . 200-30 Pas at shear rates of . 200-1200 s^{-1} at a temperature of 100°C which are a very satisfactory viscosity/shear rate ranges for ceramic injection moulding (13, 15, 17, 18, 32, 129, 170). These viscosity and shear rate values were obtained with a die of 1 mm diameter (and 20 mm length) which is much smaller than the diameter of the nozzle (= 3 mm) at the tip of the injecting barrel and therefore the actual injecting viscosities and shear rates will be much lower than the above mentioned values. Figs. 4.31-4.36 (in chapter four) show quite clearly the temperature and shear rate dependency of

viscosity, i.e. as temperature and shear rate decrease viscosity increases and vice versa. Fig. 4.31 shows that there is a critical shear rate above which dilatancy takes place causing a viscosity rise as shear rate increases which is not a suitable flow behaviour for ceramic/metallic injection moulding due to seizure problems which may occur within the barrel. The value of the critical shear rate depends on the amount of volume loading of the powder and also on the flow properties of the binder system as seen throughout chapter four.

It is also noticeable that the optimised 99.5 % alumina-PIB-MEW-LP binder mixture was moulded at a moulding temperature of 130°C which is very close to that of the optimised 99.5 % alumina-60/40 APP binder mixture (moulded at 125°C). This low moulding temperature is also another good moulding properties of the newly developed PIB-MEW-LP binder system which does not have the risk of degradation problem as reported for some binder systems (1, 51) due to their high moulding temperatures.

The visual and SEM examinations of the moulded 99.5 % alumina-PIB-MEW-LP samples showed that about 95 % (1 sample out of a batch of 20 moulded samples) of the samples were free from moulding defects. The observed moulding defects were mostly macro/micro voids (100-1000 μm) possibly due to the entrapped air or inhomogeneity of the mixture.

As mentioned earlier it became quite clear during this part of the work that the injection/moulding pressure had very small effect on the as-moulded and sintered densities since very similar results have been obtained for both injection/moulding pressures of 13.8 and 0.55 MN/m^2 during the first and second part of this work (see Tables 4.31 and 4.55 in chapter four).

5.5- Properties of the injection moulded 99.5 % alumina ceramic using the newly developed water-based polyvinyl alcohol (PVA) binder system in comparison to those of the injection moulded 99.5 % alumina ceramic using the water-based methylcellulose (Rivers) binder system

A summary of the properties of the newly developed water-based PVA (i.e. PVA + gelling agent (resorcinol) + liquid paraffin + water) binder system was also given in Table 4.55 at the end of chapter four. From this Table it can be seen that the PVA binder system has provided a volume loading of 56 % of the 99.5 % alumina powder which resulted in as-moulded and sintered densities of 91.5 and 96 % of their respective theoretical values. These values are higher than those obtained by the water-soluble methylcellulose (Rivers) binder system which provided a volume loading of 55 % of the 99.5 % alumina powder with as-moulded and sintered densities of 88 and 94 % of their respective theoretical values (see also Table 4.31). The new PVA binder system provided a debinding time of 12 h for the 5 and 6 mm thick samples which is the shortest debinding time amongst all the binder systems used during this research work including the Rivers binder system which provided a debinding time of 20 h for the 5 mm thick samples (see Table 4.31). The newly developed PVA binder system provided more rigid mouldings than the methylcellulose (Rivers) binder system and due to this rigidity there were no distortion problems during the demoulding process. There were also no adhesion problems with the PVA binder systems whereas the Rivers binder system required the use of a mould release agent for the demoulding process. A cycle time of - 1 min was used for all the PVA mouldings which was much shorter than that necessary for the methylcellulose (MC) mouldings (a gelation time of . 5 min was necessary for the complete gelation of the MC mouldings at a mould temperature of 72°C). As may have already been realised one other important

advantage of the newly developed PVA binder system over the Rivers binder system is that the PVA mixture is moulded at a moulding temperature of 72°C into a mould at room temperature with very rigid mouldings without distortion problems during demoulding whereas the MC (Rivers) binder mixture is moulded at room temperature into a hot mould at 72°C (so that to cause gelling) which is one of the main reasons for bending/distortion of the moulded samples during the demoulding (ejection) process. Visual and SEM examinations showed that more than 90 % of the moulded PVA samples were free from moulding defects and only 10 % (2 samples out of a batch of 20 moulded samples) of these samples showed macro/micro voids (~ 100-1000 μm) possibly due to the entrapped air or inhomogeneity during mixing or moulding process.

From the above discussion it is therefore quite clear that the newly developed water-based PVA binder system provided much better properties than the water-based methylcellulose (Rivers) binder system for the injection moulding of alumina powders.

5.6- Comparison between the properties of the two new binder systems developed during this work

This comparison can also be seen from Table 4.55. From this Table it is quite clear that both binder systems have provided quite satisfactory properties. However, as expected, the water-based PVA binder system provided a lower volume loading (56 % maximum) of the alumina powder than the thermoplastic-wax based PIB-MEW-LP binder system (70 % maximum) which resulted in a lower sintered density (96 % theoretical) than that provided by the PIB-MEW-LP binder system (98.5 % theoretical). As a result of this the PVA binder system caused a higher linear shrinkage (17 %) during sintering than that caused by the PIB-MEW-LP binder system (10.5 %). Other properties such as mixing, moulding and demoulding were very similar but, as expected, the PVA binder system provided a much shorter debinding time (12 h for the 5 mm thick samples) than that provided by the PIB-MEW-LP binder system (104 h for the 5 mm thick samples). These differences in properties are inevitable due to having two different types of binder systems with different properties which suggests that there is a need for compromise between very high sintered density with rather long debinding times and reasonable sintered density but with very short debinding time. The latter case is economically more viable whereas with the former case better mechanical properties are possible as will be shown and discussed in the next section (section 5.7) of this chapter.

Comparing the viscosity values of the water-based binder systems with those of the themoplastic/wax binder systems used during this work (see Figs. 4.14, 4.19, 4.32 and 4.38) it can be realised that, generally, the water-based binder systems have much higher viscosities (varying between 10-10000 Pas) than those of the thermoplastic/wax based binder systems (10-1000

Pas) within a shear rate range of 100-1200 s^{-1} and this was due to the much better and easier fluidity of the thermoplastic/wax polymers (when melted/softened) than the water-soluble polymers when mixed with ceramic/metallic powders.

5.7- Comparison between the mechanical and thermal properties obtained during this work and those by other workers for the injection moulded (and by other fabrication techniques) alumina ceramics

This section is divided into two parts. The first part compares and discusses the flexural and compressive strength results obtained during this work with those obtained by other workers. In the second part the thermal conductivity results obtained during this work are compared and discussed with those reported by other workers.

5.7.1- Comparison between the flexural and compressive strength results

This is given in Table 5.1 at the end of this chapter. From this Table it can be seen that the flexural and compressive strength results obtained during this work (see chapter four-section 4.3.1) by the injection moulding process are in good agreement with those given in the alumina book (104) obtained by the cold-dry compaction technique. This Table also shows that the flexural/bend strength results obtained during this work by the injection moulding process for the 99.5 % alumina ceramics are much higher (27-35 %) than that obtained by Mutsuddy (173) for the injection moulded 99.9 % alumina ceramic.

There are three main factors that have marked effect on the mechanical properties of ceramic materials (104) and they are as follows: composition/purity, density/porosity and particle size. As can be seen from Table 5.1 the higher the purity (i.e. the higher the % alumina content) the higher the flexural and compressive strengths and also the higher the density (i.e. the

lower the porosity) of the alumina ceramic the higher the flexural and compressive strengths. From this Table it can be seen that the compressive strength is more sensitive to purity and density variations than flexural strength.

From the above comparison it can be seen that it is therefore possible to obtain similar mechanical properties for the injection moulded alumina ceramics to those obtained by compaction processes provided that a high volume loading (. 70 %) of the alumina powder is incorporated within the binder system. Table 5.1 also shows that the injection moulded 99.5 % alumina ceramic using the PIB-MEW-LP binder system has higher flexural and compressive strengths than the injection moulded 99.5 % alumina ceramics using the 60/40 APP and/or the water-based PVA binder systems which is due to the higher sintered density (as a result of higher volume loading of the alumina powder) obtained using the PIB-MEW-LP binder system than the other two binder systems. This Table also shows that the 60/40 APP and the newly developed water-based PVA binder systems have provided comparable strength results to those obtained by the compaction process for the high purity alumina ceramics and that they provided higher flexural strength (27-29 %) than that obtained by Mutsuddy (173).

5.7.2- Comparison between the thermal conductivity results

This is given in Table 5.2 at the end of this chapter. From this Table it can be seen that the thermal conductivity results obtained for the first time during this work for the injection moulded alumina ceramics are in very good agreement with the published data in the ceramics Handbook and also with the alumina book (only for the 99.5 % and 99.7 % alumina grades). These results show quite clearly that the higher the purity of the alumina ceramic the higher the thermal conductivity and vice versa. It can also be seen that for the same alumina grade (see the 99.5 % grade in Table 5.1) the higher the sintered density (the lower the porosity) the more thermally conductive the

alumina ceramic. It can therefore be realised that thermal conductivity is very sensitive to both purity and density of the alumina ceramics. Due to this reason the injection moulded 99.5 % alumina ceramic using the PIB-MEW-LP binder system with a higher density (lower porosity) provided higher thermal conductivity (see Table 5.2) than the injection moulded 99.5 % alumina ceramics using the 60/40 APP and the water-based PVA binder systems.

5.8- Properties of the injection moulded zirconia, silicon nitride, silicon carbide and tungsten carbide-6 weight % cobalt powders using the newly developed PIB-MEW-LP binder system

A summary of these properties were given in Table 4.69 at the end of chapter four. From this Table it can be seen that the newly developed PIB-MEW-LP binder system has provided quite satisfactory properties for the above mentioned powders. These properties for each powder are discussed as follows.

1- For the first time during this work an injection moulded zirconia ceramic was obtained using the PIB-MEW-LP binder system which provided a high volume loading of 65 % of the zirconia powder resulting in a high sintered density of 96.5 % of the theoretical density.

2- This binder system provided higher volume loadings in case of the silicon nitride and the hardmetal (WC-6 wt. % Co) powders than those reported in the present literature (61, 143, 146). Sintered densities of 93 and 95 % of their theoretical values were obtained for the silicon nitride and the hardmetal respectively. However, a maximum sintered density could not be obtained for the silicon nitride due to its high sintering temperature (. 1900°C) which could not be reached during this work because of furnace limitations.

3- This binder system provided a volume loading of 60 % for the

silicon carbide powder resulting in an as-moulded density of 95 % of its theoretical value. This amount of volume loading is quite typical and comparable with those reported by other workers (143). No sintering results were obtained due to very high sintering temperature (~ 2000°C) required for the sintering of silicon carbide which could not be reached during this work because of furnace limitations. However, a sintered density of more than 95 % of the theoretical density is usually expected with a volume loading of ≥ 60 % of the silicon carbide powder (143, 144).

4- The newly developed PIB-MEW-LP binder system provided a very satisfactory mixing, moulding and demoulding properties for all the above mentioned powders. No moulding defects were found with the silicon carbide and the hardmetal moulded samples and only one silicon nitride sample (out of a batch of 12 samples) showed some macro and micro voids (100-1000 μm) and two of the zirconia moulded samples (out of a batch of 12 samples) also showed some macro and micro voids of similar type.

5- Considering the rheological properties of the above PIB-MEW-LP + powder mixtures it was found that the zirconia and silicon nitride powder-binder mixtures showed almost identical viscosities varying between 10-300 Pas within a shear rate range of 10-1200 s^{-1} at temperatures of 100-120°C which are a very suitable viscosity/shear rate ranges for the injection moulding process. The silicon carbide and the hardmetal powder-binder mixtures also showed very similar viscosities varying between 20-400 Pas within a shear rate range of 10-1200 s^{-1} at temperatures of 100-120°C which are also quite suitable viscosity/shear rate ranges for the injection moulding process.

It can therefore be concluded that the newly developed thermoplastic-wax (PIB-MEW-LP) binder system can be used quite successfully for the injection moulding of other oxide, nitride, carbide and hardmetal (cermet) powders as well as the aluminium oxide (alumina) powder which was the main oxide ceramic powder

investigated during this research work.

5.9- Properties of the injection moulded silicon nitride, tungsten carbide-6 weight % cobalt and iron-2 weight % nickel powders using the newly developed water-based PVA binder system

A summary of these properties was given in Table 4.76 at the end of chapter four. From this Table it can be seen that the newly developed water-based PVA binder system has provided quite satisfactory sintered densities of 97.5 and 94.5 % of their theoretical densities for the hardmetal (WC-6 wt. % Co) and iron-2 weight % nickel powders with very short debinding times of 7 and 7.2 h for 5 mm thick samples respectively. A sintered density of 92.5 % of the theoretical value was obtained for the silicon nitride at a sintering temperature of 1750°C with a debinding time of 12 h for 5 mm thick samples. The Edax chemical analysis of the debonded samples showed no sign of oxidation products with water and this was due to the evaporation of water at ~ 100°C during the first ramp (see Table 4.72) where no oxidation reaction is likely to take place. The temperature above which oxidation of silicon nitride takes place is ~ 600°C in air (174) and this was also prevented by debinding the silicon nitride samples under argon up to 850°C. Note that a higher sintered density would have been possible by sintering the silicon nitride at a higher temperature (~ 1900°C) but this was not possible during this work due to furnace limitations. The mixing, moulding and demoulding properties of the above powder-PVA binder mixtures were quite satisfactory and no moulding defects could be found with the moulded samples. The above moulded samples were quite rigid and there were no distortion and no adhesion problems during the demoulding process. A cycle time of less than 1 min was used for each moulding so that to obtain the complete gelation of the moulded PVA samples.

Considering the rheological properties of the above powder-binder mixtures (see Figs. 4.55, 4.56 and 4.57) it can be seen that these water-based PVA-powder mixtures have produced relatively higher viscosities (than the PIB-MEW-LP-powder mixtures) varying between ~ 100-10000 Pas within a shear rate range of ~ 10-1200 s^{-1} at a temperature of 72°C. These relatively higher viscosities are due to the poor fluidity provided by water-based binder systems, in general, which also provide lower volume loading of the powder to be injection moulded. However, these viscosities and shear rates will be reduced considerably during the injection moulding process due to the larger nozzle diameter (~ 3 mm) than that of the die (= 1 mm) used for viscosity/shear rate measurements. This size of nozzle diameter is very typical for the injection moulding of ceramic/metallic powders (15, 17, 72, 146). Amongst the above extruded PVA-powder mixtures the hardmetal and the iron-2 weight % nickel powders caused higher viscosities than the silicon nitride powder-PVA mixture reaching to ~ 25000 Pas at a shear rate of ~ 10 s^{-1} at 72°C (see Figs. 4.56 and 4.57).

From the above discussion and the related properties (see Table 4.76) it can be concluded that the newly developed water-based PVA binder system can be used quite successfully for the injection moulding of metallic (e.g. hardmetals and iron-nickel alloys) as well as ceramic (oxide and nitride) powders.

5.10- Effect of tap density (powder characteristics) on the amount of volume loading of powders (used during this work) into the PIB-MEW-LP/PVA binder systems

It is very well known (13, 15, 16, 17, 35, 106) that tap density is largely effected by powder characteristics such as particle size, particle size distribution, particle shape, surface area and flow properties of the powder. It is also very well known (1, 13, 15, 16, 17, 146, 170) that the flow properties of ceramic/metallic suspensions are controlled by three important factors: (a) the powder particle characteristics (in other words by tap density); (b) the viscosity and flow behaviour index of the organic phase and (c) the properties of the particle-fluid interfacial region. It was shown by Farris (16) that it is possible to increase the amount of a powder in an organic suspension (without increasing the viscosity of the suspension) by increasing the difference in mean particle size between coarse and fine fractions. In fact Farris showed that the volume loading of powders can be increased by - 17 % in a mix containing 75 % coarse and 25 % fines by progressively decreasing the size ratio, R = Mean fine particle size / Mean coarse particle size (see Fig. 2.3 in chapter two).

It follows therefore that another way of showing the effect of powder characteristics on the amount of volume loading of powders into an organic suspension and also on the viscosity of suspensions is by considering the tap density of the powders. It was noticed during this work that if an ideal powder (as described by Farris) does not exist then, in general, the higher the tap density of the powder the lower the amount of volume loading of that powder into the organic binders (PIB-MEW-LP/PVA, see Tables 4.77 and 4.78) and also the higher the viscosity of that powder-binder mixture (see chapter four-section 4.1.4.(c) and Figs. 4.16 and 4.17).

It must be mentioned at this stage that the aim of this work was not to repeat the work carried out by Farris (16) in order to increase the amount of a powder (e.g. alumina) in an organic binder system by increasing the difference in mean particle size between coarse and fine fractions. The aim of this work, as described previously, was to investigate/explore more systematically and also to understand more scientifically the properties of each stage in the injection moulding of a typical alumina powder using the available binder systems for which some successes had been claimed for in the literature and then use these initial findings in order to develop new binder systems which can provide not only higher volume loadings but also better moulding, demoulding and shorter debinding times than those already available with the existing binder systems. It follows therefore that although it may have been possible to increase the volume loading of the alumina powder, e.g. in the polystyrene binder system, by using the Farris way so that to obtain higher sintered densities but this would not decrease the long debinding time of 180 h (= 7.5 days, as found during this work, see Table 4.31) which is typical of polystyrene moulded samples with ≥ 5 mm thickness, and therefore not an economically viable time. It is therefore more important to have an ideal binder system since it is the organic phase which commands the broad range of properties and therefore allows a proper operation to succeed completely and not just a high voulme loading of the powder which can be achieved not only by Farris way but also by having a proper binder system incorporated with a powder having a moderate particle size distribution without an excessive concentration of particles in any narrow particle size range (35).

5.11- Torque results and related rheological flow behaviour obtained during this work for each powder-binder composition

A summary of these results are given in Tables 5.3, 5.4 and 5.5 at the end of this chapter. The details of each composition (i.e. the % volume loadings of the powders and the binders) can be seen for each binder system in chapter four (see sections 4.1, 4.2 and 4.7). From the above Tables it is quite clear that by increasing the amount of volume loading of the powder (note that composition 1 has the lowest volume loading and the last composition has the highest volume loading of the powder) in any binder system the torque value also increases. This torque value is related to the amount of shearing which takes place during the steady state mixing (the initial high transient torque levels [see Fig. 4.1-chapter four] are associated with inter-particle friction of uncoated powders) within the mixing chamber and can be used to calculate the viscosities of the powder-binder blends (15, 62). The increase in torque value therefore means an increase in viscosity of the powder-binder mixture. The above Tables also show very clearly that there is a critical torque value (also related to a critical shear rate) above which dilatant flow behaviour can be expected/predicted during the extruding and/or moulding operations. From these Tables it can be seen that usually a torque of $\geq$ 390 mg is likely to cause dilatancy during the extrusion/moulding operations and also usually a torque of $\leq$ 340 mg is a sign of pseudoplasticity which is the correct flow behaviour for the injection moulding of ceramic/metallic powders (1, 15, 17, 72). The above Tables also show that the water-based binder systems (i.e. the methylcellulose and PVA) have slightly higher torque values (. 7 %) than the thermoplastic/wax based binder systems and a similar result was also seen from the viscosity values (see section 5.8) which were generally higher for the water-based binder mixtures.

5.12- Burning properties and characteristics of the organic binders used during this work

Amongst the thermoplastic and wax binders the montanester wax (MEW) showed the most favourable burning behaviour, i.e. decomposition/volatilisation of this binder took place over a wide temperature range at an almost constant/linear rate (see Fig. 4.24 in chapter four) which is essential for a fast and defect-free burn out (1). Due to this reason a debinding time of 36 h was obtained for the 5 mm thick moulded alumina-MEW samples (see Table 4.55) which was the shortest debinding time amongst all the thermoplastic/wax binders used during this work. It is believed (146) that the broad decomposition temperature range is probably caused by the presence of the calcium salt which has been traced (176, 177) within MEW by electron probe micro-analysis. Due to the same reason some residue of calcium has been found (146) in the debonded samples. Note that the calcium salt is usually added as a thermal stabiliser to some polymers (176, 177).

The 60/40 APP binder mixture also showed similar burning characteristics to that of the MEW binder but did not provide a similar debinding time. The shortest possible debinding times provided by the 60/40 APP binder system were 107 and 78 h for 6 mm and 3 mm thick samples respectively (see Table 4.31).

From the thermogravimetric analysis (TGA data) carried out during this work for each organic material it could be understood that, in general, the temperature range of decomposition of the binders, plasticisers and lubricants used during this work was a function of molecular weight. The TGA data curves showed that the lower molecular weight materials (i.e. waxes, plasticisers and lubricants) decomposed at a lower temperature range than the higher molecular weight binders (i.e. thermoplastic binders such as ethylene vinyl acetate, polystyrene, polyacetal, polyethylene glycol, APP and PIB). This trend has also been observed by other workers (14, 146).

From the shape of the TGA curves it could be realised that the

debinding process would, in general, take place over three stages. The first stage usually took place below the softening point (~ 200°C) of the major binder and it is believed (146) that during this stage stress relieve/relaxation takes place and therefore in order to avoid stress cracking due to stress relaxation the critical heating rate should not be exceeded during the heating up period at this stage. These stresses are believed to exist within each moulded sample paticularly in thick mouldings with high binder content due to thermal expansion and contraction processes. The second debinding stage is considered to be the most critical stage during which the actual decomposition of the binders takes place and therefore more ramps with slower heating rates were used for this stage. Lubricants and plasticisers come off first and low molecular weight waxes come off next creating some pores within the sample. Most of the major binder burns out gradually during the second stage creating more voids for the third/final debinding stage during which fewer ramps and higher heating rates were applied for the complete burn out of the binders.

It was quite noticeable that the heating rates in each ramp depended on two important parameters: one was the sample thickness and the other one was the amount of binder content which together with the burning characteristic of the major binder influenced the debinding time of the thermoplastic/wax based moulded samples.

5.13- Moulding properties of the montanester wax (MEW) binder systems

It was found during the development of the new binder systems that the alumina-MEW binder mixture produced mouldings with some shrinkage cracking problems (see sections 4.2.2 and 4.2.3 in chapter four). This problem was mainly due to the high thermal expansion characteristic of the MEW which then shrinks during cooling/recrystallisation within the mould cavity (after moulding) causing shrinkage cracking of the moulded (alumina) samples. This shrinkage cracking problem was also reported by Martyn (146) for his moulded hardmetal-MEW samples. Martyn also believed that this type of cracking was due to partly the high thermal coefficient of volume expansion ($\sim 10^{-4}$ at 25°C) and more predominantly due to an increase in specific volume associated with the crystalline structure of the MEW which shrinks enormously and causes shrinkage cracking during the cooling stage within the mould cavity.

The addition of the amorphous polyisobutylene (PIB) binder to the highly crystalline MEW binder (see section 4.2.5-chapter four) was therefore carried out in order to reduce the crystallinity and hence the shrinkage level of the MEW. It was due to this binder combination that no shrinkage cracking was observed with the moulded alumina (and other powders) samples using the MEW-PIB-LP binder system. The prevention of shrinkage cracking is believed to be due to the shrinkage reduction and also extension of the phase transition of the MEW by the PIB binder. On the other hand the PIB addition caused longer debinding times (see Table 4.55) for the moulded alumina-MEW-PIB-LP (and other) samples than the single alumina-MEW moulded samples (see also Table 4.55).

The shrinkage cracking of the hardmetal-MEW moulded samples was prevented by addition of microcrystalline wax (for the same reason) to the MEW (146). This type of binder combination was also tried during this work (see chapter four-section 4.2.3) but was not successful due to still shrinkage cracking problems.

Martyn's (146) success with the MEW + microcrystalline binder combination was also partly due to the higher thermal conductivity of the hardmetal powder (than the ceramic materials) which resulted in slower cooling, i.e. less insulation of the heat and therefore better heat dissipation, and hence prevented the shrinkage cracking problem by a less strained structure. Martyn also reported that the two wax binders were quite compatible and the microcrystalline wax addition did not change the burning characteristic of the MEW and that the moulded samoles were quite tough with good handling properties.

5.14- Effects of moulding conditions and properties of the moulded rectangular test bars

It was found during this work that the injection/moulding pressure (within the range 0.55-13.8 MN/m^2) had almost no effect on the as-moulded (green) and sintered densities of the alumina samples. On the other hand other parameters such as barrel/nozzle (melt) and mould temperatures had a marked effect on the flow properties of the feedstocks and, in general, a higher melt temperature required a longer hold pressure times for the complete filling of the mould cavity and also for the complete packing of the moulded samples.

Cross section examination of the moulded rectangular alumina samples with low powder volume loadings of < 64 % showed that the density of the core regions was higher than that of the peripheral layers. This type of density variation was also reported by Martyn (146) for the moulded rectangular hardmetal samples having low powder volume fractions of < . 0.6 (= 60 %). The reason for this density changes is attributed to the low mould temperature used throughout their moulding process. As the feedstock enters the mould cavity the material immediately adjacent to the cold mould surface solidifies forming a skin which progressively increases in thickness without being subjected to the full injection pressure. At the same time the

core of the cavity remains molten for a period until the gate solidifies and therefore is subjected to the full injection pressure available. The applied pressure tends to consolidate the moulding core, compensating for any volumetric and thermal shrinkage as the moulded feedstock gradually cools. It is believed (146) that by using a higher mould temperature a higher density of the peripheral layers would be obtained due to the extension of the time period of the molten state condition within this region. However, by applying a higher mould temperature there were distortion problems during the demoulding process and to reduce the distortion problem a mould release agent was sprayed on the walls of the mould cavity (146).

This type of density variations was not observed with the moulded alumina samples having a high powder volume loading of ≥ 64 %. The water-based methylcellulose moulded samples did not show any density variations probably due to a high mould temperature of 72°C but had distortion problems during the demoulding process. The newly developed water-based PVA moulded samples also did not show any density variations probably due to a low moulding temperature of 72°C.

The major moulding defect observed during this work within some of the moulded samples was the presence of macro and micro voids of size 10-1000 μm. These voids were due to mainly entrapped air and inhomogeneity during the mixing and moulding operations. However, the occurrence of voids and density variations can also be directly attributed to the activation energy and thermal dependence of viscosity (126, 146). It is believed (126, 146) that the density variation along the moulding axis takes place as the feedstock enters the mould cavity and undergoes rapid solidification during which the rise in viscosity causes the gate area to freeze prematurely before the full pressure is applied within the cavity to compensate for volumetric shrinkage and thermal contraction.

Transverse shrinkage cracks have also been observed (146) within moulded (hardmetal) samples having relatively high powder volume fractions in a highly crystalline wax binder. It is believed

(146) that these cracks were originated from shrinkage induced stresses set up as the mouldings cooled and restrained within the mould. The stress levels are higher when the temperature differential between the melt (feedstock) and mould is high causing larger cracks.

The occurrence of voids due to air entrapments during the moulding operation may also be due to high injection rates when a jetting flow behaviour takes place. This type of flow behaviour also occurs at high shear rates during which the feedstock enters the cavity in the form of thread (see Fig. 2.13.(a) in chapter two) and is consolidated to form a coiled structure. This type of mould filling behaviour inevitably introduces air pockets in the moulded part, which are seen as voids in the sectioned samples. Filled polymers and polymers with high activation energies of viscous flow are more susceptible to jetting flow (126, 146). It is believed (146) that reducing the rate of mould filling promotes a plug type of flow during which the air is gradually removed out of the cavity by the melt front thus reducing the presence of voids.

5.15- Overall assessment of the rheological properties of the organic binders used during this work

It is believed that differences in the observed apparent viscosities of the organic binder systems are related to their respective molecular weights and amount of chain branching as also reported by other workers (15, 17, 146). Both the thermoplastic (e.g. ethylene vinyl acetate, polystyrene and atactic polypropylene, etc.) and water-based (e.g. methylcellulose and polyvinyl alcohol) binder systems showed a marked shear dependence of viscosity as the shear rate increased. This dependency was higher with low molecular weight binders having relatively narrower molecular weight distribution. The wax-binder mixtures showed near-Newtonian flow behaviour which is typical of low molecular weight binders of small molecular chain entanglement and inter-molecular attraction. However, the general trend was that the viscosity increased as the molecular weight of the binder increased. This behaviour can be mainly attributed to an increase in the Van der Waal's forces operating between molecules. It follows therefore that binders with lower molecular weights (e.g. waxes) have lower melt viscosities than binders with higher molecular weights (e.g. thermoplastics). The higher melt viscosity is mainly due to inherent molecular chain branching which effectively reduces molecular mobility.

As also reported by many other workers (1, 13, 14, 51, 146, etc.) the fundamental flow response of any powder-binder composition is dependent on the major binder used in that binder mixture. It is quite obvious that the only difference between the flow behaviour of the pure organic binder and its filled state is a substantial increase in the viscosity and more shear sensitivity of the latter which can be related to a re-alignment of the particles when the filled composition is subjected to shearing stresses (e.g. during extrusion and mixing). As shearing increases particle aggregates are gradually dispersed. This results in an increase in the amount of free binder, which

was previously immobilised between the agglomerated particles, and therefore reduces the viscosity of the mixture. As shear rate increases the particles will tend to re-align to a minimum energy state hence reducing inter-particle contacts and, as already stated, the amount of free binder in the mixture increases. In both conditions a reduction in the viscosity of the composition is likely. The two simultaneous mechanisms (as discussed above), i.e. the particle re-alignment (and de-agglomeration) and depletion of (free) binder, is known (146) as the mechanism of pseudoplastic behaviour (i.e. decrease in viscosity with shear in the filled and unfilled states). However, above a critical shear rate particle re-orientation and dispersion occurs causing inter-particle contacts which increase with the applied shear stress. Eventually a rigid mixture which cannot flow sufficiently is formed causing siezure within the extruding/moulding barrel. This is known as the mechanism of dilatant flow behaviour (i.e. increase in viscosity with shear). The critical shear rate, however, is dependent on the amount of powder loading and binder viscosity (as seen throughout the experimental results in chapter four of this thesis) and so by increasing the melt temperature the powder-binder viscosity decreases which causes the particle re-alignment to occur at a faster rate thereby eliminating inter-particle contact and hence the occurence of dilatant flow.

The observed increase in both the apparent viscosity and pseudoplasticity of compositions with high molecular weight binders (e.g. polystyrene, polyacetal, etc.) is related to a combination of chemical compatibility and an increase in the average molecular weight and molecular distribution of the binder. It is believed that addition of compatible plasticisers (such as diethyl phthalate and liquid paraffin) depresses the inter-molecular forces and therefore reduces the average molecular weight of the binder which ultimately results in low viscosity compositions.

5.16- Overall assessment of the mixing properties

It is clear from the existing literature that generally the wider the particle size distribution the higher the packing density (1, 13, 15, 16, 17, 20, etc.). As seen during the experimental work (chapter four-composition and mixing results) powders with moderate size distributions (0.1-30 μm) produced moderate feedstock compositions with easy mixing properties. As discussed earlier (in section 5.10) it was generally observed during this work that the higher the tap density of a powder the lower the volume loading of that powder into the newly developed binder systems and the more difficult the mixing process (as seen from the relatively higher steady state torque values in chapter four-mixing results). The reason for this is believed to be related to the amount of fine particles within the particulate systems, i.e. the lower the level of fine particles the easier the mixing process (the lower the energy/torque required for the mixing of that powder-binder mixture). The mixing difficulty experienced in mixing fine powders has also been reported by other workers (55, 146). Powders containing large amount of fine particles will inevitably have higher specific surface areas and consequently require a greater amount of binder so that to be coated uniformly during the mixing process. This reduces the amount of free binder (which would otherwise be available to promote composition flow) and cause an increase in the viscosity of the powder-binder mixture (resulting in higher torques during mixing). It is also believed that a de-agglomerated composition would have a higher viscosity than a comparable agglomerated mixture for the same reason, since the total surface area available in the former mixture would be greater. However, an opposite effect can also be concluded, i.e. the presence of aggregates may actually reduce the viscosity of a composition due to an increase in the amount of free binder (which would have been used for the coating of the de-agglomerated particles and as explained earlier resulting in higher viscosities).

The observed differences in the torque values (see Tables 5.3-5.5, as in the viscosities) from the Brabender plastograph is also related to the molecular weight of the binders used. It is quite obvious that the high molecular weight, high viscosity usual thermoplastic binders require a higher energy/torque for mixing than low molecular weight, low viscosity binders. Binders of low melt viscosity (e.g. waxes and the newly developed binder systems during this work) provided more effective and easier mixing than binders with relatively higher melt viscosity (e.g. polystyrene and polyacetal binders). This is due to their inherent ease of flow which reduces the need for high shearing stresses thereby reducing the incidence of wear which has been found (51, 146) to be particularly severe with highly loaded thermoplastic-based binder systems. However, it was quite clear that in order to produce a homogeneous powder-binder mixture a high shear melt mixing was generally required (so that to disperse and to de-agglomerate the powder more effectively). Small amount of binder was found to go through the rotor shaft-bearing clearance of the Brabender mixing device in the case of low viscosity compositions having a low powder volume loading. This was confirmed by subsequent thermogravimetric analysis showing a binder deficit of . 5 volume %. It was noticed that the high viscosity, high molecular weight binder systems were more capable of dispersing the agglomerates than the low viscosity, low molecular weight binders. This was due to their more standing and transferring of the high shearing stresses during the mixing operations.

5.17- Properties of the sintered parts

The microstructures of the sintered alumina samples obtained by the injection moulding process using the 60/40 APP, MEW-PIB-LP and the water-based PVA binder systems (i.e. the best binder systems during this work) showed clearly the occurrence of grain growth (see Figs. 4.38, 4.41, 4.42 and 4.43 in chapter four) which is typical of oxide ceramics due to their high sintering temperatures (104, 106). The average grain size of the 99.5 % alumina sample sintered at 1800°C was bigger than that of the 99.5 % alumina sample sintered at 1750°C (see Figs. 4.38 and 4.41) which shows the effect of a higher sintering temperature on the grain structure of sintered alumina ceramics. However, these sintered alumina microstructures were very similar to those obtained by the standard compaction techniques (see Figs. 2.33 and 2.34 in chapter two) except that there were some microporosities in the sintered structures of the injection moulded alumina samples which is believed (146) to be inevitable due to entrapped air/voids within the mouldings and also due to macro/micro voids within the debonded samples that were not removed/closed completely during the sintering process and therefore appeared as isolated closed pores within the sintered structure.

The sintered shrinkages of the alumina samples were quite linear and isotropic in all directions. Shrinkage was greater with the lower grades of alumina (88 and 95 % grades) due to the presence of the liquid phases (silica and calcia) during the sintering process which cause more shrinkage than solid state sintering (during sintering and cooling stages).

The sintered 99.5 % alumina samples obtained by the injection moulding process using the water-based methylcellulose and the PVA binder systems showed higher shrinkages than those obtained by using the thermoplastic/wax based binders and this was due to mainly their lower powder volume loadings.

No examinations of the sintered microstructures of the other

injection moulded powders were carried out. However, it is quite predictable from their near theoretical sintered densities that there will inevitably be some macro/micro porosities which is typical of the sintered microstructures obtained by the injection moulding process (146).

It was noticed that the linear shrinkages of the sintered silicon carbide, tungsten carbide-6 weight % cobalt and iron-2 weight % nickel bars were anisotropic particularly in the transverse direction of the mouldings. The work of Martyn (146) and others (178) suggest that the anisotropic shrinkage behaviour originates from streamline flow within the narrow rectangular bars. It is believed (146, 178) that during the mould filling stage the particles will be subjected to shearing stresses and tend to orientate in a direction of least resistance to flow. Consequently, asymmetric particles will tend to align with their major axis parallel to the flow direction. In contrast, their minor axis will be orientated in a direction perpendicular to the flow direction. Hence, particle concentration in the flow direction will tend to be greater than that of the transverse direction, with a corresponding reduction in the linear shrinkage.

From Tables 4.69 and 4.76 it can be seen that quite satisfactory near theoretical densities have been obtained during this work for the sintered tungsten carbide-6 weight % cobalt and iron-2 weight % nickel bars. However, even with such high densities, some macro/micro porosities are believed (146) to be inevitable within their microstructures.

Table 5.1- Comparison between the flexural and compressive strength results obtained during this work for the injection moulded alumina ceramics and those obtained by other workers by injection moulding and other fabrication processes

Source	Fabrication method	Alumina grade (%)	Density (g/cm^3)	Particle size (μm)
Practical Handbook of Materials Science, Section 6. Ceramic Materials, Table 62-2	Cold-dry compaction	99.9 (α-alumina) 99.5 96 90 85	3.96 3.87 3.72 3.6 3.41	1-6 5-50 2-20 2-10 2-12
Alumina: Processing, Properties & Applications; Springer-Verlag; 1984 (104)	Cold-dry compaction	99.7 97	3.9 3.7	4 (Ave.) 10(ave.)
Mechanical properties of injection moulded ceramics, Mutsuddy, B.C., 1987 (173)	Injection moulding	99.9	3.82	0.62 (ave.)
During this work (by injection moulding technique using the best binder systems)	MEW-PIB-LP 60/40 APP water-based PVA 60/40 APP 60/40 APP	99.5 99.5 99.5 95 88	3.81 3.71 3.71 3.57 3.45	1.4 1.4 1.4 14 23 (all ave.)

Table 5.1 continued

Source	4-point flexural/ bend strength (MN/m^2)	Compressive/ crushing strength (MN/m^2)
Practical Handbook of Materials Science, Section 6. Ceramic Materials, Table 62-2	551 380 359 338 297	3792 2620 2068 2482 1931
Alumina: Processing, Properties & Applications; Springer-Verlag; 1984 (104)	500 300	5000 3000
Mechanical properties of injection moulded ceramics, Mutsuddy, B.C., 1987 (173)	260 ± 53	——
During this work (by injection moulding using the MEW-PIB-LP, 60/40 APP, water-based PVA, 60/40 APP & 60/40 APP binder systems respectively)	401 ± 39 367 ± 43 360 ± 46 348 ± 40.5 312 ± 38	4400 ± 85.5 4101 ± 101 4000 ± 119 2910 ± 107 2405 ± 110

Table 5.2- Comparison between the thermal conductivity results obtained during this work for the injection moulded alumina ceramics and those obtained by other workers for cold-dry compacted alumina ceramics

Source	Alumina grade (%)	Thermal conductivity (KW/m°C)
Practical Handbook of Materials Science, Section 6. Ceramic Materials, Table 62-2	Single crystal 99.9 (α-alumina) 99.5 96 90 85	24.6 22 20 14 9.5 8.3
Alumina: Processing, Properties & Applications; Springer-Verlag; 1984 (104)	99.7 97	20 38
During this work by injection moulding using the MEW-PIB-LP, 60/40 APP, water-based PVA, 60/40 APP & 60/40 APP binder systems respectively	99.5 99.5 99.5 95 88	23.3 21.1 20.8 16.4 13.2

Table 5.3- Torque values and related flow behaviour for each 99.5% alumina powder-binder composition used during this work

Binder system	Composition	Torque (mg)	Flow behaviour
Ethylene vinyl acetate	1	280	Pseudoplastic
Polystyrene	1 2 3 4	250 285 325 400	Pseudoplastic . . Dilatant
Polyacetal	1 2 3	285 335 420	Pseudoplastic . Dilatant
APP (density= 0.86, M.wt.= 10600)	1 2 3	270 315 395	Pseudoplastic . Dilatant
60/40 APP	1	320	Pseudoplastic
MEW-PIB-LP	1 2 3	280 322 388	Pseudoplastic . Dilatant
Water-based methylcellulose (Rivers)	1 2 3	282 328 460	Pseudoplastic . Dilatant
Water-based PVA	1 2 3	300 320 396	Pseudoplastic . Dilatant

Table 5.4- Torque values and related flow behaviour for each zirconia, silicon nitride, silicon carbide and tungsten carbide-6 wt.% cobalt composition using the MEW-PIB-LP binder system

Powder	Composition	Torque (mg)	Flow behaviour
Zirconia	1 2 3	290 330 394	Pseudoplastic . Dilatant
Silicon nitride	1 2 3	285 320 386	Pseudoplastic . Dilatant
Silicon carbide	1 2 3	295 335 400	Pseudoplastic . Dilatant
Tungsten carbide -6 wt.% cobalt	1 2 3	292 333 397	Pseudoplastic . Dilatant

Table 5.5- Torque values and related flow behaviour for each silicon nitride, tungsten carbide-6 wt.% cobalt and iron-2 wt.% nickel composition using the water-based PVA binder system

Powder	Composition	Torque (mg)	Flow behaviour
Silicon nitride	1 2 3	300 330 400	Pseudoplastic . Dilatant
Tungsten carbide -6 wt.% cobalt	1 2 3	305 335 405	Pseudoplastic . Dilatant
Iron-2 wt.% nickel	1 2 3	300 332 403	Pseudoplastic . Dilatant

CHAPTER SIX

CHAPTER SIX

6- CONCLUSIONS AND SUGGESTIONS FOR FUTURE WORK

This chapter is divided into two sections. Section 6.1 covers the conclusions achieved from the experimental results (chapter four) during this research programme. Section 6.2 provides suggestions for further work related to this work.

6.1 CONCLUSIONS

6.1.1 From the literature review it can be concluded that there are mainly two groups of binder systems upon which the whole powder injection moulding technology is based. One group uses the usual thermoplastic/wax binders which is referred to as the Wiech process and the other group uses the water-based/soluble binders referred to as the Rivers process which are named after their respective inventers. However, as seen during the first part of the results chapter (chapter four, section 4.1) both groups of binder systems have some limitations which are due to their nature. The thermoplastic/wax-based binder systems (as seen during this work) require long debinding times (> 40 h) which makes them economically not viable for the production of thick mouldings (≥ 3 mm) whereas the water-based binder systems provide a rapid debinding time (typically < 20 h) which makes them economically viable for the production of thick mouldings, but unfortunately they suffer from mould adhesion and distortion problems during the demoulding process and also require rather long moulding cycle times which makes them less viable than the thermoplastic/wax-based binder systems. Both groups of binder systems also provide rather low sintered densities (maximum 96 % theoretical) due to rather low powder volume loading (64 % maximum) as seen during this work (section 4.1).

It follows therefore that a binder system which can provide the favourable properties of the above binder systems can significantly advance the powder injection technology and this

was the purpose of the second part (section 4.2) of this work which was achieved by developing two new binder systems.

The following sections provide the conclusions achieved from each experimental work carried out during this research programme.

6.1.2 It was found that the ethylene vinyl acetate (EVA) copolymer with a 25 % acetate content could not be used as a major binder for the injection moulding of alumina ceramics. This was due to the cracking and crumbling problems of the moulded alumina-EVA samples during the debinding process. Thermogravimetric analysis (TGA) showed that the EVA copolymer had two decomposition stages. It was found during the debinding process that the cracking and crumbling of the moulded alumina-EVA samples took place during the second (final) decomposition stage. It is believed (from TGA results) that the cracking and crumbling problems are due to the rapid and non-linear breakdown of the main ethylene chain which takes place during the second decomposition stage.

6.1.3 An optimised 99.5 % alumina-polystyrene composition with a maximum possible volume loading of 62 % of the alumina powder (having an average particle size of 1.4 μm and a particle size distribution of 0.1-10 μm) and suitable moulding properties was evaluated. Detailed experimental studies were made of each stage of the injection moulding process (IMP). An average sintered density of 95 % of the theoretical density (= 3.87 g/cm^3) and optimised debinding times of 180 and 125 h (≈ 7.5 and 5.2 days) for the 6 and 3 mm thick samples respectively were obtained with the optimised composition.

It can be concluded that the polystyrene binder system is not an economically and technically viable system for the injection moulding of alumina ceramics. This is due mainly to the long debinding periods and rather low sintered density (which is due to rather low powder volume loading into this binder system) achieved using this binder system.

6.1.4 An optimised 99.5 % alumina-polyacetal composition with a maximum possible volume loading of 56.8 % alumina powder (having the same powder characteristics as in 6.1.3) and suitable moulding properties was evaluated. Detailed experimental studies were made of each stage of the IMP. An average sintered density of 93.5 % of the theoretical density and an optimised debinding time of 129 h (≈ 5.4 days) for the 6 mm thick sample were obtained with the optimised composition.

The polyacetal binder system provided much shorter debinding time (- 50 h) but lower sintered density (due to lower volume loading) than that of the polystyrene binder system. It can be concluded that due to the very long debinding times and low sintered density the polyacetal binder system is not an economically and technically viable system for the injection moulding of alumina ceramics.

6.1.5 An optimised 99.5 % alumina-60/40 atactic polypropylene (APP) composition with a maximum possible volume loading of 64 % alumina powder (having the same powder characteristics as in 6.1.3 and 6.1.4) and very suitable moulding properties was evaluated. Detailed experimental studies were made of each stage of the IMP. It was found during the mixing process that diethyl phthalate (DEP) acted as a compatible and excellent plasticiser with the alumina powder-60/40 APP binder mixture. The 60/40 APP (+ DEP + stearic acid) binder system provided the highest sintered density of 96 % of the theoretical density and the shortest debinding times of 107 and 78 h (≈ 4.45 and 3.25 days) for the 6 and 3 mm thick samples respectively amongst the re-evaluated thermoplastic binder systems. This highest sintered density was due to the highest possible volume loading (64 %) of the alumina powder provided by the 60/40 APP binder system. However, these sintered densities provided slightly lower (-4%) flexural strengths than those obtained by other workers for the compacted 99.5 % alumina ceramics, but much better (-30%) than that obtained by another worker for the injection moulded alumina having a similar chemical composition.

It can be concluded that the 60/40 APP binder system provided

reasonable debinding times but unacceptably low sintered density which must be improved in order to have better mechanical properties.

6.1.6 88 and 95 % alumina grades were also injection moulded quite successfully using the 60/40 APP binder system with the same optimised compositions as the 99.5 % alumina-60/40 APP binder mixture. Slightly higher sintered densities (than the 99.5 % alumina) of 97 and 96.5 % of their respective theoretical densities were obtained for the 88 and 95 % alumina ceramics which were due to their higher tap densities than that of the 99.5 % alumina powder. However, due to their higher viscosities shorter mouldings were obtained with the 88 and 95 % alumina grades. Slightly lower flexural strength and very similar compressive strength results were obtained for the injection moulded 88 and 95 % alumina grades compared to those obtained by other workers for the compacted alumina ceramics having similar chemical compositions.

6.1.7 An optimised 99.5 % alumina-(water-based) methylcellulose composition (i.e. using the Rivers binder system) with a maximum possible volume loading of 55 % of the alumina powder (having the same powder characteristics as in 6.1.3) was evaluated. Detailed experimental studies were made of each stage of the IMP. This binder system provided the shortest debinding time of 20 h for the 6 mm thick samples amongst the re-evaluated binder systems. An average sintered density of 94 % of the theoretical density with a shrinkage of 18 % of the total volume were obtained with this water-based binder system. Due to the softness of the moulded samples there were distortion problems during the demoulding process and the use of a mould release agent was necessary to prevent adhesion of the mouldings. A moulding cycle time of . 5 min was required for the complete gelation of each moulding within the mould cavity.
It can be concluded that the use of the water-based methylcellulose (Rivers) binder system for the injection moulding of the 99.5 % alumina powder was not completely

satisfactory due to rather low sintered densities, distortion of the moulded samples and rather long cycle time.

6.1.8 A new thermoplastic-wax-based binder system, namely polyisobutylene (PIB) + montanester wax (MEW) + liquid paraffin (LP), was developed during the second part (section 4.2) of this research programme. This binder system provided a highest possible volume loading of 70 % of the 99.5 % alumina powder (having the same characteristics as in 6.1.3) which resulted in the highest sintered density of 98.5 % of the theoretical density (= 3.87 g/cm^3) during this work. Debinding times of 112, 104 and 80 h were obtained with this binder system for the 6, 5 and 3 mm thick samples respectively which are very similar to those obtained by the 60/40 APP binder system (which provided the shortest debinding times amongst the thermoplastic/wax-based binder systems used during this work). The sintered flexural and compressive strength results of the injection moulded 99.5 % alumina samples using the newly developed PIB-MEW-LP binder system were very similar to those obtained by the compaction process (by other workers) for the alumina ceramics having similar chemical compositions, and much better (.35%) than that obtained by another worker for the injection moulded alumina having a similar chemical composition.

The thermal conductivities of the injection moulded alumina ceramics using the newly developed MEW-PIB-LP binder system were also in good agreement with those of the compacted alumina ceramics (reported by other workers) having similar chemical compositions.

It can therefore be concluded that the newly developed PIB-MEW-LP binder system can be used as an alternative binder system to the existing thermoplastic/wax-based binder systems for the injection moulding of alumina ceramics due to the highest volume loading of the alumina powder, highest moulded and sintered densities, excellent mixing, moulding and demoulding properties provided by this binder system which all together provided very satisfactory mechanical and thermal properties.

It was found during this work that liquid paraffin acted as a highly compatible and excellent plasticiser and lubricant for the mixing of the alumina-PIB-MEW-LP binder mixture.

6.1.9 A new water-based binder system, namely polyvinyl alcohol (PVA) + gelling agent (resorcinol) + liquid paraffin + water, was also developed during the second part (section 4.2) of this work. This binder mixture dissolves in hot water at a temperature of ~ 70°C and gels upon cooling to room temperature which is useful for the production of rigid mouldings. A maximum possible volume loading of 56 % of the 99.5 % alumina powder was provided by this water-based binder system which resulted in a sintered density of 96 % of the theoretical density (= 3.87 g/cm^3) which is higher than that obtained by the water-based methylcellulose (Rivers) binder system. Due to the rigidity of the mouldings (and room temperature demoulding) there were no distortion problems during the demoulding process and also due to the lubricity provided by the solvent expulsion within the mould cavity there were no adhesion problems. A debinding time of 12 h was obtained for the 6 and 3 mm thick samples which is typical of the water-based binder systems. Comparable thermal conductivities, flexural and compressive strength results to the compacted alumina ceramics (reported by other workers) having similar chemical compositions were obtained for the sintered 99.5 % alumina samples obtained during this work by the injection moulding process using the newly developed water-based PVA binder system.

It can therefore be concluded quite clearly that the newly developed water-based PVA binder system can be used as an alternative water-based binder system to the existing water-based Rivers binder system for the injection moulding of alumina ceramics. This is due to the higher volume loading of the alumina powder, higher sintered density, shorter debinding time, better moulding, demoulding and handling properties provided by this water-based binder system which all together provided quite satisfactory mechanical and thermal properties.

6.1.10 It was found during this work that the newly developed binder systems, i.e. the MEW-PIB-LP and the water-based PVA binder systems, also provided satisfactory powder volume loading, mixing, moulding, demoulding and typical debinding properties for the injection moulding of other powders such as other oxides (e.g. zirconia), nitrides (e.g. silicon nitride), carbides (e.g. silicon carbide), hardmetals/cermets (e.g. tungsten carbide-6 weight % cobalt) and metals (e.g. iron-2 weight % nickel) as well as the alumina powder which was the main powder investigated during this work.
However, further work is required for the optimisation of the sintering conditions (temperature and time) so as to obtain the optimum sintered (and hence mechanical) properties.

6.1.11 It was found during this work that if an ideal powder (i.e. that of Farris) is not used then tap density of the powder to be injection moulded influences the amount of volume loading of the powder into the binder system. In general, it was found that the higher the tap density the lower the amount of the powder that can be incorporated into the binder system. In other words the higher the tap density the higher the amount of binder required for the moulding of that powder. It was also found that the higher the tap density of a particular powder for the same volume loading of the binder the higher the viscosity of that powder-binder mixture and also the higher the moulded and sintered densities obtained by that particular powder-binder mixture.

6.1.12 It can be concluded quite clearly from the observed steady state torque results that if a steady state torque of ≥ 380 mg is reached during the mixing stage then a dilatant flow behaviour will result (above a critical shear rate) during the extrusion process suggesting ,therefore, that mixture cannot be used as a suitable moulding composition due to poor flow within the mould cavity and also seizure within the moulding barrel.

6.1.13 It was found that the flow behaviour of the optimised compositions was pseudoplastic at their moulding temperatures. Compositions of higher powder loadings than the optimised compositions showed dilatant flow behaviour above a critical shear rate at moulding (melt) temperatures. The apparent viscosities of each composition showed quite clearly the shear and temperature dependency of viscosity.

6.1.14 The montanester wax (MEW) binder showed the most favourable burning characteristics, i.e. the widest decomposition temperature range with an almost linear burning rate, amongst the thermoplastic/wax binders used during this work. Due to this property the moulded MEW samples provided the shortest debinding time amongst the moulded thermoplastic/wax samples. However, due to high crystallinity and shrinkage of the MEW there were shrinkage cracking problems with the moulded alumina-MEW samples. This problem was prevented by the addition of the polyisobutylene (PIB) binder which was amorphous and therefore reduced the crystallinity and shrinkage of the MEW.

6.1.15 The thermogravimetric analysis (TGA results) of the organic materials used during this work showed that the lower molecular weight materials (waxes, plasticisers and lubricants) decomposed at a lower temperature range than the higher molecular weight materials (major/minor thermoplastics and waxes).

6.1.16 It was found during this work that the injection/moulding pressure (at 0.5 and 13.8 MN/m^2) has a very small effect on the (as-moulded and) sintered density and the only effective way of increasing the (as-moulded and) sintered densities was by increasing the amount of volume loading of the powder. This was in contrast to the compaction pressure which had a marked effect on the sintered densities of the alumina samples, i.e. by increasing the compaction pressure from 30 to 200 MN/m^2 the fired densities increased significantly from 90 to 99 % of the theoretical densities.

6.1.17 The majority of moulding defects appeared in the form of voids (or macro/micro cracks) within the moulded rectangular samples. It is believed that the cause of such defects was most probably due to the entrapped air and inhomogeneity during the mixing and moulding operations. Other causes such as high thermal dependency of viscosity and high activation energy of viscous flow can also be the reason for the formation of such internal defects.

External moulding defects such as sink marks and swelling were not observed with the optimised moulded compositions and only few sink marks were observed at the surfaces of some moulded compositions having a low volume loading of powders (< 56 %).

6.1.18 The debinding time for the thermoplastic/wax-based binder systems was found to be dependent on the thickness of the moulded samples and also on the amount of binder content (debinding time increased as these two parameters increased). The debinding process for the majority of the binders took place over three stages. The first stage took place below the softening temperature of the major binder and higher heating rates could be used during this stage. The second stage was the most critical stage during which most of the binder volatalised and therefore more ramps with slower heating rates were used so that to avoid crack formation due to high degassing rates. In the third (final) stage fewer ramps with higher heating rates were used (due to the presence of more voids) for the complete burn-out of the binders.

The water-based binder systems had almost similar debinding properties except that much higher heating rates could be used for each stage of the debinding process which was due to the much easier burning properties of these binders. However, the water-soluble binders were heated up to much higher temperatures (- 850°C) for their complete burn-out and it is believed that even at such a high debinding temperature there is some carbon residue left within the debonded samples although no measurements were carried out.

6.1.19 The microstructures of the sintered alumina samples obtained during this work by the injection moulding process using the newly developed and the 60/40 APP binder systems were very similar to the standard microstructures of the compacted alumina ceramics except that some macro/micro porosities were also observed which is quite inevitable for the injection moulded components.

6.1.20 Thermal conductivities of the sintered alumina samples obtained by the injection moulding process were measured for the first time during this work. It was found that they were in very good agreement (marginally better) with those published in the standard Ceramic Handbook for the compacted alumina ceramics. It was also quite clear that thermal conductivity decreased as the percentage alumina content decreased.

6.2 FUTURE WORK

6.2.1 It is strongly believed (by the author) that the newly developed thermoplastic-wax-based MEW-PIB-LP binder system has enormous potential for the injection moulding of alumina and other powders and therefore further work should be carried out in applying this binder system for a full scale production line.

6.2.2 Due to still long debinding times obtained during this work by the control of the heating rates further work should be conducted with the objective of reducing the debinding time of the MEW-PIB-LP binder system by the control of the rate of weight loss instead of the heating rates. This would require the use of a special binder-removal equipment which has been used and described elsewhere (179).

6.2.3 Further studies for improving the wetting characteristics of the MEW-PIB-LP binder system in contact with other powders such as silicon carbide, hardmetal and iron powders is believed to be of some value for providing a better mixing and moulding properties.

6.2.4 Further work in improving the powder characteristics such as particle size distribution is believed to be of some value for obtaining higher volume loadings and therefore higher sintered densities.

6.2.5 It is also very strongly believed (by the author) that the newly developed water-based PVA binder system has enormous potential for the injection moulding of oxide powders (e.g. alumina and zirconia) as well as non-oxide powders (e.g. nitrides, carbides, cermets/hardmetals and metals). This binder system must therefore be applied immediately for a full scale production line.

6.2.6 It is particularly felt necessary to improve the powder characteristics such as particle size distribution of each powder in order to achieve higher volume loadings within the water-based PVA binder system (without increasing the viscosity of the mixture) so that to obtain higher sintered densities and lower shrinkages.

6.2.7 It is strongly believed that further optimisation of the sintering conditions (temperature and time) is necessary for the injection moulded nitride, carbide, hardmetal and metallic powders so that to improve sintered densities and microstructures and therefore to obtain optimum mechanical properties.

REFERENCES

REFERENCES

(1) Edirisinghe, M.J. and Evans, J.R.G., Int. J. High Tech. Ceram. 2 (1986) 1-31.

(2) Merhar, J.R. (E.I. du pont de Nemours & Co (Inc), Remington Arms Co, Wilmington, DE 1989, USA), Metal Powder Report, vol. 45 No. 5 May 1990, 339-342.

(3) Werner Diehl, Detlev StÖver (IAW, West Germany), Metal Powder Report, vol. 45 No. 5 May 1990, 333-338.

(4) Schwartzwalder, K., Am. Ceram. Soc. Bull., 28 (1949) 459-61.

(5) Strivens, M.A., Am. Ceram. Soc. Bull., 42 (1963) 13-19.

(6) Burroughs, J.E. and Thornton, H.R., Am. Ceram. Soc. Bull., 45 (1966) 187-92.

(7) Schnittgrund, G.D., SAMPE Quarterly, July 1981, 8-13.

(8) Verduzco Bill, Metal Powder Report, vol. 45 No. 5 May 1990, 343-344.

(9) Becher, P.F., Tiegs, T.N., Advanced Ceramic Materials, 3 (2) 1988, 148-153.

(10) Warren, R., Fibre reinforced ceramic and metal matrix composites-Their potential as high temperature materials, Chalmers University of Technology, Goteborg, Sweden, 1990.

(11) Wachtman, J., Advanced materials and processing, 133 (1988) 45.

(12) Tapio Mäntylä and A.P. Nikkilä (Tampere University of Technology, Institute of materials science), Properties of construction ceramics and composites; Pressed and injection moulded, Advanced materials injection moulding and applications,

International new business and high-tech. conference, 11-15 October 1988, 1-12, Helsinki and Stockholm.

(13) Mutsuddy, B.C., Proc. Brit. Ceram. Soc., 33 (1983) 117-137.

(14) Robert W Messler Jr, Metal Powder Report, vol. 45 No. 5 May 1990, 363-370.

(15) Issitt, D.A. and James, P.J., Powder Metallurgy, vol. 29 No. 4, 1986, 259-264.

(16) Farris, R.J., Trans, Soc. Rheology, 12 (1968) 281-301.

(17) Martyn, M.T., Issit, D.A., Haworth, B., and James, P.J., Powder Metallurgy, vol. 31 No. 2, 1988, 106-112.

(18) Mangels, J.A. and Trela, W., in Advances in Ceramics, vol. 9 Ed. J. Mangels, The American Ceramic Society, Colombus, Ohio, 1984, 220-223.

(19) Lange, F.F., J. Amer. Ceram. Soc., 67, 1984, 83-89.

(20) Edirisinghe, M.J. and Evans, J.R.G., Brit. Ceram. Soc., R.W. Davidge (Ed.), 38 (1986) 67-80.

(21) Rumpf, H. and Schubert, H., In ceramic processing before firing, Onoda, G.Y., Hench, L.L. (Eds.) Wiley, New York, 1978, 357-376.

(22) London, F., Trans. Farad. Soc., 33, 1937, 8.

(23) Bernett, M.K. and Zisman, W.A., J. Coll. Interf. Sci. 28, 1968, 243.

(24) Lange, F.F., J. Amer. Ceram. Soc., 66, 1983, 396.

(25) Lange, F.F. and Metcalf, M., J. Amer. Ceram. Soc., 66 (1983) 398-406.

(26) Lange, F.F., Davis, B.I. and Aksay, I.A., J. Amer. Ceram. Soc., 66 (1983) 407-408.

(27) Di Millia, R.A. and Reed, J.S., J. Amer. Ceram. Soc., 66 (1983) 667.

(28) Frey, R.G. and Halloran, J.W., J. Amer. Ceram. Soc., 67 (1984) 199.

(29) Dynys, F.W. and Halloran, J.W., J. Amer. Ceram. Soc., 66 (1983) 655.

(30) Parish, M.V., Garcia, R.R. and Bowen, H.K., J. Mater. Sci., 20 (1985) 996-1008.

(31) Boaira, M.S. and Chaffey, C.E., Eng. Sci., 17 (1977) 715-718.

(32) Mangels, J.A. and Williams, R.A., Am. Ceram. Soc. Bull., 12 (1968) 281-301.

(33) Mooney, M., J. Coll. Sci., 6 (1951) 162.

(34) Noton, F.H., Refractories, Mc Graw-Hill, New York, 1949, 146.

(35) Adams, E.F., High temperature oxides, Part iv, Academic press, New York, 1971, 145.

(36) Sweeny, K.H. and Greckler, R.D., J. App. Phys., 25 [9], (1954) 1135-1144.

(37) Brodnyan, J.G., Trans. Soc. Rheol., III (1959) 61-68.

(38) Kitano, T., Kataoka, T. and Shirota, T., Rheol., Acta, 20 (1981) 207-209.

(39) Krieger, I.M. and Dougherty, T.J., Trans. Soc. Rheol., III (1959) 137-152.

(40) Woods, M.E. and Krieger, I.M., J. Coll. Interface Sci., 34 (1970) 91-99.

(41) Chong, J.S., Christiansen, E.B. and Baer, A.D., J. Appl. Poly. Sci., 15 (1971) 369-379.

(42) Cannon, W.R., Danforth, S.C., Flint, J.H., Haggerty, J.S. and Marra, R.A., J. Am. Ceram. Soc., 65 (1982) 330-335.

(43) Blendell, J.E., Bowen, H.K. and Coble, R.L., Am. Ceram. Soc. Bull., 63 (1984) 797-801.

(44) Lee, D.I., Trans. Soc. Rheol., 13 (1969) 273-278.

(45) Moulson, A.J., J. Mat. Sci., 14 (1979) 1017-1051.

(46) Mangels, J.A. and Williams, R.A., Am. Ceram. Soc. Bull., 62 (1983) 601-606.

(47) Matsumoto, S. and Sherman, P., J. Coll. Interface Sci., 30 (1969) 525-536.

(48) Brasted, S.J., Nawakowska, L.J., Wagstaf, I. and Walbridge, D.J., Trans. Farad. Soc., 67 (1971) 3598-3603.

(49) Willermet, P.A., Pett, R.A. and Whalen, T.J., Am. Ceram. Soc. Bull., 57 (1978) 744-747.

(50) Ayer, J.E. and Suppet, E., J. Am. Ceram. Soc., 49 (1966) 207-210.

(51) Edirisinghe, M.J. and Evans, R.G., Int. J. High Tech. Ceram. 2 (1986) 249-278.

(52) Tadmor, Z. and Gogos, C.G., Principles of powder processing, Wiley, New York, 1979, chapter 7.

(53) Lange, F.F., J. Am. Ceram. Soc., 66 (1983) 393-398.

(54) Kellet, B. and Lange, F.F., J. Am. Ceram. Soc., 67 (1984) 369-371.

(55) Messer, P.F., Trans. J. Brit. Ceram. Soc., 82 (1983) 156.

(56) Hornsby, P.R., Plastics compounding, 6 (1983) 65-70.

(57) Barringer, E.A. and Bowen, H.K., J. Am. Ceram. Soc., 65 (1982) c199-201.

(58) Billiet, R.A., Metal Powder Report, vol. 45 No. 5 May 1990, 326-332.

(59) Taylor, H.D., Am. Ceram. Soc. Bull., 45 (1966) 768-770.

(60) Mann, D.L., Technical report AFML-TR-78-200, Dec. 1978.

(61) Quackenbush, C.L., French, K. and Neil, J.T., Ceram. Eng. Sci. Proc., 3 (1982) 20-34.

(62) Brabender specification sheet, OHG DUISBURG 1988, 1-24, Engelmann & Buckham Ancillaries Ltd., William Curtis House, Alton, Hampshire.

(63) Birchall, J.D., Howard, A.J. and Kendall, K., Imperial Chemical Industries Ltd., UK, Cementitious product, Eur. Patent 0021682, 7 Jan. 1981. Date of filing: 6 Jun. 1980.

(64) Irving, H.F. and Saxton, R.L., In mixing theory and practice II, Eds. V.W. Uhl and J.B. Gray, Academic press, New York, 1967, chapter 8.

(65) Janssen, Leon P.B.M., Twin-screw extrusion, Elsevier, (Amsterdam and) Oxford, 1978.

(66) SpA Plastics Material Laboratory, UK Patent 629109, 13 Sep. 1949. Date of filing: 2 May 1946.

(67) Martelli, F., Twin screw extruders, Van Nostrand, New York, 1983.

(68) Hornsby, P.R., Plastics compounding, 6 (1983) 65-70.

(69) Abram, J., Bowman, J., Behiri, J.C. and Bonfield, W., Plast. and Rubb. Proc. and Appl., 4 (1984) 261-269.

(70) Hieber, C.A., Isayer, A.I. and Socha, L.S., Internal Report on Composites, Cornell University, 1990.

(71) Rubin, I.I., Injection moulding-Theory and practice, Wiley, New York, 1972, 1.

(72) Mutsuddy, B.C., J. Ind. Res. Dev., 25 (1983) 76-80.

(73) Sturges, R.F., UK Patent 12480, 14 Aug. 1849. Date of filing: 14 Feb. 1849.

(74) Hyatt, J.W. and Hyatt, I.S., Celluloid manufacturing Co., USA, US Patent 133229, 19 Nov. 1872.

(75) Thomas, J., Injection moulding of plastics, Reinhold, New York, 1947, chapters 1 and 2.

(76) Gastrow, H., UK Patent 424369, 20 Feb. 1935. Date of filing: 11 Dec. 1933.

(77) Burroughs, C.F., US Patent 2202140, 28 May 1940. Date of filing: 4 Aug. 1936.

(78) Rapid continuous injection of thermosetting materials, Modern Plastics, 21 (1944) 90-91.

(79) Injection-compression moulding of acrylic feeder heads, Modern Plastics, 23 (1945) 146-50.

(80) Rakas, N.J. and Cousino, W.B., Modern Plastics, 23 (1945) 146-50.

(81) Crawford, R.J., Progress in plastics engineering, Pergamon Press, London, 1981, 169-70.

(82) Fisher, E.G. and Maslen, W.A., British Plastics, 32 (1959) 417-22.

(83) Simonds, H.R. (Ed.), The Encyclopedia of Plastics Equipment, Reinhold, New York, 1964, 306.

(84) Weir, C.L. and Zimmerman, P.T., Facts and figures on ram versus screw injection, Modern Plastics, 40 (1962) 122-5 and 220.

(85) Peshek, J.R., in Advances in Ceramics, Ed. J. Mangels, vol. 9, 1984, 234-8.

(86) Stanciu, V.V., in Advances in Ceramics, Ed. J. Mangels, vol. 9, 1984, 239-40.

(87) Honstrator, R.A., Plastics Engineering, 37 (1981) 35-8.

(88) Bowden, F.P. and Tabor, D., The friction and lubrication of solids, Clarendon Press, Oxford, 1950, 294.

(89) Reinhard, M., SPE Antec, 30 (1984) 798-802.

(90) Injection moulding machine for new ceramics, Japan steel works (Hiroshima Plant), Trade literature, 1984.

(91)- Dawson, D., A.E. Turbine components Ltd., UK, Trade literature, 1986.

(92) Ohnsorg, R.W., The carborundom Co., USA, US Patent 4233256, 11 Nov. 1980. Date of filing: 18 Dec. 1978.

(93) Peltsman, I. and Peltsman, M., Interceram, 4 (1984) 56.

(94) Peltsman, I. and Peltsman, M., Ceram. Eng. and Sci. Proc., 3 (1982) 865-8.

(95) Special purpose machines, Mercia machinery sales Ltd., UK, Trade literature, 1986.

(96) Kubat, I. and Rigdahl, M., Polymer, 16 (1975) 925-9.

(97) Morrison, R.V., Discovision Assoc., USA, US Patent 4412805, 1 Nov. 1983. Date of filing: 23 Sep. 1981.

(98) Demag Kunststofftechnik, Federal Republic of Germany, UK Patent 1553924, 10 Oct. 1979. Date of filing: 23 Dec. 1976.

(99) Allan, P.S. and Bevis, M., Plast. and Rubb. Proc. and Appl., 3 (1983) 85-91.

(100) Allan, P.S. and Bevis, M., Plast. Rubb. Int., 9 (1984) 32-36.

(101) Huther, W., Motor and Turbine Union, Federal Republic of Germany, US Patent 4412804, 1 Nov. 1983. Date of filing: 4 Nov. 1981.

(102) White, J.L. and Dee, H.B., Polym. Eng. Sci., 14 [3] (1974) 212-22.

(103)- Storm, R.S., ASME Paper No. 82-GT-252, ASME International Gas Turbine Conference, Houston, TX.

(104) Dörre, E. and Hübner, H., Alumina: Processing, Properties and Applications, Materials Research and Engineering Ser., 1984, 330 P, Springer-Verlag.

(105) Rhines, F.N., Seminar on the theory of sintering, Trans. AIME, vol. 166 (1947) 474-487.

(106) Lenel, F.V., Powder Metallurgy Principles and Applications, MPIF, Princton, N.J., 1980.

(107) Cheney, R.F., Sylvania, G.T.E. and Towanda, Pa., Lecture on sintering of tungsten and molybdenum, USA (1970).

(108) English Translation: Principles of single phase sintering, Reviews on powder metallurgy and physical ceramics, vol. 1, No. 1-4 (1979).

(109) Shaw, N.J., Densification Powder Metallurgy International, vol. 21, No. 3, 1989.

(110) Johnson, A., Carlstrom, E., Hermansson, L. and Carlson, R., Proc. Brit. Ceram. Soc., 33 (1983) 139-147.

(111) Wiech, R.E., Parmatech. Corp. USA, UK Patent 1516079, 28 Jun. 1978. Date of filing: 30 Mar. 1977.

(112) Saito, K., Tanaka, T. and Hibino, T., Tokyo Shibaura Electric Co. Ltd., Japan, UK Patent 1426317, 25 Feb. 1976. Date of filing: 4 Mar. 1979.

(113) Strivens, M.A., Standard Telephone and Cables UK, UK Patent 779242, 17 July 1957. Date of filing: 7 Aug. 1953.

(114) Mutsuddy, B.C., Oxidation removal of organic binders from injection moulded ceramics, International conference on non-oxide technical and engineering ceramics, National Institute of Higher Education, Limerick, Ireland, 10-12 July 1985.

(115) Sedlazek, B., Verberger, C.G., Mark, H.F. and Fox, T.G. (Eds.), Degradation and stabilisation of polyolefins, J. Polym. Sci., Polymer Symposium No. 57, Wiley, New York 1976.

(116) Luongo, J.P., J. Polym. Sci., 42 (1960) 139-50.

(117) Canterino, P.J., Ethylene polymers, in Encyclopedia of polymer science and technology, vol. 6, Eds. H.F. Mark and N.G. Gaylord, Wiley, New York, 1967, 275-454.

(118) Adams, J.H., J. Polym. Sci., 8 (1970), 1077-90.

(119) Tsuchiya, Y. and Sumi, K., J. Polym. Sci., 7 (1969), 1599-1607.

(120) Tsuchiya, Y. and Sumi, K., J. Polym. Sci., 6 (1968), 415-24.

(121) Chaudhri, S.A., Polymer, 9 (1968) 604-8.

(122) Hansen, R.H., in Thermal stability of polymers, Ed. R.T. Conley, Marcel Dekker, New York, 1970.

(123) Reich, L. and Stivala, S.S., Elements of polymer degradation, Mc Graw Hill, New York, (1971), 10.

(124) Wiech, R.E., US Patent 4305756, 15 Dec. 1981. Date of filing: 14 Jan. 1980.

(125) Wiech, R.E., US Patent 4197118, 8 Apr. 1980. Date of filing: 12 Apr. 1976.

(126) Zhang, J.G., Edirisinghe, M.J. and Evans, J.R.G., Industrial Ceramics, vol. 9, No. 2 (1989) 72-82.

(127) Kellet, B. and Lange, F.F., J. Amer. Ceram. Soc., 67 (1984) 369-371.

(128) An oscillating pressure unit for ceramic injection moulding. Part A. Materials and Design, 8 (1987) 284-288.

(129) Edirisinghe, M.J. and Evans, J.R.G., J. Mater. Sci., 22 (1987) 269-277.

(130) Huther, W., Motor and Turbine Union, F.R.G., US Patent 4412804, 1 Nov. 1983. Date of filing: 4 Nov. 1981.

(131) Mills, N.J., Plast. & Rubb. process. & Appln., 3 (1983) 181-188.

(132) Idem, J. Mater. Sci., 22 (1987) 2267-2273.

(133) Zhang, J.G., Edirisinghe, M.J. and Evans, J.R.G., J. Mater. Sci., 23 (1988) 2115-2120.

(134) Kresser, T.O.J., Polypropylene, Reinhold, London, 1960, p. 64.

(135) Gebler, H., Kunststoffe 73 (1983) 73-76.

(136) Zhang, J.G., Edirisinghe, M.J. and Evans, J.R.G., J. Eur. Ceram. Sci., In press.

(137) Wainer, E., Thompson products Inc. Ohio, USA, US Patent 2593507, 22 Apr. 1952. Date of filing: 1 Mar. 1949.

(138) Gilissen, R. and Smolders, A., Binder removal from injection moulded ceramic bodies, Presented at 6th CIMTEC, Milan, 1989.

(139) Mutsuddy, B.C., Ceramics International, 13 (1987) 41-53.

(140) Jamet, J., Spann, J.R., Rice, R.W. and Coblenz, W.S., Ceram. Eng. Sci. Proc., 5 (1984) 677-694.

(141) Schnittgrund, G.D., SAMPE, Quarterly, 12 (1981) 8-13.

(142) Thomas J. Whalen and Carl F. Johnson, Am. Ceram. Soc. Bull., vol. 60, No. 2 (1981) 216-220.

(143) Litman, A.M., Schott, N.R. and Tozlowski, S.W., Soc. Plas. Eng. Tech., 22 (1976) 549-51.

(144) Hunold, K., Greim, J. and Lipp, A., Powder Metallurgy International, vol. 21, No. 4, 1989, 17-23.

(145) Ohnsorg, R.W., The Carburandom Co., USA, US Patent 4233256, 11 Nov. 1980. Date of filing: 18 Dec. 1978.

(146) Martyn, M.T. and James, P.J., Injection moulding of hardmetal powders using wax binder systems, Institute of Polymer Technology and Materials Engineering, Loughborough University of Technology, Loughborough, England, International New Business and High Technology Research Conference, 3-5 September 1989, Jyväskylä, Finland, 1-18.

(147) Brokin, S.I., Hardmetals production technology and research in the USSR, Ed. S.I. Bashkirov, Pergammon Press (1964).

(148) Nyce, A.C., First European Conf. on Metal, Ceramic and Cemented carbide Injection Moulding, London, Dec. 1988, IBC Technical Services Ltd., pp 1-32.

(149) Billet, R., Conf. Prod. Powd. Metall., Frankfurt, (1982) 53.

(150) Wiech, R.E., US Patent 4404166, 1983.

(151) Rivers, R.D., Cabot Corp., USA, US Patent 4113480, 12 Sep. 1978. Date of filing: 9 Dec. 1976.

(152) Lawcock, R. (GKN Technology Ltd.), Commercial production state of the art, First European Conf. on Metal, Ceramic and Cemented carbide Injection Moulding, London, Dec. 1988, IBC

Technical Services Ltd.

(153)- Barrie, I.T., Plast. Rubber Proc., June 1986.

(154) Crook, P., Rivers, R.d. and Klein, H.J., Haynes International Kokomo, IN, P/M Injection moulding of Ni steel and 316 stainless steel by the Rivers Process, Industrial Heating, May 1987, 12-15.

(155) Howatt, G.N., US Army, US Patent 2434271, 13 Jan. 1948, (30 Aug. 1944), Ceram. Abstr., 1948, April, P.93d.

(156) Ehlers, R.W., General Motors Corp., US Patent 2446872, 10 Aug. 1948, (4 Dec. 1941), Ceram. Abstr., 1949, February, P. 73a.

(157) Rogers, E.J. and Mooney, E.L., Bendix Aviation Corp., Brit. Pat. 671371, 5 Jan. 1949.

(158) Moteki Asao, Yogoyo Kyokasi Shi, 67 [768] (1959) 387-99; Ceram. Abstr. 1960, November, P. 268h.

(159) Processing breakthrough-Injection moulding high alumina components, Ceramic Age, Feb. 1962, 30-32.

(160) Strivens, M.A., UK Patent 779242, 17 July 1957. Date of filing: 7 Aug. 1953.

(161) Boroughs, J.E. and Thornton, H.R., Amer. Ceram. Bull., vol. 45, No. 2, (1966), 187-192.

(162) Herrmann, E.R., Corning glass work, USA, US Patent 323408, 8 Feb. 1966, Date of filing: 21 Nov. 1961.

(163) Newfield, S.E. and Gac, F.D., Report LA 6960, Los Alamos Scientific Lab., USA, 1978.

(164) Farrow, G. and Conciatori, A.B., Celanese Corp., USA, Eur. Patent 114746, 1 Aug. 1984. Date of filing: 19 Jan. 1984.

(165) Saito, K., Tanaka, T. and Hibino, T., Tokyo Shibaura Electric Co. Ltd., Japan, UK Patent 1426317, 25 Feb. 1976. Date of filing: 4 Mar. 1979.

(166) Pett, R.A., Rao, V.D.N. and Qaderi, S.B.A., Ford Motor Co., USA, US Patent 4265794, 5 May 1981. Date of filing: 10 Aug. 1979.

(167) Hashimoto, T., Hama, M. and Koboyashi, O., Sumitomo Chemical Co. Ltd., Japan, UK Patent 2081733, 24 Feb. 1982. Date of filing: 5 Aug. 1981.

(168) Strivens, M.A., UK Patent 808583, 4 Feb. 1959. Date of filing: 13 July 1956.

(169) Richards, G., Alumina ceramics, Review paper, Royal Worcester Industrial Ceramics Ltd., Tonyrefail, Mid Glamorgan, 120-124.

(170) Edirisinghe, M.J., Metals and Materials, vol. 6, No. 6, June 1990, 367-370.

(171) Johnson, K.P., US Patent 4765950, 1988.

(172) Dynys, F.W. and Halloran, J.W., J. Amer. Ceram. Soc., vol. 66, No. 9, (1983), 655-659.

(173) Mutsuddy, B.C., Powder Metallurgy International, vol. 19, No. 2, (1987), 43-45.

(174) Nickel, K.J., Danzer, R., Schneider, G. and Petzow, G., Powder Metallurgy International, vol. 21, No. 3, (1989), 29-33.

(175) Sarkar, N. and Greminger, G.K., Am. Ceram. Soc. Bull., 62 (1983) 1280-1288.

(176) Warth, H.A., The chemistry and technology of waxes, 2nd. Ed., Reinhold, 1956.

(177) BASF Technical Information Leaflet T1/P2798E.

(178) Spriggs, G.E., Metal Powder Report, vol. 35 No. 12, 1981, 547.

(179) Johnsson, A., Carlstrom, E., Herrmansson, L. and Carlsson, R., The Swedish Institute for Silicate Research, S-40229, Gothenburg, Sweden 17; Proc. Brit. Ceram. Soc., 33 (1983) 139-147.

(180) Pritchard, J.G., Poly (vinyl alcohol): Basic properties and uses, 1931; Published: London, Macdonald & Co., 1970.